

Environmentally Benign Method Development Towards the Synthesis of Oxygen-Containing Heterocycles

by

Jean-Marc Irvin Anthony Lawrence

B.S. Chemistry, University of Connecticut, 2017.

Submitted to the Graduate Faculty of the
Dietrich School of Arts and Sciences in partial fulfillment
of the requirements for the degree of
Doctor of Philosophy

University of Pittsburgh

2022

UNIVERSITY OF PITTSBURGH

DIETRICH SCHOOL OF ARTS AND SCIENCES

This dissertation was presented

by

Jean-Marc I. A. Lawrence

It was defended on

June 28, 2022

and approved by

Dr. Alexander Dieters, Professor, Department of Chemistry

Dr. Yiming Wang, Assistant Professor, Department of Chemistry

Dr. James Mckone, Assistant Professor, Department of Chemical and Petroleum Engineering

Thesis Advisor/Dissertation Director: Dr. Paul Floreancig, Professor, Department of Chemistry

Copyright © by Jean-Marc I. A. Lawrence

2022

Environmentally Benign Method Development Towards the Synthesis of Oxygen-Containing Heterocycles

Jean-Marc Irvin Anthony Lawrence, PhD

University of Pittsburgh, 2022

Oxygen-containing heterocycles are highly diverse and attractive targets in chemical synthesis that are prevalent in many biologically active natural products. Synthesizing these structures in an environmentally friendly manner can increase the use of these methods and their applicability in industry and medicinal chemistry. This document describes a dehydrative Re_2O_7 -catalyzed approach in the activation of 1,3- and 1,5-monoallylic diols, which generate an allylic cation intermediate that is captured by a pendent alcohol to synthesize 3,4-dihydropyrans. The 2,6-*trans*-isomer was determined to be the kinetic and thermodynamically favored isomer. A substrate scope is developed to determine the functional group tolerance, and stereocontrol is enhanced through the incorporation of a pendent stereocenter on the dihydropyran ring. Furthermore, an investigation of the mechanism is shown through the manipulation of alkene geometry and stereochemistry to discover a unique S_{Ni} mechanism.

Electrochemical oxidative C–H functionalization is an advantageous way of increasing molecular complexity with high functional group tolerance while minimizing cost and waste. Kinetically slow oxidations followed by C–C and C–O bond formation present challenges in the effective turnover of catalytic oxidants under anhydrous conditions due to low steady-state concentrations of reduced oxidant. TEMPO-based oxoammonium salts are effective hydride abstracting reagents in the oxidation of ethers, amines, and carbamates to generate excellent

electrophiles. Results described herein show that intermediate cation stability, oxidant strength, overpotential, and concentration dictate the rate of electrochemical regeneration of oxoammonium salts in the oxidation of benzylic and allylic ethers. Integrating these factors leads to a new method that synthesizes a diverse substrate scope of oxygen and nitrogen-containing heterocycles, changing the approach toward kinetically slow oxidations in future electrochemical methods.

Table of Contents

Acknowledgments	xxi
1.0 Dehydrative Re ₂ O ₇ -Catalyzed Approach to Dihydropyran Synthesis.....	1
1.1 Dihydropyrans and their Prevalence in Natural Products.....	1
1.2 Synthetic Strategies towards the Synthesis of Dihydropyrans.....	2
1.2.1 Carbon based Nucleophilic Addition into Oxocarbenium Ions.....	2
1.2.2 Ring-Closing Metathesis towards Dihydropyrans	4
1.2.3 Base Mediated Cyclodehydration towards <i>trans</i> -Dihydropyrans	5
1.3 Catalytic Dehydrative Reactions of Allylic and Benzylic Systems.....	6
1.3.1 Brønsted Acid-Catalyzed Dehydrative Reactions	7
1.3.2 Lewis Acid-Catalyzed Dehydrative Reactions	8
1.4 Rhenium Oxide-mediated Activation of Allylic and Benzylic Alcohols	11
1.4.1 Mechanistic Analysis of 1,3-Allylic Alcohol Transposition.....	11
1.4.2 Oxo-Rhenium Catalyzed Allylic Alcohol Transposition used as an Electrophilic Trapping Agent	13
1.4.3 Oxo-Rhenium Catalyzed Dehydrative Reactions in the Floreancig Group .	15
1.4.3.1 Dehydrative Reactions towards 2,6- <i>cis</i> Tetrahydropyrans and Synthetic Applications.....	15
1.4.3.2 The Use of HFIP in Oxo-Rhenium-Catalyzed Bond Forming Reactions.....	17
1.5 Dehydrative Re ₂ O ₇ -Catalyzed Approach to Dihydropyran Synthesis	19

1.5.1 Development of Substrates for Dehydrative Cyclization	20
1.5.2 Solvent Effects and Optimization of Reaction Conditions	21
1.5.3 Understanding the Kinetic and Thermodynamic Outcomes of the Reaction.	24
1.5.4 Substrate Scope	28
1.5.5 Effects of Alcohol Position and Alkene Geometry on Reaction Efficiency ...	34
1.6 Conclusions	40
2.0 Kinetics-Based Approach to Developing Electrocatalytic Variants of Slow Oxidations: Application to Hydride Abstraction-Initiated Cyclization Reactions	42
2.1 C–H Functionalization using Organic Hydride Abstracting Agents	42
2.1.1 Quinone-Based Oxidants as Hydride Abstracting Agents	43
2.1.1.1 DDQ-mediated Oxidative C–H Cleavage towards C–C Bond Formation	43
2.1.1.2 Catalytic Applications of DDQ-mediated Oxidations	45
2.1.2 Oxoammonium and Trityl Cations as Effective Hydride Abstracting Agents	47
2.1.3 Electrochemical Regeneration of Oxoammonium Species for Oxidative C–H Functionalization.....	50
2.1.3.1 Electrochemical Oxoammonium Regeneration in Alcohol Oxidation	51
2.1.3.2 Electrochemical Oxoammonium Regeneration in Bond-Forming Reactions.....	52

2.2 Kinetics-Based Approach to Developing Electrocatalytic Variants of Slow Oxidations: Application to Hydride Abstraction-Initiated Cyclization Reactions	55
2.2.1 Synthesis of Substrates as Model Systems for Electrochemical Regeneration of Oxoammonium Ions in C–C Bond-Forming Reactions	57
2.2.2 Comparing Rates of Alcohol Oxidation to Benzyl Ether Oxidation using Cyclic Voltammetry	58
2.2.3 Reaction Optimization for Successful Electrochemical Regeneration of Oxoammonium Ion	62
2.2.4 Effect of Driving Force on Catalyst Turnover	72
2.2.5 Enol Acetate Substrate Scope for Electrocatalytic Oxidative C–H Functionalization.....	79
2.2.6 Alcohol Nucleophiles in Electrocatalytic Oxidations of Benzyl Ethers.....	84
2.2.7 Effects of Concentration on Reaction Efficiency	88
2.3 Conclusions and Future Directions.....	91
Appendix A	94
Appendix B	134
Substrate Syntheses:.....	135
Appendix C	185
3.0 Bibliography	274

List of Tables

Table 1. Condition Optimization of Re₂O₇ Mediated Dehydrative Cyclization.....	22
Table 2. Substrate Scope of Dehydrative Cyclization.....	30
Table 3. Initial Electrolyte and Additive Screen	65
Table 4. Electrode and Oxidant Loading Screen	67
Table 5. Additive and Electrode Optimization of Electrocatalytic Oxidations.....	69
Table 6. Enol Acetate Substrate Scope	81
Table 7. Effects of Concentration on Reaction Efficiency.....	89
Table 8. Mosher Ester Analysis of 1.105.....	124
Table 9. Mosher Ester Analysis of 1.110.....	127
Table 10. Mosher Ester Analysis of 1.107.....	130
Table 11. Charge per mol Transferred in Each Reaction	177

List of Figures

Figure 1. Dihydropyrans in Featured Natural Products.....	1
Figure 2. NOE Correlations Confirming Structure of 1.69	22
Figure 3. pH Dependent Mechanism of Oxoammonium-Mediated Oxidation of Alcohols.	48
Figure 4. Typical Electrochemical Regeneration of Oxoammonium Ion	51
Figure 5. Oxidant Strength Based on Substituent Effects.....	54
Figure 6. Cyclic Voltammograms of 5mM Hydroxylamine (HA) in the Presence of BnOH	60
Figure 7. Cyclic Voltammogram of 5mM Hydroxylamine (HA) in the Presence of 2.32....	61
Figure 8. Cyclic Voltammogram of 2.32 and 2.34.....	64
Figure 9. Catalytic Cycle of Optimized Reaction Conditions	72
Figure 10. UV-Vis Kinetic Analysis of the Oxidation of 2.32-A	76
Figure 11. UV-Vis Kinetic Analysis of the Oxidation of 2.42-A	77
Figure 12. UV-Vis Kinetic Study of 2.42-A with Oxo-TEMPO+BF ₄ ⁻	77
Figure 13. Electrodes that are Connected to the Vial Cap.....	159
Figure 14. Electrodes used during Electrochemical Reactions.....	160
Figure 15. Example of an Electrochemical Reaction Setup on the Electrasyn 2.0	161
Figure 16. Cyclic voltammograms of 2.34 (5 mM) in the presence of BnOH (0 mM to 100 mM) in MeCN: pH 10 (0.1M HCO ₃ ⁻ /CO ₃ ²⁻) buffer (1:1).....	162
Figure 17. Cyclic Voltammograms of 2.34 (5 mM) in the presence of 2.32 (0 to 100 mM) in 0.1 M Bu ₄ NBF ₄ in MeCN.....	162

Figure 18. A) Absorbance vs time for reaction of Bobbitt's Salt with 1-A ([5] = 0.01 M; [1-A] = 0.1 M). B) Natural log of Absorbance vs time, $y = -0.005225x - 1.444$. $R^2 = 0.9991$	174
Figure 19. A) Absorbance vs time for reaction of Bobbitt's Salt with 6-A ([5] = 0.02 M; [6-A] = 0.2 M). B) Natural log of Absorbance vs time, $y = -0.002994x - 0.5704$; $R^2 = 0.9928$	174
Figure 20. A) Absorbance vs time for reaction of Oxo-TEMPO ⁺ BF ₄ ⁻ with 6-A ([8] = 0.01 M; [6-A] = 0.1 M). B) Natural log of Absorbance vs time, $y = -0.006918x - 1.461$; $R^2 = 0.9883$	175
Figure 21. Cyclic Voltammogram of 2.33	179
Figure 22. Cyclic Voltammogram of 2.42	180
Figure 23. Cyclic Voltammogram of 2.54	180
Figure 24. Cyclic Voltammogram of 2.55	181
Figure 25. Cyclic Voltammogram of 2.59	181
Figure 26. Cyclic Voltammogram of 2.60	182
Figure 27. Cyclic Voltammogram of 2.61	182
Figure 28. Cyclic Voltammogram of S2.1	183
Figure 29. Cyclic Voltammogram of S2.2	183
Figure 30. Cyclic Voltammogram of S2.4	184
Figure 31. Cyclic Voltammogram of S2.5	184

List of Schemes

Scheme 1. Traditional Ferrier Displacement	2
Scheme 2. Houk Model to Nucleophilic Addition into Planar Oxocarbenium Ions	3
Scheme 3. Synthesis of the Dihydropyran Moiety towards the Synthesis of Zincophorin	3
Scheme 4. Intramolecular Nucleophilic Addition via (<i>E</i>)-crotyl Oxonia Cope	4
Scheme 5. Ring Closing Metathesis towards Dihydropyrans	5
Scheme 6. Dehydrative Cyclization Using an Oxyphosphonium Salt	5
Scheme 7. S _N 2 displacement of a Mesylate	6
Scheme 8. Dehydrative Friedel-Crafts Alkylations Catalyzed by TfOH	7
Scheme 9. Fe(III)-Catalyzed Dehydration of Secondary Allylic Alcohols	9
Scheme 10. Synthesis of α -Benzyloxy 2,6- <i>cis</i> - Dihydropyrans	9
Scheme 11. Synthesis of 2,6- <i>cis</i> - Aryl Substituted Dihydropyrans	10
Scheme 12. Proposed Mechanistic Analysis to Support the Observed Diastereoselectivity	10
Scheme 13. Gas Chromatographic Thermodynamic Kinetic Analysis of Allylic Alcohol Transposition	12
Scheme 14. Allylic Alcohol Transposition with Enantioerosion of Stereodefined Allylic Alcohols	13
Scheme 15. Allylic Alcohol Transposition Used as an Electrophilic Trapping Agent	14
Scheme 16. Epoxides as Nucleophiles Trapping Allylic Cation Intermediates	14
Scheme 17. Dehydrative Cyclizations towards 2,6- <i>cis</i> -Tetrahydropyrans	16

Scheme 18. Re_2O_7 Dehydrative Cyclization towards 2,6- <i>cis</i> - Tetrahydropyran of Herboxidiene	16
Scheme 19. Oxo-Rhenium Catalyzed Friedel-Crafts Alkylations	17
Scheme 20. Oxo-Rhenium Catalyzed Synthesis of Nitrogen Containing Heterocycles.....	19
Scheme 21. Envisioned Route towards Dihydropyrans	19
Scheme 22. Synthesis of Base Substrates for Dehydrative Cyclization.....	20
Scheme 23. Analysis of Stereochemical Outcome of Dehydrative Cyclization	24
Scheme 24. Isopropyl Substitution to Test Kinetic Hypothesis	25
Scheme 25. Thermodynamic Control of Dehydrative Cyclization	26
Scheme 26. Illustration of $A^{1,2}$ -strain in Dihydropyrans	27
Scheme 27. Dehydrative Cyclization under Hanessian's Conditions	27
Scheme 28. Benzyloxy Stabilization of the Intermediate Leading to 1.80- <i>cis</i>	28
Scheme 29. Stereoselective Synthesis of 1.93	32
Scheme 30. Half Chair conformations of 1.94 and Expected of 1.000	33
Scheme 31. Effects of Alcohol Position and Alkene Geometry in Dehydrative Cyclization	35
Scheme 32. Synthesis of Enantiopure Homoallylic Alcohol 1.006.....	35
Scheme 33. Diastereoselective Alkyne Addition into Hydrocinnamaldehyde	36
Scheme 34. Improved Synthetic Route to 1.012	37
Scheme 35. Hypothesized Tight Ion Pair Mechanism	38
Scheme 36. Dehydrative Cyclizations towards <i>ent</i> -1.69	39
Scheme 37. $\text{S}_{\text{N}}\text{I}$ Mechanism towards <i>ent</i> -1.69	40
Scheme 38. Selective PMB Oxidation with DDQ	43

Scheme 39. Stereocontrolled Intramolecular Trapping of Oxocarbenium Ion Intermediates	44
Scheme 40. Visible Light-Mediated Oxidative Debenzylation of Benzyl Ethers	45
Scheme 41. Oxidative Regeneration of DDQ using Terminal Oxidants	46
Scheme 42. Electrochemical Regeneration of DDQ	46
Scheme 43. Oxidative Cleavage of Benzyl and Methyl Ethers using 2a	48
Scheme 44. Oxidant Screen Demonstrated on Benzyl Ethers.....	49
Scheme 45. Charge Transfer and Electrostatic Interactions between the Substrate and the Oxidant.....	50
Scheme 46. Oxidation of 1-Butanol to Butanoic Acid	51
Scheme 47. Electrochemical-Mediated Shono Oxidation of Carbamates	54
Scheme 48. Oxidative Cyclization with Electrochemical Oxoammonium Regeneration.....	57
Scheme 49. Synthesis of <i>p</i> -Methoxybenzyl Ether 2.32.....	58
Scheme 50. Envisioned Catalytic Cycle of 2a Within the Electrochemical Cell	63
Scheme 51. Synthesis of 2.42	73
Scheme 52. Comparing 2.32 to 2.42 under Optimized Conditions.....	74
Scheme 53. Stoichiometric Experiments of 2.32 and 2.42	74
Scheme 54. Electrocatalytic Oxidation of 2.42 with Oxo-TEMPO ⁺ (2d)	78
Scheme 55. Postulated Formation of Unstable Mixed Acetal	82
Scheme 56. Remote Substituent Effects in Rate of C–H Oxidation	84
Scheme 57. Synthesis of Benzyl Ether with Pendent Nucleophilic Alcohol.....	85
Scheme 58. Electrocatalytic Oxidation of Benzyl Ethers with Pendent Alcohol Nucleophiles	86

Scheme 59. Electrochemical Oxidation of Benzylidene Acetals to the Corresponding Benzoate	87
Scheme 60. Exploring Enol Acetate Nucleophile Possibilities	92
Scheme 61. Exploring Alcohol Nucleophile Possibilities	92
Scheme 62. Synthesis of Compound 1.67	95
Scheme 63. Synthesis of Compound 1.73	103
Scheme 64. Synthesis of Compound 1.75	105
Scheme 65. Synthesis of Compound 1.81	107
Scheme 66. Synthesis of 1.83	108
Scheme 67. Synthesis of Compound 1.85	110
Scheme 68. Synthesis of Compound 1.87	112
Scheme 69. Synthesis of Compound 1.89	114
Scheme 70. Synthesis of Compound 1.91	116
Scheme 71. Synthesis of Compound 1.93	118
Scheme 72. Synthesis of Compound 1.101	119
Scheme 73. Synthesis of Compound 1.102	120
Scheme 74. Synthesis of Compound 1.103	122
Scheme 75. Synthesis of Compound 1.106	123
Scheme 76. Synthesis of Compound 2.32	135
Scheme 77. Synthesis of Compound 2.33	136
Scheme 78. Synthesis of Compound 2.42	137
Scheme 79. Synthesis of Compound 2.32-A	137
Scheme 80. Synthesis of Compound 2.42-A	138

Scheme 81. Synthesis of Compound S2.1.....	139
Scheme 82. Synthesis of Compound S2.2.....	139
Scheme 83. Synthesis of Compound S2.3.....	140
Scheme 84. Synthesis of Compound S2.4.....	141
Scheme 85. Synthesis of Compound S2.5.....	142
Scheme 86. Synthesis of Compound 2.54.....	142
Scheme 87. Synthesis of Compound 2.55.....	143
Scheme 88. Synthesis of Compound 2.56.....	144
Scheme 89. Synthesis of Compound S2.6.....	144
Scheme 90. Synthesis of Compound S2.7.....	145
Scheme 91. Synthesis of Compound 2.59.....	146
Scheme 92. Synthesis of Compound 2.61.....	147
Scheme 93. Synthesis of Compound 2d.....	177

List of Equations

Equation 1. Catalyst Current Output with Respect to Concentration	62
Equation 2. Rate Constant with Respect to Observed Rate Constant and Concentration..	75
Equation 3. Eyring Equation to Determine Gibbs Free Energy of Activation	75
Equation 4. Bimolecular Rate Equation	88
Equation 5. Eyring Equation	173

List of Abbreviations

A	Angstrom	DIBAL	diisobutylaluminiumhydride
A	Amperes	DMAP	4-dimethylaminopyridine
Ac	Acetyl	DMF	Dimethyl formamide
ACT	4-acetamido-TEMPO	DMSO	Dimethyl sulfoxide
Ar	Aryl	d.r.	Diastereomeric ratio
BINOL	1,1'-bi-2-naphthol	e	Electron
Bn	Benzyl	Et	Ethyl
Bu	Butyl	ee	Enantiomeric excess
calcd.	calculated	ent	Enantiomer
CAN	Ceric ammonium nitrate	e.u.	Entropy Units
COSY	Correlation spectroscopy	F	Faraday
CSA	Camphor sulfonic acid	F/mol	Charge Transfer
CV	Cyclic Voltammetry	Fur	Tri-2-furyl
DBU	1,8-diazabicyclo[5.4.0]-undec-7-ene	h	hour(s)
DCE	1,2-dichloroethane	HA	Hydroxylamine
DDQ	2,3-dichloro-5,6-dicyano-1,4-benzoquinone	HFIP	hexafluoroisopropanol

HPLC	High-performance liquid chromatography	PMB	<i>p</i> -Methoxybenzyl
HRMS	High-resolution mass spectrometry	PMP	<i>p</i> -Methoxyphenyl
Hz	Hertz	ppm	Parts per million
IC ₅₀	Half maximal inhibitory concentration	PPTS	Pyridinium <i>p</i> -toluene sulfonate
LA	Lewis acid	<i>n</i> Pr	propyl
LDA	Lithium diisopropyl amide	<i>i</i> -Pr	isopropyl
M	Molar (mole per liter)	IR	infrared
Me	Methyl	py	pyridine
min	Minute (s)	rt	Room temperature
MOM	Methoxy Methyl	RVC	Reticular Vitreous Carbon
MTPA	α -methoxy- α -trifluoromethyl phenyl acetic acid	sat.	saturated
MS	Molecular Sieves	sec	Second (s)
NMI	<i>N</i> -methylimidazole	TBAF	Tetrabutylammonium fluoride
NMR	Nuclear magnetic Resonance	TBN	Tert butyl nitrile
NOE	Nuclear Overhauser Effect	<i>t</i> Bu	Tert-butyl
NOESY	Nuclear Overhauser Effect Spectroscopy	TBS	tertbutyldimethylsilyl
Nu	Nucleophile	TCE	2,2,2,-trichloroethanol
Ph	Phenyl	TES	triethylsilyl

Tf	Trifluoromethane sulfonyl
TFE	2,2,2-trifluoroethanol
THF	tetrahydrofuran
TLC	Thin layer chromatography
TMEDA	<i>N,N,N',N'</i> -tetramethyl,-1,2-ethylenediamine
TMS	trimethylsilyl
TOF	Turnover Frequency
TS-DPEN	<i>p</i> -Toluenesulfonyl-1,2-diphenylethanediamine
UV	Ultra violet
V	Voltage

Acknowledgments

I would like to first thank Dr. Paul Floreancig for allowing me into his group and the impeccable mentorship he provided over the years, especially while dealing with a pandemic. I would not be the scientist that I am today without his guidance. I am also very grateful for Dr. Alexander Deiters, Dr. Yiming Wang and Dr. James McKone for accepting to be on my committee and providing helpful advice and critiques during my comprehensive exam and my Ph.D defense. I would like to also thank Dr. Steve Weber, Yejin Yang, and Jenna Miller for helpful discussions and experimental advice specifically with the Kinetic Based Approach to Developing Electrocatalytic Variants of Slow Oxidations discussed in Chapter 3.

I am very grateful to all of the facilities managers at the University of Pittsburgh that have been very helpful over the years. Dr. Damodaran Krishnan Achary for helpful advice with NMR experiments and Dr. Bhaskar Godugu and his team for assistance with LC-MS and obtaining HRMS experiments over the past few years.

I am very grateful for the past and present members of the Floreancig group that I have had the privilege of working alongside. The helpful scientific discussions and friendships have truly been a blessing to be a part of. I would also like to thank all the friends that I have made over the years for their love and support: Jenna Miller, Brittany Klootwyk, Shelby Heath, Nick Cinti, Anna Healy, Savannah Albright, Kathryn Hinkelman, Mariah Meehan, Austin Durham, Austin Kilgore, Marcus Van Engen, Dr. Jordan Swisher, and Sanjeev Gautam.

Thank you to my sisters for always being there for me, and to Mikolaj Kulis for your ever loving support and friendship over the years. Lastly, I would like to thank my parents for all their

love, sacrifice and support throughout my life. Without them, I would not be where I am today.

This one is for you guys!

1.0 Dehydrative Re₂O₇-Catalyzed Approach to Dihydropyran Synthesis

1.1 Dihydropyrans and their Prevalence in Natural Products

Dihydropyrans are highly attractive synthetic targets because of their prevalence within biologically active natural products. Dihydropyrans are six-membered oxygen-containing heterocycles with an endocyclic alkene moiety. Laulimalide (Figure 1) contains two dihydropyran moieties. It has a cytotoxicity against the KB cell line with an IC₅₀ of 15 ng/mL and is a potent inhibitor of cell proliferation with IC₅₀ values between 5-12 nM against multiple drug resistant cell lines.¹⁻³ Sorangicin A, which contains a single dihydropyran unit, is a potent antibacterial agent against gram-positive and gram-negative bacteria.⁴ The endocyclic alkene in a dihydropyran can also be functionalized through C–O, C–H, and C–C bond forming reactions in a diastereoselective manner to give diversified tetrahydropyrans.

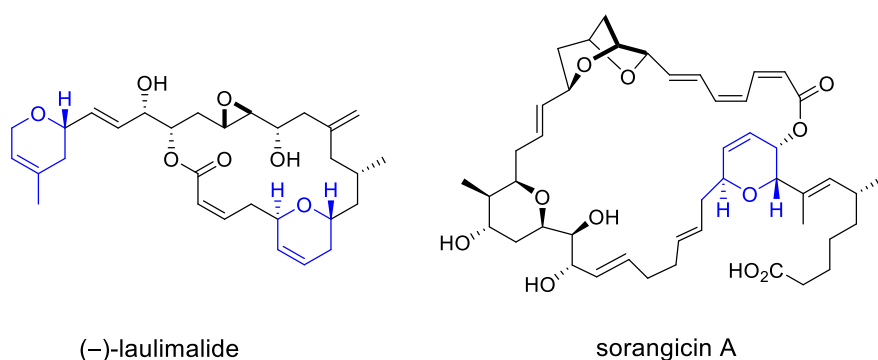


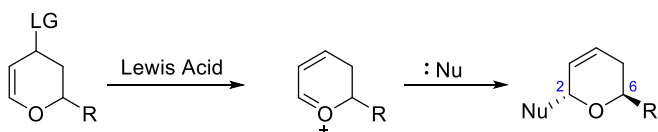
Figure 1. Dihydropyrans in Featured Natural Products

1.2 Synthetic Strategies towards the Synthesis of Dihydropyrans

Dihydropyrans (DHPs) have been made in numerous ways. The most common method is through the Ferrier reaction which consists of nucleophilic addition into unsaturated oxocarbenium ions. Other ways are through ring-closing metathesis, allylic C–H oxidation, and various dehydrative processes.^{2, 4-6}

1.2.1 Carbon based Nucleophilic Addition into Oxocarbenium Ions

Within the dihydropyran family, the 2,6-*cis*-conformer has been reported as the more thermodynamically favored isomer as the two substituents on the ring maintain an equatorial relationship, minimizing 1,3-diaxial interactions between the 2 and the 6 position.^{6, 7} Therefore to access 2,6-*trans*-isomers, kinetically favored transformations need to be used to limit thermodynamic equilibration. A common method towards the 2,6-*trans*-isomer is the Ferrier displacement with a pendent nucleophile (Scheme 1).

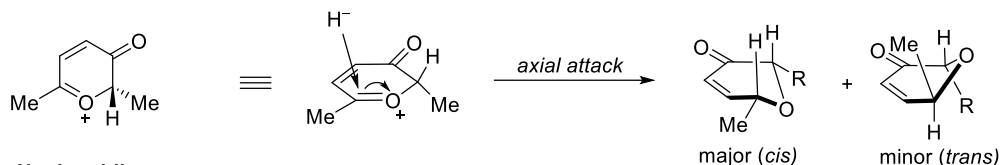


Scheme 1. Traditional Ferrier Displacement

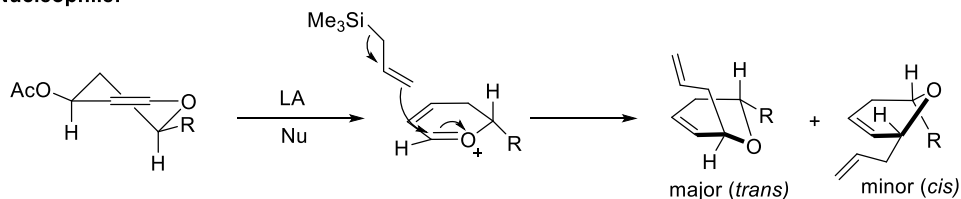
Through Lewis acid activation, an appropriate leaving group undergoes ionization to generate the oxocarbenium ion electrophile. Houk and coworkers proposed that the reactive intermediates for these types of oxocarbenium ions is planar rather than the half chair commonly seen in the formation of tetrahydropyrans (Scheme 2).⁸ Axial attack was favored by 2 kcal/mol giving *anti*-addition as the predominant pathway.⁸ Houk demonstrated that using hydride as a

nucleophile gave the 2,6-*cis*-conformer favorably. The Ferrier reaction, which involves the use of a carbon nucleophile will also favor an axial approach but results in the 2,6-*trans*-isomer as the kinetically favored product (Scheme 2).

Hydride Nucleophile:

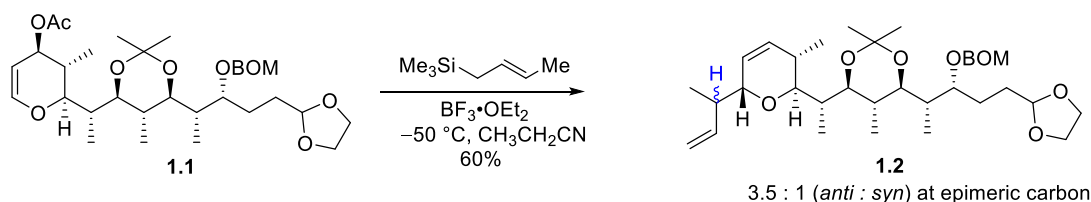


Carbon Nucleophile:



Scheme 2. Houk Model to Nucleophilic Addition into Planar Oxocarbenium Ions

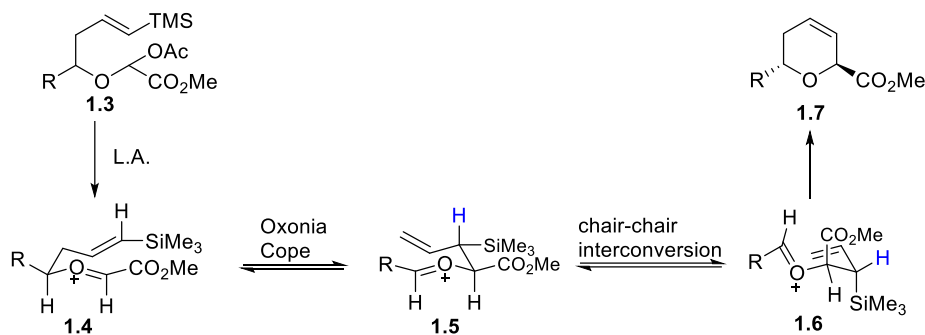
The Ferrier approach is a highly attractive method as it has high functional group tolerance and can be incorporated at later stages in a total synthesis sequence. Danishefsky and coworkers demonstrated this in the synthesis of the *trans*-dihydropyran of the natural product zincophorin (Scheme 3).⁹ Setting the allylic stereocenter at the epimeric carbon shown in **1.2** proved to be problematic but the *trans*-selectivity of the dihydropyran predominated.



Scheme 3. Synthesis of the Dihydropyran Moiety towards the Synthesis of Zincophorin

DHPs can also be synthesized through an intramolecular approach. Semeyn and coworkers used acyclic vinyl silanes to construct the DHP core, where the geometry of the alkene dictates the stereochemical relationship of the DHP (Scheme 4).⁵ In most cases, to afford a DHP with the 2,6-

trans-relationship, an (*E*)-crotyl silane must be used. Upon exposure of the substrate to a Lewis acid, an oxocarbenium ion was generated promoting a favorable oxonia-Cope rearrangement from **1.4** to **1.5** (Scheme 4).




Scheme 4. Intramolecular Nucleophilic Addition via (*E*)-crotyl Oxonia Cope

Following the oxonia-Cope, **1.5** undergoes a chair interconversion placing the silane in the axial position and the alkene in a conformation (**1.6**) that gives the (*Z*) geometry upon cyclization rather than the (*E*). Through the β -silicon effect, the electrons of the silane donate into the adjacent sp^2 carbon stabilizing the positive charge, promoting addition into the oxocarbenium ion, affording the 2,6-*trans*-isomer, **1.7**.¹⁰ If a (*Z*)-crotyl silane was used, after the oxonia-Cope rearrangement, the silane will already be axial leading to the β -silicon effect promoting fast cyclization to the 2,6-*cis*-conformer.⁵ Notwithstanding the high selectivity this method demonstrated, the acyclic precursors involved proved to be a challenge to synthesize.

1.2.2 Ring-Closing Metathesis towards Dihydropyrans


Nelson and coworkers synthesized the natural product (–) laulimalide which contains two DHP units.² The mono-substituted DHP was synthesized through a ring-closing metathesis



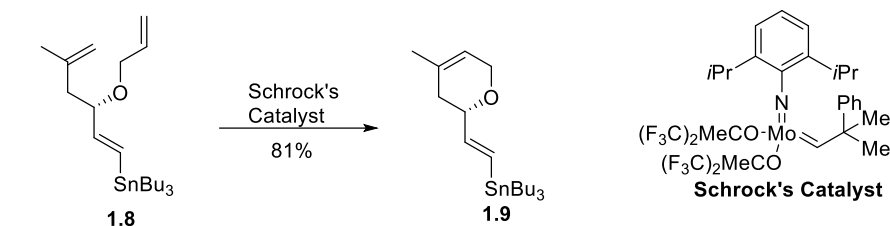
1.8

Schrock's Catalyst
 81%

1.9

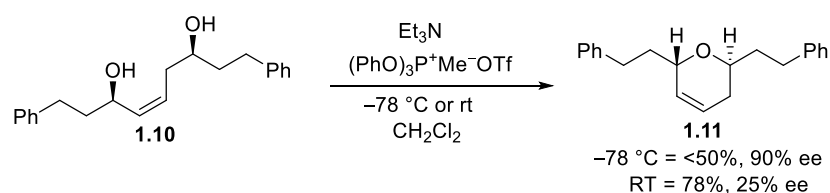


Schrock's Catalyst



the major complexities in ring construction is replicating the desired stereochemistry at the ether linkage. Although, through metathesis, the ether stereochemistry has been shown to not undergo epimerization, synthesizing secondary ethers in a stereoselective manner is difficult, especially as the complexity of the substrate increases, complicating the application of this method in more challenging systems.¹¹

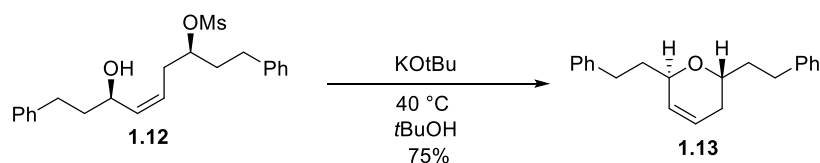
Prior efforts to synthesize 2,6-*trans*-dihydropyrans from 1,5-diols have been done using stoichiometric reagents to effectively undergo the cyclodehydration. Roush and coworkers found that a stoichiometric amount of an oxyphosphonium salt can facilitate an S_N2 reaction towards the 2,6-*trans*-DHP (Scheme 6).¹²



5

Exposure of **1.10** to the oxyphosphonium salt at room temperature gave **1.11** in 78% yield, but selective activation of a single alcohol proved difficult. This caused the enantiopurity of **1.11** to diminish drastically. When the temperature was cooled to $-78\text{ }^{\circ}\text{C}$, activation of solely the allylic alcohol increased giving 90% *ee* upon cyclization but yields were significantly diminished.¹² Although the differentiation of these alcohols was limited, the *trans:cis* ratios were excellent (as high as 20:1).¹²

To increase enantioselectivity, a classical $\text{S}_{\text{N}}2$ approach was taken by converting the homoallylic alcohol to the corresponding mesylate, **1.12** (Scheme 7). Incorporation of the mesylate allowed for stereochemical retention at the nucleophilic site and desired stereochemical inversion at the electrophilic site giving **1.13** in 75% yield as a single diastereomer. Although very good yields were observed, E2 elimination became a concern under these conditions where approximately 10% of diene was formed.¹²



Scheme 7. $\text{S}_{\text{N}}2$ displacement of a Mesylate

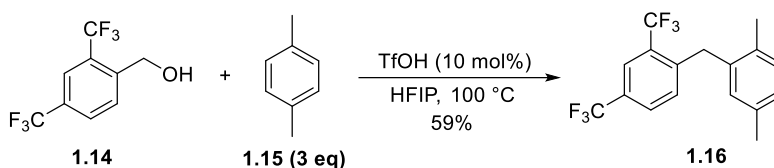
1.3 Catalytic Dehydrative Reactions of Allylic and Benzylic Systems

Catalytic dehydration of allylic and benzylic alcohols is an environmentally benign method that can be used to generate cationic intermediates which can be captured by pendent nucleophiles to construct new bonds. Prior methods for activating alcohols for substitution reactions involve

functional group interconversion to stoichiometric electrophilic intermediates such as sulfonate esters, alkyl halides, or phosphonium salts, all of which undergo traditional S_N2 or S_N1 substitution. Although these functional groups have proven to be extremely useful in synthetic pathways, they require installation immediately before functionalization and their byproducts are less environmentally friendly, making dehydrative reactions from the alcohol more attractive. These methods would utilize both Brønsted acid and Lewis acid catalysis to promote ionization to form a stabilized carbocation either through allylic or benzylic stabilization.

1.3.1 Brønsted Acid-Catalyzed Dehydrative Reactions

Brønsted acid-catalyzed reactions can be used for C–C, C–O, and C–N bond formation reactions in high catalytic efficiency. Moran and coworkers¹³ (Scheme 8) explored the Friedel-Crafts alkylation by activating electron-poor benzyl alcohols with a catalytic amount of triflic acid (TfOH). The use of 1,1,1,3,3,3-hexafluoroisopropanol (HFIP) was imperative in the reaction because, in the presence of sufficiently strong Brønsted acid donors, it acted as an H-bond acceptor resulting in the formation of higher order HFIP-acid aggregates. These aggregates combined with the strong dipole moment and polar protic properties of HFIP led to further stabilization of the benzyl cation intermediates formed, which expanded the scope to encompass many electron-poor benzyl alcohols including those bearing a CN, NO₂, CF₃ and even bis-NO₂ and bis-CF₃ groups.

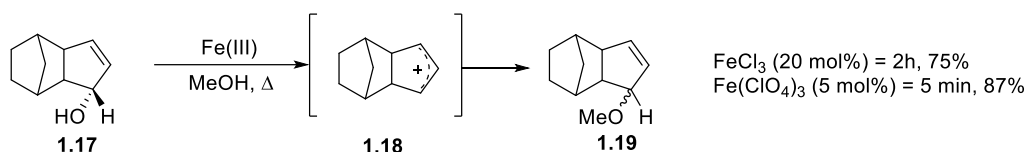


Scheme 8. Dehydrative Friedel-Crafts Alkylations Catalyzed by TfOH

1.3.2 Lewis Acid-Catalyzed Dehydrative Reactions

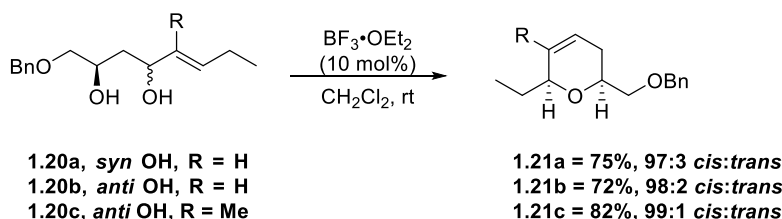
Many Lewis acids in literature have been known to activate allylic alcohols. Soft Lewis acids such as gold and palladium can easily form complexes with electron-rich species such as alkenes and alkynes, giving them electrophilic character and promoting subsequent attack by intramolecular or intermolecular nucleophiles.^{7, 14-20} Hard Lewis acids prefer the formation of hard ion pairs, rather than coordination to π -bonds, as their bonds are formed primarily through electrostatic interactions. With the high positive charge of Lewis acids and the high electronegativity of the Lewis bases, the ion pairing bond is favored over the metal to ligand π -bond. Therefore, when hard Lewis acids are subjected to allylic alcohols, they react with the alcohol directly, which will undergo dehydration to form stabilized allylic cation intermediates. Many hard Lewis acids exist, however, Fe(III) species, Bi(OTf)₃ and BF₃•OEt₂ have primarily been used in many of these processes.^{7, 21-25}

Initial efforts by Salehi and coworkers demonstrate that Fe(III) species, specifically FeCl₃ or Fe(ClO₄)₃, can be used in catalytic loadings with allylic alcohols to generate allylic cation intermediates, and undergo solvolysis by the respective alcohol solvent to yield the corresponding allylic ether (Scheme 9).²⁶ Exposure of enantiopure **1.17** to the reaction conditions gave a product consistent with an allylic cationic intermediate, as racemate **1.19** was the only product observed.²⁶ Although enantiopurity was lost, these reactions proceeded very efficiently. An increase in reactivity was observed when using the more Lewis acidic Fe(ClO₄)₃, where the reaction times were significantly reduced and higher yields were observed. This method was extended to secondary benzylic alcohols as well but showed no reactivity with primary benzyl alcohols.



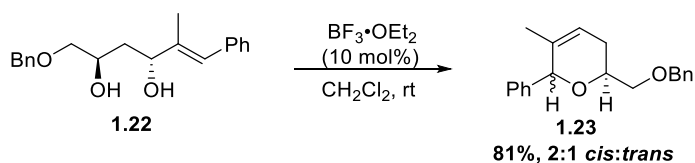
Scheme 9. Fe(III)-Catalyzed Dehydration of Secondary Allylic Alcohols

Oxygen and nitrogen-containing heterocycles are common structures synthesized through hard Lewis acid catalysis. Cossy and coworkers initiated these efforts in the FeCl₃-catalyzed dehydrative approach to 2,6-*cis*-tetrahydropyrans and 2,6-*cis*-piperidines.²² Hanessian and coworkers continued the endeavor in hard Lewis acid catalysis towards the synthesis of dihydropyrans. Upon exposing BF₃•OEt₂ to 1,3-allylic diols **1.20**, the 2,6-*cis*-dihydropyran **1.21** was produced as the predominant isomer in very high diastereoselectivity and moderate yields (Scheme 10).



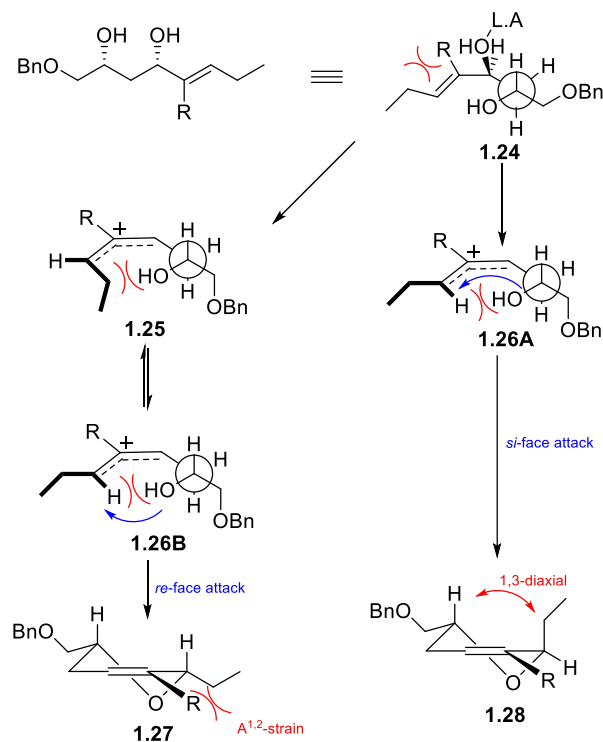
Scheme 10. Synthesis of α-Benzyloxy 2,6-*cis*- Dihydropyrans

The stereochemical relationship between the alcohols proved to be inconsequential to the outcome of the reaction, suggesting that the reaction proceeds via an allylic cation intermediate. Applying the method to the (*Z*)-olefin, resulted in the same outcome of product **1.21c** to give further support of an allylic cation intermediate. Expanding the scope to cinnamyl cations seemed to complicate results, as the diastereoselectivity diminished greatly from 97:3 to 2:1 *cis:trans* (Scheme 11).



Scheme 11. Synthesis of 2,6-*cis*- Aryl Substituted Dihydropyrans

The favored 2,6-*cis*-selectivity in these reactions was explained based on the stereochemical models in Scheme 12. They demonstrated that the *re*-face attack in **1.26B** was allegedly favored over the higher energy *si*-face attack in **1.26A**, despite the $\text{A}^{1,2}$ strain observed in the 2,6-*cis*-isomer, **1.27** (Scheme 12). Further developments in our work provided an alternative explanation for the *cis*-isomer selectivity which is described in section 1.5.3.



Scheme 12. Proposed Mechanistic Analysis to Support the Observed Diastereoselectivity

1.4 Rhenium Oxide-mediated Activation of Allylic and Benzylic Alcohols

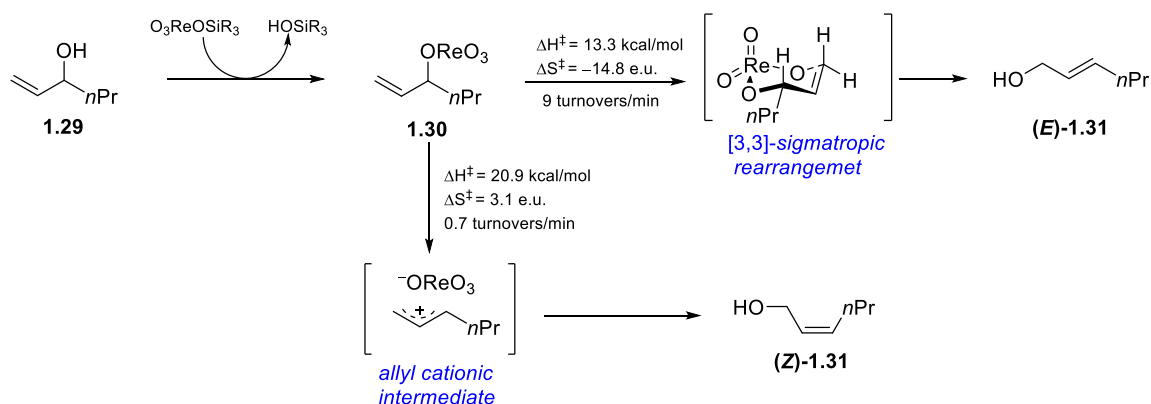
Rhenium oxide, like other hard Lewis acids, reacts with allylic alcohols to form allylic cation intermediates. As a high oxidation state oxo-metal catalyst, rhenium oxide can facilitate allylic alcohol and silyl ether [1,3]-transposition without competitive oxidation.²⁷ This transposition will provide access to synthetically challenging allylic alcohols via a more easily accessible regioisomer, reducing the overall step count in a sequence. Other oxo-metal catalysts such as vanadium and chromium demonstrate similar capabilities in the [1,3]-transposition of allylic alcohols, but harsh reaction conditions and subsequent oxidation to the corresponding enone can limit the synthetic applications of these metals.

1.4.1 Mechanistic Analysis of 1,3-Allylic Alcohol Transposition

Early work by Chabardes and coworkers demonstrated the use of an oxo-vanadium catalyst in allylic alcohol transposition.²⁸ The proposed mechanism for transposition was through the formation of a vanadate ester intermediate which was followed by a [3,3]-sigmatropic rearrangement via a chair-like transition state. However, this did not explain some of the side reactions observed such as elimination and racemization, prompting further mechanistic studies.²⁷

To better understand oxo-rhenium catalyzed allylic alcohol transposition, Osborne and coworkers investigated this mechanism using gas chromatography to study the kinetics of **1.29** (Scheme 13).²⁹ Subjection of $\text{O}_3\text{ReOSiR}_3$ to **1.29** afforded perrhenate ester **1.30** which proceeds through a [3,3]-sigmatropic rearrangement to give (*E*)-**1.31** or a cationic pathway to give (*Z*)-**1.31**. The formation of (*E*)-**1.31** had an enthalpy of activation of 13.3 kcal/mol and an entropic energy

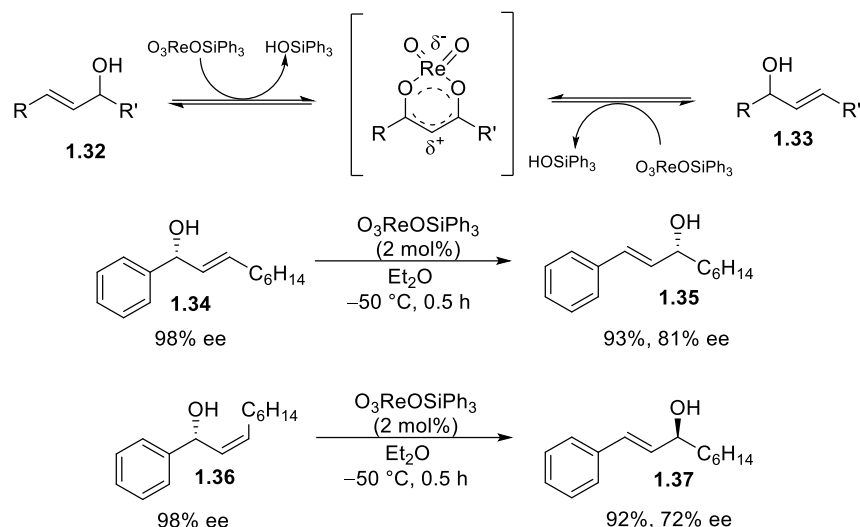
of activation of -14.8 e.u., whereas the formation of **(Z)-1.31** had an enthalpic energy of activation of 20.9 kcal/mol and an entropic energy of activation of 3.1 e.u.²⁹ The low entropies of activation in the formation of **(E)-1.31** suggested a closed cyclic transition state, whereas the positive entropic values observed in the formation of **(Z)-1.31** stems from possible dissociation of the perrhenate anion leading to an allyl cation intermediate (Scheme 14).²⁹ This became more clear as **(Z)-1.31** was formed at higher rates when more polar solvents were used, because of stabilization of the cationic intermediate.



Scheme 13. Gas Chromatographic Thermodynamic Kinetic Analysis of Allylic Alcohol Transposition

To further investigate Osborne's kinetic analysis, Grubbs and coworkers studied the isomerization of allylic alcohols using $\text{O}_3\text{ReOSiPh}_3$ as a catalyst. At low catalyst loadings, successful isomerization of various allylic alcohols was observed under mild conditions and in high yield (Scheme 14).²⁷ When the method was expanded to enantioenriched substrates, loss of enantiopurity was observed, suggesting that the allylic cationic intermediate was a competing pathway even at cold temperatures (Scheme 14). Although enantioerosion proved to be an issue,

both the [3,3]-sigmatropic rearrangement and the allylic cation intermediate are viable pathways that can be exploited in future synthetic endeavors.²⁷



Scheme 14. Allylic Alcohol Transposition with Enantioerosion of Stereodefined Allylic Alcohols

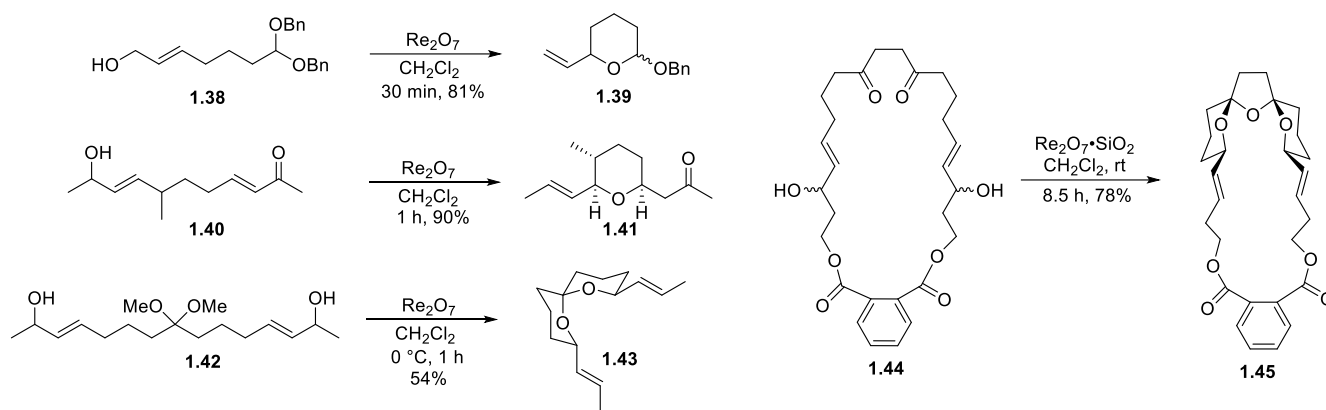
1.4.2 Oxo-Rhenium Catalyzed Allylic Alcohol Transposition used as an Electrophilic

Trapping Agent

The ability of rhenium(VII) to facilitate [3,3]-sigmatropic rearrangements inspired numerous studies of electrophilic trapping in the Floreancig Group where the allylic alcohol acts as a pendent nucleophile. The group began with exploratory studies in the synthesis of tetrahydropyrans, **1.39** and **1.41**, from allylic alcohols reacting with acetal and ketone electrophiles respectively in high yield and diastereocontrol.³⁰ This method was expanded by incorporating two allylic alcohols in the synthesis of spiroketal (**1.43**) and even more complex bis-spiroketal (**1.45**),

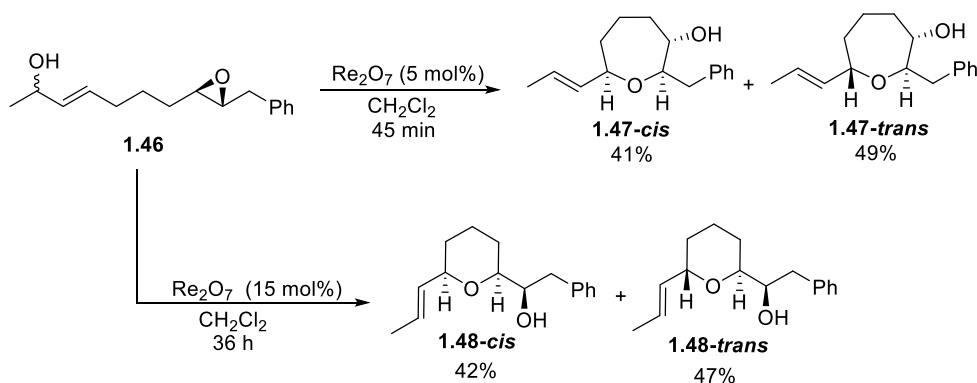
which utilized a tethering strategy on the olefins of the allylic alcohols to achieve stereocontrol.

(Scheme 15).³⁰⁻³²



Scheme 15. Allylic Alcohol Transposition Used as an Electrophilic Trapping Agent

Enantioenriched epoxides were initially used as electrophiles to access stereodefined products because of their inability to equilibrate.^{32, 33} However, subjecting **1.46** to 5 mol% Re_2O_7 surprisingly afforded oxepanes **1.47-*cis*** and **1.47-*trans***, which can only be made through ionization of the allylic alcohol to an allylic cation intermediate followed by trapping with the epoxide.³³ Upon prolonged exposure of **1.46** to the reaction conditions at higher catalyst loadings, **1.47** equilibrated to the allylic cation intermediate and was recaptured to afford the 6-*exo*-trig cyclized tetrahydropyrans **1.48** in high yield with little enantioerosion observed (Scheme 16).



Scheme 16. Epoxides as Nucleophiles Trapping Allylic Cation Intermediates

The selectivity between the 2,6-*cis*- and 2,6-*trans*-tetrahydropyrans can theoretically be a controlled process upon prolonged exposure of the products to the reaction conditions. When Re_2O_7 was resubjected to **1.48-*cis*** and **1.48-*trans***, initially the tetrahydropyrans did not equilibrate. Masking the free hydroxy group as a methyl ether led to the 1:1 mixture of isomers completely equilibrating to the 2,6-*cis*-isomer.³³ This demonstrated that an allylic cation intermediate was a viable pathway that can be exploited in future methods.

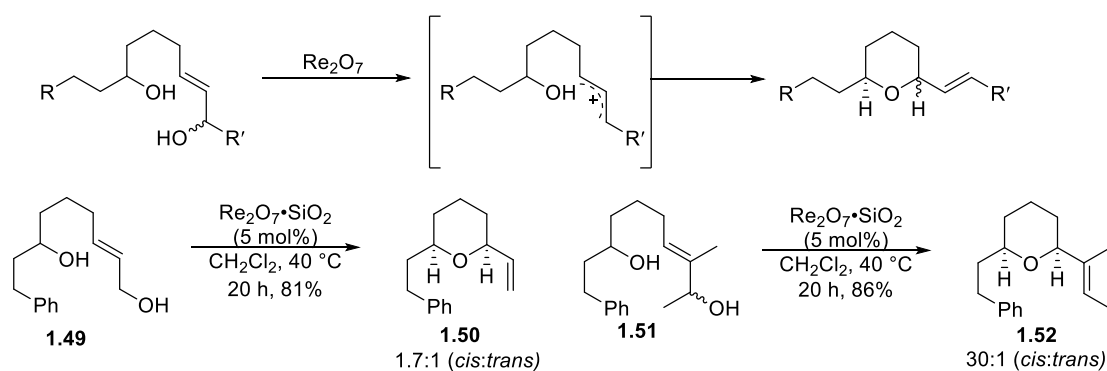
1.4.3 Oxo-Rhenium Catalyzed Dehydrative Reactions in the Floreancig Group

Inspired by the nucleophilic addition of epoxides into allylic cation intermediates observed previously, the Floreancig group developed multiple methods that use allylic alcohols as electrophiles that can be captured by pendent intramolecular and intermolecular nucleophiles.³³⁻³⁶ These methods involved a number of C–C, C–O, C–N and C–S bond forming reactions that constructed molecules with increased molecular complexity from simple starting materials.³⁵⁻³⁷

1.4.3.1 Dehydrative Reactions towards 2,6-*cis* Tetrahydropyrans and Synthetic

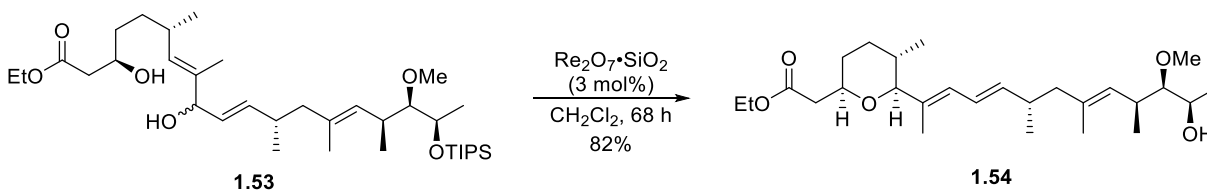
Applications

The expansion of allylic alcohols as electrophiles began with the subjection of Re_2O_7 to a 1,7-monoallylic diol which ionized to the corresponding allylic cation and was captured at the proximal end of the cation by a pendent alcohol (Scheme 17). This produced a series of tetrahydropyrans as a mixture of *cis*- and *trans*-isomers with the 2,6-*cis*-isomer predominating.³⁷ The only observed side reaction was E1 elimination which results in the formation of the corresponding diene.



Scheme 17. Dehydrative Cyclizations towards 2,6-*cis*-Tetrahydropyrans

When primary allylic alcohol **1.49** was subjected to Re_2O_7 supported on silica gel, cyclization gave **1.50** with very little diastereocontrol (Scheme 17). However, as secondary allylic alcohol **1.51** was subjected to the conditions, **1.52-*cis*** was formed as the major isomer in a 30:1 (*cis:trans*) ratio.³⁷ The increased stabilization from the secondary allylic cation intermediate led to improved yields and higher rates of isomerization. To test the synthetic utility of the method, this was further applied to the construction of the tetrahydropyran core of the natural product, herboxidiene (Scheme 18).³⁷ This showcased that the method has high functional group compatibility and can be implemented at later stages within a synthetic route.



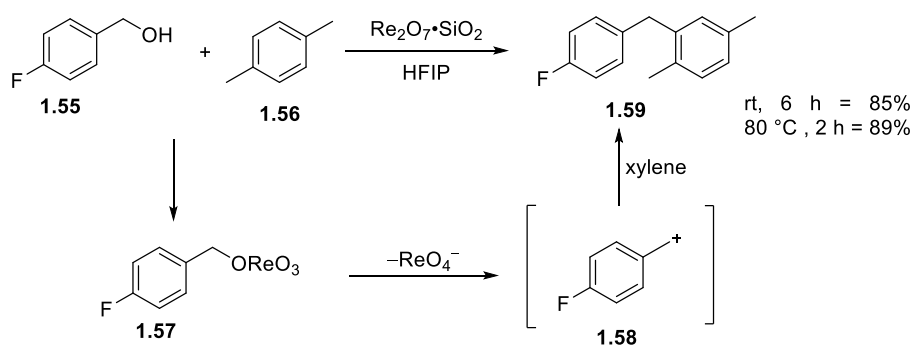
Scheme 18. Re_2O_7 Dehydrative Cyclization towards 2,6-*cis*- Tetrahydropyran of Herboxidiene

With the pK_a of perhenic acid (the active catalyst species) being around -1 , a control experiment was done with *p*-TsOH to ensure allylic alcohol ionization was not a Brønsted acid

catalyzed process. This resulted in a slower transformation and extensive side products showcasing the high selectivity of oxo-rhenium species in allylic alcohol activation.³⁷

1.4.3.2 The Use of HFIP in Oxo-Rhenium-Catalyzed Bond Forming Reactions.

Similar to work done by Moran and coworkers (Section 1.3.1), the Floreancig group studied oxo-rhenium catalysis in intermolecular Friedel-Crafts alkylations.^{13, 35} This method involved the activation of benzylic alcohols by Re_2O_7 to synthesize diarylmethanes, like **1.59**, via a benzylic cation intermediate (**1.58**) that was captured by *p*-xylene as the nucleophile (Scheme 19).³⁵



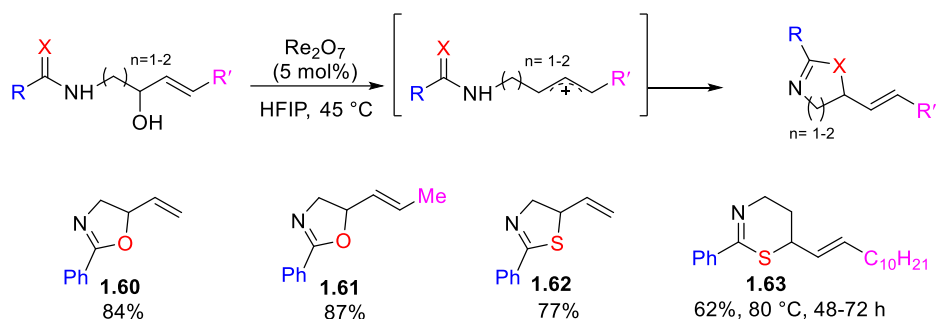
Scheme 19. Oxo-Rhenium Catalyzed Friedel-Crafts Alkylations

Unlike the dehydrative cyclizations in Section 1.4.3.1, 1,1,1,3,3,3-hexafluoroisopropanol (HFIP) was necessary for efficient reactivity. HFIP is a polar protic solvent with a high dielectric constant and high polarizability, which promotes ionization of the perrhenate ester intermediate (**1.57**), increasing the overall concentration of stabilized benzylic cation intermediate (**1.58**) in solution. The significant hydrogen bond donating abilities of the solvent allows it to sequester water, which prevents hydrolysis of the benzylic cation and dampens the nucleophilicity of the benzyl alcohol, limiting alcohol dimerization to form the benzyl ether.³⁵ When conducted in

dichloroethane, the reaction was less efficient, resulting in a 29% yield of benzyl ether in addition to the Friedel-Crafts product.

In the presence of base, when 2,6-di-*tert*-butylpyridine was used, no reaction was observed, supporting that perrhenic acid (HReO_3) was the active catalyst species. When Re_2O_7 was substituted with HReO_3 , improvements in yields were observed. To study whether this was solely a Brønsted acid-catalyzed process, TfOH was substituted for HReO_3 . Although similar yields were observed, the reactions proceeded at slower rates. This demonstrated that although ionization via Brønsted acid catalysis can't be ruled out as a competing pathway, ionization via perrhenate ester formation predominated.

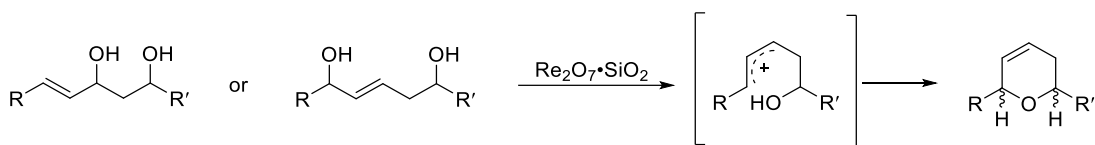
Understanding the significant role that HFIP played in the stabilization of benzylic cation intermediates,³⁵ and its ability to sequester water, the Floreancig group expanded their efforts to synthesizing nitrogen containing heterocycles.³⁶ They demonstrated that when allylic alcohols were used as precursors to allylic cation intermediates, they could be captured by the oxygen or sulfur of an amide or thioamide to form the corresponding heterocyclic moiety. These were very efficient reactions, giving oxazolines **1.60** and **1.61**, thiazoline **1.62**, and thiazine **1.63** in high yield (Scheme 20).³⁶ HFIP was imperative for successful cyclization as it stabilized the allylic cation intermediates, sequestered water and mitigated the basicity of the amides preventing quenching of perrhenic acid. When the reaction was conducted in dichloromethane, depreciated yields were observed, possibly due to the diminished cation stability.



Scheme 20. Oxo-Rhenium Catalyzed Synthesis of Nitrogen Containing Heterocycles

1.5 Dehydrative Re₂O₇-Catalyzed Approach to Dihydropyran Synthesis

The Floreancig group, as mentioned previously, has done extensive work with oxo-rhenium catalysis, especially using allylic alcohols as electrophiles through a dehydrative ionization pathway.^{32, 35-37} Previous dehydrative cyclizations involved the activation of 1,7-monoallylic diols which proceeded through an ionization pathway to give 2,6-*cis*-tetrahydropyrans bearing an exocyclic alkene (Section 1.4.3.1, Scheme 17).³⁷ This transformation inspired an alternative reaction pathway where a nucleophilic alcohol reacts with the distal end of the allylic cation to give dihydropyrans containing an endocyclic alkene. Through the oxo-rhenium catalyzed ionization pathway, this approach gives these products from 1,3- and 1,5-diols (Scheme 21).



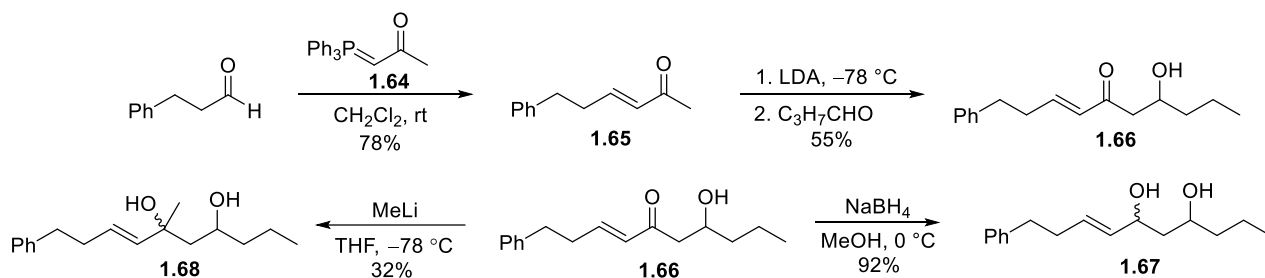
Scheme 21. Envisioned Route towards Dihydropyrans

This cyclization poses a few challenges. For cyclization to occur, the alkene must ionize or the geometry must flip from (*E*) to (*Z*) for cyclization to occur, requiring a boat-type transition

state. Therefore, the barrier of rotation for the allylic cation must be relatively low for favorable interconversion between the (*E*)- and (*Z*)-isomers. Elimination could be a competitive pathway if the lifetime of the cation is not long enough to undergo isomerization, so stabilization of the cationic intermediate is key. This study focuses on the synthesis of 3,4-dihydropyrans, reaction optimization, mechanistic analysis, and scope diversification.

1.5.1 Development of Substrates for Dehydrative Cyclization

Initial work by the Floreancig group proved experimentally that secondary and tertiary allylic cations showed greater ionizing ability than primary allylic cations, therefore **1.67** and **1.68** both are precursors to these cations (Scheme 22).^{34, 37, 38} The initial substrate design focused on substrates with primarily alkyl functionality that contained easily distinguishable NMR signals and sufficient molecular weight to not be volatile. Substrates **1.67** and **1.68** were synthesized using a divergent approach.



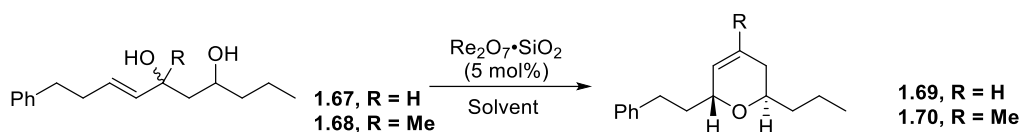
Scheme 22. Synthesis of Base Substrates for Dehydrative Cyclization

A Wittig reaction between hydrocinnamaldehyde and Wittig reagent, **1.64** produced known α,β -unsaturated ketone³⁹ **1.65** in 78% yield. An aldol reaction between **1.65** and butyraldehyde gave β -hydroxy ketone **1.66** in 55% yield. Reduction of ketone **1.66** with NaBH₄ gave diol **1.67** in 92% yield and methyllithium addition into the carbonyl of **1.66** gave **1.68** in 32% yield.

1.5.2 Solvent Effects and Optimization of Reaction Conditions

Initially, the cyclization proved to be difficult due to the reaction's sensitivity to solvent. Previously reported Re_2O_7 reactions were performed in dichloromethane.³⁷ However, when **1.67** as a mixture of diastereomers was subjected to 5 mol% $\text{Re}_2\text{O}_7 \cdot \text{SiO}_2$ with dichloromethane as a solvent at room temperature, poor yields and significant elimination was observed with less than 14% of dihydropyran **1.69** being isolated (Entry 1, Table 1). This result could be attributed to the instability of the allylic cation intermediate, as a similar issue was observed for the benzylic and allylic alcohols in section 1.4.3.2.³⁵ To rectify this issue, the carbocation was stabilized through the use of a more polar protic solvent. As shown previously, HFIP stabilizes the benzylic and allylic cation intermediates because of its high dipole moment, hydrogen bond donating ability, and non-nucleophilic nature, making it the ideal candidate.^{35, 36}

When **1.67** was subjected to the reaction conditions with HFIP as the solvent, the yield improved significantly, giving **1.69** in 40% yield in a 3:1 (*trans:cis*) diastereomeric ratio in less than ten minutes (Entry 2, Table 1). Similarly, **1.68** under these conditions gave a 55% yield of **1.70** in a 2:1 (*trans:cis*) mixture of diastereomers (Entry 8, Table 1).³⁴ Using ^1H NMR analysis, the stereochemistry based on coupling constants were assigned, and this stereochemistry was confirmed by 2D- ^1H -NOESY experiments (Figure 2). Since no clear byproducts were observed, the lower yields were attributed to non-specific decomposition.



Entry	Product	Solvent	Temperature (°C)	Yield (%)	d.r. (<i>trans</i> : <i>cis</i>)
1	1.69	CH ₂ Cl ₂	rt	<14	-
2	1.69	HFIP	rt	40	3:1
3	1.69	HFIP/MeNO ₂ (4:1)	rt	66	-
4	1.69	HFIP/MeNO ₂ (7:3)	rt	54	-
5	1.69	HFIP/MeNO ₂ (9:1)	rt	71	3.3 : 1
6	1.69	HFIP/MeCN (9:1)	rt	trace	-
7	1.69	MeCN	rt	NR	-
8	1.70	HFIP	rt	55	2:1
9	1.70	HFIP/MeNO ₂ (9:1)	rt	69	1.5:1
10	1.70	HFIP/MeNO ₂ (4:1)	rt	57	-
11	1.70	HFIP/MeCN (4:1)	rt	57	5.4:1
12	1.70	HFIP/MeCN (9:1)	rt	74	2.5:1

Table 1. Condition Optimization of Re₂O₇ Mediated Dehydrative Cyclization

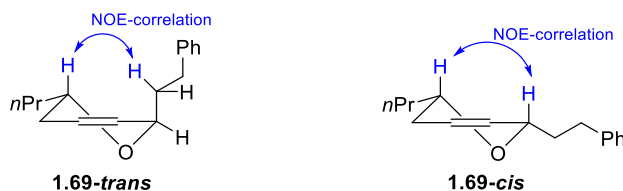


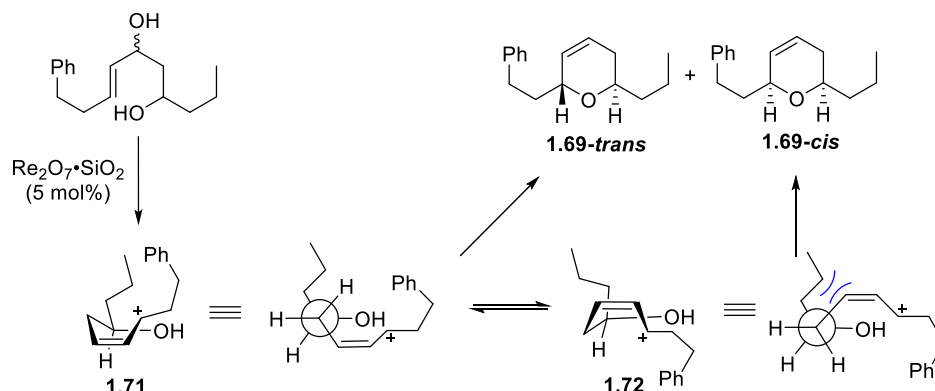
Figure 2. NOE Correlations Confirming Structure of 1.69

Inspired by the dehydrative processes of Hall and coworkers, mixtures of HFIP/MeNO₂ were attempted.⁴⁰ This led to significant improvements in yield and cleanliness of the reaction, with 9:1 HFIP:MeNO₂ being the optimal solvent mixture (Entry 5, Table 1), giving **1.69** in 71% yield in a 3.3:1 (*trans:cis*) selectivity within five minutes.³⁴ The exact effect nitromethane had on the reaction was elusive, however, it was proposed that the carbocation was greater stabilized in this mixture leading to a cleaner reaction and more efficient cyclization. In the HFIP:MeNO₂ solvent mixtures, a side product that was observed with **1.68** was the hydration of the tertiary carbocation as the quantity of MeNO₂ increased. This was minimized when more HFIP was present in the mixture, suggesting that HFIP's ability to sequester water played a significant role in the overall reaction efficiency. When **1.68** was exposed to 5 mol% Re₂O₇•SiO₂ in a 9:1 mixture of HFIP:MeNO₂, **1.70** was synthesized in 69% yield in a 1.5:1 (*trans:cis*) d.r. (Entry 9) within 5 minutes.

Further solvent studies investigated MeCN, a solvent with a similar dielectric constant to nitromethane. This solvent improved only reactions forming a tertiary allylic cation upon ionization (**1.68** to **1.70**) (Entries 11 and 12). Efforts to synthesize **1.69** under the conditions with MeCN as the solvent were unsuccessful as no reaction was observed (Entries 6 and 7). The exact reason for MeCN inhibiting the reaction was unclear; however, studies by Floreancig and coworkers in the oxo-rhenium catalyzed synthesis of nitrogen-containing heterocycles demonstrated that HFIP was also a better solvent for their dehydrative cyclization.³⁶ Therefore, the generally more applicable 9:1 mixture of HFIP:MeNO₂ was used moving forward.³⁴

1.5.3 Understanding the Kinetic and Thermodynamic Outcomes of the Reaction.

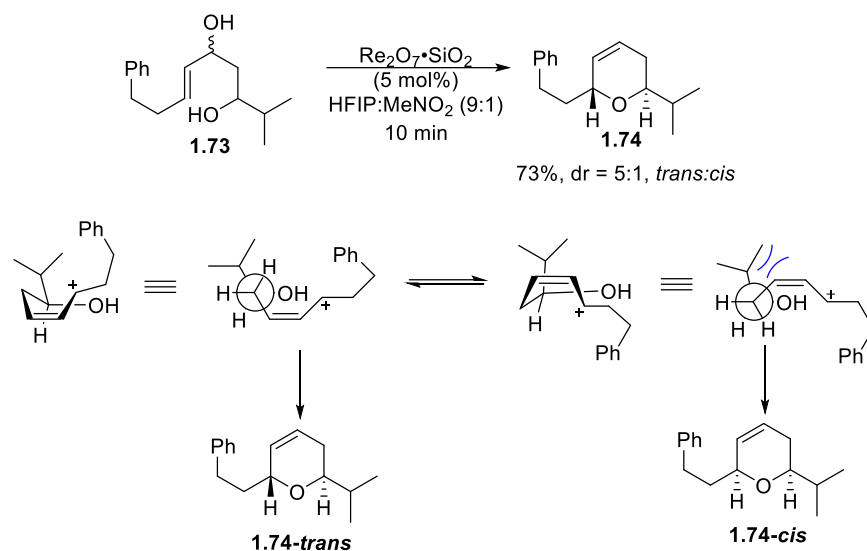
Previous reports show that the *trans*-isomer predominates under kinetic control.^{2, 4, 6, 9} As mentioned, when **1.67** was subjected to 5 mol% $\text{Re}_2\text{O}_7 \cdot \text{SiO}_2$, **1.69** was synthesized in 71% yield in a 3.3:1 (*trans*:*cis*) mixture of diastereomers.³⁴ To further understand the stereochemical outcome of the reaction, we postulated that for cyclization to occur, the reaction must proceed through a boat-like transition state to afford the *cis*-endocyclic alkene of the dihydropyran (Scheme 23). Analyzing the reactive intermediates that lead to each product, we hypothesize that intermediate **1.72** leading to the 2,6-*cis*-isomer is disfavored due to the gauche interactions in the Newman projection observed between the propyl chain of the nucleophilic alcohol and the allylic cation.³⁴ To minimize the gauche interactions observed in **1.72**, the *anti*-relationship in **1.71** between the propyl chain and the allylic cation is preferred, forming **1.69-*trans*** as the major product.³⁴



Scheme 23. Analysis of Stereochemical Outcome of Dehydrative Cyclization

To test the hypothesis that the gauche interactions cause the observed selectivity, the propyl chain was replaced with an isopropyl group to see if there is greater selectivity for the *trans*-isomer (**1.73**, Scheme 24). Once **1.73** was subjected to the reaction conditions, the d.r. increased to 5:1 (*trans*:*cis*) of **1.74** in 73% yield (Scheme 24).³⁴ This illustrates that the isopropyl group introduced

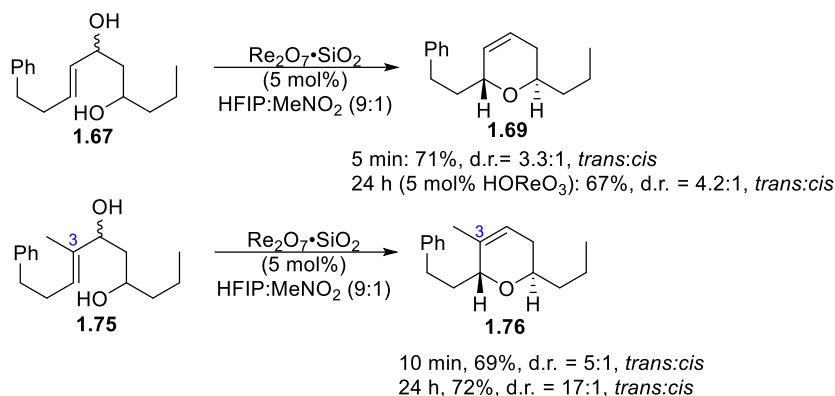
a greater degree of torsional strain in the intermediate that leads to the 2,6-*cis*-isomer of **1.74**, making this pathway less favored, resulting in greater selectivity for the 2,6-*trans*-isomer.



Scheme 24. Isopropyl Substitution to Test Kinetic Hypothesis

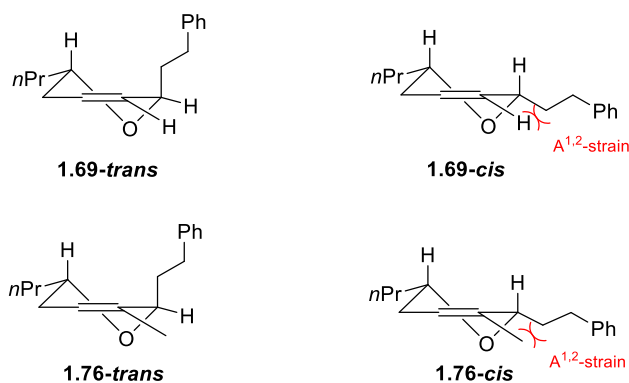
Previous reports of Lewis acid-mediated preparations of dihydropyrans demonstrated that the 2,6-*trans*-isomer was formed through kinetic control.^{2, 9} Reactions under thermodynamic control initially formed a mixture of *cis*- and *trans*-isomers that equilibrated to favor the *cis*-isomer.^{2, 4-7, 9, 37} The 3.3:1 (*trans:cis*) d.r. of **1.69** and the 5:1 (*trans:cis*) d.r. of **1.74** were the kinetic stereochemical outcomes of these reactions, as they were stopped upon consumption of starting material. Equilibration to the thermodynamically favored isomer is typically seen after prolonged exposure of the diastereomeric mixture to the reaction conditions. To determine if there was a thermodynamic preference for a single isomer, time course experiments were performed and the diastereomeric outcomes were analyzed after 24 hours. In this reaction, HOREO₃ was substituted for Re₂O₇ as it is significantly more cost effective and not moisture sensitive as it is sold as a 76.5% wt solution in water. Substrate **1.67** was subjected to 5 mol% HOREO₃ (Scheme 25) for 24 hours and gave a 67% yield of **1.69** in a 4.2:1 (*trans:cis*) d.r., showing an increase in the selectivity for

the *trans*-isomer after prolonged exposure. This proved that HOREO₃ was a good catalyst for the prolonged exposure studies,³⁴⁻³⁶ and successful results also suggested that this was the active catalyst in the dehydrative cyclization.



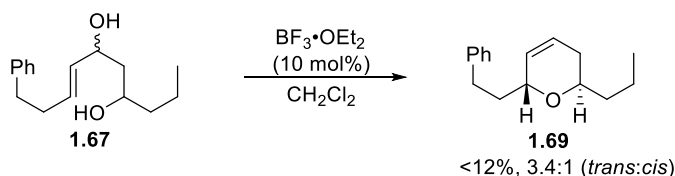
Scheme 25. Thermodynamic Control of Dehydrative Cyclization

To better understand the diastereoselectivity observed for the 24 hour experiment forming **1.69**, a similar experiment was conducted with **1.75** to explore the effects of A^{1,2} strain by introducing a methyl group at the C3-position (Scheme 25). When the reaction was stopped upon consumption of starting material, a 69% yield of **1.76** was observed with a 5:1 (*trans:cis*) ratio. Upon prolonged exposure for 24 hours, **1.76** was observed in a 72% yield with a 17:1 (*trans:cis*) diastereomeric ratio. As seen from the half chair conformations of the products (Scheme 26), the 2,6-*cis*-isomer of **1.76** exhibits significant A^{1,2}-strain between the methyl group on the alkene and the adjacent pseudo-equatorial hydrocinnamyl chain. This strain destabilized the *cis*-isomer and drives the equilibrium to the 2,6-*trans*-isomer, which explains the results observed with prolonged exposure to Re₂O₇. Compound **1.69-cis** exhibits A^{1,2}-strain but to a lesser degree, explaining the small increase in diastereoselectivity from 3.3:1 (*trans:cis*) to 4.2:1 (*trans:cis*).³⁴



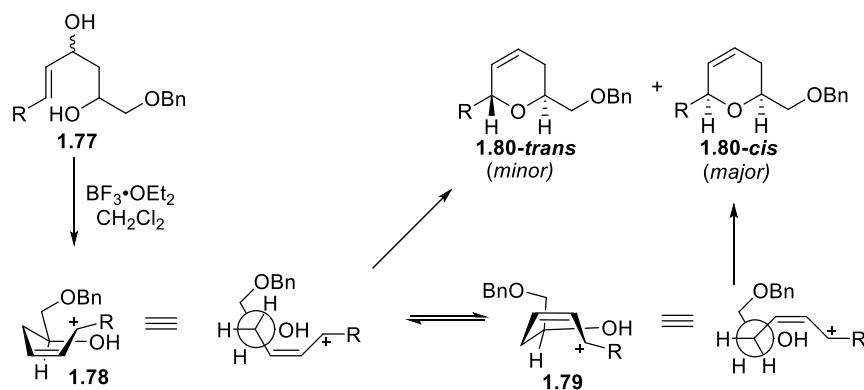
Scheme 26. Illustration of A^{1,2}-strain in Dihydropyrans

The results observed with the Re_2O_7 chemistry contradict previous work done by Hanessian and coworkers illustrated in section 1.3.2.1.⁷ Hanessian demonstrated that the 2,6-*cis*-dihydropyran was favored over the 2,6-*trans*-isomer when $\text{BF}_3 \cdot \text{OEt}_2$ was used as a Lewis acid to catalyze the cyclization. Notably, all of the substrates used in this study were 1,3-monoallylic diols that contained an α -benzyloxy group adjacent to the nucleophilic alcohol.⁷ This led us to investigate whether the stereochemical outcomes observed in our reactions were a result of substrate control, or the effects of HFIP. To test this, **1.67** was subjected to Hanessian's exact conditions (Scheme 27), resulting in a low yield of **1.69** (<12%) with the 2,6-*trans*-isomer still being favored upon cyclization (3.4:1, *trans*:*cis*).^{7, 34} To see if the *cis*-isomer would predominate upon prolonged exposure, **1.69-*trans*** was subjected to the reported conditions, but after 18 hours, no equilibration was observed.³⁴



Scheme 27. Dehydrative Cyclization under Hanessian's Conditions

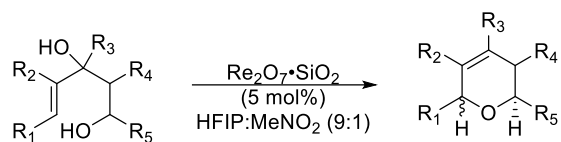
These results support that the stereochemical outcome of our reactions was primarily through substrate control and the α -benzyloxy substituent in Hanessian's study must have played a role in the selectivity they observed for the 2,6-*cis*-dihydropyran. Upon examining Hanessian's substrate using our boat-like transition state models, we proposed that the benzyloxy group sits proximal to the allylic cation in the intermediate leading to the *cis*-isomer (**1.79**, Scheme 28). This would allow for electrostatic interactions from the oxygen of the benzyl ether to stabilize the allylic cation intermediate (Scheme 28). Therefore, this stabilization could supersede other steric interactions to give **1.80-*cis*** as the major isomer.³⁴



Scheme 28. Benzyloxy Stabilization of the Intermediate Leading to 1.80-*cis*

1.5.4 Substrate Scope

With an understanding of the stereochemical outcomes of the reaction, the scope was expanded to include various 1,3-monoallylic diols. Each substrate was subjected to 5 mol% Re_2O_7 or HOREO_3 and was monitored until starting material was consumed unless otherwise specified.



Entry	Substrate	Product	Yield (%)	d.r (<i>trans:cis</i>)
1 ^a	 1.68	 1.70	68	1.5:1
2 ^{a,b}	 1.68	 1.70	79	2:1
3	 1.81	 1.82	79	1.7:1
4	 1.83	 1.84	62	-
5	 1.85	 1.86	74	5:1
6	 1.87	 1.88	59	1.5:1
7	 1.89	 1.90	55	1:1

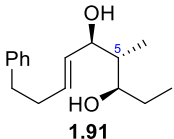
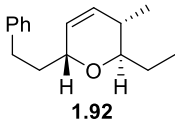
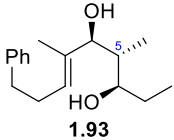
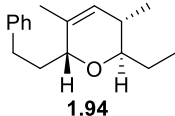
8	 1.91	 1.92	47	<i>c</i>
9	 1.93	 1.94	77	<i>c</i>

Table 2. Substrate Scope of Dehydrative Cyclization

^a 5 mol% HOREO₃, ^b Subjected for 24 h. ^c A single stereoisomer was isolated.

In Entries 1 and 2, 5 mol% HOREO₃ was used instead of Re₂O₇ in the ionization of tertiary alcohol **1.68**. We observed that there was no change in the previous yields and diastereoselectivity from those observed with Re₂O₇•SiO₂ in section **1.5.2**, reinforcing that HOREO₃ was the active catalyst species in the reaction, and both catalysts can be used interchangeably. Subjecting **1.68** to 5 mol% HOREO₃ for 24 hours gave **1.70**, which equilibrated from 1.5:1 to 2:1 (*trans:cis*) (Entry 2, Table 2).³⁴ Much like **1.69**, **1.70** does not exhibit much A^{1,2} strain. This lead us to postulate that the small amount of stereochemical equilibration observed can be attributed to minimizing steric interactions in the reactive conformation, forcing rapid ring closure.³⁴

The isopropyl group in **1.81** was introduced in hopes of increasing selectivity for *trans*-isomer. However, no change in selectivity was observed from incorporating the isopropyl substitution, although the yield was much improved (Entry 3, Table 2). Understanding that tertiary cations were significantly more stabilized, we wanted to expand the scope to monosubstituted dihydropyrans. Inspired by the monosubstituted dihydropyran in (–) laulimalide,² **1.83** was subjected to the developed conditions and gave **1.84** in 62% yield with no loss of enantiopurity observed (Entry 4, Table 2).³⁴ This showcased the possibility that this method could be

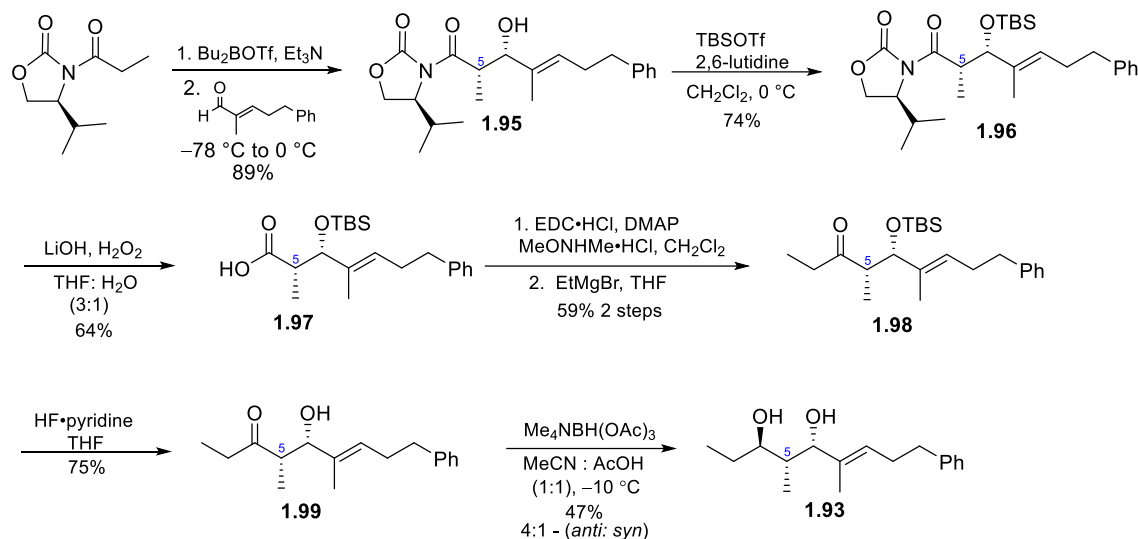
implemented as a strategy for the installation of monosubstituted dihydropyrans in natural product syntheses.

Oxo-rhenium catalyzed benzyl alcohol activation demonstrated by Floreancig and coworkers inspired us to investigate the synthesis of isochromans. Exposure of **1.85** to $\text{Re}_2\text{O}_7 \cdot \text{SiO}_2$ resulted in isochroman **1.86** in 74% yield as a 5:1 (*trans*:*cis*) mixture of diastereomers (Entry 5, Table 2).³⁴ Introduction of heteroatom functionality on the nucleophilic side chain led to further challenges. When a primary TBS-ether was incorporated at the terminus of the propyl side chain, **1.87** (Entry 6, Table 2), upon ionization, the 6-*exo*-cyclization of the allylic cation intermediate proceeded faster than the 6-*endo*-cyclization to afford **1.88** even whilst the primary alcohol was protected as a silyl ether. The nucleophile that captured the allylic cation intermediate was unclear, as either the silyl ether or the deprotected primary alcohol can act as a nucleophile. Standard conditions afforded a mixture of **1.88** and the corresponding secondary silyl ether that resulted from silyl transfer. To prevent silyl ether formation, upon consumption of starting material NH_4F was used to quench the reaction and as a fluoride source, giving **1.88** in 59% yield as a 1.5:1 mixture of diastereomers.

Incorporation of a methyl ester group led to a less efficient cyclization, but still afforded **1.90** in 55% yield in a 1:1 (*trans*:*cis*) ratio (Entry 7, Table 2).³⁴ The inductive effect of the methyl ester may dampen the nucleophilicity of the pendent alcohol, leading to more competitive elimination type pathways. The methyl ester also may stabilize the allylic cation in the intermediate that leads to the *cis*-isomer, similarly to the α -benzyloxy substituents in Hanessian's work, which could explain the lack of stereocontrol.

Lastly, we expanded the substitution on the dihydropyran ring, as many natural products such as sorangicin A incorporate a non-equilibrating stereocenter at the C5 position.⁴ A methyl

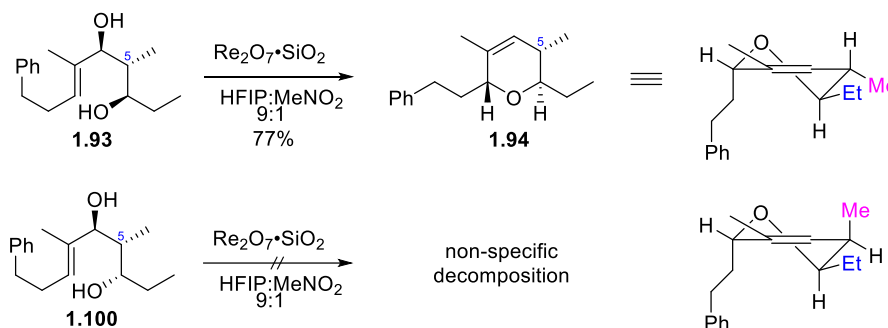
stereocenter at that C5 position was chosen (Entries 8 and 9, Table 2). To stereoselectively install the methyl group, a diastereoselective aldol reaction was done with Bu₂BOTf and 3-pentanone, but this led to poor *syn:anti* diastereocontrol which could be problematic during cyclization. Therefore, a new route was designed using Evan's oxazolidinone to set the stereocenter (Scheme 29).⁴¹



Scheme 29. Stereoselective Synthesis of 1.93

Starting with known acyl oxazolidinone, an Evan's aldol reaction was performed with the α,β -unsaturated aldehyde illustrated to give **1.95** in 89% yield. The allylic alcohol was protected as the silyl ether followed by *in situ* generated LiOOH deprotection of the oxazolidinone in 74% and 64% yield respectively to give carboxylic acid **1.97**. Acid **1.97** was acylated with *N,O*-dimethylhydroxylamine to give the Weinreb amide followed by an ethyl Grignard addition to give β -hydroxy ketone **1.98** in 59% yield over two steps. The silyl ether was deprotected using HF·pyridine followed by an Evans-Saksena reduction to afford *anti*-diol **1.93**. Compound **1.91** was synthesized in a similar manner.⁴²

Compounds **1.91** and **1.93** were both synthesized with a 1,3-*anti*-relationship between the alcohols. Subjection to 5 mol% $\text{Re}_2\text{O}_7 \cdot \text{SiO}_2$ favorably gave **1.92** and **1.93** as single diastereomers in 47% and 77% yield respectively (Table 2, Entries 8 and 9).³⁴ Surprisingly, the 1,3-*anti* relationship was necessary for cyclization to be successful. When 1,3-*syn* diol, **1.100** (Scheme 30) was subjected to the conditions, only unspecific decomposition without cyclization was observed. These results indicate a match versus mismatch case based on the product outcomes of the two diastereomers. In **1.92** and **1.94**, the methyl group and the ethyl side chain were both equatorial. However, successful cyclization of **1.100** would result in an axial-equatorial relationship between the methyl group and the ethyl group (Scheme 30). Although both conformations contain gauche interactions, the energetic penalty of the axial orientation may have been too severe for cyclization to occur.



Scheme 30. Half Chair conformations of 1.94 and Expected of 1.000

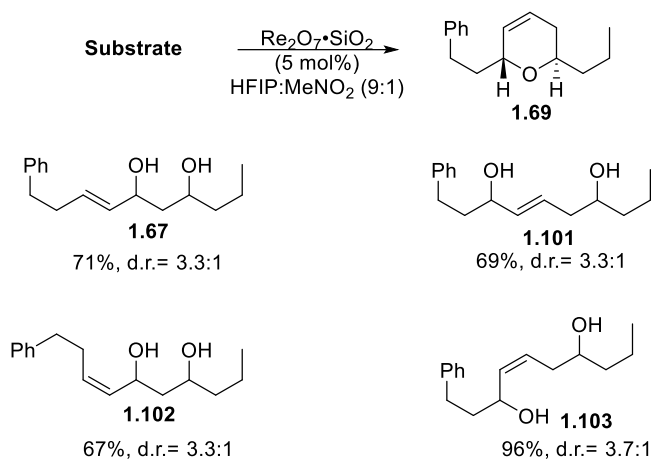
The rate of cyclization of **1.91** and **1.93** was much faster than most substrates. This increase in rate could be attributed to a reactive rotamer effect where the stereochemistry of the methyl group exhibits the right conformation required for efficient cyclization. This hypothesis is supported by Bruice and coworkers who determined that geminal substitution enhanced the rate of both ring closure and ring opening of cyclic anhydrides.⁴³

1.5.5 Effects of Alcohol Position and Alkene Geometry on Reaction Efficiency

Previous work by Roush and coworkers (Section 1.2.3) reported that an allylic cation intermediate was not completely necessary in the synthesis of 2,6-*trans*-dihydropyrans, as their (*Z*)-1,5-diol monoallylic diols proceeded through an S_N2 pathway rather than an S_N1.¹² Therefore it was necessary for us to examine how other isomers could affect the outcome of the reaction. With the conditions and substrate scope developed, constitutional isomers of **1.67** were explored (Scheme 32) to further understand the dehydrative cyclization. In principle, **1.69** can be made from four possible precursors: two isomers can be derived from regioisomeric forms of the diol, and the other two can be derived from two possible alkene geometries. The objective of this study was to determine if the geometric and regioisomeric relationship of the alkenes and alcohols respectively could directly affect the efficiency of the reaction.

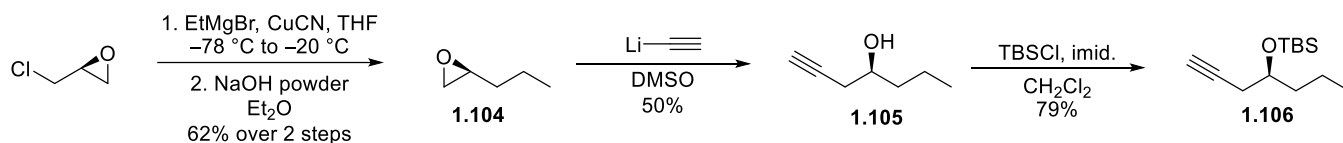
To begin the study, diastereomeric mixtures of **1.101**, **1.102**, and **1.103** were synthesized, each were subjected to Re₂O₇•SiO₂, and stopped upon consumption of starting material (Scheme 31). Theoretically for cyclization to occur, substrates **1.67**, **1.101** and **1.102** each would require ionization prior to cyclization as the alkene either needs to transpose or rotate to the (*Z*)-confirmation required for cyclization.³⁴ Subjection of **1.67**, **1.101** and **1.102** to Re₂O₇ resulted in similar yields and identical stereocontrol (Scheme 32). However **1.103** reacted significantly more efficiently and with slightly improved diastereocontrol, raising the question of whether it proceeded through an alternative mechanistic pathway to the other substrates.³⁴ Compound **1.103** contains the 1,5-diol relationship and the (*Z*)-olefin required for cyclization. Therefore the superior efficiency of **1.103** could be explained by either S_N2 displacement of the perrhenate ester

intermediate by the nucleophilic alcohol or a more likely S_N1 pathway via a tight ion pair intermediate because of its preorganized confirmation for cyclization.



Scheme 31. Effects of Alcohol Position and Alkene Geometry in Dehydrative Cyclization

To test this hypothesis, single diastereomers of **1.103** were synthesized, one assuming the stereochemical relationship for the traditional S_N2 /tight ion pair type pathway, to give an increase in the diastereomeric ratio, and the other which should completely ionize and give the stereocontrol observed in **1.67**, **1.101**, and **1.102** (3.3:1, *trans:cis*).

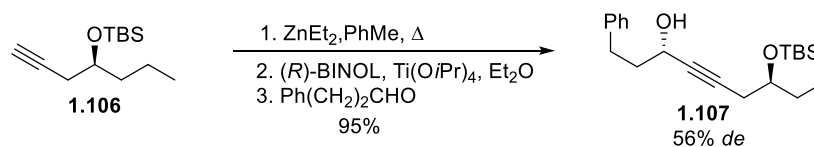


Scheme 32. Synthesis of Enantiopure Homoallylic Alcohol **1.106**

Efforts to synthesize these single diastereomers began using (*S*)-epichlorohydrin (Scheme 32). Ethyl magnesium bromide addition catalyzed by copper (I) cyanide was added into the less-hindered face of the epoxide to give the corresponding secondary alcohol.³⁴ The epoxide was reformed through S_N2 displacement of the chloride to give **1.104** in 62% yield over two steps. This was followed by lithium acetylide opening to give homopropargylic alcohol **1.105** in 98% *ee*

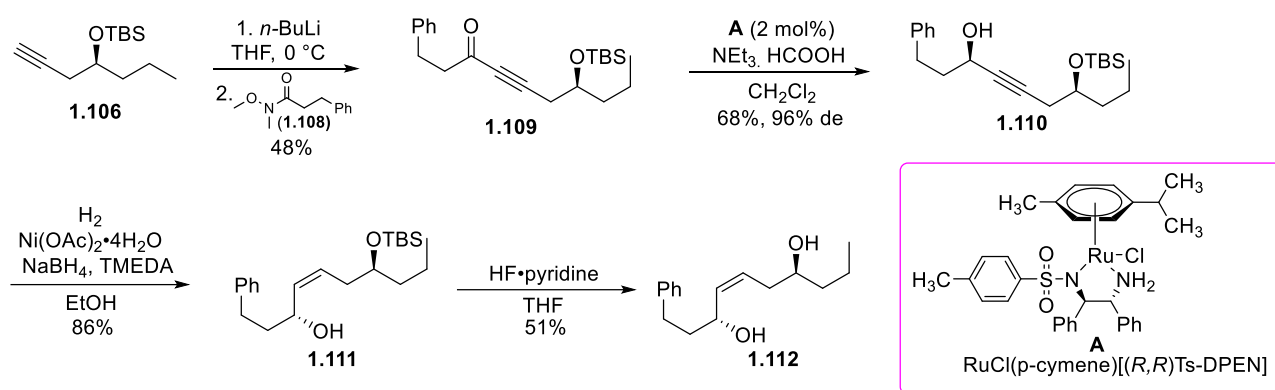
determined by Mosher ester analysis.⁴⁴ Finally, the secondary alcohol was protected as the silyl ether giving **1.106** in 79% yield.³⁴

To initially set the stereochemistry of the allylic alcohol, we envisioned using chemistry developed by Pu and coworkers which involved enantioselective alkyne additions into aldehydes.⁴⁵ A diastereoselective addition of **1.106** into hydrocinnamaldehyde gave **1.107** in 95% yield but in 56% *de* (Scheme 33). Although the reaction gave great yields, it required four equivalents of **1.106** and exhibited poor diastereocontrol determined by Mosher ester analysis.⁴⁴ This may be due to off-site coordination by titanium to the silyl ether instead of completely coordinating to BINOL. Off-site coordination can disrupt the transition state for addition, resulting in poor stereocontrol.



Scheme 33. Diastereoselective Alkyne Addition into Hydrocinnamaldehyde

Unfortunately, low diastereocontrol of the alkyne addition could skew the results of the mechanistic analysis. Instead, the synthesis was redesigned in order to introduce the propargylic alcohol via a Noyori reduction of a propargylic ketone, which has shown to have much greater stereocontrol (Scheme 34).⁴⁶



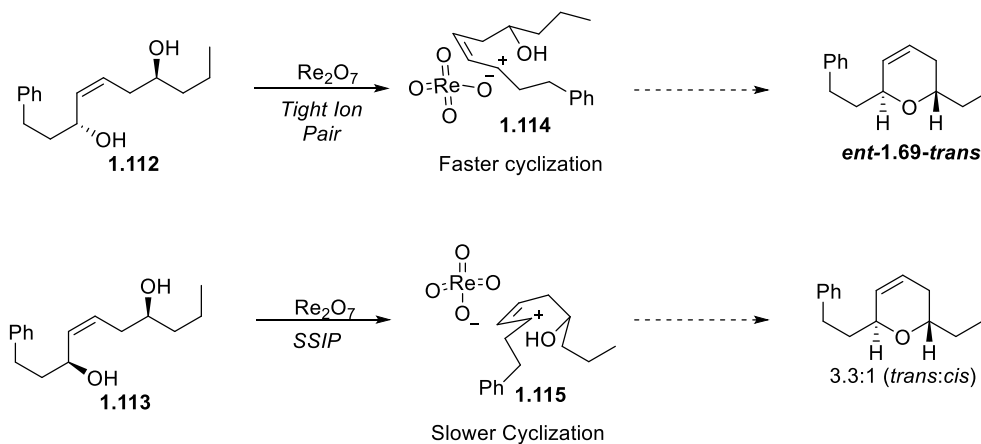
Scheme 34. Improved Synthetic Route to 1.012

Compound **1.106** was deprotonated and added into known Weinreb amide, **1.108**,⁴⁷ to give propargyl ketone **1.109**. The ketone was reduced using the Noyori reduction to give the (*R*)-propargylic alcohol in 68% yield and 96% *de* determined by Mosher ester analysis.^{34, 44, 46} The alkyne was selectively reduced to the (*Z*)-olefin using the nickel boride reduction developed by Brown and coworkers followed by HF•pyridine deprotection of the silyl ether to give **1.112** (Scheme 34).^{34, 48} Diastereomer **1.113** was synthesized in a similar manner, substituting the (*R,R*)-TsDPEN catalyst for the (*S,S*)-TsDPEN catalyst.³⁴

As mentioned previously, it was hypothesized that **1.103** may be going through an S_N1 tight ion pair mechanism which would behave similarly to a typical S_N2 reaction. A tight ion pair mechanism is an S_N1 reaction that proceeds with inversion of stereochemistry, where the perhenate anion forms an ion pair with the allylic cation locking the reactive intermediate (**1.114**, Scheme 35).⁴⁹ Therefore, the diastereomer that would favor the tight ion pair pathway would undergo a fast cyclization and inversion of stereochemistry to give the 2,6-*trans*-diastereomer. The other diastereomer would have difficulty in attacking the cation from this position due to steric interactions between the cation and the propyl chain. To alleviate this strain, the perhenate anion would need to completely dissociate from the allylic cation, generating a solvent separated ion pair

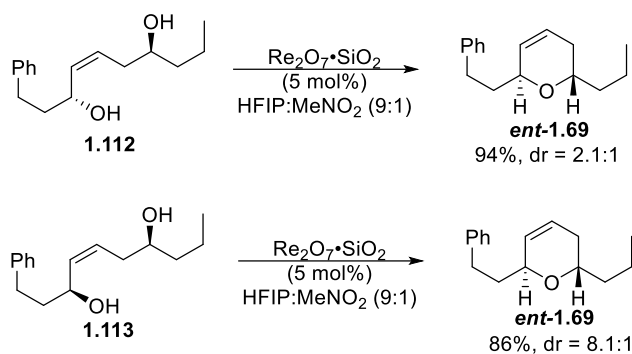
(SSIP) (**1.115**, Scheme 35).⁴⁹ Breaking the tight ion pair would remove the locked conformation, giving the nucleophile access to the cation as it adopts a conformation analogous to the boat transition proposed earlier, resulting in a similar stereochemical outcome observed with racemate **1.69** (3.3:1, *trans:cis*).

We predicted that **1.112** would proceed through a tight ion pair mechanism, through intermediate **1.114** because the alcohol is sitting proximal to the cation (Scheme 35).³⁴ This would result in back side attack, giving predominantly the 2,6-*trans*-isomer with inversion of stereochemistry.³⁴ Compound **1.113** however would sit in an unfavorable conformation for cyclization as the alcohol would not be able to attack the cation effectively, **1.115**. Therefore, in order for it to cyclize it would need to form a solvent separated ion pair and proceed through a similar reactive intermediate to **1.67**, **1.101** and **1.102**, giving a similar outcome to the racemate (3.3:1, *trans:cis*).³⁴



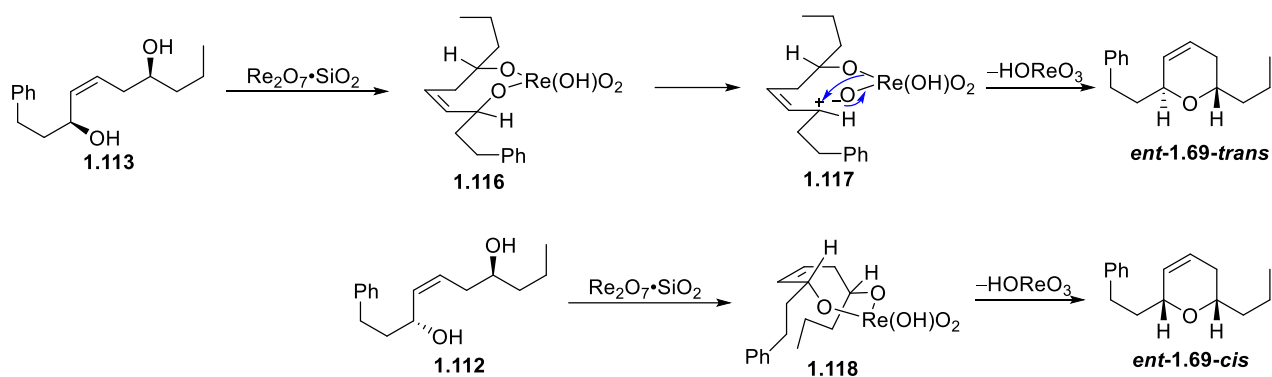
Scheme 35. Hypothesized Tight Ion Pair Mechanism

With an understanding of this mechanistic hypothesis, both diastereomers were subjected to $\text{Re}_2\text{O}_7 \cdot \text{SiO}_2$ and stopped upon immediate consumption of starting material. The reactions were analyzed and the outcome was surprising.



Scheme 36. Dehydrative Cyclizations towards *ent*-1.69

When **1.112** was subjected to 5 mol% Re_2O_7 , **ent-1.69** was isolated in 94% yield with a 2.1:1 (*trans*:*cis*) d.r. (Scheme 36). However, **1.113** under identical conditions gave an 86% yield of **ent-1.69** but in a 8.1:1 (*trans*:*cis*) d.r.³⁴ Each reaction was run in identical 5 min intervals and previous equilibration studies have shown that epimerization was negligible at short reaction intervals, indicating that these results operated under kinetic control. This led us to believe that **1.113** was actually proceeding through an S_{Ni} pathway, via a cyclic perrhenate ester intermediate with retention of stereochemistry.⁵⁰⁻⁵³ This would explain the increased diastereocontrol observed with **1.113**, as it forms cyclic perrhenate ester **1.116**, which dissociates to form tight ion pair **1.117** that cyclizes faster than bond rotation resulting in the 2,6-*trans*-isomer and subsequent loss of HOREO_3 (Scheme 37). However, upon subjection of **1.112** to $\text{Re}_2\text{O}_7 \cdot \text{SiO}_2$, cyclic perrhenate ester **1.118** forms, which would breakdown into the 2,6-*cis*-isomer rather than the 2,6-*trans*-. The lower selectivity observed indicated that the tight-ion pair intermediate (Scheme 35) could not be completely ruled out, however, the increase in *cis*-selectivity compared to the racemate indicated that the S_{Ni} mechanism competed with this pathway (Scheme 37).³⁴



Scheme 37. S_{Ni} Mechanism towards *ent*-1.69

The high yield and diastereocontrol observed with **1.113** showcased the efficiency of the S_{Ni} mechanism making this component of the method a strong candidate for total synthesis applications. These cyclic perhenate esters could be potential intermediates prior to ionization in 1,3-diols as well. However, any stereochemical information would be lost as the allylic cation was formed so it can adopt the proper conformation for cyclization.³⁴

1.6 Conclusions

We demonstrated that dihydropyrans can be prepared through a dehydrative process from 1,3- and 1,5-allylic diols using catalytic amounts of $\text{Re}_2\text{O}_7 \cdot \text{SiO}_2$ or HOREO_3 . This occurs through a cationic intermediate in which a pendent alcohol reacts with the distal end of the generated allylic cation. This process favors the 2,6-*trans*-selectivity in good yield and moderate stereocontrol. We discovered that the *trans*-isomer was the kinetic product based on a boat-type transition state, which through torsional strain destabilized the intermediate leading to the *cis*-isomer. The 2,6-*trans*-isomer was also thermodynamically favored due to $\text{A}^{1,2}$ strain minimization. Substitution on the C5 position of the ring led to a single *trans*-isomer isolated as the kinetic product and

monosubstituted dihydropyrans were synthesized with no loss of enantiopurity. Constitutional isomers of a substrate led to identical products which demonstrated that once ionization occurred, 1,3-(*E*)-, 1,3-(*Z*)-, and 1,5-(*E*)-monoallylic diols all proceeded in equal efficiency and diastereoselectivity. However, 1,5-(*Z*)-monoallylic diols exhibited greater diastereocontrol and reaction efficiency. Synthesis of the single diastereomers of these 1,5-(*Z*) monoallylic diols led to a study that discovered a unique S_Ni mechanistic pathway with stereochemical retention through a cyclic perrhenate diester intermediate leading to increased *trans*-selectivity.

2.0 Kinetics-Based Approach to Developing Electrocatalytic Variants of Slow Oxidations: Application to Hydride Abstraction-Initiated Cyclization Reactions

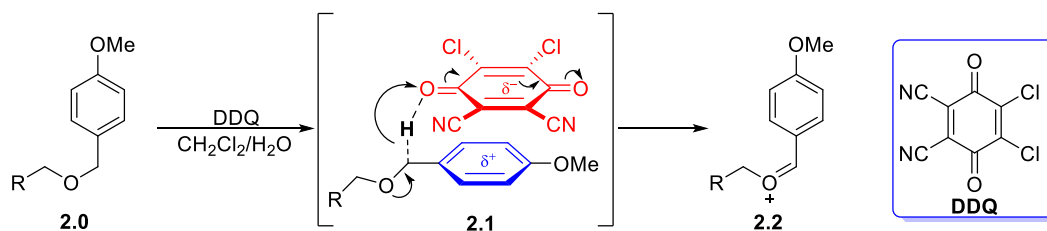
2.1 C–H Functionalization using Organic Hydride Abstracting Agents

C–H functionalization is a unique and advantageous strategy for improving step economy in syntheses while introducing structural complexity. Oxidative C–H functionalization can involve hydride abstractions to promote C–C, C–O, C–N, or C–X bond formation, capitalizing on the overall redox economy. This method bypasses functional group manipulation and minimizes byproduct formation. With minimum waste generation, maximized step economy, and high functional group tolerance, C–H functionalization has been a useful strategy in total synthesis and in the industrial world.^{54, 55}

Traditionally, oxidative C–H functionalization employs transition metal catalysts that proceed through hydride abstraction or hydrogen atom abstraction. Although efficient, these require directing groups to mitigate poor regioselectivity and enhance the overall catalytic efficiency of the system.⁵⁶ In recent years, many organic hydride abstracting agents have been developed as a means of generating carbocation intermediates which have shown great promise as they can be used to construct new bonds from simple starting materials, introducing molecular complexity to the substrate.

2.1.1 Quinone-Based Oxidants as Hydride Abstracting Agents

Quinone-based oxidants are commonly used as hydride abstracting agents with many synthetic applications. A common oxidant that has been used in this effort is 2,3-dichloro-5,6-dicyano-*p*-benzoquinone (DDQ). DDQ has been a prominent oxidant in the cleavage of benzyl ethers and has been incorporated into numerous total syntheses over the years. This proceeds through a hydride abstraction mechanism at the benzylic position which was supported by a computational study by Floreancig, Liu and coworkers (Scheme 38).⁵⁷ The computational data showed that hydride abstraction to the oxygen atom as DDQ stacks over the π -system, a mechanism involving transition state **2.1** was kinetically and thermodynamically favored over hydrogen atom and single electron transfer mechanisms. Therefore **2.0** undergoes hydride abstraction to form oxocarbenium ion **2.2**, which in most synthetic applications, are hydrolyzed to release the corresponding alcohol.

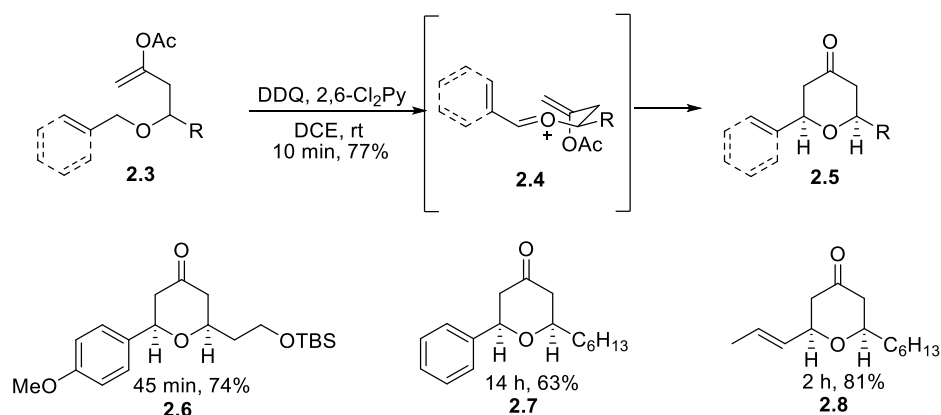


Scheme 38. Selective PMB Oxidation with DDQ

2.1.1.1 DDQ-mediated Oxidative C–H Cleavage towards C–C Bond Formation

Oxocarbenium ions like **2.2**, under anhydrous conditions can be utilized as intermediates in bond forming reactions. These reactions can be either bimolecular or intramolecular processes, showcasing the diverse synthetic utility of the cationic intermediates being generated.

The Floreancig group initiated their efforts in DDQ-mediated oxidations with the oxidation of allylic and benzylic ethers, focusing on intramolecular trapping of the generated oxocarbenium ion. Upon subjection of **2.3** to DDQ, hydride abstraction occurred to give oxocarbenium ion **2.4**. This then cyclized via a chair-like transition state in which the oxocarbenium ion in intermediate **2.4** adopts an (*E*)-geometry, and is captured by the pendent enol acetate nucleophile to give pyranone **2.5** as a single diastereomer (Scheme 39). The acylium ion that was lost was scavenged by 2,6-dichloropyridine, preventing Friedel-Crafts acylations with electron-rich arenes.⁵⁸



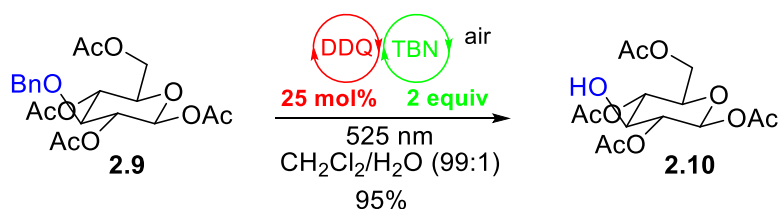
Scheme 39. Stereocontrolled Intramolecular Trapping of Oxocarbenium Ion Intermediates

An array of pyranones could be synthesized from substrates that vary in oxidation potential. Oxidation of allylic ethers was similarly efficient, as demonstrated by **2.8** which was synthesized in 81% yield in 2 hours (Scheme 39). The difference in reactivity between **2.6** and **2.7** was a result of the greater cation stability and high charge transfer ability of the *p*-methoxybenzyl ether. Allylic ether **2.8** had much greater cation stability than **2.7** due to electron donation from the methyl group compared to benzyl ether **2.7**, leading to much faster reaction times.⁵⁸ These excellent results sparked numerous studies within the group which focused on different nucleophiles, electrophiles, and tethering strategies to broaden the applications of DDQ-mediated oxidations towards various heterocyclic moieties and targets for total synthesis.⁵⁹⁻⁶⁸

2.1.1.2 Catalytic Applications of DDQ-mediated Oxidations

While DDQ-mediated oxidations of benzylic and allylic ethers shown previously have many applications that introduce molecular complexity through a simple hydride abstraction, these oxidations required stoichiometric amounts of DDQ. This can generate substantial waste when used in quantitative amounts, driving the development of reactions in which catalytic quantities can be used. In order to use DDQ in a catalytic amount, the reduced hydroquinone (DDQH₂) needs to be oxidized by a stoichiometric oxidant to regenerate the quinone. This has previously been accomplished via the use of terminal oxidants, aerobic oxidation, or electrochemical oxidation.^{65, 69, 70}

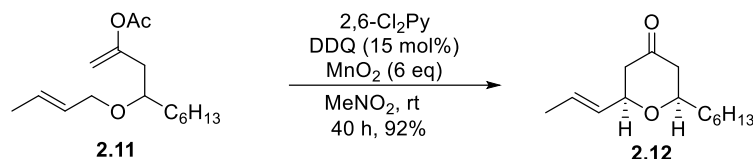
A modernized approach to catalysis was conducted by Seeberger and Pieber, who used visible light in a cooperative catalytic cycle with catalytic DDQ, *t*-butyl nitrite (TBN), and oxygen as a stoichiometric oxidant for the deprotection of benzyl ethers.⁶⁹ TBN was used as a thermolytic or photolytic source of NO which was oxidized by atmospheric oxygen to NO₂. Upon oxidation of the benzyl ether **2.9** with DDQ, NO₂ was used to re-oxidize DDQH₂ back to DDQ, restarting the catalytic cycle leading to **2.10** in 95% yield (Scheme 40).⁶⁹



Scheme 40. Visible Light-Mediated Oxidative Deprotection of Benzyl Ethers

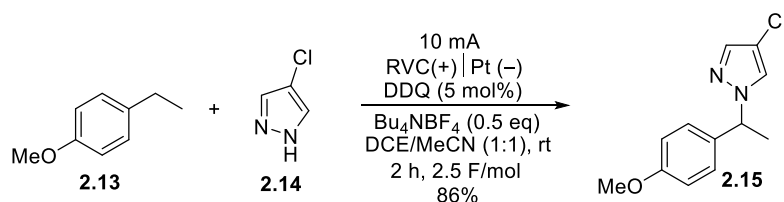
Catalytic amounts of DDQ can also be regenerated using stoichiometric metal oxides as terminal oxidants. This was demonstrated by the Floreancig group, who applied this to their work in benzylic and allylic ether oxidations (Scheme 41).⁵⁸ A catalytic amount of DDQ was subjected

to **2.11** and six equivalents of MnO_2 were used as a terminal oxidant to give pyranone **2.12** within 40 hours in 92% yield.⁶⁵ Lead(IV) oxide was also a competent oxidant in these transformations but, due to the toxicity of lead, MnO_2 was chosen as the preferred oxidant. More reactive and less toxic oxidants such as ceric ammonium nitrate (CAN) can also be used as a terminal oxidant but as a stoichiometric oxidant this can be quite expensive.⁷¹



Scheme 41. Oxidative Regeneration of DDQ using Terminal Oxidants

While terminal oxidants were effective in regenerating DDQ from DDQH_2 , an alternative is the use of electrochemical methods. Using electricity to turnover DDQ may be a more affordable process as the reagents are simply electrons. The other benefit is the functional group tolerance of this method as the conditions can be altered to selectively oxidize the mediator, being DDQ, rather than the substrate. Wang and coworkers demonstrated this through the electrochemical amination of benzylic C–H bonds (Scheme 42). The benzylic position of **2.13** was oxidized by DDQ to the corresponding benzylic cation and was captured by **2.14** to yield **2.15** in 86%.⁷⁰ This process was extremely efficient and could be conducted on a gram scale and run at 66 mA for 8 hours to afford **2.15** in 79% yield.



Scheme 42. Electrochemical Regeneration of DDQ

DDQ has proven to have many synthetic applications in both stoichiometric and catalytic amounts. However the rate of hydride abstraction can be dependent on numerous factors as demonstrated by Miller and coworkers.⁷² They investigated a number of hydride abstracting agents that can be used to generate identical oxocarbenium ion intermediates which is further elaborated in Section 2.1.2. Although each oxidant can generate the same cation, the kinetics of each oxidant is affected differently by sterics, electronics, and oxidation potential of the substrate.⁷²

2.1.2 Oxoammonium and Trityl Cations as Effective Hydride Abstracting Agents

Oxoammonium ions and triphenylmethyl (trityl) cations are two other oxidants that have shown to be effective hydride abstracting agents in oxidative C–H functionalization reactions. Oxoammonium ions specifically are very attractive as they are mild oxidants that exhibit high functional group compatibility.

Oxoammonium ions, specifically Bobbitt's salt (**2a**, Figure 3), have been shown to have significant applications in alcohol oxidations. These oxidations were typically run under basic conditions. Bailey and Wiberg investigated this through a computational study modeling the oxidation of alcohols by oxoammonium ions under basic and acidic or neutral conditions.⁷³ The study concluded that at high pH, the oxidation proceeded via nucleophilic addition of the alcohol into the nitrogen atom of the oxoammonium species followed by deprotonation by the oxygen atom (**2.16**) (Figure 3). On the other hand, at lower pH (**2.17**) the oxoammonium oxidized the alcohol via hydride abstraction, where cation stability dictated the reactivity of the substrate (Figure 3).⁷³

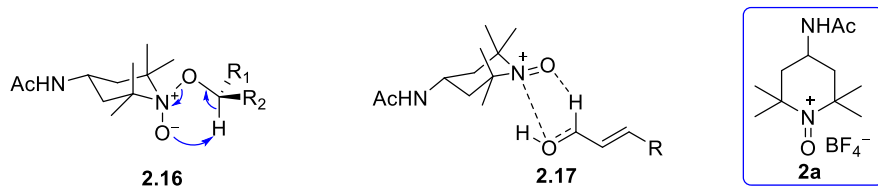
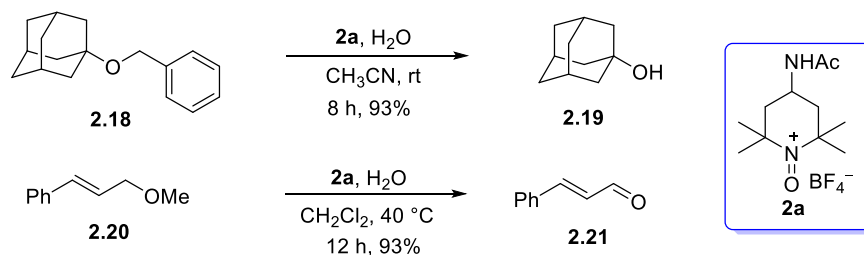


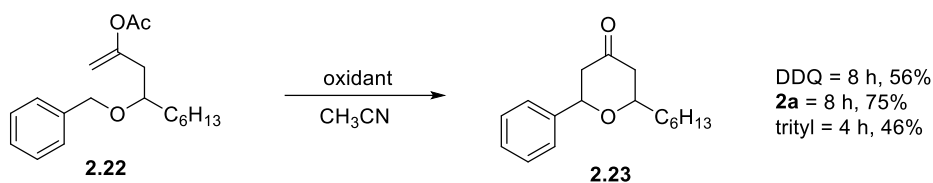
Figure 3. pH Dependent Mechanism of Oxoammonium-Mediated Oxidation of Alcohols

Unlike alcohols and amines, non-nucleophilic species cannot undergo oxidation via **2.16** regardless of the pH of the solution. Therefore these will oxidize via hydride abstraction similar to **2.17**. Leadbeater and Bailey expanded the applications of oxoammonium ions to the oxidation of allylic and benzylic ethers using a stoichiometric amount of Bobbitt's Salt (**2a**) (Scheme 43).^{74, 75} Once Bobbitt's salt was subjected to **2.18** and **2.20**, the oxocarbenium ions generated were hydrolyzed by water to release alcohol **2.19** and benzaldehyde, and aldehyde **2.21** and methanol respectively.



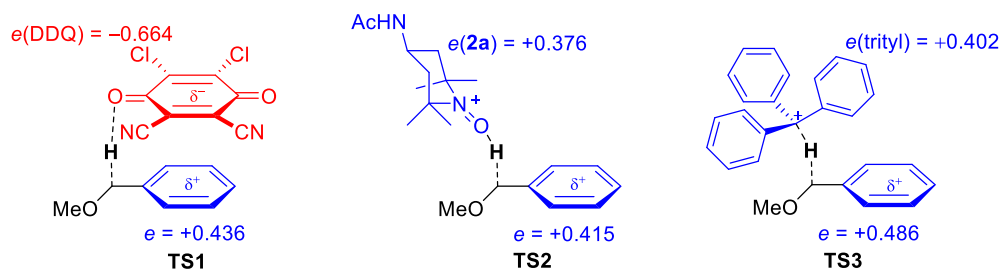
Scheme 43. Oxidative Cleavage of Benzyl and Methyl Ethers using 2a

Miller and coworkers expanded on the synthetic utility of this oxidation towards generating oxocarbenium and iminium-type intermediates for C–C bond formation. In a more in-depth analysis of initial work by Floreancig and coworkers (Scheme 44), the effects of oxidant compatibility with various substrates were examined.⁷² They demonstrated that DDQ, Bobbitt's salt and trityl cation were effective in the hydride abstraction of benzylic ethers. However, as geometries, oxidation potential, and electronics of the substrates varied, the reactivity of the oxidants differed. (Scheme 44).



Scheme 44. Oxidant Screen Demonstrated on Benzyl Ethers

With the aid of computational models, the transition states of each oxidant were examined to understand experimental trends (Scheme 45). The computed natural populated analysis (NPA) charges shown illustrate the degree of charge transfer between the oxidant and the substrate (Scheme 45). In **TS1**, DDQ exhibits the greatest amount of charge transfer, whereas in **TS2** and **TS3** charge transfer was negligible, illustrating that π -stacking is required for effective hydride abstraction with DDQ. This stacking also increases the effects of sterics in the transition state with DDQ, while Bobbitt's salt and trityl cation remain distal to the oxidation site. Therefore, from the trends observed computationally and experimentally, Bobbitt's salt and trityl cation oxidation rates were solely dependent on cation stability, whereas DDQ was dependent on charge transfer, cation stability, and steric interactions. This resulted in Bobbitt's salt being a kinetically faster hydride abstracting agent than DDQ overall. Trityl cation saw enhanced reactivity compared to Bobbitt's salt, leading to more oxidative decomposition. Therefore Bobbitt's salt was determined to be the optimal oxidant because of its kinetics, which is beneficial when progressing towards catalytic methods.



Scheme 45. Charge Transfer and Electrostatic Interactions between the Substrate and the Oxidant

2.1.3 Electrochemical Regeneration of Oxoammonium Species for Oxidative C–H

Functionalization

Oxoammonium ions have been examined in the catalytic oxidation of alcohols and amines. Once reacted with the substrate, the reduced hydroxylamine species was regenerated with a terminal oxidant. Numerous methodologies in the past have been developed using stoichiometric terminal oxidants such as bleach⁷⁶ or CuCl and oxygen for the regeneration of TEMPO in alcohol oxidations.⁷⁷ Although beneficial, these methods require excessive amounts of these reagents. An alternative is the use of electrochemistry to turnover the reduced oxidant through anodic oxidation *in situ* without the use of other expensive terminal oxidants. The catalytic cycle these proceed through depends on the starting catalyst. For example, starting at the nitroxyl radical requires oxidation to the oxoammonium ion at the anode prior to reacting with the substrate. Once the oxoammonium ion is generated, it will oxidize the substrate and be reduced to the corresponding hydroxylamine (Figure 4). This is followed by a $2e^-$ oxidation at the anode to regenerate the oxoammonium species. In an electrochemical cell, reduction at the cathode must occur

simultaneously to keep the current flowing effectively. Typically in these oxidative processes, the common reaction at the cathode is proton reduction to release hydrogen gas (Figure 4).

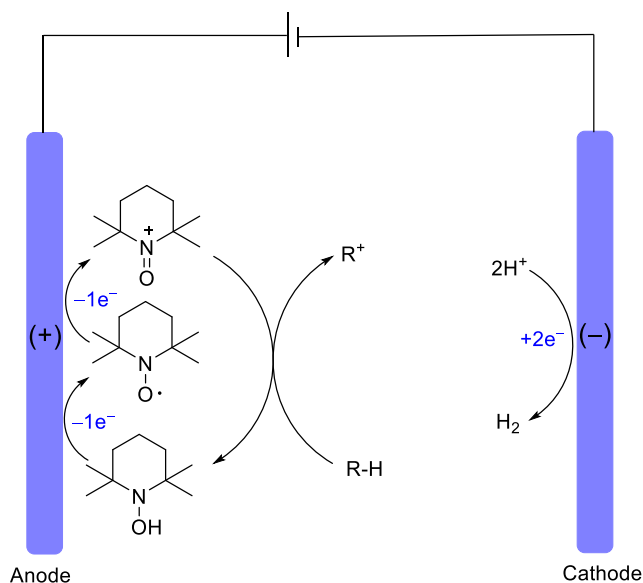
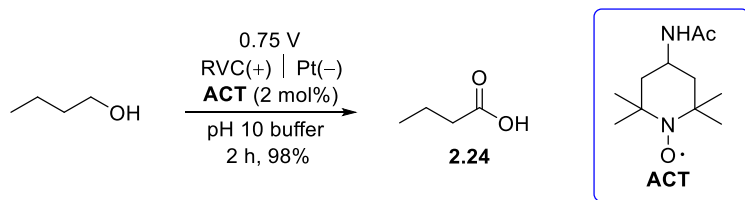


Figure 4. Typical Electrochemical Regeneration of Oxoammonium Ion

2.1.3.1 Electrochemical Oxoammonium Regeneration in Alcohol Oxidation

The electrochemical oxidation of alcohols to aldehydes and carboxylic acids with TEMPO-based oxidants has been rigorously studied by Stahl and coworkers.⁷⁸⁻⁸¹ Although these reactions were pH dependent, they were extremely efficient. In one example, 2 mol% of 4-acetamido-TEMPO (ACT) was used as an oxidant precursor to oxidize 1-butanol at 0.75 V within two hours in pH 10 buffer to give butanoic acid (**2.24**) in almost quantitative yield (Scheme 46).



Scheme 46. Oxidation of 1-Butanol to Butanoic Acid

Alcohols react readily with oxoammonium species under basic conditions, a trend that was clear in the cyclic voltammograms taken by Stahl and coworkers. The voltammograms showed spikes in the current with over a 300% increase as the pH increased from pH 9 to pH 12.⁸¹ This meant that oxidant was being consumed so quickly that there was constant oxidation of reduced hydroxylamine occurring at the anode. This subsequently increased the turnover rate of catalyst in the oxidation of 1-butanol with ACT as they calculated an increase in turnover frequency (TOF) from 552 TOF (h^{-1}) at pH 9 to 2010 TOF (h^{-1}) at pH 11.^{81, 82} This increase in the rate of oxidation as pH increases can be attributed to the alcohol oxidation mechanism under basic conditions proposed by Bailey and Wiberg in Section 2.1.2.⁷³ Therefore, this increase in the rate of oxidation explains the low potentials required for high catalyst turnover and maximized current flow in Stahl's oxidations.

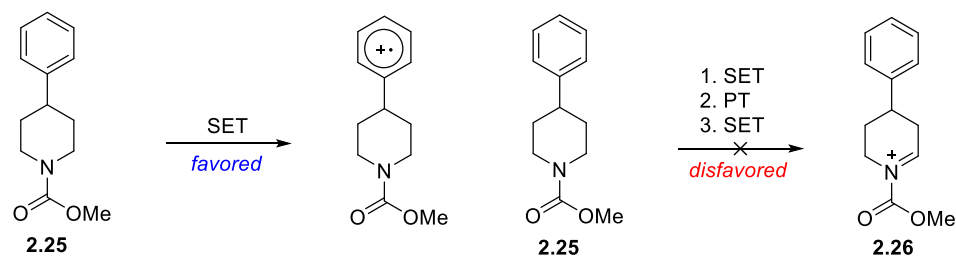
2.1.3.2 Electrochemical Oxoammonium Regeneration in Bond-Forming Reactions

Alcohol oxidation is an extremely efficient process, and due to the enhanced reactivity under high pH aqueous environments, the turnover rate and conductance within the electrochemical cell is very high.^{78, 80, 81} These fast oxidations generate large steady-state concentrations of reduced hydroxylamine which results in high activity at the anode, allowing for current to flow well at low voltages. Non-nucleophilic substrates, such as ethers, are unable to attack the nitrogen center of the oxoammonium ion the same way as alcohols. This will result in ethers being more difficult to oxidize, causing slower consumption of the oxidant, limiting the concentration of reduced hydroxylamine at the anode during the course of the reaction. This will make it difficult for current to flow in the cell, restricting the electrochemical regeneration of the

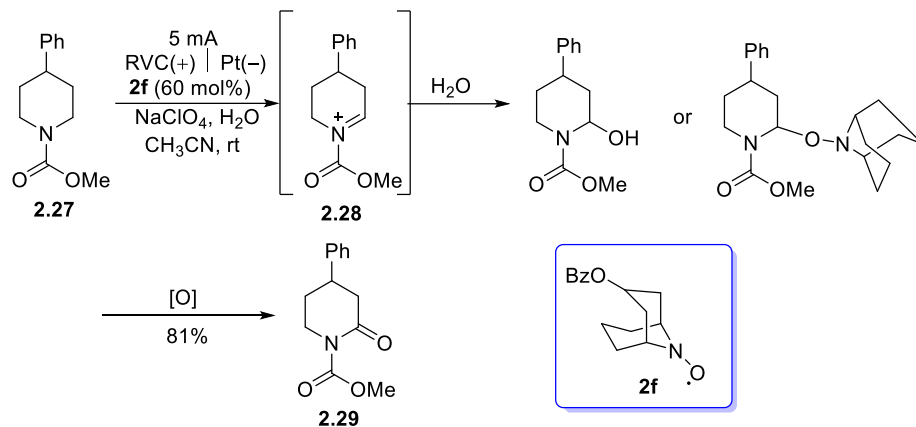
oxoammonium species. Therefore, oxidations of these types of systems pose a significant challenge.

Amides and carbamates are two examples of difficult functional groups to oxidize due to the destabilized acyl-iminium species that are formed. Stahl and coworkers demonstrated the ability to perform the challenging Shono oxidation of carbamates using a bicyclic oxyl radical mediator, benzoyloxy-ABNO (**2f**) (Scheme 47).⁸³ Typically electrochemical Shono oxidations on carbamates were performed using direct electrolysis. This involves a single electron transfer to the carbamate, the loss of a proton, then another single electron transfer to generate the acyl-iminium ion.⁸³ However, introducing aromatic substitution on the piperidine ring led to preferred single electron transfer on the arene rather than the nitrogen of the carbamate (Scheme 47).^{83, 84} Therefore, under these circumstances, an electrochemical mediator can be used to effectively perform redox events at a lower voltage than the oxidation potential of the substrate while controlling the site of oxidation. This allows for enhancements in functional group compatibility and scope.

Direct Oxidation:



Mediated Oxidation:



Scheme 47. Electrochemical-Mediated Shono Oxidation of Carbamates

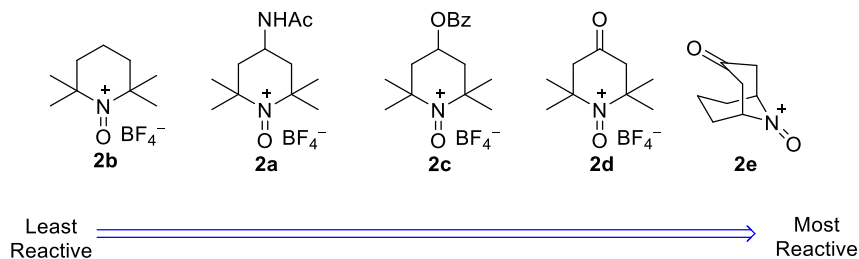


Figure 5. Oxidant Strength Based on Substituent Effects

The oxidizing strength of oxoammonium salts can also be tuned based on the electron withdrawing or donating groups incorporated (Figure 5). Bicyclic oxoammonium species display similar reactivity to the TEMPO based oxidants based on oxidation potential (Figure 5); however, because its bicyclic structure sits flanked behind the N-O bond, the oxidation site is more

accessible. This makes them better oxidants for sterically encumbered substrates. Using 60 mol% of **2f** at a constant current of 5 mA, carbamate **2.25** was oxidized to the iminium species **2.26**. This was then captured by water or the hydroxylamine and underwent a subsequent oxidation to generate the lactam **2.29** (Scheme 47).⁸³

Unlike the alcohol oxidations, these reactions were much slower and required 60 mol% compared to 2 mol% in the alcohol oxidations. This illustrates that hydride abstraction of cyclic carbamates was challenging and slow reacting, resulting in lower concentrations of reduced hydroxylamine during the course of the reaction. This reduces the amount of current flowing in the cell, requiring larger concentrations of nitroxyl mediator to circumvent the low turnover rates.

2.2 Kinetics-Based Approach to Developing Electrocatalytic Variants of Slow Oxidations:

Application to Hydride Abstraction-Initiated Cyclization Reactions

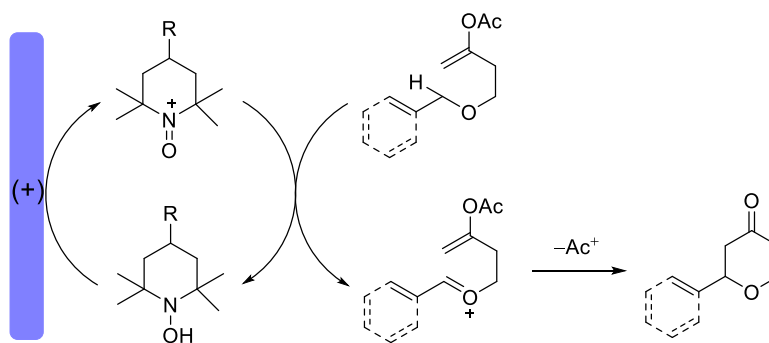
Electrochemical regeneration of catalytic oxidants in kinetically slow redox reactions poses a significant issue due to the overall low concentrations of reduced oxidant within the cell. This leads to the inability to maintain current flow or to prevent spikes in potential shifting towards direct oxidation of the substrate. The Floreancig group has done significant work in C–H abstraction of benzylic and allylic ethers in the generation of new C–C bonds which recently expanded to include the use of oxoammonium salts and trityl cations as effective oxidants.^{58, 60-68, 72, 85-87} Additionally, Stahl and coworkers have done extensive work in electrocatalytic C–H oxidations with oxoammonium salts as mediators, however, they have primarily focused their approach in alcohol oxidations in aqueous media.^{79-83, 88-90} The limited applications in anhydrous

organic solvent involve the use of easily oxidizable piperidines, replicating the efficiency seen in the oxidations of alcohols in aqueous media.⁹¹

This led us to investigate the oxidative C–H functionalization of benzylic and allylic ethers for C–C and C–O bond formation in the electrochemical cell, using a catalytic amount of oxoammonium salt as a mediator (Scheme 48). Although the mediator looks unnecessary at first glance, the substrate and product are similar in structure, with the product still containing an oxidizable C–H bond. Therefore both substrate and product could competitively oxidize at the anode during direct oxidation if a mediator were not used. The mediator allows for these reactions to be conducted at lower potentials, mitigating direct oxidation at the anode which can lead to high energy radical cation intermediates. Oxoammonium salts were investigated as potential mediators, due to the functional group and substrate compatibility along with the lower toxicity and environmental impact.

Although these reactions could be done using stoichiometric amounts of oxidant, conducting them on industrial scales will lead to large amounts of waste generated, which could be a problematic for the expense and ease of purification. Electrochemical regeneration of these oxidants in catalytic quantities, with reactions only costing \$0.07 per KWh, is a more cost effective way of conducting these reactions at larger scales, while simultaneously lowering the amount of waste generated. However, with electrochemistry being an emerging field, electrocatalysis of reactions that involve slow hydride abstractions has not been addressed by the synthetic community. With its numerous applications for C–C or C–O bond formation in total synthesis and the ability to introducing structural complexity in one step, this has motivated us to develop a method in which these hydride abstractions can be done in a cost-effective but efficient manner.

A possible complication is intermediate cation stability. With the end goal being C–C or C–O bond formation, any water present in the reaction would hydrolyze the cationic intermediate, so the chemical rate accelerating property of water observed in Stahl’s work could not be used.⁸³ Under those circumstances, the rate of substrate oxidation is the defining factor in effective catalyst turnover. The substrate scope envisioned in this endeavor would incorporate substrates of varying cation stability, which can affect the observed reaction rates, resulting in substrate-dependent concentrations of reduced oxidant within the electrochemical cell. Therefore, this study focused on the interplay between intermediate cation stability, oxidant strength, overpotential, and how concentration affects scalability in the successful electrochemical regeneration of oxoammonium salts in the oxidative C–H functionalization of allylic and benzylic ethers.⁹²

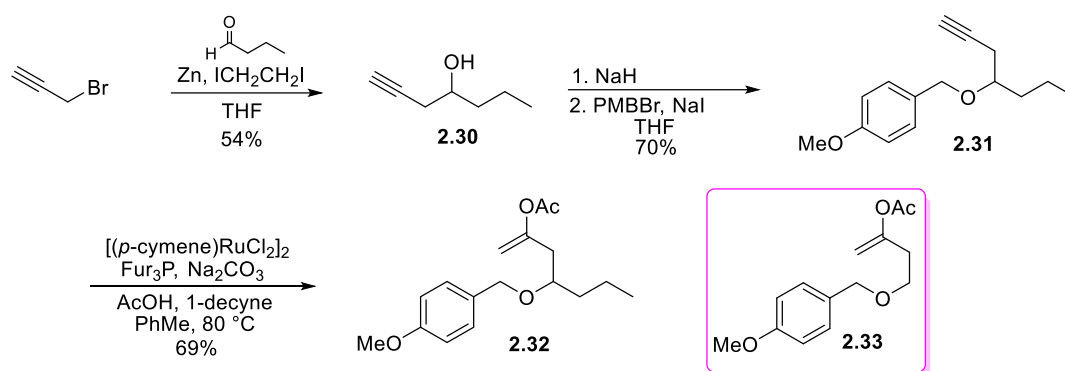


Scheme 48. Oxidative Cyclization with Electrochemical Oxoammonium Regeneration

2.2.1 Synthesis of Substrates as Model Systems for Electrochemical Regeneration of Oxoammonium Ions in C–C Bond-Forming Reactions

We began our studies by synthesizing two *p*-methoxybenzyl ethers as the model substrates. These were selected as the substrates to model our initial screens because the *p*-methoxybenzyl ether stabilizes the cation intermediate very well. These molecules were efficiently synthesized in

two to three steps. This began with a Barbier reaction between propargyl bromide and butyraldehyde to give **2.30** in 54% yield (Scheme 49).⁹³ Deprotonation of the alcohol followed by addition of *p*-methoxybenzyl bromide and a catalytic amount of sodium iodide gave *p*-methoxybenzyl ether **2.31**. Lastly, a regiocontrolled Ru-catalyzed Markovnikov addition of acetic acid into the alkyne gave enol acetate **2.32** in 69% yield.^{92, 94, 95} An analogous substrate **2.33** was synthesized in a similar manner, starting with 3-butyn-1-ol instead of secondary alcohol **2.30**. (Scheme 49/Appendix B)



Scheme 49. Synthesis of *p*-Methoxybenzyl Ether 2.32

2.2.2 Comparing Rates of Alcohol Oxidation to Benzyl Ether Oxidation using Cyclic Voltammetry

Stahl utilized cyclic voltammetry as a means of comparing the effects of pH on the performance of alcohol oxidations in the presence of the ACT nitroxyl radical.^{80, 81} They observed that as the alcohol reacted more rapidly with the *in situ* generated oxoammonium ion, the current output at the oxidation potential of the nitroxyl radical dramatically increased. This was also examined in terms of the concentration dependency of the substrate. In examining the cyclic

voltammetry (CV) time scale, they observed a dramatic increase in the anodic peak current (>500% increase) as the concentration of substrate increased relative to a constant concentration of the nitroxyl mediator.^{80, 81} This increase in anodic peak current means that there is a saturated amount of reduced hydroxylamine at the anode that needs to be oxidized, increasing activity at the anode, reiterating that alcohol oxidation under basic conditions is a kinetically fast redox event.

Given that cyclic voltammetry can be used in this way, we envisioned that this could be used to understand how much slower the oxidation of ethers under anhydrous conditions were compared to alcohol oxidation under aqueous conditions. Two studies were conducted to identify the magnitude of the increase in current upon the oxidation of *N*-(1-hydroxy-2,2,6,6-tetramethylpiperidin-1-yl)acetamide, **2.34**, the reduction product of Bobbitt's salt. The first demonstrated the oxidation of benzyl alcohol under a variant of Stahl's conditions, where the only difference was the hydroxylamine (Figure 6). An initial CV scan was taken with only hydroxylamine **2.34** at 5mM in a 1:1 mixture of MeCN and pH 10 buffer vs 3M Ag/AgCl. This was followed by 25 mM increment additions of benzyl alcohol to the solution and a CV scan was taken of each.⁹² This was repeated under anhydrous conditions using **2.32** vs 0.01M Ag/AgNO₃. (Figure 7).

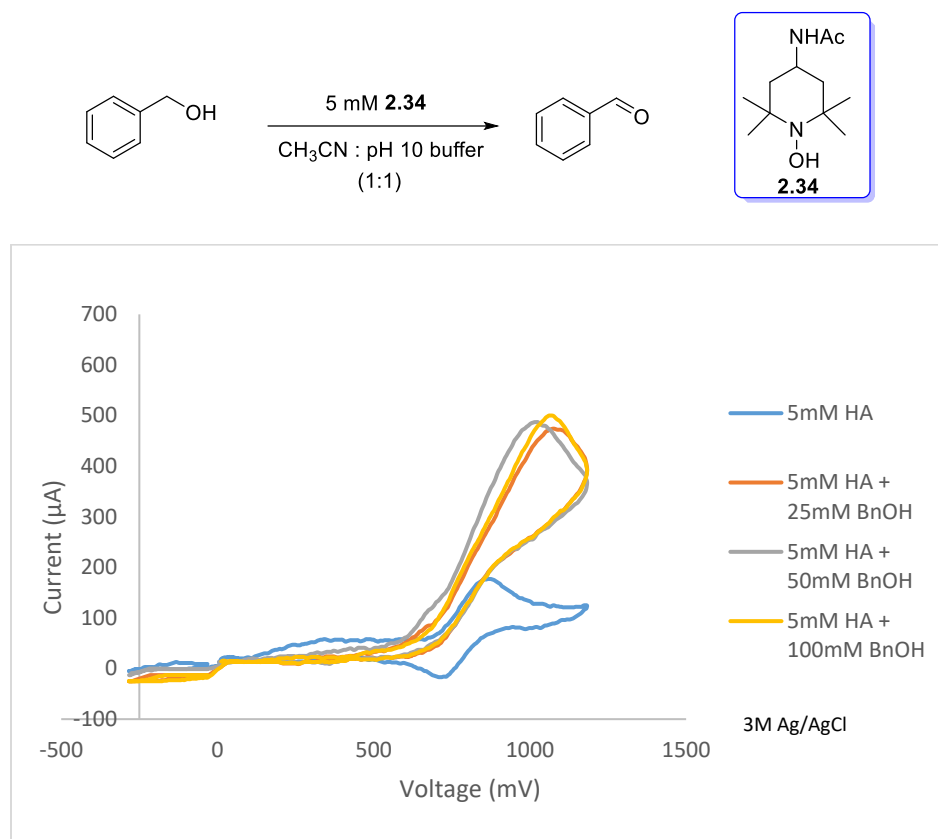


Figure 6. Cyclic Voltammograms of 5mM Hydroxylamine (HA) in the Presence of BnOH

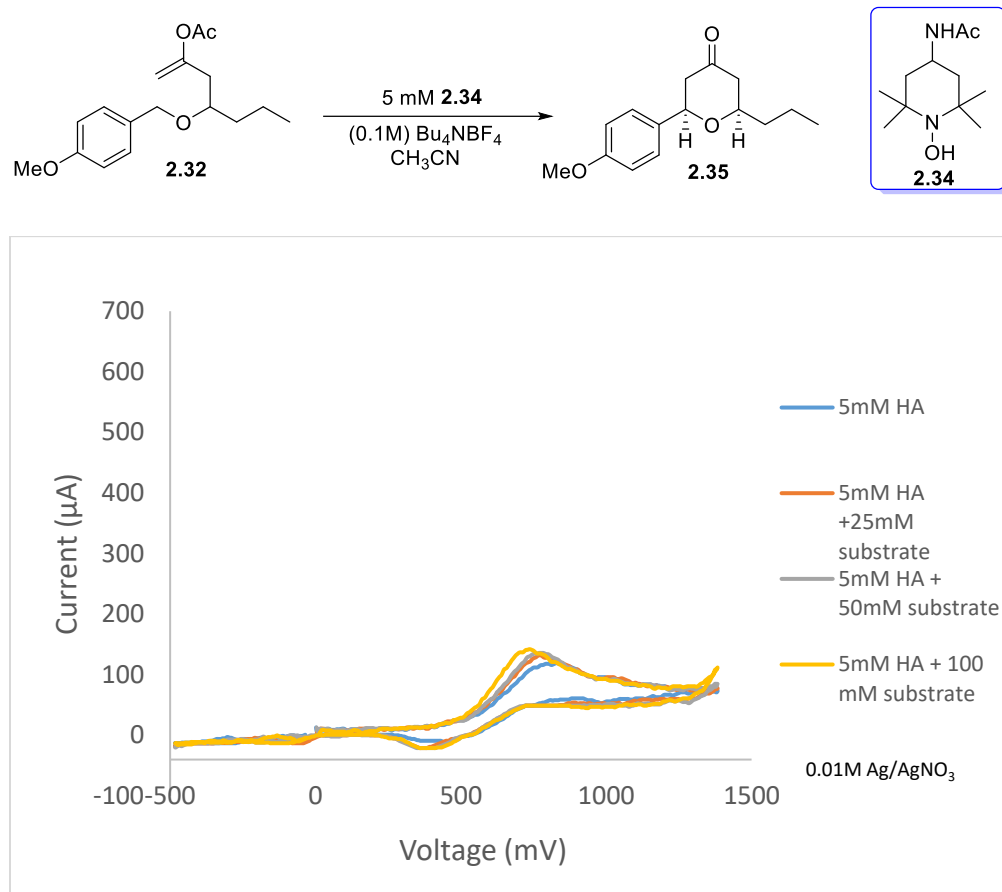


Figure 7. Cyclic Voltammogram of 5mM Hydroxylamine (HA) in the Presence of 2.32

During the CV time scale, the hydroxylamine species undergoes a $2e^-$ oxidation to the oxoammonium ion, which reacts with the substrate accordingly, regenerating the hydroxylamine which can be oxidized again. Upon the 25 mM addition of benzyl alcohol to Stahl's conditions, a 190% increase in anodic current was observed with minimal increases in higher concentrations of benzyl alcohol, illustrating that the reaction rate reached saturation. However, under the anhydrous conditions, at 100 mM of **2.32** there was only a 20% increase in anodic current.⁹² Regardless of the difference in reaction conditions, the anodic currents were directly proportional to the concentration of hydroxylamine present in the cell. This was supported by Savéant and coworkers who demonstrated that the current output by the catalyst is given by Equation 1, where C_H is the

bulk concentration of hydroxylamine, F is Faraday's constant, A is the electrode surface area, and D_A is the diffusion coefficient, illustrating that current is directly proportional to the concentration of hydroxylamine in the cell.^{81, 96}

$$I_{cat} = nFAC_H(D_A k_{obs} C_A)^{1/2}$$

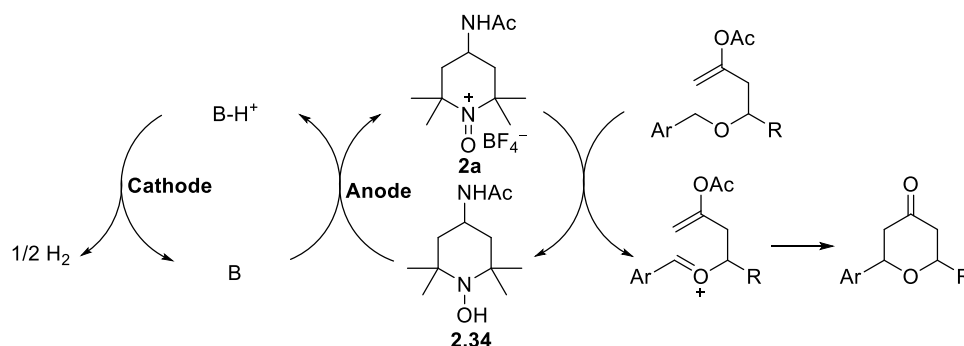
Equation 1. Catalyst Current Output with Respect to Concentration

Therefore, it was concluded that with only a 20% increase in current, the rate of hydride abstraction of **2.32** was very slow in comparison to alcohol oxidations. This indicated the difficulty in turning over Bobbitt's salt electrochemically under anhydrous conditions.⁹²

2.2.3 Reaction Optimization for Successful Electrochemical Regeneration of Oxoammonium Ion

Initial efforts began with a variation on Stahl's oxoammonium regeneration for the cyanation of piperidines via an iminium ion intermediate.⁹¹ Two types of experiments can be run, constant potential (voltage) or constant current. When an experiment was run under constant potential, the current is the dependent variable, with current decreasing as substrate is consumed. In constant current experiments, the system will adjust in voltage in order to maintain the current at which the reaction was set to. This can lead to spikes in potential resulting in undesired redox events. Constant potential experiments can be useful when substrates and products have similar redox potentials. This can be set to control the applied voltage, preventing undesired over-oxidation or reduction in the cell. However, the decrease in current over time as the concentration of substrate decreases can cause reactions to not proceed to full completion.⁹⁷

The envisioned catalytic cycle (Scheme 50) began with Bobbitt's salt (**2a**), would oxidizing the benzyl ether to generate the oxocarbenium ion, which would then be captured by an intramolecular enol acetate to give the resulting pyranone. The reduced hydroxylamine will be oxidized at the anode, while at the cathode, a proton source will be deprotonated to release hydrogen gas. The base that was generated *in situ* will deprotonate the hydroxylamine and restart the catalytic cycle.



Scheme 50. Envisioned Catalytic Cycle of 2a Within the Electrochemical Cell

Prior to exposure of the substrate to electrochemical conditions, it was imperative to determine the oxidation potentials of the substrate and hydroxylamine to understand what voltages could afford single electron transfer to the substrate itself. From the cyclic voltammogram (Figure 8), the reversible oxidation of the hydroxylamine species had an oxidation potential of 0.79 V vs 0.01M Ag/AgNO₃ and substrate **2.32** had an oxidation potential of 2.07 V vs 0.01M Ag/AgNO₃.⁹² Based on the acting potentials during reaction optimization, it was possible to determine whether product formation was a result of direct electrolysis to the substrate or catalyst turnover.

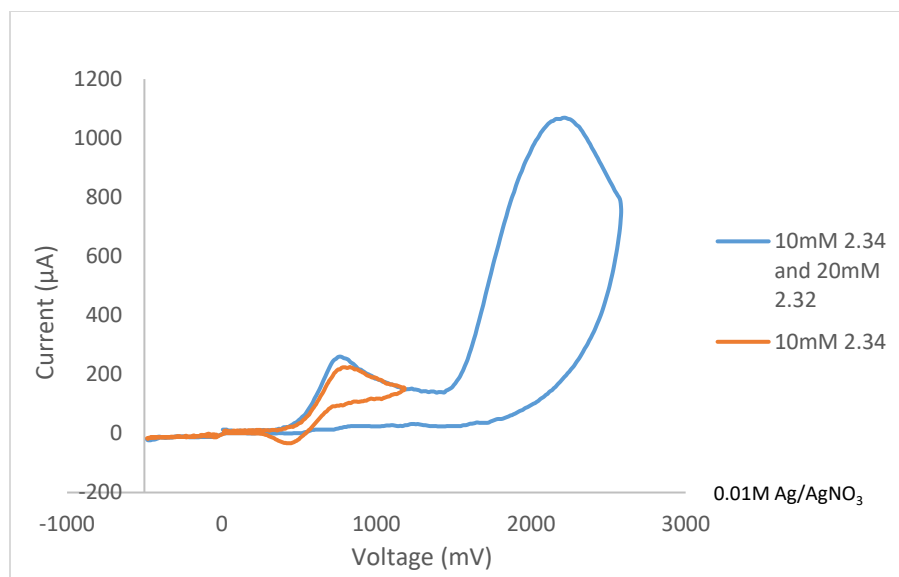
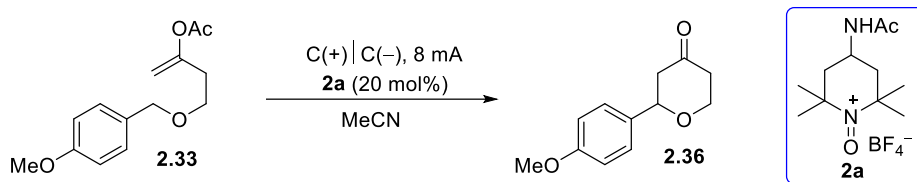


Figure 8. Cyclic Voltammogram of 2.32 and 2.34

The process began by screening electrolytes and the presence of an additive when 20 mol% Bobbitt's salt (**2a**) was subjected to **2.33** using graphite electrodes (Table 3). When the reaction was run without an additive at 8 mA constant current, **2.36** was produced in 24% yield. The lack of product formation with little starting material recovered indicated significant oxidative decomposition occurred. This was likely a result of the high potentials observed in the reaction.⁹² Stahl demonstrated that the addition of HFIP aided in turnover at the cathode, as it was a proton source that could be reduced to form the corresponding alkoxide.⁹¹ This aids in the deprotonation of the hydroxylamine to help promote oxidation at the anode. The addition of HFIP as well as tetrabutylammonium tetrafluoroborate (Bu₄NBF₄) as an electrolyte gave the best results. The reaction was run at 8 mA with 0.1M Bu₄NBF₄, 1 equivalent of HFIP, and 20 mol% Bobbitt's salt to give 51% of **2.36**, 8.5% of anisaldehyde, which results from hydrolysis of the oxocarbenium, and 7% recovered **2.33**.⁹² Although promising, the voltages at which these constant current experiments operated was approximately 3.5 V. This was much higher than the oxidation potential

of the substrate, which indicated that the yield was a result of direct oxidation of the substrate by the anode rather than the turnover of Bobbitt's salt.



Conditions	Electrolyte	Additive (1 eq)	NMR Yield (%)	% Aldehyde	% SM
8 mA	Bu ₄ NPF ₆	none	24	-	-
8 mA	Bu ₄ NPF ₆	HFIP	35	13	12
8 mA	NaClO ₄	HFIP	39	9.5	23
8 mA	Bu ₄ NBF ₄	HFIP	51	8.5	7

Table 3. Initial Electrolyte and Additive Screen

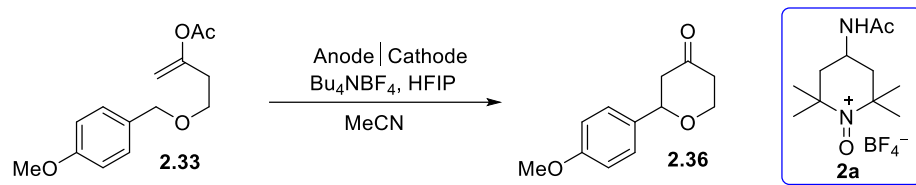
Stahl and coworkers demonstrated in their CVs that at higher concentrations of substrate, this can lead to faster consumption of oxidant. In order to maximize the substrate to catalyst ratio, the catalyst loadings were lowered to 5 mol%, but this endeavor was fruitless, as the acting potentials were still very high. This led to inconsistent yields and high potentials, indicating that direct oxidation of the substrate by the anode was still occurring.

In order to better understand the issue at hand, different electrodes were screened as each material can interact differently with each reagent within the electrochemical cell. A recent review by Heard and Lennox illustrated that the electrode material used can dictate how well hydrogen and oxygen evolution occurred at each electrode.⁹⁸ Based on this information, platinum had a higher reduction potential than graphite for hydrogen evolution, indicating that using a platinum electrode at the cathode would more easily reduce protons than graphite.⁹⁸ A screen of electrodes

was conducted at both the anode and the cathode to try and improve reaction efficiency and to afford turnover rather than direct electrolysis of the substrate.

Using a graphite anode and a platinum plated cathode still consistently afforded high acting potentials with 5 mol% Bobbitt's Salt (Table 4). The first change in conditions was to platinum foil electrodes (purer source of platinum) at both the anode and cathode, 20 mol% Bobbitt's salt, and the use of a reference electrode (Table 4).⁹² A practical guide from Baran and coworkers described the use of the reference electrode as unnecessary in constant current experiments, however, those experiments primarily focused on direct oxidations of the substrate.⁹⁷ Due to the constraints of our system, lower potentials were required to prevent direct oxidation of the substrate by the anode, so using the reference electrode gave a more accurate analysis of the acting potentials during the course of the reaction to ensure only catalyst was being turned over.

When the reaction was run under these conditions at 8 mA, it immediately displayed very high potentials, so the potential was lowered to 4 mA. The acting potentials were below 2.2 V with the use of a reference electrode, which was much more reasonable, and the conservation of starting material was much improved. Each reaction was stopped once potentials spiked to ensure direct oxidation was not a factor. Again with no more than 30% oxidation observed and inconsistent reaction times, it was concluded that minimal turnover occurred (Table 4). This led us to hypothesize that the true problem was not oxidation at the anode, but the effective reduction of the proton source at the cathode. If that balance was not achieved, then potentials would continue to rise to maintain the current, oxidizing the species in the largest concentration, which in this case was the substrate.



Current	2a (mol%)	Time (h)	Anode	Cathode	NMR Yield (%)	Aldehyde(%)	SM(%)
^a 8 mA	5	3	C	Pt Plated	29	6	28
^a 4 mA	20	1	Pt	Pt	24	10	66
^b 4 mA	20	3.5	Pt	Pt	21	4	75

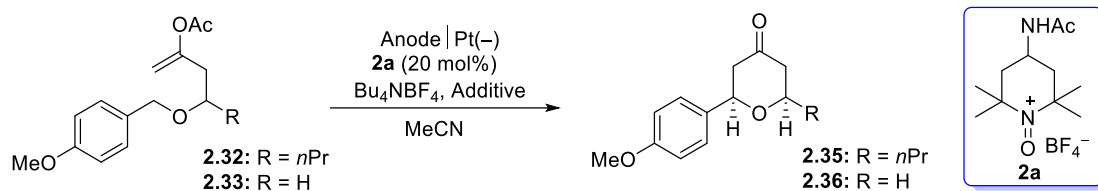
Table 4. Electrode and Oxidant Loading Screen

^a Without reference electrode, ^b With reference electrode.

Understanding that controlling reduction at the cathode was the potential issue in successful turnover, a number of additives were screened with platinum foil electrodes to determine the best source of protons for reduction at the cathode (Table 5). HFIP as mentioned previously seemed to be a poor additive for proton reduction in our system (Entry 1, Table 5). Previous examples in literature have also employed 2,2,2-trifluoroethanol (TFE) as a proton source, which inspired us to attempt these conditions.^{99, 100} Initial improvements in reactivity were seen with one full turnover of catalyst observed in 1.25 h, yielding 33% of **2.36** and 7% *p*-methoxybenzaldehyde upon addition of two equivalents of TFE (Entry 2, Table 5). Increasing to three equivalents gave optimal and repeatable results at 66% yield of **2.36**, 8% aldehyde and 24% recovered **2.33** (Entry 3, Table 5).⁹² More than three equivalents of TFE seemed to be detrimental to the reaction. This was possibly due to hydrogen bonding to the benzyl ether, which pulls electron density away from the ether oxygen. This would destabilize the resulting cation, making the benzylic C–H more difficult to abstract (Entry 4, Table 5).

The significant improvement seen with the use of TFE over HFIP prompted the question of whether inductive effects played a role in the effective reduction at the cathode. When 2,2,2-trichloroethanol (TCE) was used, it could not supersede TFE as an additive, giving 40% of **2.36** after 1 hour before potentials spiked. This is possibly due to TCE being more electron-rich than TFE, resulting in a more negative reduction potential, which makes it more difficult to reduce (Entry 5, Table 5). Amine bases unfortunately could not be used, as their oxidation potentials were too low (1.26V vs 0.01M Ag/AgNO₃ for *N*-methylimidazole) leading to direct oxidation at the anode, and therefore no reaction observed (Entry 6, Table 5). Lastly, the conditions were studied in the absence of catalyst to compare the results of direct oxidation (Entry 7, Table 5). Direct oxidation led to high acting potentials, low yield, and decomposition observed in 4.5 hours compared to the 3 hours in the presence of **2a** (Entry 3, Table 5).⁹² Therefore, we can conclude that the 66% yield of **2.36** and 6% anisaldehyde was a result of successful turnover of **2a** and not direct oxidation.

With these optimized conditions in hand (Entry 3, Table 5), other substrates were attempted, although full consumption of starting material was not achieved. However, when other substrates were attempted under these conditions, low yields, substrate and product decomposition, electrode fouling, and significant potential increases were observed. With the possibility that this may be an electrode compatibility issue, the anode was changed from platinum back to graphite and the reaction was run under constant potential conditions to ensure oxidative decomposition did not take place.



Entry	Compound	Conditions	Anode (+)	Additive (equiv)	Time (h)	% Yield of Product ^a	% of Aldehyde	% of SM recovered
1	2.33	4 mA	Pt	HFIP (1)	3.5	21	4	75
2	2.33	5 mA	Pt	TFE (2)	1.25	33	7	55
3	2.33	5 mA	Pt	TFE (3)	3	66	6	21
4	2.33	5 mA	Pt	TFE (3.5)	1.5	32	4	42
5	2.33	5 mA	Pt	TCE (3)	1	40	4	49
6	2.33	5 mA	Pt	NMI	-	NR	-	-
7 ^b	2.33	5 mA	Pt	TFE (3)	4.5	14	1	47
8	2.33	1.6 V	C	TFE (3)	8	55	14	16
9 ^c	2.32	1.6 V	C	TFE (3)	8	65	-	-
10 ^c	2.32	1.7 V	C	TFE (3)	4	52	-	-
11 ^b	2.32	1.6 V	C	TFE (3)	-	NR	-	-

Table 5. Additive and Electrode Optimization of Electrocatalytic Oxidations

^a NMR yields vs TMSOMe in C₆D₆, ^b No Catalyst, ^c Isolated Yields.

During constant current experiments, the voltage typically stabilized between 1.5-1.9 V (vs 0.01M Ag/AgNO₃), so selecting a voltage within this range seemed optimal. As a result, these reactions were conducted at 1.6 V (vs 0.01M Ag/AgNO₃) to begin. Thankfully, this was a success

as **2.33** was exposed to 20 mol% Bobbitt's salt at 1.6 V over 8 hours to give **2.35** in 55% yield, 14% hydrolysis, and 16% **2.33** recovered (Entry 8, Table 5). This was attempted with **2.32** and similarly resulted in 65% isolated yield of **2.35** but with minimal hydrolysis and full consumption of starting material being observed (Entry 9, Table 5).⁹² Despite the increased length in reaction time, these conditions led to a much cleaner reaction and provided consistent results. Increasing the potential to 1.7 V (vs 0.01M Ag/AgNO₃) increased the rate of the reaction as expected but afforded more decomposition, resulting in depreciated yields (Entry 10, Table 5). Moving forward, the reactions were conducted at 1.6 V (vs 0.01M Ag/AgNO₃) with a graphite anode and a platinum foil cathode.⁹²

Conducting these experiments at 1.6 V (vs 0.01M Ag/AgNO₃) seemed necessary. The hydroxylamine has a peak oxidation potential of 0.79 V (vs 0.01M Ag/AgNO₃), but when reactions were conducted at 0.8 V, which was deemed sufficient in alcohol oxidation, current died off rapidly, causing turnover to fail. This suggested that not enough energy was present in the system to drive the reaction. With the oxidation potential of the substrate being 2.07 V (vs 0.01M Ag/AgNO₃), conducting these reactions at 1.6 V (vs 0.01M Ag/AgNO₃) was sufficient for oxidation of the hydroxylamine but not the substrate. Thus, no reaction was observed in the absence of Bobbitt's salt (Entry 11, Table 5), leading to the conclusion that overpotential played a significant role in the effective turnover at 1.6 V (vs 0.01M Ag/AgNO₃).⁹²

Overpotential is the potential that is required beyond what is necessary by thermodynamics to drive a reaction at a practical rate.⁸⁴ This phenomenon is reaction dependent and can vary significantly as observed in the Shono oxidations conducted by Clausen and coworkers which was performed at 2.0 V (vs Ag/AgCl) to oxidize keto-ABNO.¹⁰¹ Overpotential can also be affected by the electrode materials used. Increasing the overpotential will provide more energy in the reaction

system. Slow electron transfer processes require larger overpotentials in order to increase the rate of electron transfer. Therefore, conducting reactions with an ample overpotential can increase the rate of catalyst turnover, which proved to be a significant issue when the concentration of hydroxylamine at the anode was low.

Another interesting observation was the need for these reactions to be vigorously stirred at 800 RPM. At lower RPMs current dropped and did not flow as efficiently. This suggests that mass transport within the electrochemical cell was an issue. The electrochemical cell is made up of three phases: the anodic layer surrounding the anode itself, the cathodic layer surrounding the cathode, and the bulk phase which exists between the two electrodes. When oxidation occurs at the anode, the oxoammonium ion travels to the bulk phase of the solution and reacts with substrate, and the reduced form travels back to the anodic layer. Ineffective mass transport of these species can lead to undesired redox events which can slow the rate of oxidation, but also lead to catalyst decomposition, supporting the need for 20 mol% of the oxidant.

With this knowledge, successful conditions were developed for electrochemical regeneration of Bobbitt's salt under anhydrous conditions. The final catalytic cycle for the optimized conditions (Figure 9) involved oxidation of the benzyl ether resulting in the formation of the hydroxylamine and the corresponding oxocarbenium ion, which was then trapped by the enol acetate to give the corresponding pyranone. At the platinum foil cathode, reduction of TFE released hydrogen gas and the TFE alkoxide. This then deprotonated the hydroxylamine, and a $2e^-$ oxidation occurs at the graphite anode to regenerate the oxoammonium ion restarting the catalytic cycle.⁹² With the optimized conditions in hand, the substrate scope for the method was expanded.

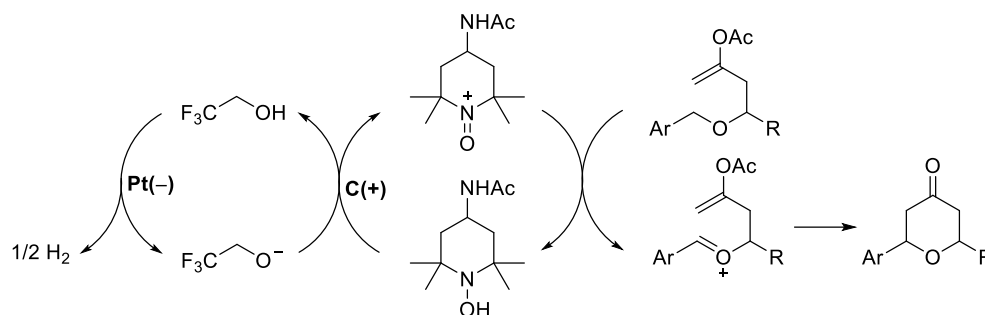
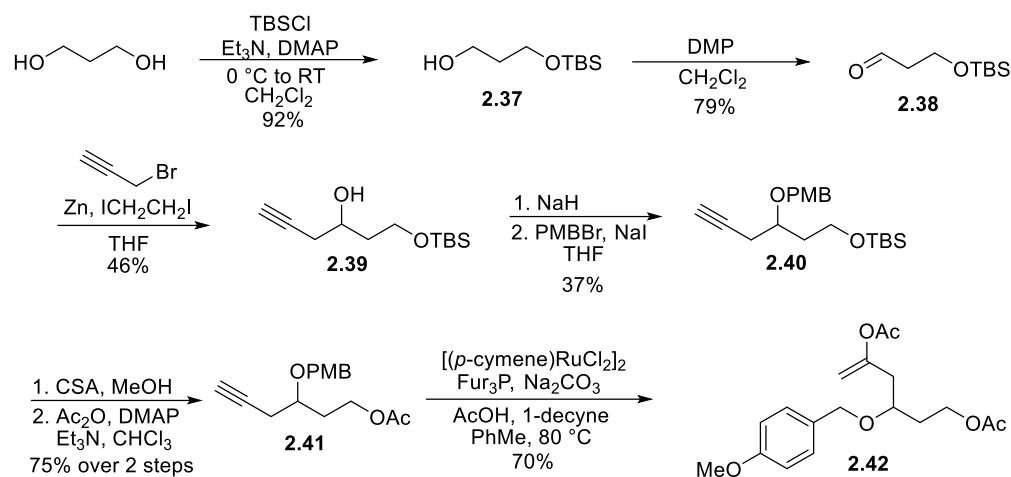


Figure 9. Catalytic Cycle of Optimized Reaction Conditions

2.2.4 Effect of Driving Force on Catalyst Turnover

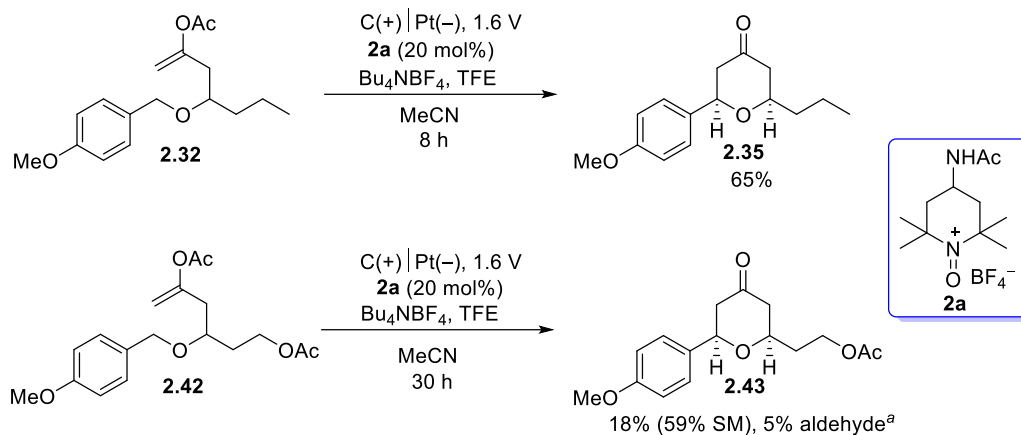
As a result of the successful cyclization of compound **2.32** to **2.35**, initial efforts to expand the substrate scope began by incorporating a terminal acetoxy group on the propyl chain (Scheme 51). This strategically introduced heteroatom functionality to the substrate while mimicking the 1,3-diol relationship commonly seen in polyketide based natural products. The synthetic route began with a silyl ether protection of 1,3-propanediol to give **2.37** (Scheme 51). The primary alcohol was oxidized to the corresponding aldehyde followed by a Barbier reaction with propargyl bromide to give homopropargylic alcohol **2.39** in 46% yield.⁹³ The *p*-methoxybenzyl ether was installed in 37% yield, followed by deprotection of the silyl group and acetylation of the resulting primary alcohol gave acetate **2.41** in 75% yield over two steps. Lastly, Ru-catalyzed Markovnikov addition of acetic acid into the alkyne led to substrate **2.42** in 70% yield.^{92, 94, 95} The acetoxy group was used in **2.42** rather than the silyl ether protecting group because of its ability to help dampen the nucleophilicity of the oxygen. Although nucleophilic attack of the oxocarbenium by the silyl ether has not been observed with this system as shown in section **2.1.1.1**, the use of the acetate

removes this possibility, and also introduces an alternative protecting group strategy for total synthesis applications.



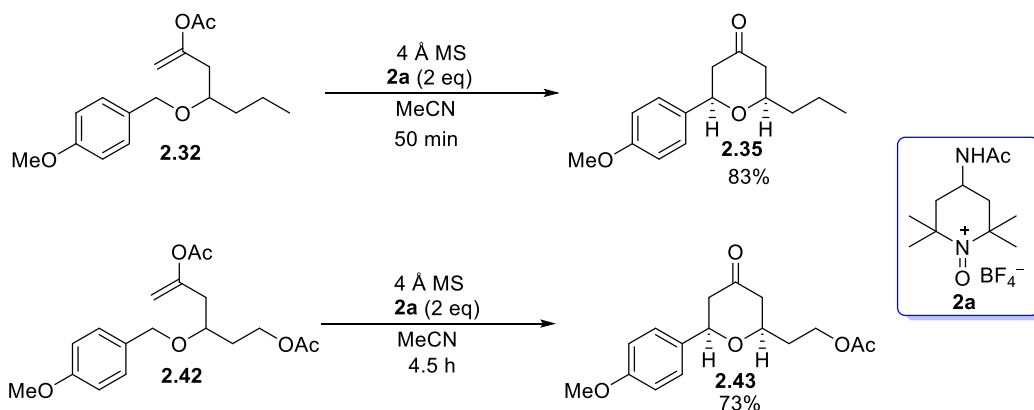
Scheme 51. Synthesis of 2.42

When **2.42** was subjected to the optimized conditions, the reaction proceeded extremely slowly with very little current flowing in the electrochemical cell, yielding 18% of **2.43** and 5% of anisaldehyde with 59% of **2.42** recovered (Scheme 52). Since the rate-determining step of these reactions is hydride abstraction, it was postulated that the remote acetoxy group inductively withdrew electron density from the ether linkage, resulting in the destabilization of the intermediate oxocarbenium ion.⁹² This made it more difficult for the benzyl ether to undergo hydride abstraction resulting in slower reactions with Bobbitt's salt (**2a**). The slower rate of reaction reduces the steady-state concentration of hydroxylamine at the anode, causing less current to flow in the electrochemical cell and limiting the turnover of oxidant. Therefore with the goal being to expand these to substrates with varying degrees of cation stability, this could be problematic.



Scheme 52. Comparing 2.32 to 2.42 under Optimized Conditions

To determine if the rate of hydride abstraction was the cause of the diminished reactivity, **2.32** and **2.42** were both subjected to 2 equivalents of Bobbitt's salt (**2a**) and were monitored until starting material was fully consumed. It was observed that **2.32** was fully consumed to give **2.35** in 83% yield within 50 minutes (Scheme 53).⁹² However, **2.42** took 4.5 hours to proceed to completion, giving **2.43** in 73% yield. Since **2.42** took almost five times longer to consume starting material, it was clear that remote effects of the acetoxymethyl group played a significant role in the rate of hydride abstraction.



Scheme 53. Stoichiometric Experiments of 2.32 and 2.42

To gain further information on the effects of remote substitutions on hydride abstraction, simplified benzyl ethers, **2.32-A** and **2.42-A** were synthesized and kinetic studies on the oxidations of each were conducted (Figures 10 and 11).⁹² Using UV-Vis spectroscopy, pseudo-first order kinetic experiments were conducted with respect to the oxidant, as the substrate concentration was considered negligible due to its abundance. The experiments were conducted by subjecting one equivalent of Bobbitt's Salt (**2a**) to 10 equivalents of each substrate separately and the relationship of the observed consumption of oxidant over time was plotted. The slope of the natural log of this relationship gave the observed rate constant. From this, the rate constant (*k*) was calculated with respect to the concentration of the substrate (Equation 2):

$$k = -\frac{k_{obs}}{[Substrate]}$$

Equation 2. Rate Constant with Respect to Observed Rate Constant and Concentration

The calculated rate constant was then substituted into the Eyring equation (Equation 3) to determine the Gibbs free energy of the transition state for the oxidation of each compound to its corresponding reaction intermediate.

$$\Delta G^\ddagger = -RT \ln \left(\frac{kh}{k_B T} \right)$$

Equation 3. Eyring Equation to Determine Gibbs Free Energy of Activation

From the kinetic studies, it was determined that **2.42-A** ($\Delta G^\ddagger = 19.9$ kcal/mol) (Figure 11) had a transition state free energy 0.7 kcal/mol higher than the transition state free energy of **2.32-A** ($\Delta G^\ddagger = 19.2$ kcal/mol) (Figure 10). This supported the greater than 70% reduction in reaction rate observed when **2.42** was subjected to the electrochemical conditions.⁹²

In Stahl's alcohol oxidations, he demonstrated that the turnover rate of the catalyst can be increased when the driving force for oxidation increases.⁸¹ In other words, the stronger the oxidant,

the faster the substrate can be consumed, increasing the overall rate of the reaction. This led us to explore the use of the stronger oxidant, Oxo-TEMPO⁺BF₄⁻ (**2d**) as an alternative.

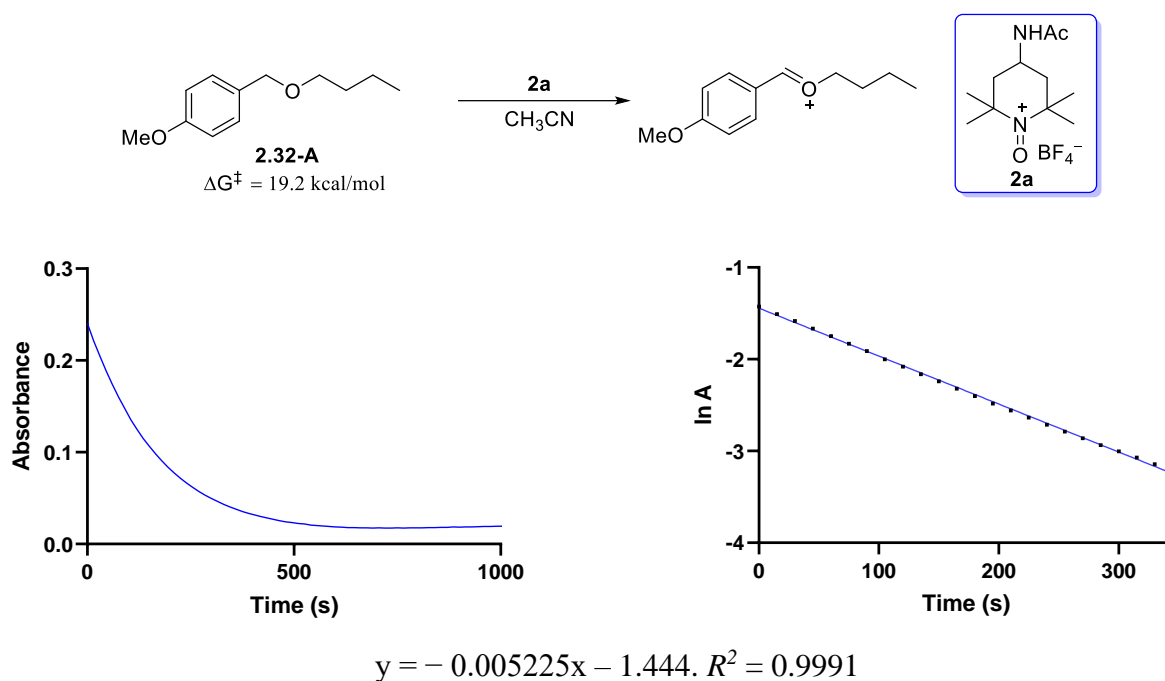


Figure 10. UV-Vis Kinetic Analysis of the Oxidation of 2.32-A

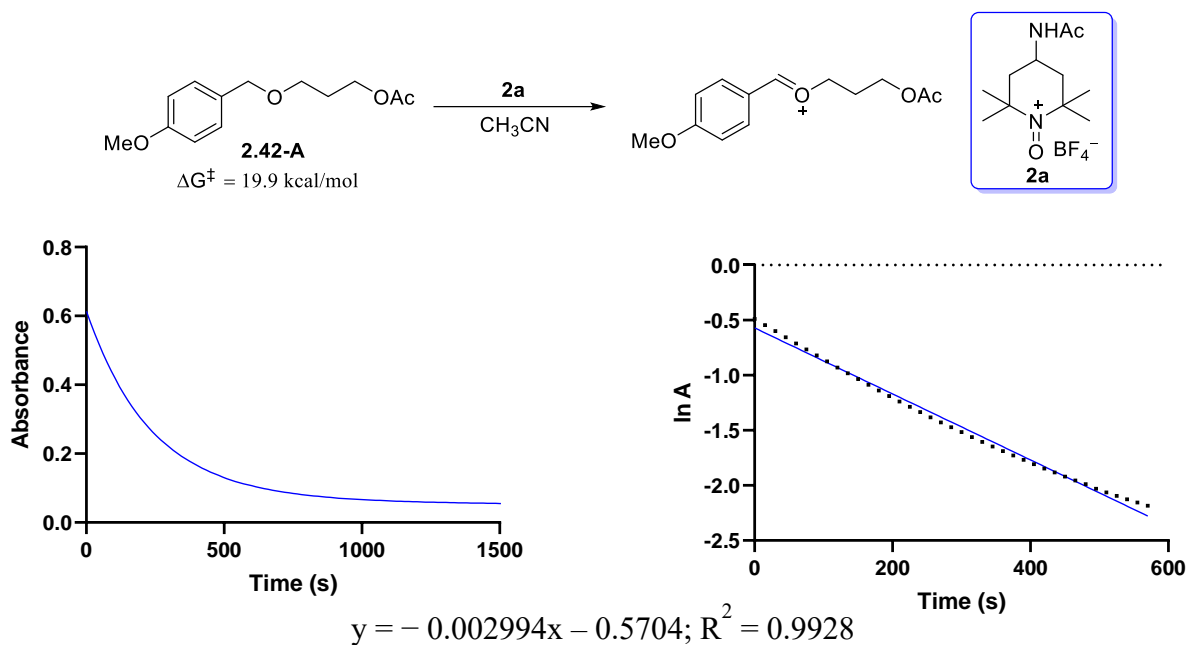


Figure 11. UV-Vis Kinetic Analysis of the Oxidation of 2.42-A

To determine whether Oxo-TEMPO⁺BF₄[−] (**2d**) was effective in increasing the driving force, the kinetic study was repeated substituting Bobbitt's salt (**2a**) with **2d** (Figure 12). These results were encouraging as it showed that the transition state free energy for the hydride abstraction of **2.42-A** with **2d** was lowered by 0.9 kcal/mol (19.0 kcal/mol).

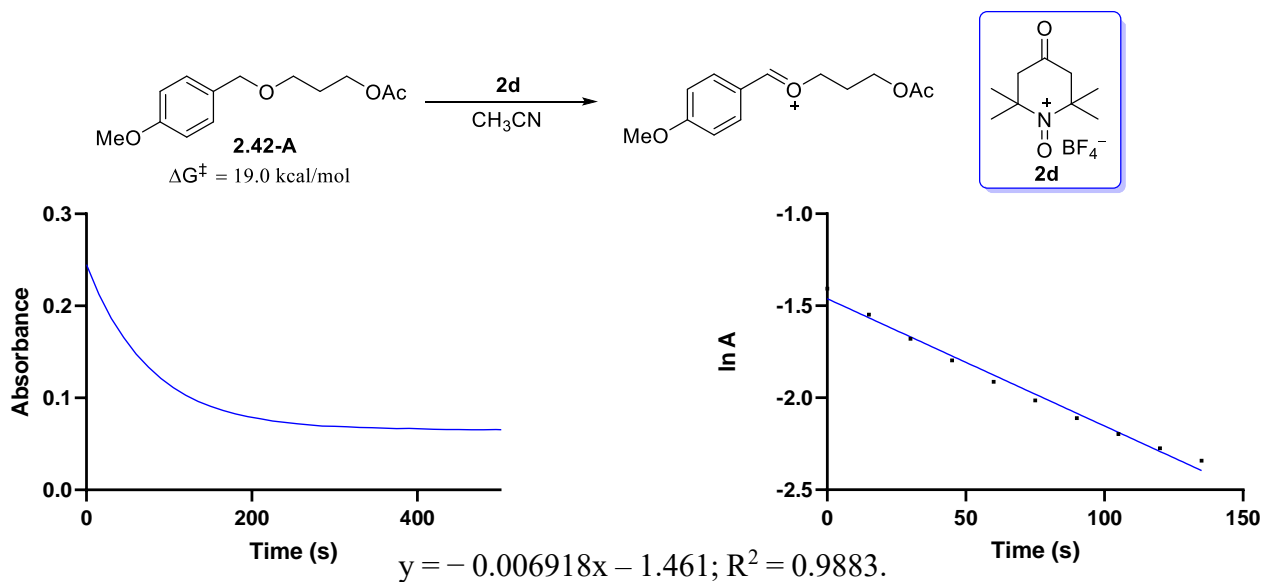
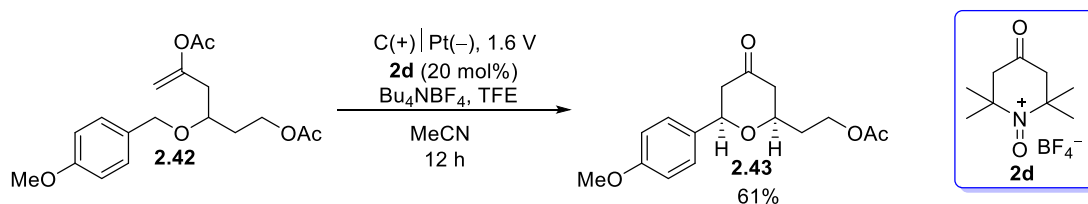


Figure 12. UV-Vis Kinetic Study of 2.42-A with Oxo-TEMPO⁺BF₄[−]

Therefore, **2.42** was subjected to the optimized electrochemical conditions substituting the oxidant for 20 mol% Oxo-TEMPO⁺BF₄⁻ (**2d**). This resulted in a significant increase in reaction rate and maintained current flow in the electrochemical cell, leading to the successful electrochemical regeneration of the oxidant. This led to full consumption of **2.42** within 12 hours to afford **2.43** in 61% yield (Scheme 54). From this result, it was concluded that increasing the driving force for oxidation increased the rate of consumption of **2.42** and in turn resulted in a greater concentration of reduced hydroxylamine in the electrochemical cell. Increasing the steady-state concentration of hydroxylamine helped current flow within the cell as there was sufficient hydroxylamine for the anode to oxidize, effectively turning over of catalyst. Although the oxidation potential of **2d** (0.87 V vs 0.01M Ag/AgNO₃) was higher than **2a** (0.79 V vs 0.01M Ag/AgNO₃), which made it more difficult to oxidize, conducting the reactions at 1.6 V was sufficient to oxidize the hydroxylamine of **2d**.

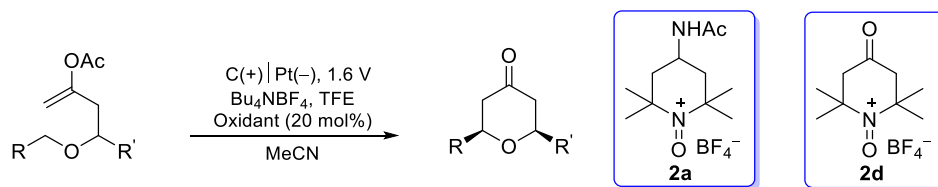


Scheme 54. Electrocatalytic Oxidation of 2.42 with Oxo-TEMPO⁺ (2d**)**

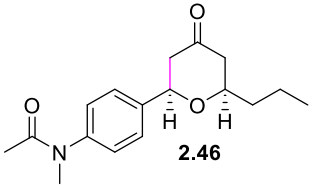
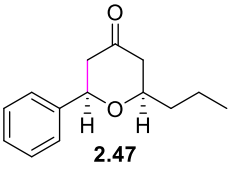
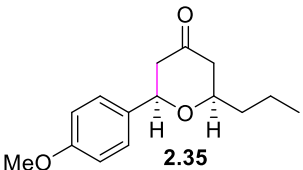
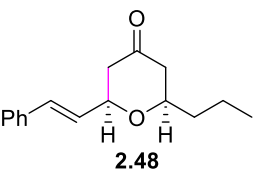
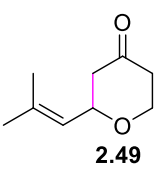
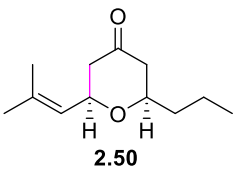
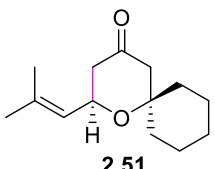
This significant result demonstrated the ability to conduct electrocatalytic oxidative C–H functionalization on even slower reacting substrates. Traditionally, only one catalyst is designed for an entire scope due to the specificity of electrochemically-driven redox reactions. However, the successful oxidation of **2.42** by **2d** can broadly expand the substrate scope and functional group compatibility of the method, signifying that the oxidant of choice can be tuned to the reactivity of the substrate.

2.2.5 Enol Acetate Substrate Scope for Electrocatalytic Oxidative C–H Functionalization

The successful oxidation of **2.32** using Bobbitt's Salt (**2a**) and **2.42** using Oxo-TEMPO⁺BF₄[−] (**2d**) demonstrated that a variety of benzyl and allyl ethers could be compatible with the method. The scope of benzylic and allylic ethers were chosen based on the stability of their cationic intermediates, each were first subjected to a stoichiometric amount of **2a** and monitored until starting material was fully consumed. The time in which it took for the reactions to complete was used as a guide to determine the oxidant that would be used for the respective substrate's electrochemical reaction. If the stoichiometric reaction was completed within 2 hours, **2a** was used as the electrochemical oxidant. Any reaction that took longer than 2 hours, required the use of **2d** as the electrochemical oxidant. The duration of reactions using stoichiometric **2a** along with the electrocatalytic results are illustrated in Table 6.



Entry	Product	Time [h] (2 eq, 2a)	Oxidant, time (h)	Yield %
1	 2.44	1	2a , 10	61
2 ^a	 2.45	3	2d , 12	68

3 ^b	 2.46	24	2d, 30	54
4 ^c	 2.47	23	2d, 30	73
5 ^b	 2.35	50 min	ACT, 16	70 (23% hydrolysis)
6	 2.48	45 min	2a, 10	58
7	 2.49	25 min	2a, 6.5	58 (31% hydrolysis)
8	 2.50	25 min	2a, 8	67
9	 2.51	0.5	2a, 6	70

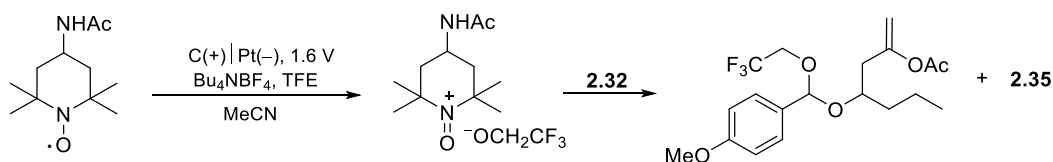
10	 2.52	2	2a, 13	71
11	 2.53	4.5	2d, 10	75

Table 6. Enol Acetate Substrate Scope

^a Conducted at 1.7 V, ^bNMR yield vs 2,5-dibromo-1-nitrobenzene, ^c30 mol% oxidant.

A wide range of substrates were examined. Silyloxy-substituted benzyl ethers were attempted as a means of having similar reactivity to a *p*-methoxybenzyl ether but could be more easily deprotected in a synthetic sequence. The silyloxy-substituted benzyl ether was compatible under the electrochemical conditions with no observation of quinone methide formation, yielding **2.44** in 61% (Entry 1). To continue with electron-rich arenes, **2.35** could also be synthesized using the nitroxyl radical, ACT, as the mediator rather than the pre-oxidized oxoammonium ion. This involved *in situ* oxidation at the anode prior to addition of the substrate as the radical can react with nucleophilic functional groups. These reactions had much greater mass recovery as **2.35** was isolated in 70% yield and 23% hydrolysis to anisaldehyde observed (Entry 5). This increase in hydrolysis compared to prior reactions was attributed to the excess generation of trifluoroethoxide at the cathode prior to addition of the substrate. It was believed that this behaved as a competitive nucleophile, adding into the oxocarbenium ion to form an unstable mixed acetal which broke down into anisaldehyde (Scheme 55). Efforts to mitigate this issue included addition of catalytic

quantities of HBF₄, but this only led to significant substrate decomposition due to the super-acidic nature of HBF₄.



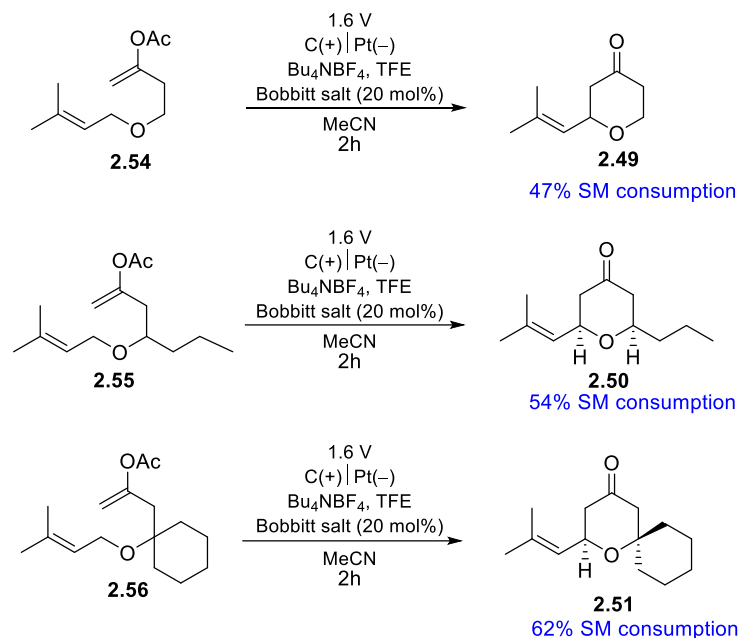
Scheme 55. Postulated Formation of Unstable Mixed Acetal

Moving to less reactive arenes, the need for Oxo-TEMPO⁺BF₄⁻ (**2d**) became necessary as seen with Entries 2 to 4. Although methyl groups act as electron-donating groups, its inductive donation did not contribute much to the stability of the resulting oxocarbenium ion, as seen from the stoichiometric experiment (Entry 2). Therefore using **2d** as the electrochemical oxidant, the reaction was conducted at 1.7 V (vs 0.01M Ag/AgNO₃) and still cleanly yielded **2.45** in 68%. The limits of the methodology were reached with Entries 3 and 4.

Understanding that tertiary amines have low oxidation potentials, *N*-methylacetamidobenzyl ether was used instead to prevent off-site oxidation and was believed to have similar inductive properties to a methyl group (Entry 3). Yet based on its slow reactivity, it seemed to behave like an electron withdrawing group, possibly due to the electrons from the amide nitrogen flowing towards the carbonyl rather than the arene. This carbonyl species was hypothesized to be twisted out of planarity with the arene due to electronic destabilization by the aromatic ring and possible minimization of steric interactions between the aromatic ring and the carbonyl. This is commonly seen in anilides as mentioned by Liu and coworkers.¹⁰² Therefore the electron flow from the nitrogen is moving towards the carbonyl of the amide instead of towards the benzylic position, resulting in the nitrogen acting as an inductive withdrawing group, in accord with its electronegativity, destabilizing the benzylic ether. Even under these circumstances, within

30 hours, **2.46** was synthesized in 54% yield and only 16% of the starting material remained (Entry 3). Similar reactivity was seen with benzyl ether **2.47**, synthesized in 69% yield with 13% hydrolysis and 16% starting material after 30 hours. To remedy the incomplete consumption of starting material, 10 mol% more of **2d** was added to the reaction (30 mol% total oxidant) as the current began to decline, and full consumption of starting material was observed after 30 hours giving **2.47** in 73% isolated yield (Entry 4).

Allylic ether oxidations proceeded just as effectively as most electron-rich arenes, all reacting electrochemically with Bobbitt's salt (**2a**) (Entries 6-10). Cinnamyl ethers demonstrated similar reactivity to PMB-ethers as **2.48** was formed in 58% yield in 10 hours (Entry 6). As expected, the prenyl ether stabilized the cationic intermediate well through inductive donation by the allylic methyl group, but slight remote substituent effects were observed in Entries 7-9, with 9 being the fastest. Although one would anticipate that the Thorpe-Ingold Effect plays a role, it is not the case as the Thorpe-Ingold Effect promotes the rate of cyclization, while the rate determining step of this reaction is hydride abstraction. To take a closer look at these remote effects, the consumption of starting material for each substrate after 2 hours was analyzed by crude NMR (Scheme 56). From the data collected, it was determined that **2.54** was the slowest to react with 47% consumption at 2 hours, and **2.56** was the fastest with 62% consumption at 2 hours, but the overall difference between them was quite small. The reason for the increase in the rate of reactivity was elusive, but it was postulated to be remote inductions that increased the electron density around the allylic C-H bond which led to faster rates of hydride abstraction.



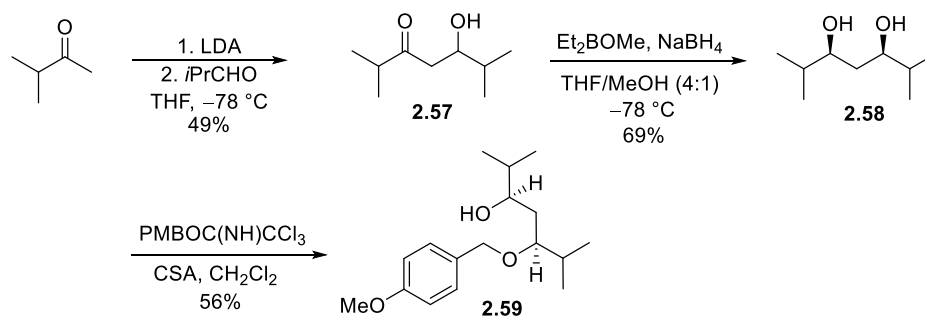
Scheme 56. Remote Substituent Effects in Rate of C–H Oxidation

Incorporation of a vinyl silane onto the alkene proved that steric effects at the site of oxidation was inconsequential to the rate of hydride abstraction as **2a** was used to synthesize **2.52** in 71% yield in 13 hours (Entry 10). This substrate was also significant as it proved that vinyl silanes, although electron-rich olefins, were tolerated under electrochemical conditions and could be used as a handle for functionalization of the alkene via cross-coupling. Allylic carbamates were also suitable substrates for the electrochemical conditions, although they were less reactive and required **2d** to proceed to completion. Upon subjection to the optimized conditions this resulted in **2.53** in 75% isolated yield (Entry 11).

2.2.6 Alcohol Nucleophiles in Electrocatalytic Oxidations of Benzyl Ethers

In order to further expand the substrate scope, other nucleophiles were investigated to trap the oxocarbenium ions generated in these reactions. Amines unfortunately oxidize too easily and

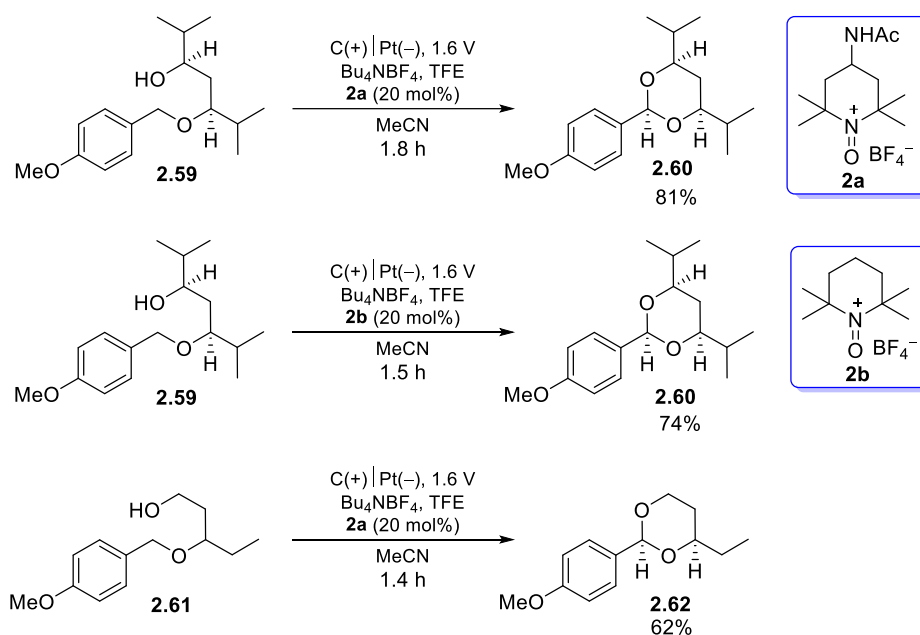
may undergo single electron transfer at the anode more easily under the developed conditions. This led us to look into alcohols as nucleophiles. Alcohol oxidations have two different mechanisms of oxidation under neutral pH vs basic pH as described in section 2.1.2 (Figure 3) proposed by Bailey and Wiberg.⁷³ Therefore, this led us to question whether selective oxidation of the benzyl ether can be controlled over the oxidation of the alcohol under the optimized electrochemical conditions. To do so, 3-methyl-2-butanone underwent an aldol reaction into isobutyraldehyde to give β -hydroxyketone **2.57** (Scheme 57). A *syn*-selective Narasaka-Prasad reduction using diethylmethoxyborane and sodium borohydride gave **2.58** in 69% yield.¹⁰³ Lastly using the *p*-methoxybenzyl acetimidate as an electrophile, *p*-methoxybenzyl ether **2.59** was synthesized in 56% yield.



Scheme 57. Synthesis of Benzyl Ether with Pendent Nucleophilic Alcohol

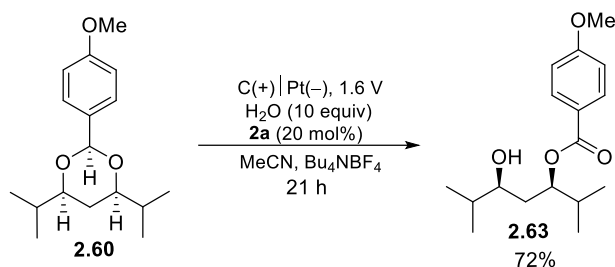
Once **2.59** was subjected to the electrochemical conditions, it underwent rapid cyclization to benzylidene acetal **2.60** in 81% yield within 1.8 hours, with no observation of alcohol oxidation (Scheme 58). The significant increase in reactivity was a shock, but indicated that the free alcohol played a significant role in the increased rate of reactivity. It was postulated that the pendent alcohol not only acted as a nucleophile, but its lone pairs donated electron density into the σ^* orbital of the benzylic C–H. This further stabilized the transition state, increasing the rate of hydride abstraction with Bobbitt's salt (**2a**). This substrate was so reactive that even the less

reactive oxidant $\text{TEMPO}^+\text{BF}_4^-$ (**2b**) could be used and efficiently undergo electrochemical regeneration to give **2.60** in 74% yield within 1.5 hours (Scheme 58). Understanding that secondary alcohols were successful, expanding the method to primary alcohols seemed worthwhile, as they are better nucleophiles, but could be more susceptible to oxidation. Surprisingly, upon subjection of **2.61** to the electrochemical conditions, **2.62** was synthesized in 62% yield with the only byproduct being hydrolysis to anisaldehyde in 29% yield. No alcohol oxidation to the corresponding aldehyde was observed.



Scheme 58. Electrocatalytic Oxidation of Benzyl Ethers with Pendent Alcohol Nucleophiles

In the initial oxidation of **2.59** with Bobbitt's salt, a byproduct that was observed was a second oxidation of **2.60** to the corresponding benzoate. This was a surprising outcome, as over oxidation was not observed in any of the pyranones synthesized and sparked great interest. Therefore to push the reaction to where this would be the outcome, **2.60** was resubjected to the electrochemical conditions substituting 3 equivalents of TFE for 10 equivalents of water. After 21 hours, this efficiently yielded **2.63** in 72% isolated yield (Scheme 59).



Scheme 59. Electrochemical Oxidation of Benzylidene Acetals to the Corresponding Benzoate

Alcohol nucleophiles and enol acetate nucleophiles showed large differences in total charge transfer within the reactions. The charge transfer for the slowest cyclization to give **2.47** was 21.4 F/mol whereas, in the cyclization to give **2.59**, it was significantly lower as only 1.91 F/mol was passed.⁹² Charge transfer refers to the total amount of charge (F) required to complete a transformation per mole of substrate. When determining the amount of charge transfer required in a reaction, this can be simplified to a net 2e⁻ process that requires 2 F/mol of charge to be passed. Therefore, with 20 mol% oxidant being supplied in these reactions, the minimum amount of charge that was required for these reactions was 1.6 F/mol.

Based on the total charge transfer for each reaction (Appendix B), the data illustrated that faster oxidations were significantly more efficient and resulted in more effective charge transfer, possibly due to the saturation of hydroxylamine concentration at the anode. Although the slower, less efficient oxidations displayed a constant current flowing in the reaction, this could be attributed to unaccountable redox events occurring with the oxidant at the cathode. These undesired redox events could lead to catalyst degradation over time, slowing down the reaction further. Unfortunately, these are limitations of an undivided cell. This can be circumvented through the use of a divided cell, however, to mitigate this issue in the interim, higher catalyst loadings can be beneficial when less reactive substrates are used.

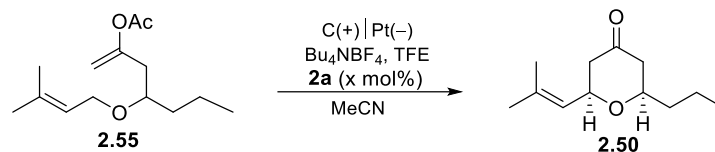
2.2.7 Effects of Concentration on Reaction Efficiency

After analyzing a diverse substrate scope, it was equally important to investigate these reactions on a 1 mmol scale to determine the practicality of the method on larger scales. Previously, the optimized conditions in Table 6 were conducted at 0.067 M. This was necessary in order for sufficient exposure of the electrodes in the electrochemical cell. However, when conducted at 1 mmol scale, apparatus constraints led to the experiments being run at 0.1 M. For this study the substrate that was examined was **2.50**. When **2.55** was subjected to the developed conditions at 0.067M this led to a 67% yield of **2.50** in 8 hours (Table 7, Entry 1). Similarly when the reaction was repeated at a 1 mmol scale with identical reaction conditions at 0.1 M concentration this afforded **2.50** in 64% isolated yield in 10 hours. (Table 7, Entry 2). Unexpectedly, the current in the electrochemical cell was significantly higher than previously observed, which indicated that substrate was being consumed at a faster rate, increasing the concentration of hydroxylamine at the anode. When examining the bimolecular rate equation, the rate of the reaction is dependent on the concentrations of the reactants (Equation 4). Therefore, as the concentration increases, the rate of the reaction should increase, resulting in higher currents flowing in the electrochemical cell.

$$Rate = k [A][B]$$

Equation 4. Bimolecular Rate Equation

Having higher currents flowing in the cell led us to study the effects of concentration and its role on reaction efficiency and catalyst loading (Table 7).



Entry	[2.55] (M)	2a (mol%)	Potential (V)	Yield (%)	2.55 Recovered (%)	Charge Transfer (F/mol)
1 ^a	0.067	20	1.6	67	-	4.42
2 ^a	0.10	20	1.6	64	-	3.10
3 ^a	0.10	10	1.6	63	-	3.31
4 ^b	0.20	5	1.6	27	61	1.12
5 ^b	0.20	20	1.4	59	30	2.12
6 ^b	0.10	20	1.4	56	28	2.15
7 ^b	0.067	20	1.4	38	54	1.08

Table 7. Effects of Concentration on Reaction Efficiency

^a Isolated Yields, ^b NMR Yield vs 2,5-dibromonitrobenzene.

With the current density much greater in the reactions at higher concentration, the catalyst loading was lowered to determine if current can flow as efficiently and the reaction could proceed to completion. The catalyst loading was decreased to 10 mol% which increased the length of time for the reaction, but full consumption of starting material was observed in 16 hours to give **2.50** in 63% yield (Table 7, Entry 3). Seeing that the catalyst concentration could be halved at 0.1 M, this was halved again to 5 mol% catalyst loading at 0.2 M was attempted, but this led to only 27% of **2.50** with 61% of **2.55** recovered (Table 7, Entry 4). Although the reaction couldn't proceed to completion, there were five successful turnovers of oxidant before current diminished, which was

more than the total of 4 turnovers required with 20 mol% Bobbitt's salt, indicating that concentration increased the efficiency and ability to turnover oxidant.

Increasing the concentration of the reaction lowered the amount of oxidant necessary for the reactions to proceed to completion. This phenomenon led us to question whether the overpotential applied in the reactions could follow a similar trend. The overpotential applied in the reactions at 0.067 M was necessary under those conditions to drive the reaction to completion, but at higher concentrations, this may not be the case. To test this hypothesis, the potential was lowered to 1.4 V at both 0.2 M and 0.1 M (Table 7, Entries 5 and 6), giving 59% and 56% of **2.50** with 30% and 28% of **2.55** recovered respectively. Both experiments failed to undergo full consumption of starting material before the current diminished, yet the cleanliness and mass recovery of the reaction was significantly higher, as majority of the unreacted starting material remained. This was still a significant improvement compared to 0.067M at 1.4 V only yielding 38% of **2.50** before current diminished (Table 7, Entry 7). Although the reactions at 1.4 V failed to proceed to completion, the increase in concentration resulted in further starting material consumption and displayed slightly diminished yields compared to Entries 1-3. Therefore, in terms of practicality in scale up, if greater mass recovery was preferred, lower voltages can be applied, whereas if full consumption of starting material was desired, 1.6 V can be applied.

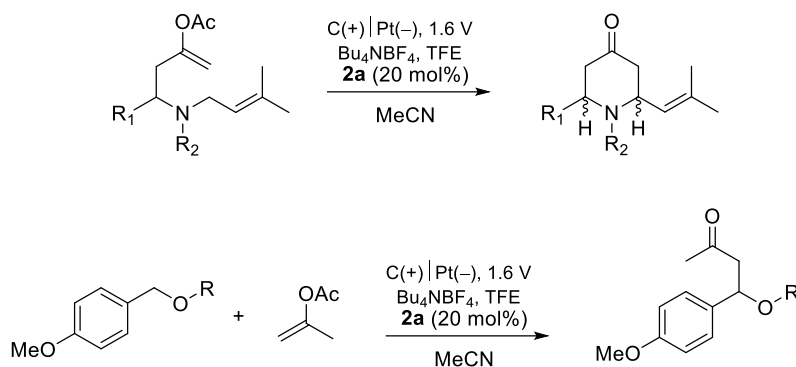
Increasing concentration demonstrated similar charge transfer effects as those seen with the alcohol nucleophiles. The charge transfer required in the formation of **2.50** at 0.067M was 4.42 F/mol whereas at 0.1 M it was 3.1 F/mol. This increase in concentration could lead to greater mass transport to the electrode surface leading to an increased concentration of hydroxylamine at the anode. Therefore, the improvement in overall charge transfer in reactions at higher concentrations showcase an increase in reaction efficiency.⁹²

2.3 Conclusions and Future Directions

An efficient and multi-applicational method was developed towards the electrochemical regeneration of oxoammonium ions under anhydrous conditions for oxidative C–H functionalization. Allylic and benzylic ethers underwent hydride abstraction to generate an oxocarbenium ion intermediate which was then captured by pendent enol acetate or alcohol nucleophiles to form new C–C and C–O bonds respectively using a catalytic amount of oxidant. These reactions were conducted under constant potential, which increased reaction times, but eliminated product decomposition at higher voltages and ensured that the catalytic oxidant was the sole species undergoing redox events. Although the potential applied was much larger than the oxidation potential of the oxidant, this overpotential was necessary to increase the rate of catalyst turnover and maintain ample currents during the reaction. This was significant as it demonstrated a more atom economical and environmentally benign route to oxygen- and nitrogen- containing heterocycles.

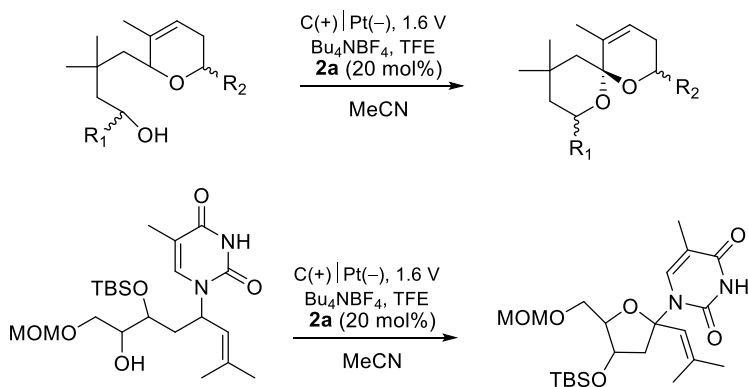
The rates of these hydride abstractions were dictated by the stability of the cations derived from the benzylic or allylic ethers, with slower hydride abstractions requiring a stronger oxidant for efficient turnover. An increase in reaction rate was also observed upon increasing the concentration of the reactions, leading to lower catalyst loadings. These reactions can also be run at lower potentials with similar yields, but starting material will fail to be consumed before current diminishes. Therefore, increasing the concentration demonstrated an increase in the rate of reactions which led to improved reaction efficiency, supported by the lower degree of charge transfer necessary to push the reaction to completion.

This methodology provided a basis for understanding the electrocatalysis of slow hydride abstractions and can be applied to more complex reactions that mimic this redox activity such as the synthesis of piperidine analogs and in bimolecular reactions using external nucleophiles (Scheme 60).



Scheme 60. Exploring Enol Acetate Nucleophile Possibilities

A number of C–C, C–O, and C–N bond-forming reactions could also be explored especially focusing on the increased reactivity of pendent alcohol nucleophiles that were observed in the formation of the benzylidene acetals. These could be used as a means of synthesizing spiroketals which are common moieties in natural products^{62, 104} as well as unnatural nucleoside analogs that contain quaternary centers (Scheme 61).



Scheme 61. Exploring Alcohol Nucleophile Possibilities

Although stoichiometric methods have already been developed for some of these reactions,^{66, 68, 85} using electrocatalysis would provide a more environmentally friendly and inexpensive route to these types of products, especially on the production scale.

Appendix A

Supporting Information: Dehydrative Re_2O_7 -Catalyzed Approach to Dihydropyran

Synthesis

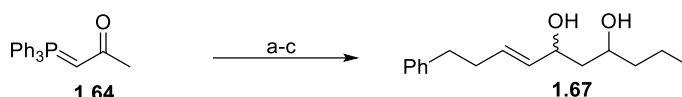
(^1H NMR) and carbon (^{13}C NMR) nuclear magnetic resonance spectra were taken on a Bruker Avance 300 spectrometer at 300 MHz and 75 MHz respectively, a Bruker Avance 400 spectrometer at 400 MHz and 100 MHz, a Bruker Avance 500 spectrometer at 500 MHz and 125 MHz, or a Bruker Avance 600 spectrometer at 600 MHz and 150 MHz as specified. The chemical shifts are reported in parts per million (ppm) on the delta (δ) scale. The solvent peak was used as a reference value, for ^1H NMR: CDCl_3 = 7.26 ppm, C_6D_6 = 7.16 ppm or $\text{C}_3\text{D}_6\text{O}$ = 2.05 ppm, for ^{13}C NMR: CDCl_3 = 77.16 ppm, C_6D_6 = 128.06 ppm or $\text{C}_3\text{D}_6\text{O}$ = 29.84 ppm and 206.26 ppm. Data are reported as follows: m = multiplet, s = singlet; d = doublet; t = triplet; dd = doublet of doublets; dt = doublet of triplets; ddq = doublet of doublet of quartets; ddd = doublet of doublet of doublets etc. Infrared (IR) spectra were taken on a Nicolet IR200 FT-IR spectrometer with an ATR attachment. Methylene chloride was distilled under N_2 from CaH_2 . Diethyl Ether and tetrahydrofuran were distilled over sodium/benzophenone under N_2 . Hexafluoroisopropanol (HFIP) was purchased from Oakwood Chemicals and distilled over 3\AA molecular sieves and stored in a desiccator. Analytical TLC was performed on E. Merck pre-coated (25 mm) silica gel 60 F254 plates. Visualization was done under UV (254 nm) or by staining by staining (95mL ethanol, 3mL conc. H_2SO_4 , 2mL acetic acid, 5mL anisaldehyde). Flash chromatography was done using SiliCycle SiliaFlash P60 40-63 μm 60 \AA silica gel. Reagent grade ethyl acetate, diethyl ether, dichloromethane, methanol, and hexanes (commercial mixture) were purchased from Fisher

Scientific and were used as-is for chromatography. All reactions were performed in flame-dried glassware under a positive pressure of either Ar or N₂ with magnetic stirring unless noted otherwise. All reagents were purified according to “Purification of Laboratory Chemicals Sixth edition”. Re₂O₇•SiO₂ was prepared according to a literature protocol.³³

General cyclization protocol

To a solvent mixture of a 9:1 ratio of HFIP:MeNO₂ (0.10 M) in a flame dried 1 dram vile (Chemglass CG-4904-05 with a polypropylene screw cap containing a PTFE faced silicone septum) was added the corresponding diol. Re₂O₇ (9.1%, w/w, on SiO₂, 0.05 eq) was added to the mixture and the reaction was run at ambient temperature and monitored by TLC until starting material was consumed. The reaction mixture was then diluted with dichloromethane and filtered through a short silica pipet column (approx. 2 cm). The column was flushed 3x with EtOAc and then the crude mixture was isolated under reduced pressure. The mixture was purified by flash column chromatography. Diastereomeric ratios were determined by crude ¹H NMR analysis. Further purification was done for product characterization if necessary.

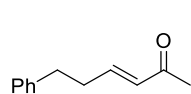
Experimental Protocols



Reagents and conditions

a) **1.64**, Ph(CH₂)₂CHO CH₂Cl₂, 78%. b) LDA, THF, -78 °C (ii) *n*-PrCHO, -78 °C, 55%
c) NaBH₄, MeOH, 0 °C, 92%.

Scheme 62. Synthesis of Compound 1.67



(*E*)-6-Phenylhex-3-en-2-one (**1.65**)

Compound **1.64** (3.9 g, 12.2 mmol) was added to a flame dried round bottom flask then was dissolved in CH₂Cl₂ (20 mL, 0.5 M) and cooled to 0 °C. Distilled 3-phenylpropionaldehyde (1.3 mL, 10.2 mmol) was added dropwise, and the reaction was stirred for

18 h. The crude mixture was isolated under reduced pressure, dry-loaded onto silica gel and purified by column chromatography (0 to 10% EtOAc in hexanes) to produce **1.65** as a colorless oil (1.38 g, 78%).

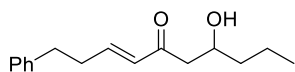
¹H NMR (300 MHz, CDCl₃) δ 7.33 – 7.27 (m, 2H), 7.25 – 7.15 (m, 3H), 6.82 (dt, *J* = 15.9, 6.8 Hz, 1H), 6.10 (dt, broad, *J* = 15.9, 1.5 Hz, 1H), 2.80 (t, *J* = 8.1 Hz, 2H), 2.59 – 2.51 (m, 2H), 2.23 (s, 3H).

¹³C NMR (75 MHz, CDCl₃) δ 198.7, 147.2, 140.8, 131.9, 128.7, 128.5, 126.4, 34.6, 34.2, 27.0.

IR (ATR, neat) 3027, 2927, 1672, 1627, 1497, 1453, 1427, 1359, 1253, 1186, 1088, 975, 746, 698 cm⁻¹.

HRMS (TOF MS ES⁺) *m/z* calcd. for C₁₂H₁₅O [M+H]⁺ 175.1123, found 175.1094.

(*E*)-7-Hydroxy-1-phenyldec-3-en-5-one (1.66)



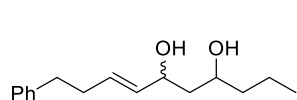
A flame dried round bottom flask was charged with anhydrous THF (32 mL, 0.25 M). Diisopropylamine was added and the mixture was cooled to –78 °C. A solution of n-BuLi (5.4 mL, 1.6 M, 8.69 mmol) was added dropwise and the reaction stirred for 15 min. Ketone **1.65** (1.37 g, 7.90 mmol), was then added dropwise and stirred for 30 min at the same temperature. Butyraldehyde (0.77 mL, 8.61 mmol) was then added dropwise and the reaction was monitored by TLC. The reaction mixture was quenched with saturated NH₄Cl at –78 °C, the organic layer was separated and the aqueous layer was extracted with Et₂O (3x). The ether fractions were combined and washed with brine, dried with MgSO₄, filtered and solvent was removed under reduced pressure. The crude mixture was then purified by flash column chromatography (10% EtOAc in hexanes to 20% EtOAc in hexanes), and **1.66** was isolated as a colorless oil (1.08 g, 55%).

¹H NMR (400 MHz, CDCl₃) δ 7.33 – 7.27 (m, 2H), 7.24 – 7.15 (m, 3H), 6.88 (dt, *J* = 15.9, 6.8 Hz, 1H), 6.11 (dt, *J* = 15.9, 1.4 Hz), 4.12 – 4.03 (m, 1H), 3.13 (d, *J* = 3.3 Hz, 1H), 2.80 (t, *J* = 7.7 Hz, 2H), 2.72 (dd, *J* = 17.3, 2.7 Hz, 1H), 2.60 (dd, *J* = 17.2, 8.9 Hz, 1H), 2.58 – 2.52 (m, 2H), 1.58 – 1.44 (m, 2H), 1.44 – 1.32 (m, 2H), 0.93 (t, 7.0 Hz, 3H).

¹³C NMR (100 MHz, CDCl₃) δ 201.2, 147.5, 140.7, 131.2, 128.7, 128.5, 126.4, 67.6, 46.3, 38.8, 34.5, 34.3, 18.8, 14.1.

IR (ATR, neat) 3445, 3028, 2930, 1659, 1626, 1496, 1453, 1290, 1182, 1124, 1071, 1014, 972, 901, 845, 745, 698 cm⁻¹.

HRMS (TOF MS ES⁺) *m/z* calcd. for C₁₆H₂₃O₂ [M+H]⁺ 247.1698, found 247.1689.



(*E*)-10-Phenyldec-7-ene-4,6-diol (1.67**)**

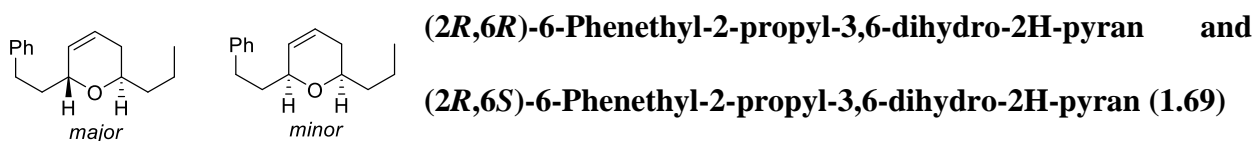
A solution of ketone **1.66** (0.200 g, 0.812 mmol) in methanol (18 mL, 0.045 M) was added to a flame dried round bottom flask. The solution was cooled to 0 °C, then NaBH₄ (61 mg, 1.62 mmol) was added and the reaction stirred for 1 h. The reaction mixture was quenched with brine, and extracted with EtOAc (3 x 15 mL). The combined organic layers were dried over MgSO₄, filtered, and concentrated under reduced pressure. The isolated crude mixture was purified by flash column chromatography (40% EtOAc in hexanes) to obtain **1.67** (0.185 g, 92%) as a colorless oil.

¹H NMR (400 MHz, CDCl₃) δ 7.31 – 7.25 (m, 2H), 7.21 – 7.14 (m, 3H), 5.77 – 5.66 (m, 1H), 5.59 – 5.45 (m, 1H), 4.39 (dt, *J* = 6.0, 6.0 Hz, 0.4H), 4.30 (dt, *J* = 7.2, 7.2 Hz, 0.6H), 3.90 – 3.79 (m, 1H), 2.87 (s, 0.6H), 2.75 – 2.67 (m, 2H), 2.42 (s, 0.4H), 2.36 (dt, *J* = 15.5, 7.8 Hz, 2H), 1.69 – 1.62 (m, 1H), 1.61 – 1.55 (m, 1H), 1.52 – 1.28 (m, 4H), 0.93 (t, *J* = 6.9 Hz, 3H).

^{13}C NMR (100 MHz, CDCl_3) δ 141.8, 141.7, 133.4, 133.3, 130.9, 130.7, 128.6, 128.6, 128.4, 126.0, 73.8, 72.2, 70.7, 69.1, 43.4, 42.7, 40.4, 39.8, 35.7, 35.6, 34.0, 34.0, 19.0, 18.7, 14.2, 14.2.

IR (ATR, neat) 3351, 3027, 2929, 2868, 1494, 1451, 1319, 1127, 1069, 1025, 971, 841, 745, 698 cm^{-1} .

HRMS (ESI) m/z calcd. for $\text{C}_{16}\text{H}_{24}\text{O}_2\text{Na}$ $[\text{M}+\text{Na}]^+$ 271.6685, found 271.1666.



The general cyclization procedure was followed with **1.67** (24.0 mg, 0.0966 mmol) in HFIP/ MeNO_2 (9:1, 0.97 mL, 0.1M). To this, $\text{Re}_2\text{O}_7 \cdot \text{SiO}_2$ (25.7 mg, 9.1%, 0.00483 mmol) was added and the reaction was stirred for 5 min. The mixture was diluted with CH_2Cl_2 and filtered through a short silica pipette column. The column was flushed with EtOAc (3x) and the solvent was removed under reduced pressure. The crude mixture was purified by flash column chromatography (5% Et_2O in hexanes to 10% Et_2O in hexanes) to afford **1.69** (15.8 mg, 71%, d.r. = 3.3:1) as a colorless oil.

***Trans*-isomer (slower eluting, major)**

^1H NMR (400 MHz, C_6D_6) δ 7.20 – 7.16 (m, 2H), 7.16 – 7.13 (m, 2H), 7.11 – 7.05 (m, 1H), 5.65 (dddd, J = 10.2, 5.1, 2.5, 2.5 Hz, 1H), 5.48 (ddt, J = 10.2, 4.1, 1.4 Hz, 1H), 4.14 – 4.08 (m, 1H), 3.56 (tt, J = 8.4, 4.2 Hz, 1H), 2.82 (ddd, J = 13.6, 9.8, 4.8 Hz, 1H), 2.64 (ddd, J = 13.6, 9.6, 7.2 Hz, 1H), 1.96 – 1.86 (m, 1H), 1.86 – 1.77 (m, 1H), 1.75 – 1.67 (m, 1H), 1.65 – 1.50 (m, 3H), 1.45 – 1.33 (m, 1H), 1.33 – 1.23 (m, 1H), 0.91 (t, J = 7.3 Hz, 3H).

^{13}C NMR (100 MHz, C_6D_6) δ 142.7, 130.4, 129.0, 128.7, 126.1, 124.3, 71.6, 67.1, 38.1, 36.1, 32.7, 31.3, 19.4, 14.4.

IR (ATR, neat) 3062, 3027, 2956, 2927, 2871, 1603, 1495, 1454, 1091, 1073, 747, 696 cm^{-1} .

HRMS (ESI) m/z calcd. for $\text{C}_{16}\text{H}_{23}\text{O}$ $[\text{M}+\text{H}]^+$ 231.1743, found 231.1749.

***Cis*-isomer (faster eluting, minor)**

^1H NMR (400 MHz, C_6D_6) δ 7.19 – 7.17 (m, 1H), 7.15 – 7.11 (m, 3H), 7.09 – 7.04 (m, 1H), 5.67 (dddd, $J = 10.0, 5.5, 2.2, 2.2$ Hz, 1H), 5.47 (ddt, $J = 10.1, 2.7, 1.3$ Hz, 1H), 4.08 – 4.01 (m, 1H), 3.41 (ddt, $J = 12.3, 4.7, 3.3$ Hz, 1H), 2.85 (ddd, $J = 13.7, 9.5, 5.4$ Hz, 1H), 2.79 (ddd, $J = 13.7, 9.2, 7.2$ Hz, 1H), 1.94 – 1.82 (m, 2H), 1.80 – 1.71 (m, 1H), 1.66 – 1.61 (m, 1H), 1.61 – 1.50 (m, 2H), 1.44 – 1.29 (m, 2H), 0.91 (t, $J = 7.2$ Hz, 3H).

^{13}C NMR (100 MHz, C_6D_6) δ 142.8, 130.9, 128.9, 126.0, 125.1, 74.0, 73.7, 38.7, 37.9, 31.9, 31.8, 19.2, 14.4.

IR (ATR, neat) 3062, 3026, 2955, 2926, 2870, 1603, 1496, 1454, 1318, 1094, 1081, 747, 698 cm^{-1} .

HRMS (ESI) m/z calcd. for $\text{C}_{16}\text{H}_{23}\text{O}$ $[\text{M}+\text{H}]^+$ 231.1743, found 231.1750.

24 h Reaction

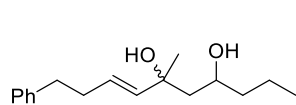
To **1.67** (18.9 mg, 0.0761 mmol) in HFIP/ MeNO_2 (9:1, 0.76 mL, 0.10 M) in a flame dried 1 dram vile (Chemglass CG-4904-05 with a polypropylene screw cap containing a PTFE faced silicone septum) was added HOREO_3 (0.58 μL , 76.5% solution in H_2O , 0.00381 mmol) using a calibrated μL pipette. The reaction stirred for 24 h, then was diluted with CH_2Cl_2 and filtered through a short silica pipette column. The column was flushed with EtOAc (3x) and the solvent was removed under reduced pressure. The crude mixture was purified by flash column chromatography (5% Et_2O in hexanes to 10% Et_2O in hexanes) to afford **1.69** (11.7 mg, 67%, d.r. = 4.2:1) as a colorless oil.

Mmol Scale Reaction

The general Re_2O_7 cyclization procedure was followed with **1.67** (0.285 g, 1.15 mmol) in HFIP: MeNO_2 (9:1, 11.5 mL, 0.1M). To this was added $\text{Re}_2\text{O}_7 \cdot \text{SiO}_2$ (0.278 g, 10%, 0.0574 mmol) and the reaction was stirred for 10 min. The mixture was diluted with CH_2Cl_2 and filtered through a silica pad in a fritted filter. The silica pad was flushed with EtOAc (3 x 10 mL), transferred to a round bottom flask, and the solvent was removed under reduced pressure. The crude mixture was purified by flash column chromatography (5% Et_2O in hexanes to 10% Et_2O in hexanes) to afford **1.69** (0.153 g, d.r. = 3.5:1, 58% yield) as a colorless oil.

$\text{BF}_3 \cdot \text{OEt}_2$ -Catalyzed Reaction

To CH_2Cl_2 solution (1.1 mL) in a flame-dried 1 dram vile (Chemglass CG-4904-05 with a polypropylene screw cap containing a PTFE faced silicone septum) was added compound **1.67** (16.7 mg, 0.0672 mmol) and $\text{BF}_3 \cdot \text{OEt}_2$ (0.83 μL , 0.0067 mmol) using a calibrated μL pipette. The reaction was stirred for 18 h, then the solvent was removed under reduced pressure. The crude mixture was purified by flash column chromatography (5% Et_2O in hexanes to 10% Et_2O in hexanes) to afford **1.69** along with an unknown impurity (1.8 mg, <12% yield, d.r. = 3.4:1, *trans:cis*) as a colorless oil.



(E)-6-Methyl-10-phenyldec-7-ene-4,6-diol (**1.68**)

To a flame dried round bottom flask was added LiBr (0.17 g, 1.97 mmol). The flask was purged with argon and a solution of ketone **1.66**, (0.32 g, 1.31 mmol) in THF (37 mL, 0.035M) was added. The mixture was cooled to -78°C and a solution of MeLi (1.2 mL, 1.6M, 2.0 mmol) was added dropwise and the reaction was stirred for 1 h. The reaction was quenched

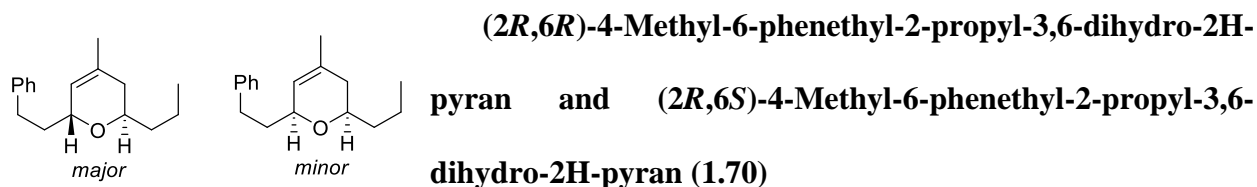
with NH_4Cl and the mixture was diluted with EtOAc. The organic layer separated, then the aqueous layer was further extracted with EtOAc (3 x 20 mL). The combined organic layers were washed with brine and dried over Na_2SO_4 , then solvent was removed under reduced pressure. Purification by flash column chromatography (30% EtOAc in hexanes) afforded **1.68** as a 1:1 mixture of diastereomers (0.109 g, 32%) as a colorless oil.

^1H NMR (500 MHz, CDCl_3) δ 7.31 – 7.25 (m, 2H), 7.21 – 7.15 (m, 3H), 5.72 (dt, $J = 15.5$, 6.8 Hz, 0.5H), 5.68 (dt, $J = 15.9$, 6.8 Hz, 0.5H), 5.56 (dt, $J = 15.6$, 1.2 Hz, 0.5H), 5.45 (dt, $J = 15.5$, 1.4 Hz, 0.5H), 4.02 – 3.96 (m, 0.5H), 3.67 – 3.60 (m, 0.5H), 2.77 – 2.65 (m, 2H), 2.46 – 2.38 (m, 1H), 2.38 – 2.32 (m, 1H), 1.62 (dd, $J = 14.5$, 2.7 Hz, 0.5H), 1.60 (dd, $J = 14.1$, 2.7 Hz, 0.5H), 1.54 – 1.42 (m, 2H), 1.42 – 1.35 (m, 1.5H), 1.33 (s, 1.5H), 1.32 – 1.24 (m, 1.5H), 1.23 (s, 1.5H), 0.93 (t, $J = 7.1$ Hz, 1.5H), 0.90 (t, $J = 7.0$ Hz, 1.5H).

^{13}C NMR (150 MHz, CDCl_3) δ 142.0, 141.9, 138.9, 136.7, 128.7, 128.6, 128.4, 128.3, 127.6, 126.8, 126.0, 125.9, 73.8, 73.4, 70.0, 69.0, 47.3, 47.1, 40.5, 40.5, 35.9, 35.9, 34.1, 33.9, 30.7, 26.9, 18.7, 18.6, 14.3, 14.2.

IR (ATR, neat) 3334, 2958, 2929, 2871, 1453, 1434, 1370, 1263, 1182, 1128, 1075, 1027, 970, 841, 746, 697 cm^{-1} .

HRMS (ESI) m/z calcd. for $\text{C}_{17}\text{H}_{26}\text{O}_2\text{Na}$ $[\text{M}+\text{Na}]^+$ 285.1825, found 285.1822.



To a solution of a **1.68** (16.9 mg, 0.0644 mmol) in HFIP/ MeNO_2 (9:1, 0.64 mL, 0.1M) was added HOREO_3 (0.50 μL , 76.5% solution in H_2O , 0.0032 mmol) and the mixture was stirred for 5 min.

The reaction mixture was diluted with CH₂Cl₂ and filtered through a short silica gel pipette column. The column was flushed with EtOAc (3x) and the solvent was removed under reduced pressure. The crude mixture was purified by flash column chromatography (5% Et₂O in hexanes to 10% Et₂O in hexanes) to afford **1.70** (10.7 mg, 68%, dr = 1.5:1) as an inseparable colorless oil.

¹H NMR (400 MHz, CDCl₃) δ 7.31 – 7.24 (m, 2H), 7.23 – 7.14 (m, 3H), 5.40 – 5.35 (m, 0.6H), 5.32 – 5.28 (m, 0.4H), 4.17 – 4.09 (m, 0.6H), 4.03 – 3.95 (m, 0.4H), 3.68 (tt, *J* = 8.5, 4.5 Hz, 0.6H), 3.48 (tt, *J* = 11.0, 4.3 Hz, 0.3H), 2.86 – 2.77 (m, 1H), 2.75 – 2.63 (m, 1H), 1.97 – 1.83 (m, 2H), 1.83 – 1.72 (m, 1H), 1.69 (s, 3H), 1.65 – 1.58 (m, 1H), 1.54 – 1.47 (m, 1H), 1.47 – 1.37 (m, 2H), 0.99 – 0.91 (m, 3H).

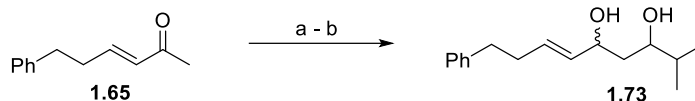
¹³C NMR (100 MHz, CDCl₃) δ 142.6, 142.5, 132.9, 131.9, 128.7, 128.6, 128.5, 128.4, 125.8, 125.7, 124.1, 123.4, 73.9, 73.9, 72.1, 67.4, 38.4, 37.9, 37.6, 36.5, 35.9, 32.6, 31.6, 23.4, 23.1, 19.2, 18.9, 14.3.

IR (ATR, neat) 3023, 2955, 2924, 2867, 1453, 1376, 1253, 1077, 1029, 906, 883, 747, 700 cm⁻¹.

HRMS (ESI) *m/z* calcd. for C₁₇H₂₅O [M+H]⁺ 245.1899, found 245.1899.

24 h Reaction

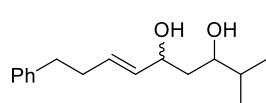
To a solution of a **1.68** (15.9 mg, 0.0609 mmol) in HFIP/MeNO₂ (9:1, 0.6 mL, 0.1M) was added HOREO3 (0.45 μL, 76.5% solution in H₂O, 0.003 mmol) and the mixture was stirred for 24 h. The reaction mixture was diluted with CH₂Cl₂ and filtered through a short silica gel pipette column. The column was flushed with EtOAc (3x) and the solvent was removed under reduced pressure. The crude mixture was purified by flash column chromatography (5% Et₂O in hexanes to 10% Et₂O in hexanes) to afford pyran **1.70** (11.7 mg, 79%, d.r. = 2:1) as a colorless oil.



Reagents and conditions

a) LDA, -78°C , then *i*PrCHO, 63%. b) NaBH₄, MeOH, 0°C , 67%.

Scheme 63. Synthesis of Compound 1.73



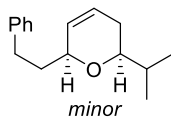
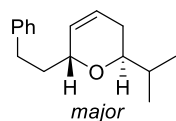
(*E*)-2-Methyl-9-phenylnon-6-ene-3,5-diol (1.73)

¹H NMR (500 MHz, CDCl₃) δ 7.32 – 7.25 (m, 2H), 7.21 – 7.15 (m, 3H), 5.77 – 5.67 (m, 1H), 5.55 (ddt, $J = 15.3, 6.2, 1.3$ Hz, 0.3H), 5.50 (ddt, $J = 15.3, 6.8, 1.3$ Hz, 0.7H), 4.39 (dt, $J = 7.2, 7.2$ Hz, 0.3H), 4.31 (dt, $J = 7.4, 7.4$ Hz, 0.7H), 3.64 – 3.54 (m, 1H), 2.84 (s, 1H), 2.75 – 2.66 (m, 2H), 2.42 – 2.30 (m, 2H), 1.72 – 1.58 (m, 2H), 1.58 – 1.54 (m, 1H), 0.94 – 0.89 (m, 6H).

¹³C NMR (125 MHz, CDCl₃) δ 141.8, 133.5, 133.4, 130.8, 130.6, 128.6, 128.6, 128.5, 128.4, 126.0, 77.3, 74.0, 73.9, 70.8, 40.0, 39.6, 35.7, 35.6, 34.3, 34.0, 33.9, 18.6, 18.3, 17.8, 17.6.

IR (ATR, neat) 3383, 3026, 2941, 1495, 1449, 1329, 1270, 1141, 1051, 971, 905, 850, 745, 698, 501 cm⁻¹.

HRMS (ESI) m/z calcd. for C₁₆H₂₄O₂Na [M+Na]⁺ 271.6685, found 271.1667.



(2*S*,6*R*)-2-Isopropyl-6-phenethyl-3,6-dihydro-2H-pyran and

(2*S*,6*S*)-2-Isopropyl-6-phenethyl-3,6-dihydro-2H-pyran

(1.74)

The general cyclization procedure was followed with **1.73** (22.6 mg, 0.0910 mmol) in HFIP/MeNO₂ (9:1, 0.91 mL, 0.1M). To this, Re₂O₇•SiO₂ (24.2 mg, 9.1%, 0.00455 mmol) was added and the reaction was stirred for 10 min. The mixture was diluted with CH₂Cl₂ and filtered through a short silica pipette column. The column was flushed with EtOAc (3x) and the solvent was

removed under reduced pressure. The crude mixture was purified by flash column chromatography (5% Et₂O in hexanes to 10% Et₂O in hexanes) to afford **1.74** (15.3 mg, 73%, d.r. = 5:1) as a colorless oil.

***Trans*-isomer (slower eluting, major)**

¹H NMR (400 MHz, C₆D₆) δ 7.21 – 7.17 (m, 4H), 7.11 – 7.06 (m, 1H), 5.69 – 5.63 (m, 1H), 5.48 (ddt, *J* = 10.2, 3.0, 1.5 Hz, 1H), 4.14 (dt, *J* = 9.8, 2.8 Hz, 1H), 3.21 (ddd, *J* = 10.1, 6.7, 3.3 Hz, 1H), 2.84 (ddd, *J* = 14.1, 9.4, 4.6 Hz, 1H), 2.62 (ddd, *J* = 13.6, 9.6, 7.3 Hz, 1H), 1.96 – 1.84 (m, 2H), 1.73 – 1.61 (m, 2H), 1.58 – 1.48 (m, 1H), 1.09 (d, *J* = 6.6 Hz, 3H), 0.86 (d, *J* = 6.8 Hz, 3H).

¹³C NMR (100 MHz, C₆D₆) δ 142.7, 130.3, 128.9, 128.7, 126.1, 124.4, 72.3, 35.9, 33.2, 32.8, 28.7, 19.1, 18.9.

IR (ATR): 3028, 2956, 2925, 2872, 1604, 1496, 1454, 1384, 1194, 1091, 1074, 1029, 939, 749 cm⁻¹.

HRMS (ESI) *m/z* calcd. for C₁₆H₂₃O [M+H]⁺ 231.1743, found 231.1743.

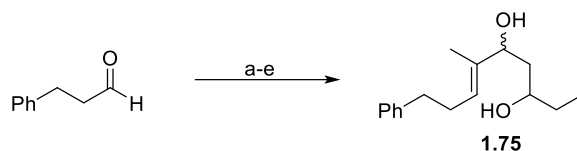
***Cis*-isomer (faster eluting, minor)**

¹H NMR (500 MHz, C₆D₆) δ 7.23 – 7.17 (m, 3H), 7.14 – 7.04 (m, 2H), 5.70 – 5.65 (m, 1H), 5.46 (ddt, *J* = 10.1, 2.7, 1.3 Hz, 1H), 4.06 – 3.98 (m, 1H), 3.08 (ddd, *J* = 10.4, 7.1, 3.4 Hz, 1H), 2.88 – 2.75 (m, 2H), 1.95 – 1.82 (m, 2H), 1.79 – 1.64 (m, 3H), 1.06 (d, *J* = 6.7 Hz, 3H), 0.85 (d, *J* = 6.8 Hz, 3H).

¹³C NMR (125 MHz, C₆D₆) δ 142.8, 130.9, 129.0, 128.6, 126.0, 125.2, 79.0, 74.1, 37.9, 33.6, 31.9, 28.8, 18.9, 18.4.

IR (ATR) 3027, 2956, 2924, 2854, 1603, 1496, 1454, 1361, 1259, 1191, 1095, 1062, 1030, 974, 747 cm⁻¹.

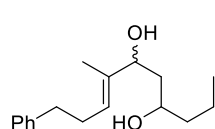
HRMS (ESI) *m/z* calcd. for C₁₆H₂₃O [M+H]⁺ 231.1743, found 231.1745.



Reagents and conditions

a) $\text{Ph}_3\text{P}=\text{C}(\text{Me})\text{C}(\text{H})\text{O}$, PhMe , $80\text{ }^\circ\text{C}$, 79%. b) MeLi , Et_2O , $-78\text{ }^\circ\text{C}$, 78%. c) $(\text{COCl})_2$, Et_3N , DMSO , CH_2Cl_2 , $-78\text{ }^\circ\text{C}$, 67%. d) LDA , THF , $-78\text{ }^\circ\text{C}$, then $n\text{-PrCHO}$, 73%. e) NaBH_4 , MeOH , $0\text{ }^\circ\text{C}$, 60%.

Scheme 64. Synthesis of Compound 1.75



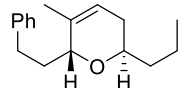
(E)-7-Methyl-10-phenyldec-7-ene-4,6-diol (1.75)

^1H NMR (500 MHz, CDCl_3) δ 7.30 – 7.26 (m, 2H), 7.21 – 7.15 (m, 3H), 5.52 (t, $J = 7.1\text{ Hz}$, 0.4H), 5.47 (t, $J = 7.1\text{ Hz}$, 0.6H), 4.29 (dd, $J = 7.7, 3.4\text{ Hz}$, 0.4H), 4.24 (dd, $J = 9.3, 3.5\text{ Hz}$, 0.6H), 3.85 – 3.75 (m, 1H), 2.72 – 2.62 (m, 2H), 2.41 – 2.29 (m, 2H), 1.72 (ddd, $J = 14.5, 7.9, 2.9\text{ Hz}$, 0.6H), 1.64 – 1.56 (m, 2.4H), 1.56 (s, 2H), 1.54 (s, 1.2H), 1.51 – 1.32 (m, 4H), 0.93 (t, $J = 7.0\text{ Hz}$, 3H).

^{13}C NMR (125 MHz, CDCl_3) δ 142.2, 142.1, 138.2, 138.0, 128.6, 128.4, 126.0, 125.3, 124.5, 78.7, 74.7, 72.4, 69.3, 41.6, 40.7, 40.4, 39.7, 35.8, 29.8, 29.5, 19.0, 18.7, 14.2, 12.6, 11.8.

IR (ATR, neat) 3402, 3027, 2928, 1495, 1405, 1315, 1074, 1027, 910, 746, 698, 664 cm^{-1} .

HRMS (ESI) m/z calcd. for $\text{C}_{17}\text{H}_{26}\text{O}_2\text{Na}$ $[\text{M}+\text{Na}]^+$ 285.1825, found 285.1824.



(2R,6R)-5-Methyl-6-phenethyl-2-propyl-3,6-dihydro-2H-pyran (1.76)

The general cyclization procedure was followed with **1.75** (17.8 mg, 0.0678 mmol) in $\text{HFIP}/\text{MeNO}_2$ (9:1, 0.68 mL, 0.1M). To this, $\text{Re}_2\text{O}_7 \cdot \text{SiO}_2$ (18.0 mg, 9.1%, 0.00339 mmol) was added and the reaction was stirred for 24 h. The mixture was diluted with CH_2Cl_2 and filtered through a short silica pipette column. The column was flushed with EtOAc (3x) and the solvent was removed under reduced pressure. The crude mixture was purified by flash column

chromatography (5% Et₂O in hexanes to 10% Et₂O in hexanes) to afford **1.76** (12.0 mg, 72%, d.r. = 17:1) as a colorless oil.

¹H NMR (500 MHz, C₆D₆) δ 7.23 – 7.17 (m, 4H), 7.11 – 7.06 (m, 1H), 5.39 – 5.35 (m, 1H), 4.02 – 3.96 (m, 1H), 3.57 (tt, J = 8.7, 4.0 Hz, 1H), 2.97 (ddd, J = 13.8, 9.7, 4.3 Hz, 1H), 2.72 (ddd, J = 13.6, 9.5, 7.5 Hz, 1H), 1.94 – 1.82 (m, 2H), 1.80 – 1.69 (m, 2H), 1.69 – 1.58 (m, 2H), 1.48 – 1.41 (m, 1H), 1.40 (s, 3H), 1.37 – 1.28 (m, 1H), 0.93 (t, J = 7.3 Hz, 3H).

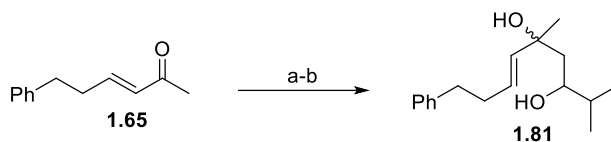
¹³C NMR (125 MHz, C₆D₆) δ 142.5, 135.8, 128.6, 128.3, 127.9, 125.7, 119.4, 74.8, 66.3, 38.0, 33.6, 32.4, 31.5, 20.0, 19.5, 19.2, 14.1.

IR (ATR) 3026, 2956, 2928, 2870, 1603, 1496, 1454, 1435, 1377, 1090, 1066, 1028, 969, 807, 748 cm⁻¹.

HRMS (ESI) m/z calcd. for C₁₇H₂₅O [M+H]⁺ 245.1899, found 245.1898.

10 min Reaction

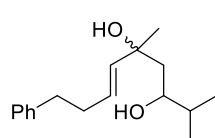
The general cyclization procedure was followed with **1.75** (17.1 mg, 0.0652 mmol) in HFIP/MeNO₂ (9:1, 0.65 mL, 0.1M). To this, Re₂O₇•SiO₂ (18.0 mg, 9.1%, 0.00326 mmol) was added and the reaction was stirred for 10 min. The mixture was diluted with CH₂Cl₂ and filtered through a short silica pipette column. The column was flushed with EtOAc (3x) and the solvent was removed under reduced pressure. The crude mixture was purified by flash column chromatography (5% Et₂O in hexanes to 10% Et₂O in hexanes) to afford **1.76** (11.0 mg, 69%, d.r. = 5:1) as a colorless oil.



Reagents and conditions

a) LDA, THF, -78°C , then $i\text{PrCHO}$, 63%. b) MeLi, LiBr, Et_2O , -78°C , 40%.

Scheme 65. Synthesis of Compound 1.81



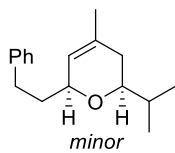
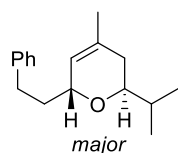
(*E*)-2,5-Dimethyl-9-phenylnon-6-ene-3,5-diol (1.81)

^1H NMR (500 MHz, CDCl_3) δ 7.30 – 7.25 (m, 2H), 7.21 – 7.15 (m, 3H), 5.73 (dt, $J = 15.4$, 6.8 Hz, 0.6H), 5.69 (dt, $J = 15.5$, 6.6 Hz, 0.4H), 5.56 (dt, $J = 15.6$, 1.2 Hz, 0.4 H), 5.43 (dt, $J = 15.4$, 1.4 Hz, 0.6H), 3.74 (ddd, $J = 10.5$, 5.3, 1.9 Hz, 0.4H), 3.39 (ddd, $J = 10.8$, 5.3, 1.9 Hz, 0.6H), 2.82 – 2.67 (m, 2H), 2.48 – 2.39 (m, 1H), 2.39 – 2.32 (m, 1H), 1.67 – 1.44 (m, 3H), 1.33 (s, 1.2H), 1.23 (s, 1.7H), 0.92 (d, $J = 6.6$ Hz, 1.8H), 0.90 (d, $J = 6.6$ Hz, 1.2H), 0.84 (d, $J = 6.9$ Hz, 1.9H), 0.83 (d, $J = 6.9$ Hz, 1.4H).

^{13}C NMR (125 MHz, CDCl_3) δ 142.0, 141.9, 139.0, 136.8, 128.7, 128.7, 128.6, 128.4, 128.3, 127.6, 126.7, 126.0, 74.8, 73.9, 73.6, 73.2, 43.9, 43.6, 35.9, 34.3, 34.3, 34.1, 33.9, 30.8, 26.8, 18.4, 18.3, 17.7, 17.6.

IR (ATR, neat) 3354, 3027, 2919, 1453, 1367, 1267, 1179, 1071, 972, 859, 746, 698, 541 cm^{-1} .

HRMS (ESI) m/z calcd. for $\text{C}_{17}\text{H}_{26}\text{O}_2\text{Na}$ $[\text{M}+\text{H}]^+$ 285.1820, found 285.1820.



(2*S*,6*R*)-2-Isopropyl-4-methyl-6-phenethyl-3,6-dihydro-2H-pyran and (2*S*,6*S*)-2-Isopropyl-4-methyl-6-phenethyl-3,6-dihydro-2H-pyran (1.82)

The general cyclization procedure was followed with **1.81** (20.2 mg, 0.0769 mmol) in HFIP/ MeNO_2 (9:1, 0.77 mL, 0.1M). To this, $\text{Re}_2\text{O}_7 \cdot \text{SiO}_2$ (20.5 mg, 9.1%, 0.00385 mmol) was

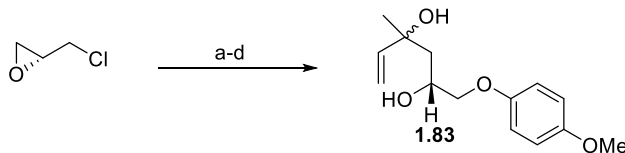
added and the reaction was stirred for 10 min. The mixture was diluted with CH₂Cl₂ and filtered through a short silica pipette column. The column was flushed with EtOAc (3x) and the solvent was removed under reduced pressure. The crude mixture was purified by flash column chromatography (5% Et₂O in hexanes to 10% Et₂O in hexanes) to afford **1.82** (14.8 mg, 79%, d.r. = 1.7:1) as an inseparable colorless oil.

¹H NMR (500 MHz, C₆D₆) δ 7.20 – 7.16 (m, 4H), 7.11 – 7.05 (m, 1H), 5.23 – 5.19 (m, 1H), 4.20 – 4.14 (m, 0.6H), 4.04 – 3.98 (m, 0.4H), 3.23 (td, J = 6.8, 3.2 Hz, 0.6H), 3.07 (td, J = 7.1, 3.6 Hz, 0.4H), 2.90 – 2.84 (m, 1H), 2.84 – 2.77 (m, 0.4H), 2.66 (ddd, J = 13.6, 9.8, 7.2 Hz, 0.6H), 1.95 – 1.80 (m, 2H), 1.81 – 1.76 (m, 0.4H), 1.75 – 1.68 (m, 1H), 1.60 – 1.57 (m, 1H), 1.56 (s, 3H), 1.11 (d, J = 6.7 Hz, 1.8H), 1.09 (d, J = 6.7 Hz, 1.2H), 0.92 – 0.88 (m, 3H).

¹³C NMR (125 MHz, C₆D₆) δ 142.9, 142.8, 132.5, 131.7, 129.0, 128.9, 128.7, 128.6, 128.4, 126.1, 126.0, 124.7, 124.1, 79.1, 74.1, 72.5, 72.4, 38.2, 36.1, 33.6, 33.6, 33.5, 33.2, 32.9, 32.0, 23.4, 23.2, 19.1, 19.0, 18.9, 18.5.

IR (ATR): 3027, 2959, 2926, 1603, 1496, 1453, 1380, 1365, 1284, 1220, 1189, 1075, 849, 747, 698 cm⁻¹.

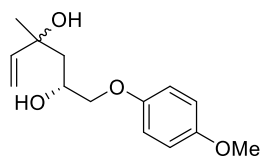
HRMS (ESI) m/z calcd. for C₁₇H₂₅O [M+H]⁺ 245.1899, found 245.1892.



Reagents and conditions

a) *p*-MeOPhOH, K₂CO₃, Na₂S₂O₄, KI, Acetone, reflux, 35%, b) 2-methyl-1,3-dithiane, *n*-BuLi, THF, –30 °C, 55%, c) PhI(OTFA)₂, MeCN, H₂O, 0 °C, 45%, d) CH₂=CHMgBr, THF, 0 °C, 47%.

Scheme 66. Synthesis of 1.83



(2R)-1-(4-Methoxyphenoxy)-4-methylhex-5-ene-2,4-diol (1.83)

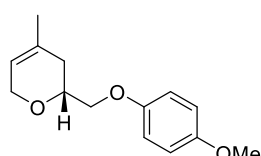
¹H NMR (500 MHz, CDCl₃) δ 6.88 – 6.80 (m, 4H), 5.99 (dd, *J* = 17.3, 10.7 Hz, 0.4H), 5.93 (dd, *J* = 17.2, 10.7 Hz, 0.6H), 5.40 (dd, *J* = 17.2, 1.4 Hz, 0.6H), 5.28 (dd, *J* = 17.3, 1.0 Hz, 0.4H), 5.18 (dd, *J* = 10.7, 1.4 Hz, 0.6H), 5.07 (dd, *J* = 10.7, 1.0 Hz, 0.4H), 4.41 – 4.34 (m, 0.4H), 4.28 – 4.21 (m, 0.6H), 3.90 – 3.84 (m, 1H), 3.84 – 3.79 (m, 1H), 3.83 – 3.79 (m, 1H), 3.77 (s, 3H), 3.47 (s, 0.6H), 3.29 (d, *J* = 2.1 Hz, 0.4H), 3.12 (d, *J* = 2.3 Hz, 0.6H), 2.83 (s, 0.4H), 1.88 (dd, *J* = 14.4, 10.8 Hz, 0.4H), 1.83 (dd, *J* = 14.5, 9.8 Hz, 0.6H), 1.74 (dd, *J* = 14.6, 3.0 Hz, 0.4H), 1.70 (dd, *J* = 14.5, 1.9 Hz, 0.6H), 1.42 (s, 1.4H), 1.33 (s, 1.8H).

¹³C NMR (125 MHz, CDCl₃) δ 154.3, 154.3, 152.8, 152.8, 145.6, 143.9, 115.7, 115.7, 114.8, 113.1, 111.8, 74.0, 73.3, 73.1, 73.0, 68.8, 68.1, 55.9, 43.4, 43.1, 30.2, 27.1.

IR (ATR, neat) 3328, 2931, 1641, 1505, 1447, 1410, 1288, 1225, 1176, 1108, 1036, 926, 826, 737, 596, 522 cm⁻¹.

HRMS (ESI) *m/z* calcd. for C₁₄H₁₉O₃ [M–OH]⁺ 235.1329, found 235.1318.

[α]_D²⁵ = –3.3 (*c* = 1.0, CHCl₃)



(R)-2-((4-Methoxyphenoxy)methyl)-4-methyl-3,6-dihydro-2H-pyran

(1.84)

The general cyclization procedure was followed with **1.83** (9.4 mg, 0.037 mmol) in HFIP/MeNO₂ (9:1, 0.37 mL, 0.1M). To this, Re₂O₇•SiO₂ (9.9 mg, 9.1%, 0.0019 mmol) was added and the reaction was stirred for 20 min. The mixture was diluted with CH₂Cl₂ and filtered through a short silica pipette column. The column was flushed with EtOAc (3x) and the solvent was removed under reduced pressure. The crude mixture was purified by flash column

chromatography (10% EtOAc in hexanes to 15% EtOAc in hexanes) to afford **1.84** (5.4 mg, 62%) as a colorless oil.

¹H NMR (500 MHz, CDCl₃) δ 6.91 – 6.86 (m, 2H), 6.85 – 6.80 (m, 2H), 5.47 – 5.44 (m, 1H), 4.25 – 4.21 (m, 2H), 4.04 – 3.99 (m, 1H), 3.96 – 3.88 (m, 2H), 3.77 (s, 3H), 2.19 – 2.11 (m, 1H), 1.95 – 1.88 (m, 1H), 1.73 (s, 3H).

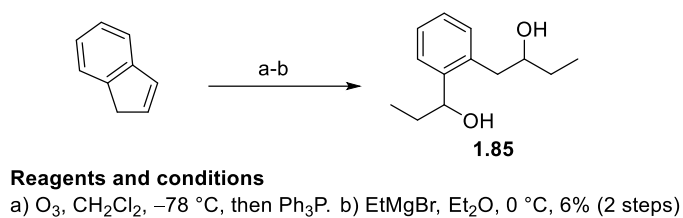
¹³C NMR (125 MHz, CDCl₃) δ 154.1, 153.2, 131.3, 119.9, 115.9, 114.7, 72.3, 71.7, 66.1, 55.9, 32.2, 23.2.

IR (ATR, neat): 2921, 2855, 2832, 1506, 1453, 1382, 1287, 1229, 1136, 1039, 941, 824, 748 cm⁻¹

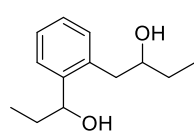
HRMS (TOF MS ES⁺) *m/z* calcd. for C₁₄H₁₈O₃ [M]⁺ 234.1256, found 234.1244.

$[\alpha]_D^{25} = -1.1$ (c = 0.2, CHCl₃)

HPLC analysis: The sample was analyzed with a Phenomenex Lux 5u Cellulose-3 column using 5% iPrOH in hexane as a solvent with a flow rate of 0.5 mL/min. Retention time (major) = 11.46 min, retention time (minor) = 12.91 min.



Scheme 67. Synthesis of Compound 1.85



1-(2-(1-Hydroxypropyl)phenyl)butan-2-ol (**1.85**)

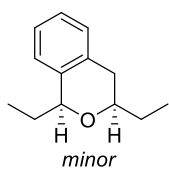
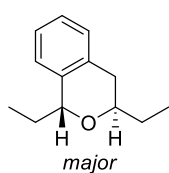
¹H NMR (500 MHz, CDCl₃) δ 7.47 – 7.42 (m, 0.4H), 7.40 – 7.36 (m, 0.6H), 7.27 – 7.21 (m, 2H), 7.19 – 7.15 (m, 1H), 4.85 (dd, *J* = 7.6, 6.1 Hz, 0.4H), 4.80 (dd, *J* = 7.5, 6.0 Hz, 0.6H), 3.75 (tt, *J* = 8.1, 4.3 Hz, 0.6H), 3.69 – 3.63 (m, 0.4H), 2.93 (dd, *J* = 14.0, 3.9 Hz, 0.6H),

2.88 (dd, $J = 14.0, 9.9$ Hz, 0.4H), 2.81 (dd, $J = 13.9, 8.5$ Hz, 0.6H), 2.75 (dd, $J = 14.0, 3.1$ Hz, 0.4H), 2.62 (s, 2H) 1.99 – 1.89 (m, 0.4H), 1.89 – 1.80 (m, 1H), 1.79 – 1.72 (m, 0.6H), 1.69 – 1.49 (m, 2H), 1.01 (t, $J = 7.5$ Hz, 1.8H), 1.00 (t, $J = 6.8$ Hz, 1.2H), 0.97 (t, $J = 6.7$ Hz, 1.2 H), 0.94 (t, $J = 7.4$ Hz, 1.8H).

^{13}C NMR (125 MHz, CDCl_3) δ 142.9, 142.7, 137.5, 136.1, 131.1, 130.3, 127.7, 127.5, 127.0, 126.9, 126.9, 125.9, 75.3, 74.2, 73.4, 70.8, 39.5, 39.2, 31.4, 30.8, 30.2, 29.3, 14.3, 11.0, 10.8, 10.3, 10.2.

IR (ATR, neat) 3328, 3062, 2963, 2932, 2876, 1488, 1453, 1378, 1265, 1092, 1054, 1008, 971, 753 cm^{-1} .

HRMS (ESI) m/z calcd. for $\text{C}_{13}\text{H}_{20}\text{O}_2$ $[\text{M}+\text{H}]^+$ 209.1536, found 209.1543.



(1R,3R)-1,3-Diethylisochromane and (1S,3R)-1,3-Diethylisochromane (1.86**)**

The general cyclization procedure was followed with **1.85** (25.0 mg, 0.120 mmol) in HFIP/ MeNO_2 (9:1, 1.2 mL, 0.1M). To this, $\text{Re}_2\text{O}_7 \cdot \text{SiO}_2$ (32 mg, 9.1%, 0.0060 mmol) was added and the reaction was stirred for 15 min. The mixture was diluted with CH_2Cl_2 and filtered through a short silica pipette column. The column was flushed with EtOAc (3x) and the solvent was removed under reduced pressure. The crude mixture was purified by flash column chromatography (5% Et_2O in hexanes) to afford **1.86** (17 mg, 74%, d.r. = 5:1) as an inseparable colorless oil.

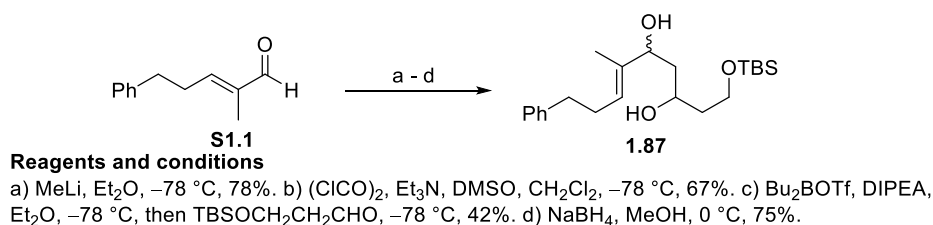
^1H NMR (400 MHz, C_6D_6) δ 7.09 – 7.00 (m, 2H), 6.96 – 6.89 (m, 1H), 6.83 – 6.77 (m, 1H), 4.68 (dd, $J = 10.6, 3.3$ Hz, 0.8H), 4.65 – 4.62 (m, 0.13H), 3.56 (ddt, $J = 9.8, 8.0, 4.0$ Hz, 0.8H), 3.36 – 3.28 (m, 0.15H), 2.58 (dd, $J = 15.9, 11.2$ Hz, 0.15H), 2.51 (dd, $J = 16.0, 9.9$ Hz, 0.8H), 2.39 (dd,

$J = 16.1, 3.5$ Hz, 0.8H), 2.37 – 2.31 (m, 0.14H), 2.08 – 1.97 (m, 0.16H), 1.87 – 1.71 (m, 1H), 1.70 – 1.49 (m, 2H), 1.49 – 1.35 (m, 1H), 1.09 (t, $J = 7.4$ Hz, 2.3H), 1.05 (t, $J = 7.4$ Hz, 0.7H), 0.99 (t, $J = 7.4$ Hz, 2.3H), 0.97 (t, $J = 7.5$ Hz, 0.7H).

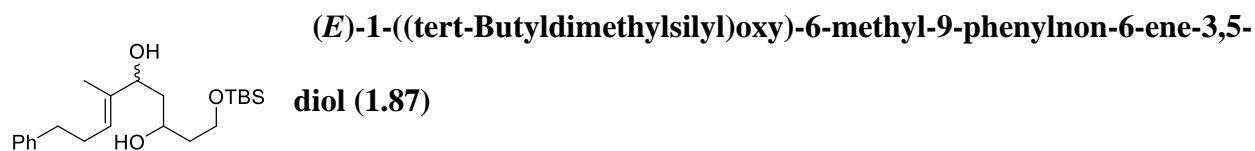
^{13}C NMR (100 MHz, C_6D_6) δ 139.4, 138.8, 135.1, 133.9, 129.1, 128.2, 127.9, 126.4, 126.3, 126.0, 125.7, 124.6, 77.8, 76.2, 75.6, 68.7, 35.1, 34.6, 29.5, 29.1, 29.0, 11.2, 10.5, 10.2, 9.5.

IR (ATR, neat) 3023, 2962, 2928, 2874, 1453, 1377, 1358, 1199, 1114, 1053, 998, 955, 880, 750, 739, 544 cm^{-1} .

HRMS (ESI) m/z calcd. for $\text{C}_{18}\text{H}_{19}\text{O}$ $[\text{M}+\text{H}]^+$ 191.1430, found 191.1431.



Scheme 68. Synthesis of Compound 1.87

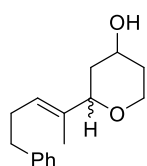


^1H NMR (400 MHz, CDCl_3) δ 7.31 – 7.24 (m, 2H), 7.21 – 7.15 (m, 3H), 5.53 (t, $J = 6.5$ Hz, 0.5H), 5.50 (t, $J = 6.5$ Hz, 0.5H), 4.30 (dd, $J = 8.4, 3.0$ Hz, 0.5H), 4.26 (dd, $J = 9.3, 2.9$ Hz, 0.5H), 4.12 – 4.03 (m, 1H), 3.95 – 3.87 (m, 1H), 3.86 – 3.79 (m, 1H), 2.71 – 2.62 (m, 2H), 2.39 – 2.28 (m, 2H), 1.88 – 1.73 (m, 1H), 1.73 – 1.61 (m, 3H), 1.57 (s, 1.6H), 1.55 (s, 1.6H), 0.90 (s, 9H), 0.09 (s, 6H).

^{13}C NMR (100 MHz, CDCl_3) δ 142.3, 138.0, 137.9, 128.6, 128.4, 125.9, 125.0, 124.5, 78.0, 74.2, 72.9, 70.2, 63.1, 62.5, 42.2, 41.3, 39.0, 38.2, 35.9, 35.8, 29.7, 29.6, 26.0, 18.3, 18.2, 12.4, 11.9, $-5.4, -5.4$.

IR (ATR): 3378, 2949, 2928, 2856, 1462, 1453, 1360, 1306, 1253, 1083, 1005, 938, 834, 775, 747, 698, 663 cm^{-1} .

HRMS (ESI) m/z calcd. for $\text{C}_{22}\text{H}_{39}\text{O}_3\text{Si}$ $[\text{M}+\text{H}]^+$ 379.2663, found 379.2654.



(E)-2-(5-Phenylpent-2-en-2-yl)tetrahydro-2H-pyran-4-ol (1.88)

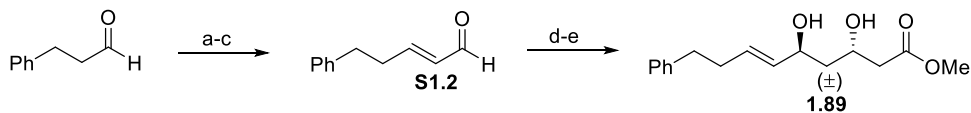
The general cyclization procedure was followed with **1.87** (20.4 mg, 0.0539 mmol) in HFIP/ MeNO_2 (9:1, 0.54 mL, 0.1M). To this, $\text{Re}_2\text{O}_7 \cdot \text{SiO}_2$ (14 mg, 9.1%, 0.0027 mmol) was added and the reaction was stirred for 45 min. NH_4F (6 mg, 0.16 mmol) was added and the reaction was stirred for an additional 1 h. The mixture was diluted with CH_2Cl_2 and filtered through a short silica pipette column. The column was flushed with EtOAc (3x) and the solvent was removed under reduced pressure. The crude mixture was purified by flash column chromatography (20% EtOAc in hexanes to 40% EtOAc in hexanes) to afford **1.88** (7.8 mg, 59%, d.r. = 1.5:1) as an inseparable colorless oil.

^1H NMR (500 MHz, CDCl_3) δ 7.30 – 7.25 (m, 2H), 7.20 – 7.15 (m, 3H), 5.53 – 5.47 (m, 1H), 4.28 (dt, J = 6.2, 3.1 Hz, 0.4H), 4.12 (dd, J = 11.3, 1.5 Hz, 0.4H), 4.06 (ddd, J = 11.9, 5.2, 1.7 Hz, 0.6H), 3.92 (td, J = 12.1, 2.2 Hz, 0.4H), 3.86 – 3.78 (m, 1H), 3.64 (d, J = 11.3 Hz, 0.6H), 3.44 (td, J = 12.1, 2.2 Hz, 0.4H), 2.72 – 2.61 (m, 2H), 2.39 – 2.30 (m, 2H), 1.95 – 1.83 (m, 1.8H), 1.73 (ddd, J = 14.0, 11.3, 2.7 Hz, 0.6H), 1.65 – 1.63 (m, 0.4H), 1.60 (m, 3H), 1.56 – 1.47 (m, 1.4H), 1.43 – 1.35 (m, 0.8H).

^{13}C NMR (125 MHz, CDCl_3) δ 142.3, 142.2, 136.3, 135.8, 128.6, 128.4, 128.4, 125.9, 125.9, 125.8, 125.3, 81.4, 76.6, 68.6, 66.0, 64.4, 62.6, 40.2, 37.5, 35.8, 35.7, 35.7, 33.1, 29.7, 29.7, 12.6.

IR (ATR) 3388, 3026, 2923, 2856, 1603, 1496, 1453, 1372, 1265, 1248, 1218, 1191, 1068, 1029, 987, 881, 837, 735, 698, 598 cm^{-1} .

HRMS (ESI) m/z calcd. for $C_{16}H_{23}O_2$ $[M+H]^+$ 247.1693, found 247.1693.

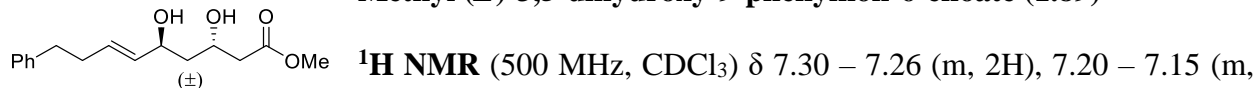


Reagents and conditions

a) $(MeO)_2P(O)CH_2CO_2Me$, LiCl, DBU, CH_3CN , 0 °C to rt, 84%. b) DIBAL-H, CH_2Cl_2 , -78 °C to rt, 58%. c) $(ClCO)_2$, DMSO, Et_3N , CH_2Cl_2 , -78 °C, 73%. d) Methyl acetoacetate, NaH, $n-BuLi$, THF, -78 °C, 58%, b) $Me_4NB(OAc)_3H$, MeCN, AcOH, -20 °C, 63%.

Scheme 69. Synthesis of Compound 1.89

Methyl (*E*)-3,5-dihydroxy-9-phenylnon-6-enoate (1.89)

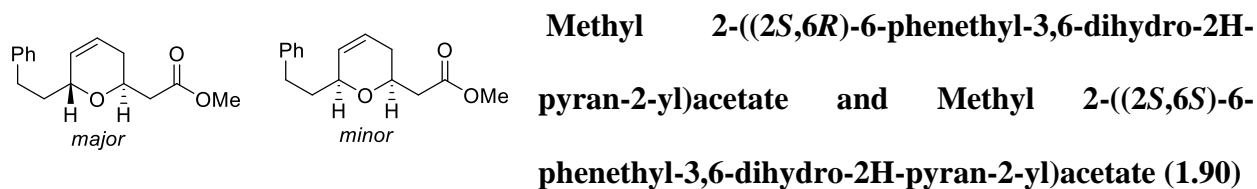


1H NMR (500 MHz, $CDCl_3$) δ 7.30 – 7.26 (m, 2H), 7.20 – 7.15 (m, 3H), 5.73 (dt, J = 15.4, 7.2 Hz, 1H), 5.53 (ddt, J = 15.4, 6.5, 1.2 Hz, 1H), 4.42 – 4.35 (m, 1H), 4.28 (ddt, J = 12.5, 8.1, 4.0 Hz, 1H), 3.72 (s, 3H), 3.36 (d, J = 3.4 Hz, 1H), 2.71 (t, J = 7.7 Hz, 2H), 2.55 – 2.47 (m, 2H), 2.46 – 2.42 (m, 1H), 2.37 (dd, J = 14.8, 7.3 Hz, 2H), 1.73 (ddd, J = 14.3, 9.1, 3.5 Hz, 1H), 1.61 (ddd, J = 14.6, 7.8, 3.1 Hz, 1H).

^{13}C NMR (125 MHz, $CDCl_3$) δ 173.3, 141.8, 131.1, 130.9, 128.6, 128.4, 126.0, 70.1, 65.7, 51.9, 42.3, 41.2, 35.7, 34.0.

IR (ATR, neat) 3423, 3032, 2927, 2858, 1710, 1452, 1434, 1370, 1349, 1246, 1158, 1063, 1034, 970, 847, 748, 699 cm^{-1} .

HRMS (ESI) m/z calcd. for $C_{16}H_{21}O$ $[M-OH]^+$ 261.1485, found 261.1475.



The general cyclization procedure was followed with **1.89** (22.0 mg, 0.079 mmol) in HFIP/ $MeNO_2$ (9:1, 0.79 mL, 0.1M). To this, $Re_2O_7 \cdot SiO_2$ (21 mg, 9.1%, 0.0040 mmol) was added and the reaction

was stirred for 10 min. The mixture was diluted with CH₂Cl₂ and filtered through a short silica pipette column. The column was flushed with EtOAc (3x) and the solvent was removed under reduced pressure. The crude mixture was purified by flash column chromatography (5% EtOAc in hexanes to 10% EtOAc in hexanes) to afford **1.90** (11.3 mg, 55%, d.r. = 1:1) as a colorless oil.

***Trans*-Isomer (slower eluting)**

¹H NMR (400 MHz, C₆D₆) δ 7.36 – 7.18 (m, 3H), 7.14 – 6.94 (m, 2H), 5.56 – 5.49 (m, 1H), 5.39 (ddt, *J* = 10.3, 3.9, 1.3 Hz, 1H), 4.18 (tt, *J* = 8.6, 4.3 Hz, 1H), 4.10 – 4.04 (m, 1H), 3.37 (s, 3H), 2.90 (ddd, *J* = 13.3, 10.2, 4.7 Hz, 1H), 2.61 (ddd, *J* = 13.5, 9.7, 7.2 Hz, 1H), 2.50 (dd, *J* = 15.2, 9.0, Hz, 1H), 2.16 (dd, *J* = 15.2, 4.2 Hz, 1H), 1.96 (dddd, *J* = 14.3, 9.9, 9.8, 4.6 Hz, 1H), 1.80 – 1.60 (m, 2H), 1.51 (dddd, *J* = 13.8, 10.4, 6.9, 3.4 Hz, 1H).

¹³C NMR (100 MHz, C₆D₆) δ 171.4, 142.8, 130.3, 129.1, 128.7, 126.1, 123.5, 72.1, 64.7, 51.1, 40.6, 36.1, 32.5, 30.3.

IR (ATR) 3028, 2922, 1739, 1603, 1496, 1436, 1353, 1277, 1212, 1149, 1030, 876, 798, 698 cm⁻¹.

HRMS (ESI) *m/z* calcd. for C₁₆H₂₁O₃ [M+H]⁺ 261.1485, found 261.1494.

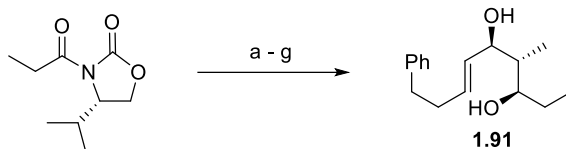
***Cis*-Isomer (faster eluting)**

¹H NMR (400 MHz, C₃D₆O) δ 7.34 – 7.27 (m, 2H), 7.27 – 7.22 (m, 2H), 7.22 – 7.17 (m, 1H), 5.87 – 5.81 (m, 1H), 5.70 (ddt, *J* = 10.2, 2.7, 1.3 Hz, 1H), 4.15 – 4.07 (m, 1H), 4.00 (tt, *J* = 10.2, 3.3, Hz, 1H), 3.71 (s, 3H), 2.80 – 2.67 (m, 2H), 2.57 (d, *J* = 7.0 Hz, 2H), 2.08 – 1.98 (m, 2H), 1.85 – 1.71 (m, 2H).

¹³C NMR (100 MHz, C₃D₆O) δ 172.0, 143.2, 131.2, 129.5, 129.2, 126.6, 125.2, 74.5, 71.6, 51.8, 41.6, 38.2, 31.9, 31.4.

IR (ATR) 3028, 2948, 2919, 1738, 1603, 1436, 1277, 1213, 1068, 1039, 874, 748 cm⁻¹.

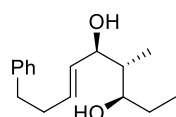
HRMS (ESI) m/z calcd. for $C_{16}H_{21}O_3$ $[M+H]^+$ 261.1485, found 261.1496.



Reagents and conditions

a) Bu_2BOTf , Et_3N , CH_2Cl_2 , $-78\text{ }^\circ\text{C}$, then **S1.2**, $-78\text{ }^\circ\text{C}$ to $0\text{ }^\circ\text{C}$, 63%. b) $TBSOTf$, 2,6-lutidine, CH_2Cl_2 , 83%. c) $LiOH$, H_2O_2 , THF, H_2O , 78%. d) $HN(OMe)Me\cdot HCl$, $EDC\cdot HCl$, iPr_2Et , DMAP, CH_2Cl_2 , 82%. e) $EtMgBr$, THF, $0\text{ }^\circ\text{C}$ to rt, 88%. f) $HF\cdot$ pyridine, THF, 83%. g) $Me_4NB(OAc)_3H$, MeCN, AcOH, $-10\text{ }^\circ\text{C}$, 64%.

Scheme 70. Synthesis of Compound 1.91



(3R,4R,5R, E)-4-Methyl-9-phenylnon-6-ene-3,5-diol (1.91)

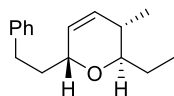
1H NMR (500 MHz, $CDCl_3$) δ 7.31 – 7.24 (m, 2H), 7.21 – 7.14 (m, 3H), 5.70 (dtd, $J = 15.5, 6.6, 1.1$ Hz, 1H), 5.56 (ddt, $J = 15.5, 6.3, 1.2$ Hz, 0.9H), 5.51 – 5.39 (m, 0.2H), 4.36 – 4.32 (m, 0.1H), 4.30 (dd, $J = 6.2, 2.0$ Hz, 0.8H), 3.76 (ddd, $J = 7.8, 6.0, 1.8$ Hz, 0.2H), 3.45 (td, $J = 7.7, 3.7$ Hz, 0.8H), 2.75 – 2.68 (m, 2H), 2.40 (dt, $J = 15.1, 7.5$ Hz, 2H), 1.77 – 1.51 (m, 2H), 1.51 – 1.38 (m, 1H), 0.95 (t, $J = 7.4$ Hz, 2.5H), 0.92 (t, $J = 7.4$ Hz, 0.5H), 0.86 (d, $J = 7.1$ Hz, 0.5H), 0.80 (d, $J = 7.1$ Hz, 2.4H).

^{13}C NMR (125 MHz, $CDCl_3$) δ 141.8, 132.2, 131.6, 130.8, 130.7, 128.6, 128.5, 128.4, 125.9, 76.3, 75.3, 41.9, 41.3, 35.7, 34.1, 28.1, 27.2, 20.8, 12.5, 12.6, 9.6, 4.9.

IR (ATR, neat) 3332, 3023, 2971, 2882, 1494, 1453, 1426, 1377, 1332, 1134, 1029, 966, 748, 698 cm^{-1} .

HRMS (ESI) m/z calcd. for $C_{16}H_{24}O_2Na$ $[M+Na]^+$ 271.1669, found 271.1665.

$[\alpha]_D^{25} = +31.8$ ($c = 0.4$, $CHCl_3$)



(2*R*,3*S*,6*R*)-2-Ethyl-3-methyl-6-phenethyl-3,6-dihydro-2H-pyran (1.92)

The general cyclization procedure was followed with **1.91** (17.2 mg, 0.066 mmol) in HFIP/MeNO₂ (9:1, 0.66 mL, 0.1M). To this, Re₂O₇•SiO₂ (17 mg, 9.1%, 0.0033 mmol) was added and the reaction was stirred for 5 min. The mixture was diluted with CH₂Cl₂ and filtered through a short silica pipette column. The column was flushed with EtOAc (3x) and the solvent was removed under reduced pressure. The crude mixture was purified by flash column chromatography (5% EtOAc in hexanes to 10% EtOAc in hexanes) to afford **1.92** (7.6 mg, 47%) as a colorless oil.

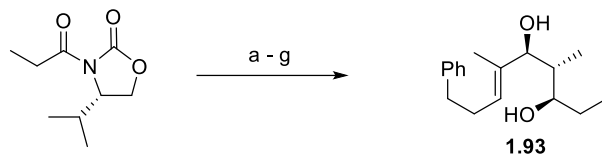
¹H NMR (500 MHz, C₆D₆) δ 7.22 – 7.17 (m, 3H), 7.11 – 7.06 (m, 2H), 5.49 (dt, *J* = 10.0, 2.1 Hz, 1H), 5.45 (dt, *J* = 10.2, 2.2 Hz, 1H), 4.11 – 4.06 (m, 1H), 3.13 (td, *J* = 7.7, 3.9 Hz, 1H), 2.84 (ddd, *J* = 14.1, 10.0, 4.7 Hz, 1H), 2.66 (ddd, *J* = 13.7, 9.7, 7.2 Hz, 1H), 1.99 – 1.91 (m, 1H), 1.91 – 1.83 (m, 1H), 1.61 – 1.56 (m, 1H), 1.56 – 1.49 (m, 2H), 1.09 (t, *J* = 7.4 Hz, 3H), 0.81 (d, *J* = 7.1 Hz, 3H).

¹³C NMR (125 MHz, C₆D₆) δ 142.7, 130.9, 129.4, 128.9, 128.7, 126.1, 75.8, 70.8, 36.2, 34.3, 32.7, 30.2, 26.2, 18.2, 10.8.

IR (ATR) 3027, 2963, 2930, 2875, 1603, 1496, 1453, 1378, 1265, 1088, 1044, 995, 875, 737, 698 cm⁻¹.

HRMS (ESI) *m/z* calcd. for C₁₆H₂₃O [M+H]⁺ 231.1743, found 231.1734.

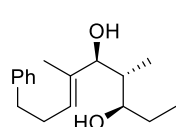
[α]_D²⁵ = +79.8 (c = 0.2, CHCl₃)



Reagents and conditions

a) Bu₂BOTf, Et₃N, CH₂Cl₂, -78 °C, then **S1.1**, -78 °C to 0 °C, 89%. b) TBSOTf, 2,6-lutidine, CH₂Cl₂, 74%, c) LiOH, H₂O₂, THF, H₂O, 64%. d) HN(OMe)Me·HCl, EDC·HCl, *i*Pr₂Et, DMAP, CH₂Cl₂. e) EtMgBr, THF, 0 °C to rt, 59% over 2 steps. f) HF·pyridine, THF, 75%. g) Me₄NB(OAc)₃H, MeCN, AcOH, -10 °C, 47%.

Scheme 71. Synthesis of Compound 1.93



(3*R*,4*R*,5*S*,*E*)-4,6-Dimethyl-9-phenylnon-6-ene-3,5-diol (1.93)

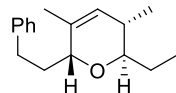
¹H NMR (500 MHz, CDCl₃) δ 7.30 – 7.26 (m, 2H), 7.21 – 7.16 (m, 3H), 5.59 – 5.53 (m, 0.2H), 5.53 – 5.48 (ddd, *J* = 7.2, 1.3, 1.3 Hz, 0.9H), 4.42 – 4.38 (m, 0.2H), 4.36 – 4.31 (m, 0.8H), 3.72 – 3.64 (m, 0.2H), 3.54 (ddd, *J* = 7.3, 5.2, 5.2 Hz, 0.8H), 2.73 – 2.64 (m, 2H), 2.45 – 2.33 (m, 2H), 1.70 (dq, *J* = 14.8, 7.1, 1.9 Hz, 1H), 1.65 – 1.54 (m, 2H), 1.51 (s, 3H), 0.98 (t, *J* = 7.1 Hz, 3H), 0.83 (d, *J* = 7.1 Hz, 2.3H), 0.78 (m, 0.5H).

¹³C NMR (125 MHz, CDCl₃) δ 142.3, 136.4, 128.6, 128.4, 126.0, 125.9, 124.3, 123.8, 80.6, 75.5, 39.1, 38.6, 36.0, 35.9, 29.8, 29.7, 28.4, 28.2, 14.0, 13.6, 10.7, 10.7, 10.5, 10.1, 4.9.

IR (ATR) 3331, 3024, 2928, 2868, 1603, 1493, 1452, 1320, 1125, 1023, 909, 843, 744, 697, 574, 509 cm⁻¹.

HRMS (TOF MS ES⁺) *m/z* calcd. for C₁₇H₂₅O₂ [M-H]⁺ 261.1855, found 261.1878.

[α]_D²⁵ = +4.3 (c = 2.1, CHCl₃)



(2*R*,3*S*,6*R*)-2-Ethyl-3,5-dimethyl-6-phenethyl-3,6-dihydro-2H-pyran (1.94)

The general cyclization procedure was followed with **1.93** (3.5 mg, 0.013 mmol) in HFIP/MeNO₂ (9:1, 0.13 mL, 0.1M). To this, Re₂O₇·SiO₂ (3.5 mg, 9.1%, 0.00066 mmol) was added and the reaction was stirred for 5 min. The mixture was diluted with CH₂Cl₂ and filtered through a short silica pipette column. The column was flushed with EtOAc (3x) and the solvent

was removed under reduced pressure. The crude mixture was purified by flash column chromatography (5% EtOAc in hexanes to 10% EtOAc in hexanes) to afford pyran **1.94** (2.5 mg, 77%) as a colorless oil.

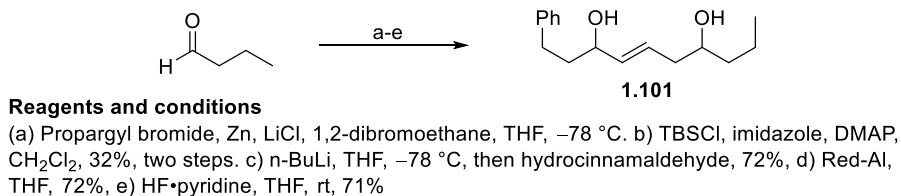
¹H NMR (500 MHz, CDCl₃) δ 7.32 – 7.27 (m, 2H), 7.25 – 7.22 (m, 2H), 7.21 – 7.16 (m, 1H), 5.28 (dq, *J* = 4.3, 1.4 Hz, 1H), 3.96 – 3.92 (m, 1H), 3.13 (td, *J* = 8.8, 2.5 Hz, 1H), 2.91 (ddd, *J* = 14.0, 9.9, 4.4 Hz, 1H), 2.70 (ddd, *J* = 13.7, 9.9, 7.2 Hz, 1H), 2.08 – 1.99 (m, 1H), 1.93 – 1.78 (m, 2H), 1.73 (dq, *J* = 13.8, 8.8, 2.6 Hz, 1H), 1.60 (s, 3H), 1.45 (ddq, *J* = 14.4, 9.3, 7.1 Hz, 1H), 1.07 (t, *J* = 7.3 Hz, 3H), 0.92 (d, *J* = 7.0 Hz, 3H).

¹³C NMR (125 MHz, CDCl₃) δ 142.6, 134.9, 128.7, 128.5, 126.5, 125.8, 75.3, 74.9, 34.8, 33.6, 32.5, 26.2, 19.8, 18.2, 11.1.

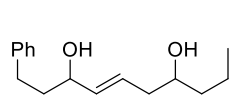
IR (ATR) 3025, 2923, 2853, 1500, 1448, 1351, 1229, 1145, 1031, 899, 748, 699 cm⁻¹.

HRMS (ESI) *m/z* calcd. for C₁₇H₂₅O [M-H]⁺ 245.1905, found 245.1916.

[α]_D²⁵ = -11.0 (c = 0.6, CHCl₃)



Scheme 72. Synthesis of Compound 1.101



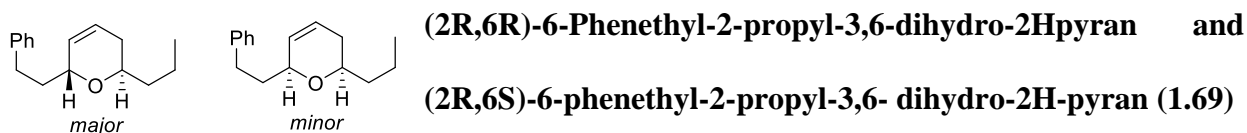
(*E*)-1-Phenyldec-4-ene-3,7-diol (1.101)

¹H NMR (400 MHz, CDCl₃) δ 7.33 – 7.25 (m, 2H), 7.24 – 7.15 (m, 3H), 5.77 – 5.56 (m, 2H), 4.18 – 4.06 (m, 1H), 3.72 – 3.60 (m, 1H), 2.80 – 2.62 (m, 2H), 2.33 – 2.22 (m, 1H), 2.19 – 2.09 (m, 1H), 1.92 – 1.77 (m, 2H), 1.54 – 1.42 (m, 2H), 1.42 – 1.23 (m, 2H), 0.99 – 0.90 (m, 3H).

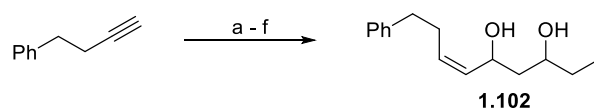
^{13}C NMR (100 MHz, CDCl_3) δ 142.0, 136.4, 136.4, 128.6, 128.5, 128.1, 127.9, 126.0, 72.2, 72.2, 70.9, 40.5, 40.3, 39.3, 39.2, 38.9, 31.9, 18.9, 14.3, 14.2.

IR (ATR, neat) 3333, 3027, 2955, 2928, 2869, 1453, 1313, 1122, 1057, 1026, 971, 745, 698, 543 cm^{-1} .

HRMS (ESI) m/z calcd. for $\text{C}_{16}\text{H}_{24}\text{O}_2\text{Na}$ $[\text{M}+\text{Na}]^+$ 271.1669, found 271.1666.



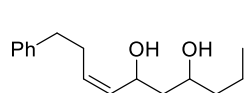
The general cyclization procedure was followed with **1.101** (20.7 mg, 0.083 mmol) in HFIP/ MeNO_2 (9:1, 0.83 mL, 0.1M). To this, $\text{Re}_2\text{O}_7 \cdot \text{SiO}_2$ (22.2 mg, 9.1%, 0.00417 mmol) was added and the reaction was stirred for 5 min. The mixture was diluted with CH_2Cl_2 and filtered through a short silica pipette column. The column was flushed with EtOAc (3x) and the solvent was removed under reduced pressure. The crude mixture was purified by flash column chromatography (5% Et_2O in hexanes to 10% Et_2O in hexanes) to afford **1.69** (13.3 mg, 69%, d.r. = 3.3:1) as a colorless oil.



Reagents and conditions

a) $n\text{-BuLi}$, DMF, THF, -78°C , 49%. b) LDA, 2-butanone, THF, -78°C , 56%. c) TBSCl, imidazole, CH_2Cl_2 , 63%. d) NaBH_4 , MeOH, 0°C , 71%. e) H_2 , $\text{Ni}(\text{OAc})_2 \cdot 4\text{H}_2\text{O}$, NaBH_4 , TMEDA, EtOH, 73%. f) $\text{HF} \cdot \text{Py}$, THF, rt, 67%.

Scheme 73. Synthesis of Compound 1.102



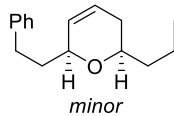
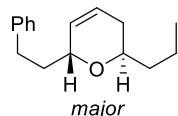
(Z)-10-Phenyldec-7-ene-4,6-diol (1.102)

^1H NMR (500 MHz, CDCl_3) δ 7.31 – 7.26 (m, 2H), 7.22 – 7.15 (m, 3H), 5.53 – 5.45 (m, 1.3H), 5.38 (t, J = 9.5, 1.2 Hz, 0.6H), 4.56 (td, J = 7.6, 3.7 Hz, 0.3H), 4.45 (td, J = 9.2, 3.3 Hz, 0.6H), 3.87 – 3.81 (m, 0.3H), 3.75 – 3.67 (m, 0.6H), 2.83 (s, 0.5H), 2.75 – 2.59 (m, 2H), 2.52 – 2.33 (m, 2H), 2.25 (s, 0.3H), 2.01 (s, 0.5H), 1.73 (s, 0.3H), 1.60 – 1.22 (m, 6H), 0.96 – 0.88 (m, 3H).

^{13}C NMR (125 MHz, CDCl_3) δ 141.6, 133.3, 133.2, 130.4, 130.1, 128.9, 128.8, 128.5, 126.2, 72.0, 69.0, 68.6, 65.6, 43.2, 42.9, 40.3, 39.8, 35.8, 35.8, 29.8, 29.8, 19.0, 18.7, 14.2.

IR (ATR, neat) 3337, 3022, 2929, 2867, 1602, 1494, 1451, 1310, 1126, 1069, 1026, 840, 739, 698 cm^{-1} .

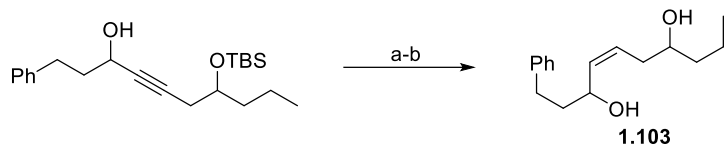
HRMS (ESI) m/z calcd. for $\text{C}_{16}\text{H}_{24}\text{O}_2\text{Na}$ $[\text{M}+\text{Na}]^+$ 271.1668, found 271.1666.



(2R,6R)-6-Phenethyl-2-propyl-3,6-dihydro-2H-pyran and

(2R,6S)-6-Phenethyl-2-propyl-3,6-dihydro-2H-pyran (1.69)

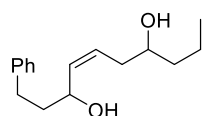
The general Re_2O_7 cyclization procedure was followed with **1.102** (16.0 mg, 0.064 mmol) in HFIP/ MeNO_2 (9:1, 0.64 mL, 0.1M). To this, $\text{Re}_2\text{O}_7 \cdot \text{SiO}_2$ (17.1 mg, 9.1%, 0.00322 mmol) was added and the reaction was stirred for 5 min. The mixture was diluted with CH_2Cl_2 and filtered through a short silica pipette column. The column was flushed with EtOAc (3x) and the solvent was removed under reduced pressure. The crude mixture was purified by flash column chromatography (5% Et_2O in hexanes to 10% Et_2O in hexanes) to afford **1.69** (10.0 mg, 67%, d.r. = 3.3:1) as a colorless oil.



Reagents and conditions

a) H_2 , $\text{Ni}(\text{OAc})_2 \cdot 4\text{H}_2\text{O}$, NaBH_4 , TMEDA, EtOH, 51%. b) $\text{HF} \cdot \text{Py}$, THF, 59%.

Scheme 74. Synthesis of Compound 1.103



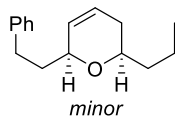
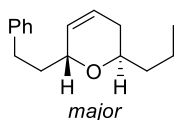
(Z)-1-Phenyldec-4-ene-3,7-diol (1.103)

^1H NMR (500 MHz, CDCl_3) δ 7.30 – 7.25 (m, 2H), 7.22 – 7.15 (m, 3H), 5.72 – 5.56 (m, 2H), 4.41 (ddt, $J = 13.3, 7.5, 6.0$ Hz, 1H), 3.71 (tt, $J = 5.8, 4.9$ Hz, 0.5H), 3.66 – 3.56 (m, 0.6H), 2.79 – 2.61 (m, 2H), 2.43 – 2.07 (m, 3H), 2.00 – 1.89 (m, 1H), 1.86 – 1.72 (m, 1H), 1.53 – 1.28 (m, 5H), 0.94 (t, $J = 6.1$ Hz, 3H).

^{13}C NMR (125 MHz, CDCl_3) δ 142.1, 142.1, 135.9, 129.5, 128.6, 128.5, 127.9, 125.9, 125.9, 70.8, 70.5, 66.8, 66.1, 39.9, 38.9, 38.8, 38.7, 35.8, 34.9, 31.9, 31.9, 19.2, 19.0, 14.2.

IR (ATR, neat) 3327, 2955, 2928, 2869, 1453, 1378, 1276, 1121, 1059, 1013, 911, 875, 747, 697 cm^{-1} .

HRMS (ESI) m/z calcd. for $\text{C}_{16}\text{H}_{24}\text{O}_2\text{Na}$ $[\text{M}+\text{Na}]^+$ 271.1668, found 271.1667.

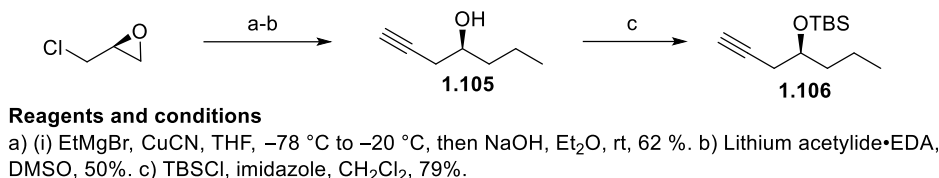


(2R,6R)-6-Phenethyl-2-propyl-3,6-dihydro-2H-pyran and

(2R,6S)-6-Phenethyl-2-propyl-3,6-dihydro-2H-pyran (1.69)

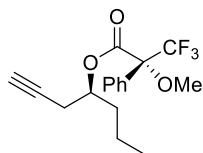
The general Re_2O_7 cyclization procedure was followed with **1.103** (18.4 mg, 0.0741 mmol) in $\text{HFIP}/\text{MeNO}_2$ (9:1, 0.74 mL, 0.1M). To this, $\text{Re}_2\text{O}_7 \cdot \text{SiO}_2$ (17.9 mg, 9.1%, 0.00370 mmol) was added and the reaction was stirred for 5 min. The mixture was diluted with CH_2Cl_2 and filtered through a short silica pipette column. The column was flushed with EtOAc (3x) and the solvent was removed under reduced pressure. The crude mixture was purified by flash column

chromatography (5% Et₂O in hexanes to 10% Et₂O in hexanes) to afford **1.69** (16.4 mg, 96%, d.r. = 3.7:1) as a colorless oil.



Scheme 75. Synthesis of Compound 1.106

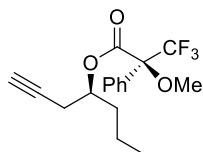
Mosher Ester Analysis of Compound 1.105⁴⁴



To a solution of pyridine (24.0 μ L, 0.301 mmol) in CH₂Cl₂ (1.4 mL, 0.07M) was added alcohol **1.105** (10.9 mg, 0.097 mmol), followed by (*S*)-(+)-MTPA-Cl (34.6 μ L, 0.185 mmol). The reaction mixture was stirred for 2 h. The reaction mixture was quenched with water, and the organic layer was partitioned with Et₂O. The ether layer was isolated and was dried over Na₂SO₄. The crude mixture was concentrated in vacuo and purified by flash column chromatography (10% EtOAc in hexanes) provided the (*R*)-Mosher ester.

¹H NMR (400 MHz, CDCl₃) δ 7.57 – 7.53 (m, 2H), 7.42 – 7.38 (m, 3H), 5.18 (tt, *J* = 6.7, 5.7 Hz, 1H), 3.55 (s, 3H), 2.57 – 2.46 (m, 2H), 1.93 (t, *J* = 2.6 Hz, 1H), 1.82 – 1.69 (m, 2H), 1.47 – 1.31 (m, 2H), 0.94 (t, *J* = 7.4 Hz, 3H).

¹⁹F NMR (376 MHz, CDCl₃) δ -71.4 ppm (minor, 0.04 F), -71.6 ppm. (major, 3 F)

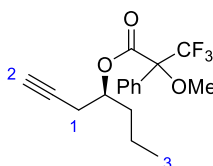


To a solution of **1.105** (10 mg, 0.0892 mmol) in CH₂Cl₂ (1.4 mL, 0.064M) was added (*S*)-MTPA-OH (64.7 mg, 0.276 mmol) and DMAP (33.7 mg, 0.276 mmol). DCC (56 mg, 0.276 mmol) was then added and the reaction was stirred for 18 h. The resulting suspension was filtered through a cotton plug, and the solvent was removed

in vacuo. Purification by flash column chromatography (10% EtOAc in hexanes) provided the (*S*)-Mosher ester.

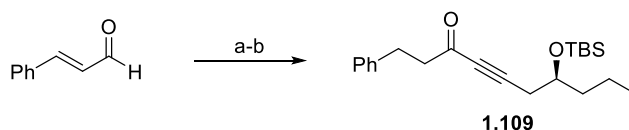
¹H NMR (400 MHz, CDCl₃) δ 7.61 – 7.57 (m, 2H), 7.45 – 7.34 (m, 3H), 5.19 (tt, 6.7, 5.3 Hz, 1H), 3.61 (s, 3H), 2.62 (dq, *J* = 17.1, 2.7, 1H), 2.53 (dq, *J* = 17.2, 2.9 Hz, 1H), 2.03 (t, *J* = 2.7 Hz, 1H), 1.78 – 1.68 (m, 1H), 1.67 – 1.59 (m, 1H), 1.32 – 1.15 (m, 4H), 0.86 (t, *J* = 7.4 Hz, 3H).

¹⁹F NMR (376 MHz, CDCl₃) δ –71.4 ppm (major, 3F), –71.7 ppm (minor, 0.04 F).



H#	δ (<i>S</i>)-MTPA Ester	δ (<i>R</i>)-MTPA Ester	Δδ = δ(<i>S</i>) – δ(<i>R</i>)
1	2.548	2.514	+ 0.034
2	2.011	1.927	+ 0.084
3	0.833	0.943	– 0.110

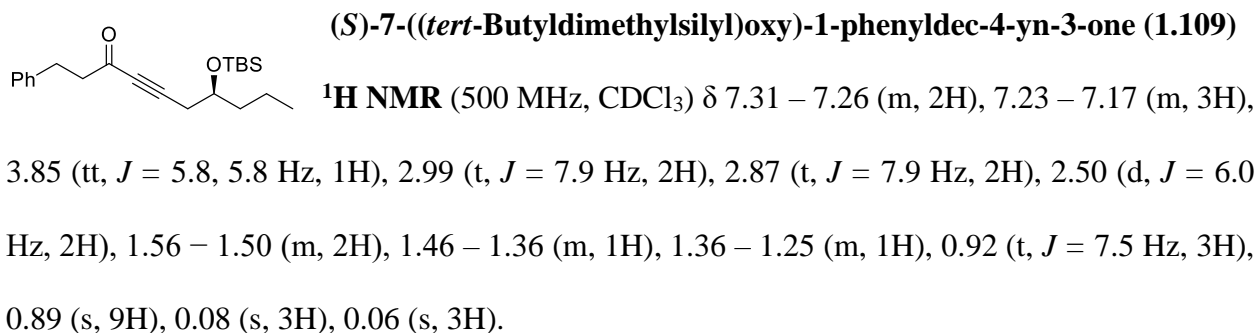
Table 8. Mosher Ester Analysis of 1.105



Reagents and conditions

a) TMSCN, DBU, THF, then MeON(H)Me, Et₃N, 63%. b) **1.105**, *n*-BuLi, THF, –78 °C, 48%.

Scheme A-1. Synthesis of Compound 1.109



¹³C NMR (125 MHz, CDCl₃) δ 187.0, 140.5, 128.7, 128.5, 126.4, 92.2, 82.2, 70.2, 47.1, 39.4, 30.1, 28.1, 18.5, 18.2, 14.2, −4.4, −4.5.

IR (ATR, neat) 2932, 2859, 2213, 1675, 1462, 1363, 1252, 1087, 1040, 975, 933, 835, 775, 699, 562 cm^{−1}.

HRMS (ESI) *m/z* calcd. for C₂₂H₃₅O₂Si [M+H]⁺ 359.2401, found 359.2385.

[α]_D²⁵ = −24.4 (c = 1.2, CHCl₃)



A solution of ketone **1.109** (0.374 g, 1.04 mmol) under argon in CH₂Cl₂ (3.1 mL, 0.34 M) was cooled to 0 °C. RuCl(*p*-cymene)[(*R,R*)-Ts-DPEN], (0.0132 g, 0.0208 mmol), and triethylamine (0.45 mL, 3.22 mmol) were added to the flask, followed by formic acid (0.27 mL, 7.28 mmol) in CH₂Cl₂ (2 mL). The reaction was stirred overnight at ambient temperature. Upon completion, some of the CH₂Cl₂ was removed under reduced pressure, and the reaction mixture was then diluted with pentane. K₂CO₃ (0.604 g, 4.37 mmol) and MgSO₄ (0.376 g, 3.12 mmol) were added simultaneously. The mixture was stirred for 2 h, then was diluted with CH₂Cl₂ and filtered through a short silica pad. The silica pad was rinsed with Et₂O twice and the combined organics were isolated under reduced pressure. The crude mixture was further purified by column chromatography (15% EtOAc in hexanes) to yield **1.110** (0.256 g, 68%) in 96% de confirmed by Mosher ester analysis.

¹H NMR (400 MHz, CDCl₃) δ 7.32 – 7.25 (m, 2H), 7.24 – 7.17 (m, 3H), 4.41 – 4.33 (m, 1H), 3.79 (tt, *J* = 5.9, 5.8 Hz, 1H), 2.79 (t, *J* = 7.9 Hz, 2H), 2.43 – 2.31 (m, 2H), 2.07 – 1.94 (m, 2H), 1.79 (d, *J* = 4.4 Hz, 1H), 1.67 – 1.57 (m, 1H), 1.57 – 1.49 (m, 1H), 1.49 – 1.37 (m, 1H), 1.37 – 1.24 (m, 1H), 0.92 (t, *J* = 7.5 Hz, 3H), 0.90 (s, 9H), 0.08 (s, 3H), 0.07 (s, 3H).

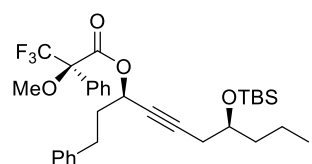
^{13}C NMR (100 MHz, CDCl_3) δ 141.6, 128.6, 128.5, 126.1, 83.3, 82.6, 70.9, 62.2, 39.7, 39.1, 27.8, 26.0, 18.6, 18.2, 14.3, -4.3 , -4.5 .

IR (ATR, neat) 3026, 2955, 2929, 2857, 1603, 1462, 1496, 1471, 1455, 1361, 1252, 1083, 1040, 1006, 936, 834, 774, 754 cm^{-1} .

HRMS (ESI) m/z calcd. for $\text{C}_{22}\text{H}_{37}\text{O}_2\text{Si}$ $[\text{M}+\text{H}]^+$ 361.2557, found 361.2559.

$[\alpha]_D^{25} = -10.0$ ($c = 0.5$, CHCl_3)

Mosher Ester Analysis of Compound **1.110**⁴⁴

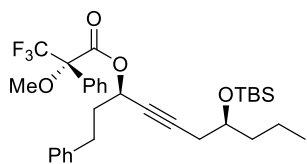


To a solution of **1.110** (7.10 mg, 0.0197 mmol) in CH_2Cl_2 (0.31 mL, 0.064M) was added (*R*)- MTPA-OH (14.2 mg, 0.0610 mmol) and DMAP (1 crystal). DCC (12.6 mg, 0.0610 mmol) was then added and

the reaction was stirred for 18 h. The resulting suspension was filtered through a cotton plug, and the solvent was removed in vacuo. Purification by flash column chromatography on silica gel (10% EtOAc in hexanes) provided (*R*)-Mosher ester.

^1H NMR (400 MHz, CDCl_3) δ 7.62 – 7.56 (m, 2H), 7.44 – 7.37 (m, 3H), 7.30 – 7.27 (m, 1H), 7.26 – 7.24 (m, 1H), 7.22 – 7.16 (m, 1H), 7.13 – 7.07 (m, 2H), 5.55 (tt, $J = 6.5$, 1.9 Hz, 2H), 3.78 (tt, $J = 9.3$, 5.8 Hz, 1H), 3.60 (s, 3H), 2.69 (ddd, $J = 14.0$, 9.4, 6.3 Hz, 1H), 2.61 (ddd, $J = 13.8$, 9.0, 6.8 Hz, 1H), 2.43 – 2.32 (m, 2H), 2.16 – 2.00 (m, 2H), 1.61 – 1.47 (m, 3H), 1.47 – 1.35 (m, 1H), 1.35 – 1.20 (m, 2H), 0.89 (t, $J = 7.4$ Hz, 3H), 0.88 (s, 9H), 0.06 (s, 3H), 0.05 (s, 3H).

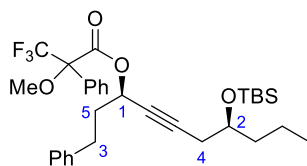
^{19}F NMR (376 MHz, CDCl_3) δ -71.5 ppm (major, 3F), -71.8 ppm (minor, 0.05F).



To a solution of **1.110** (6.10 mg, 0.0169 mmol) in CH₂Cl₂ (0.26 mL, 0.064M) was added (*S*)-MTPA-OH (12.3 mg, 0.0524 mmol) and DMAP (1 crystal). DCC (10.8 mg, 0.0524 mmol) was then added and the reaction was stirred for 18 h. The resulting suspension was filtered through a cotton plug, and the solvent was removed in vacuo. Purification by flash column chromatography on silica gel (10% EtOAc in hexanes) provided (*S*)-Mosher ester.

¹H NMR (400 MHz, CDCl₃) δ 7.59 – 7.52 (m, 2H), 7.45 – 7.37 (m, 3H), 7.33 – 7.26 (m, 2H), 7.24 – 7.19 (m, 1H), 7.19 – 7.14 (m, 2H), 5.54 (tt, *J* = 6.5, 1.9 Hz, 1H), 3.76 (tt, *J* = 9.0, 5.9 Hz, 1H), 3.56 (s, 3H), 2.80 (dt, *J* = 14.1, 6.9 Hz, 1H), 2.74 (dt, *J* = 14.0, 7.0 Hz, 1H), 2.40 – 2.29 (m, 2H), 2.22 – 2.06 (m, 2H), 1.56 – 1.46 (m, 3H), 1.46 – 1.38 (m, 1H), 1.38 – 1.27 (m, 2H), 0.89 (t, 7.4 Hz, 3H), 0.87 (s, 9H), 0.04 (s, 6H).

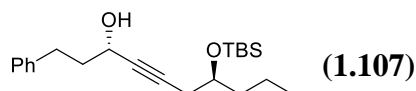
¹⁹F NMR (376 MHz, CDCl₃) δ –71.5 ppm (minor, 0.06F), –71.8 ppm (major, 3F).



H#	δ (<i>S</i>)-MTPA Ester	δ (<i>R</i>)-MTPA Ester	Δ δ= δ(<i>S</i>) – δ (<i>R</i>)
1	5.536	5.555	– 0.019
2	3.752	3.769	– 0.017
3	2.805	2.695	+ 0.110
3'	2.730	2.627	+ 0.103
4	2.348	2.376	– 0.028
5	2.140	2.083	+ 0.057

Table 9. Mosher Ester Analysis of 1.110

(3*S*,7*S*)-7-((*tert*-Butyldimethylsilyl)oxy)-1-phenyldec-4-yn-3-ol



A solution of ketone **1.109** (0.500 g, 1.39 mmol) under argon in CH₂Cl₂ (3.2 mL, 0.34 M) was cooled to 0 °C. RuCl(*p*-cymene)[(*S,S*)-Ts-DPEN], (0.0177 g, 0.0278 mmol), and triethylamine (0.61 mL, 4.31 mmol) were added to the flask, followed by formic acid (0.37 mL, 9.73 mmol) in 2 mL of CH₂Cl₂ and the reaction was stirred overnight at ambient temperature. Upon completion, some of the CH₂Cl₂ was removed under reduced pressure, and the reaction mixture was then diluted with pentane. K₂CO₃ (0.633 g, 4.58 mmol) and MgSO₄ (0.394 g, 3.27 mmol) were added simultaneously. The mixture was stirred for 2 h. The mixture was diluted with CH₂Cl₂ and filtered through a short silica pad. The silica pad was rinsed with Et₂O twice and the combined organics were isolated under reduced pressure. The crude mixture was further purified by column chromatography (15% EtOAc in hexanes) to yield **1.107** (0.37 g, 75%), in 96% de confirmed by Mosher ester analysis.

¹H NMR (500 MHz, CDCl₃) δ 7.31 – 7.26 (m, 2H), 7.23 – 7.17 (m, 3H), 4.37 (ddt, *J* = 11.9, 6.2, 1.9 Hz, 1H), 3.79 (tt, *J* = 6.6, 5.2 Hz, 1H), 2.79 (t, *J* = 7.9, 2H), 2.41 – 2.31 (m, 2H), 2.09 – 1.94 (m, 2H), 1.71 (d, *J* = 5.4 Hz, 1H), 1.62 – 1.55 (m, 1H), 1.55 – 1.46 (m, 1H), 1.45 – 1.38 (m, 1H), 1.37 – 1.27 (m, 1H), 0.92 (t, *J* = 7.5 Hz, 3H), 0.89 (s, 9H), 0.08 (s, 3H), 0.06 (s, 3H).

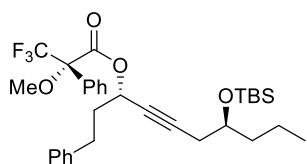
¹³C NMR (125 MHz, CDCl₃) δ 141.6, 128.6, 128.5, 126.1, 83.3, 82.6, 80.0, 62.2, 39.7, 39.2, 31.6, 27.8, 26.0, 18.6, 18.2, 14.3, – 4.3, – 4.5.

IR (ATR, neat): 3027, 2929, 2953, 2856, 1604, 1495, 1272, 1359, 1252, 1140, 1081, 1044, 900, 835, 774, 748, 698 cm⁻¹.

HRMS (TOF MS ES⁺) *m/z* calcd. for C₂₂H₃₅O₂Si [M–H]⁺ 359.2406, found 359.2421.

[α]_D²⁵ = – 13.2 (c = 0.4, CHCl₃)

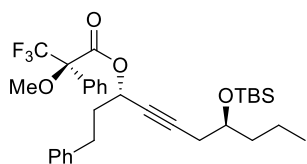
Mosher Ester Analysis of Compound **1.107**⁴⁴



To a solution of **1.107** (9.6 mg, 0.0266 mmol) in CH₂Cl₂ (0.42 mL, 0.064M) was added (*S*)-MTPA-OH (19.3 mg, 0.0825 mmol) and DMAP (10.8 mg, 0.0825 mmol). DCC (17.0 mg, 0.0825 mmol) was then added and the reaction was stirred for 18 h. The resulting suspension was filtered through a cotton plug, and the solvent was removed in vacuo. Purification by flash column chromatography on silica gel (10% EtOAc in hexanes) provided (*S*)-Mosher ester.

¹H NMR (400 MHz, CDCl₃) δ 7.62 – 7.54 (m, 2H), 7.45 – 7.37 (m, 3H), 7.31 – 7.26 (m, 1H), 7.26 – 7.23 (m, 1H), 7.22 – 7.16 (m, 1H), 7.12 – 7.06 (m, 2H), 5.54 (tt, *J* = 6.5, 1.9 Hz, 1H), 3.78 (tt, *J* = 5.8, 5.7 Hz, 1H), 3.60 (s, 3H), 2.73 – 2.57 (m, 2H), 2.39 (ddd, *J* = 16.6, 5.1, 1.9 Hz, 1H), 2.35 (ddd, *J* = 16.7, 6.6, 1.9 Hz, 1H), 2.16 – 2.00 (m, 2H), 1.60 – 1.56 (m, 1H), 1.55 – 1.47 (m, 2H), 1.47 – 1.36 (m, 1H), 0.88 (t, *J* = 7.3 Hz, 3H), 0.88 (s, 9H), 0.06 (s, 3H), 0.05 (s, 3H).

¹⁹F NMR (376 MHz, CDCl₃) δ –71.5 ppm (major, 3F), –71.8 ppm (minor, 0.05F).

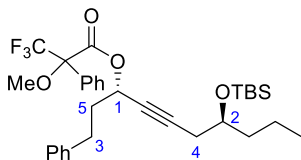


To a solution of **1.107** (8.7 mg, 0.0241 mmol) in CH₂Cl₂ (0.38 mL, 0.064M) was added (*R*)-MTPA-OH (17.5 mg, 0.0747 mmol) and DMAP (9.13 mg, 0.0747 mmol). DCC (15.4 mg, 0.0747 mmol) was then added and the reaction was stirred for 18 h. The resulting suspension was filtered through a cotton plug, and the solvent was removed in vacuo. Purification by flash column chromatography on silica gel (10% EtOAc in hexanes) provided (*R*)-Mosher ester.

¹H NMR (400 MHz, CDCl₃) δ 7.44 – 7.38 (m, 3H), 7.32 – 7.27 (m, 2H), 7.23 – 7.14 (m, 3H), 5.54 (tt, *J* = 9.9, 1.8 Hz, 1H), 3.76 (tt, *J* = 5.9, 5.7 Hz, 1H), 3.56 (s, 3H), 2.83 – 2.70 (m, 2H), 2.37 (ddd,

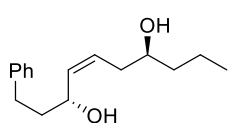
$J = 16.7, 5.5, 1.9$ Hz, 1H), 2.32 (ddd, $J = 16.8, 6.6, 1.9$ Hz, 1H), 2.22 – 2.07 (m, 2H), 1.61 – 1.54 (m, 2H), 1.54 – 1.45 (m, 1H), 1.45 – 1.36 (m, 1H), 0.88 (t, $J = 7.2$ Hz, 3H), 0.87 (s, 9H), 0.06 (s, 3H), 0.05 (s, 3H).

^{19}F NMR (376 MHz, CDCl_3) δ –71.5 ppm (minor, 0.06F), –71.8 ppm (major, 3F).



H#	δ (S)-MTPA Ester	δ (R)-MTPA Ester	$\Delta \delta = \delta(\text{S}) - \delta(\text{R})$
1	5.539	5.534	+ 0.005
2	3.778	3.758	+ 0.020
3	2.652	2.765	– 0.113
4	2.394	2.369	+ 0.025
4'	2.350	2.325	+ 0.025
5	2.082	2.140	– 0.058

Table 10. Mosher Ester Analysis of 1.107



(3R,7S,Z)-1-Phenyldec-4-ene-3,7-diol (1.112)

To a flask charged with a stir bar was added $\text{Ni}(\text{OAc})_2 \cdot 4\text{H}_2\text{O}$ (0.0549 g, 0.221 mmol). The flask was flushed under an atmosphere of H_2 . Ethanol (2.2 mL, 0.2 M) was added and the solution was stirred vigorously. Within 30 s, a solution of 1M NaBH_4 in ethanol (0.18 mL, 0.176 mol), stabilized by two drops of 0.1M NaOH , was added and the reaction stirred for 5 min. TMEDA (46.0 μL , 0.309 mmol) was added and the solution stirred again for 5 min. Alkyne **1.110** (0.16 g, 0.441 mmol) was added and the reaction was monitored by TLC and NMR analysis until all of the starting material was consumed. Once consumed, the reaction vessel was opened and quenched with water. The mixture was added to a separatory funnel and the aqueous layer was

extracted with EtOAc (3 x 15 mL) and the organic layers were combined. The combined organic layers were washed with brine, dried with Na₂SO₄ and concentrated under reduced pressure to afford the crude (Z)-alkene (0.139 g, 86% yield) as a colorless oil.

The alkene (0.138 g, 0.381 mmol) was dissolved in THF (5 mL, 0.0767 M) and added to a 50 mL polypropylene tube. To this was added a 70% solution of HF•pyridine (0.70 mL, 19.0 mmol), and the reaction was stirred overnight. The reaction mixture was then cooled to 0 °C and quenched with saturated NaHCO₃. The mixture was transferred to a separatory funnel and the aqueous layer was extracted with EtOAc (3 x 15 mL). The organic layers were combined, dried over MgSO₄, filtered, and concentrated. The crude mixture was then purified by column chromatography (30% EtOAc in hexanes to 40% EtOAc in hexanes) to afford diol **1.112** (0.048 g, 51% yield).

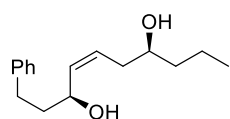
¹H NMR (400 MHz, CDCl₃) δ 7.31 – 7.25 (m, 2H), 7.23 – 7.15 (m, 3H), 5.67 (dd, *J* = 11.0, 7.4 Hz, 1H), 5.60 (dt, *J* = 10.8, 6.8 Hz, 1H), 4.42 (dt, *J* = 7.3, 6.7 Hz, 1H), 3.73 (tt, *J* = 9.1, 5.3 Hz, 1H), 2.74 (ddd, *J* = 13.6, 9.4, 6.3 Hz, 1H), 2.67 (ddd, *J* = 13.5, 8.9, 6.4 Hz, 1H), 2.39 (ddd, *J* = 14.3, 7.4, 4.7 Hz, 1H), 2.21 (dt, *J* = 14.1, 6.7 Hz, 1H), 1.99 – 1.89 (m, 1H), 1.87 – 1.73 (m, 1H), 1.51 – 1.39 (m, 3H), 1.39 – 1.29 (m, 1H), 0.93 (t, *J* = 7.0 Hz, 3H).

¹³C NMR (100 MHz, CDCl₃) δ 142.1, 135.9, 128.6, 128.5, 128.0, 126.0, 70.8, 66.7, 38.9, 38.8, 35.0, 31.9, 19.2, 14.2.

IR (ATR, neat) 3331, 3022, 2927, 2867, 1603, 1494, 1452, 1316, 1121, 1015, 909, 837, 744, 698 cm⁻¹.

HRMS (ESI) *m/z* calcd. for C₁₆H₂₄O₂Na [M+Na]⁺ 271.1669, found 271.1666.

[α]_D²⁵ = + 13.0 (c = 1.0, CHCl₃)



(3S,7S,Z)-1-Phenyldec-4-ene-3,7-diol (1.113)

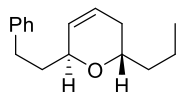
¹H NMR (400 MHz, CDCl₃) δ 7.31 – 7.25 (m, 2H), 7.23 – 7.15 (m, 3H), 5.67 (dd, *J* = 10.8, 8.5 Hz, 1H), 5.60 (dt, *J* = 10.5, 6.1 Hz, 1H), 4.40 (dt, *J* = 7.1, 7.1 Hz, 1H), 3.64 – 3.56 (m, 1H), 2.72 (ddd, *J* = 13.8, 9.8, 6.2 Hz, 1H), 2.67 (ddd, *J* = 13.8, 9.7, 6.0 Hz, 1H), 2.29 (ddd, *J* = 14.1, 9.6, 9.6 Hz, 1H), 2.12 (dddd, *J* = 13.8, 6.0, 3.0, 1.2 Hz, 1H), 2.00 – 1.90 (m, 1H), 1.83 – 1.72 (m, 1H), 1.53 – 1.31 (m, 5H), 0.94 (t, 7.04 Hz, 3H).

¹³C NMR (75 MHz, CDCl₃) δ 142.1, 135.9, 129.5, 128.6, 128.5, 125.9, 70.6, 66.1, 39.9, 38.7, 35.8, 31.9, 19.0, 14.2.

IR (ATR, neat) 3327, 2954, 2927, 2868, 1494, 1453, 1376, 1273, 1124, 1027, 910, 876, 747, 698 cm⁻¹.

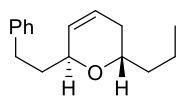
HRMS (ESI) *m/z* calcd. for C₁₆H₂₃O [M–OH]⁺ 231.1743, found 231.1735.

$[\alpha]_D^{25} = +11.6$ (*c* = 0.4, CHCl₃)



(2S,6S)-6-Phenethyl-2-propyl-3,6-dihydro-2H-pyran (*ent*-1.69)

The general cyclization procedure was followed with **1.112** (15.2 mg, 0.0612 mmol) which was dissolved in HFIP/MeNO₂ (9:1, 0.61 mL, 0.1M). To this, Re₂O₇•SiO₂ (10%, 14.8 mg, 0.00306 mmol) was added and the reaction was stirred for 5 min. The reaction mixture was diluted with CH₂Cl₂ and filtered through a short silica pipette column. The column was flushed with EtOAc (3x) and the crude mixture isolated under reduced pressure. The mixture was purified by flash chromatography (5% Et₂O in hexanes to 10% Et₂O in hexanes) to afford ***ent*-1.69** (13.3 mg, 94%, d.r. = 2.1:1) as a colorless oil.



(2*S*,6*S*)-6-Phenethyl-2-propyl-3,6-dihydro-2*H*-pyran (*ent*-1.69)

The general Re_2O_7 cyclization procedure was followed with **1.113** (13.5 mg, 0.0544 mmol), which was dissolved in HFIP/ MeNO_2 (9:1, 0.54 mL, 0.1M). To this, $\text{Re}_2\text{O}_7 \cdot \text{SiO}_2$ (10%, 13.2 mg, 0.00272 mmol) was added and the reaction was monitored until complete consumption of starting material (5 min). The reaction mixture was diluted with CH_2Cl_2 and filtered through a short silica pipette column. The column was flushed with EtOAc (3x) and the crude mixture isolated under reduced pressure. The mixture was purified by flash chromatography (5% Et_2O in hexanes to 10% Et_2O in hexanes) to afford pyran ***ent*-1.69** (10.8 mg, 86%, dr = 8.1:1) as a colorless oil.

HPLC analysis – diastereocontrol: The sample was analyzed with a Phenomenex Lux 5u Cellulose-3 column using 5% *i*PrOH in hexane as a solvent. Retention time (*cis*) = 3.67 min, retention time (*trans*) = 4.22 min.

HPLC analysis – enantiocontrol: The sample was analyzed with a Phenomenex Lux 5u Cellulose-3 column using 3.5% *i*PrOH in hexane as a solvent. Retention time (minor) = 7.82 min, retention time (major) = 8.67 min.

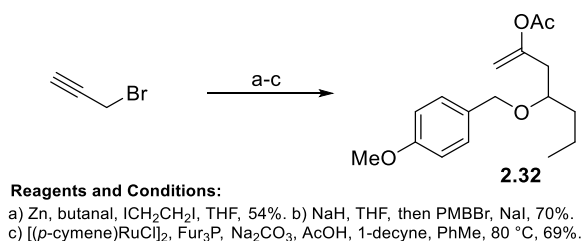
Appendix B

General Information

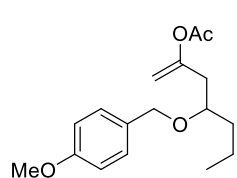
(^1H NMR) and carbon (^{13}C NMR) nuclear magnetic resonance spectra were taken on a Bruker Avance 300 spectrometer at 300 MHz and 75 MHz respectively, a Bruker Avance 400 spectrometer at 400 MHz and 100 MHz, or a Bruker Avance 500 spectrometer at 500 MHz and 125 MHz as specified. The chemical shifts are reported in parts per million (ppm) on the delta (δ) scale. The solvent peak was used as a reference value, for ^1H NMR: $\text{CDCl}_3 = 7.26$ ppm, $\text{C}_6\text{D}_6 = 7.16$ ppm, $\text{CF}_3\text{COOD} = 11.5$ ppm or for ^{13}C NMR: $\text{CDCl}_3 = 77.16$ ppm, $\text{C}_6\text{D}_6 = 128.06$ ppm, $\text{CF}_3\text{COOD} = 164.2$ and 116.6 ppm. Data are reported as follows: m = multiplet, s = singlet; d = doublet; t = triplet; dd = doublet of doublets; dt = doublet of triplets; ddq = doublet of doublet of quartets; ddd = doublet of doublet of doublets etc. Infrared (IR) spectra were taken on a Nicolet IR200 FT-IR spectrometer with an ATR attachment. Methylene chloride and acetonitrile were distilled under N_2 from CaH_2 . Diethyl Ether and tetrahydrofuran were distilled over sodium/benzophenone under N_2 . 2,2,2-Trifluoroethanol was purchased from Sigma Aldrich and used as is. Bobbitt's Salt, 4-acetamido-2,2,6,6-tetramethylpiperidine 1-oxyl and Tetrabutyl ammonium tetrafluoroborate were purchased from TCI Chemicals, stored in a desiccator and used as is. All electrodes and Electrasyn 2.0 were purchased from IKA Works and used as is. The platinum wire counter electrode used in CV experiments was fashioned from platinum wire (0.01mm diameter, 1 m) 99.997% (metal basis) from Thermo Scientific, and wrapped around an IKA electrode attachment. Analytical TLC was performed on E. Merck pre-coated (25 mm) silica

gel 60 F254 plates. Visualization was done under UV (254 nm) or by staining by staining (95mL ethanol, 3mL conc. H₂SO₄, 2mL acetic acid, 5mL anisaldehyde). Flash chromatography was done using SiliCycle SiliaFlash P60 40-63 μ m 60 Å silica gel. Reagent grade ethyl acetate, diethyl ether, dichloromethane, methanol, and hexanes (commercial mixture) were purchased from Fisher Scientific and were used as is for chromatography. All reactions were performed in flame-dried glassware under a positive pressure of either Ar or N₂ with magnetic stirring unless noted otherwise. All reagents were purified according to “Purification of Laboratory Chemicals Sixth edition”.

Substrate Syntheses:



Scheme 76. Synthesis of Compound 2.32



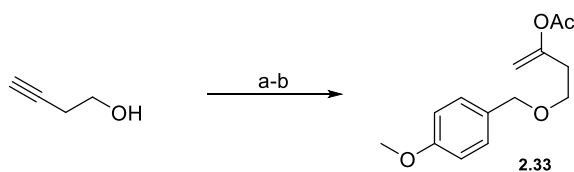
4-((4-Methoxybenzyl)oxy)hept-1-en-2-yl acetate (1)

IR (ATR, neat): 2957, 2870, 1753, 1665, 1613, 1513, 1462, 1368, 1300, 1244, 1178, 1031, 871, 819, 755, 585, 510 cm⁻¹.

¹H NMR (500 MHz, CDCl₃): δ 7.26, (d, *J* = 8.6 Hz, 2H), 6.86 (d, *J* = 8.7 Hz, 2H), 4.83 – 4.78 (m, 2H), 4.48 (d, *J* = 11.0 Hz, 1H), 4.41 (d, *J* = 11.1 Hz, 1H), 3.80 (s, 3H), 3.53 (tt, *J* = 8.9, 5.8 Hz, 1H), 2.51 (dd, *J* = 14.9, 6.5 Hz, 1H), 2.42 (dd, *J* = 15.0, 5.6 Hz, 1H), 2.08 (s, 3H), 1.57 – 1.48 (m, 2H), 1.48 – 1.38 (m, 1H), 1.38 – 1.28 (m, 1H), 0.90 (t, *J* = 7.2 Hz, 3H).

¹³C NMR (125 MHz, CDCl₃): δ 169.3, 159.3, 153.8, 130.9, 129.5, 113.8, 103.8, 75.9, 70.9, 55.4, 38.5, 36.4, 21.3, 18.7, 14.2.

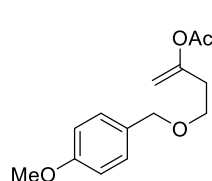
HRMS (ESI): *m/z* calcd. for C₁₇H₂₄O₄Na [M + Na]⁺ 315.1567, found 315.1562.



Reagents and Conditions:

a) NaH, THF, then PMBBBr, Bu₄NI, 70%. b) [(*p*-cymene)RuCl₂]₂, Fur₃P, Na₂CO₃, AcOH, 1-decyne, PhMe, 80 °C, 74%.

Scheme 77. Synthesis of Compound 2.33



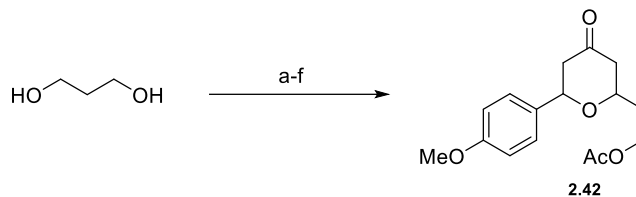
4-((4-Methoxybenzyl)oxy)but-1-en-2-yl acetate (2.33)

IR (ATR, neat): 2861, 1752, 1611, 1669, 1513, 1460, 1367, 1300, 1243, 1212, 1174, 1094, 1026, 961, 877, 818, 756, 580, 516 cm⁻¹.

¹H NMR (400 MHz, CDCl₃): δ 7.26 (d, *J* = 8.4 Hz, 2H), 6.88 (d, *J* = 8.6 Hz, 2H), 4.80 (s, 2H), 4.45 (s, 2H), 3.80 (s, 3H), 3.56 (t, *J* = 6.6 Hz, 2H), 2.53 (t, *J* = 6.5 Hz, 2H), 2.10 (s, 3H).

¹³C NMR (100 MHz, CDCl₃): δ 169.3, 159.4, 153.6, 130.4, 129.5, 113.9, 103.0, 72.8, 66.9, 55.4, 34.1, 21.2.

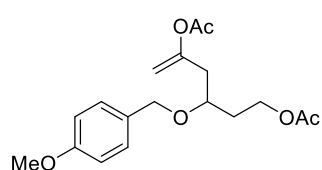
HRMS (ESI): *m/z* calcd. for C₁₄H₁₉O₄ [M + H]⁺ 251.1278, found 251.1267.



Reagents and Conditions:

a) Et₃N, TBSCl, DMAP THF, 0 °C to rt, 92%. b) DMP, CH₂Cl₂, 79%. c) Zn, propargyl bromide, ICH₂CH₂I, THF, 46%. d) NaH, THF, then PMBBR, 37%. e) CSA, MeOH, CH₂Cl₂, 0 °C to rt, then Ac₂O, DMAP, Et₃N, CHCl₃, 75% over two steps. f) [(*p*-cymene)RuCl₂]₂, Fur₃P, Na₂CO₃, AcOH, 1-decyne, PhMe, 80 °C, 70%.

Scheme 78. Synthesis of Compound 2.42



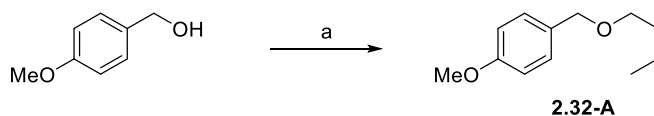
3-((4-Methoxybenzyl)oxy)hex-5-ene-1,5-diyl diacetate (2.42)

IR (ATR, neat): 2917, 1736, 1665, 1612, 1586, 1513, 1465, 1368, 1302, 1243, 1198, 1173, 1033, 966, 877, 820, 755, 637, 606, 518 cm⁻¹.

¹H NMR (400 MHz, CDCl₃): δ 7.25 (d, *J* = 9.1 Hz, 2H), 6.86 (d, *J* = 8.7 Hz, 2H), 4.84 (s, 1H), 4.82 (s, 1H), 4.52 (d, *J* = 11.0 Hz, 1H), 4.37 (d, *J* = 11.0 Hz, 1H), 4.15 (t, *J* = 6.4 Hz, 2H), 3.80 (s, 3H), 3.67 – 3.59 (m, 1H), 2.56 (dd, *J* = 14.9, 5.9 Hz, 1H), 2.46 (dd, *J* = 15.1, 6.4 Hz, 1H), 2.09 (s, 3H), 2.00 (s, 3H), 1.94 – 1.78 (m, 2H).

¹³C NMR (100 MHz, CDCl₃): δ 171.6, 169.2, 159.4, 153.1, 130.4, 129.7, 113.9, 104.3, 72.8, 71.1, 61.4, 55.4, 38.3, 33.3, 21.2, 21.1.

HRMS (ESI): *m/z* calcd. for C₁₈H₂₅O₆ [M + H]⁺ 337.1646, found 337.1651.

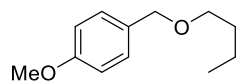


Reagents and Conditions:

a) NaH, THF, then BuBr, 78%.

Scheme 79. Synthesis of Compound 2.32-A

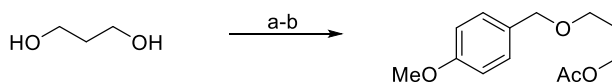
1-(Butoxymethyl)-4-methoxybenzene (2.32-A)



¹H NMR (400 MHz, CDCl₃) δ 7.26 (d, *J* = 8.7 Hz, 2H), 6.88 (d, *J* = 8.7 Hz, 2H), 4.43 (s, 2H), 3.80 (s, 3H), 3.44 (t, *J* = 6.6 Hz, 2H), 1.63 – 1.54 (m, 2H), 1.45 – 1.32 (m, 2H), 0.91 (t, *J* = 7.4 Hz, 3H).

¹³C NMR (100 MHz, CDCl₃) δ 159.2, 131.0, 129.3, 113.9, 72.6, 70.1, 55.4, 32.0, 19.5, 14.1.

These data match literature values.¹⁰⁵



Reagents and Conditions:

a) NaH, THF, then PMBBBr, Bu₄NI, 71%. b) Ac₂O, pyr., CH₂Cl₂, 85%.

Scheme 80. Synthesis of Compound 2.42-A

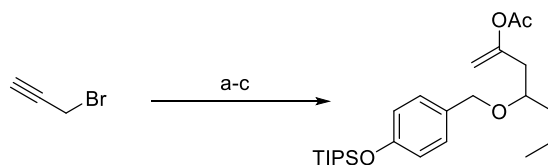
3-((4-Methoxybenzyl)oxy)propyl acetate (2.42-A)

IR (ATR, neat): 3004, 2956, 2864, 1733, 1612, 1586, 1512, 1458, 1365, 1297, 1242, 1172, 1098, 1032, 818, 751, 607, 514 cm⁻¹.

¹H NMR (400 MHz, CDCl₃): δ 7.25 (d, *J* = 8.1 Hz, 2H), 6.88 (d, *J* = 8.6 Hz, 2H), 4.44 (s, 2H), 4.17 (t, *J* = 6.5 Hz, 2H), 3.80 (s, 3H), 3.52 (t, *J* = 6.2 Hz, 2H), 2.03 (s, 3H), 1.92 (p, *J* = 6.4 Hz, 2H).

¹³C NMR (100 MHz, CDCl₃): δ 171.3, 159.3, 130.5, 129.4, 113.9, 72.8, 66.5, 61.9, 55.4, 29.2, 21.1.

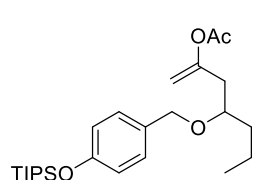
HRMS (ESI): *m/z* calcd. for C₁₃H₂₂O₄N [M + NH₄]⁺ 256.1543, found 256.1545.



Reagents and Conditions:

a) Zn, Butyraldehyde, $\text{ICH}_2\text{CH}_2\text{I}$, THF, 54%. b) (i) NaH, THF, then *p*-TIPSO-BnBr, 27%.
c) [(*p*-cymene) RuCl_2] $_2$, Fur_3P , Na_2CO_3 , AcOH, 1-decyne, PhMe, 80 °C, 43%.

Scheme 81. Synthesis of Compound S2.1



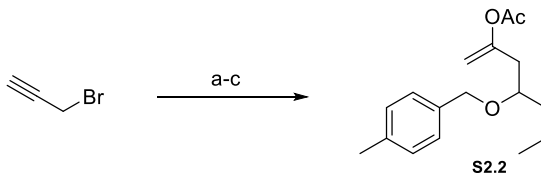
4-((4-((Triisopropylsilyl)oxy)benzyl)oxy)hept-1-en-2-yl acetate (S2.1)

IR (ATR, neat): 2945, 2867, 1756, 1665, 1609, 1509, 1463, 1368, 1262, 1202, 1071, 1012, 910, 881, 828, 679, 508 cm^{-1} .

^1H NMR (500 MHz, CDCl_3): δ 7.18 (d, J = 8.4 Hz, 2H), 6.83 (d, J = 8.5 Hz, 2H), 4.80 (d, J = 1.3 Hz, 1H), 4.79 (s, 1H), 4.47 (d, J = 11.2 Hz, 1H), 4.40 (d, J = 11.2 Hz, 1H), 3.51 (tt, J = 6.0, 5.9 Hz, 1H), 2.51 (dd, J = 14.9, 6.4 Hz, 1H), 2.42 (dd, J = 14.9, 5.7 Hz, 1H), 2.08 (s, 3H), 1.58 – 1.48 (m, 2H), 1.48 – 1.37 (m, 1H), 1.37 – 1.29 (m, 1H), 1.29 – 1.20 (m, 3H), 1.13 – 1.06 (m, 18H), 0.88 (t, J = 7.2 Hz, 3H).

^{13}C NMR (125 MHz, CDCl_3): δ 169.3, 155.7, 153.9, 131.2, 129.4, 119.8, 103.7, 75.9, 71.0, 38.5, 36.4, 31.1, 21.2, 18.7, 18.1, 14.2, 12.8.

HRMS (ESI): m/z calcd. for $\text{C}_{25}\text{H}_{41}\text{O}_4\text{Si}$ [$\text{M} - \text{H}$] $^+$ 433.2769, found 433.2769.

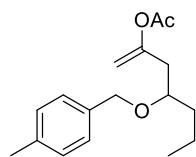


Reagents and Conditions:

a) Zn, Butyraldehyde, $\text{ICH}_2\text{CH}_2\text{I}$, THF, 54%. b) NaH, THF, then *p*-Me-BnBr, 78%.
c) [(*p*-cymene) RuCl_2] $_2$, Fur_3P , Na_2CO_3 , AcOH, 1-decyne, PhMe, 80 °C, 54%.

Scheme 82. Synthesis of Compound S2.2

4-((4-Methylbenzyl)oxy)hept-1-en-2-yl acetate (S2.2)

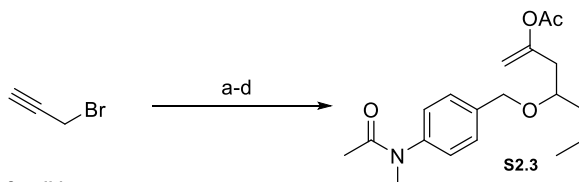


IR (ATR, neat): 2981, 2971, 2884, 1754, 1665, 1517, 1462, 1369, 1200, 1186, 1074, 1026, 965, 871, 801, 753, 588, 473 cm^{-1} .

^1H NMR (300 MHz, CDCl_3): δ 7.24 (d, J = 7.9 Hz, 2H), 7.14 (d, J = 7.8 Hz, 2H), 4.82 (s, 2H), 4.53 (d, J = 11.3 Hz, 1H), 4.45 (d, J = 11.2 Hz, 1H), 3.54 (tt, J = 5.9, 5.8 Hz, 1H), 2.53 (dd, J = 15.0, 6.2 Hz, 1H), 2.43 (dd, J = 15.0, 5.8 Hz, 1H), 2.34 (s, 3H), 2.09 (s, 3H), 1.63 – 1.46 (m, 2H), 1.46 – 1.26 (m, 2H), 0.91 (t, J = 7.1 Hz, 3H).

^{13}C NMR (75 MHz, CDCl_3): δ 169.2, 153.8, 137.3, 135.7, 129.1, 128.0, 103.7, 76.1, 71.1, 38.4, 36.4, 21.3, 21.2, 18.7, 14.2.

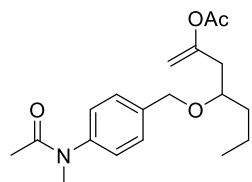
HRMS (ESI): m/z calcd. for $\text{C}_{17}\text{H}_{24}\text{O}_3\text{Na}$ [$\text{M} + \text{Na}$] $^+$ 299.1618, found 299.1617.



Reagents and Conditions:

a) Zn, Butyraldehyde, $\text{ICH}_2\text{CH}_2\text{I}$, THF, 54%. b) $p\text{-NHAc-PhCH}_2\text{OC(NH)CCl}_3$, TFOH (5 mol%), CH_2Cl_2 , 47%. c) NaH, DMF, then MeI, 77%. d) [$p\text{-cymene}$] RuCl_2I_2 , Fur_3P , Na_2CO_3 , AcOH, 1-decyne, PhMe, 80 $^\circ\text{C}$, 54%.

Scheme 83. Synthesis of Compound S2.3



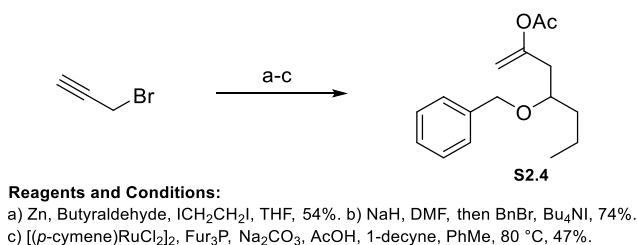
4-((4-(N-Methylacetamido)benzyl)oxy)hept-1-en-2-yl acetate (S2.3)

IR (ATR, neat): 2959, 2935, 2873, 1753, 1718, 1660, 1602, 1512, 1423, 1371, 1204, 1084, 1018, 975, 920, 868, 829, 707, 599, 559 cm^{-1} .

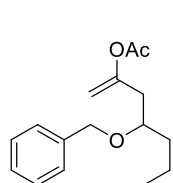
^1H NMR (400 MHz, CDCl_3): δ 7.39 (d, J = 8.2 Hz, 2H), 7.15 (d, J = 8.2 Hz, 2H), 4.83 (s, 2H), 4.56 (d, J = 11.5 Hz, 1H), 4.50 (d, J = 11.5 Hz, 1H), 3.58 (tt, J = 6.0, 6.0 Hz, 1H), 3.24 (s, 3H), 2.53 (dd, J = 15.0, 6.6 Hz, 1H), 2.45 (dd, J = 14.9, 5.4 Hz, 1H), 2.10 (s, 3H), 1.86 (s, 3H), 1.63 – 1.51 (m, 2H), 1.51 – 1.42 (m, 1H), 1.42 – 1.30 (m, 1H), 0.91 (t, J = 7.2 Hz, 3H).

^{13}C NMR (100 MHz, CDCl_3): δ 170.7, 169.2, 153.6, 144.0, 138.5, 129.1, 127.1, 103.9, 70.7, 38.5, 37.3, 36.4, 22.6, 21.3, 18.7, 14.2.

HRMS (ESI): m/z calcd. for $\text{C}_{19}\text{H}_{28}\text{O}_4\text{N}$ $[\text{M} + \text{H}]^+$ 334.2013, found 334.2018.



Scheme 84. Synthesis of Compound S2.4



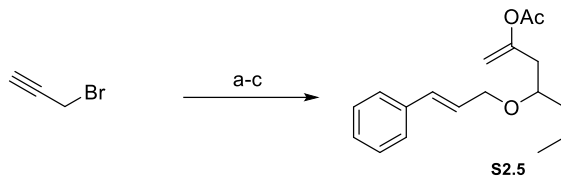
4-(Benzyloxy)hept-1-en-2-yl acetate (S2.4)

IR (ATR, neat): 3031, 2959, 2934, 2872, 1754, 1665, 1496, 1454, 1432, 1368, 1187, 1088, 1062, 1030, 965, 917, 871, 734, 696, 606, 465 cm^{-1} .

^1H NMR (500 MHz, CDCl_3): δ 7.36 – 7.31 (m, 4H), 7.29 -7.26 (m, 1H), 4.82 (s, 2H), 4.56 (d, $J = 11.4\text{ Hz}$, 1H), 4.49 (d, $J = 11.4\text{ Hz}$, 1H), 4.49 (d, $J = 11.5\text{ Hz}$, 1H), 3.55 (tt, $J = 6.0, 5.9\text{ Hz}$, 1H), 2.53 (dd, $J = 14.9, 6.5\text{ Hz}$, 1H), 2.44 (dd, $J = 14.9, 5.6\text{ Hz}$, 1H), 2.08 (s, 3H), 1.62 – 1.50 (m, 2H), 1.50 – 1.40 (m, 1H), 1.40 – 1.31 (m, 1H), 0.90 (t, $J = 7.3\text{ Hz}$, 3H).

^{13}C NMR (125 MHz, CDCl_3): δ 169.3, 153.8, 138.8, 128.4, 128.0, 127.7, 103.8, 76.3, 71.3, 38.4, 36.4, 21.2, 18.7, 14.3.

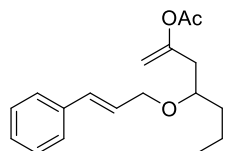
HRMS (ESI): m/z calcd. for $\text{C}_{16}\text{H}_{23}\text{O}_3$ $[\text{M} + \text{H}]^+$ 263.1642, found 263.1643.



Reagents and Conditions:

a) Zn, Butyraldehyde, $\text{ICH}_2\text{CH}_2\text{I}$, THF, 54%. b) NaH, THF, then *trans*-cinnamyl bromide, 72%.
c) [(*p*-cymene) RuCl_2] $_2$, Fur_3P , Na_2CO_3 , AcOH, 1-decyne, PhMe, 80 °C, 39%.

Scheme 85. Synthesis of Compound S2.5



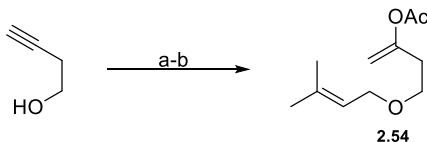
4-(Cinnamyloxy)hept-1-en-2-yl acetate (S2.5)

IR (ATR, neat): 3028, 2958, 2933, 2872, 1753, 1665, 1496, 1450, 1369, 1202, 1117, 1048, 1019, 873, 865, 745, 692 cm^{-1} .

^1H NMR (400 MHz, CDCl_3): δ 7.40 – 7.36 (m, 2H), 7.34 – 7.28 (m, 2H), 7.26 – 7.20 (m, 1H), 6.59 (d, J = 16.2 Hz, 1H), 6.27 (dt, J = 15.9, 6.1 Hz, 1H), 4.82 (s, 2H), 4.19 (ddd, J = 12.5, 6.1, 1.1 Hz, 1H), 4.14 (ddd, J = 12.6, 6.1, 1.1 Hz, 1H), 3.53 (tt, J = 5.9, 5.8 Hz, 1H), 2.49 (dd, J = 14.9, 6.5 Hz, 1H), 2.42 (dd, J = 14.9, 5.6 Hz, 1H), 2.10 (s, 3H), 1.57 – 1.49 (m, 2H), 1.49 – 1.41 (m, 1H), 1.41 – 1.31 (m, 1H), 0.93 (t, J = 7.2 Hz, 3H).

^{13}C NMR (100 MHz, CDCl_3): δ 169.3, 153.8, 136.9, 132.2, 128.7, 127.7, 126.7, 126.6, 103.8, 76.2, 70.0, 38.6, 36.5, 21.3, 18.7, 14.3.

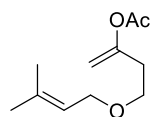
HRMS (ESI): m/z calcd. for $\text{C}_{18}\text{H}_{25}\text{O}_3$ $[\text{M} + \text{H}]^+$ 289.1798, found 289.1799.



Reagents and Conditions:

a) NaH, DMF, then prenyl bromide, 78%. b) [(*p*-cymene) RuCl_2] $_2$, Fur_3P , Na_2CO_3 , AcOH, 1-decyne, PhMe, 80 °C, 70%.

Scheme 86. Synthesis of Compound 2.54

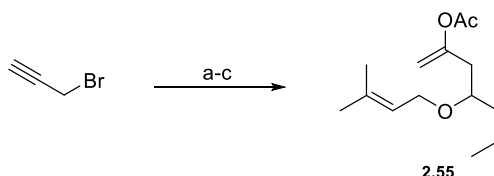


4-((3-Methylbut-2-en-1-yl)oxy)but-1-en-2-yl acetate (2.54)

^1H NMR (400 MHz, CDCl_3): δ 5.33 (t, J = 6.2 Hz, 1H), 4.80 (s, 1H), 4.79 (s, 1H), 3.96 (d, J = 6.8 Hz, 2H), 3.54 (t, J = 6.7 Hz, 2H), 2.50 (t, J = 6.6 Hz, 2H), 2.13 (s, 3H), 1.74 (s, 3H), 1.67 (s, 3H).

^{13}C NMR (100 MHz, CDCl_3): δ 169.3, 153.7, 137.2, 121.1, 102.9, 67.4, 67.0, 34.1, 25.9, 21.2, 18.1.

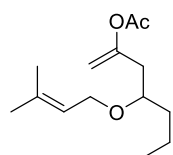
These spectroscopic data match literature values.⁷²



Reagents and Conditions:

a) Zn, Butyraldehyde, $\text{ICH}_2\text{CH}_2\text{I}$, THF, 54%. b) NaH, THF, then prenyl bromide, NaI, 54%. c) [p -cymene] RuCl_2 , Fur_3P , Na_2CO_3 , AcOH, 1-decyne, PhMe, 80 °C, 62%.

Scheme 87. Synthesis of Compound 2.55



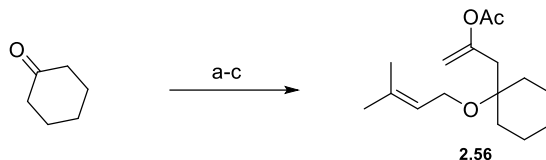
4-((3-Methylbut-2-en-1-yl)oxy)hept-1-en-2-yl acetate (2.55)

IR (ATR, neat): 2933, 2872, 1756, 1666, 1436, 1369, 1198, 1117, 1052, 1020, 917, 780, 587 cm^{-1} .

^1H NMR (500 MHz, CDCl_3): δ 5.36 – 5.30 (m, 1H), 4.79 (s, 2H), 3.99 (dd, J = 11.1, 7.0 Hz, 1H), 3.93 (dd, J = 11.1, 7.1 Hz, 1H), 3.42 (tt, J = 8.9, 5.9 Hz, 1H), 2.46 (dd, J = 14.9, 6.5 Hz, 1H), 2.36 (dd, J = 14.9, 5.6 Hz, 1H), 2.13 (s, 3H), 1.73 (s, 3H), 1.66 (s, 3H), 1.52 – 1.45 (m, 2H), 1.45 – 1.38 (m, 1H), 1.38 – 1.28 (m, 1H), 0.91 (t, J = 7.2 Hz, 3H).

^{13}C NMR (125 MHz, CDCl_3): δ 169.2, 153.9, 136.8, 121.6, 103.6, 76.0, 65.8, 38.7, 36.6, 25.9, 21.3, 18.8, 18.1, 14.2.

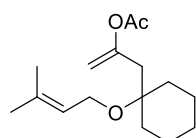
HRMS (ESI): m/z calcd. for $\text{C}_{14}\text{H}_{24}\text{O}_3$ $[\text{M} + \text{Na}]^+$ 263.1618, found 263.1619.



Reagents and Conditions:

a) Propargyl Bromide, Mg, HgCl₂, 53%. (b) NaH, DMF, then prenyl bromide, Bu₄Ni, 54%.
c) [(*p*-cymene)RuCl₂]₂, Fur₃P, Na₂CO₃, AcOH, 1-decyne, PhMe, 80 °C, 23%.

Scheme 88. Synthesis of Compound 2.56



3-(1-((3-Methylbut-2-en-1-yl)oxy)cyclohexyl)prop-1-en-2-yl acetate (2.56)

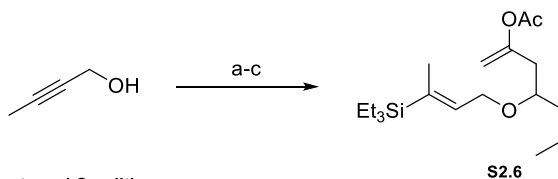
IR (ATR, neat): 2930, 2858, 1754, 1663, 1449, 1368, 1195, 1168, 1053, 1021,

957, 871, 783, 751, 718, 680, 596, 538, 482 cm⁻¹.

¹H NMR (500 MHz, CDCl₃): δ 5.35 – 5.29 (m, 1H), 4.84 (d, *J* = 1.2 Hz, 1H), 4.79 (d, *J* = 0.9 Hz, 1H), 3.84 (d, *J* = 6.6 Hz, 2H), 2.42 (s, 2H), 2.11 (s, 3H), 1.83 – 1.76 (m, 2H), 1.73 (s, 3H), 1.66 (s, 3H), 1.63 – 1.58 (m, 1H), 1.57 – 1.52 (m, 2H), 1.48 – 1.40 (m, 2H), 1.40 – 1.32 (m, 2H), 1.28 – 1.17 (m, 1H).

¹³C NMR (125 MHz, CDCl₃): δ 169.4, 153.1, 135.3, 122.2, 105.1, 74.9, 57.5, 40.9, 34.6, 26.0, 25.9, 22.1, 21.4, 18.2.

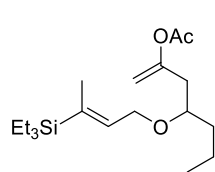
HRMS (ESI): *m/z* calcd. for C₁₆H₂₆O₃Na [*M* + Na]⁺ 289.1774, found 289.1776.



Reagents and Conditions:

a) Et₃SiH, H₂PtCl₆•6H₂O, THF, 50 °C, 24%, b) Cl₃CCN, NaH, Et₂O, then secondary homopropargylic alcohol, TfOH, 30%. c) [(*p*-cymene)RuCl₂]₂, Fur₃P, Na₂CO₃, HOAc, 1-decyne, PhMe, 80 °C, 47%.

Scheme 89. Synthesis of Compound S2.6



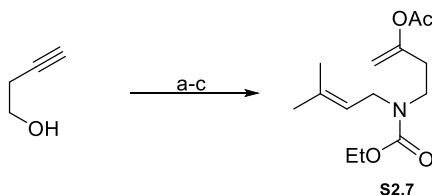
(*E*)-4-((3-(Triethylsilyl)but-2-en-1-yl)oxy)hept-1-en-2-yl acetate (S2.6)

IR (ATR, neat): 2955, 2911, 2875, 1758, 1665, 1458, 1369, 1199, 1087, 1043, 1018, 965, 870, 717, 669, 587 cm^{-1} .

^1H NMR (400 MHz, CDCl_3): δ 5.79 (tq, $J = 5.5, 1.8$ Hz, 1H), 4.79 (s, 2H), 4.14 (dd, $J = 12.7, 5.5$ Hz, 1H), 4.10 (dd, $J = 12.9, 5.6$ Hz, 1H), 3.44 (tt, $J = 5.9, 5.8$ Hz, 1H), 2.47 (dd, $J = 14.9, 6.3$ Hz, 1H), 2.38 (dd, $J = 14.9, 5.7$ Hz, 1H), 2.13 (s, 3H), 1.66 (s, 3H), 1.54 – 1.46 (m, 2H), 1.46 – 1.38 (m, 1H), 1.38 – 1.28 (m, 1H), 0.91 (t, $J = 7.8$ Hz, 12H), 0.59 (q, $J = 7.9$ Hz, 6H).

^{13}C NMR (100 MHz, CDCl_3): δ 169.3, 153.9, 137.8, 136.3, 103.7, 76.4, 66.0, 38.5, 36.5, 21.3, 18.8, 15.6, 14.3, 7.6, 2.6.

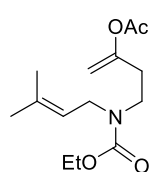
HRMS (ESI): m/z calcd. for $\text{C}_{19}\text{H}_{37}\text{O}_3\text{Si}$ $[\text{M} + \text{H}]^+$ 341.2507, found 341.2508.



Reagents and Conditions:

a) TsCl , Et_3N , Et_2O , then NaN_3 , DMF, 70 $^\circ\text{C}$, then Ph_3P , Et_2O , then H_2O , then ClCO_2Et , Et_3N , CH_2Cl_2 , 45%. b) NaH , DMF, then prenyl bromide, 87%. c) $[(p\text{-cymene})\text{RuCl}]_2$, Fur_3P , Na_2CO_3 , AcOH , 1-decyne, PhMe , 80 $^\circ\text{C}$, 62%.

Scheme 90. Synthesis of Compound S2.7



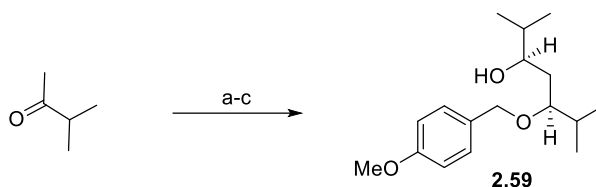
4-((Ethoxycarbonyl)(3-methylbut-2-en-1-yl)amino)but-1-en-2-yl acetate (S2.7)

IR (ATR, neat): 2933, 2106, 1757, 1694, 1671, 1471, 1421, 1370, 1194, 1106, 1018, 960, 922, 879, 770, 721, 639, 590 cm^{-1} .

^1H NMR (400 MHz, CDCl_3): δ 5.22 – 5.07 (m, 1H), 4.83 – 4.69 (m, 2H), 4.12 (q, $J = 7.1$ Hz, 2H), 3.93 – 3.77 (m, 2H), 3.41 – 3.25 (m, 2H), 2.50 – 2.37 (m, 2H), 2.13 (s, 3H), 1.72 (s, 3H), 1.67 (s, 3H), 1.24 (t, $J = 7.1$ Hz, 3H).

¹³C NMR (100 MHz, CDCl₃): δ 169.2, 156.3, 153.8, 120.5, 103.1, 61.3, 44.9, 25.9, 21.2, 17.9, 14.8.

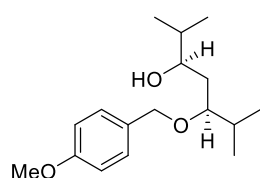
HRMS (ESI): *m/z* calcd. for C₁₄H₂₄O₄N [M + H]⁺ 270.1700, found 270.1701.



Reagents and Conditions:

a) LDA, -78 °C, THF, then *i*PrCHO, 49%. b) Et₂BOMe, NaBH₄, -78 °C, THF, MeOH, 69%.
c) PMBOC(NH)CCl₃, CSA, CH₂Cl₂, 56%.

Scheme 91. Synthesis of Compound 2.59



(3*S*,5*R*)-5-((4-Methoxybenzyl)oxy)-2,6-dimethylheptan-3-ol (2.59)

IR (ATR, neat): 3489, 2959, 2873, 1612, 1514, 1465, 1386, 1302, 1247, 1174, 1034, 958, 820, 757, 580, 512 cm⁻¹.

¹H NMR (500 MHz, CDCl₃): δ 7.26 (d, *J* = 8.6 Hz, 2H), 6.87 (d, *J* = 8.7 Hz, 2H), 4.59 (d, *J* = 10.8 Hz, 1H), 4.37 (d, *J* = 10.7 Hz, 1H), 3.79 (s, 3H), 3.76 (s, 1H), 3.56 – 3.50 (m, 2H), 2.18 – 2.10 (m, 1H), 1.68 – 1.60 (m, 1H), 1.52 (dt, *J* = 14.7, 2.7 Hz, 1H), 1.46 (dt, *J* = 14.6, 9.7 Hz, 1H), 0.93 (d, *J* = 6.9 Hz, 3H), 0.90 (d, *J* = 7.0 Hz, 3H), 0.90 (d, *J* = 6.8 Hz, 3H), 0.90 (d, *J* = 6.8 Hz, 3H).

¹³C NMR (125 MHz, CDCl₃): δ 159.4, 130.3, 129.6, 114.1, 85.4, 70.8, 55.4, 34.1, 32.0, 29.4, 18.8, 18.5, 17.6, 16.1.

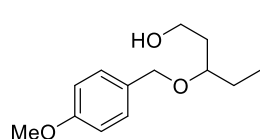
HRMS (ESI): *m/z* calcd. for C₁₇H₂₉O₃ [M + H]⁺ 281.2111, found 281.2111.



Reagents and Conditions:

a) NaH, THF, 0 °C, then TIPSCl, rt, 85%, b) (ClCO)₂, DMSO, Et₃N, CH₂Cl₂, -78 °C, 100%.
c) EtMgBr, THF, 0 °C to rt, 72%. d) NaH, THF, then PMBBR, Bu₄Ni, 35%. (e) TBAF, THF, 64%.

Scheme 92. Synthesis of Compound 2.61



3-((4-Methoxybenzyl)oxy)pentan-1-ol (2.61)

IR (ATR, neat): 3375, 2935, 2875, 1612, 1513, 1464, 1349, 1302, 1245,

1173, 1033, 924, 820, 746, 579, 515 cm⁻¹.

¹H NMR (400 MHz, CDCl₃): δ 7.27 (d, *J* = 8.5 Hz, 2H), 6.88 (d, *J* = 8.6 Hz, 2H), 4.54 (d, *J* = 11.1 Hz, 1H), 4.41 (d, *J* = 11.1 Hz, 1H), 3.80 (s, 3H), 3.80 – 3.69 (m, 2H), 3.62 – 3.55 (m, 1H), 1.83 – 1.72 (m, 2H), 1.72 – 1.53 (m, 2H), 0.92 (t, *J* = 7.5 Hz, 3H).

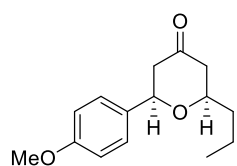
¹³C NMR (100 MHz, CDCl₃): δ 159.4, 130.7, 129.6, 114.0, 79.6, 70.7, 61.2, 55.4, 35.5, 26.1, 9.4.

HRMS (ESI): *m/z* calcd. for C₁₃H₁₉O₃ [M – H]⁺ 223.1329, found 223.1331.

Cyclization Reactions: Stoichiometric Oxidant

General Oxidation Protocol A

To a flame-dried 1 dram vile (Chemglass CG-4904-05 with a polypropylene screw cap containing a PTFE faced silicone septum) with a stir bar was added the substrate in freshly distilled MeCN (0.1 M). To this, 4Å molecular sieves were added (1 mass eq) and stirred for 2 min. Bobbitt's Salt (2 equiv) was added to the solution, and the reaction mixture was stirred until starting material was consumed. The reaction mixture was diluted with CH₂Cl₂ and transferred to a round bottom flask. The solvent was removed under reduced pressure and the crude mixture was purified by column chromatography to give the desired product.



2-(4-Methoxyphenyl)-6-propyltetrahydro-4H-pyran-4-one (2.35)

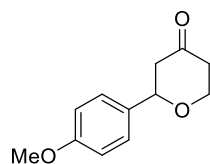
Synthesized according to general oxidation protocol A using **2.32** (17.4 mg, 0.0595 mmol), 4Å molecular sieves (17.4 mg) and Bobbitt's Salt (35.7 mg, 0.119 mmol) in MeCN (0.6 mL, 0.1 M). The reaction mixture was stirred for 50 min then purified by column chromatography (10% Et₂O to 30% Et₂O in hexanes) to yield **2.35** (12.3 mg, 83%) as a colorless oil.

IR (ATR, neat): 2971, 2981, 2907, 1716, 1613, 1514, 1463, 1354, 1304, 1246, 1176, 1063, 1032, 954, 826, 767, 660, 555, 510 cm⁻¹.

¹H NMR (400 MHz, C₆D₆): δ 7.13 (d, *J* = 8.6 Hz, 2H), 6.78 (d, *J* = 8.7 Hz, 2H), 4.22 (dd, *J* = 11.7, 2.5 Hz, 1H), 3.35 – 3.26 (m, 1H), 3.29 (s, 3H), 2.48 (app dt, *J* = 14.2, 2.3 Hz, 1H), 2.23 (ddd, *J* = 14.0, 11.7, 0.6 Hz, 1H), 2.19 (app dt, *J* = 14.2, 2.2 Hz, 1H), 1.93 (dd, *J* = 13.8, 11.8 Hz, 1H), 1.55 – 1.43 (m, 1H), 1.43 – 1.30 (m, 1H), 1.28 – 1.14 (m, 2H), 0.79 (t, *J* = 7.2 Hz, 3H).

¹³C NMR (100 MHz, C₆D₆): δ 204.8, 159.8, 134.1, 127.2, 114.1, 78.5, 77.0, 54.8, 50.0, 47.8, 38.8, 18.8, 14.2.

HRMS (ESI): *m/z* calcd. for C₁₅H₂₁O₃ [M + H]⁺ 249.1485, found 249.1484.



2-(4-Methoxyphenyl)tetrahydro-4H-pyran-4-one (2.36)

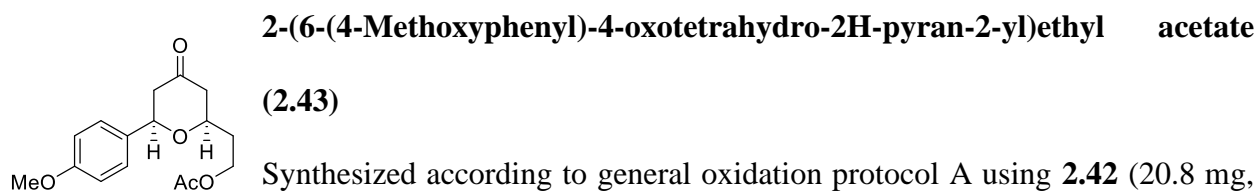
Synthesized according to general oxidation protocol A using **2.33** (18.9 mg, 0.0755 mmol), 4Å molecular sieves (18.9 mg) and Bobbitt's salt (45.3 mg, 0.151 mmol) in MeCN (0.76 mL, 0.1 M). The reaction mixture was stirred for 1.25 h then purified by column chromatography (10% Et₂O to 30% Et₂O in hexanes) to yield **2.36** (11.1 mg, 71%) as an off-white sticky solid.

IR (ATR, neat): 2978, 2889, 1708, 1463, 1384, 1249, 1154, 1079, 955, 828 cm^{-1} .

^1H NMR (400 MHz, C_6D_6): δ 7.11 (d, J = 8.6 Hz, 2H), 6.77 (d, J = 8.7 Hz, 2H), 4.16 (dd, J = 11.2, 2.6 Hz, 1H), 3.82 (ddd, J = 11.3, 7.3, 1.5 Hz, 1H), 3.29 (s, 3H), 3.20 (app td, J = 11.8, 2.9 Hz, 1H), 2.43 (app dt, J = 14.3, 2.3 Hz, 1H), 2.24 (dd, J = 13.9, 11.6 Hz, 1H), 2.11 (ddd, J = 14.2, 12.4, 7.8 Hz, 1H), 2.00 – 1.91 (m, 1H).

^{13}C NMR (100 MHz, C_6D_6): δ 204.9, 159.8, 133.7, 127.3, 114.1, 79.4, 66.4, 54.8, 50.2, 42.1.

HRMS (ESI): m/z calcd. for $\text{C}_{12}\text{H}_{15}\text{O}_3$ $[\text{M} + \text{H}]^+$ 207.1016, found 207.1016.

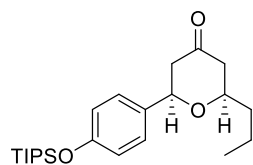


IR (ATR, neat): 2966, 1734, 1717, 1613, 1515, 1367, 1239, 1177, 1148, 1106, 1058, 1031, 828, 764 cm^{-1} .

^1H NMR (400 MHz, CDCl_3): δ 7.29 (d, J = 8.7 Hz, 2H), 6.91 (d, J = 8.6 Hz, 2H), 4.60 (dd, J = 10.7, 3.6 Hz, 1H), 4.32 – 4.19 (m, 2H), 3.94 – 3.86 (m, 1H), 3.81 (s, 3H), 2.66 – 2.53 (m, 2H), 2.51 – 2.36 (m, 2H), 2.11 – 1.99 (m, 1H), 2.03 (s, 3H), 1.99 – 1.88 (m, 1H).

^{13}C NMR (100 MHz, CDCl_3): δ 206.5, 171.0, 159.5, 132.8, 127.0, 114.0, 78.4, 74.2, 60.9, 55.4, 49.4, 47.7, 35.4, 21.0.

HRMS (ESI): m/z calcd. for $\text{C}_{16}\text{H}_{21}\text{O}_5$ $[\text{M} + \text{H}]^+$ 293.1384, found 293.1383.



2-Propyl-6-(4-((triisopropylsilyl)oxy)phenyl)tetrahydro-4H-pyran-4-one (2.44)

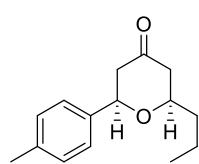
Synthesized according to general oxidation protocol A using **S2.1** (17.1 mg, 0.0393 mmol), 4Å molecular sieves (17.1 mg) and Bobbitt's Salt (23.6 mg, 0.0787 mmol) in MeCN (0.39 mL, 0.1 M). The reaction mixture was stirred for 1 h then purified by column chromatography (5% Et₂O to 15% Et₂O in hexanes) to yield **2.44** (11.1 mg, 72%) as a colorless oil.

IR (ATR, neat): 2945, 2867, 1720, 1610, 1511, 1464, 1343, 1263, 1153, 1065, 910, 882, 830, 710, 682, 661 cm⁻¹.

¹H NMR (500 MHz, C₆D₆): δ 7.12 (d, *J* = 8.5 Hz, 2H), 6.92 (d, *J* = 8.6 Hz, 1H), 4.22 (dd, *J* = 11.7, 2.5 Hz, 1H), 3.30 (ddt, *J* = 14.3, 7.2, 2.2 Hz, 1H), 2.48 (app dt, *J* = 14.2, 2.3 Hz, 1H), 2.24 – 2.16 (m, 2H), 1.92 (dd, *J* = 13.9, 11.9 Hz, 1H), 1.52 – 1.42 (m, 1H), 1.41 – 1.32 (m, 1H), 1.26 – 1.13 (m, 5H), 1.12 – 1.07 (m, 18H), 0.79 (t, *J* = 7.2 Hz, 3H).

¹³C NMR (125 MHz, C₆D₆): δ 204.7, 156.0, 134.7, 127.2, 120.0, 78.4, 77.0, 49.9, 47.8, 38.8, 18.8, 18.1, 14.2, 13.0.

HRMS (ESI): *m/z* calcd. for C₂₃H₃₉O₃Si [M + H]⁺ 391.2663, found 391.2662.



2-Propyl-6-(p-tolyl)tetrahydro-4H-pyran-4-one (2.45)

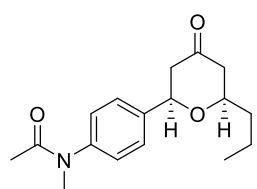
Synthesized according to general oxidation protocol A using **S2.2** (45.6 mg, 0.196 mmol), 4Å molecular sieves (45.6 mg) and Bobbitt's Salt (0.118 g, 0.392 mmol) in MeCN (2 mL, 0.1 M). The reaction mixture was stirred for 3 h then purified by column chromatography (5% Et₂O to 15% Et₂O in hexanes) to yield **2.45** (26 mg, 57%) as a white sticky solid.

IR (ATR, neat): 2959, 2931, 2870, 1713, 1516, 1464, 1344, 1324, 1290, 1253, 1156, 1135, 1061, 957, 803, 664, 552, 528, 492 cm^{-1} .

^1H NMR (500 MHz, C_6D_6): δ 7.14 (d, J = 8.0 Hz, 2H), 6.99 (d, J = 7.9 Hz, 2H), 4.24 (dd, J = 11.7, 2.6 Hz, 1H), 3.33 – 3.26 (m, 1H), 2.49 (ddd, J = 14.2, 2.5, 2.1 Hz, 1H), 2.22 (ddd, J = 14.2, 11.8, 0.9 Hz, 1H), 2.18 (app dt, J = 14.1, 2.2 Hz, 1H), 2.10 (s, 3H), 1.92 (ddd, J = 14.1, 11.7, 0.6 Hz, 1H), 1.52 – 1.43 (m, 1H), 1.41 – 1.31 (m, 1H), 1.27 – 1.15 (m, 2H), 0.79 (t, J = 7.2 Hz, 3H).

^{13}C NMR (125 MHz, C_6D_6): δ 204.7, 139.1, 137.3, 129.3, 125.9, 78.6, 77.0, 50.0, 47.8, 38.8, 21.1, 18.8, 14.1.

HRMS (ESI): m/z calcd. for $\text{C}_{15}\text{H}_{21}\text{O}_2$ $[\text{M} + \text{H}]^+$ 233.1536, found 233.1544.



***N*-Methyl-*N*-(4-(4-oxo-6-propyltetrahydro-2H-pyran-2-yl)phenyl)acetamide (**2.46**)**

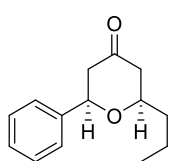
Synthesized according to general oxidation protocol A using **S2.3** (23.8 mg, 0.0714 mmol), 4Å molecular sieves (23.8 mg) and Bobbitt's Salt (42.8 mg, 0.142 mmol) in MeCN (0.71 mL, 0.1 M). The reaction mixture was stirred for 24 h then purified by column (40% EtOAc in hexanes to 40% hexanes in EtOAc) to yield **2.46** (12.1 mg, 59%) as a colorless oil.

IR (ATR, neat): 3038, 2958, 2921, 2870, 1717, 1658, 1607, 1512, 1419, 1377, 1345, 1292, 1138, 1018, 1007, 976, 906, 834, 742, 623, 580, 539, 498 cm^{-1} .

^1H NMR (500 MHz, CDCl_3): δ 7.43 (d, J = 8.7 Hz, 2H), 7.20 (d, J = 8.2 Hz, 2H), 4.67 (dd, J = 11.6, 2.3 Hz, 1H), 3.79 (ddt, J = 13.9, 7.1, 2.3 Hz, 1H), 3.25 (s, 3H), 2.66 (app dt, J = 14.3, 2.1 Hz, 1H), 2.56 – 2.45 (m, 2H), 2.38 (dd, J = 14.1, 11.6 Hz, 1H), 1.88 (s, 3H), 1.81 – 1.73 (m, 1H), 1.65 – 1.59 (m, 1H), 1.59 – 1.50 (m, 1H), 1.50 – 1.40 (m, 1H), 0.96 (t, J = 7.3 Hz, 3H).

¹³C NMR (125 MHz, CDCl₃): δ 206.7, 170.7, 144.3, 140.7, 127.4, 127.1, 78.0, 49.6, 47.8, 38.6, 37.3, 29.8, 22.6, 18.7, 14.1.

HRMS (ESI): *m/z* calcd. for C₁₇H₂₄O₃N [M + H]⁺ 290.1751, found 290.1755.



2-Phenyl-6-propyltetrahydro-4H-pyran-4-one (2.47)

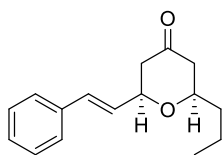
Synthesized according to general oxidation protocol A using **S2.4** (18.4 mg, 0.0701 mmol), 4Å molecular sieves (18.4 mg) and Bobbitt's Salt (42.1 mg, 0.140 mmol) in MeCN (0.7 mL, 0.1 M). The reaction mixture was stirred for 23 h then purified by (2.5% Et₂O to 10% Et₂O in hexanes) to yield **2.47** (12.3 mg, 80%) as a colorless oil.

IR (ATR, neat): 3033, 2959, 2872, 1717, 1497, 1454, 1346, 1311, 1291, 1256, 1235, 1153, 1118, 1059, 1028, 953, 918, 752, 697, 676, 614, 555, 492 cm⁻¹.

¹H NMR (500 MHz, C₆D₆): δ 7.20 – 7.17 (m, 2H), 7.15 – 7.12 (m, 2H), 7.10 – 7.05 (m, 1H), 4.21 (dd, *J* = 11.8, 2.6 Hz, 1H), 3.28 (ddt, *J* = 14.4, 7.3, 2.2 Hz, 1H), 2.45 (app dt, *J* = 14.2, 2.3 Hz, 1H), 2.20 – 2.12 (m, 2H), 1.89 (dd, *J* = 14.1, 11.7 Hz, 1H), 1.51 – 1.42 (m, 1H), 1.40 – 1.29 (m, 1H), 1.26 – 1.13 (m, 2H), 0.79 (t, *J* = 7.3 Hz, 3H).

¹³C NMR (125 MHz, C₆D₆): δ 204.5, 142.0, 128.6, 125.8, 78.6, 77.0, 49.9, 47.8, 38.7, 18.8, 14.1.

HRMS (ESI): *m/z* calcd. for C₁₄H₁₉O₂ [M + H]⁺ 219.1380, found 219.1382.



(E)-2-Propyl-6-styryltetrahydro-4H-pyran-4-one (2.48)

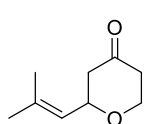
Synthesized according to general oxidation protocol A using **S2.5** (40.3 mg, 0.140 mmol), 4Å molecular sieves (40.3 mg) and Bobbitt's Salt (83.9 mg, 0.279 mmol) in MeCN (1.4 mL, 0.1 M). The reaction mixture was stirred for 45 min then purified by column (2.5% Et₂O to 10% Et₂O in hexanes) to yield **2.48** (14.5 mg, 42%) as a colorless oil.

IR (ATR, neat): 3027, 2959, 2932, 2871, 1717, 1496, 1450, 1341, 1318, 1231, 1159, 1053, 965, 836, 746, 692, 538, 489 cm^{-1} .

^1H NMR (500 MHz, C_6D_6): δ 7.22 – 7.19 (m, 2H), 7.13 – 7.08 (m, 2H), 7.07 – 7.03 (m, 1H), 6.49 (dd, J = 16.0, 0.8 Hz, 1H), 6.03 (dd, J = 16.0, 5.6 Hz, 1H), 3.83 (dddd, J = 11.7, 5.6, 2.6, 1.4 Hz, 1H), 3.29 – 3.21 (m, 1H), 2.29 (app dt, J = 14.1, 2.3 Hz, 1H), 2.16 (app dt, J = 14.2, 2.2 Hz, 1H), 2.05 (ddd, J = 14.1, 11.8, 0.8 Hz, 1H). 1.89 (ddd, J = 14.0, 11.5, 1.1 Hz, 1H), 1.52 – 1.43 (m, 1H), 1.43 – 1.34 (m, 1H), 1.30 – 1.14 (m, 2H), 0.81 (t, J = 7.3 Hz, 3H).

^{13}C NMR (125 MHz, C_6D_6): δ 204.5, 137.1, 130.6, 129.4, 128.9, 126.9, 77.3, 76.8, 48.0, 47.9, 38.8, 30.1, 18.8, 14.2.

HRMS (ESI): m/z calcd. for $\text{C}_{16}\text{H}_{21}\text{O}_2$ $[\text{M} + \text{H}]^+$ 245.1536, found 245.1534.



2-(2-Methylprop-1-en-1-yl)tetrahydro-4H-pyran-4-one (2.49)

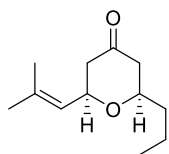
Synthesized according to general oxidation protocol A using **2.54** (33.2 mg, 0.167 mmol), 4Å molecular sieves (33.2 mg) and Bobbitt's Salt (0.101g, 0.335 mmol) in MeCN (1.7 mL, 0.1 M). The reaction mixture was stirred for 25 min then purified by column chromatography (10% Et_2O to 20% Et_2O in hexanes) to yield **2.49** (9.6 mg, 37%) as a colorless oil.

IR (ATR, CH_2Cl_2): 2965, 2857, 1717, 1614, 1616, 1464, 1368, 1243, 1177, 1151, 1060, 1033, 880, 764 cm^{-1} .

^1H NMR (300 MHz, C_6D_6): δ 5.22 – 5.16 (m, 1H), 4.03 (ddd, J = 10.8, 7.8, 3.0 Hz, 1H), 3.76 (ddd, J = 11.3, 7.1, 1.9 Hz, 1H), 3.15 (app td, J = 11.6, 3.1 Hz, 1H), 2.26 (ddd, J = 14.4, 2.8, 2.1 Hz, 1H), 2.14 – 2.00 (m, 2H), 1.91 (ddt, J = 14.4, 3.2, 1.9 Hz, 1H), 1.48 (d, J = 1.3 Hz, 3H), 1.35 (d, J = 1.2 Hz, 3H).

^{13}C NMR (75 MHz, C_6D_6): δ 204.6, 135.6, 125.6, 75.3, 66.1, 48.7, 42.3, 25.5, 18.2.

HRMS (ESI): m/z calcd. for $C_9H_{15}O_2$ $[M + H]^+$ 155.1067, found 155.1067.



2-(2-Methylprop-1-en-1-yl)-6-propyltetrahydro-4H-pyran-4-one (2.50)

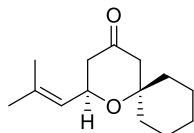
Synthesized according to general oxidation protocol A using **2.55** (21.4 mg, 0.089 mmol), 4Å molecular sieves (21.4 mg) and Bobbitt's Salt (53.4 mg, 0.178 mmol) in MeCN (0.89 mL, 0.1 M). The reaction mixture was stirred for 25 min then purified by column chromatography (5% Et₂O to 15% Et₂O in hexanes) to yield **2.50** (10.8 mg, 62%) as a colorless oil.

IR (ATR, neat): 2933, 2962, 2873, 1718, 1451, 1377, 1316, 1259, 1240, 1214, 1160, 1130, 1050, 939, 865, 819, 544, 492, 457 cm⁻¹.

¹H NMR (500 MHz, C₆D₆): δ 5.23 – 5.18 (m, 1H), 4.07 (ddd, J = 11.6, 7.9, 3.0 Hz, 1H), 3.26 – 3.20 (m, 1H), 2.28 (app dt, J = 14.2, 2.3 Hz, 1H), 2.15 (app dt, J = 14.1, 2.2 Hz, 1H), 2.07 (ddd, J = 14.2, 11.5, 0.7 Hz, 1H), 1.89 (ddd, J = 14.1, 11.5, 0.8 Hz, 1H), 1.50 (d, J = 1.0 Hz, 3H), 1.49 – 1.40 (m, 1H), 1.40 – 1.33 (m, 1H), 1.37 (d, J = 1.2 Hz, 3H), 1.27 – 1.19 (m, 1H), 1.19 – 1.10 (m, 1H), 0.78 (t, J = 7.3 Hz, 3H).

¹³C NMR (125 MHz, C₆D₆): δ 205.1, 135.4, 126.0, 76.6, 74.4, 48.2, 48.0, 38.9, 25.5, 18.8, 18.2, 14.1.

HRMS (ESI): m/z calcd. for $C_{12}H_{21}O_2$ $[M + H]^+$ 197.1536, found 197.1539.



2-(2-Methylprop-1-en-1-yl)-1-oxaspiro[5.5]undecan-4-one (2.51)

Synthesized according to general oxidation protocol A using **2.56** (21.8 mg, 0.0818 mmol), 4Å molecular sieves (21.8 mg) and Bobbitt's Salt (49.1 mg, 0.164 mmol) in MeCN (0.82 mL, 0.1 M). The reaction mixture was stirred for 30 min then purified by column

chromatography (2.5% Et₂O to 20% Et₂O in hexanes) to yield **2.51** (8.9 mg, 49%) as a low melting white solid.

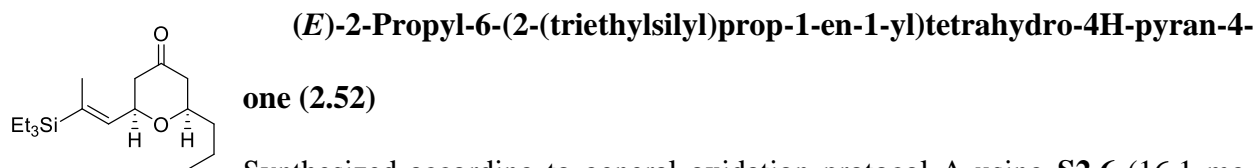
IR (ATR, neat): 2930, 2858, 1717, 1444, 1408, 1376, 1306, 1260, 1204, 1158, 1044, 977, 915, 866, 834, 752, 693, 588, 554, 524, 498 cm⁻¹.

¹H NMR (400 MHz, C₆D₆): δ 5.25 (d, *J* = 7.9 Hz, 1H), 4.43 (ddd, *J* = 11.0, 8.0, 3.0 Hz, 1H), 2.26 (app dt, *J* = 13.8, 2.4 Hz, 1H), 2.14 (dd, *J* = 13.4, 1.6 Hz, 1H), 2.06 (dd, *J* = 14.0, 11.4 Hz, 1H), 2.01 (d, *J* = 13.6 Hz, 1H), 1.84 – 1.72 (m, 1H), 1.72 – 1.59 (m, 2H), 1.52 (s, 3H), 1.48 – 1.35 (m, 2H) 1.41 (s, 3H), 1.31 – 1.18 (m, 2H), 1.18 – 1.08 (m, 1H), 1.08 – 0.94 (m, 2H).

¹³C NMR (100 MHz, C₆D₆): δ 205.6, 134.7, 126.7, 75.9, 67.3, 52.8, 48.0, 39.7, 31.8, 25.7, 25.7, 21.9, 21.5, 18.1.

HRMS (ESI): *m/z* calcd. for C₁₄H₂₃O₂ [M + H]⁺ 223.1693, found 223.1694.

Melting point: 34.8 – 35.8 °C



Synthesized according to general oxidation protocol A using **S2.6** (16.1 mg, 0.0473 mmol), 4Å molecular sieves (16.1 mg) and Bobbitt's Salt (28.4 mg, 0.0946 mmol) in MeCN (0.47 mL, 0.1 M). The reaction mixture was stirred for 2 h then purified by column (2.5% Et₂O to 10% Et₂O in hexanes) to yield **2.52** (11.2 mg, 80%) as a colorless oil.

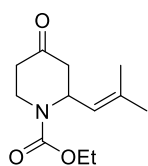
IR (ATR, neat): 3017, 2955, 2910, 2874, 1721, 1458, 1416, 1338, 1255, 1236, 1160, 1053, 1008, 962, 726, 668, 582, 548, 471 cm⁻¹.

¹H NMR (400 MHz, CDCl₃): δ 5.73 (dq, *J* = 7.2, 1.7 Hz, 1H), 4.46 (ddd, *J* = 8.8, 6.9, 5.3 Hz, 1H), 3.68 – 3.59 (m, 1H), 2.41 – 2.33 (m, 2H), 2.33 – 2.21 (m, 2H), 1.75 – 1.63 (m, 1H), 1.69 (d, *J* =

1.6 Hz, 3H), 1.55 – 1.45 (m, 2H), 1.45 – 1.33 (m, 1H). 0.93 (t, $J = 7.3$ Hz, 3H), 0.91 (t, $J = 7.8$ Hz, 9H), 0.60 (q, $J = 7.9$ Hz, 6H).

^{13}C NMR (100 MHz, CDCl_3): δ 207.6, 139.2, 137.3, 74.2, 48.0, 47.6, 38.7, 18.7, 15.9, 14.1, 7.5, 2.5.

HRMS (ESI): m/z calcd. for $\text{C}_{17}\text{H}_{33}\text{O}_2\text{Si}$ $[\text{M} + \text{H}]^+$ 297.2244, found 297.2246.



Ethyl 2-(2-methylprop-1-en-1-yl)-4-oxopiperidine-1-carboxylate (18)

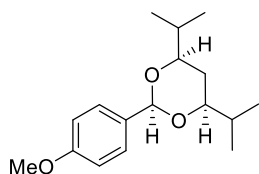
Synthesized according to general oxidation protocol A using **S2.7** (23.3 mg, 0.0865 mmol), 4Å molecular sieves (23.3 mg) and Bobbitt's Salt (51.9 mg, 0.173 mmol) in MeCN (0.87 mL, 0.1 M). The reaction mixture was stirred for 4.5 h then purified by column (15% EtOAc to 30% EtOAc in hexanes) to yield **2.53** (13.8 mg, 71%) as a colorless oil.

IR (ATR, neat): 2976, 2913, 1689, 1420, 1384, 1304, 1240, 1170, 1113, 1055, 1021, 991, 835, 767 cm^{-1} .

^1H NMR (500 MHz, CDCl_3): δ 5.41 – 5.31 (m, 1H), 5.16 – 5.11 (m, 1H), 4.32 – 4.23 (m, 1H), 4.23 – 4.14 (m, 2H), 3.34 (ddd, $J = 13.7, 11.7, 3.8$ Hz, 1H), 2.67 (dd, $J = 14.3, 6.6$ Hz, 1H), 2.50 (ddd, $J = 15.1, 11.7, 7.0$ Hz, 1H), 2.37 (ddt, $J = 15.3, 4.1, 2.0$ Hz, 1H), 2.29 (dt, $J = 14.3, 2.1$ Hz, 1H), 1.71 (s, 6H), 1.29 (t, $J = 7.1$ Hz, 3H).

^{13}C NMR (125 MHz, CDCl_3): δ 208.0, 155.1, 121.5, 61.8, 50.3, 46.5, 41.0, 39.0, 25.8, 18.3, 14.7.

HRMS (ESI): m/z calcd. for $\text{C}_{12}\text{H}_{20}\text{O}_3\text{N}$ $[\text{M} + \text{H}]^+$ 226.1438, found 226.1440.



(4R,6S)-4,6-Diisopropyl-2-(4-methoxyphenyl)-1,3-dioxane (2.60)

Synthesized according to general oxidation protocol A using **2.59** (19.1 mg, 0.0681 mmol), 4Å molecular sieves (19.1 mg) and Bobbitt's Salt (40.8 mg,

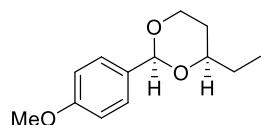
0.136 mmol) in MeCN (0.68 mL, 0.1 M). The reaction mixture was stirred for 35 min then purified by (5% EtOAc to 20% EtOAc in hexanes) to yield **2.60** (9.5 mg, 50%) as a colorless oil and **2.63** (8.3 mg, 41%) as a colorless oil.

IR (ATR, neat): 2959, 2874, 2837, 1615, 1589, 1517, 1465, 1383, 1345, 1301, 1246, 1169, 1091, 1034, 912, 827, 775, 671, 593, 511 cm^{-1} .

^1H NMR (500 MHz, CDCl_3): δ 7.44 (d, J = 8.6 Hz, 2H), 6.88 (d, J = 8.8 Hz, 2H), 5.44 (s, 1H), 3.80 (s, 3H), 3.45 (ddd, J = 11.1, 6.8, 2.3 Hz, 2H), 1.85 – 1.74 (m, 2H), 1.60 (dt, J = 12.8, 2.3 Hz, 1H), 1.35 (dt, J = 12.6, 11.3 Hz, 1H), 1.02 (d, J = 6.8 Hz, 6H), 0.95 (d, J = 6.9 Hz, 6H).

^{13}C NMR (125 MHz, CDCl_3): δ 159.7, 132.2, 127.4, 113.6, 100.3, 82.0, 55.4, 33.2, 30.9, 18.7, 18.2.

HRMS (ESI): m/z calcd. for $\text{C}_{17}\text{H}_{27}\text{O}_3$ $[\text{M} + \text{H}]^+$ 279.1955, found 279.1956.



4-Ethyl-2-(4-methoxyphenyl)-1,3-dioxane (2.62)

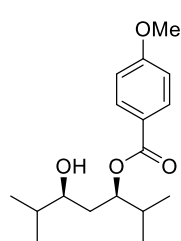
Synthesized according to general oxidation protocol A using **2.61** (16.6 mg, 0.074 mmol), 4Å molecular sieves (16.6 mg) and Bobbitt's Salt (44.0 mg, 0.148 mmol) in MeCN (0.74 mL, 0.1 M). The reaction mixture was stirred for 20 min then purified by (10% EtOAc to 30% EtOAc in hexanes) to yield **2.62** (4.6 mg, 28%) as a colorless oil.

IR (ATR, neat): 2963, 2839, 1615, 1588, 1517, 1463, 1395, 1362, 1301, 1243, 1162, 1102, 1073, 1032, 974, 897, 826, 781, 659, 594, 548, 526 cm^{-1} .

^1H NMR (400 MHz, CDCl_3): δ 7.46 – 7.40 (m, 2H), 6.91 – 6.86 (m, 2H), 5.47 (s, 1H), 4.25 (ddd, J = 11.4, 5.0, 1.1 Hz, 1H), 3.94 (ddd, J = 12.3, 11.5, 2.6 Hz, 1H), 3.80 (s, 3H), 3.77 – 3.69 (m, 1H), 1.84 – 1.73 (m, 1H), 1.73 – 1.64 (m, 1H), 1.63 – 1.48 (m, 2H), 0.98 (t, J = 7.5 Hz, 3H).

¹³C NMR (100 MHz, CDCl₃): δ 159.9, 131.7, 127.5, 113.7, 101.2, 101.2, 78.6, 67.2, 55.4, 55.4, 31.0, 29.1, 9.6.

HRMS (ESI): *m/z* calcd. for C₁₃H₁₉O₃ [M + H]⁺ 223.1329, found 223.1331.



5-Hydroxy-2,6-dimethylheptan-3-yl 4-methoxybenzoate (2.63)

To a 1 dram vile (Chemglass CG-4904-05 with a polypropylene screw cap containing a PTFE faced silicone septum) with a stir bar was added **2.60** (15.3 mg, 0.055 mmol) dissolved in MeCN (0.55 mL, 0.1 M). To this, H₂O (10 uL, 0.55 mmol, 10 equiv) was added (1 mass eq). Bobbitt's Salt (33 mg, 0.110 mmol, 2 equiv) was added to the solution, and the reaction mixture was stirred for 1.5 h. The reaction mixture was diluted with CH₂Cl₂ and transferred to a round bottom flask. The solvent was removed under reduced pressure and the crude mixture was purified by column chromatography (10% EtOAc to 20% EtOAc in hexanes) to give **2.63** (13.8 mg, 85%) as a colorless oil.

IR (ATR, neat): 3464, 2981, 2971, 2884, 1690, 1605, 1511, 1464, 1420, 1388, 1166, 1099, 1029, 956, 846, 770, 696, 613 cm⁻¹.

¹H NMR (400 MHz, CDCl₃): δ 8.00 (d, *J* = 8.8 Hz, 2H), 6.92 (d, *J* = 8.8 Hz, 2H), 5.05 (ddd, *J* = 6.8, 5.0, 5.0 Hz, 1H), 3.86 (s, 3H), 3.53 (dt, *J* = 8.6, 4.3 Hz, 1H), 2.25 (s, 1H), 2.08 – 1.95 (m, 1H), 1.86 (ddd, *J* = 14.7, 4.7, 3.9 Hz, 1H), 1.80 – 1.72 (m, 1H), 1.72 – 1.65 (m, 1H), 1.00 (d, *J* = 6.6 Hz, 3H), 0.99 (d, *J* = 6.4 Hz, 3H), 0.92 (d, *J* = 6.2 Hz, 3H), 0.90 (d, *J* = 6.4 Hz, 3H).

¹³C NMR (100 MHz, CDCl₃): δ 166.7, 163.6, 131.8, 123.1, 113.8, 77.9, 74.9, 55.6, 36.4, 33.7, 32.2, 18.9, 18.8, 17.5, 17.0.

HRMS (ESI): *m/z* calcd. for C₁₇H₂₇O₄ [M + H]⁺ 295.1904, found 295.1905.

Electrochemical oxidations

Electrodes and Electrasyn Setup for Bulk Electrolysis Reactions:



Figure 13. Electrodes that are Connected to the Vial Cap



Figure 14. Electrodes used during Electrochemical Reactions

.



Figure 15. Example of an Electrochemical Reaction Setup on the Electrasyn 2.0

Cyclic Voltammetry Studies:

All cyclic voltammetry studies were conducted at room temperature using the IKA Electrasyn 2.0. The experiments were carried out using a three electrode cell set up in which a 3 mm glassy carbon working electrode and a platinum wire counter electrode were used. For experiments in aqueous solution, potentials were measured versus an Ag/AgCl reference electrode and for those in organic solution, potentials were measured versus Ag/AgNO₃ (0.01 M AgNO₃, 0.1 M Bu₄NBF₄ in MeCN).

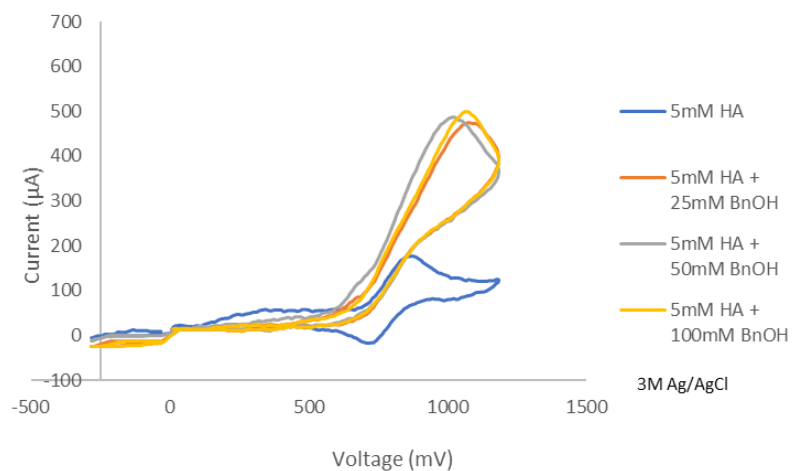


Figure 16. Cyclic voltammograms of 2.34 (5 mM) in the presence of BnOH (0 mM to 100 mM) in MeCN: pH 10 (0.1M HCO₃⁻/CO₃²⁻) buffer (1:1)

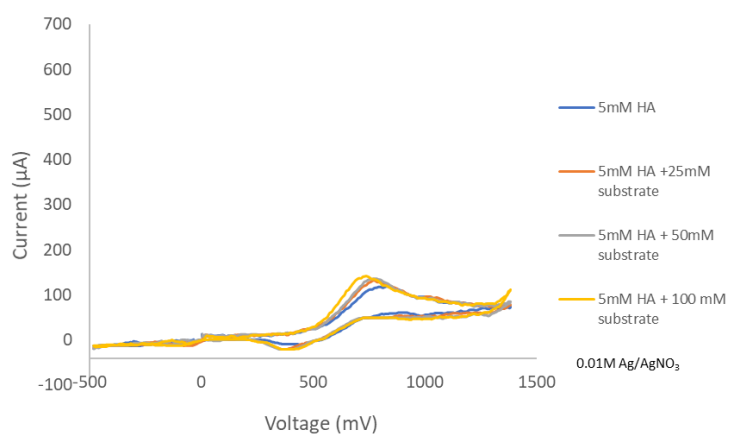
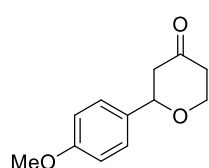


Figure 17. Cyclic Voltammograms of 2.34 (5 mM) in the presence of 2.32 (0 to 100 mM) in 0.1 M Bu₄NBF₄ in MeCN

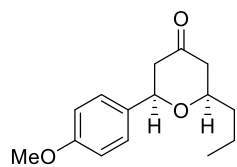
General oxidation procedure B

An IKA Electrasyn vial (5 mL) was charged with a stir bar and a solution of the substrate in freshly distilled MeCN (0.067 M). Bu₄NBF₄ (0.1 M, 1.5 equiv) and 2,2,2-trifluoroethanol (3 equiv) were added to the solution in no particular order. The oxidant (0.20 equiv) was added and the vial was shaken lightly to dissolve the solids. The Electrasyn vial cap equipped with a graphite anode, platinum foil cathode and a reference electrode (Ag/AgNO₃, 0.01 M AgNO₃, 0.1 M Bu₄NBF₄ in MeCN) was inserted into the reaction mixture and secured tightly to the vial. The reaction mixture was set to react at a constant potential of 1.6 V, stirring at 800 rpm and monitored by TLC until starting material was consumed or the current flowing through the cell was less than 2.5 mA. Once completed, the vial cap was removed and the electrodes were rinsed with CH₂Cl₂ into a round bottom flask. The reaction mixture was transferred to the same flask using CH₂Cl₂ and the solvent removed under reduced pressure. The crude material was purified by column chromatography to yield the desired product.



2-(4-Methoxyphenyl)tetrahydro-4H-pyran-4-one (**2.36**)

General oxidation protocol B was followed with **2.33** (67.7 mg, 0.270 mmol), Bu₄NBF₄ (0.133 g, 0.1 M), 2,2,2-trifluoroethanol (59 μ L, 0.810 mmol, 3 equiv.) and Bobbitt's salt (16.2 mg, 0.054 mmol, 0.2 equiv.) in MeCN (4 mL, 0.067 M). The reaction mixture was electrolyzed at 1.6 V for 8 h (4.89 F/mol) to yield **2.36** (55%, ¹H NMR yield relative to Me₃SiOMe as an internal standard). Spectral data matched those from the stoichiometric oxidation.

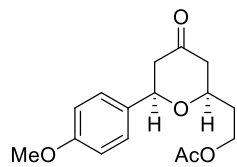


2-(4-Methoxyphenyl)-6-propyltetrahydro-4H-pyran-4-one (**2.35**)

General oxidation protocol B was followed with **2.32** (87.5 mg, 0.299 mmol), Bu₄NBF₄ (0.147 g, 0.1 M), 2,2,2-trifluoroethanol (65 μL, 0.897 mmol, 3 equiv.) and Bobbitt's salt (17.9 mg, 0.0598 mmol, 0.2 equiv.) in MeCN (4.5 mL, 0.0667 M). The reaction mixture was electrolyzed at 1.6 V for 8 h (4.79 F/mol). Once completed, the crude material was purified by column chromatography (5% Et₂O to 30% Et₂O in hexanes) to yield **2.35** (48.5 mg, 65%) as a colorless oil. Spectral data matched those from the stoichiometric oxidation.

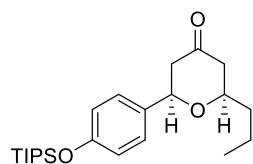
Using 4-acetamido-2,2,6,6-tetramethylpiperidine 1-oxyl (ACT)

An IKA Electrasyn vial (5 mL) was flame dried and charged with a stir bar. ACT (12.4 mg, 0.058 mmol) and Bu₄NBF₄ (0.143 g, 1.5 equiv., 0.1 M final concentration) were dissolved in MeCN (2.9 mL). Following this, 2,2,2-trifluoroethanol (63 μL, 0.870 mmol, 3 equiv.) was added to the solution and the Electrasyn vial cap equipped with a graphite anode, platinum foil cathode and a reference electrode (Ag/AgNO₃, 0.01 M AgNO₃, 0.1 M Bu₄NBF₄ in MeCN) was inserted into the reaction mixture, and secured tightly to the vial. The reaction mixture was set to react at a constant potential of 1.6 V, stirring at 800 rpm for 15 min or until current begins to drop. At this point, a solution of **2.32** (84.7 mg, 0.29 mmol) in 1.4 mL of MeCN was transferred to the reaction vial. The reaction was stirred for 16 h (11.85 F/mol) to yield **2.35** (70%, ¹H NMR yield relative to 2,5-dibromo-1-nitrobenzene as an internal standard).



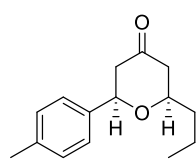
2-(6-(4-Methoxyphenyl)-4-oxotetrahydro-2H-pyran-2-yl)ethyl acetate (2.43)

General oxidation protocol A was followed with **2.42** (91.1 mg, 0.271 mmol), Bu₄NBF₄ (0.135 g, 0.1 M), 2,2,2-trifluoroethanol (59 μL, 0.813 mmol, 3 equiv.) and Oxo-TEMPO⁺ BF₄⁻ (13.9 mg, 0.0542 mmol, 0.2 equiv.) in MeCN (4.1 mL, 0.0667 M). The reaction mixture was electrolyzed at 1.6 V for 12 h (7.38 F/mol). Once completed, the crude material was purified by column chromatography (15% EtOAc to 30% EtOAc in hexanes) to yield **2.43** (48 mg, 61%) as a colorless oil. Spectral data matched those from the stoichiometric oxidation.



2-Propyl-6-(4-((triisopropylsilyl)oxy)phenyl)tetrahydro-4H-pyran-4-one (2.44)

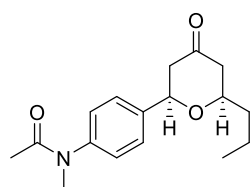
General oxidation protocol B was followed with **S2.1** (0.112 g, 0.258 mmol), Bu₄NBF₄ (0.127 g, 0.1 M), 2,2,2-trifluoroethanol (56 μL, 0.774 mmol, 3 equiv.) and Bobbitt's salt (15.5 mg, 0.0516 mmol, 0.2 equiv.) in MeCN (3.9 mL, 0.0667 M). The reaction mixture was electrolyzed at 1.6 V for 10 h (5.46 F/mol). Once completed, the crude material was purified by column chromatography (5% Et₂O to 15% Et₂O in hexanes) to yield **2.44** (61.6 mg, 61%) as a colorless oil. Spectral data matched those from the stoichiometric oxidation.



2-Propyl-6-(p-tolyl)tetrahydro-4H-pyran-4-one (2.45)

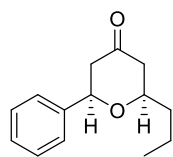
General oxidation protocol B was followed with **S2.2** (82.6 mg, 0.299 mmol), Bu₄NBF₄ (0.148 g, 0.1 M), 2,2,2-trifluoroethanol (64 μL, 0.897 mmol, 3 equiv.) and Oxo-TEMPO⁺ BF₄⁻ (15.4 mg, 0.0598 mmol, 0.2 equiv.) in MeCN (4.5 mL, 0.0667 M). The reaction mixture was electrolyzed at 1.7 V for 12 h (6.82 F/mol). Once completed, the crude

material was purified by column chromatography (5% Et₂O to 15% Et₂O in hexanes) to yield **2.45** (47.1 mg, 68%) as a white sticky solid. Spectral data matched those from the stoichiometric oxidation.



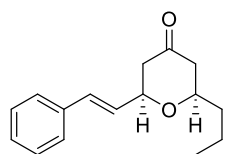
***N*-Methyl-*N*-(4-(4-oxo-6-propyltetrahydro-2H-pyran-2-yl)phenyl)acetamide (**2.46**)**

General oxidation protocol B was followed with **S2.3** (0.101 g, 0.303 mmol), Bu₄NBF₄ (0.149 g, 0.1 M), 2,2,2-trifluoroethanol (66 µL, 0.909 mmol, 3 equiv.) and Oxo-TEMPO⁺ BF₄⁻ (15.6 mg, 0.0606 mmol, 0.2 equiv.) in MeCN (4.5 mL, 0.0667 M). The reaction mixture was electrolyzed at 1.6 V for 30 h (20.59 F/mol) to yield **2.46** (54%, ¹H NMR yield relative to 2,5-dibromo-1-nitrobenzene as an internal standard). Spectral data matched those from the stoichiometric oxidation.



2-Phenyl-6-propyltetrahydro-4H-pyran-4-one (2.47**)**

General oxidation protocol B was followed with **S2.4** (73.1 mg, 0.279 mmol), Bu₄NBF₄ (0.138 g, 0.1 M), 2,2,2-trifluoroethanol (60 µL, 0.837 mmol, 3 equiv.) and **2d** (14.3 mg, 0.0558 mmol, 0.2 equiv.) in MeCN (4.2 mL, 0.0667 M). The reaction mixture was electrolyzed at 1.6 V for 15 h. At this point, additional **2d** (7.2 mg, 0.0279 mmol, 0.1 equiv) was added to the reaction mixture and was electrolyzed at 1.6 V for a further 15 h (11.7 F/mol total). Once completed the crude material was purified by column chromatography (5% to 10% Et₂O in hexanes) to yield **2.47** (44.5 mg, 73%) as a colorless oil. Spectral data matched those from the stoichiometric oxidation.

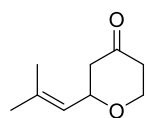


(E)-2-Propyl-6-styryltetrahydro-4H-pyran-4-one (2.48)

General oxidation protocol B was followed with **S2.5** (86.5 mg, 0.3 mmol),

Bu₄NBF₄ (0.148 g, 0.1 M), 2,2,2-trifluoroethanol (65 μL, 0.9 mmol, 3 equiv.)

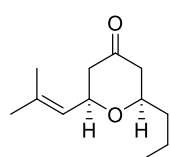
and Bobbitt's salt (18.0 mg, 0.06 mmol, 0.2 equiv.) in MeCN (4.5 mL, 0.0667 M). The reaction mixture was electrolyzed at 1.6 V for 10 h (5.43 F/mol). Once completed, the crude material was purified by column chromatography (2.5% Et₂O to 10% Et₂O in hexanes) to yield **2.48** (42.7 mg, 58%) as a colorless oil. Spectral data matched those from the stoichiometric oxidation.



2-(2-Methylprop-1-en-1-yl)tetrahydro-4H-pyran-4-one (2.49)

General oxidation protocol B was followed with **2.54** (57.6 mg, 0.291 mmol),

Bu₄NBF₄ (0.144 g, 0.1 M), 2,2,2-trifluoroethanol (63 μL, 0.873 mmol, 3 equiv.) and Bobbitt's salt (17.5 mg, 0.0582 mmol, 0.2 equiv.) in MeCN (4.4 mL, 0.0667 M). The reaction mixture was electrolyzed at 1.6 V for 6.5 h (5.27 F/mol). Once completed, the crude material was purified by column chromatography (10% Et₂O to 30% Et₂O in hexanes) to yield **2.49** (26.2 mg, 58%) as a colorless oil. Spectral data matched those from the stoichiometric oxidation.



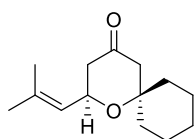
2-(2-Methylprop-1-en-1-yl)-6-propyltetrahydro-4H-pyran-4-one (2.50)

General oxidation protocol B was followed with **2.55** (72.1 mg, 0.3 mmol),

Bu₄NBF₄ (0.148 g, 0.1 M), 2,2,2-trifluoroethanol (65 μL, 0.9 mmol, 3 equiv.) and

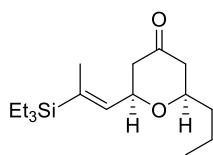
Bobbitt's salt (18.0 mg, 0.06 mmol, 0.2 equiv.) in MeCN (4.5 mL, 0.0667 M). The reaction mixture was electrolyzed at 1.6 V for 8 h (4.42 F/mol). Once completed, the crude material was purified

by column chromatography (5% Et₂O to 15% Et₂O in hexanes) to yield **2.50** (39.2 mg, 67%) as a colorless oil. Spectral data matched those from the stoichiometric oxidation.



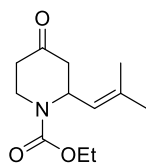
2-(2-Methylprop-1-en-1-yl)-1-oxaspiro[5.5]undecan-4-one (2.51)

General oxidation protocol B was followed with **2.56** (73.2 mg, 0.275 mmol), Bu₄NBF₄ (0.136 g, 0.1 M), 2,2,2-trifluoroethanol (60 μL, 0.825 mmol, 3 equiv.) and Bobbitt's salt (16.5 mg, 0.055 mmol, 0.2 equiv.) in MeCN (4.1 mL, 0.0667 M). The reaction mixture was electrolyzed at 1.6 V for 6 h (4.62 F/mol). Once completed, the crude material was purified by column chromatography (5% Et₂O to 15% Et₂O in hexanes) to yield **2.51** (42.9 mg, 70%) as a white solid. Spectral data matched those from the stoichiometric oxidation.



(E)-2-Propyl-6-(2-(triethylsilyl)prop-1-en-1-yl)tetrahydro-4H-pyran-4-one (2.52)

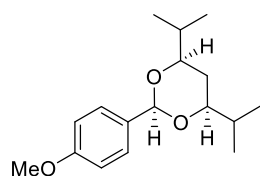
General oxidation protocol B was followed with **S2.6** (83.2 mg, 0.244 mmol), Bu₄NBF₄ (0.121 g, 0.1 M), 2,2,2-trifluoroethanol (53 μL, 0.732 mmol, 3 equiv.) and Bobbitt's salt (14.7 mg, 0.0489 mmol, 0.2 equiv.) in MeCN (3.7 mL, 0.0667 M). The reaction mixture was electrolyzed at 1.6 V for 13 h (7.48 F/mol). Once completed, the crude material was purified by column chromatography (2.5% Et₂O to 10% Et₂O in hexanes) to yield **2.52** (51.2 mg, 71%) as a colorless oil. Spectral data matched those from the stoichiometric oxidation.



Ethyl 2-(2-methylprop-1-en-1-yl)-4-oxopiperidine-1-carboxylate (2.53)

General oxidation protocol B was followed with **S2.7** (80.3 mg, 0.298 mmol), Bu₄NBF₄ (0.147 g, 0.1 M), 2,2,2-trifluoroethanol (65 μL, 0.894 mmol, 3 equiv.) and

Oxo-TEMPO⁺ BF₄⁻ (15.3 mg, 0.0596 mmol, 0.2 equiv.) in MeCN (4.5 mL, 0.0667 M). The reaction mixture was electrolyzed at 1.6 V for 10 h (7.94 F/mol). Once completed, the crude material was purified by column chromatography (10% EtOAc to 30% EtOAc in hexanes) to yield **2.53** (50.2 mg, 75%) as a colorless oil. Spectral data matched those from the stoichiometric oxidation.



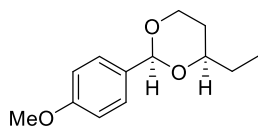
(4*R*,6*S*)-4,6-Diisopropyl-2-(4-methoxyphenyl)-1,3-dioxane (2.60)

Using Bobbitt's Salt:

General oxidation protocol B was followed with **2.59** (75.5 mg, 0.269 mmol), Bu₄NBF₄ (0.133 g, 0.1 M), 2,2,2-trifluoroethanol (58 μL, 0.801 mmol, 3 equiv.) and Bobbitt's salt (16.2 mg, 0.0538 mmol, 0.2 equiv.) in MeCN (4.0 mL, 0.0667 M). The reaction mixture was electrolyzed at 1.6 V for 1.8 h (2.05 F/mol). Once completed, the crude material was purified by column chromatography (10% Et₂O to 20% Et₂O in hexanes) to yield **2.60** (60.9 mg, 81%) as a colorless oil and **2.63** (8.5 mg, 10%) as a colorless oil. Spectral data matched those from the stoichiometric oxidation.

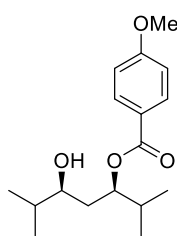
Using TEMPO⁺BF₄⁻:

General oxidation protocol B was followed with **2.59** (81.8 mg, 0.292 mmol), Bu₄NBF₄ (0.144 g, 0.1 M), 2,2,2-trifluoroethanol (63 μL, 0.876 mmol, 3 equiv.) and TEMPO⁺BF₄⁻ (14.2 mg, 0.0583 mmol, 0.2 equiv.) in MeCN (4.4 mL, 0.0667 M). The reaction mixture was electrolyzed at 1.6 V for 1.5 h (1.91 F/mol). Once completed, the crude material was purified by column chromatography (10% Et₂O to 20% Et₂O in hexanes) to yield **2.60** (60.5 mg, 74%) as a colorless oil.



4-Ethyl-2-(4-methoxyphenyl)-1,3-dioxane (**2.62**)

General oxidation protocol B was followed with **2.61** (62.7 mg, 0.28 mmol), Bu₄NBF₄ (0.138 g, 0.1 M), 2,2,2-trifluoroethanol (61 μL, 0.84 mmol, 3 equiv.) and Bobbitt's salt (16.8 mg, 0.056 mmol, 0.2 equiv.) in MeCN (4.2 mL, 0.0667 M). The reaction mixture was electrolyzed at 1.6 V for 1.4 h (2.07 F/mol). Once completed, the crude material was purified by column chromatography (5% EtOAc to 20% EtOAc in hexanes) to yield **2.62** (38.6 mg, 62%) as a colorless oil. Spectral data matched those from the stoichiometric oxidation.



5-Hydroxy-2,6-dimethylheptan-3-yl 4-methoxybenzoate (**2.63**)

To an IKA 5 mL vial was added **2.60** (52.9 mg, 0.190 mmol) in MeCN (2.85 mL, 0.0667 M). Bu₄NBF₄ (93.8 mg, 0.1 M), and H₂O (17.1 μL, 0.950 mmol, 5 equiv.) were added to the solution. Bobbitt's salt (11.4 mg, 0.0380 mmol, 0.2 equiv.) was then added and the vial shaken lightly to dissolve the oxidant. The Electrasyn vial cap equipped with a graphite anode, platinum foil cathode and a reference electrode (0.01 M AgNO₃, 0.1 M Bu₄NBF₄ in MeCN) was inserted into the reaction mixture, and secured tightly to the vial. The reaction mixture was electrolyzed at 1.6 V for 9 h (8.84 F/mol) stirring at 800 rpm. At this point, more H₂O (17.1 μL, 0.950 mmol, 5 equiv.) was added to the reaction mixture and stirred for 12 h (10.23 F/mol). Once completed, the Electrasyn vial cap was removed, and the electrodes rinsed with CH₂Cl₂ into a round bottom flask. The reaction mixture was transferred to the same flask using CH₂Cl₂ and the solvent removed under reduced pressure. The crude material was purified by column chromatography (10% to 20% EtOAc in hexanes) to yield **2.63** (40 mg, 72%) as a colorless oil. Spectral data matched those from the stoichiometric oxidation.

1 mmol Experiments

(20 mol% catalyst, 1.6 V, 0.1 M)

To a flame dried IKA 10 mL vial with a stir bar was added **2.55** (0.242 g, 1.01 mmol) in MeCN (10 mL, 0.1 M). Bu₄NBF₄ (0.329 g, 0.1 M), and 2,2,2-trifluoroethanol (0.22 mL, 3.03 mmol, 3 equiv.) were added to the solution. Bobbitt's salt (60.6 mg, 0.202 mmol, 0.2 equiv.) was then added and the vial shaken lightly to dissolve the oxidant. The Electrasyn vial cap equipped with a graphite anode, platinum foil cathode and a reference electrode (0.01 M AgNO₃, 0.1 M Bu₄NBF₄ in MeCN) was inserted into the reaction mixture and secured tightly to the vial. The reaction mixture was electrolyzed at 1.6 V for 10 h (3.10 F/mol) stirring at 800 rpm. Once completed, the Electrasyn vial cap was removed, and the electrodes rinsed with CH₂Cl₂ into a round bottom flask. The reaction mixture was transferred to the same flask using CH₂Cl₂ and the solvent removed under reduced pressure. The crude material was purified by column chromatography (5% Et₂O to 15% Et₂O in hexanes) to yield **2.50** (0.127 g, 64%) as a colorless oil.

(10 mol% catalyst, 1.6 V, 0.1 M)

To a flame dried IKA 10 mL vial with a stir bar was added **2.55** (0.241 g, 1.00 mmol) in MeCN (10 mL, 0.1 M). Bu₄NBF₄ (0.329 g, 0.1 M), and 2,2,2-trifluoroethanol (0.22 mL, 3.00 mmol, 3 equiv.) were added to the solution. Bobbitt's salt (30.0 mg, 0.10 mmol, 0.1 equiv.) was then added and the vial shaken lightly to dissolve the oxidant. The Electrasyn vial cap equipped with a graphite anode, platinum foil cathode and a reference electrode (0.01 M AgNO₃, 0.1 M Bu₄NBF₄ in MeCN) was inserted into the reaction mixture and secured tightly to the vial. The reaction mixture was electrolyzed at 1.6 V for 16 h (3.31 F/mol) stirring at 800 rpm. Once completed, the Electrasyn vial cap was removed, and the electrodes rinsed with CH₂Cl₂ into a round bottom flask. The

reaction mixture was transferred to the same flask using CH_2Cl_2 and the solvent removed under reduced pressure. The crude material was purified by column chromatography (5% Et_2O to 15% Et_2O in hexanes) to yield **2.50** (0.123 g, 63%) as a colorless oil.

(20 mol% catalyst, 1.4 V, 0.1 M)

To a flame dried IKA 10 mL vial with a stir bar was added **2.55** (0.241 g, 1.00 mmol) in MeCN (10 mL, 0.1 M). Bu_4NBF_4 (0.329 g, 0.1 M), and 2,2,2-trifluoroethanol (0.22 mL, 3.00 mmol, 3 equiv.) were added to the solution. Bobbitt's salt (60.0 mg, 0.20 mmol, 0.2 equiv.) was then added and the vial shaken lightly to dissolve the oxidant. The Electrasyn vial cap equipped with a graphite anode, platinum foil cathode and a reference electrode (0.01 M AgNO_3 , 0.1 M Bu_4NBF_4 in MeCN) was inserted into the reaction mixture, and secured tightly to the vial. The reaction mixture was electrolyzed at 1.4 V for 13 h (2.15 F/mol) stirring at 800 rpm to give **2.50** (56%, ^1H NMR yield relative to 2,5-dibromo-1-nitrobenzene as an internal standard).

(20 mol% catalyst, 1.4 V, 0.2 M)

To a flame dried IKA 5 mL vial with a stir bar was added **2.55** (0.241 g, 1.00 mmol) in MeCN (5 mL, 0.2 M). Bu_4NBF_4 (0.165 g, 0.1 M), and 2,2,2-trifluoroethanol (0.22 mL, 3.00 mmol, 3 equiv.) were added to the solution. Bobbitt's salt (60.0 mg, 0.20 mmol, 0.2 equiv.) was then added and the vial shaken lightly to dissolve the oxidant. The Electrasyn vial cap equipped with a graphite anode, platinum foil cathode and a reference electrode (0.01 M AgNO_3 , 0.1 M Bu_4NBF_4 in MeCN) was inserted into the reaction mixture, and secured tightly to the vial. The reaction mixture was electrolyzed at 1.4 V for 12 h (2.12 F/mol) stirring at 800 rpm to give **2.50** (59%, ^1H NMR yield relative to 2,5-dibromo-1-nitrobenzene as an internal standard).

(20 mol% catalyst, 1.4 V, 0.0667 M)

To a flame dried IKA 5 mL vial with a stir bar was added **2.55** (69.3 mg, 0.288 mmol) in MeCN (4.3 mL, 0.0667 M). Bu₄NBF₄ (0.142 g, 0.1 M), and 2,2,2-trifluoroethanol (62 μ L, 0.864 mmol, 3 equiv.) were added to the solution. Bobbitt's salt (17.3 mg, 0.0576 mmol, 0.2 equiv.) was then added and the vial shaken lightly to dissolve the oxidant. The Electrasyn vial cap equipped with a graphite anode, platinum foil cathode and a reference electrode (0.01 M AgNO₃, 0.1 M Bu₄NBF₄ in MeCN) was inserted into the reaction mixture and secured tightly to the vial. The reaction mixture was electrolyzed at 1.4 V for 3 h (1.08 F/mol) stirring at 800 rpm to give **2.50** (38%, ¹H NMR yield relative to 2,5-dibromo-1-nitrobenzene as an internal standard).

Kinetics Studies

General Procedure for Rate Constant Determination

Absorbance data was collected using an Evolution 600 UV-Visible Spectrophotometer at 25 °C and at 456 nm for Bobbitt's Salt (**2a**), and 381 nm for Oxo-TEMPO⁺ (**2b**). The oxidant (1 eq) and substrate (10 eq) were added to dry MeCN to reach the final concentration denoted in each plot. A decrease in absorbance as a function of time was measured, and its natural log of that relationship gave the slope $-k_{obs}$. The biomolecular rate constant k , was calculated by dividing k_{obs} by substrate concentration. From this, using the Eyring equation shown below, the ΔG^\ddagger was calculated:

$$\Delta G^\ddagger = -RT \ln \left(\frac{kh}{k_B T} \right)$$

Equation 5. Eyring Equation

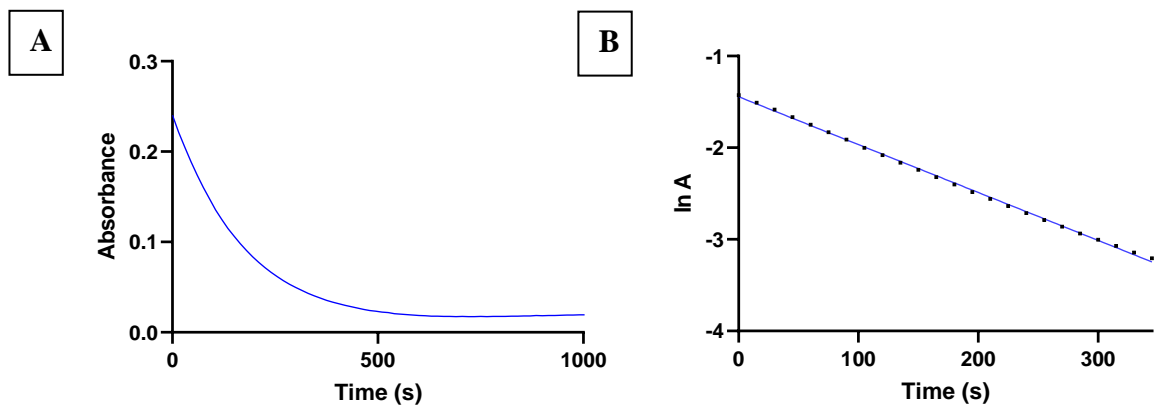


Figure 18. A) Absorbance vs time for reaction of Bobbitt's Salt with 1-A ($[5] = 0.01$ M; $[1-A] = 0.1$ M). B) Natural log of Absorbance vs time, $y = -0.005225x - 1.444$. $R^2 = 0.9991$

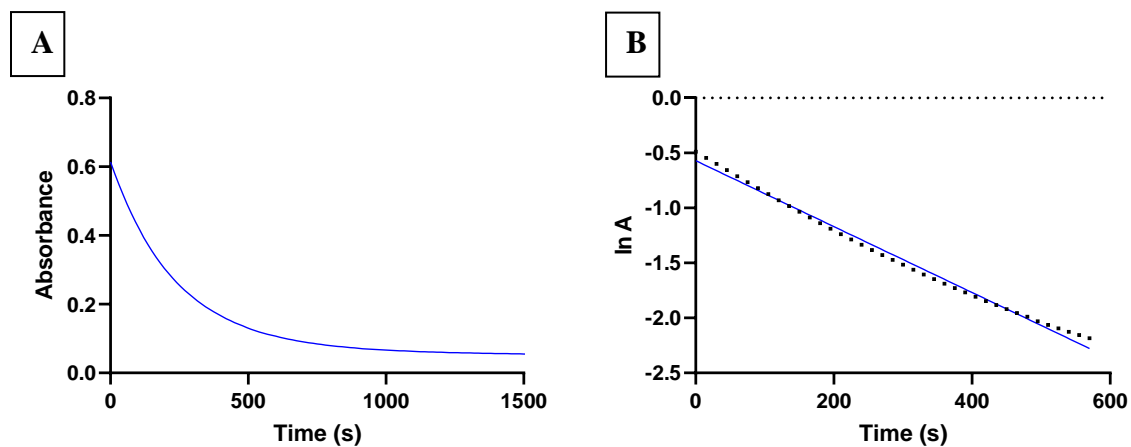


Figure 19. A) Absorbance vs time for reaction of Bobbitt's Salt with 6-A ($[5] = 0.02$ M; $[6-A] = 0.2$ M). B) Natural log of Absorbance vs time, $y = -0.002994x - 0.5704$; $R^2 = 0.9928$

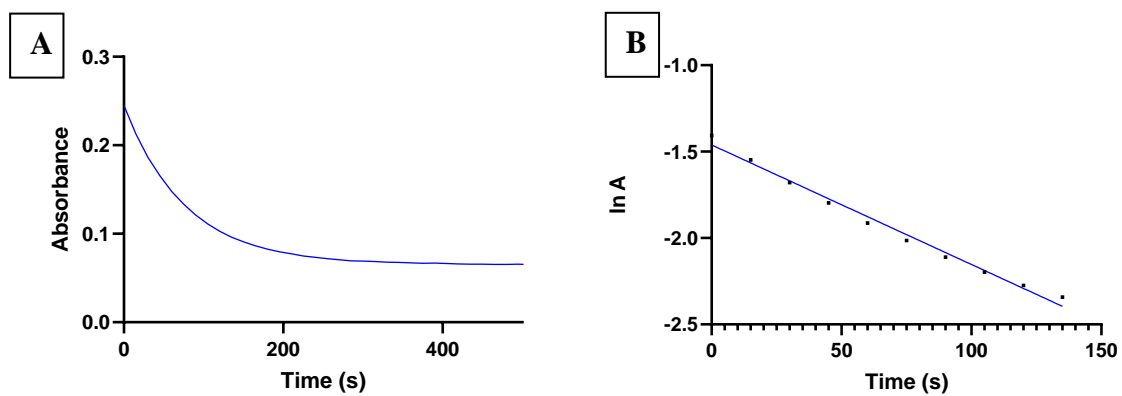
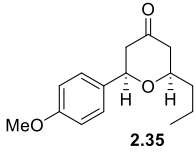
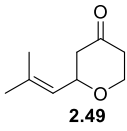
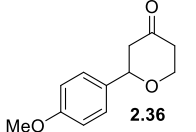
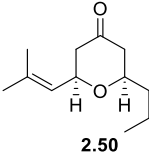
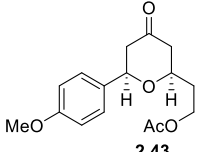
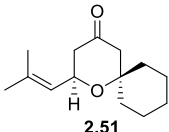
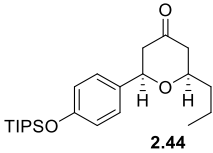
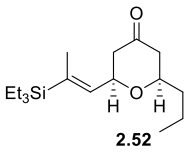
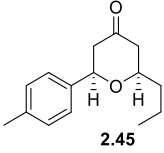
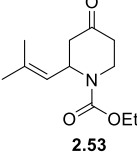
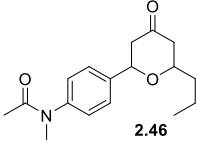
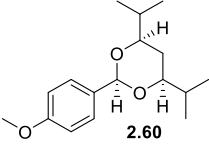


Figure 20. A) Absorbance vs time for reaction of Oxo-TEMPO⁺ BF₄⁻ with 6-A ([8] = 0.01 M; [6-A] = 0.1 M). B) Natural log of Absorbance vs time, $y = -0.006918x - 1.461$; $R^2 = 0.9883$.

Compound	Time (h)	F/mol	Compound	Time (h)	F/mol
 2.35	5: 8 ACT: 16	5: 4.79 ACT: 11.85	 2.49	6.5	5.27
 2.36	8	4.89	 2.50	0.0667 M: 8 0.1 M (20 mol%): 10 0.1 M (10 mol%): 16	4.42 3.10 3.31
 2.43	12	7.38	 2.51	6	4.62
 2.44	10	5.46	 2.52	13	7.48
 2.45	12	6.82	 2.53	10	7.94
 2.46	30	20.59	 2.60	5 : 1.8 TEMPO⁺: 1.5	5: 2.05 TEMPO⁺: 1.91

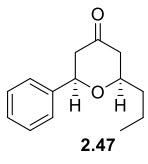
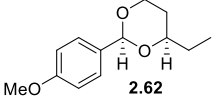
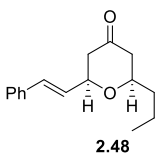
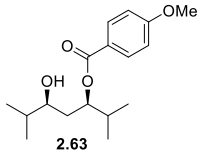
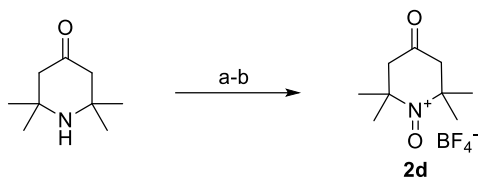
 2.47	30 (20 mol%) 30 (30 mol%)	21.39 11.7	 2.62	1.4	2.07
 2.48	10	5.43	 2.63	21	19.07

Table 11. Charge per mol Transferred in Each Reaction

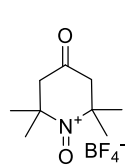
Synthesis of Oxoammonium Salts:



Reagents and Conditions:

- a) EDTA, Na₂WO₄·2H₂O, H₂O₂, MeOH, H₂O, 52%
b) HBF₄, Et₂O, 0 °C, 37%

Scheme 93. Synthesis of Compound 2d



Oxo-TEMPO⁺BF₄⁻ (2d)

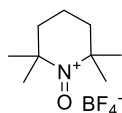
IR (ATR, neat): 2981, 1727, 1473, 1380, 1248, 1157, 1094, 1034, 520, 475 cm⁻¹.

¹H NMR (500 MHz, CF₃COOD): δ 3.79 (s, 4H), 1.91 (s, 12H).

¹³C NMR (125 MHz, CF₃COOD): δ 204.3, 103.5, 50.9, 31.0.

HRMS (ESI): *m/z* calcd. for C₉H₁₆O₂N⁺ [M]⁺ 170.1176, found 170.1178.

Melting point: 101 °C (decomposition).¹⁰⁶



TEMPO⁺BF₄⁻ (2b)

To a solution of TEMPO (2 g, 12.8 mmol) stirring in H₂O (5.1 mL) was added HBF₄ (50% in H₂O, 2 mL, 14.6 mmol) dropwise over 30 min. Upon addition, Commercial bleach (6% wt NaOCl, 2.0 mL, 6.4 mmol) was added dropwise over 3 h while vigorously stirring. Once all the bleach was added, NaBF₄ (1.41 g, 12.8 mmol) was added and the reaction mixture stirred for 10 min and then cooled to 0 °C continuing to stir for 2 h. The resulting bright yellow solid was collected via vacuum filtration and was left to dry under vacuum overnight yielding, TEMPO⁺BF₄⁻ (1.21 g, 50%), as a bright yellow powder.

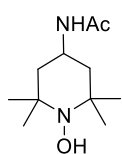
IR (ATR, neat): 2981, 1628, 1471, 1385, 1238, 1035, 760, 522, 474 cm⁻¹.

¹H NMR (500 MHz, CF₃COOD): δ 2.67 – 2.61 (m, 4H), 2.60 – 2.51 (m, 2H), 1.77 (s, 12H).

¹³C NMR (125 MHz, CF₃COOD): δ 107.5, 42.9, 31.1, 18.0.

HRMS (ESI): *m/z* calcd. for C₉H₁₈ON⁺ [M]⁺ 156.1383, found 156.1384.

Melting point: 175.8 °C (decomposition).^{106, 107}



***N*-(1-hydroxy-2,2,6,6-tetramethylpiperidin-4-yl)acetamide (2.34)**

To a suspension of ACT (0.2 g, 0.938 mmol) in water (2.6 mL, 0.36 M) charged with a stir bar was added sodium ascorbate (0.316 g, 1.59 mmol). The suspension was stirred until completely decolorized and a white precipitate appeared. The aqueous suspension was extracted with EtOAc twice, and the organic layers combined. The combined organic layer was washed with water and dried over MgSO₄. This was decanted into a round bottom flask and solvent removed under reduced pressure to give **2.34** (66 mg, 33%) as an off white solid.

IR (ATR, neat): 3307, 2978, 1640, 1620, 1563, 1370, 1322, 1248, 1175, 1096, 978, 612, 546, 489 cm^{-1} .

^1H NMR (300 MHz, CDCl_3): δ 5.17 (s, 1H), 4.26 – 4.08 (m, 1H), 1.96 (s, 3H), 1.87 (dd, $J = 12.0$, 3.5 Hz, 2H), 1.30 (app t, $J = 12.4$ Hz, 2H), 1.20 (s, 6H), 1.18 (s, 6H).

^{13}C NMR (75 MHz, CDCl_3): δ 168.9, 58.8, 45.4, 40.7, 32.1, 23.4, 19.3.

HRMS (ESI): m/z calcd. for $\text{C}_{17}\text{H}_{27}\text{O}_4$ $[\text{M} + \text{H}]^+$ 215.1754, found 215.1758.

Melting point: 160.4 – 162.9 $^{\circ}\text{C}$.

Obtainable CVs of other Substrates:

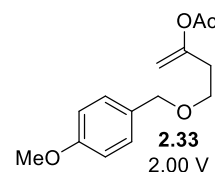
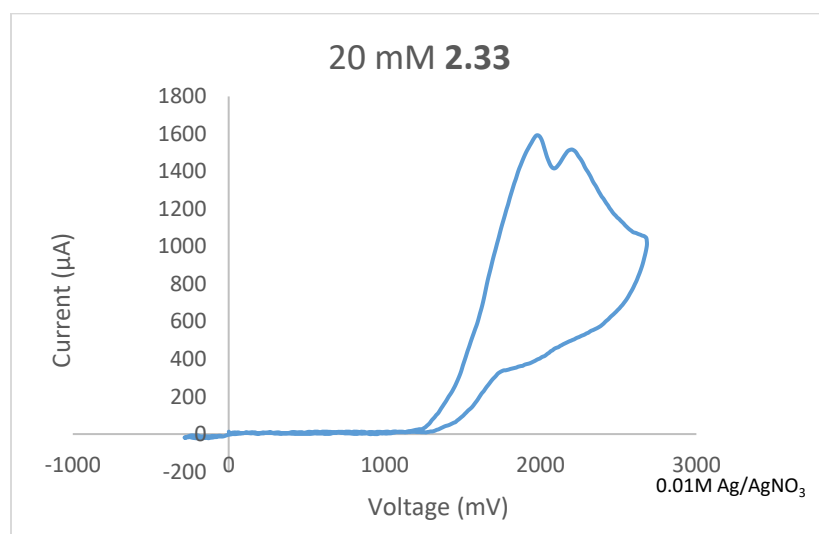


Figure 21. Cyclic Voltammogram of 2.33

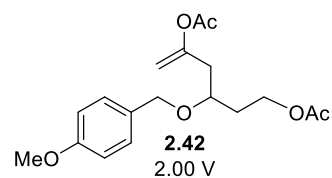
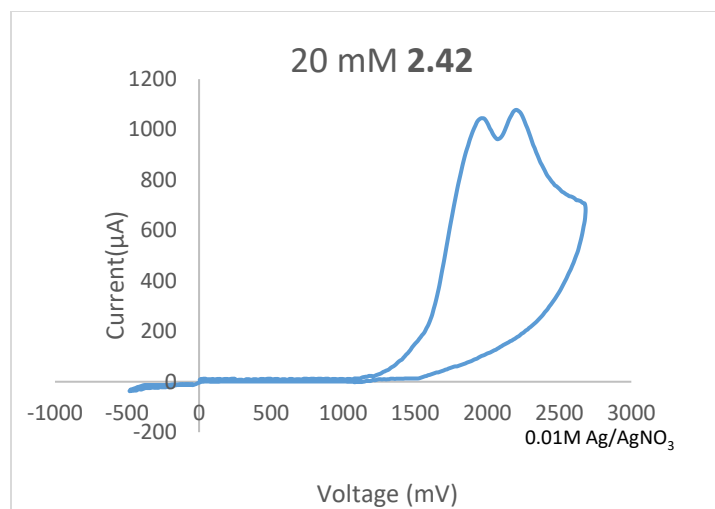


Figure 22. Cyclic Voltammogram of 2.42

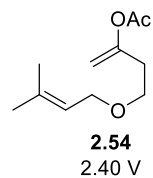
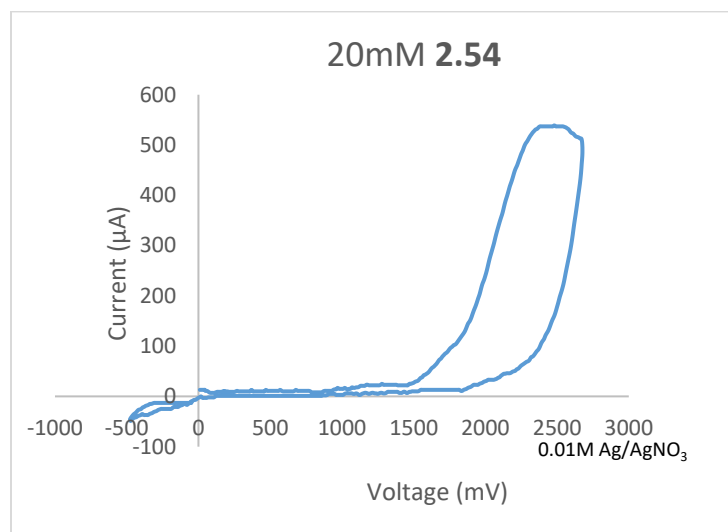


Figure 23. Cyclic Voltammogram of 2.54

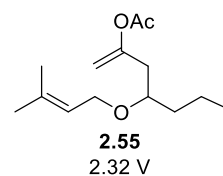
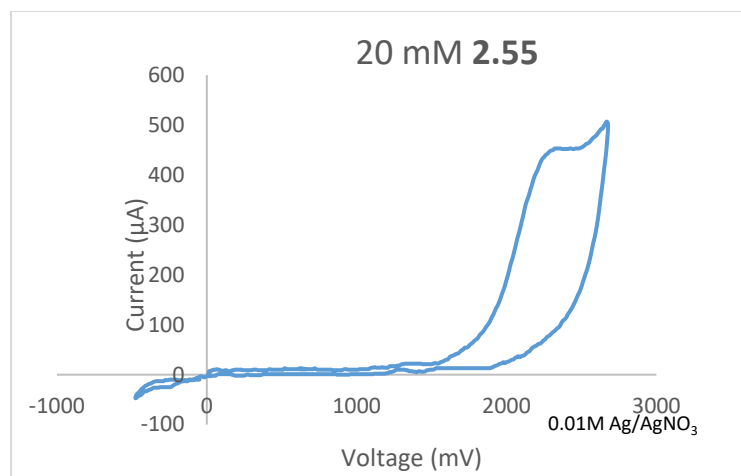


Figure 24. Cyclic Voltammogram of 2.55

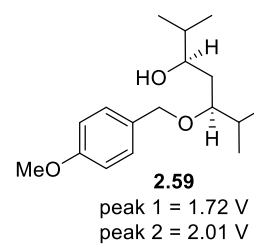
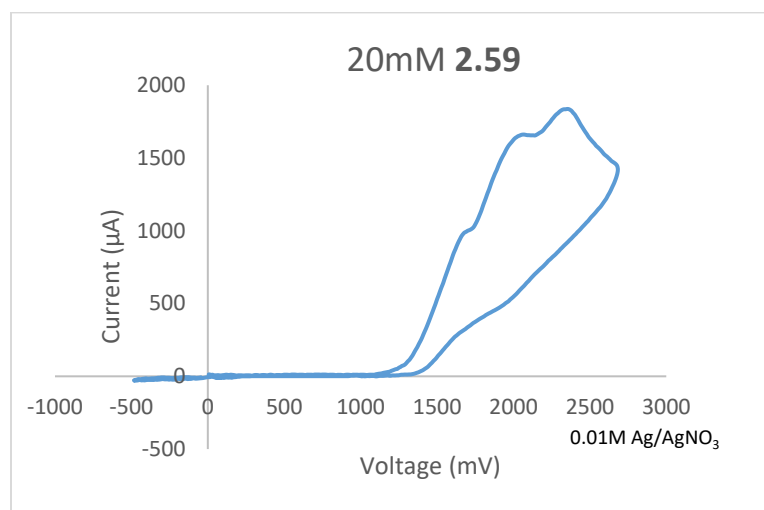


Figure 25. Cyclic Voltammogram of 2.59

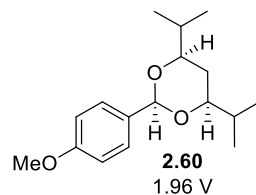
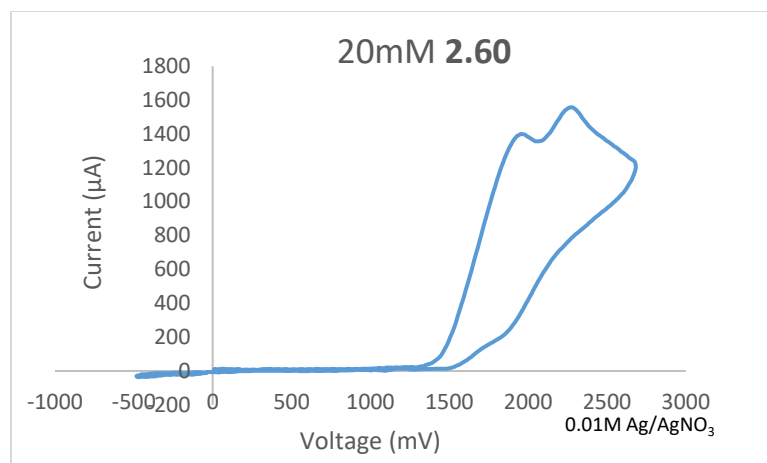


Figure 26. Cyclic Voltammogram of 2.60

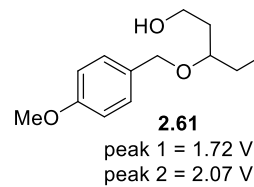
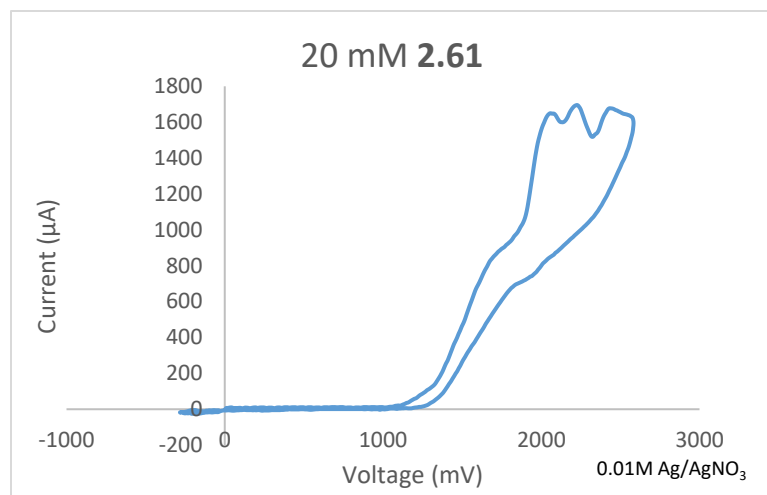


Figure 27. Cyclic Voltammogram of 2.61

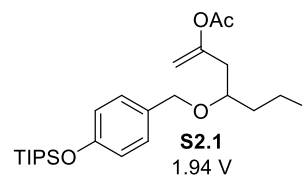
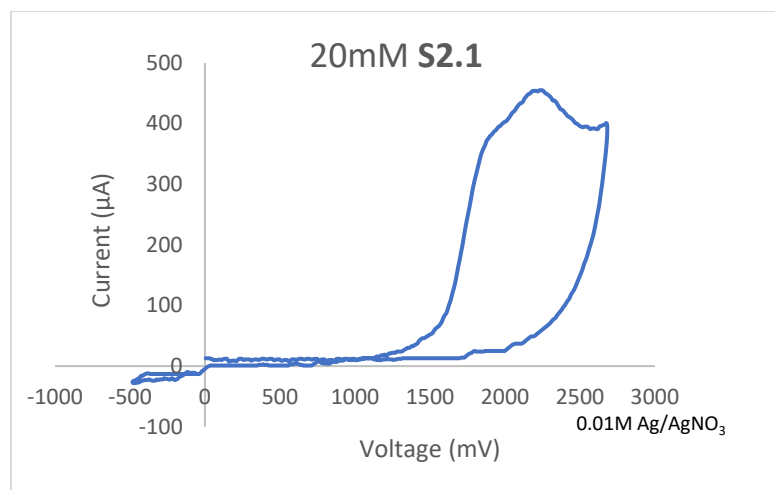


Figure 28. Cyclic Voltammogram of S2.1

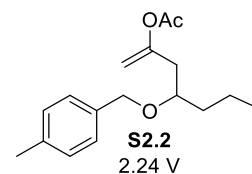
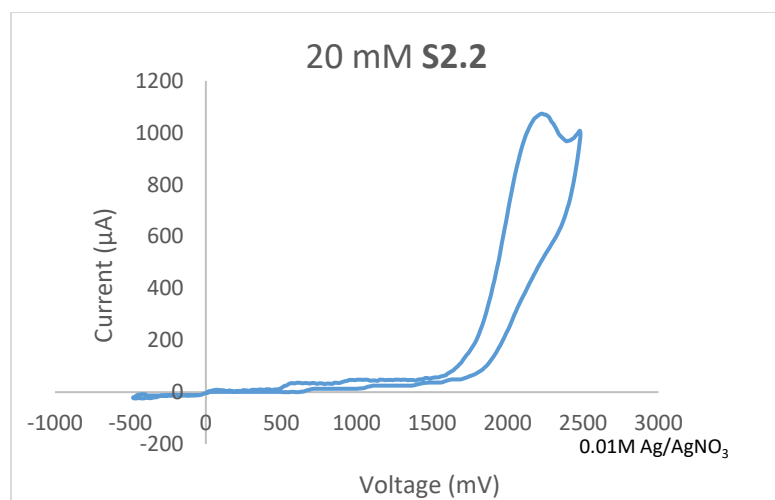


Figure 29. Cyclic Voltammogram of S2.2

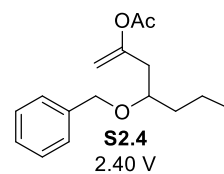
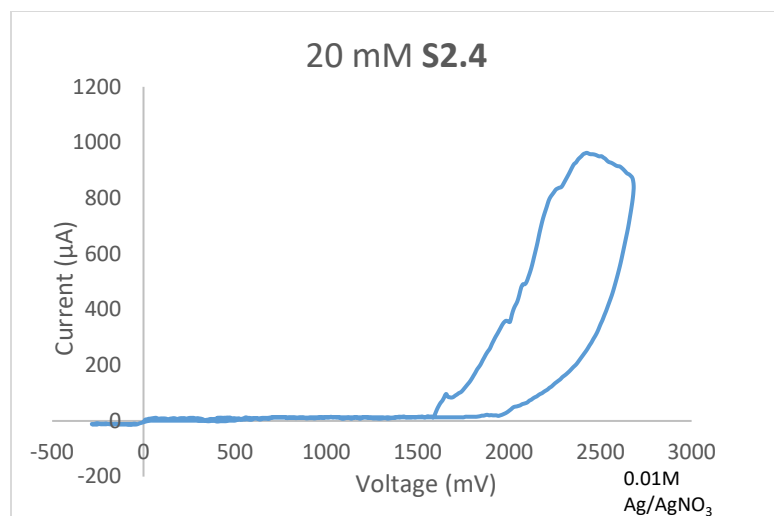


Figure 30. Cyclic Voltammogram of S2.4

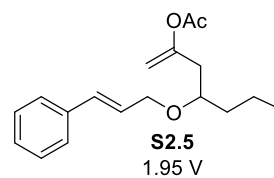
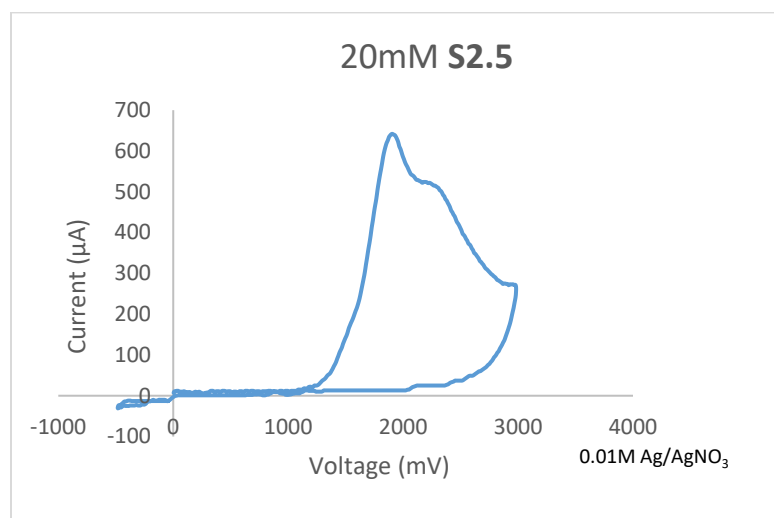
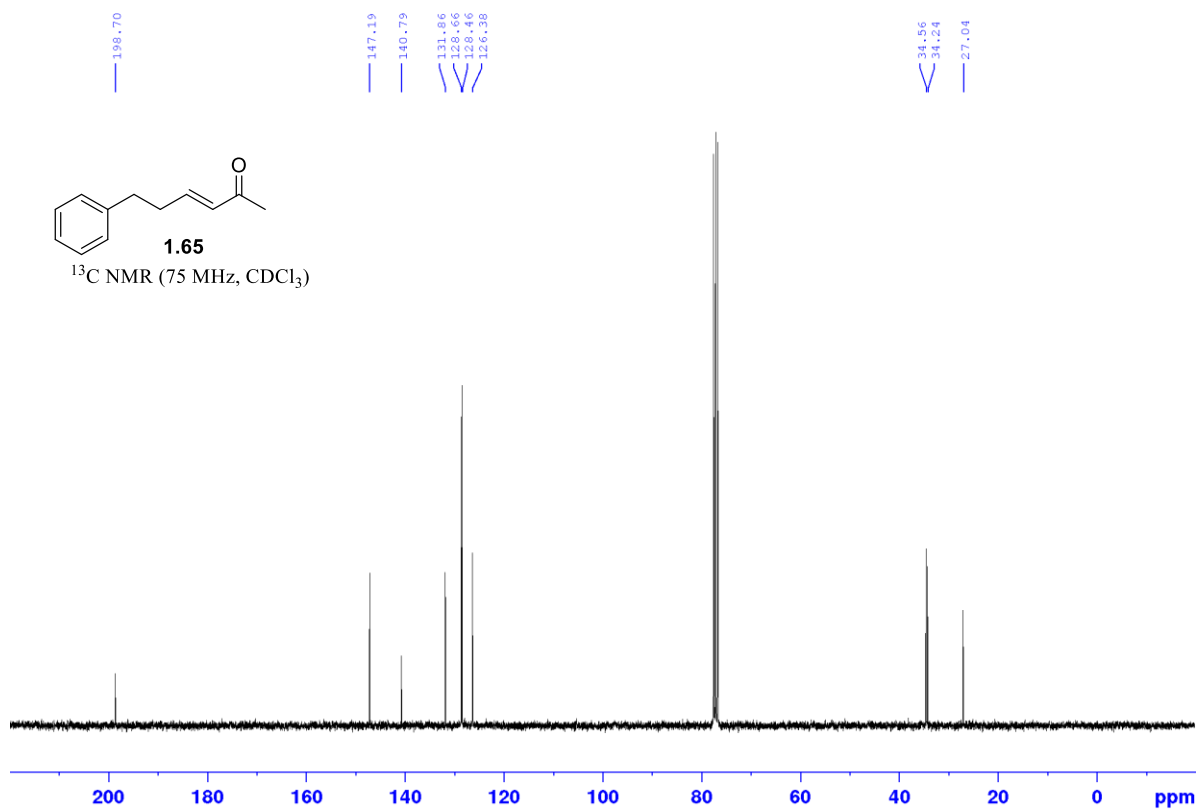
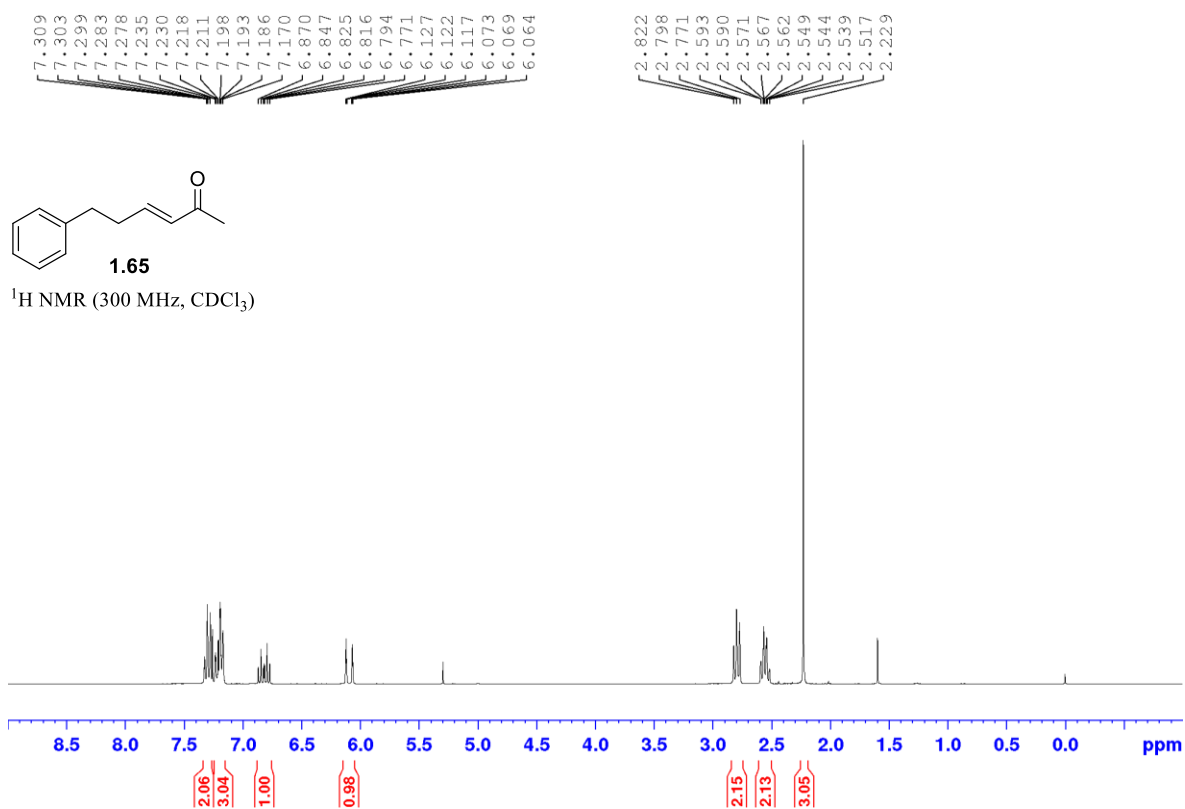
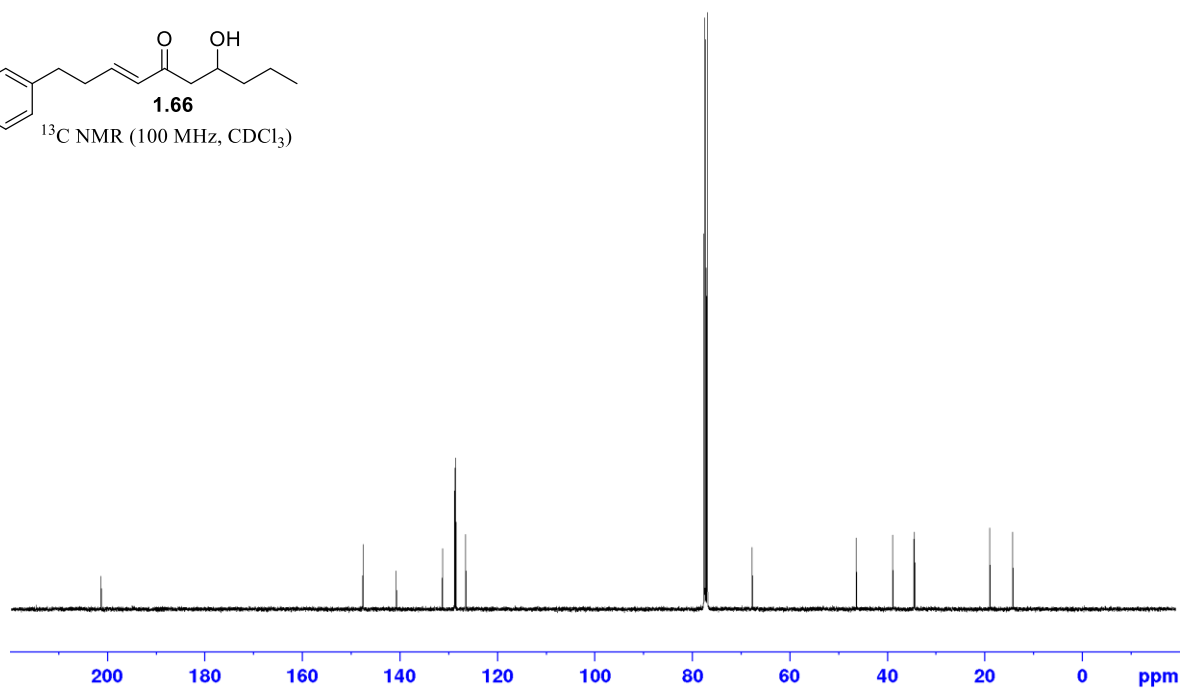
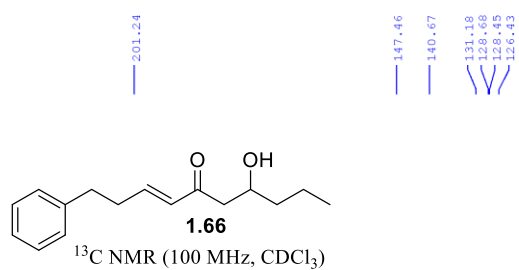
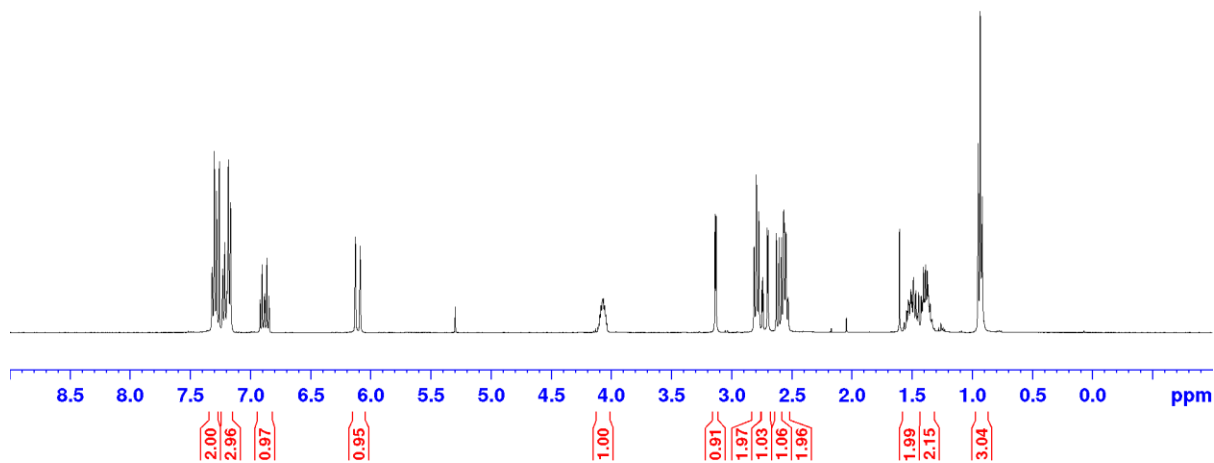
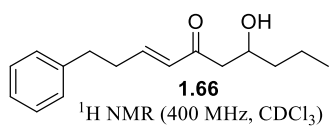


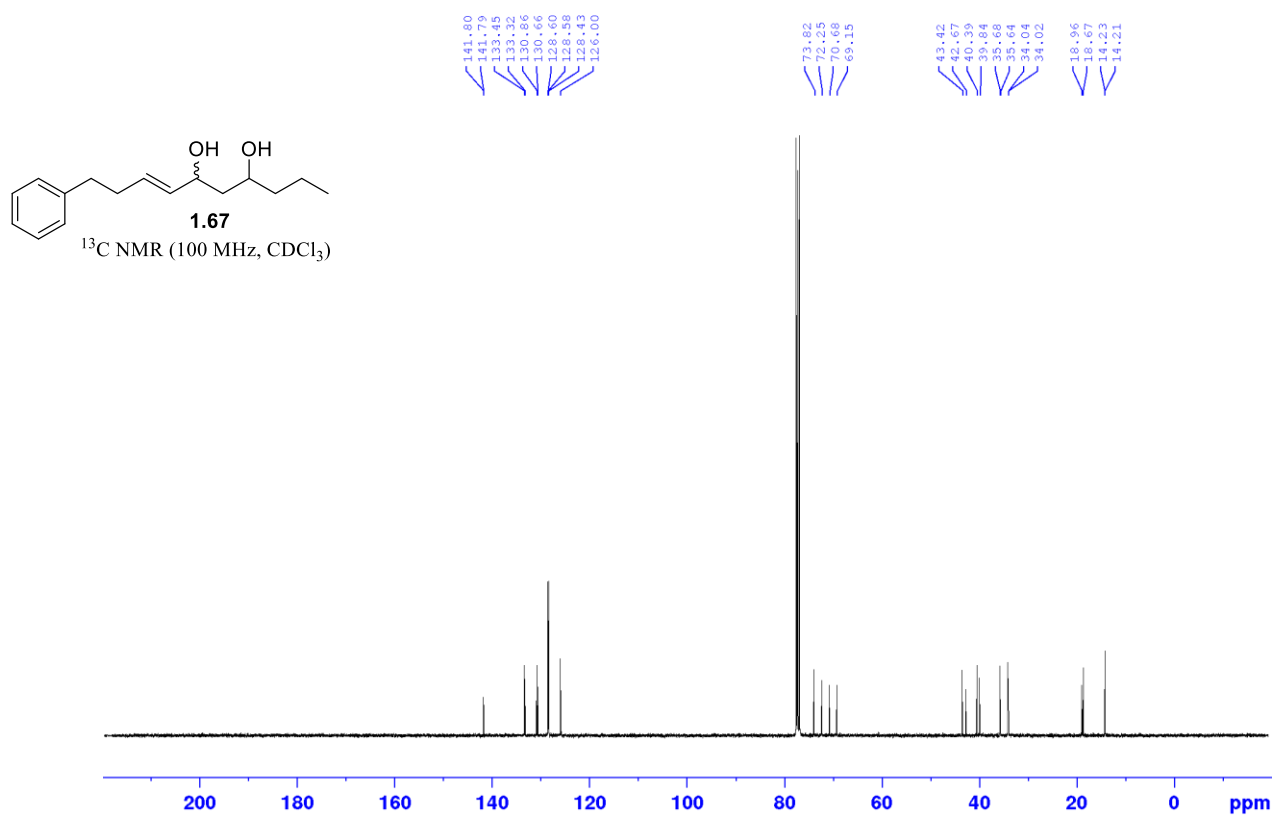
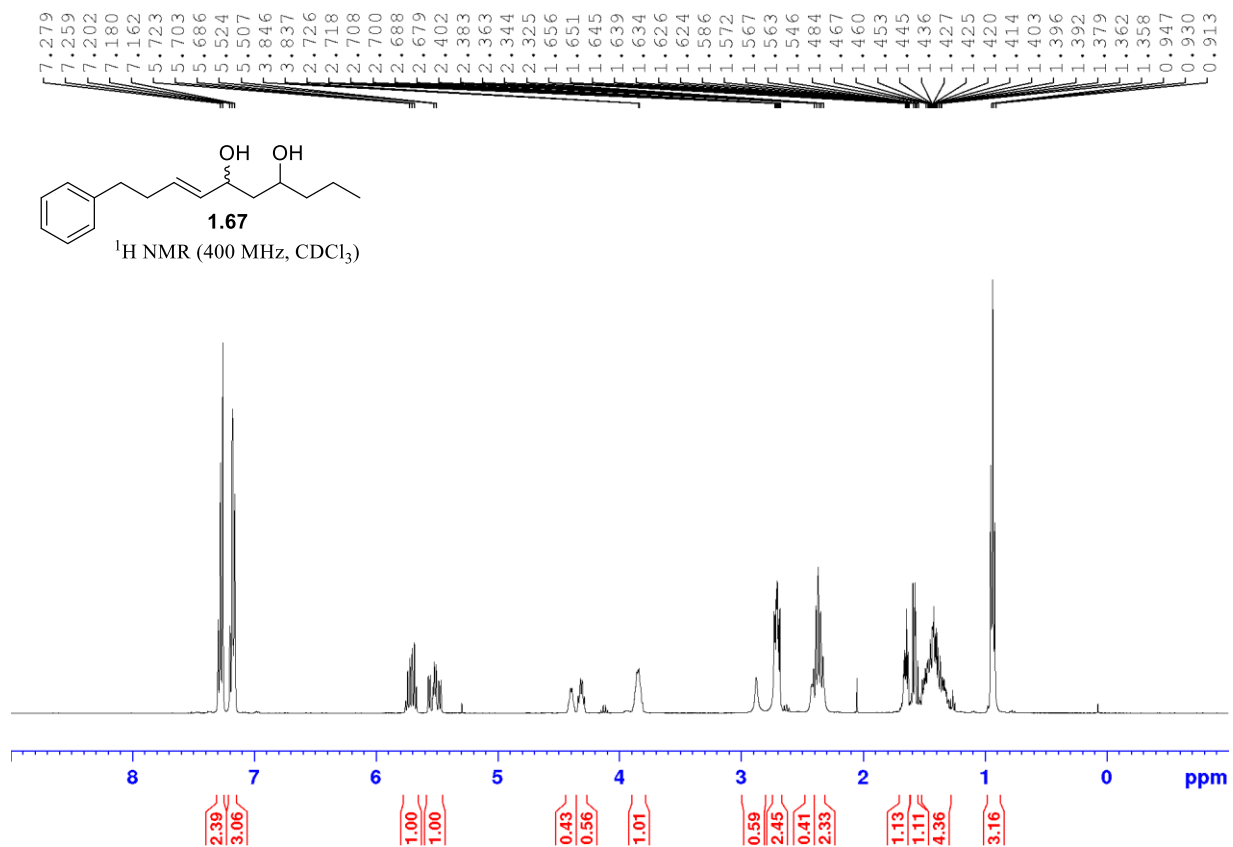
Figure 31. Cyclic Voltammogram of S2.5

Appendix C

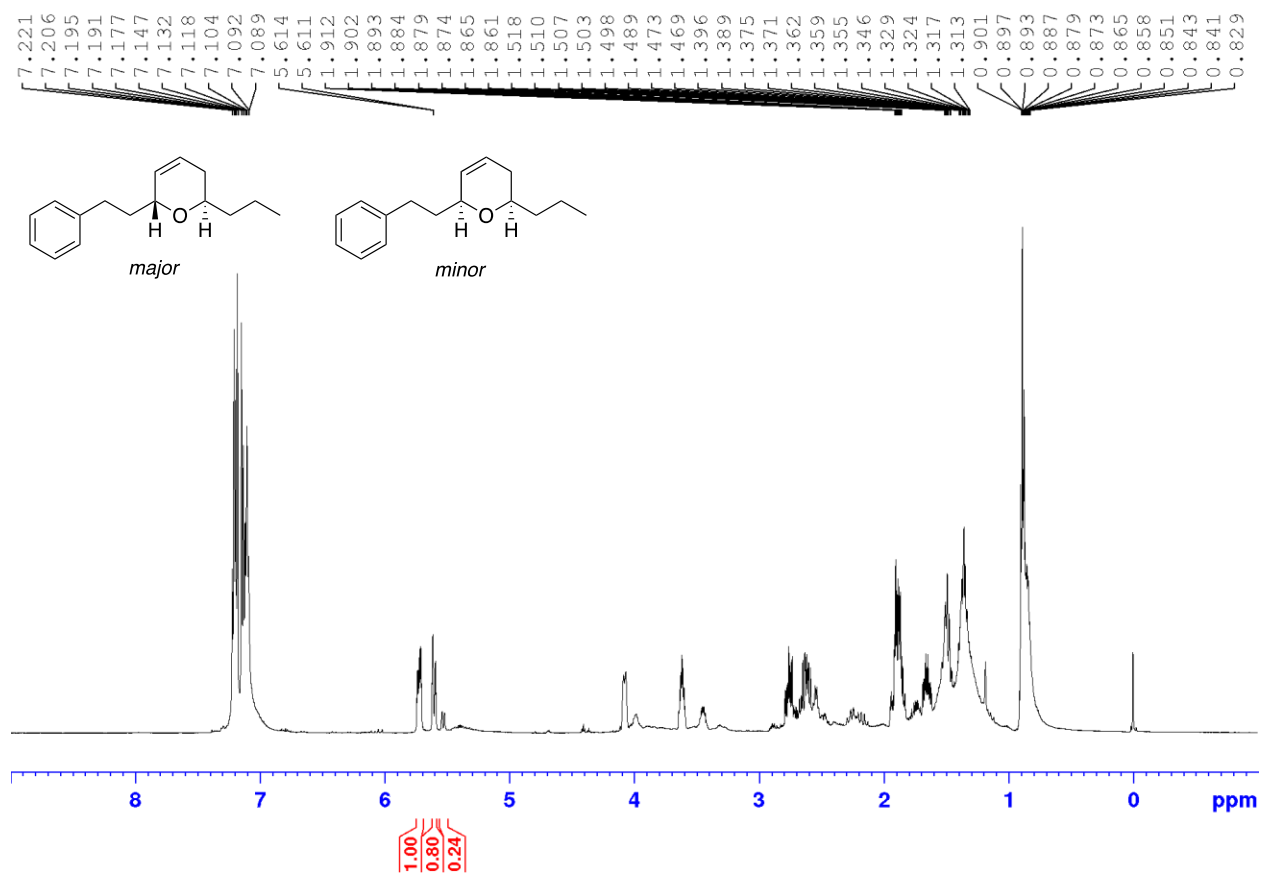
NMR Spectra and HPLC Traces

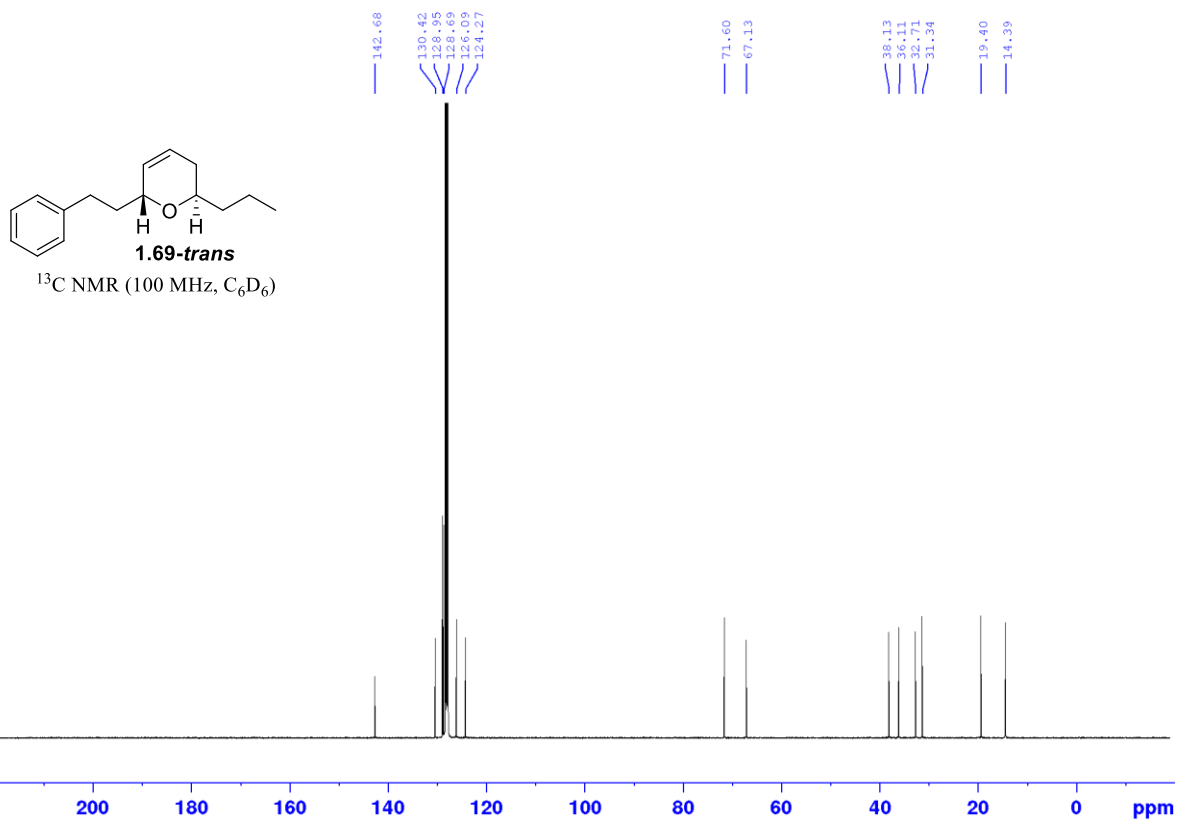
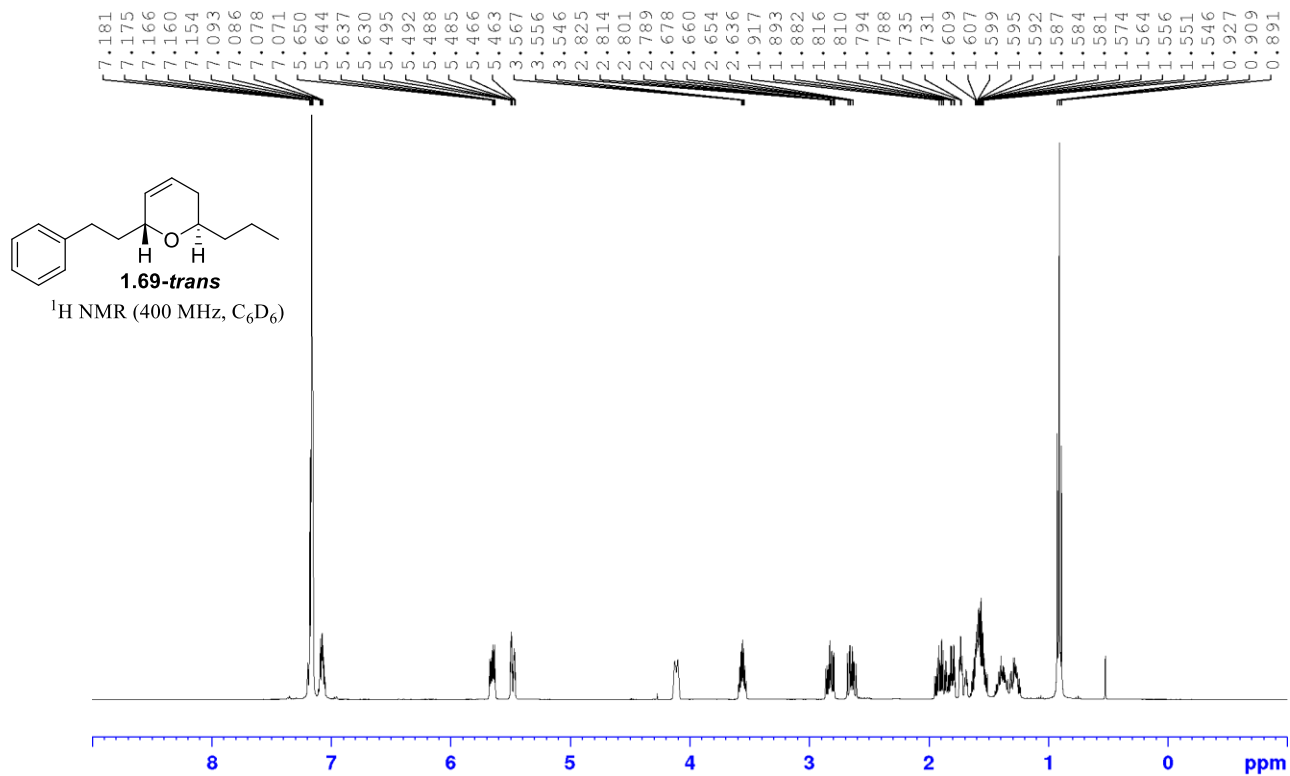




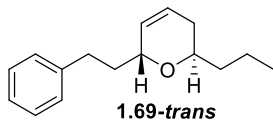


Crude Cyclization Product

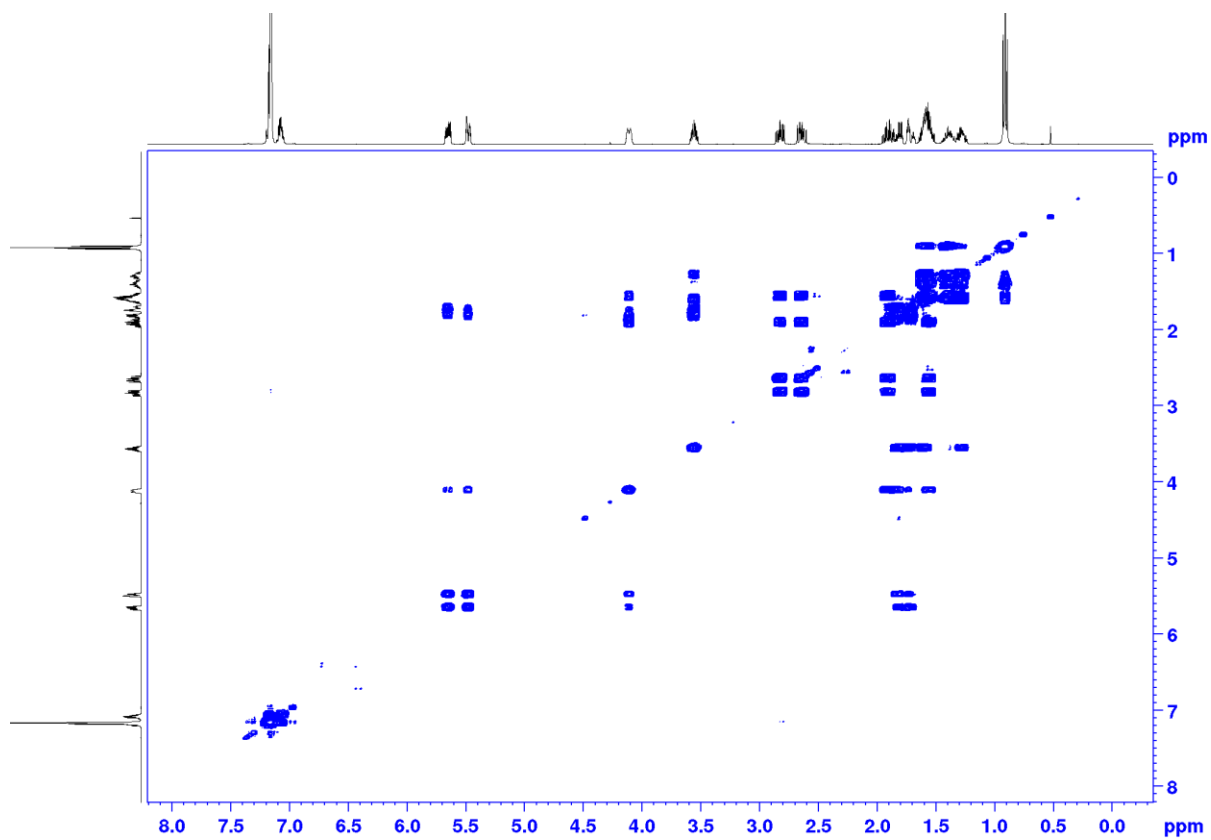




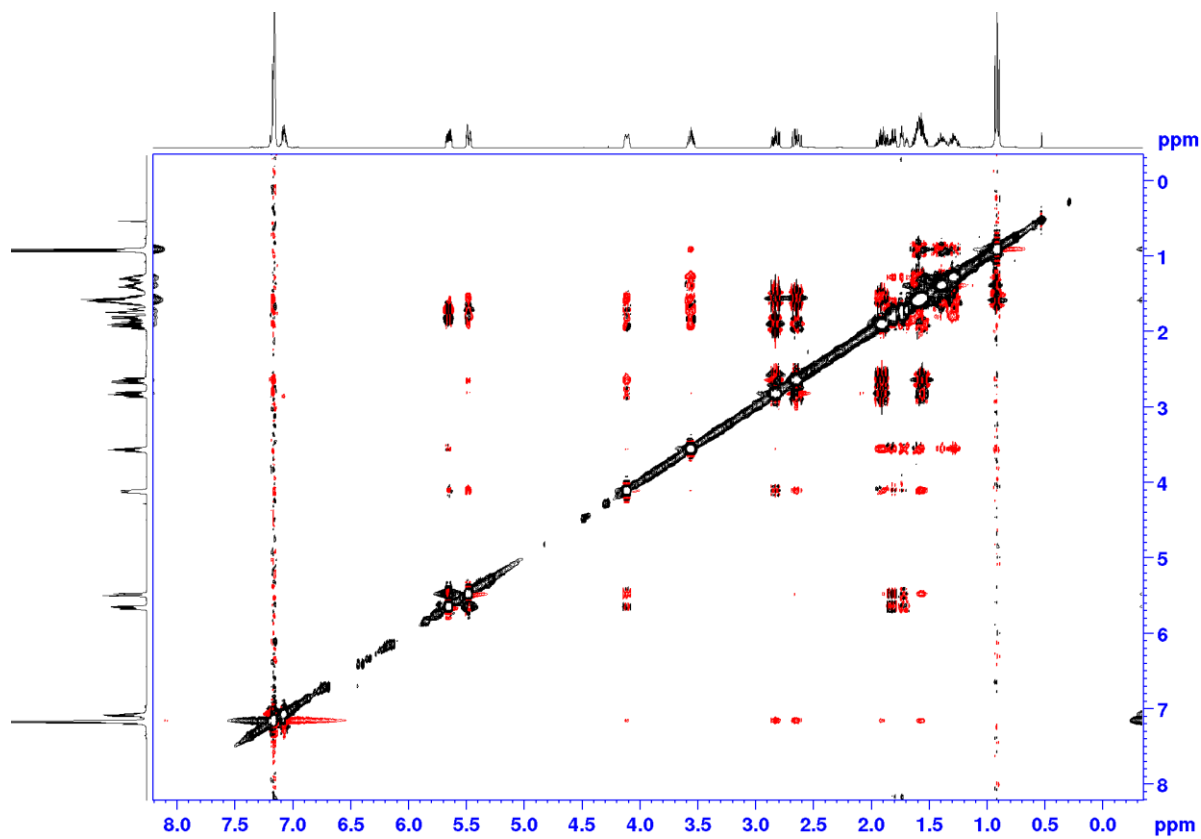
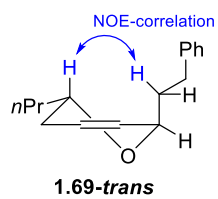
COSY Spectrum



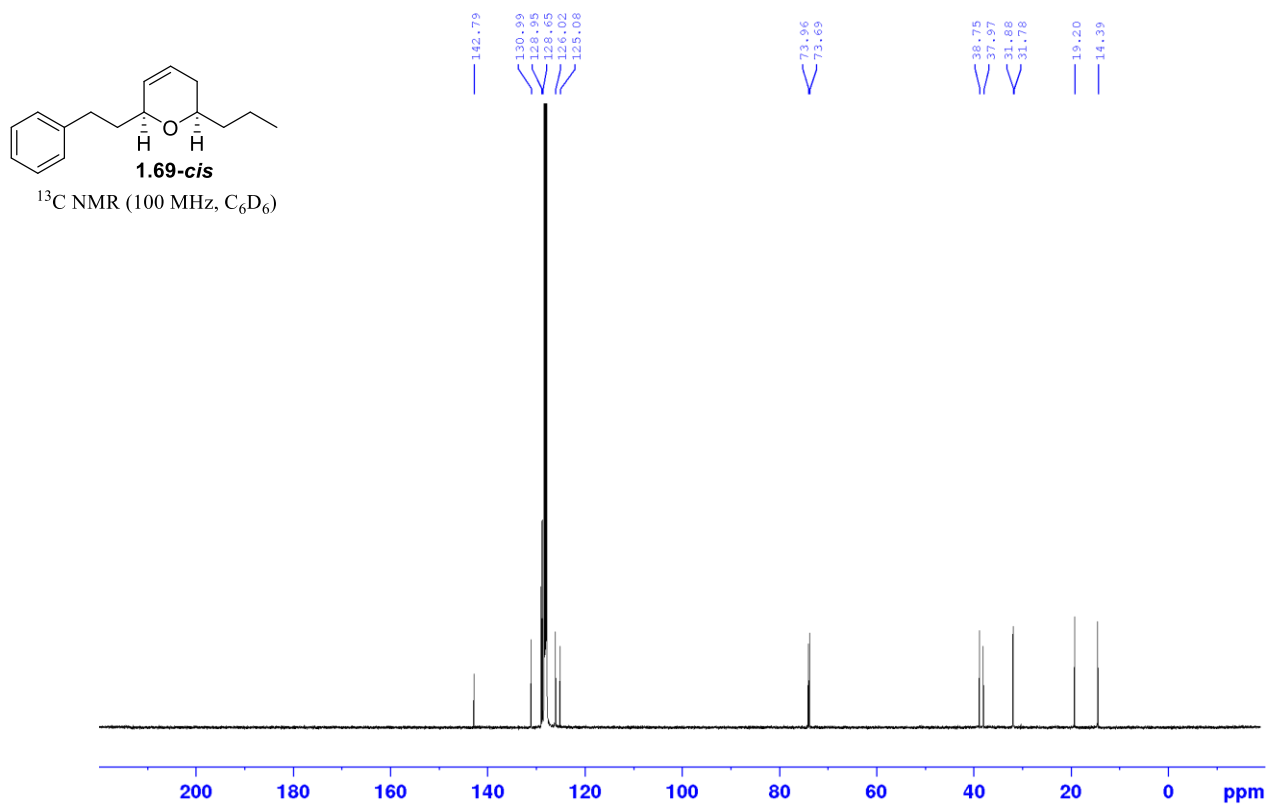
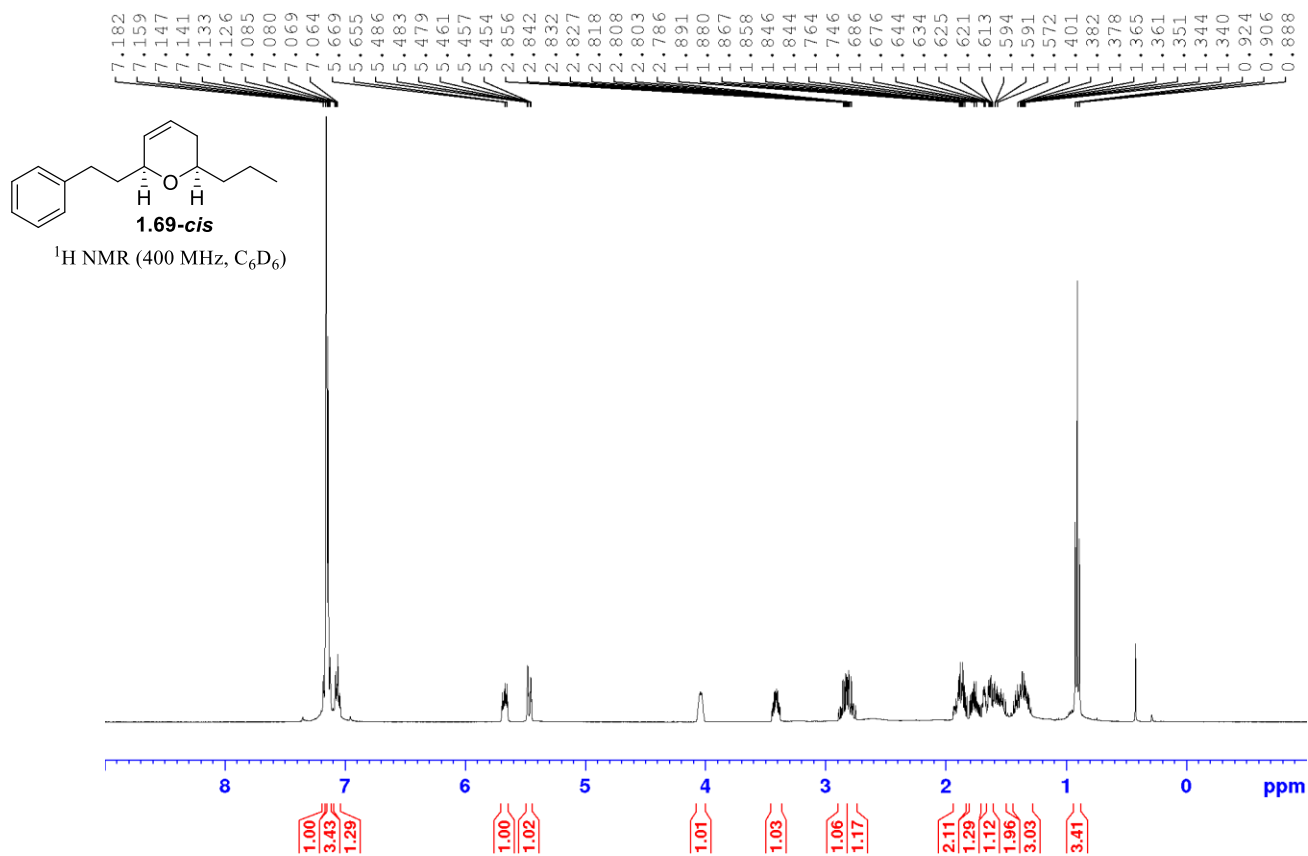
¹H-COSY NMR (400 MHz, C₆D₆)



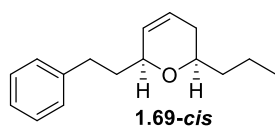
NOESY Spectrum



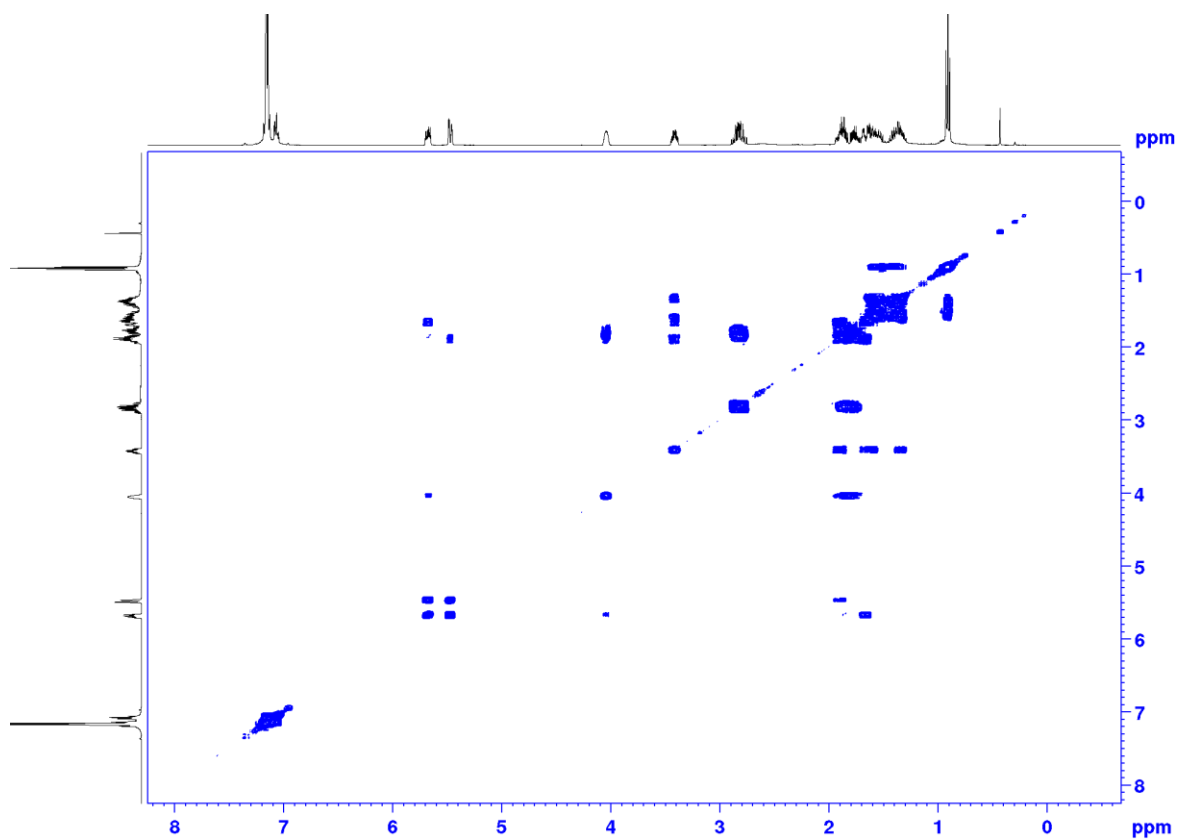
NOESY (400 MHz, C₆D₆)



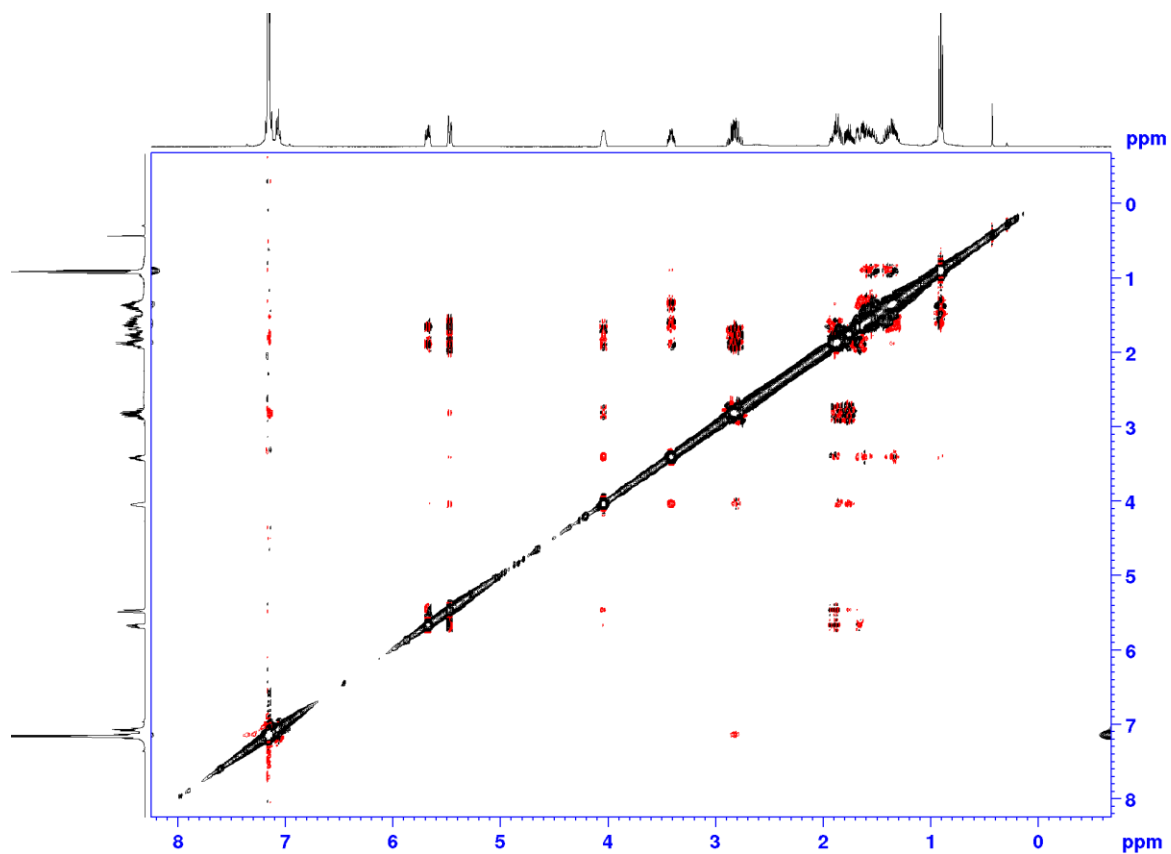
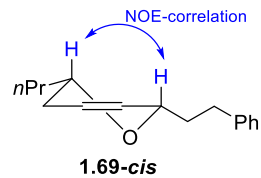
COSY Spectrum



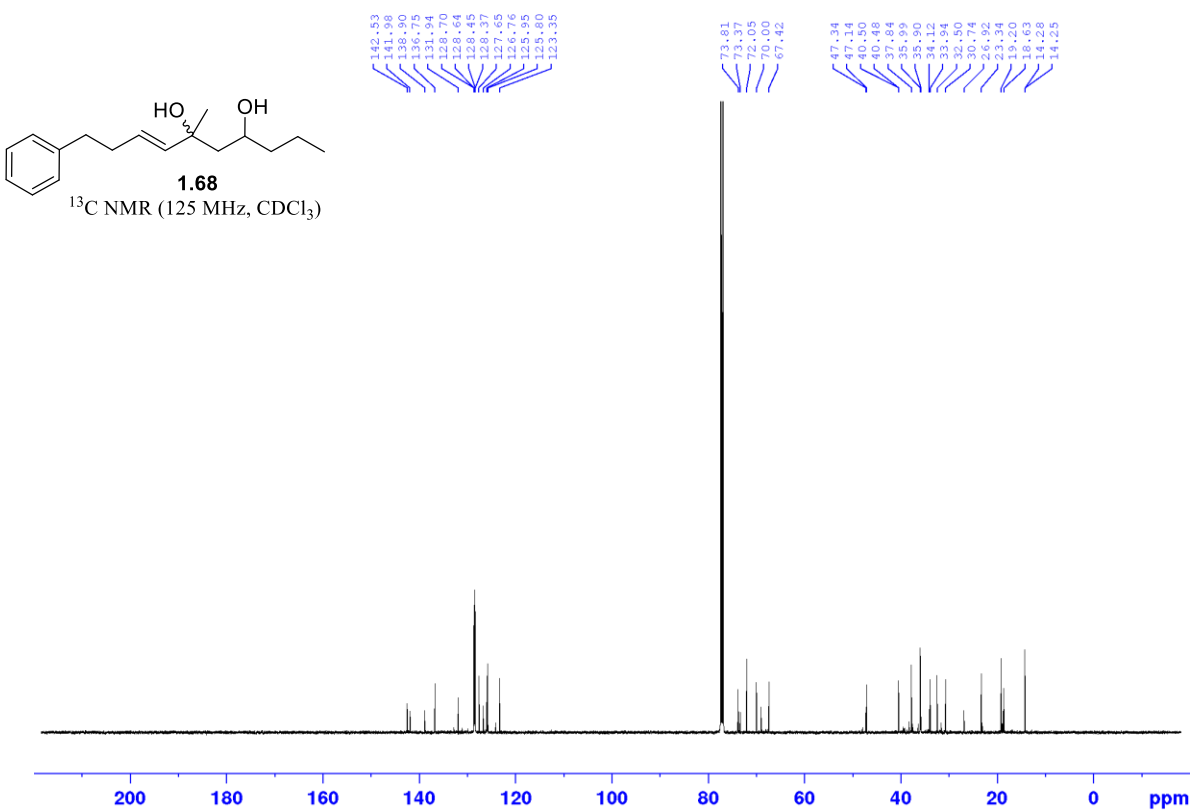
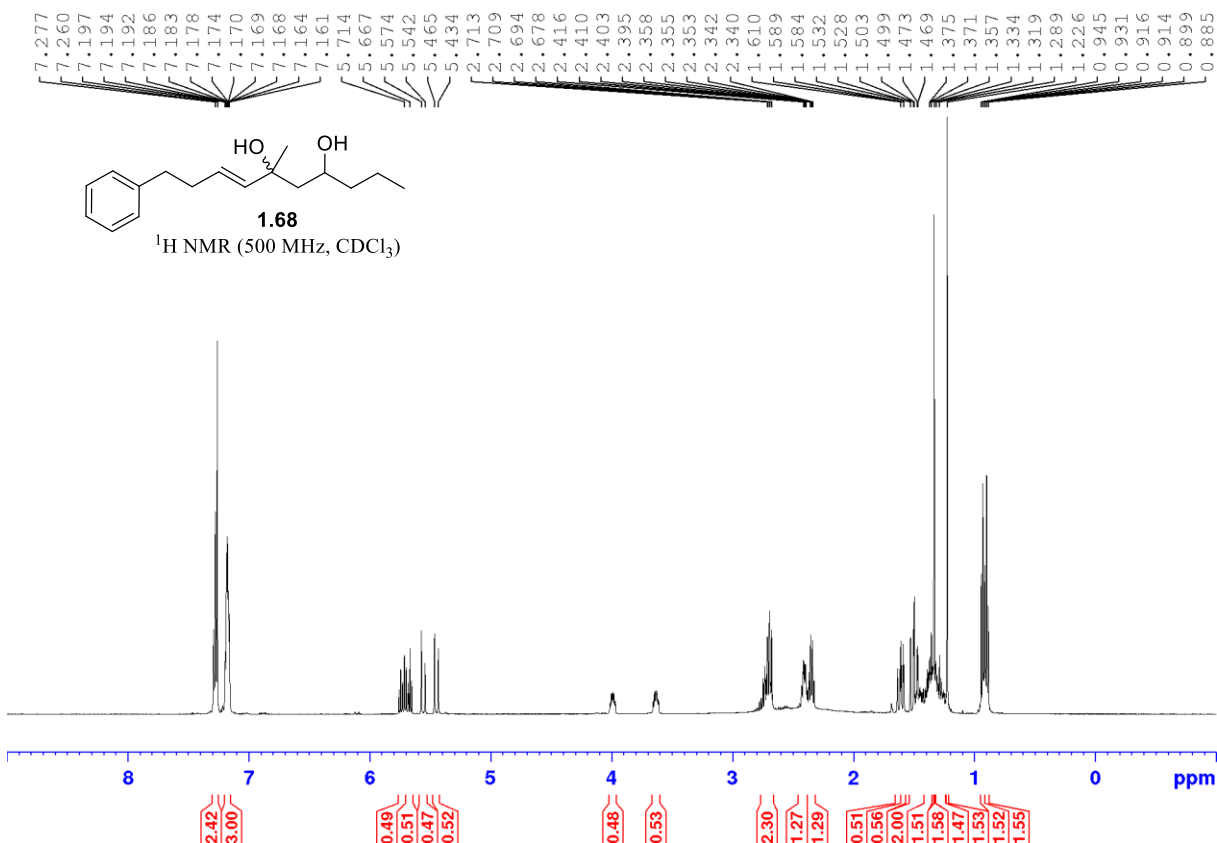
¹H-COSY NMR (400 MHz, C₆D₆)

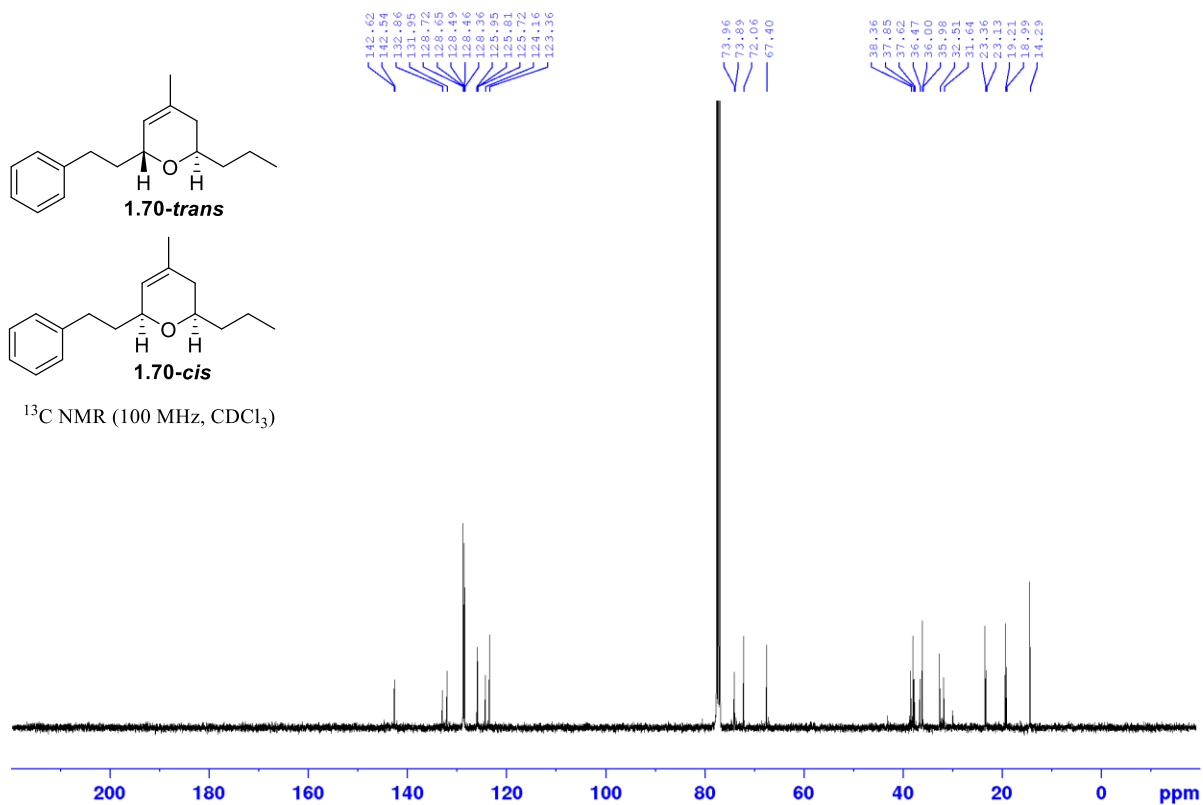
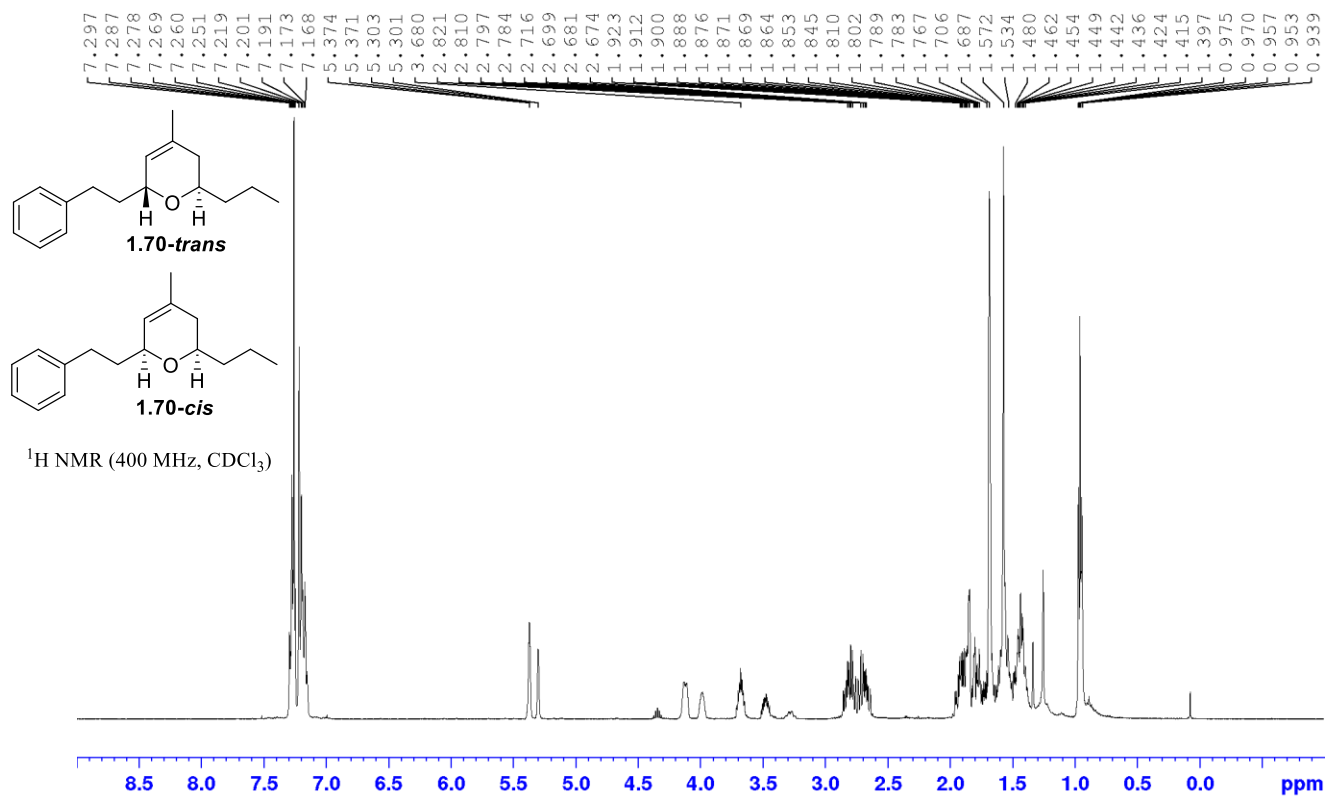


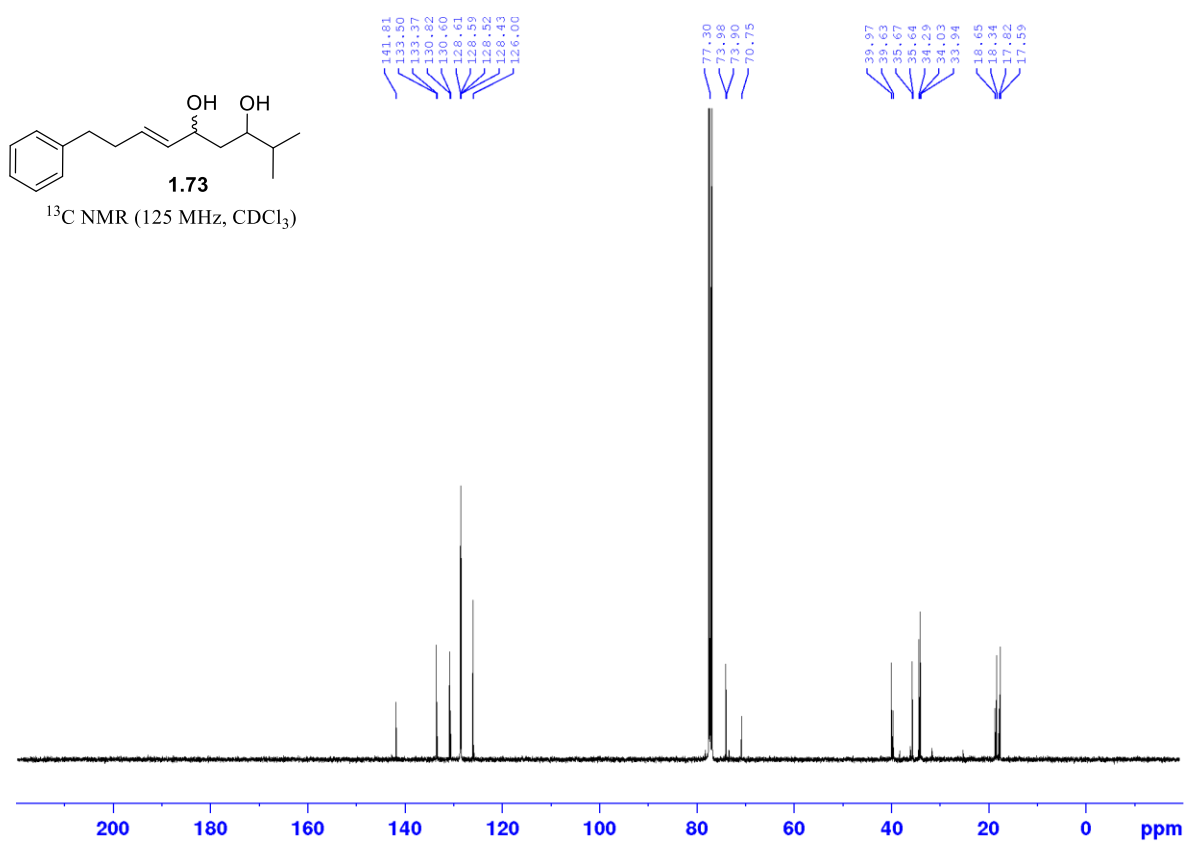
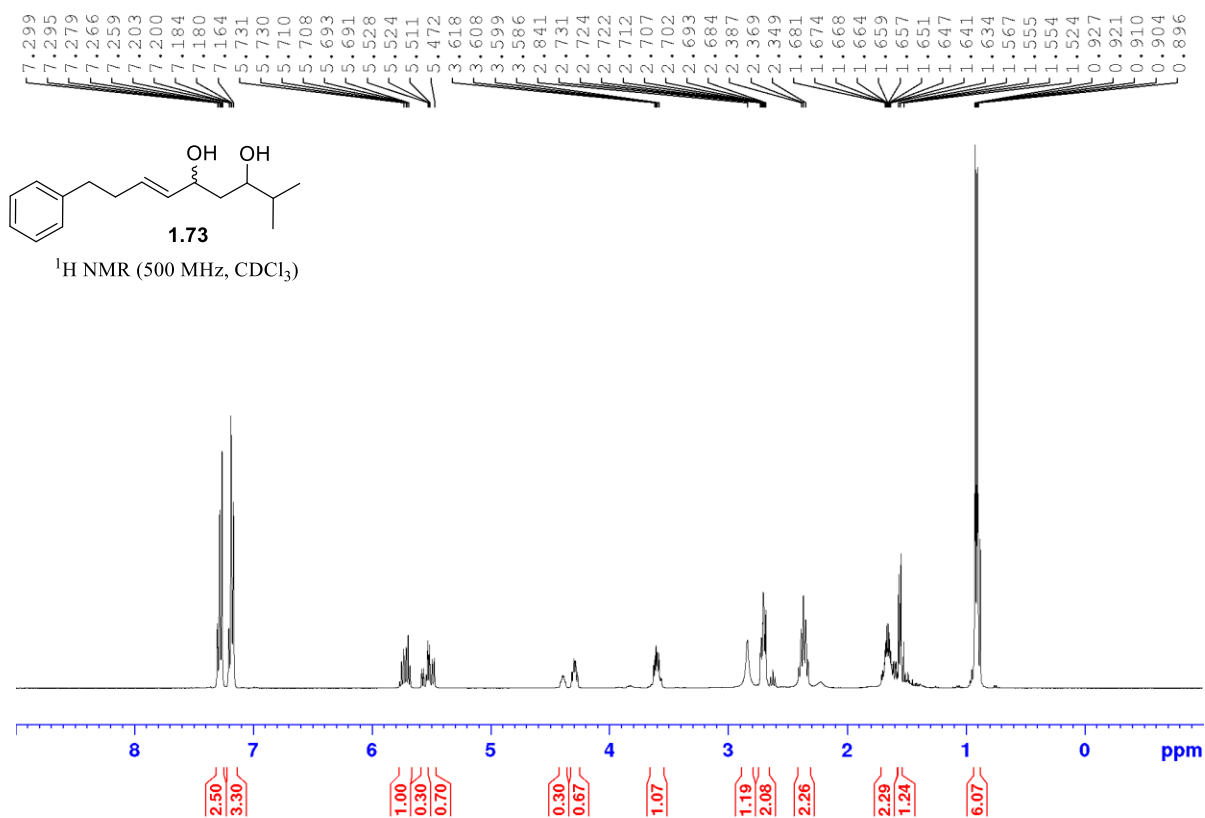
NOESY Spectrum

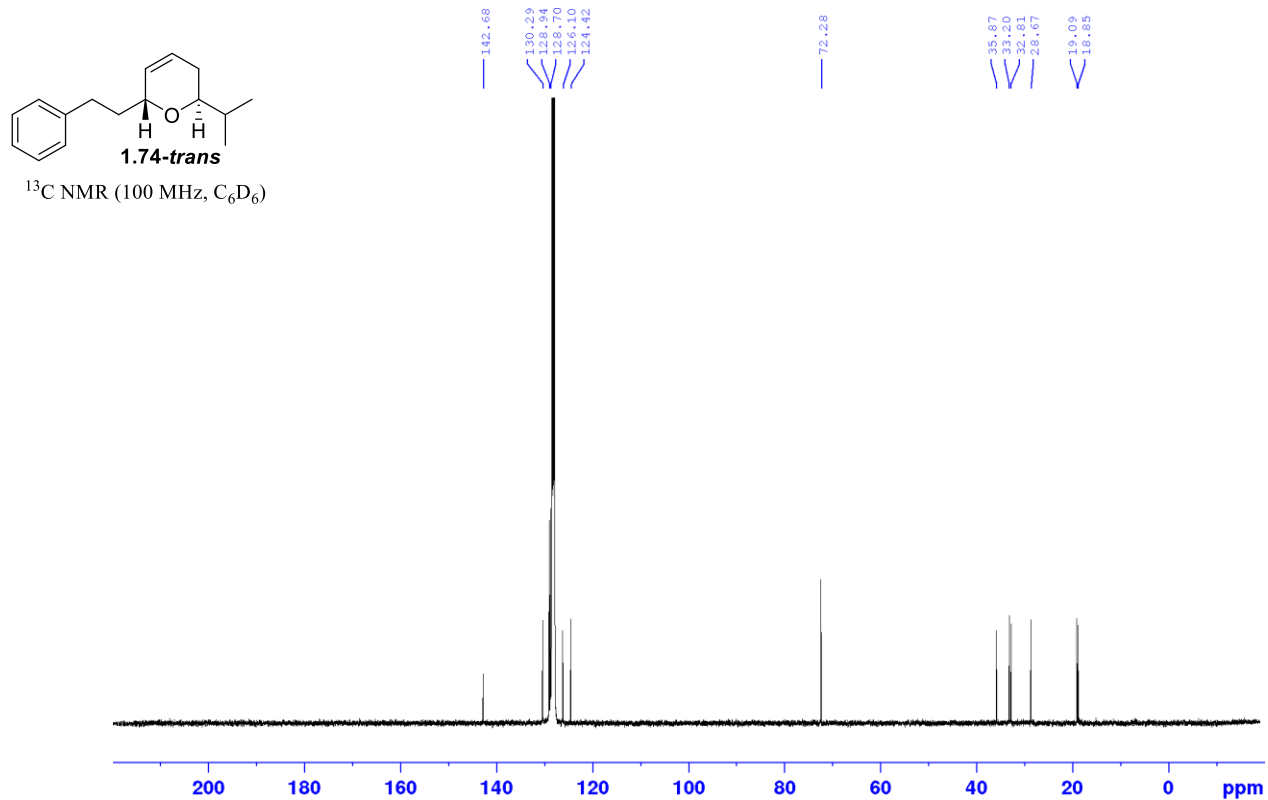
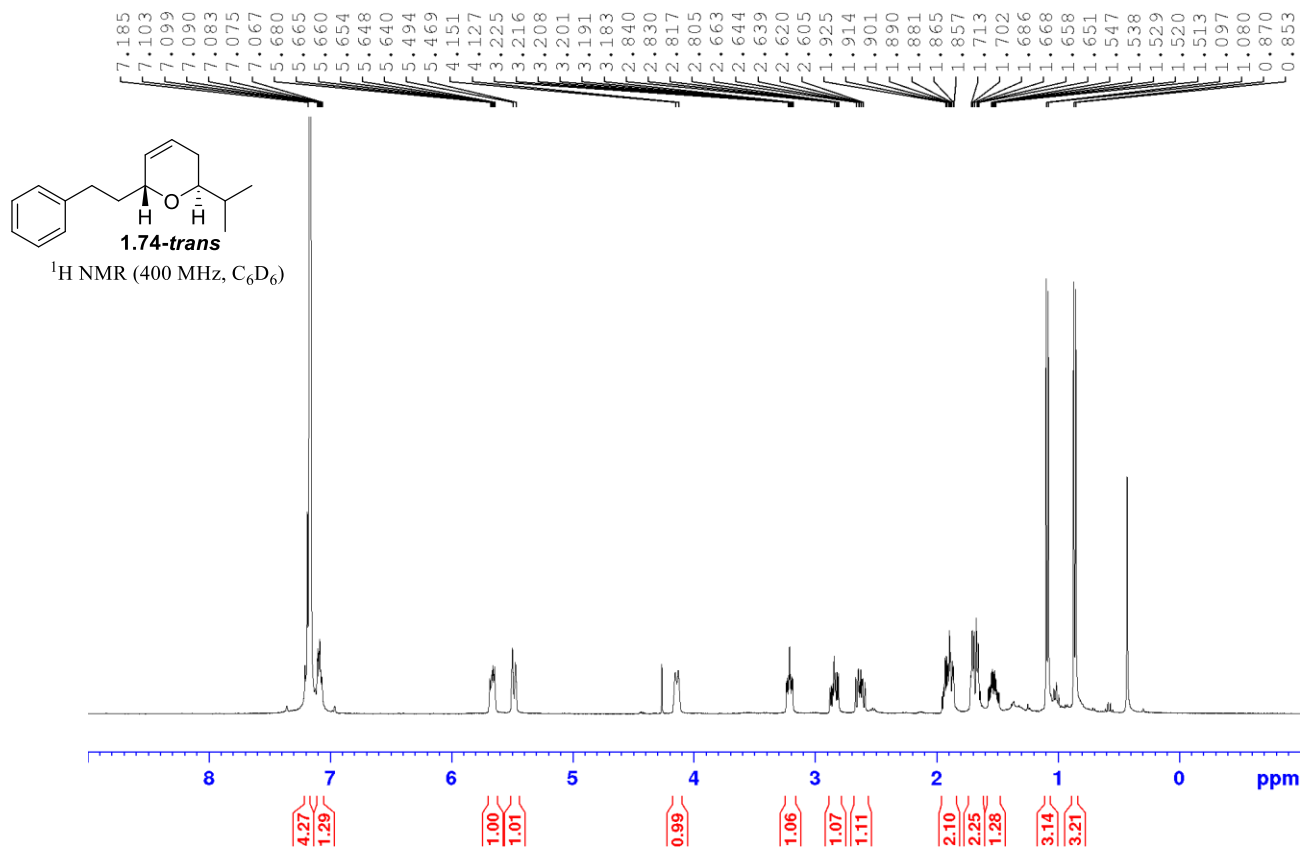


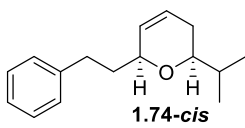
NOESY (400 MHz, C₆D₆)



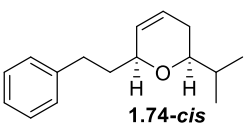
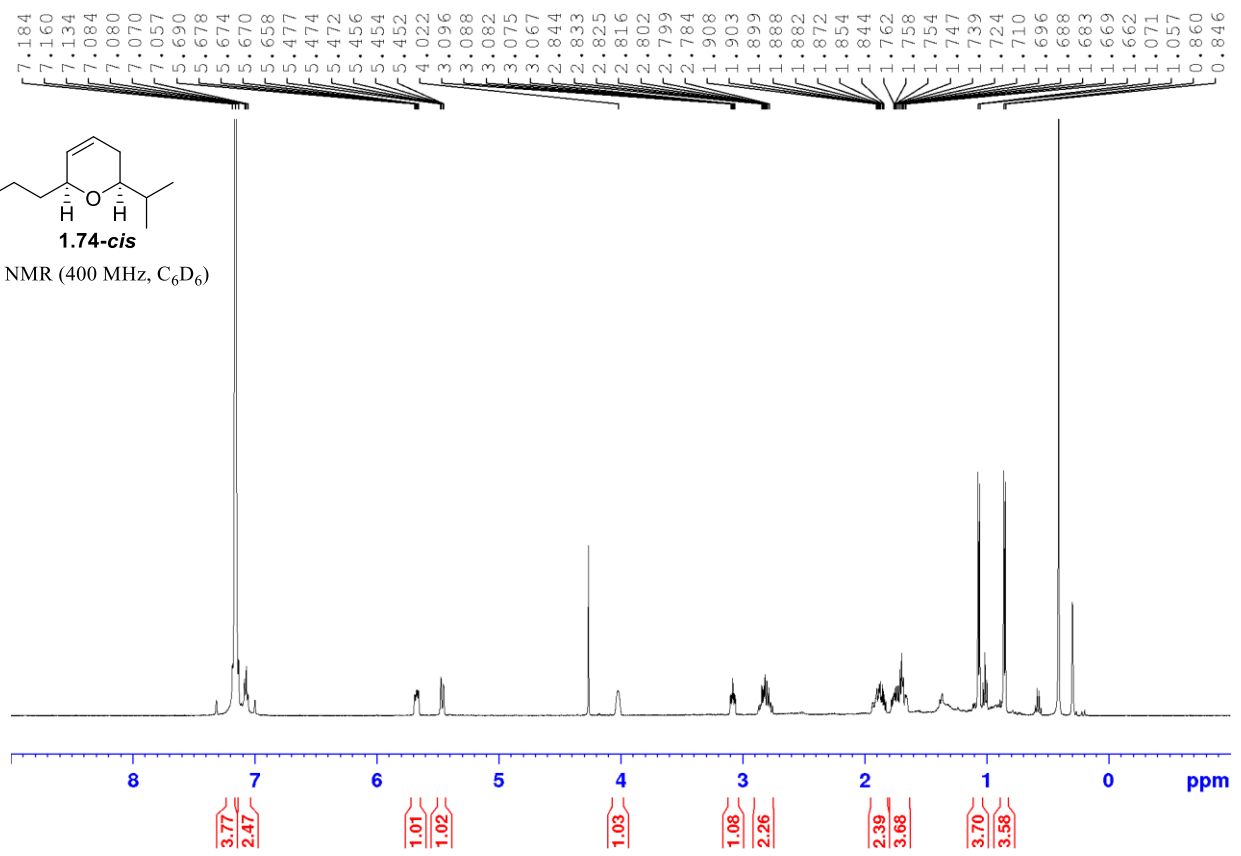




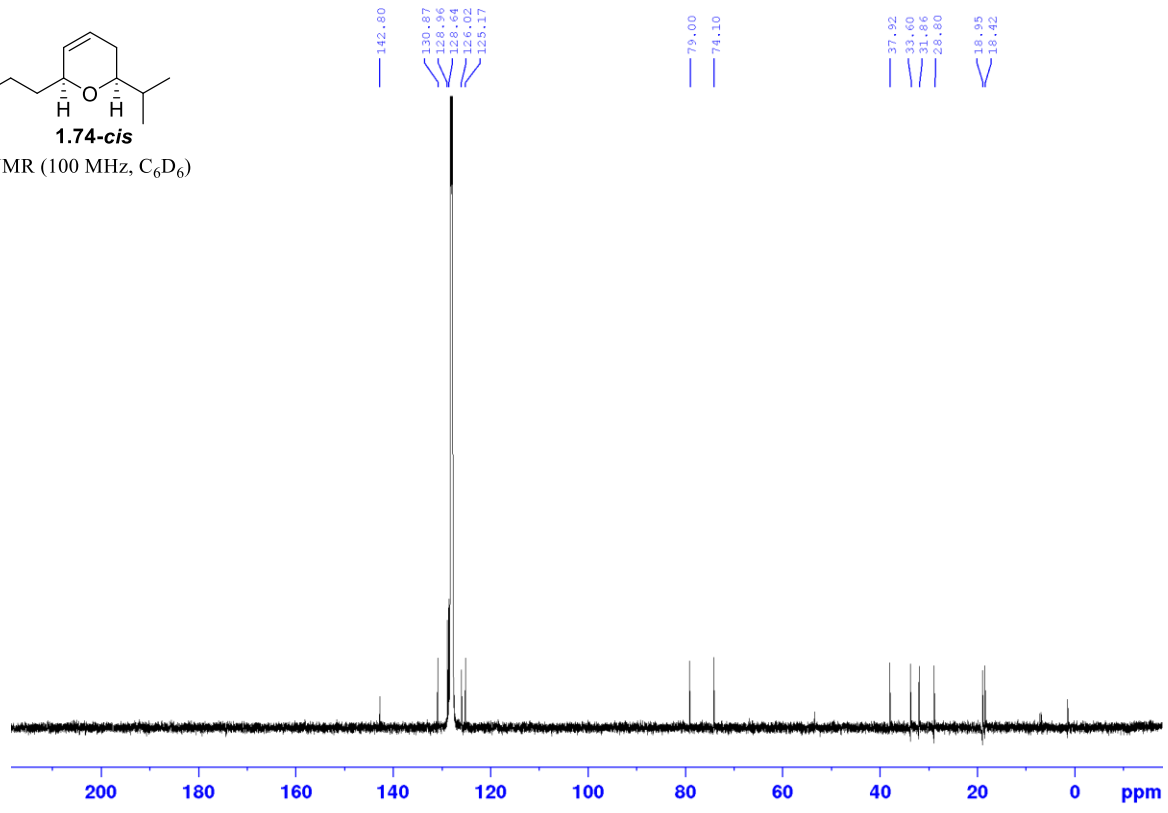


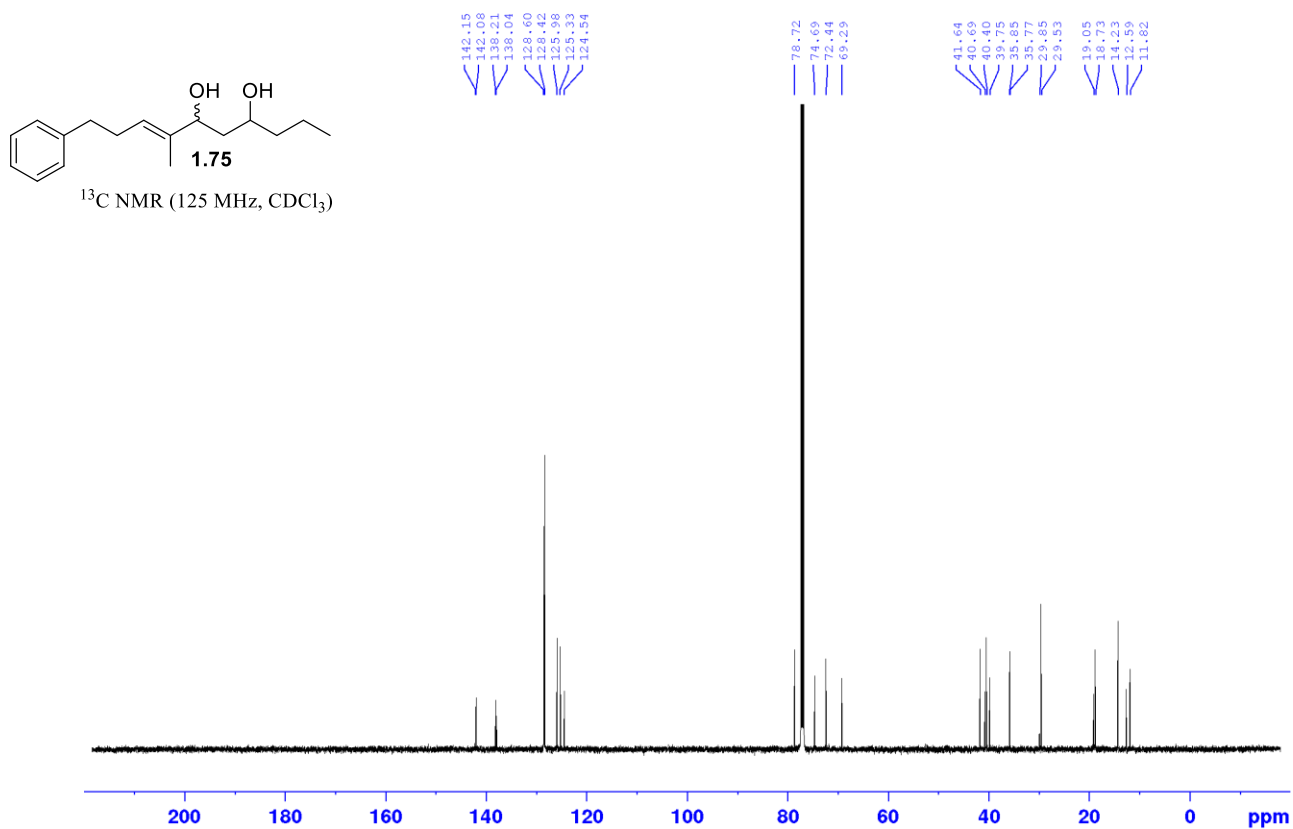
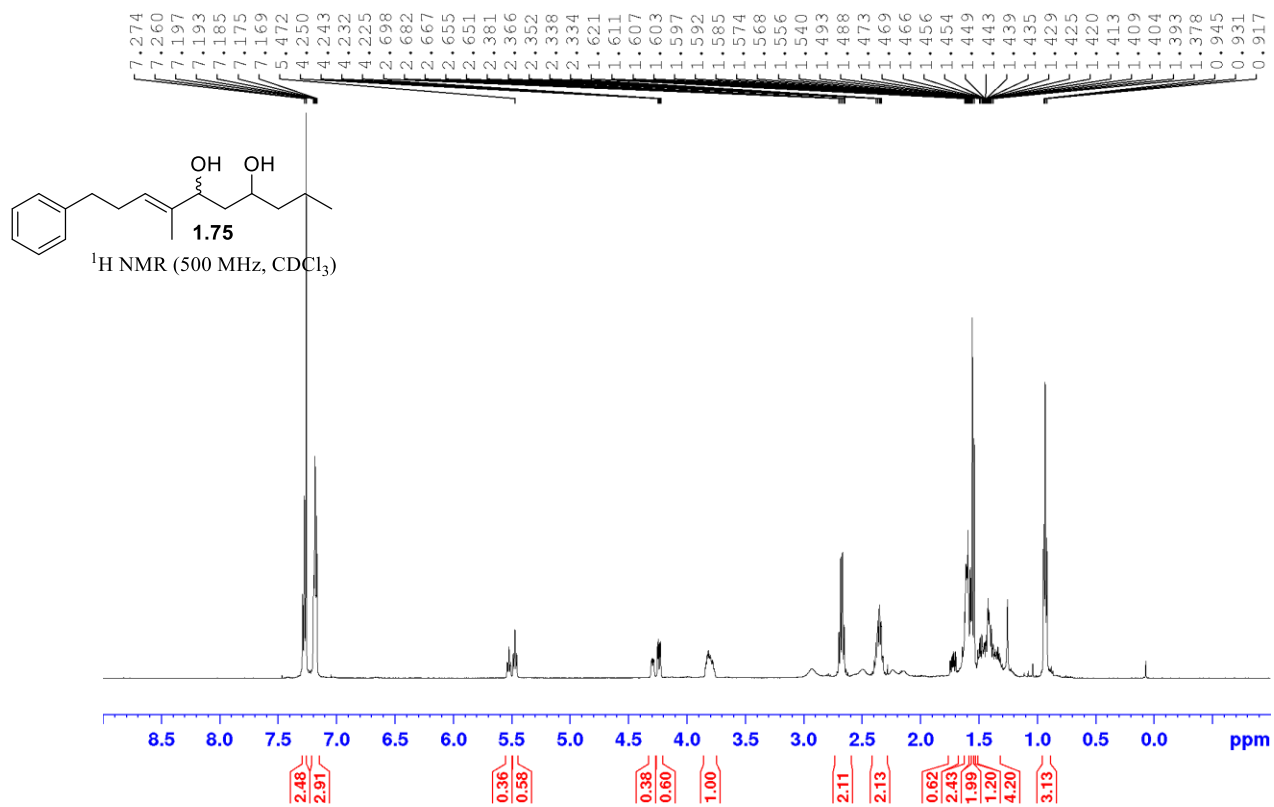


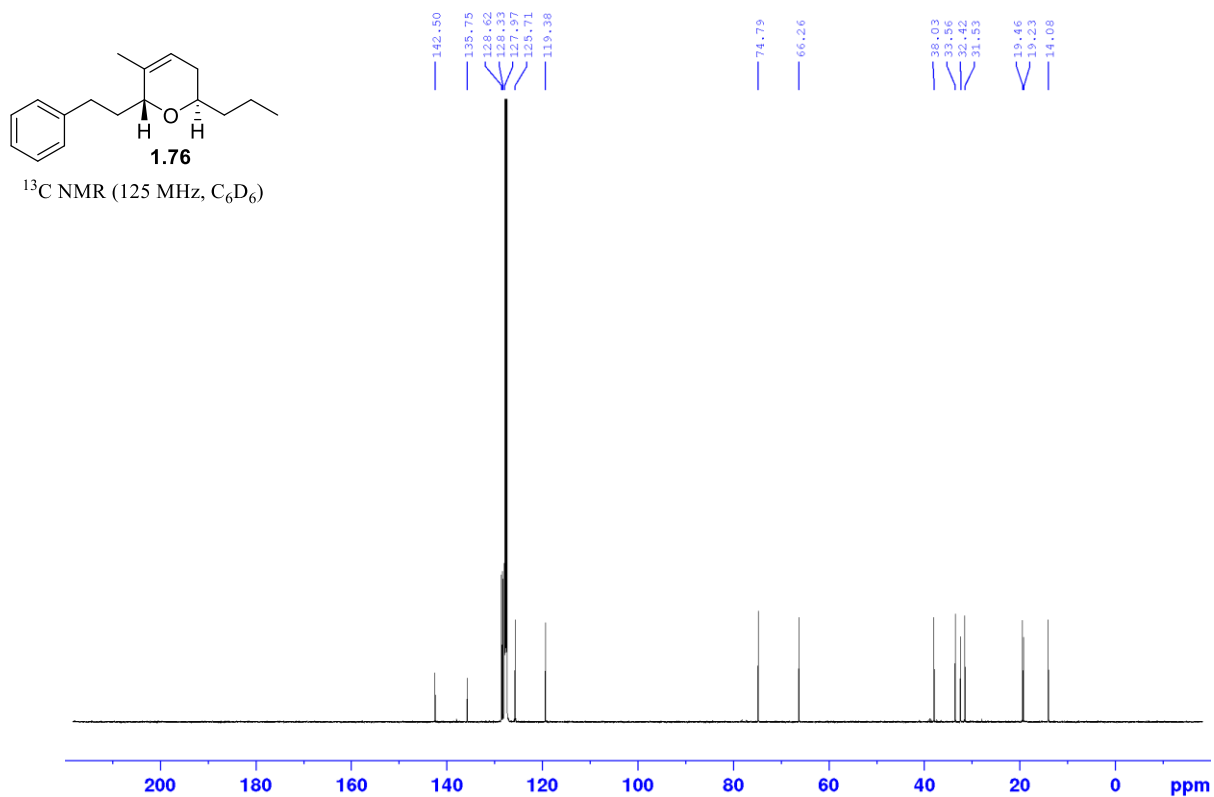
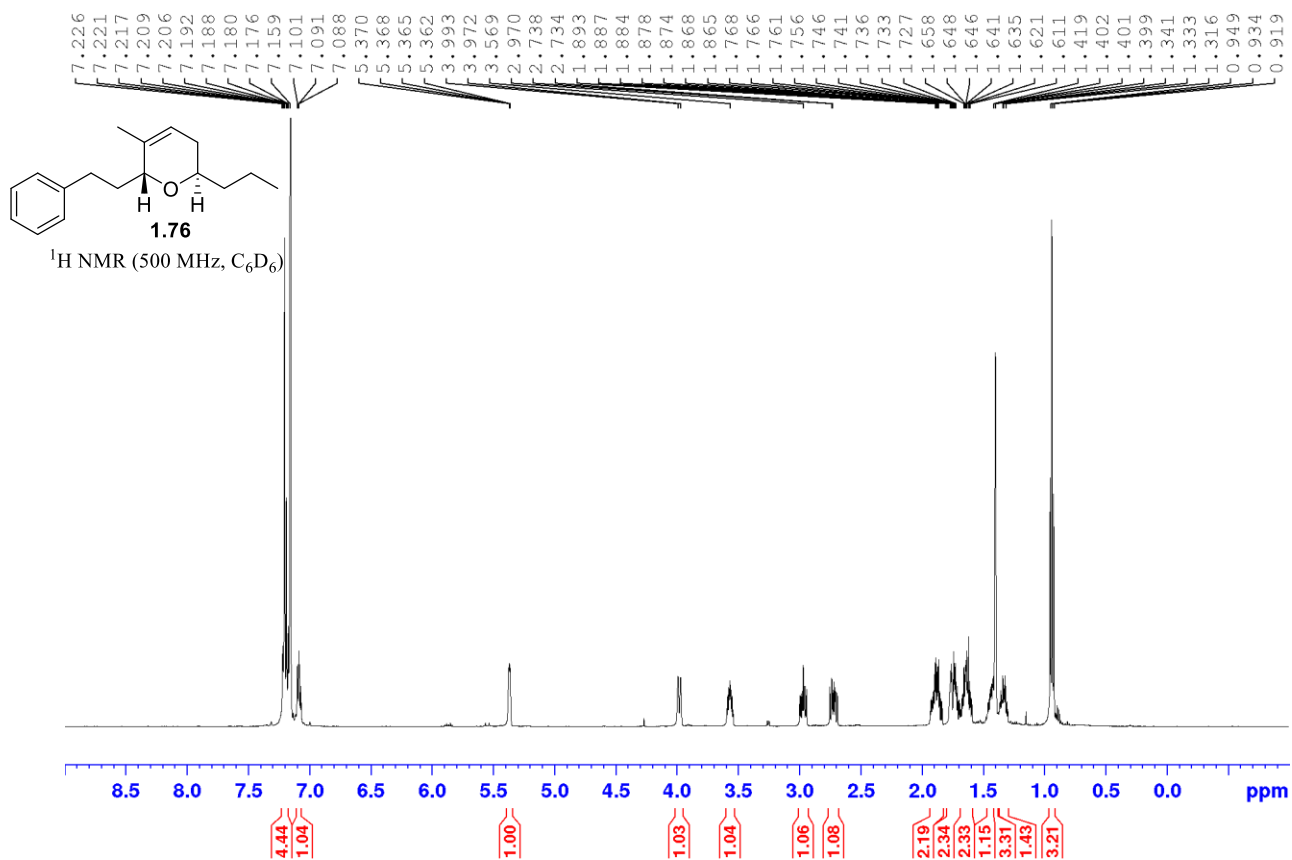
¹H NMR (400 MHz, C₆D₆)

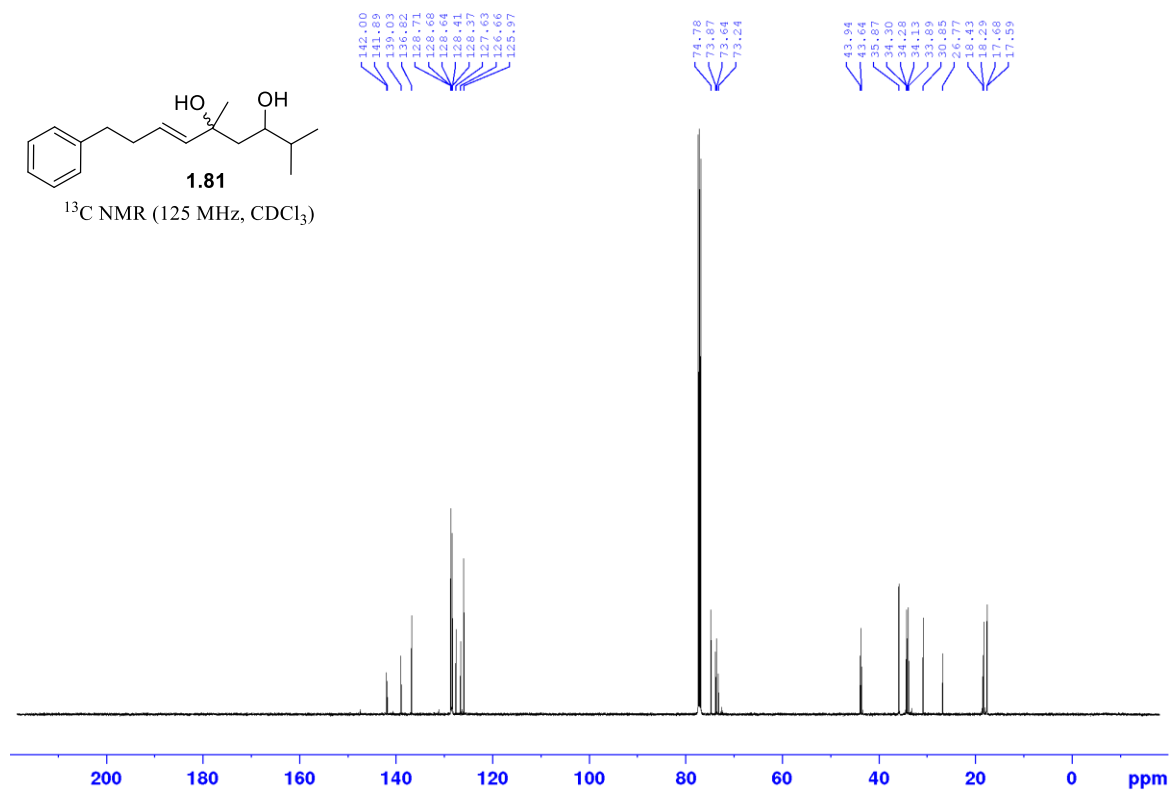
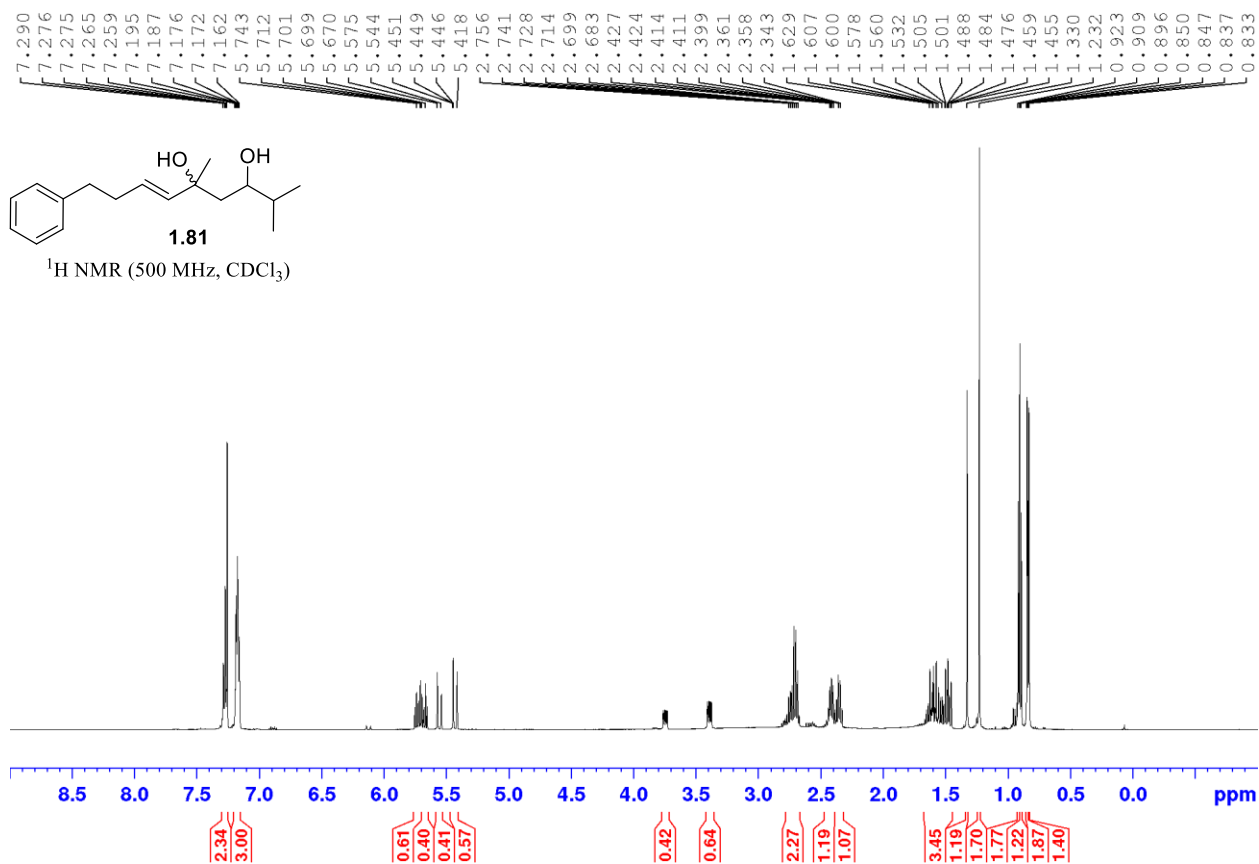


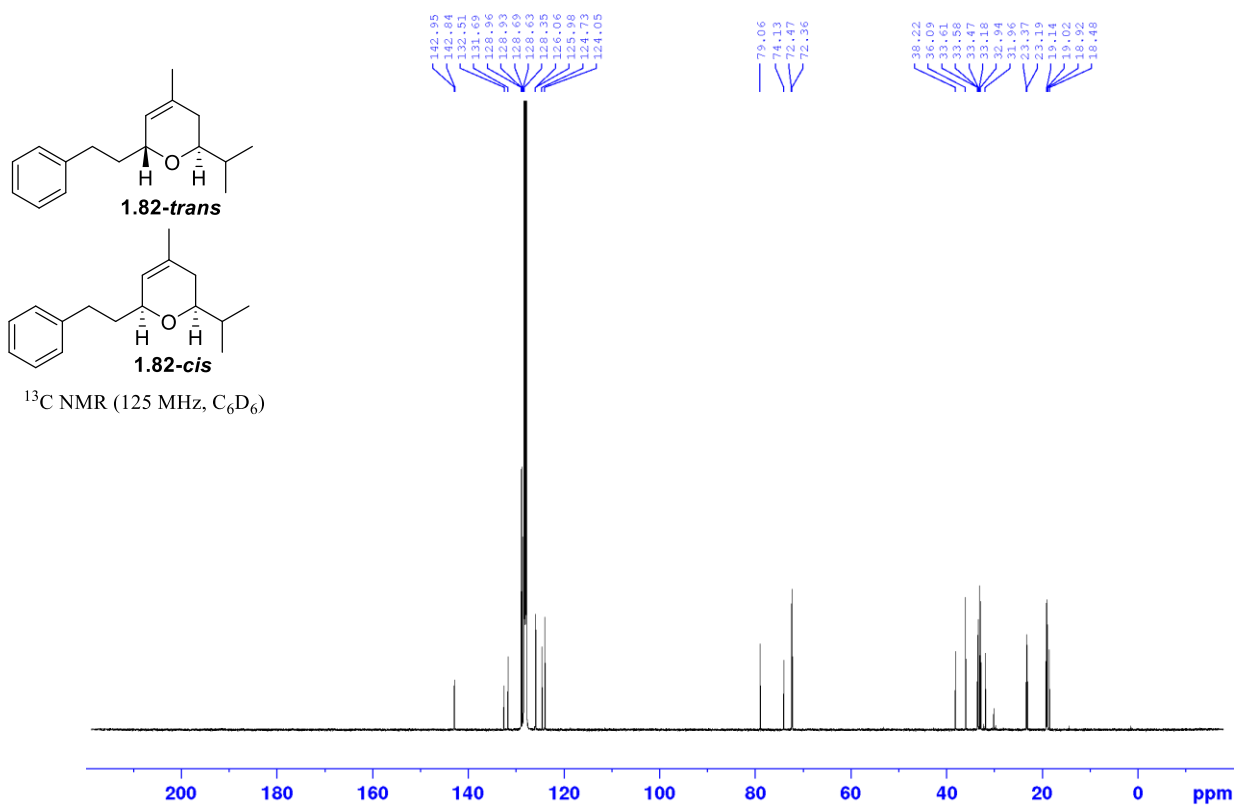
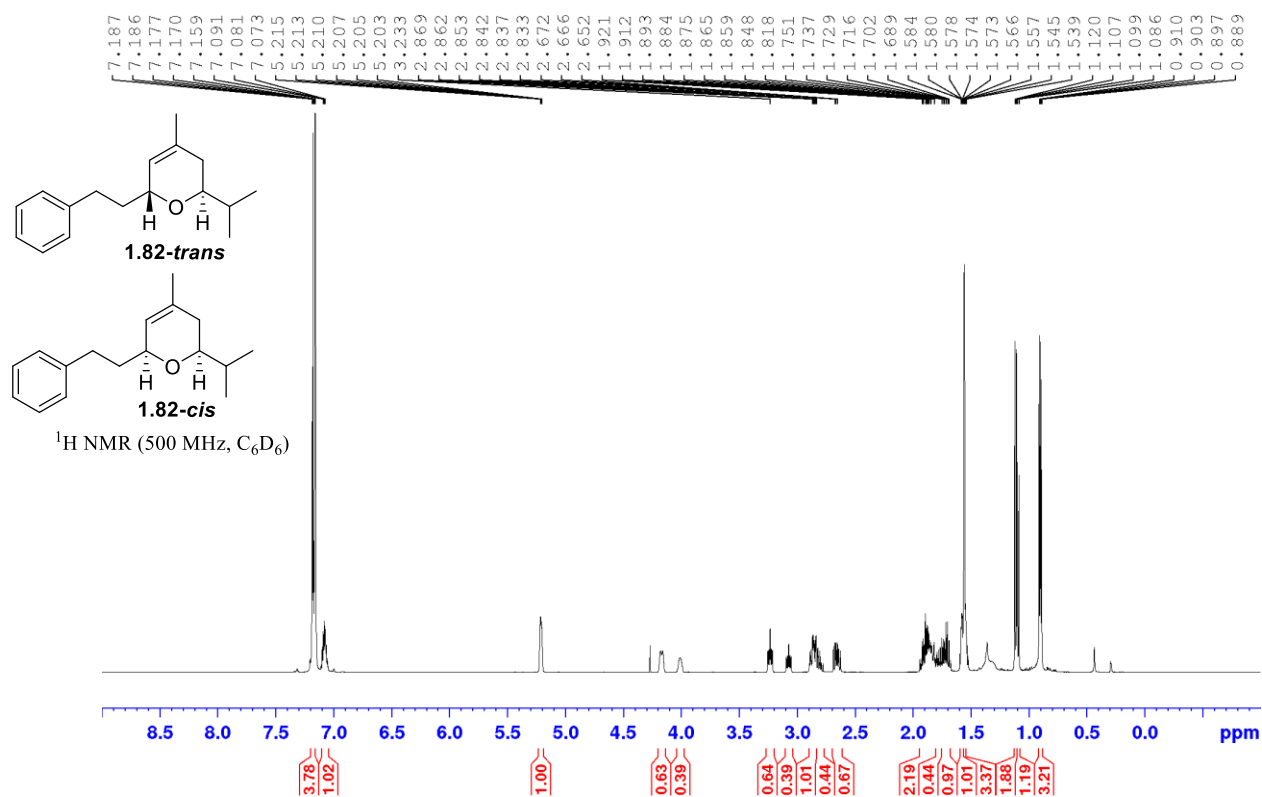
¹³C NMR (100 MHz, C₆D₆)

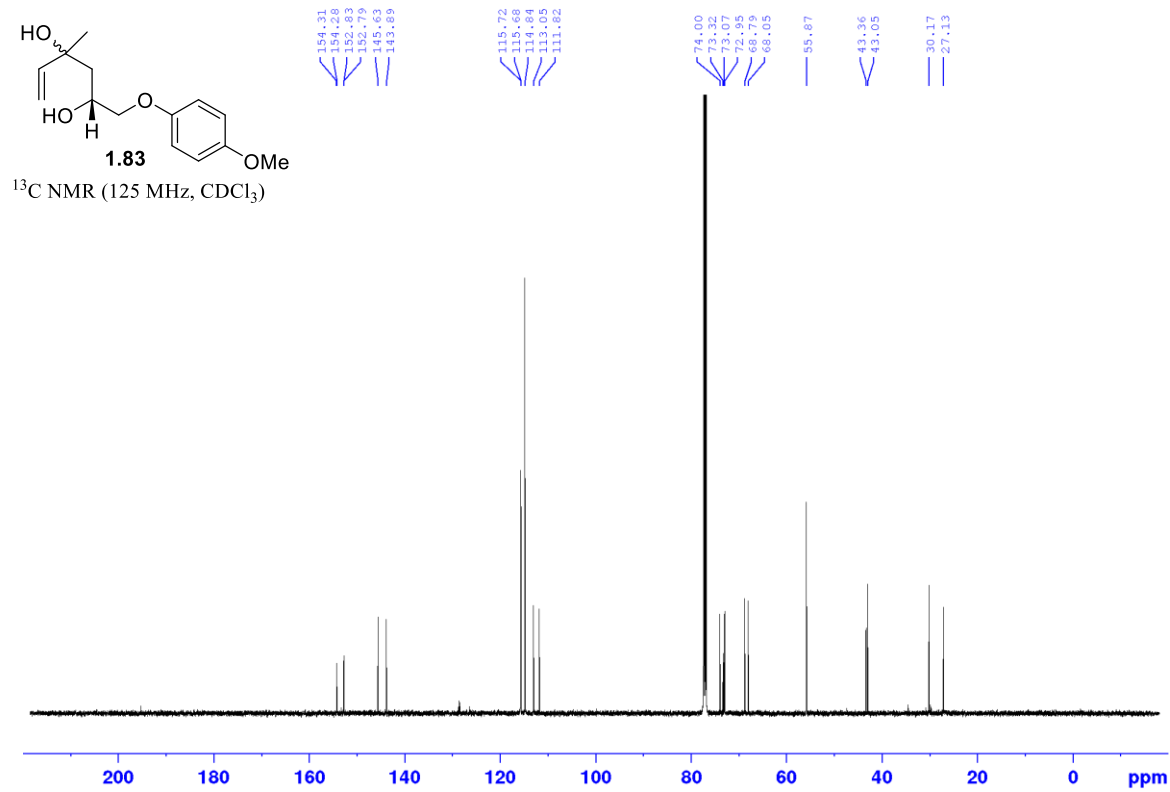
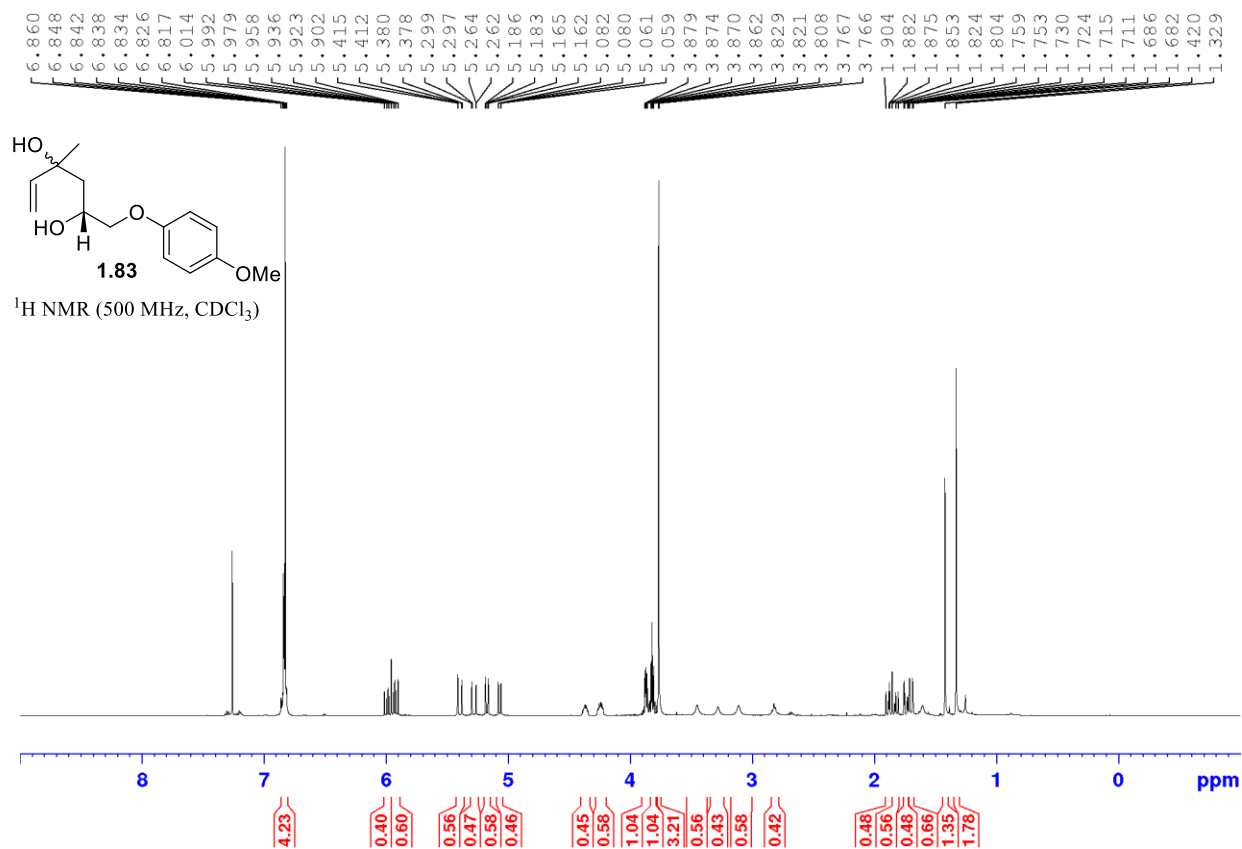


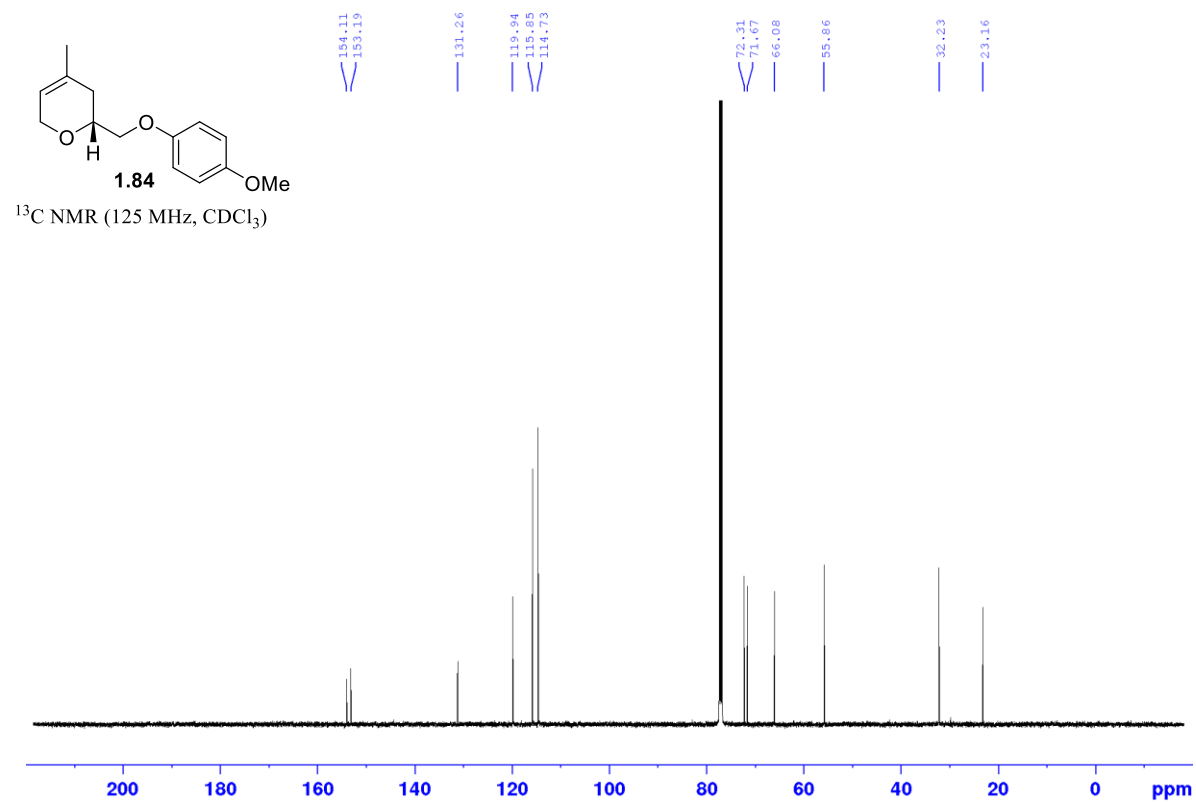
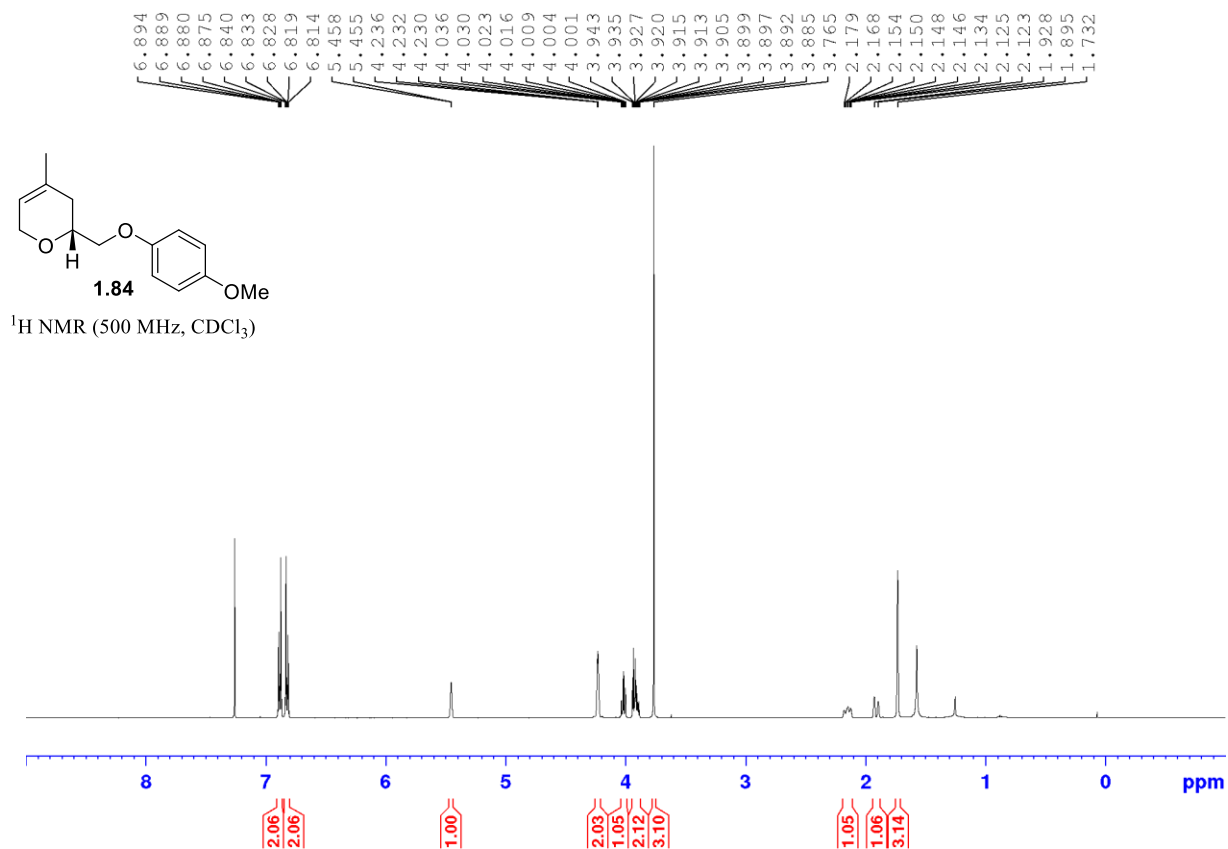




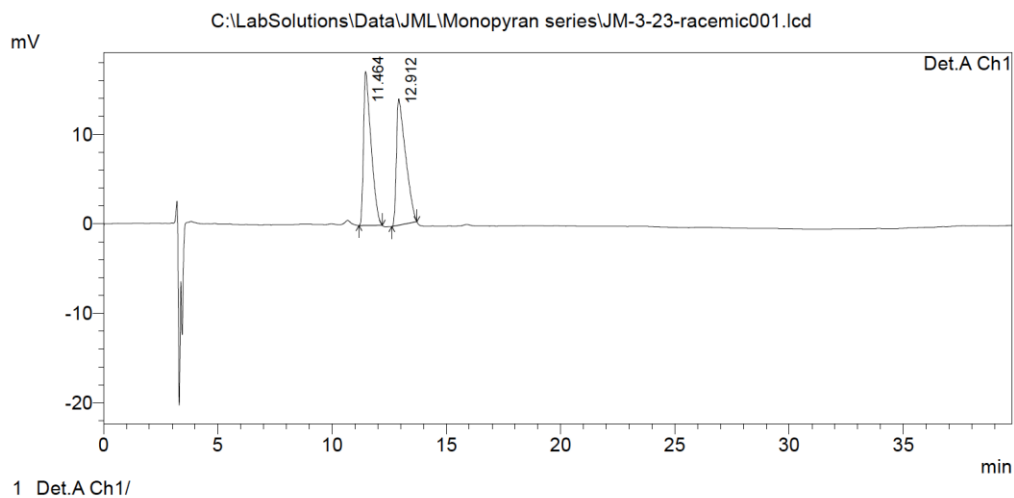








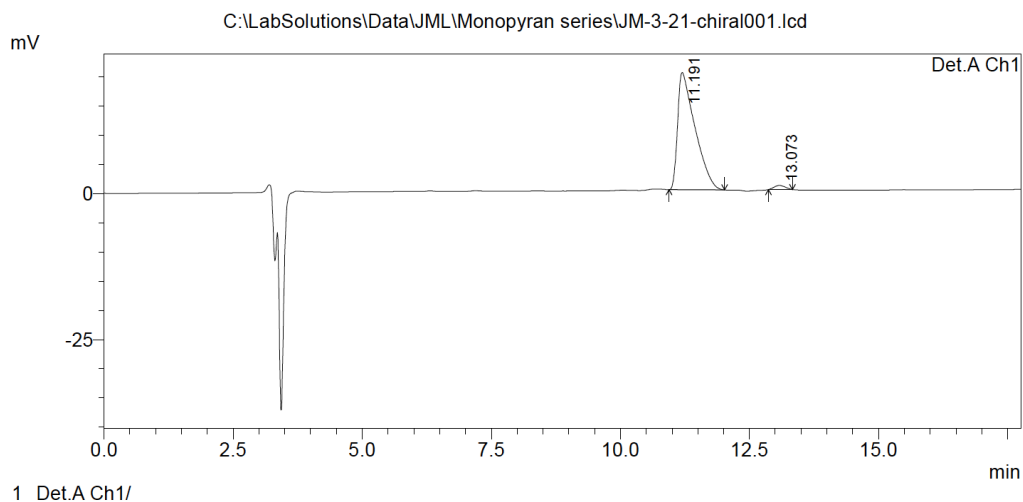
HPLC analysis of racemic **1.84**



PeakTable

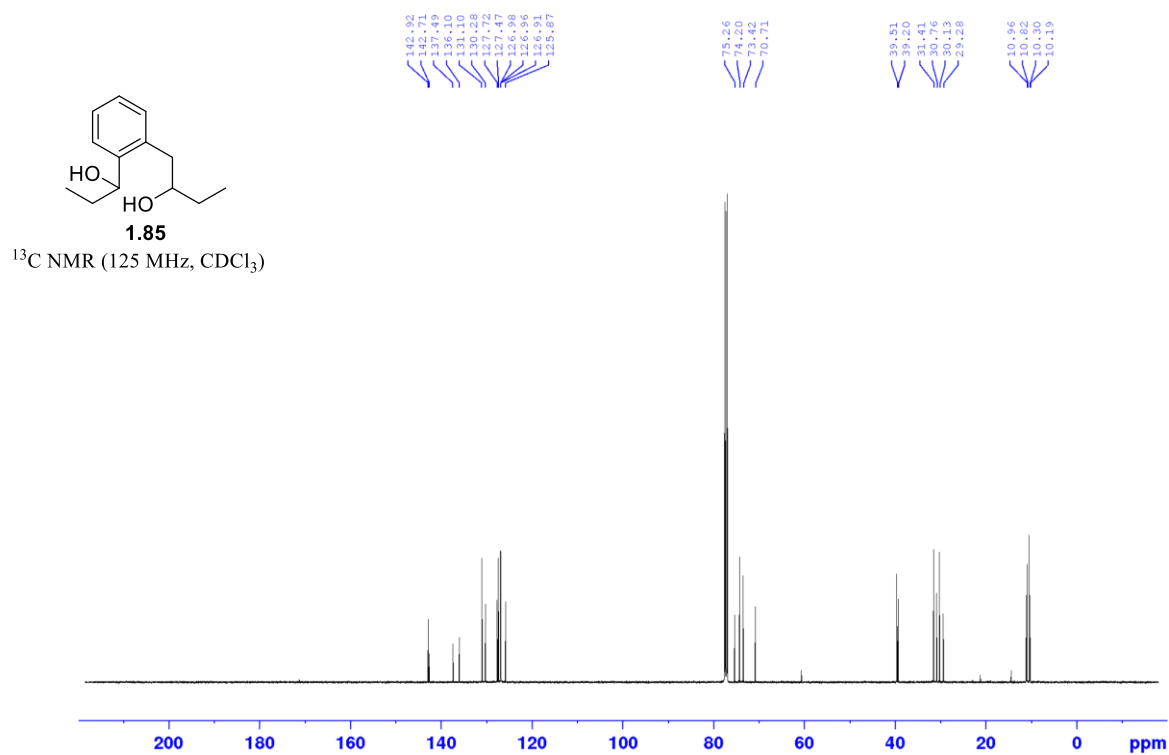
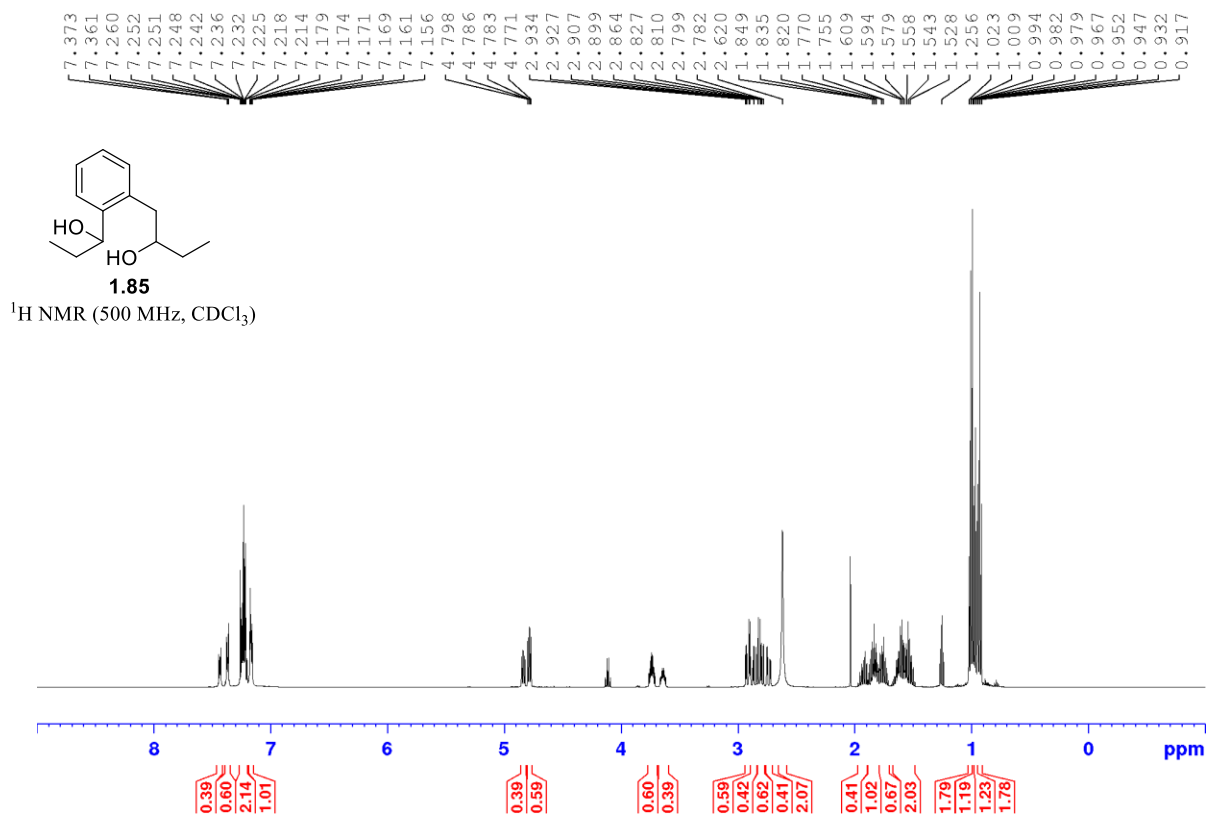
Peak#	Ret. Time	Area	Height	Area %	Height %
1	11.464	392813	17188	50.057	54.884
2	12.912	391921	14128	49.943	45.116
Total		784734	31316	100.000	100.000

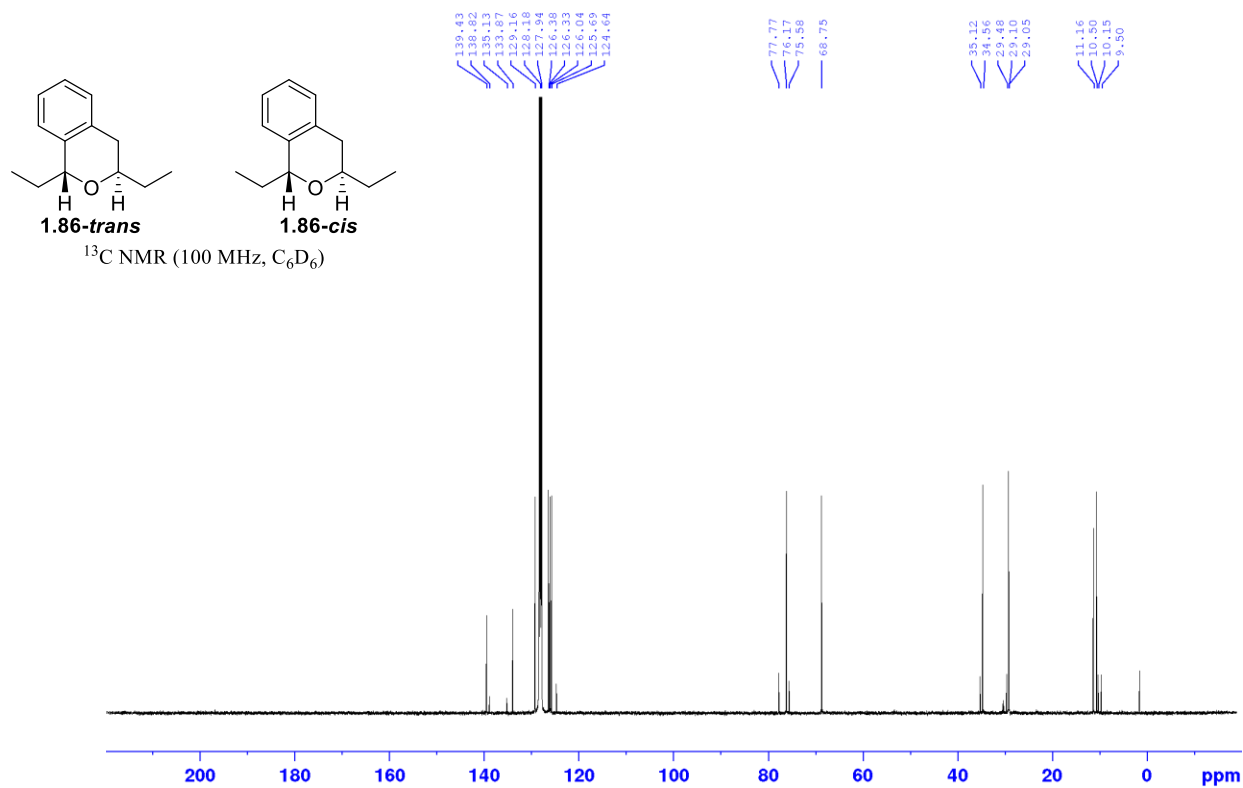
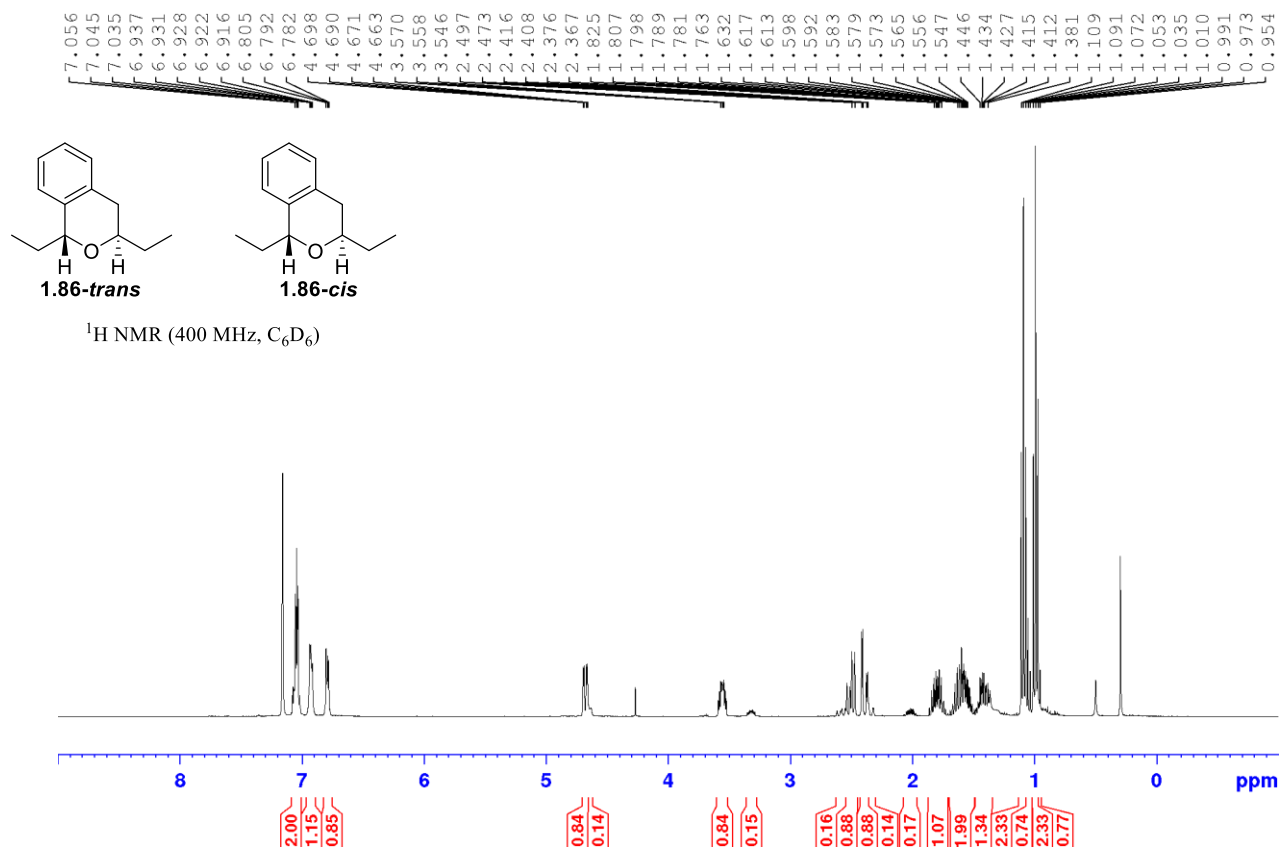
HPLC analysis of enantiomerically enriched **1.84**

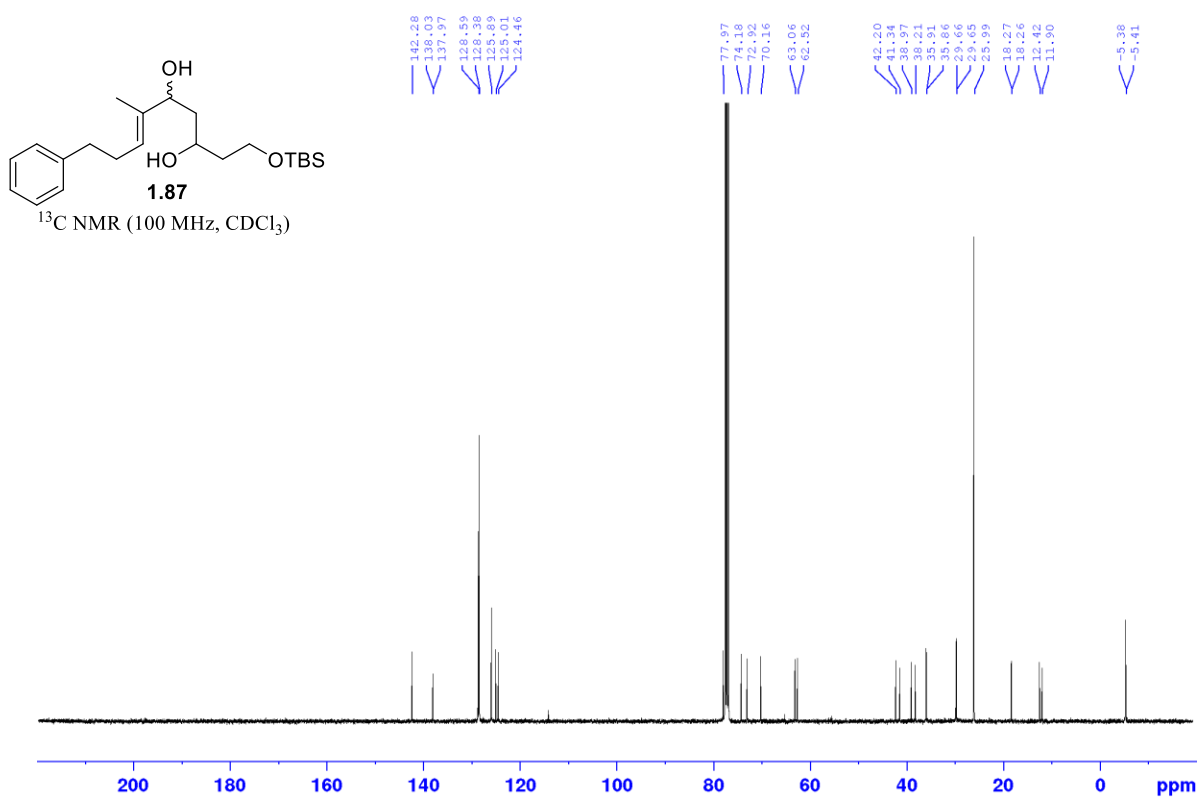
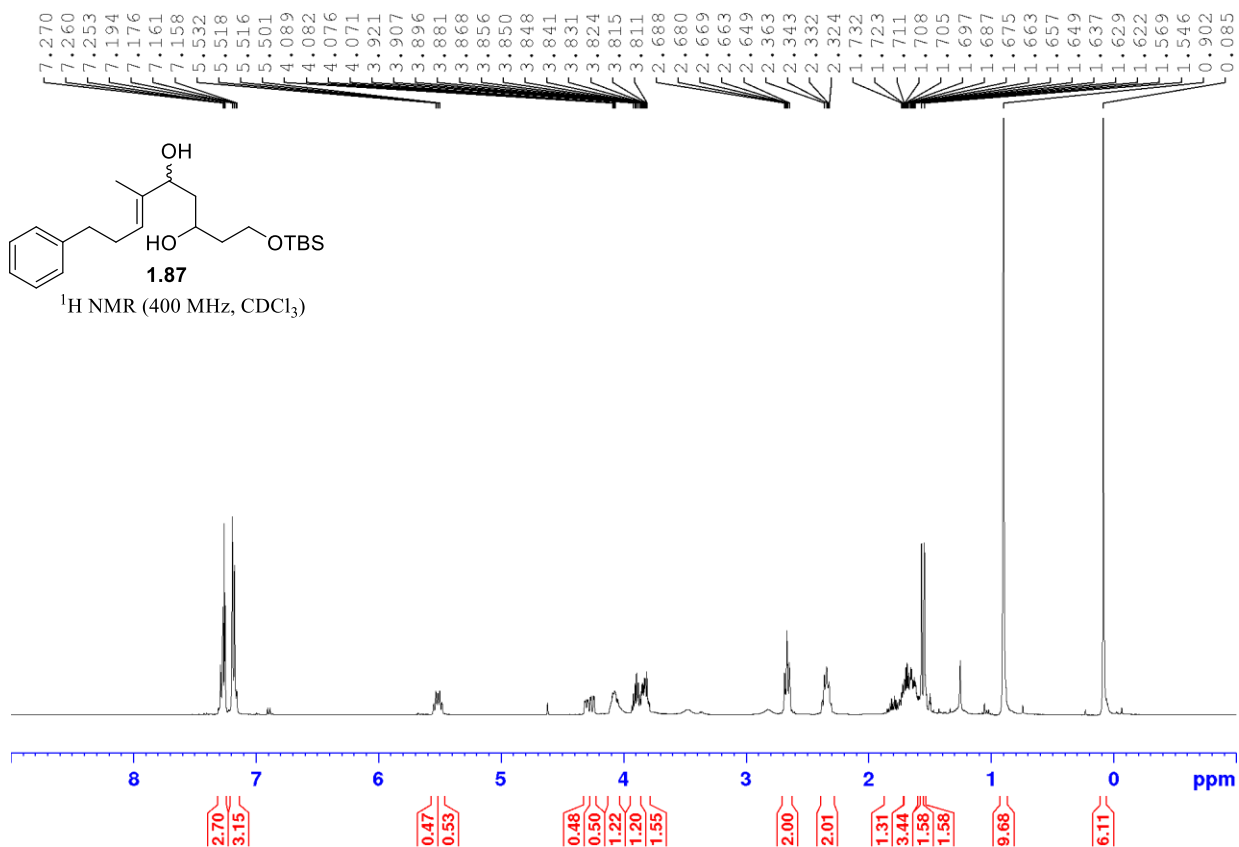


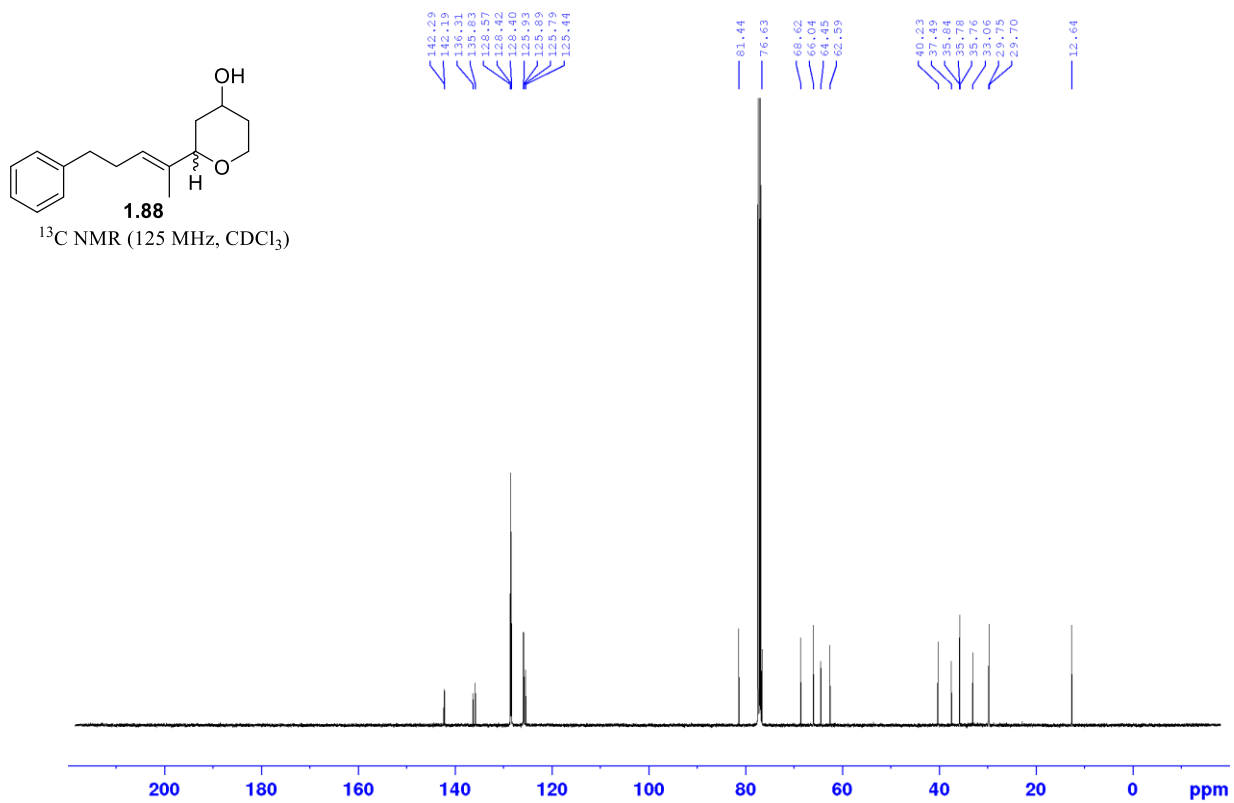
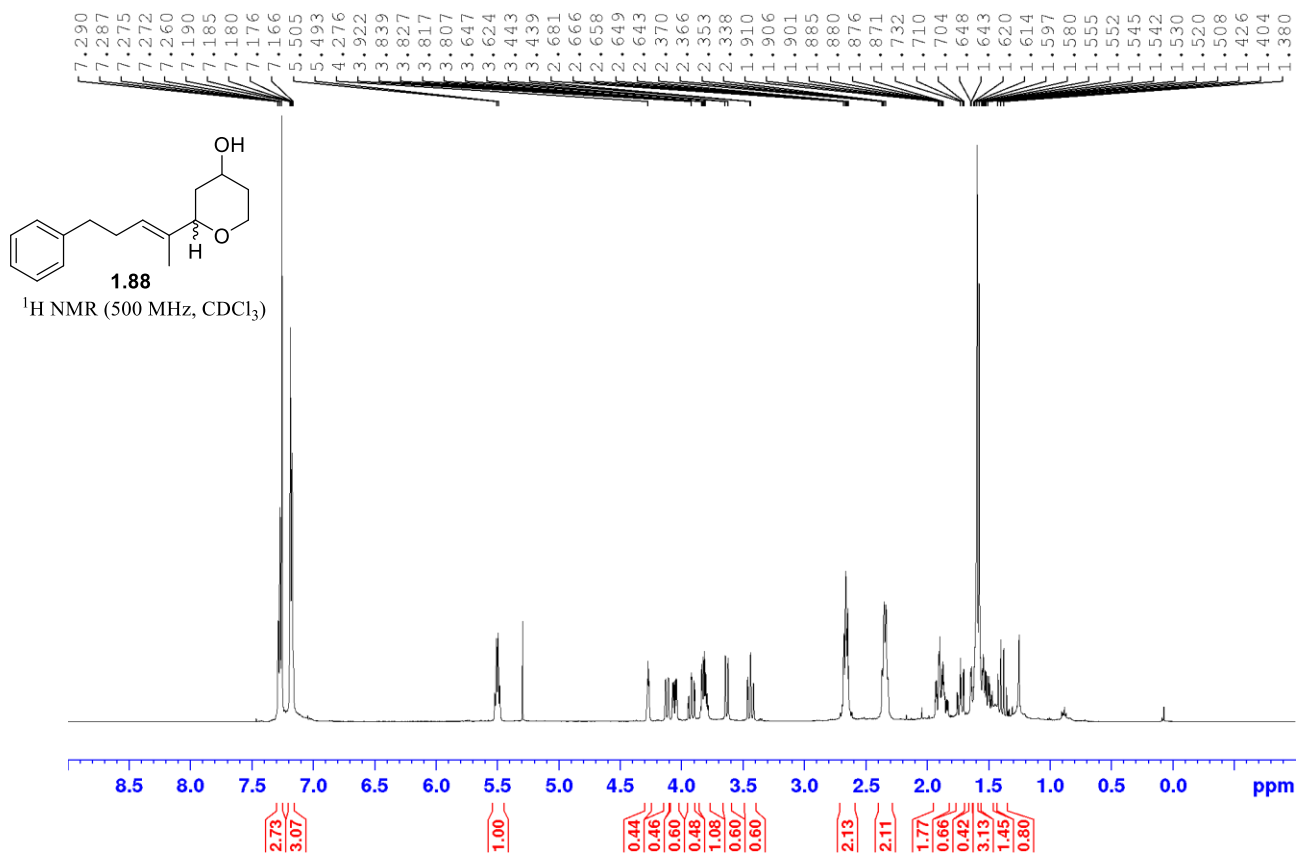
PeakTable

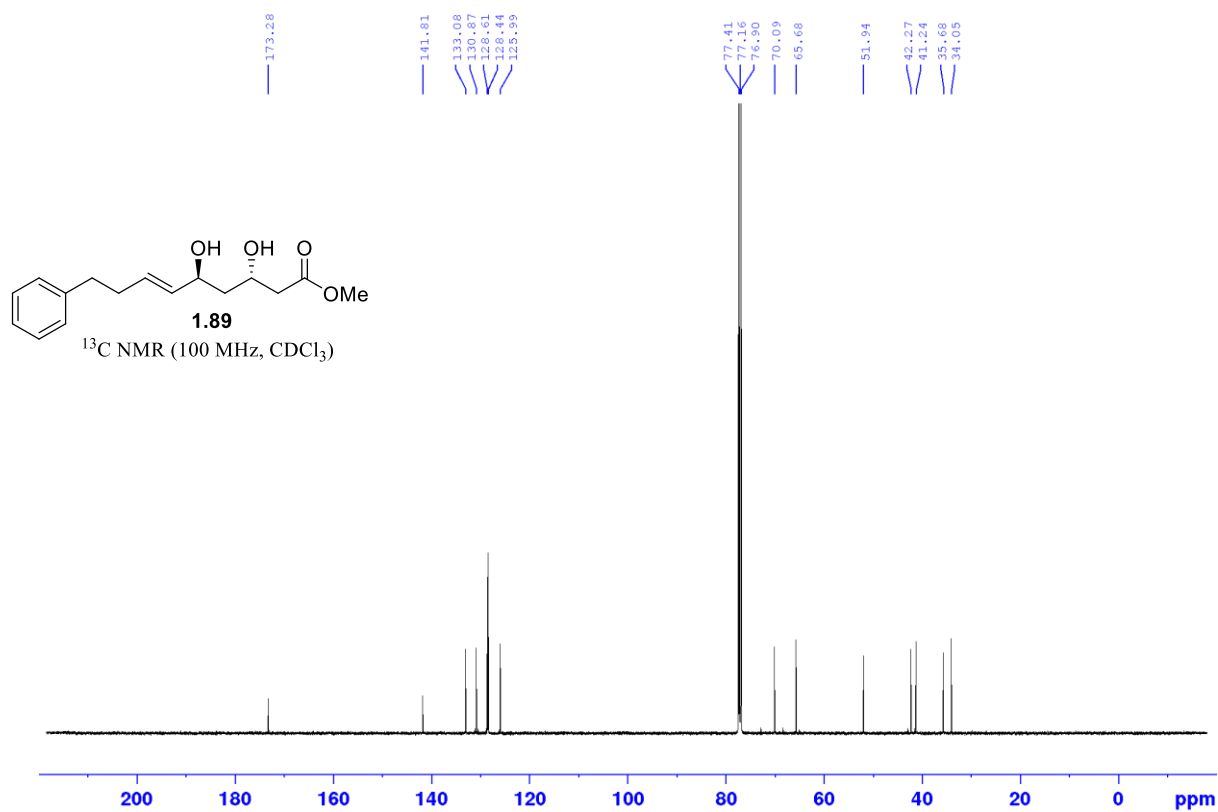
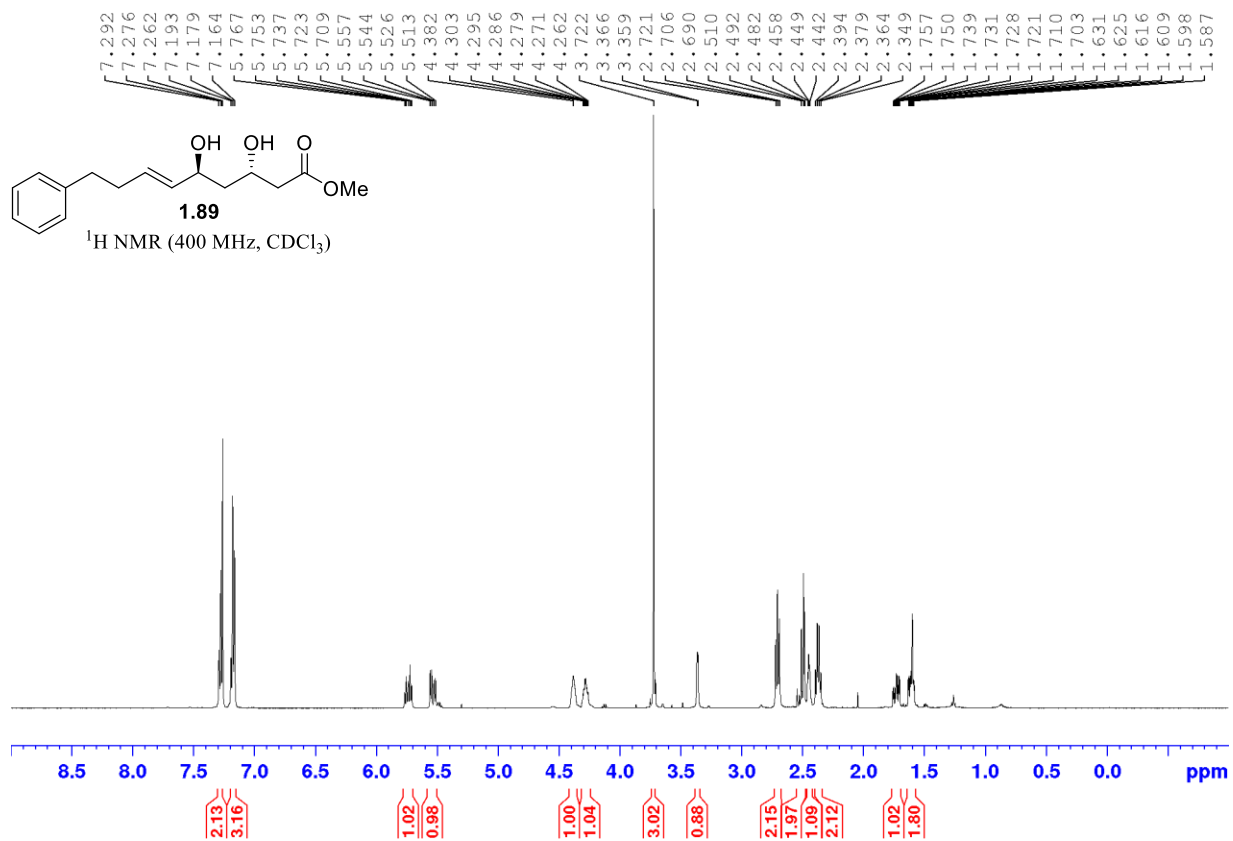
Peak#	Ret. Time	Area	Height	Area %	Height %
1	11.191	469551	20064	97.839	96.645
2	13.073	10369	697	2.161	3.355
Total		479919	20761	100.000	100.000

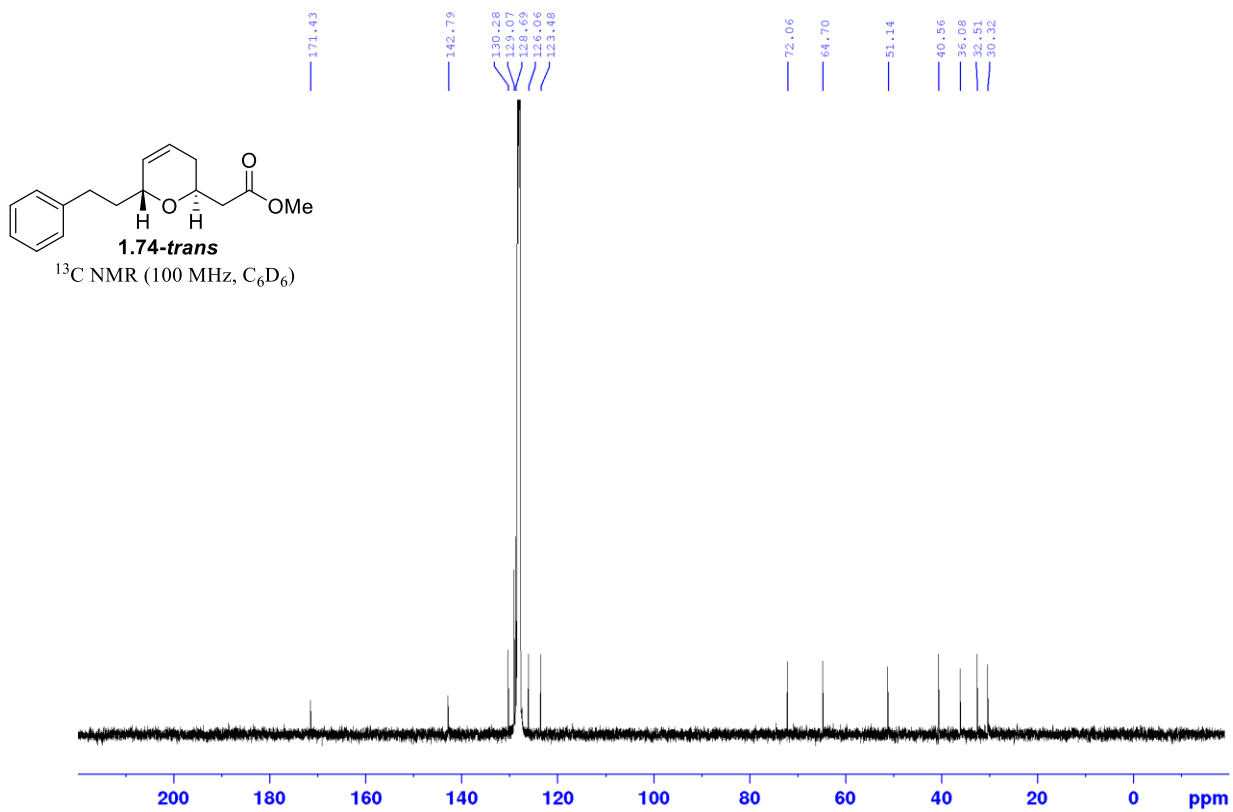
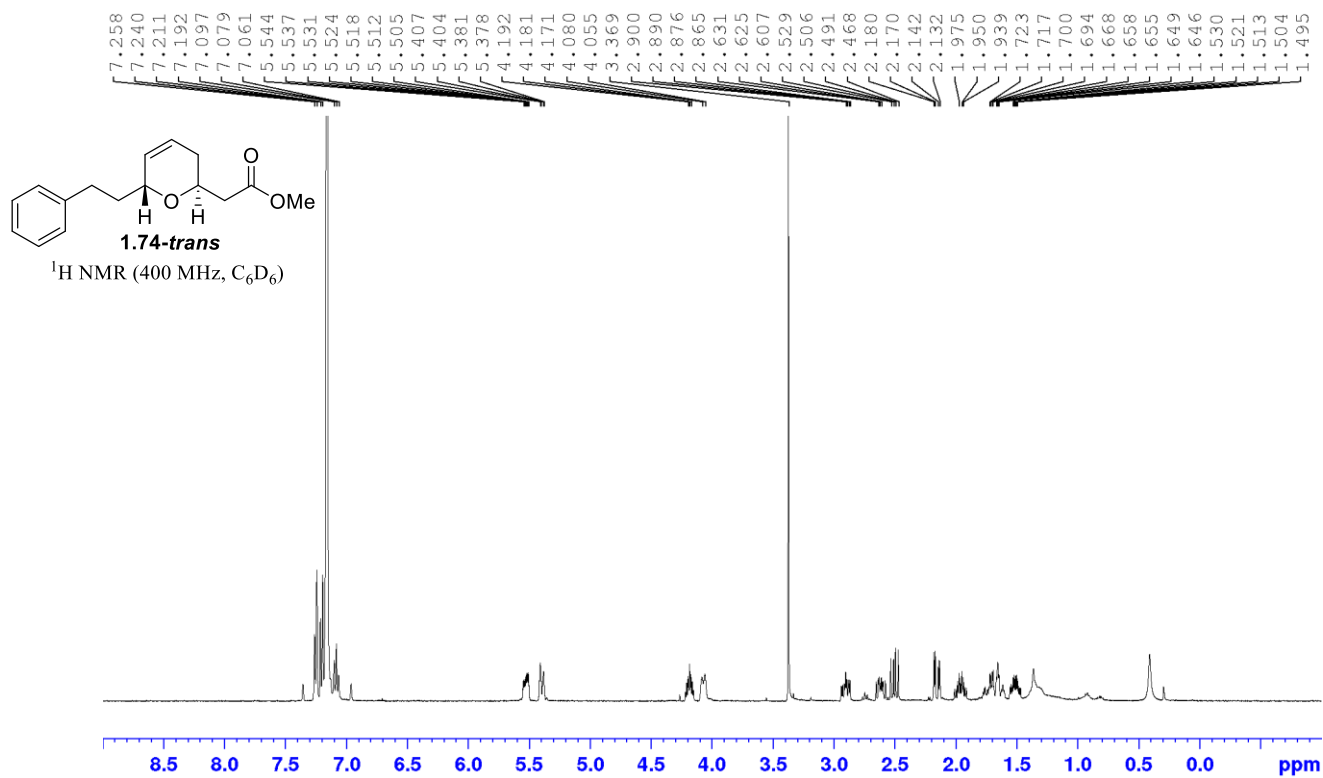


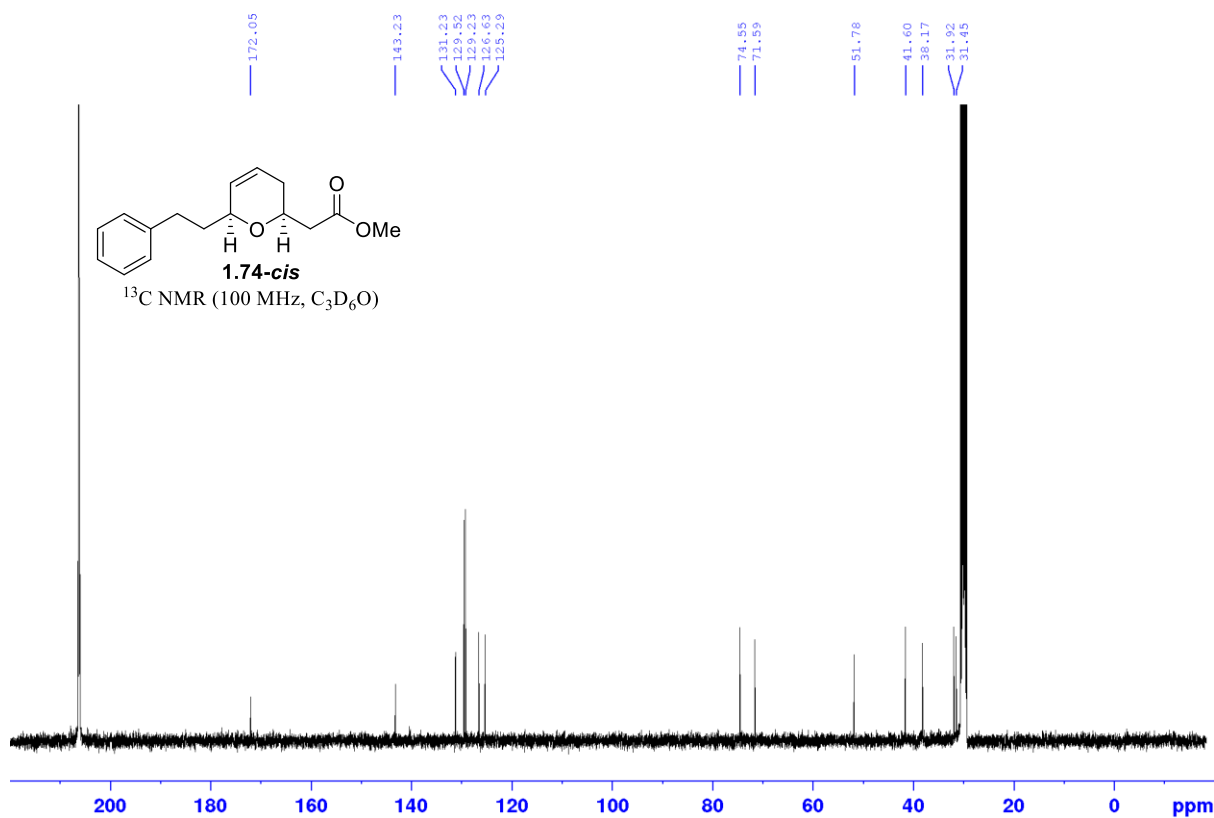
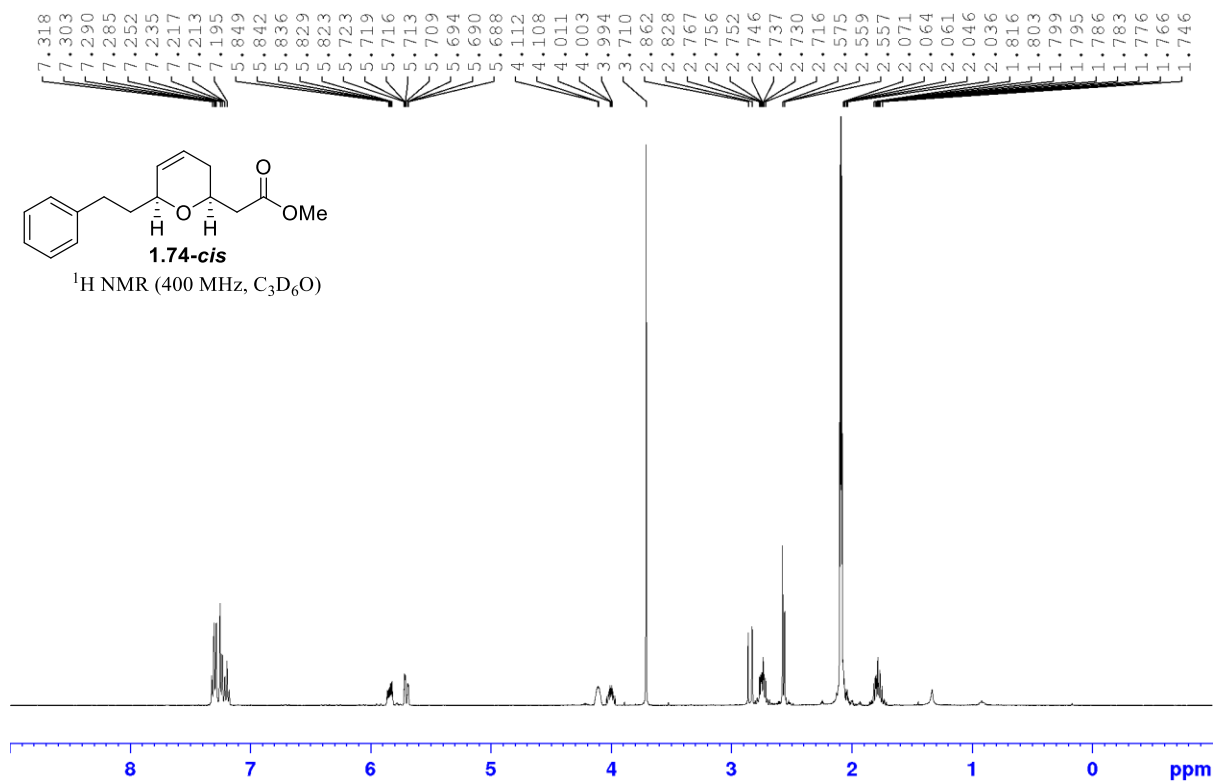


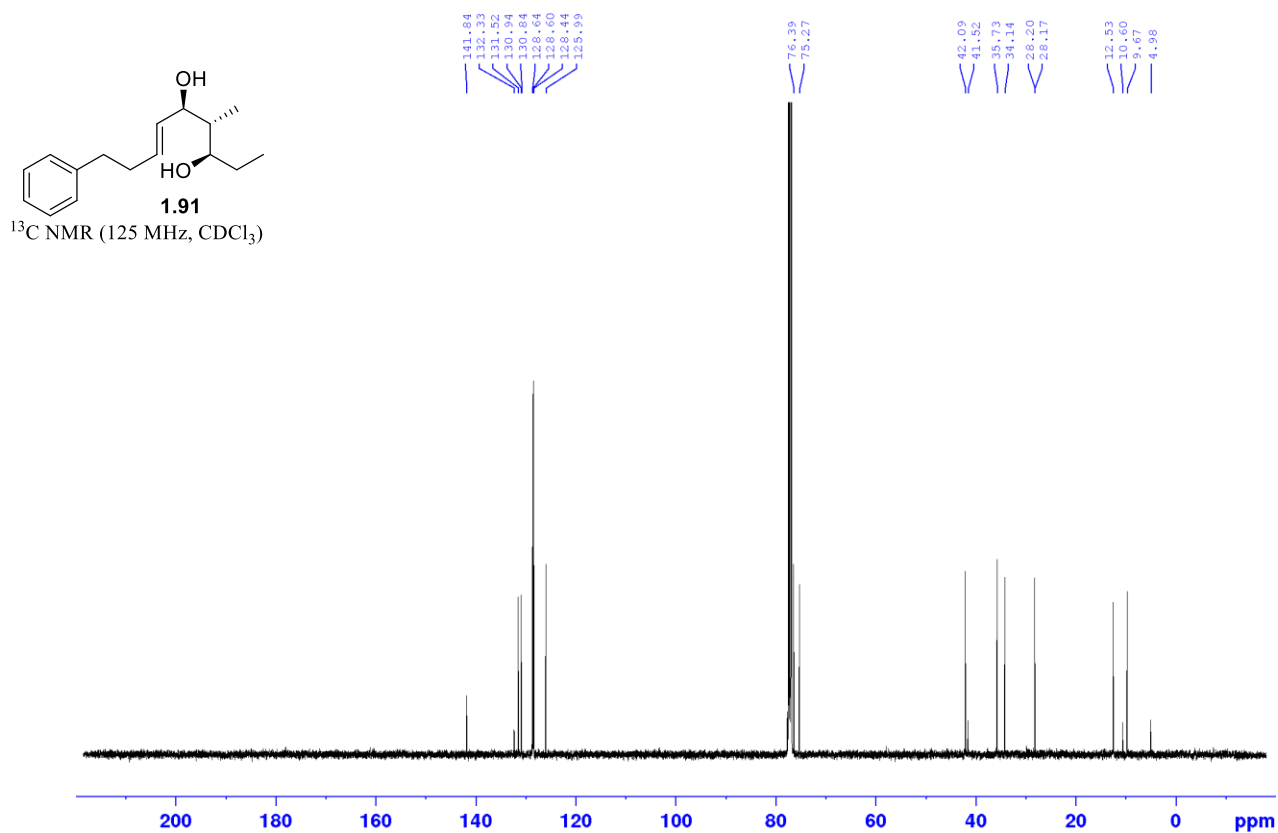
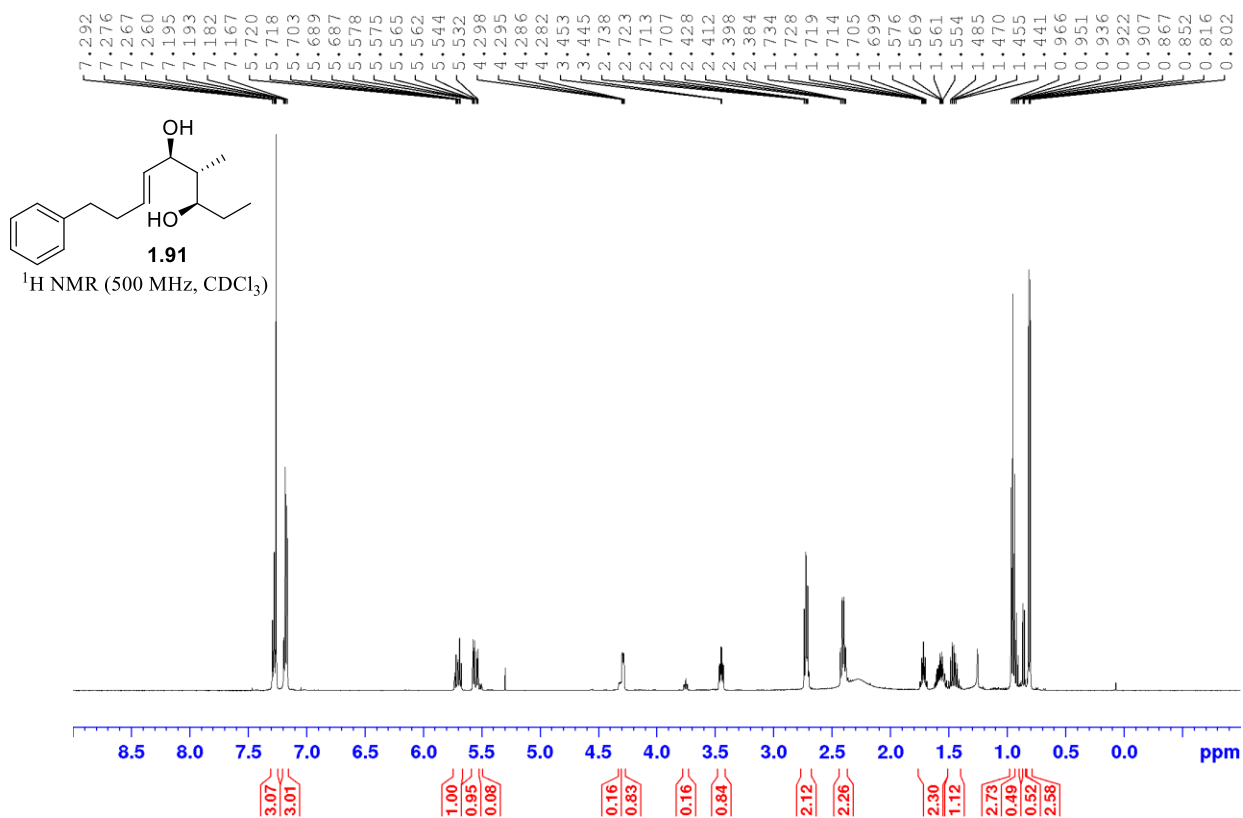


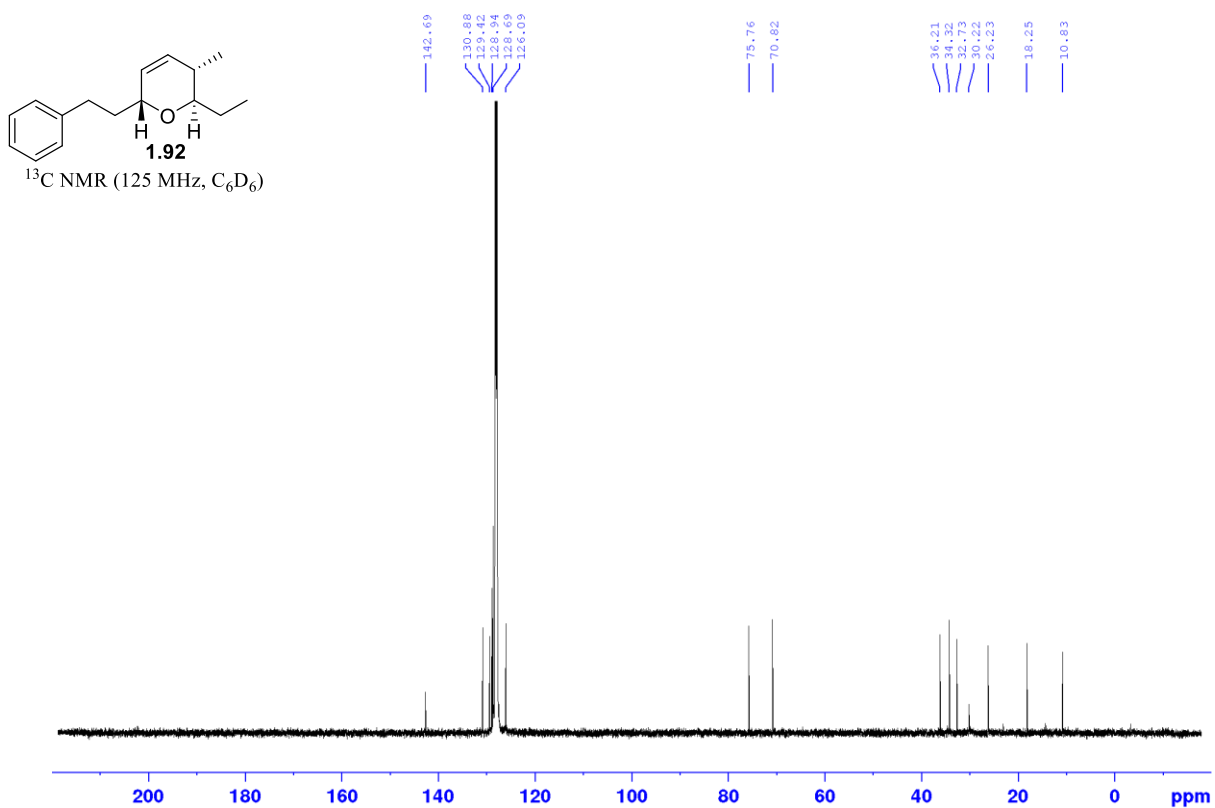
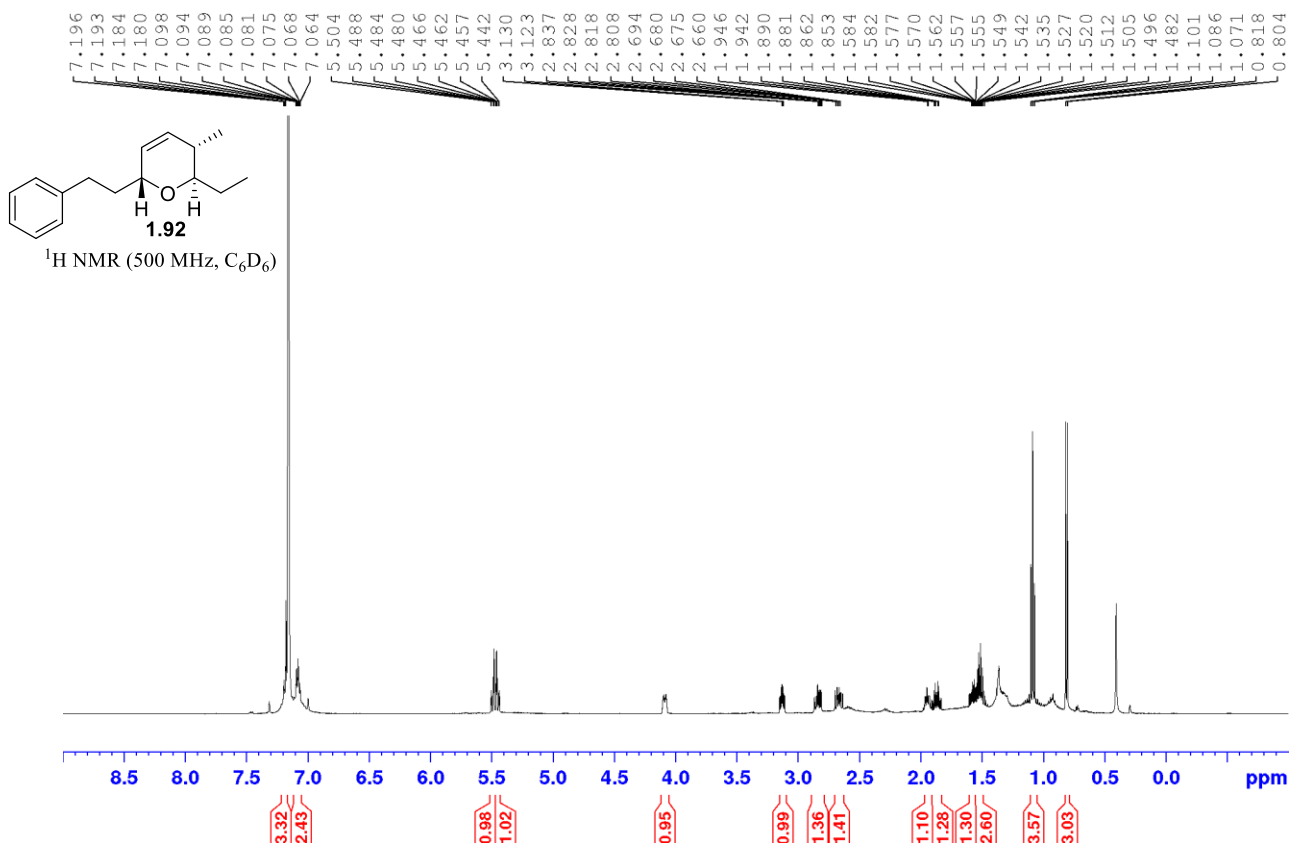


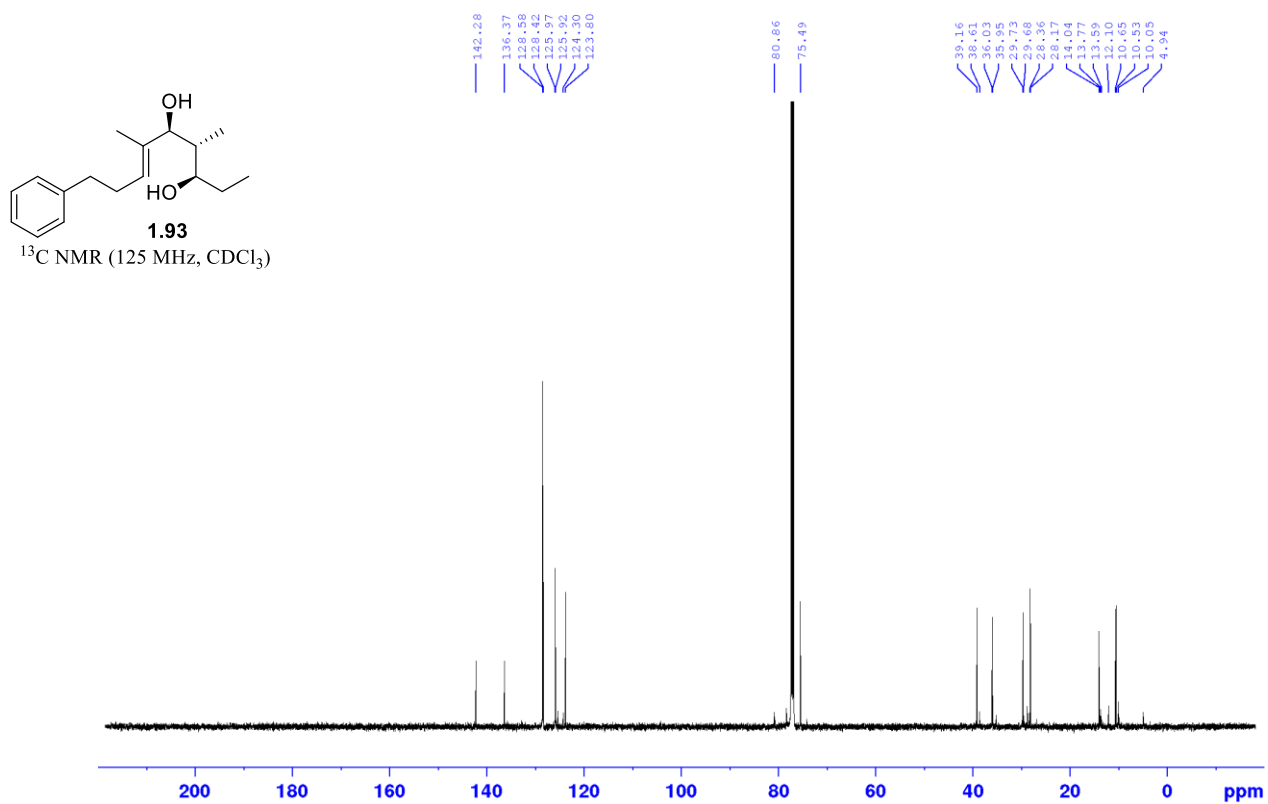
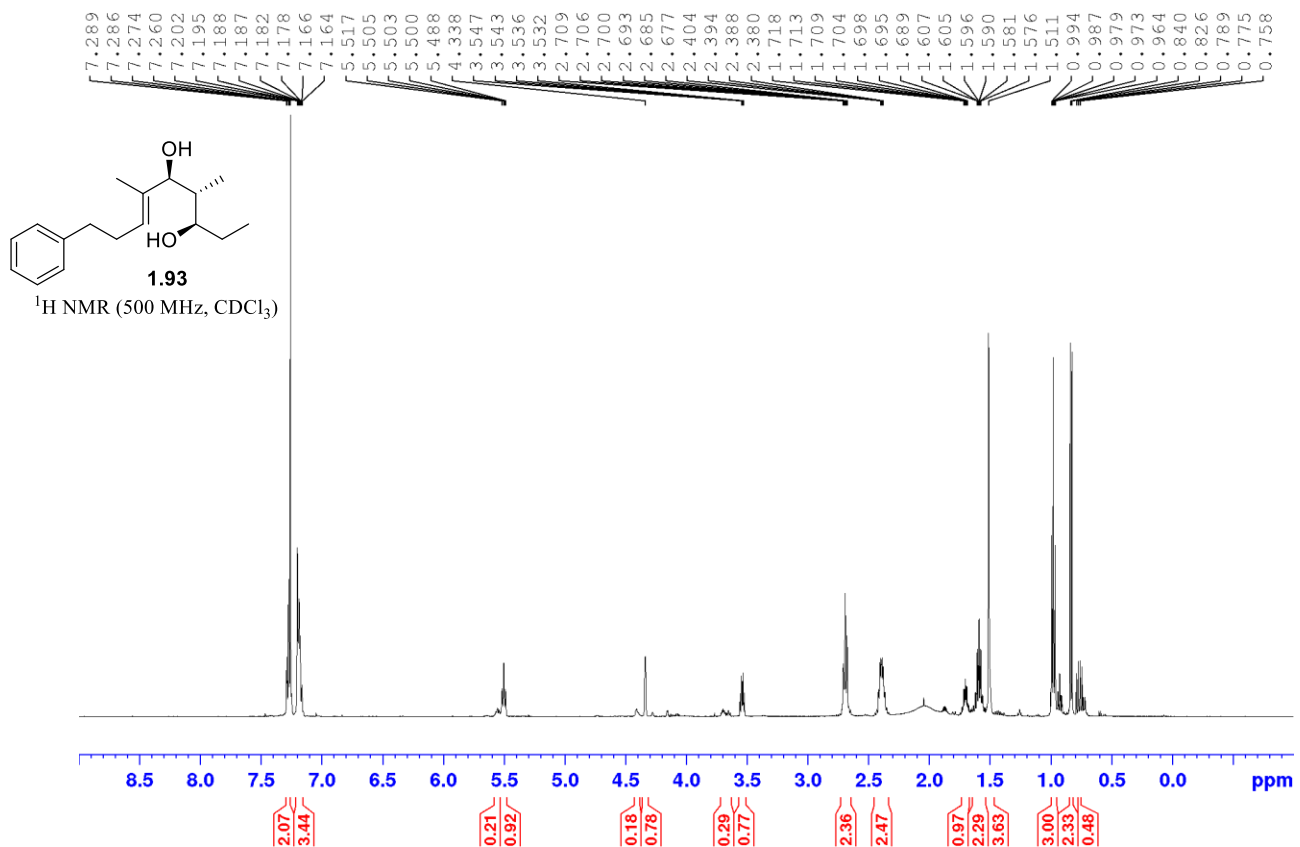


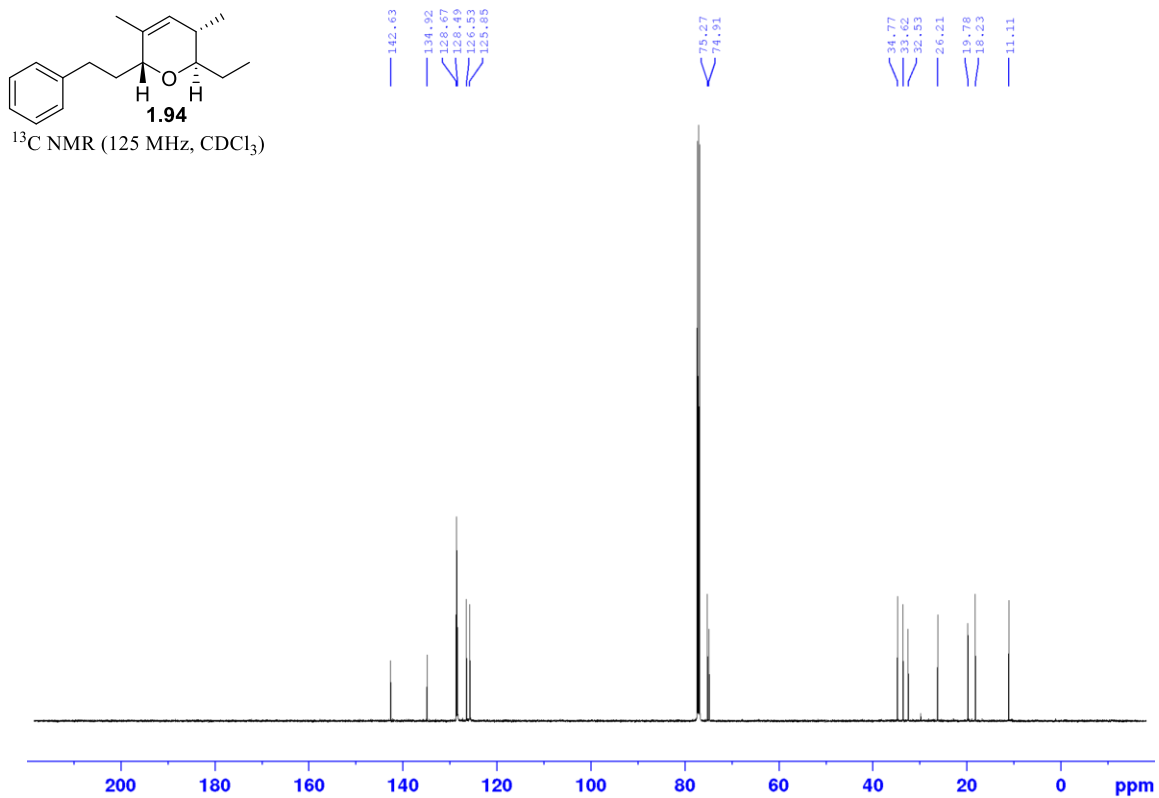
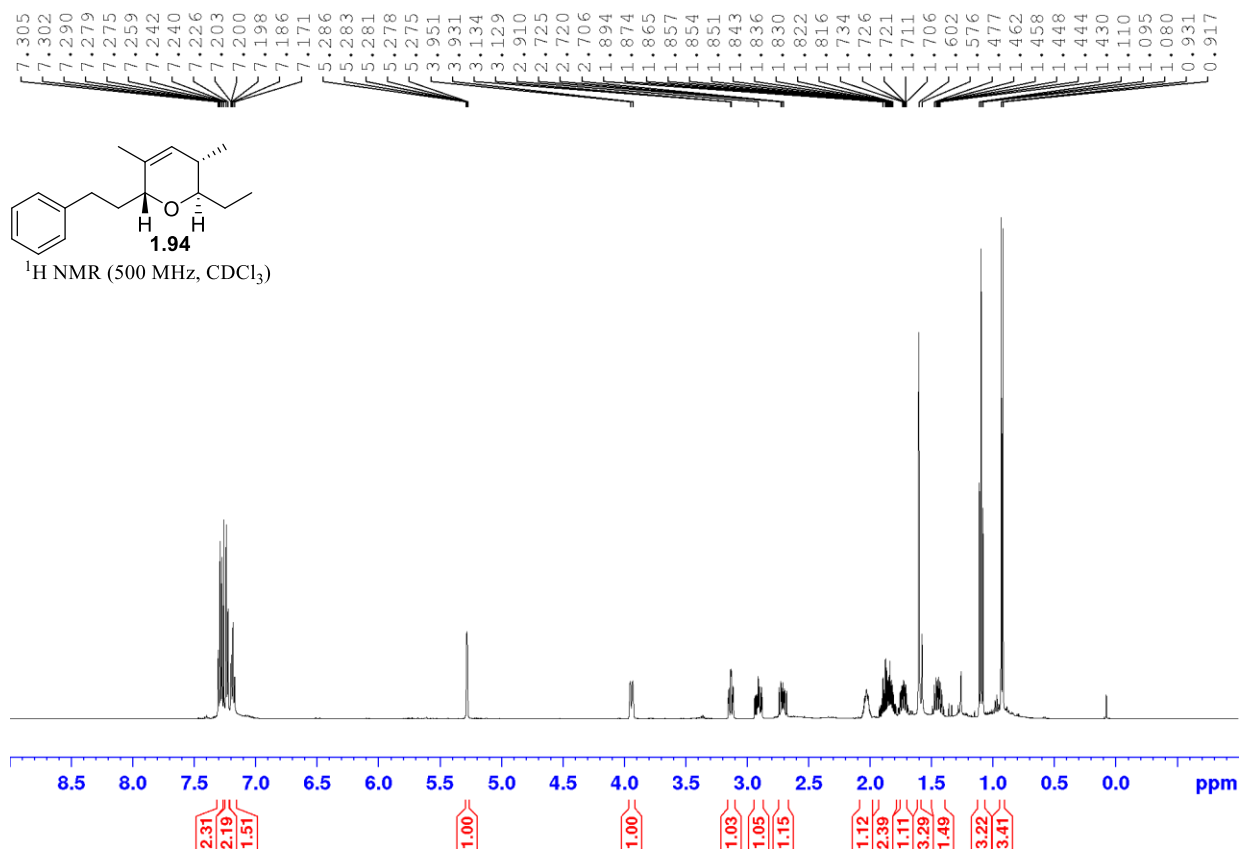


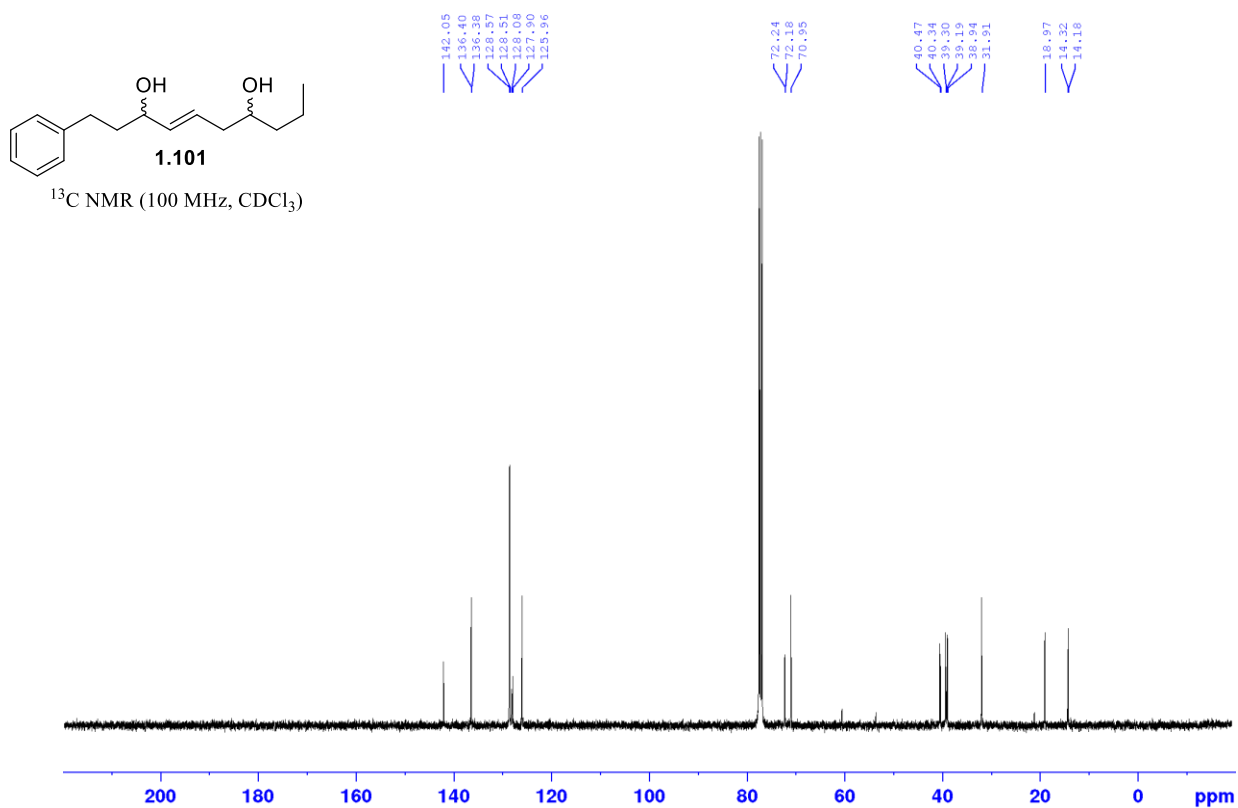
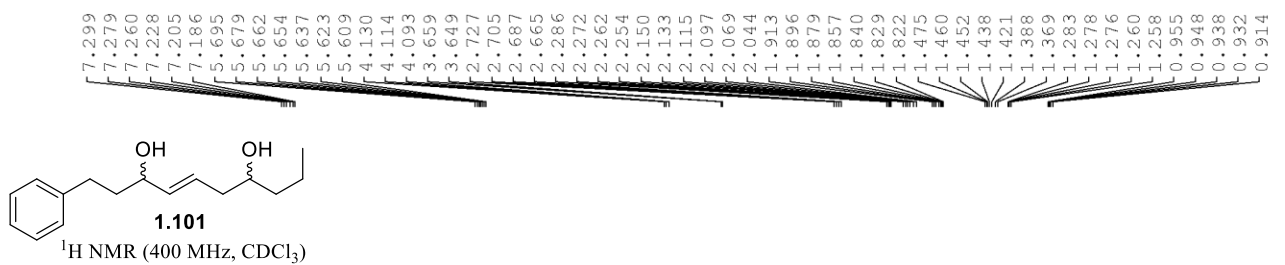


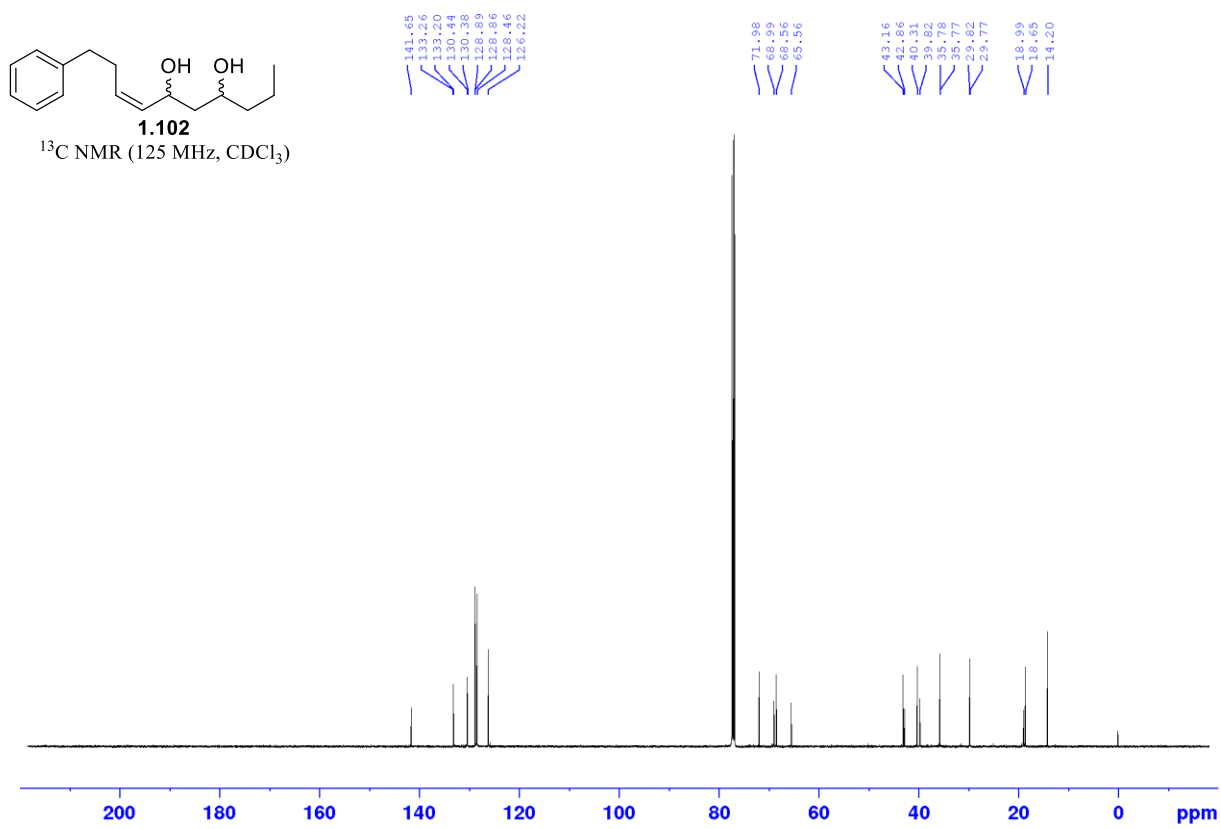
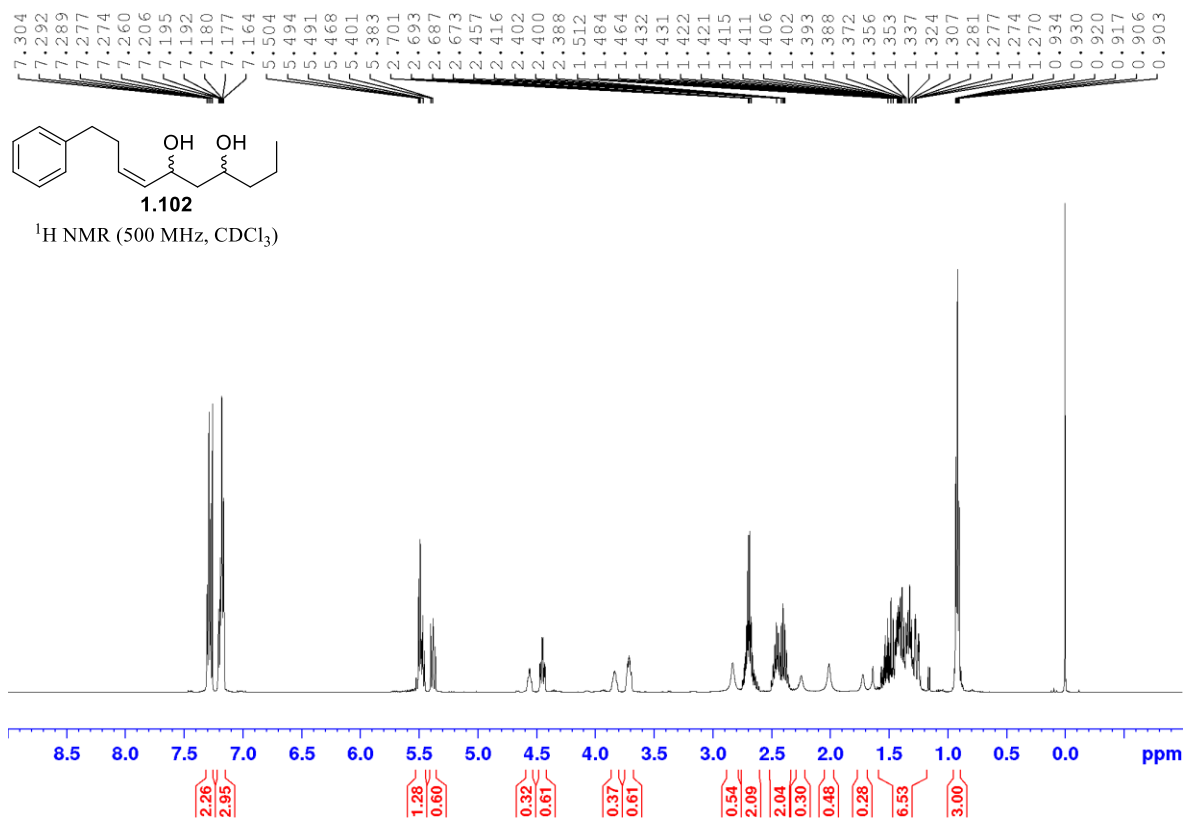


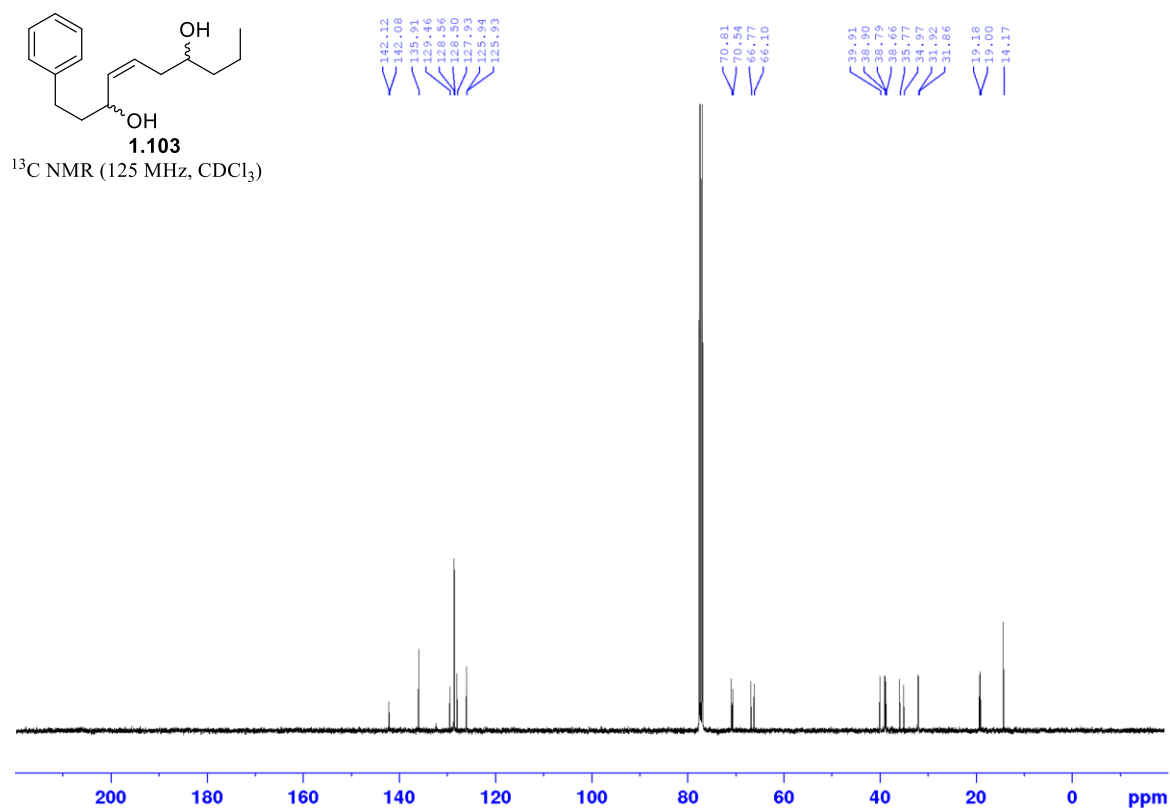
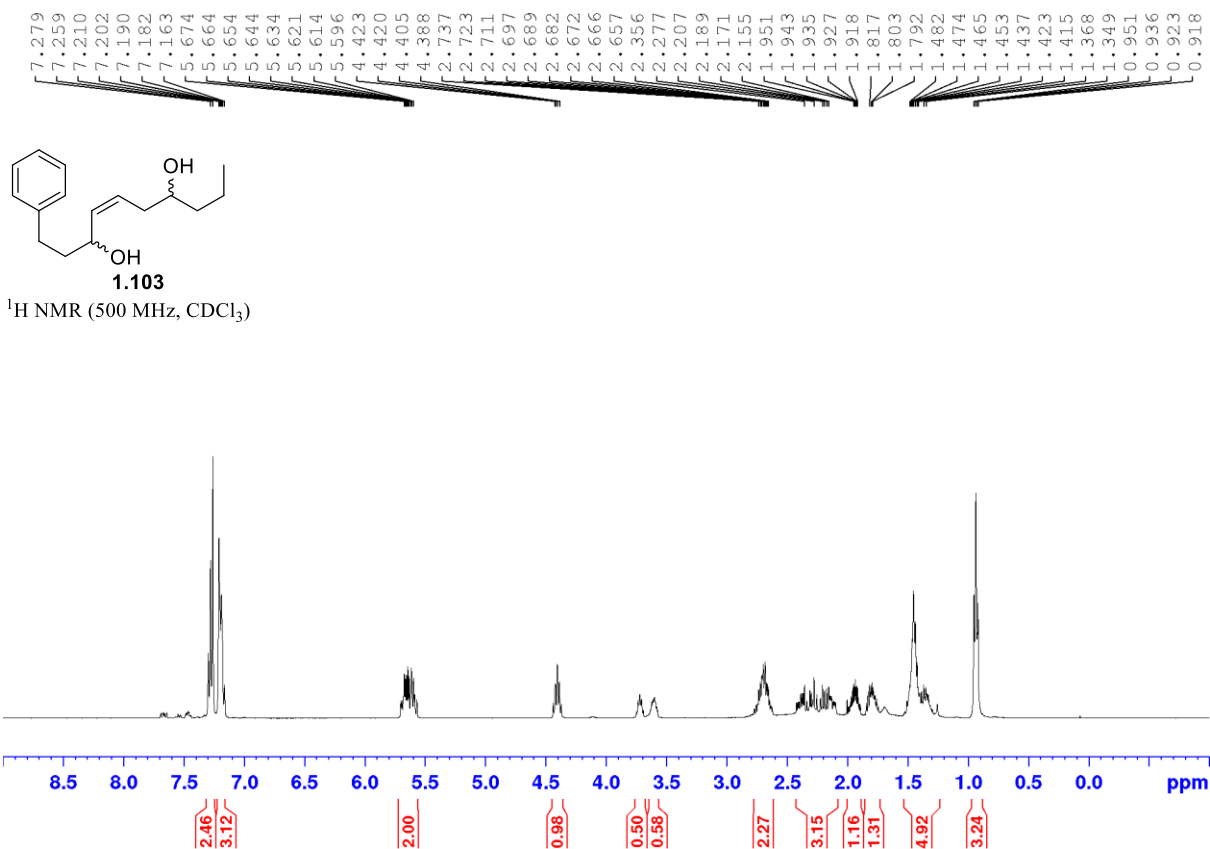


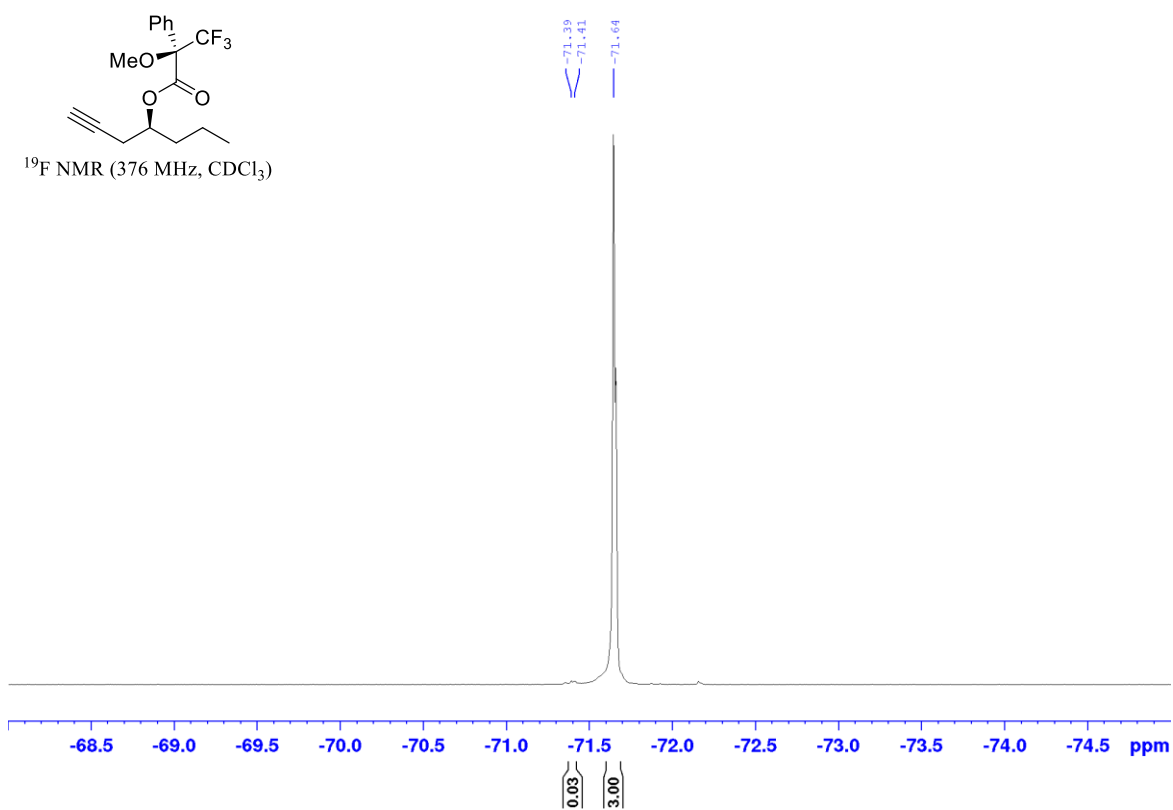
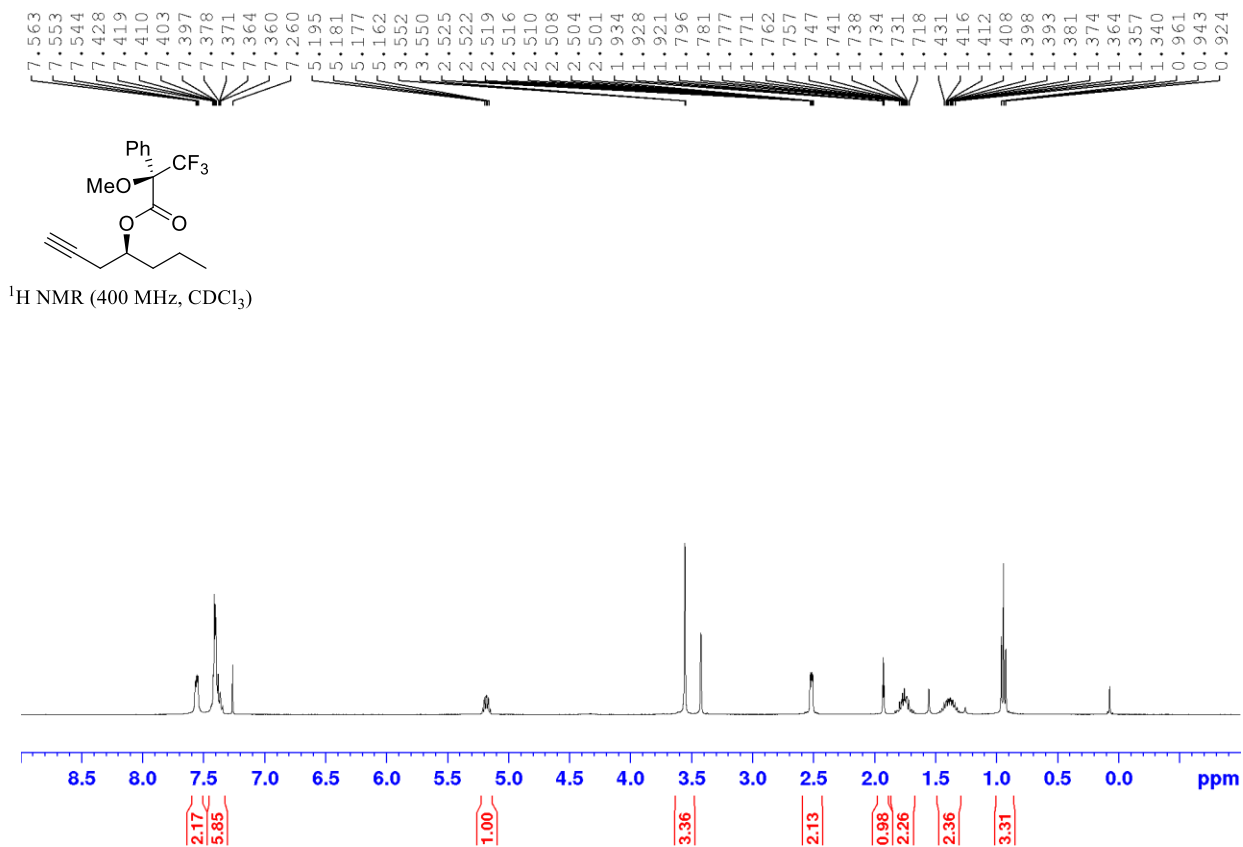


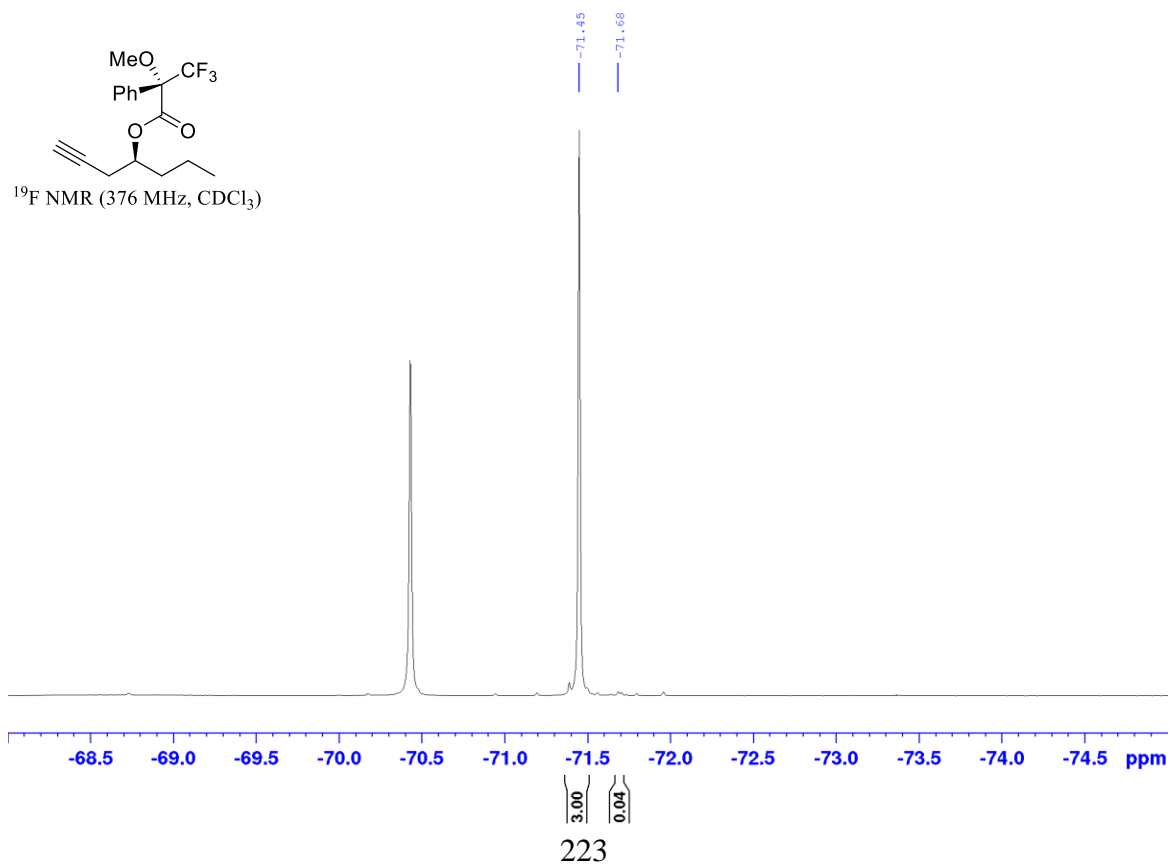
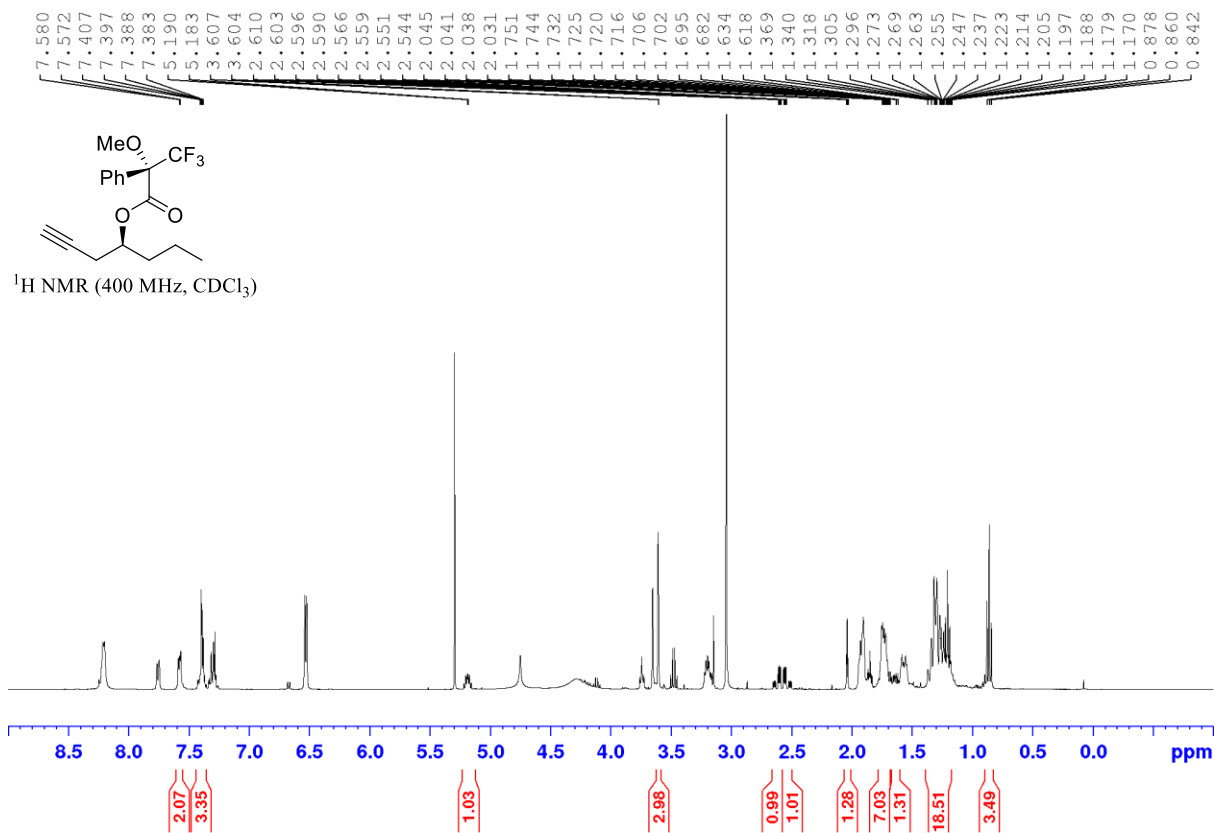


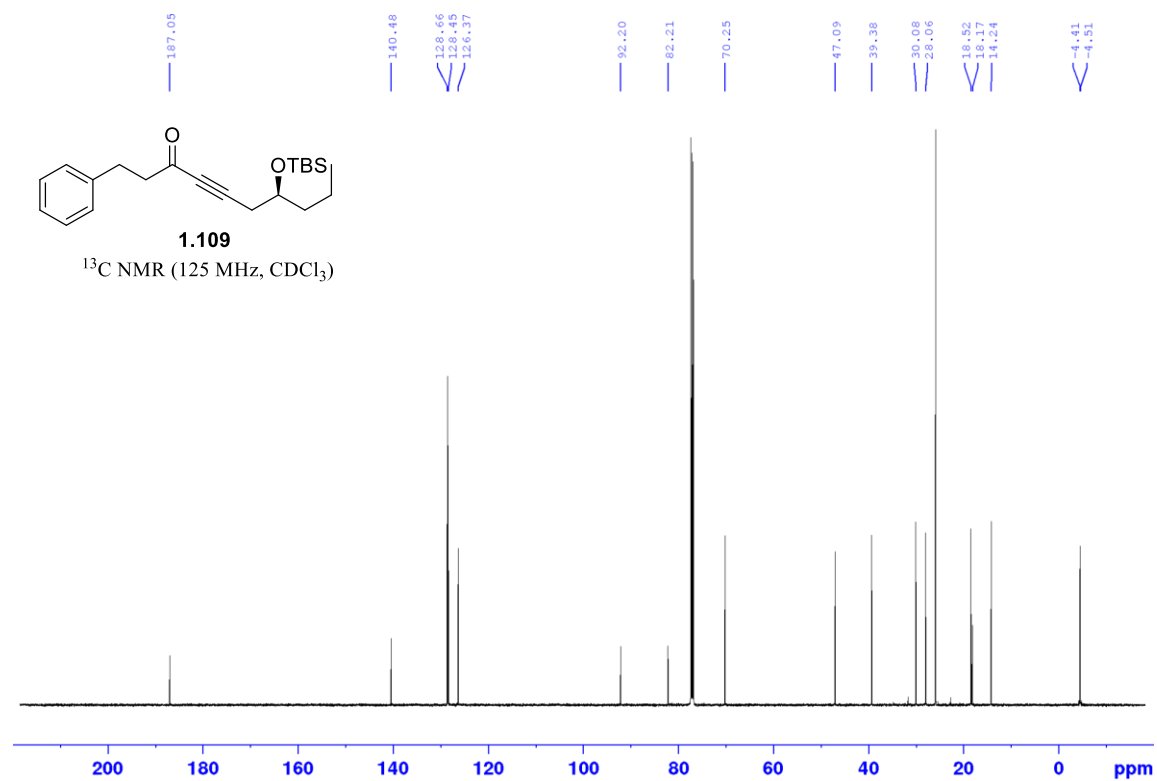
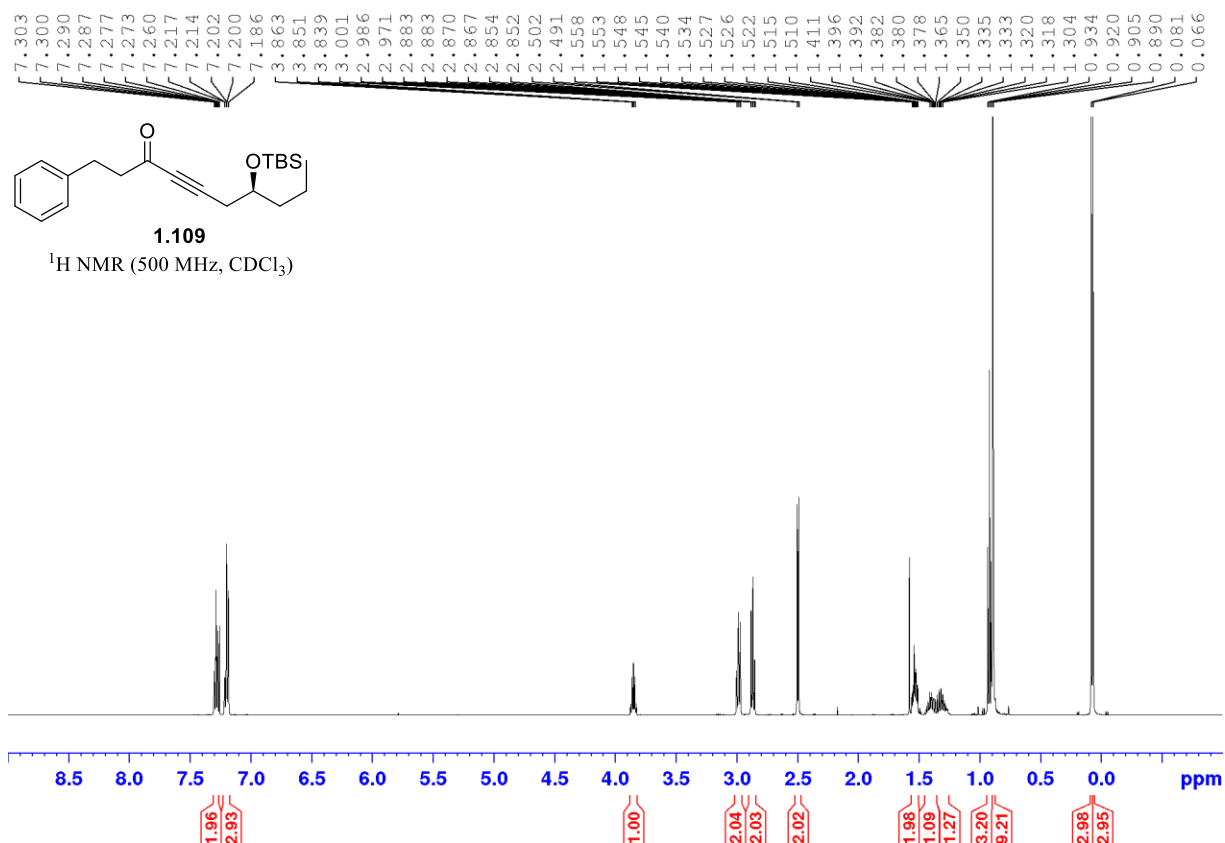


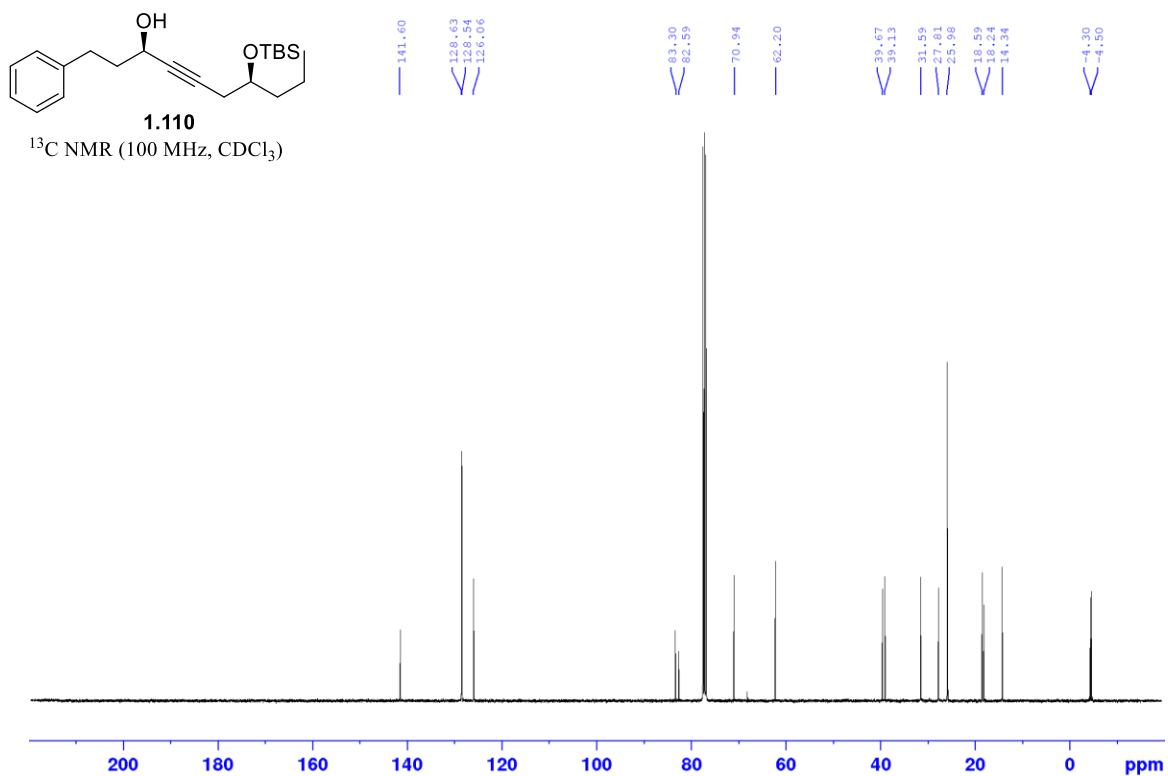
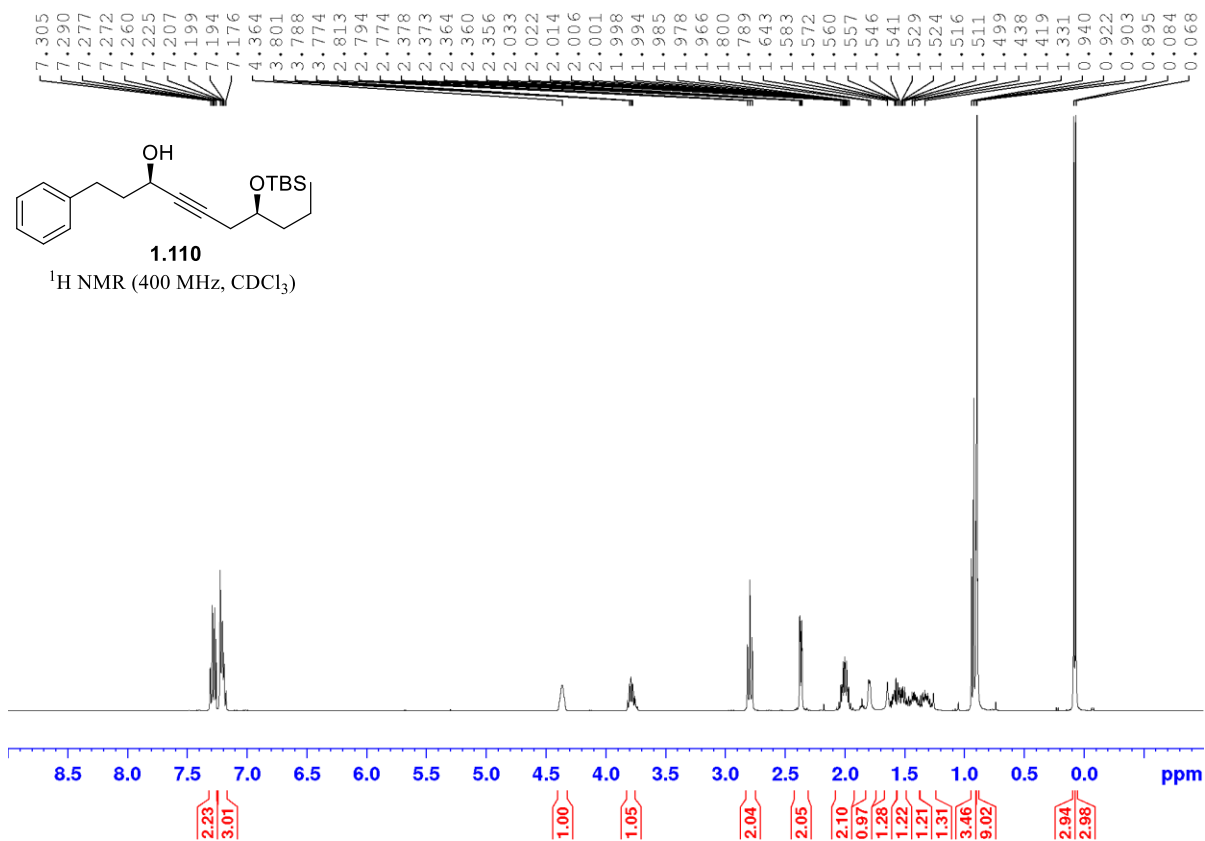


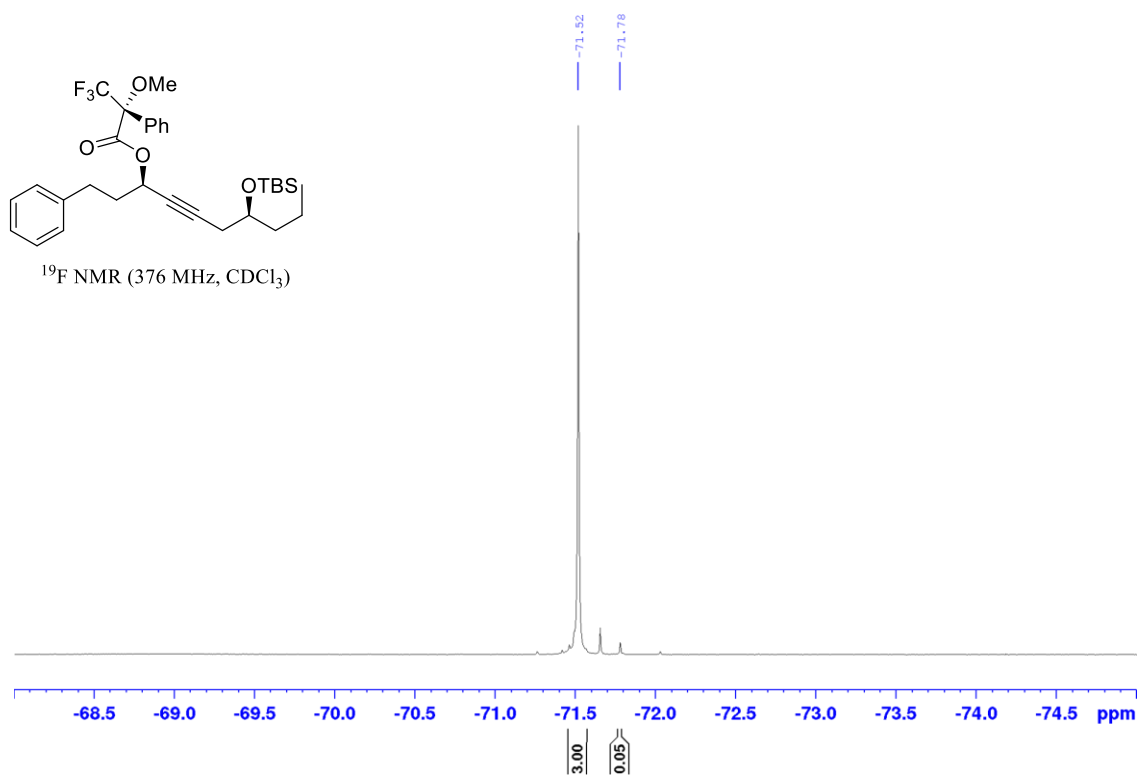
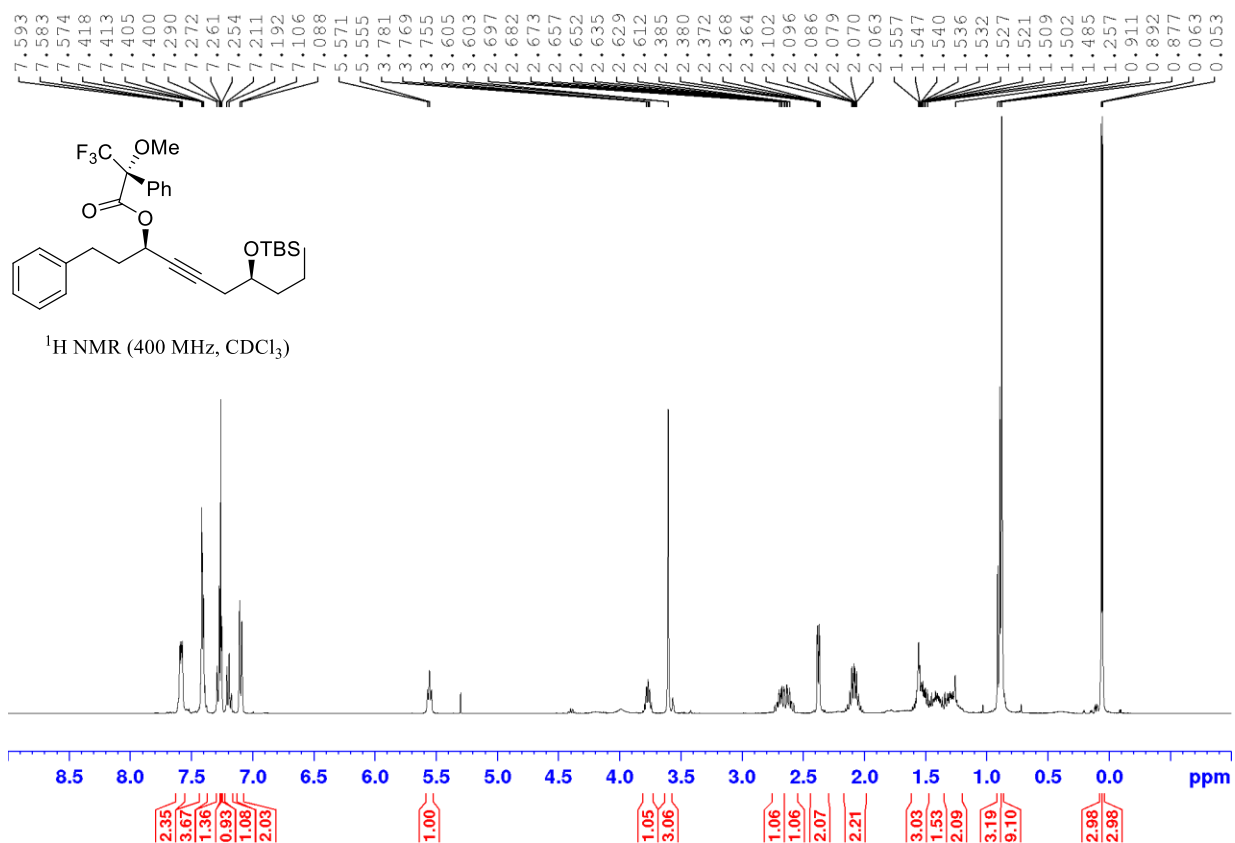


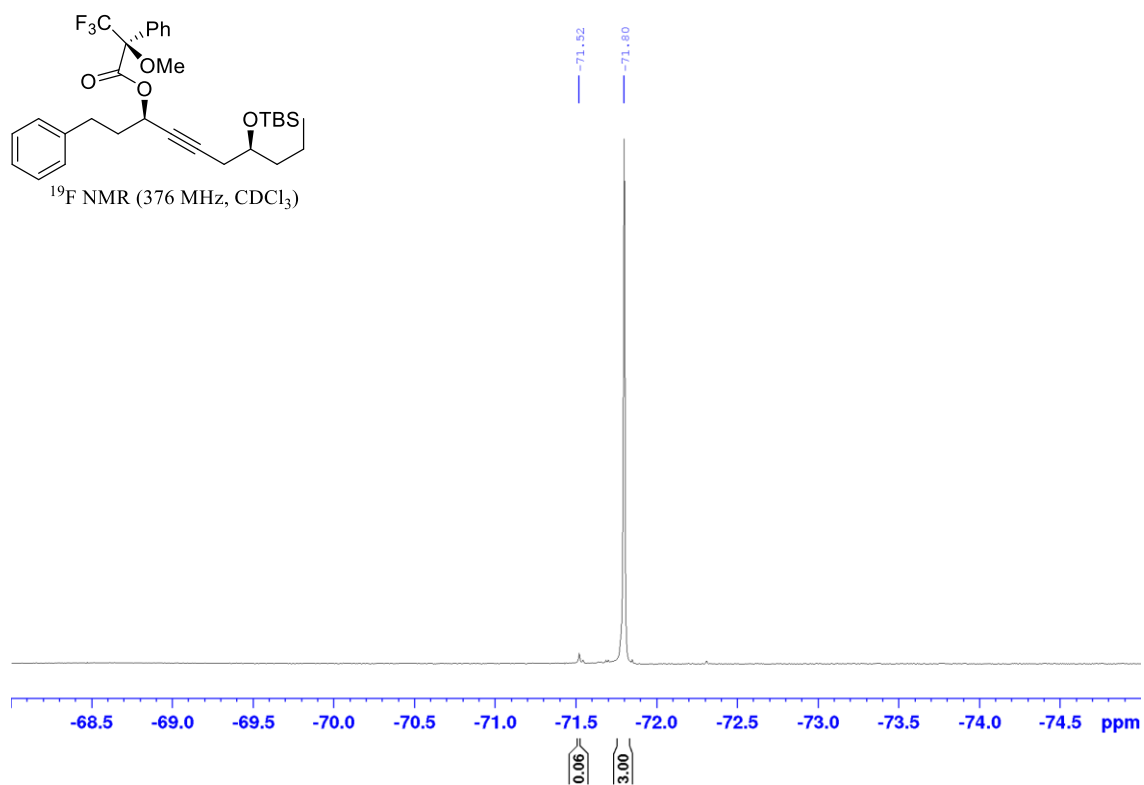
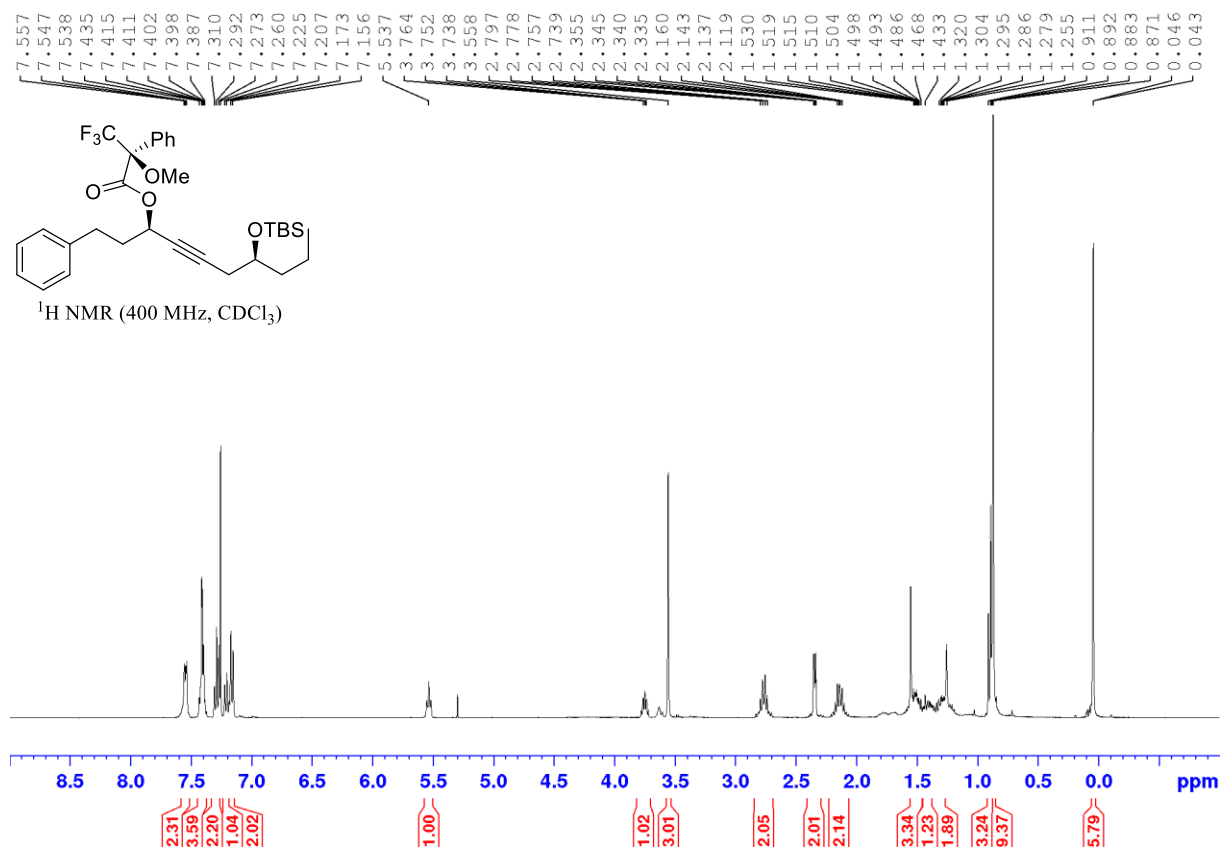


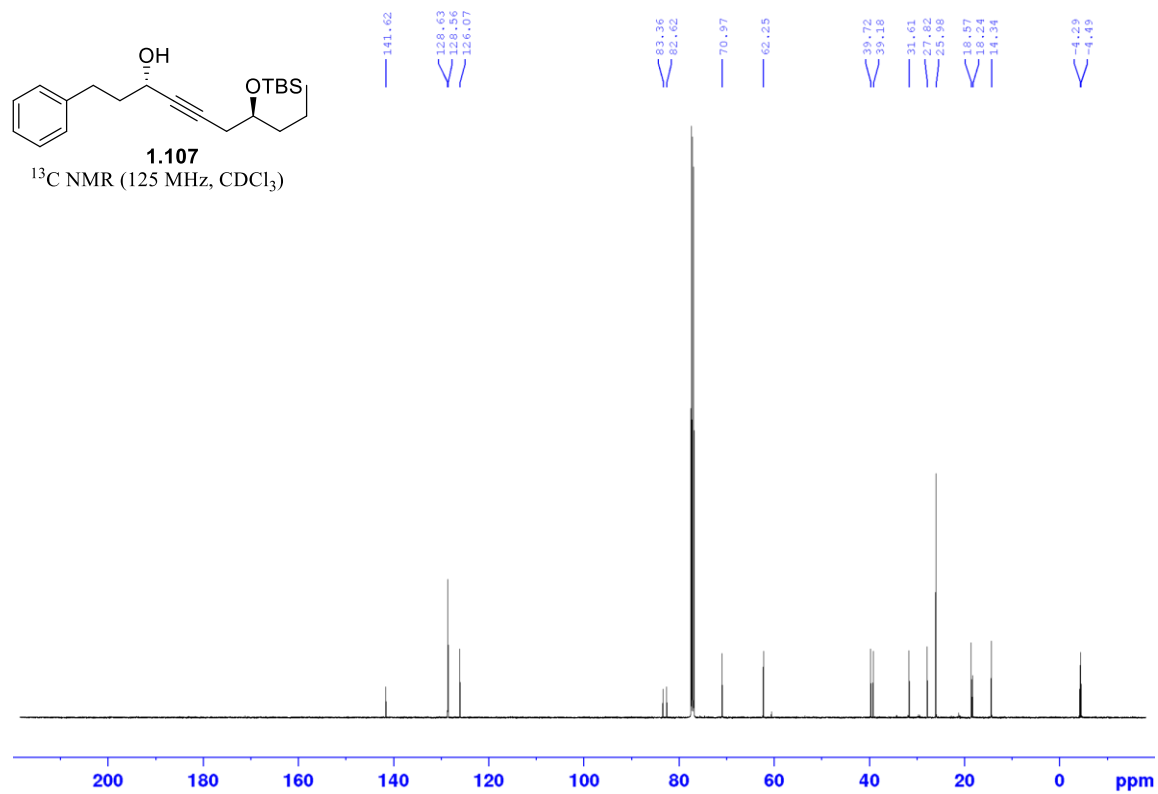
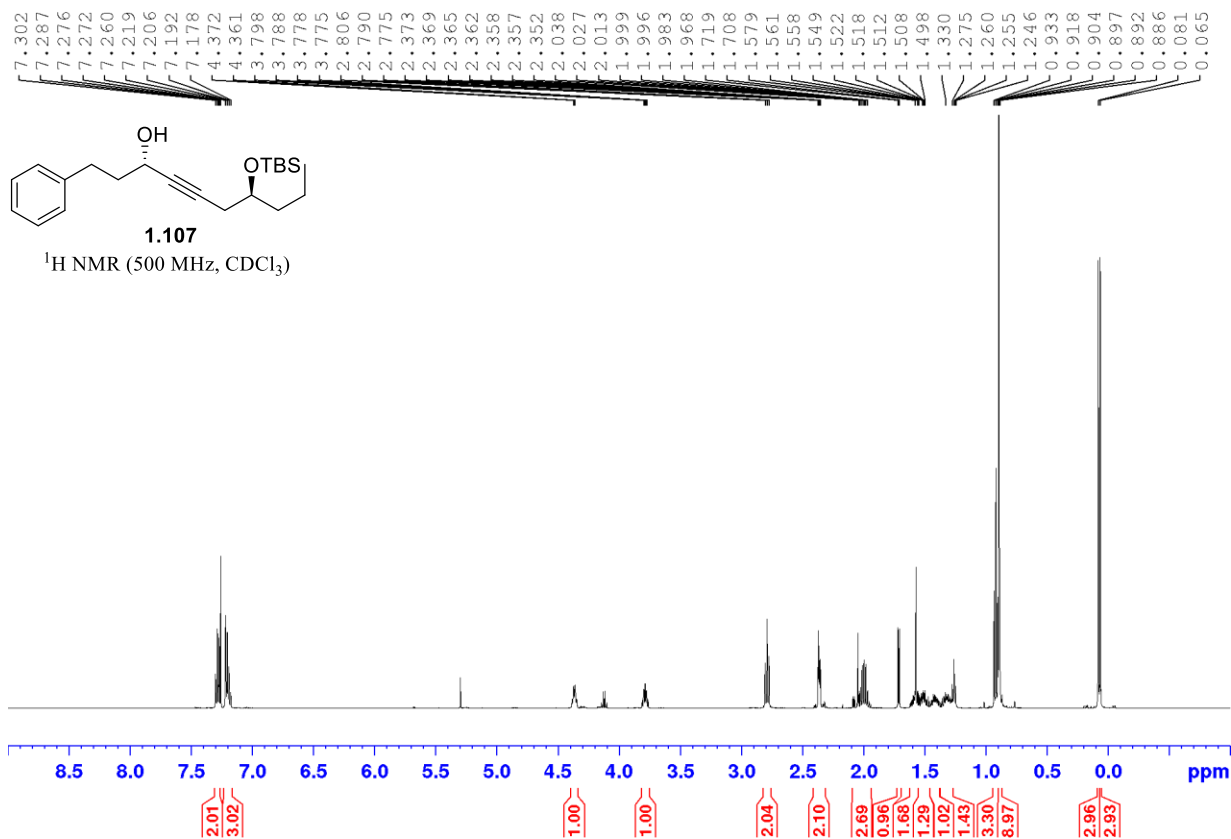


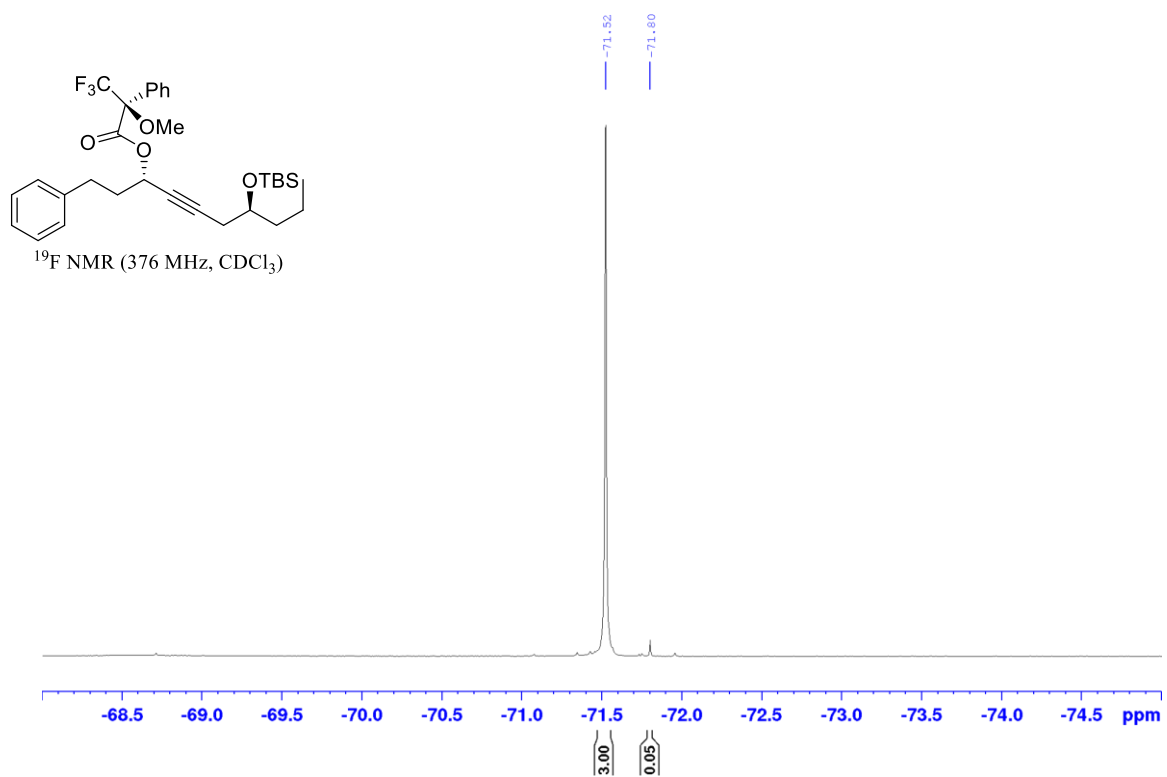
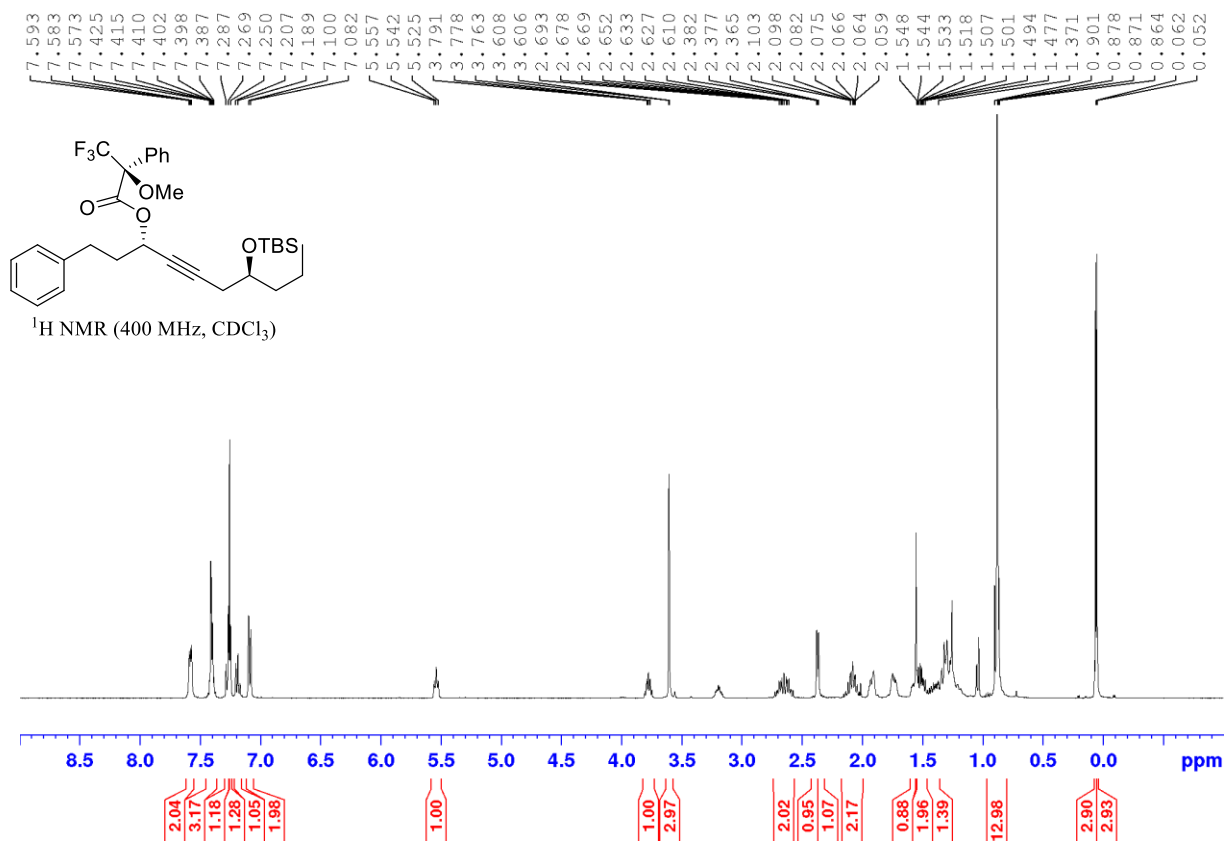


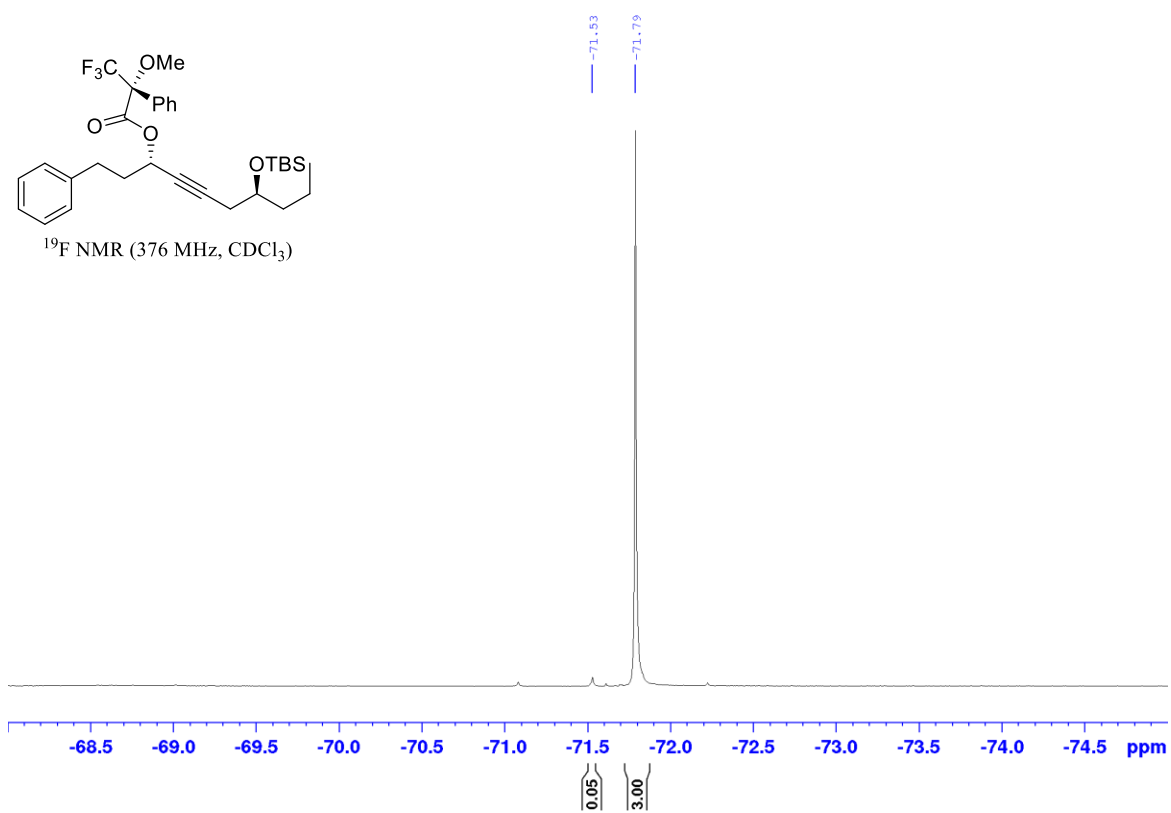
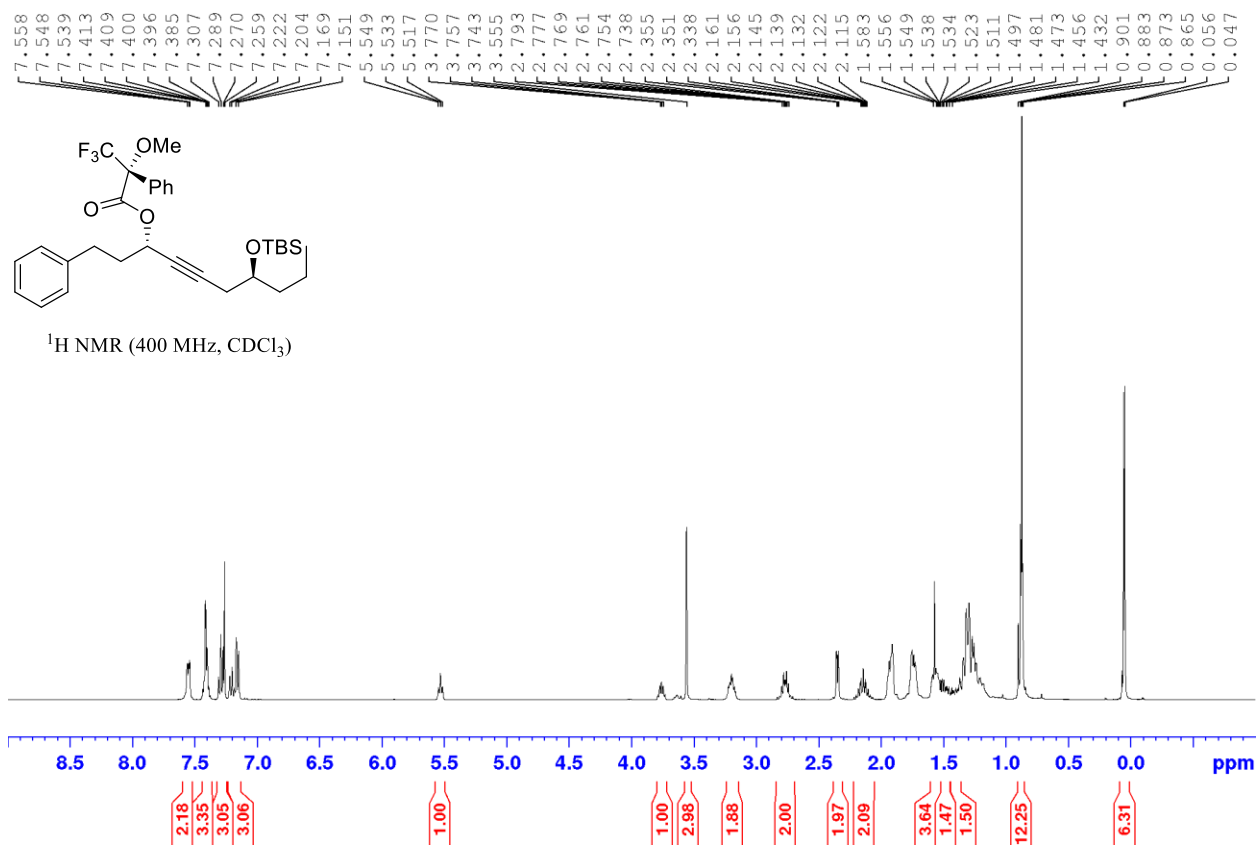


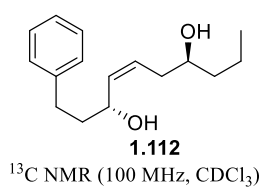
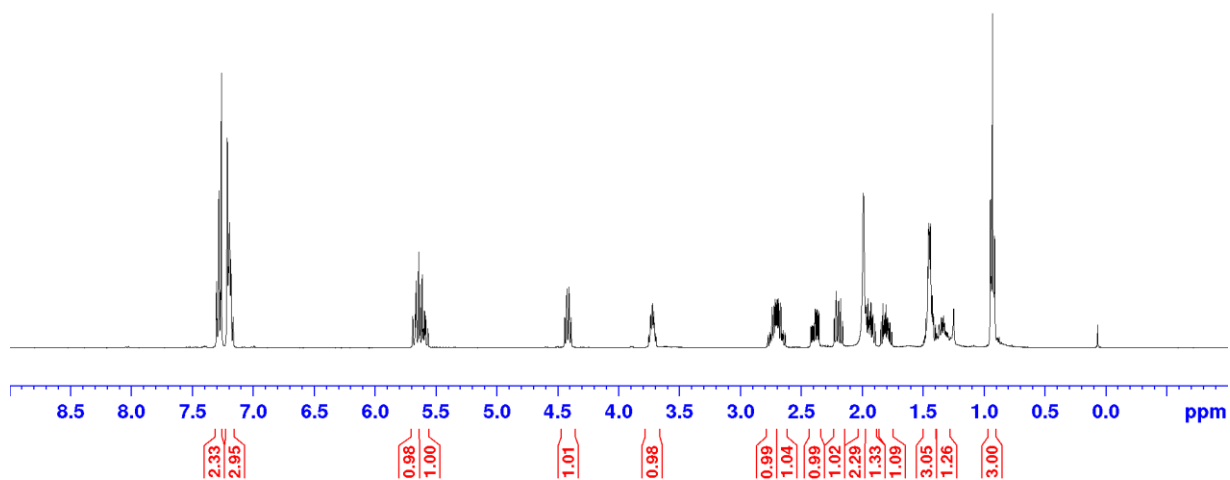
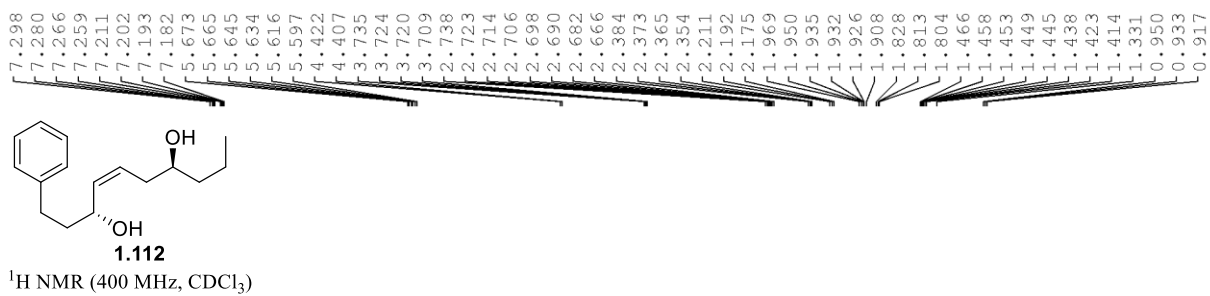


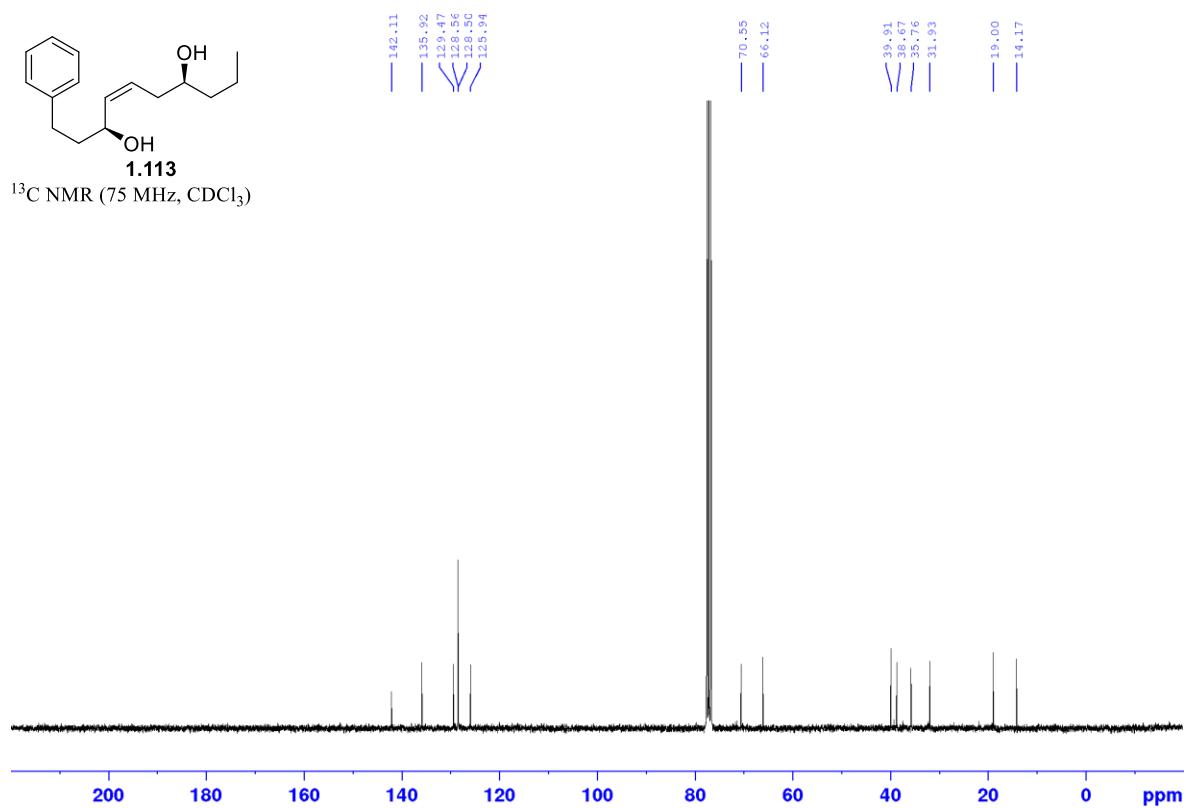
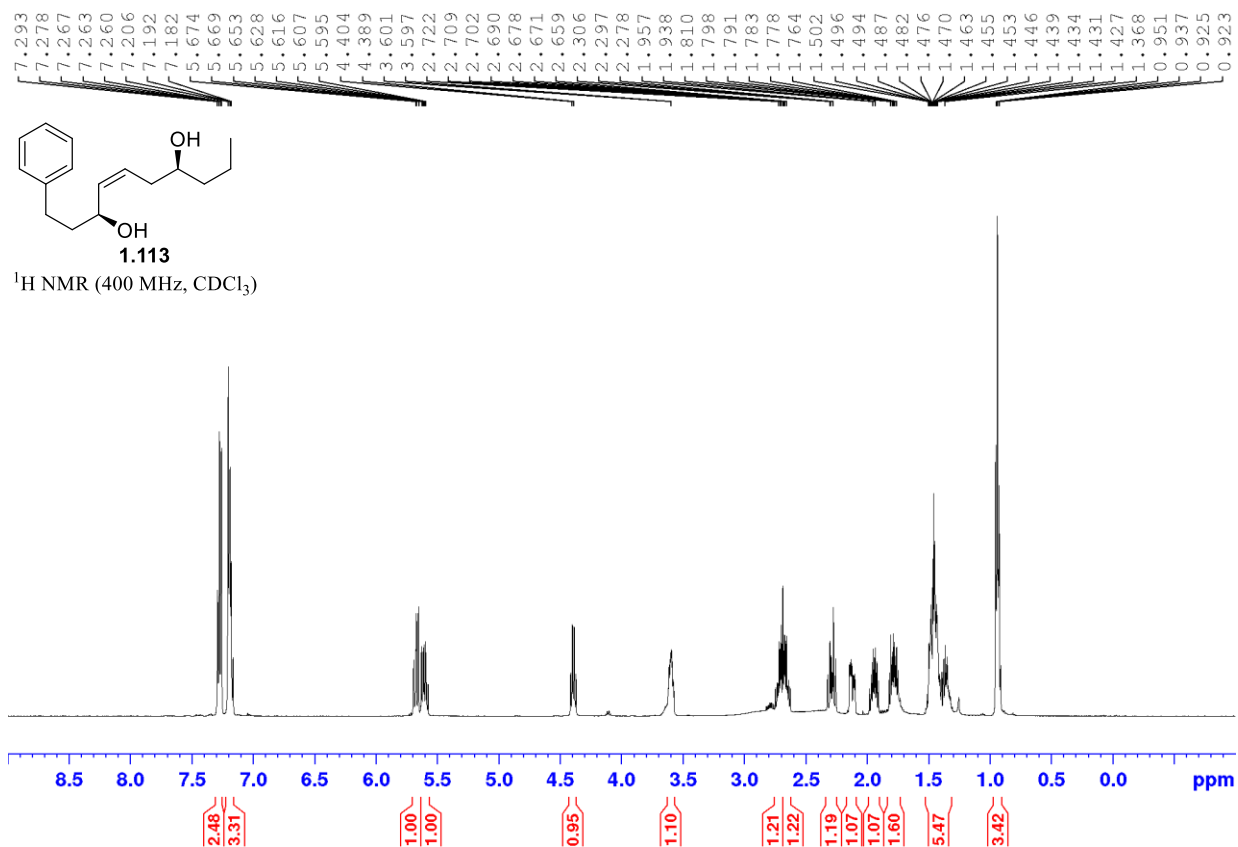


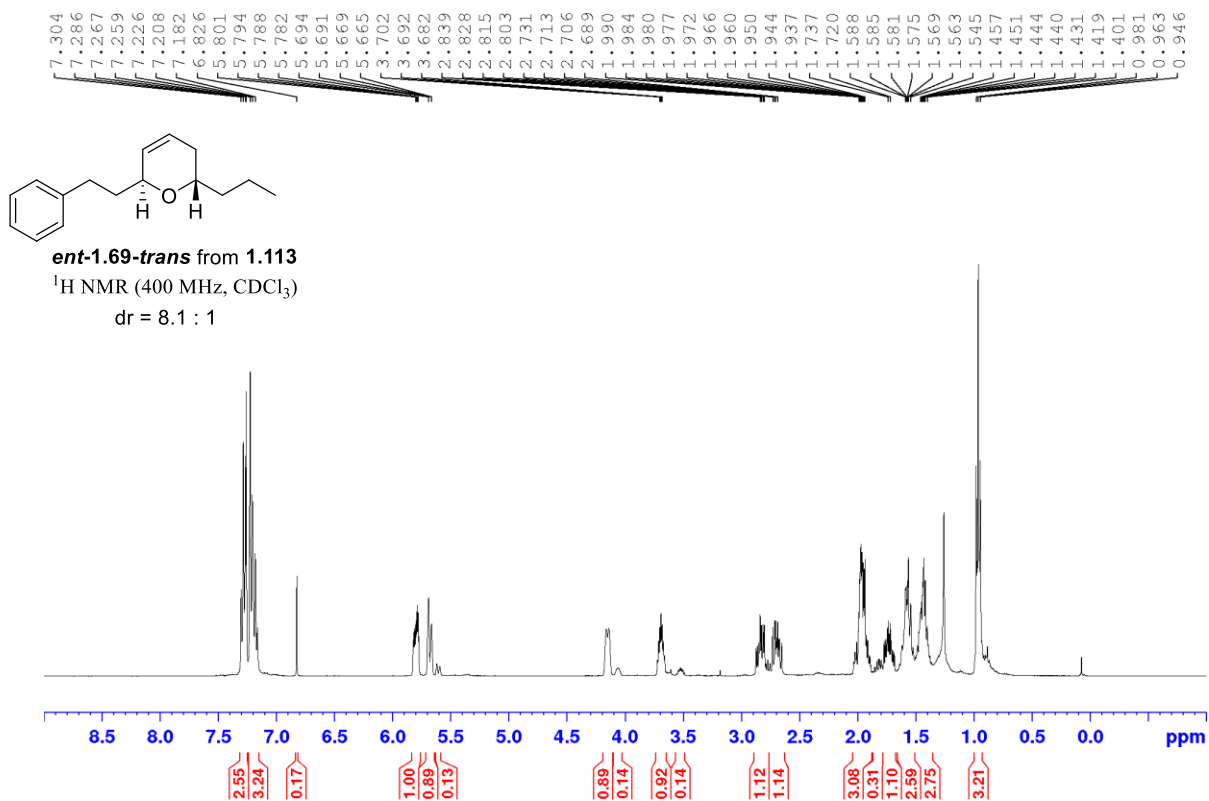
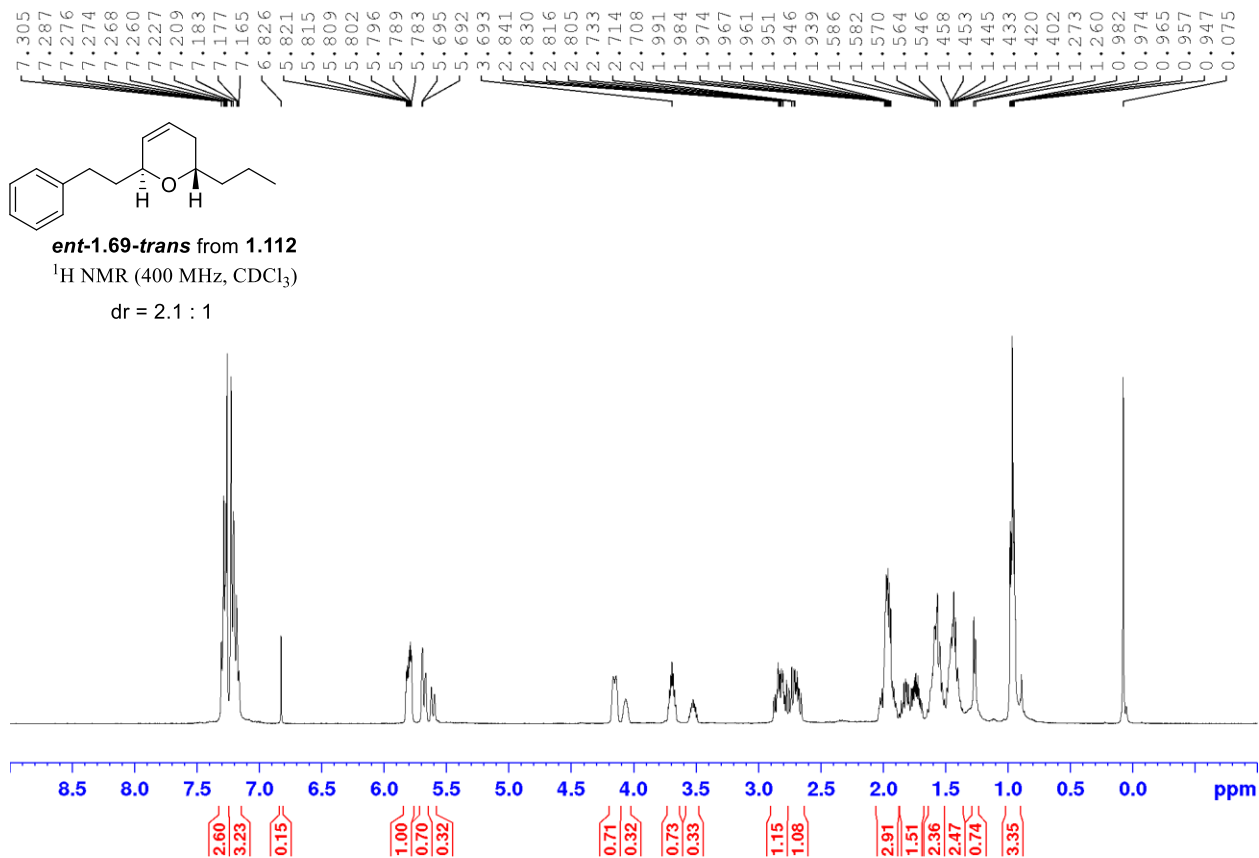




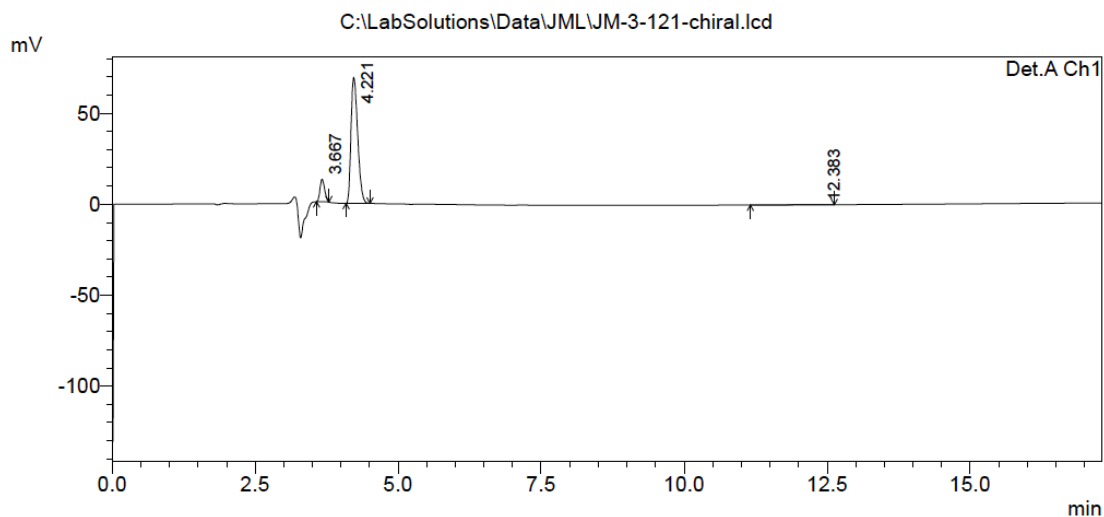








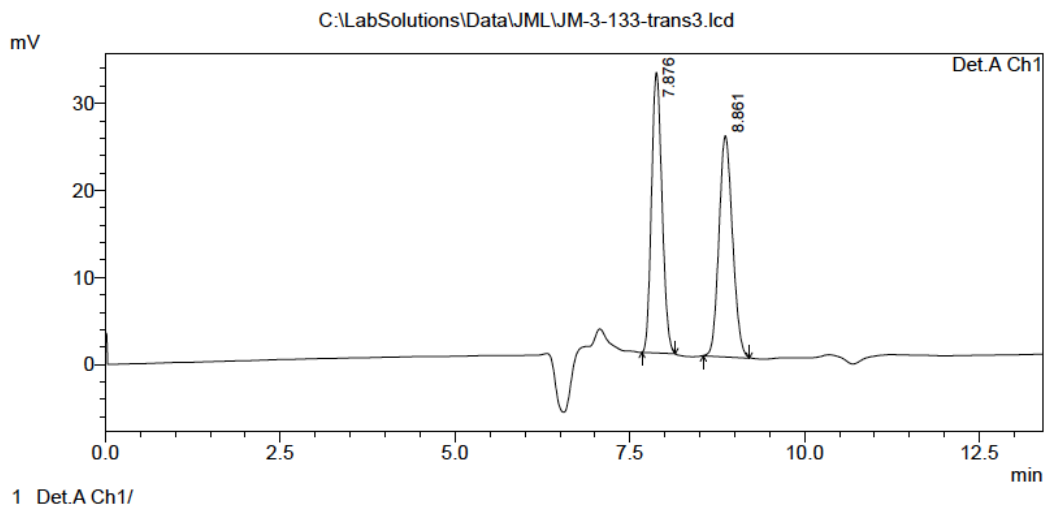
HPLC of the cyclization of 1.113 to *ent*-1.69 to determine diastereoselectivity.



PeakTable

Peak#	Ret. Time	Area	Height	Area %	Height %
1	3.667	69397	12296	10.935	15.063
2	4.221	562862	69290	88.692	84.884
3	12.383	2368	43	0.373	0.052
Total		634627	81629	100.000	100.000

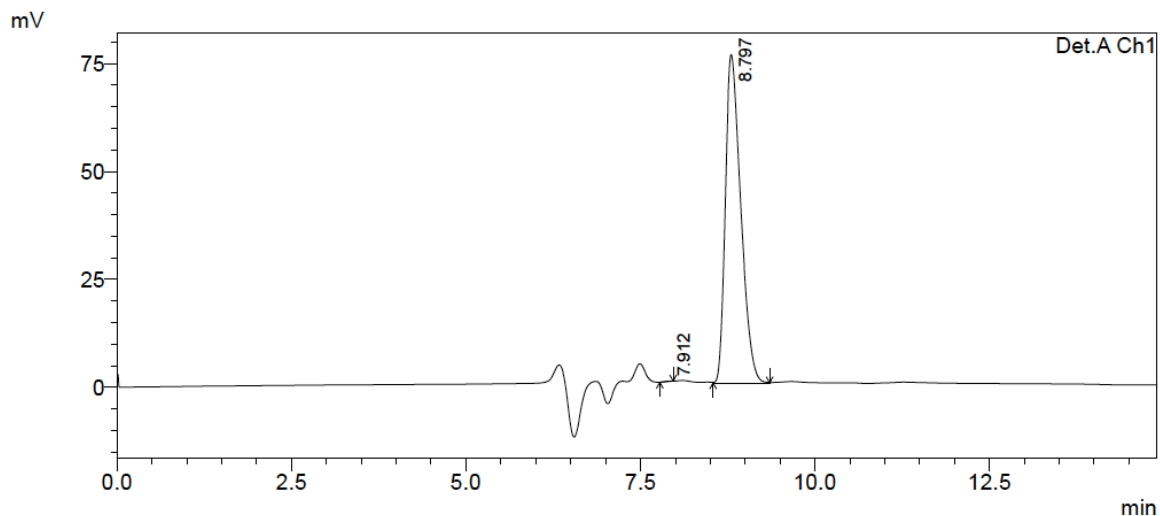
HPLC of racemic 1.69-*trans*.



PeakTable

Peak#	Ret. Time	Area	Height	Area %	Height %
1	7.876	337121	32242	49.465	55.909
2	8.861	344414	25426	50.535	44.091
Total		681535	57668	100.000	100.000

HPLC of *ent*-1.69-*trans* from 1.113 to determine enantiopurity.



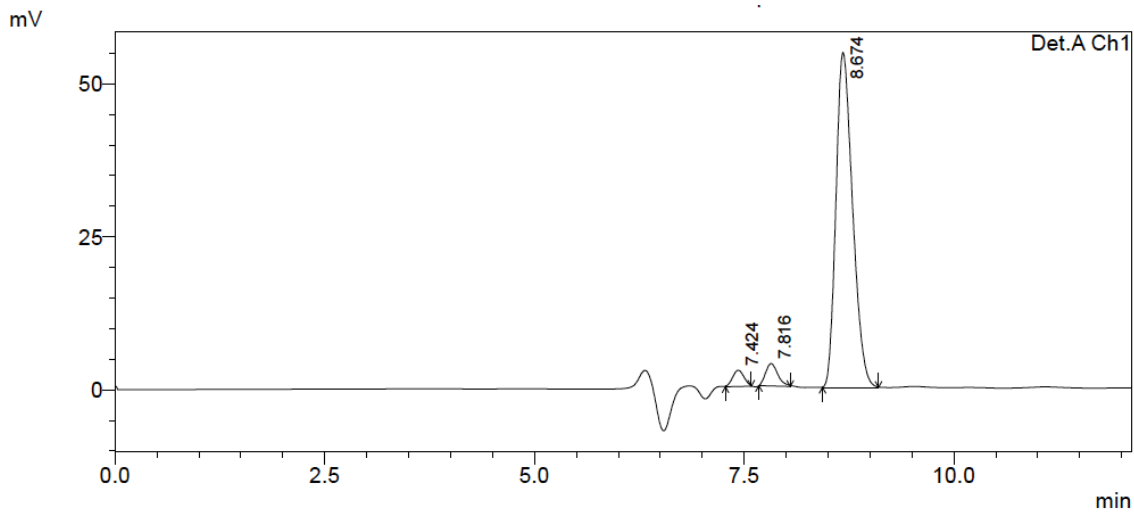
1 Det.A Ch1/

PeakTable

Detector A Ch1

Peak#	Ret. Time	Area	Height	Area %	Height %
1	7.912	1116	133	0.095	0.175
2	8.797	1170479	76115	99.905	99.825
Total		1171595	76248	100.000	100.000

HPLC of *ent*-1.69-*trans* from 1.113, spiked with the enantiomer of 1.69-*trans*.

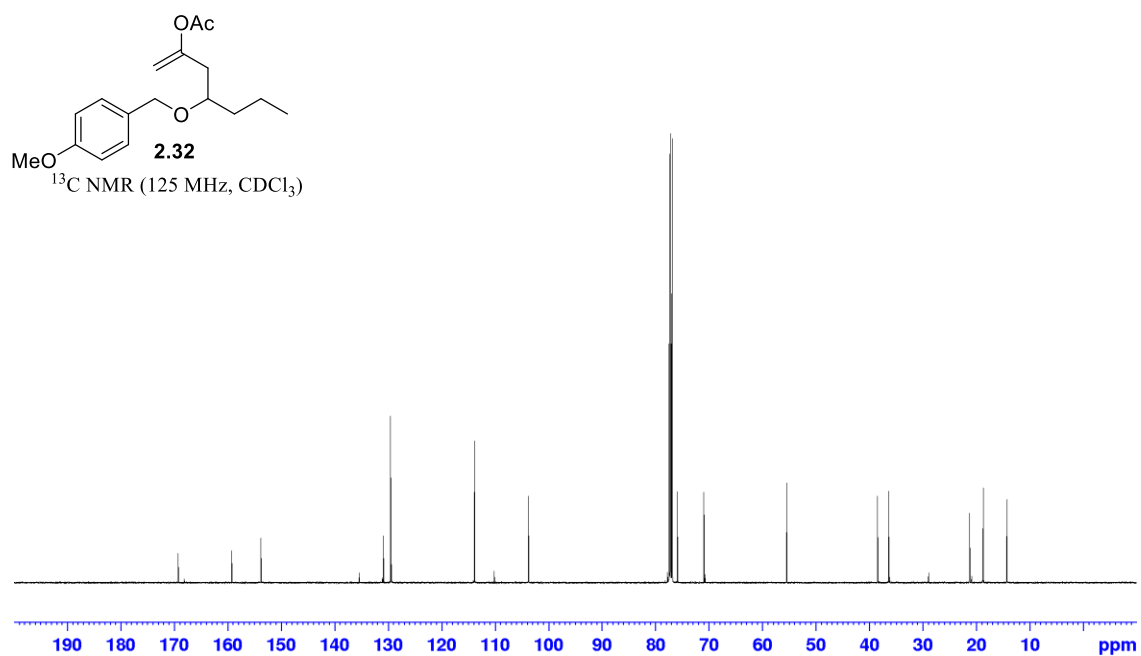
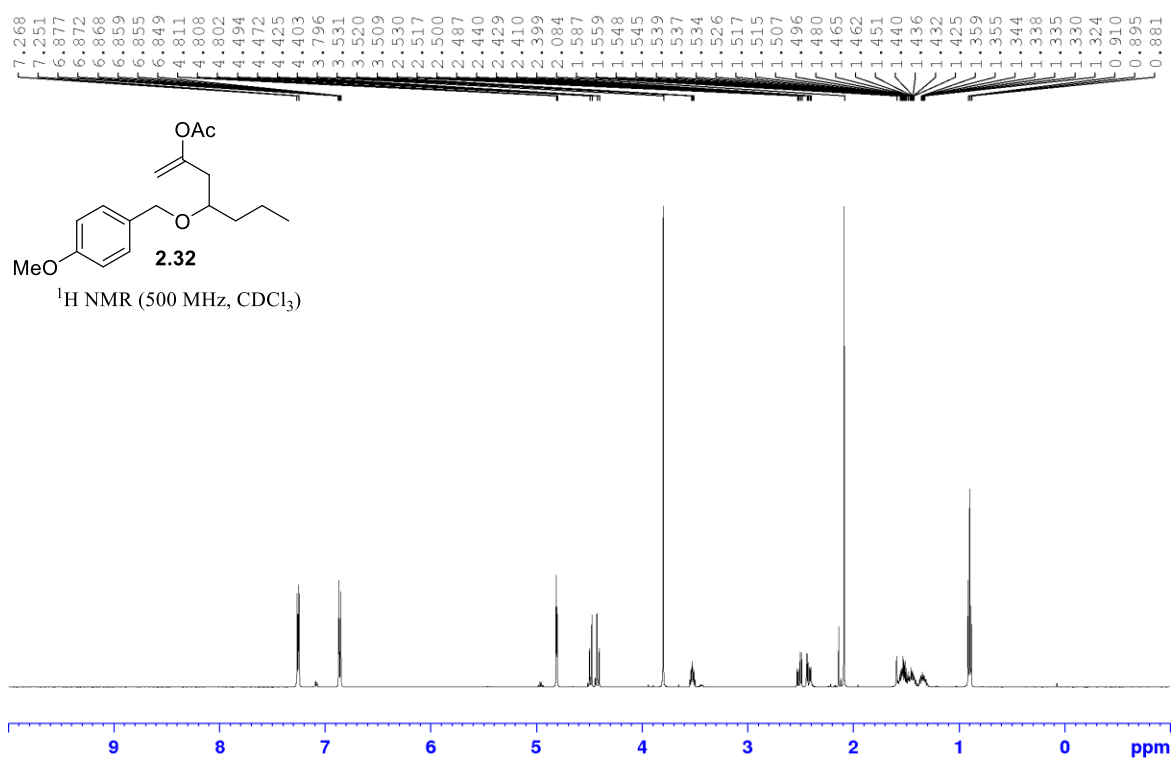


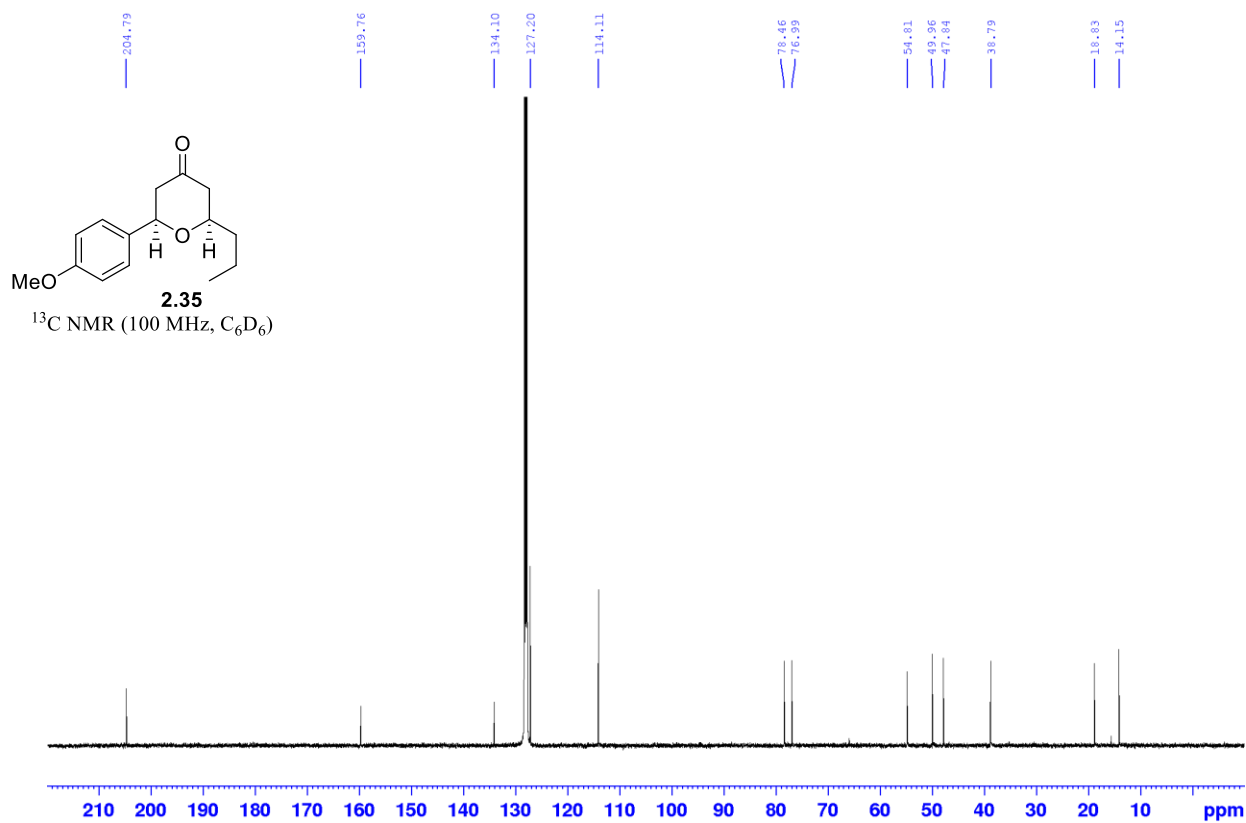
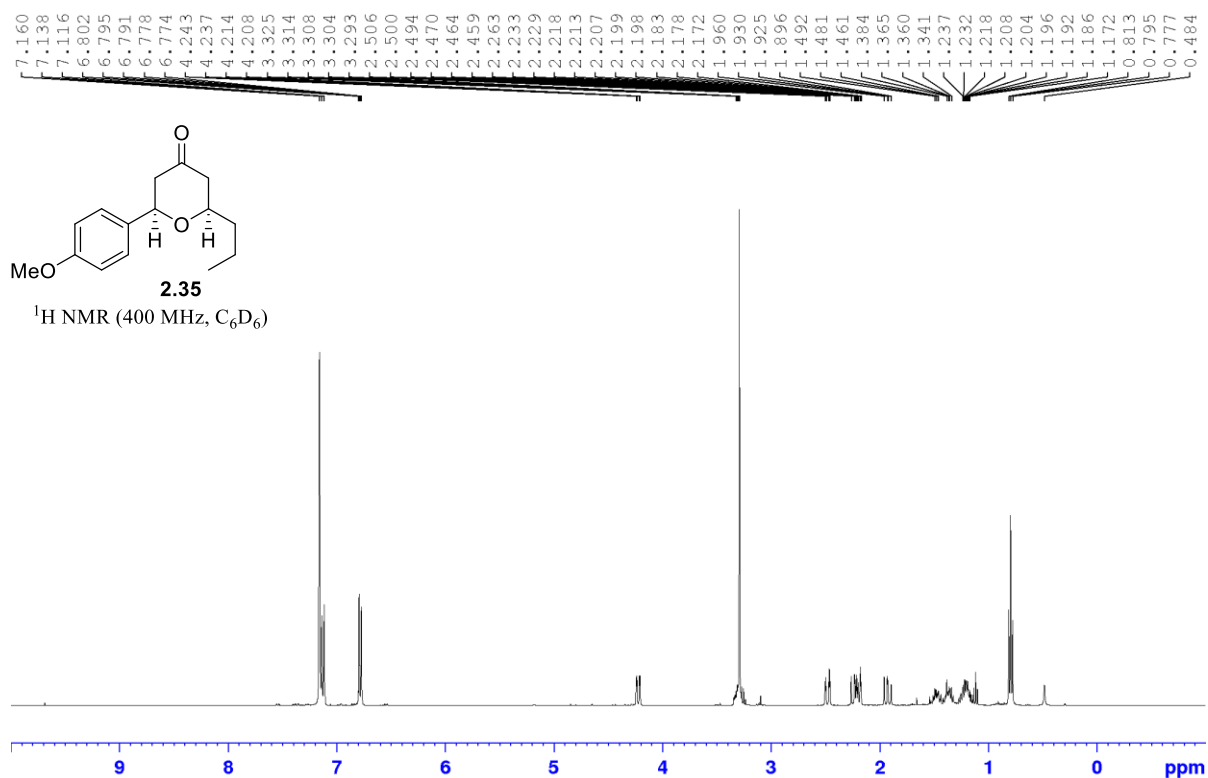
1 Det.A Ch1/

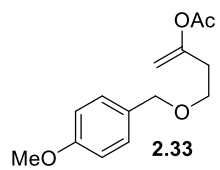
PeakTable

Detector A Ch1

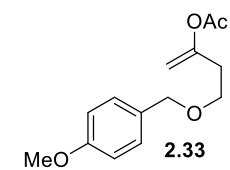
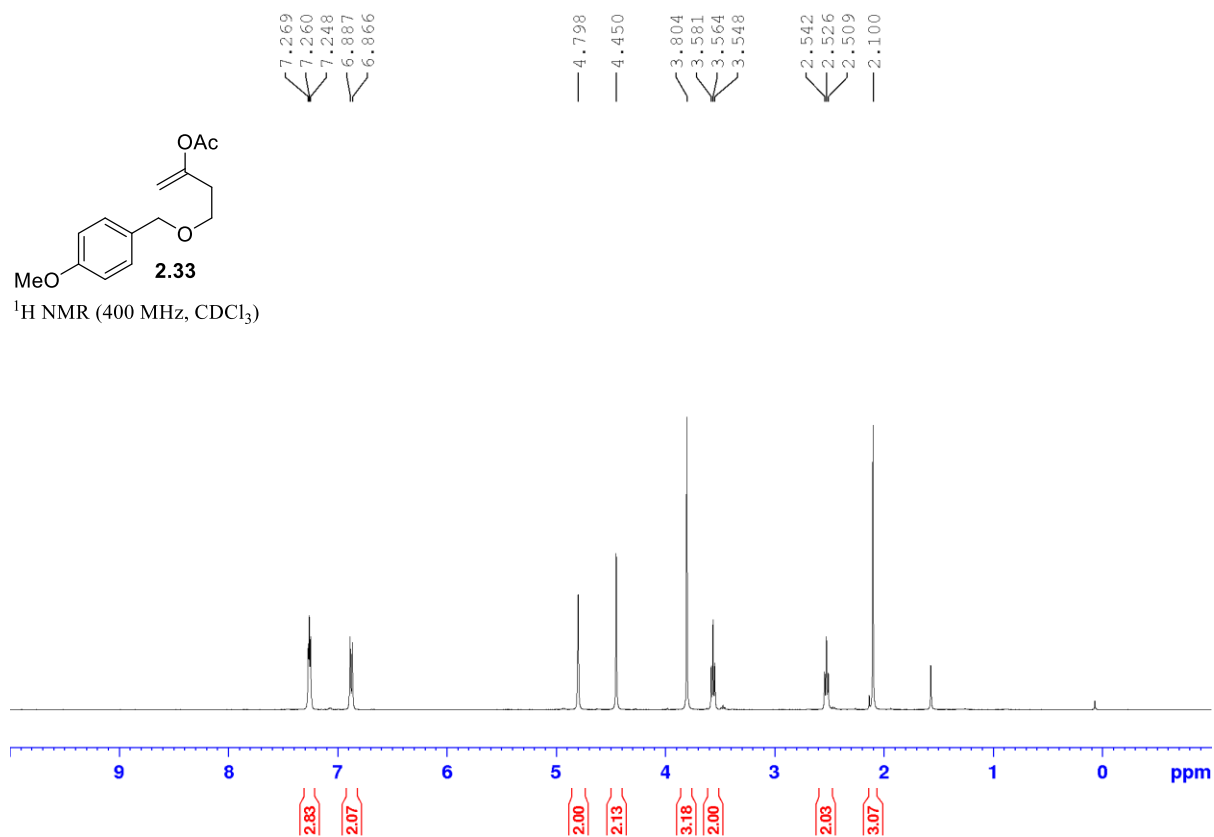
Peak#	Ret. Time	Area	Height	Area %	Height %
1	7.424	24671	2643	3.019	4.330
2	7.816	37269	3658	4.561	5.991
3	8.674	755142	54753	92.419	89.680
Total		817081	61054	100.000	100.000



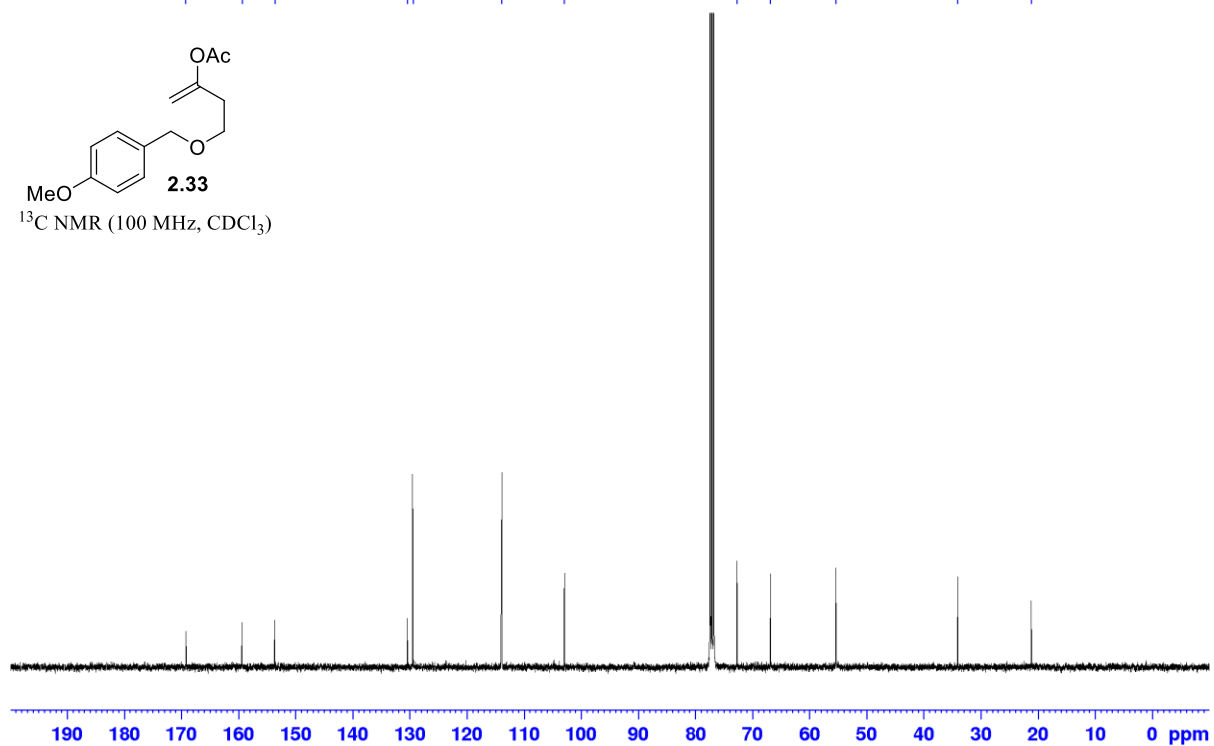


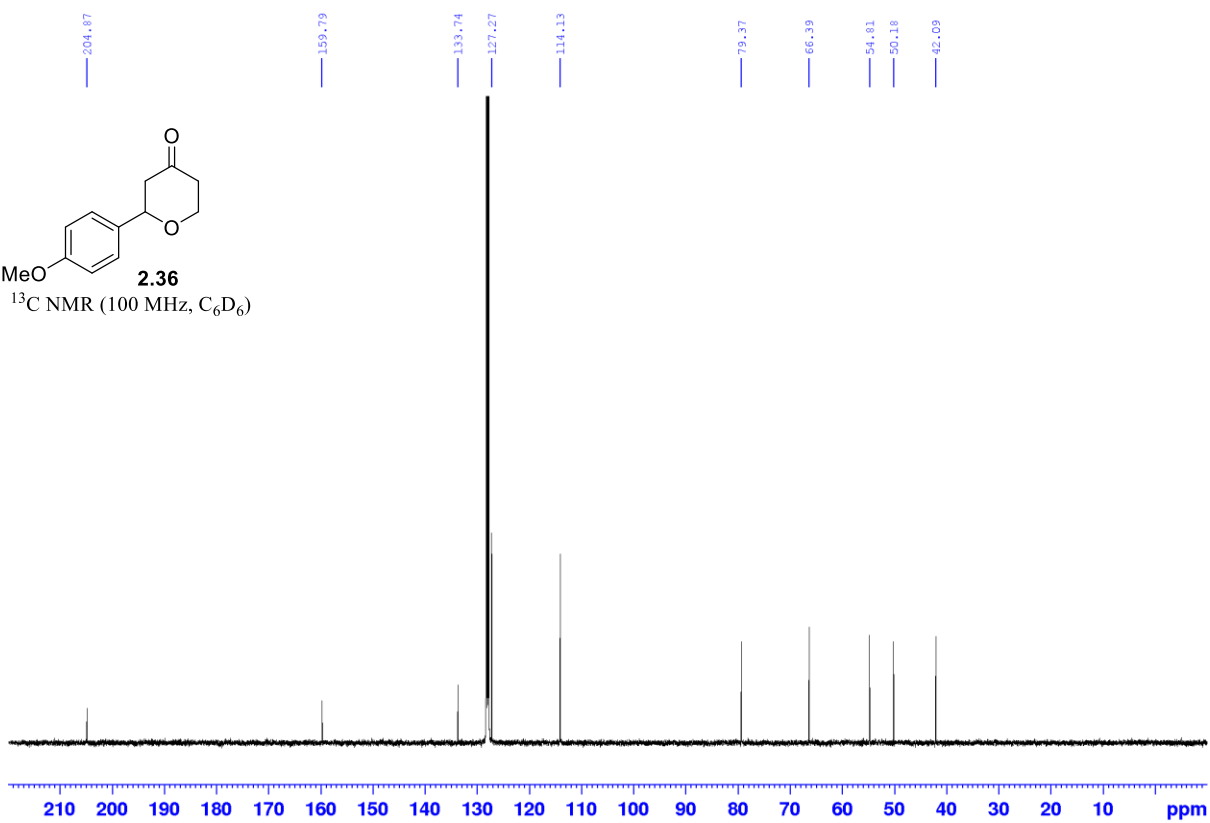
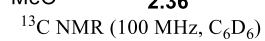
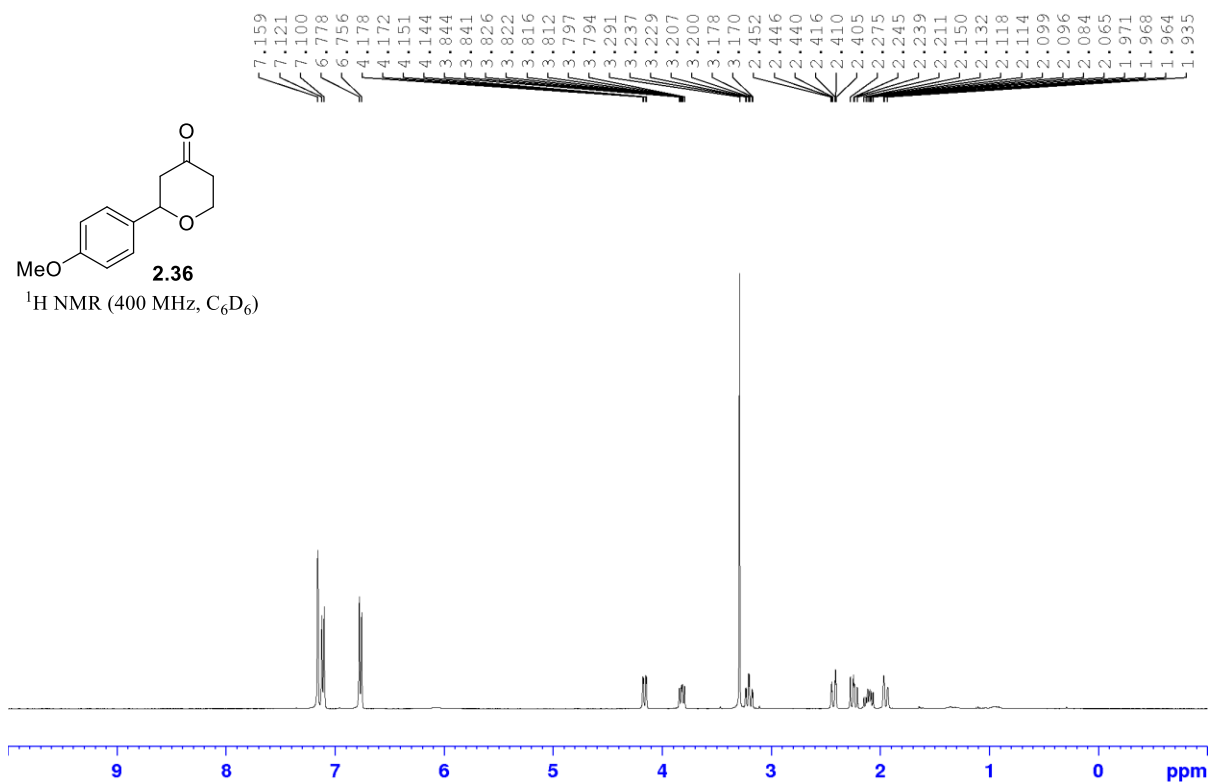
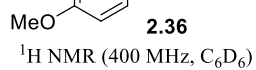


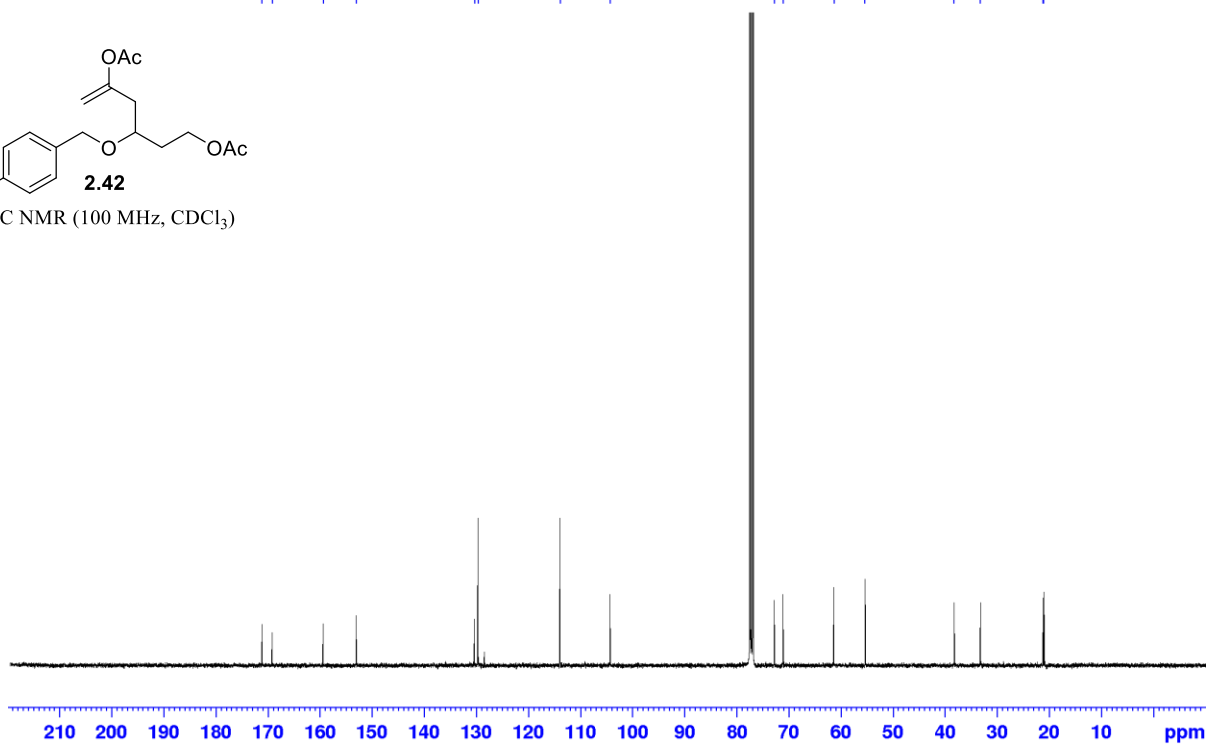
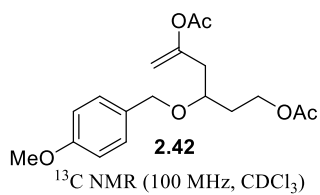
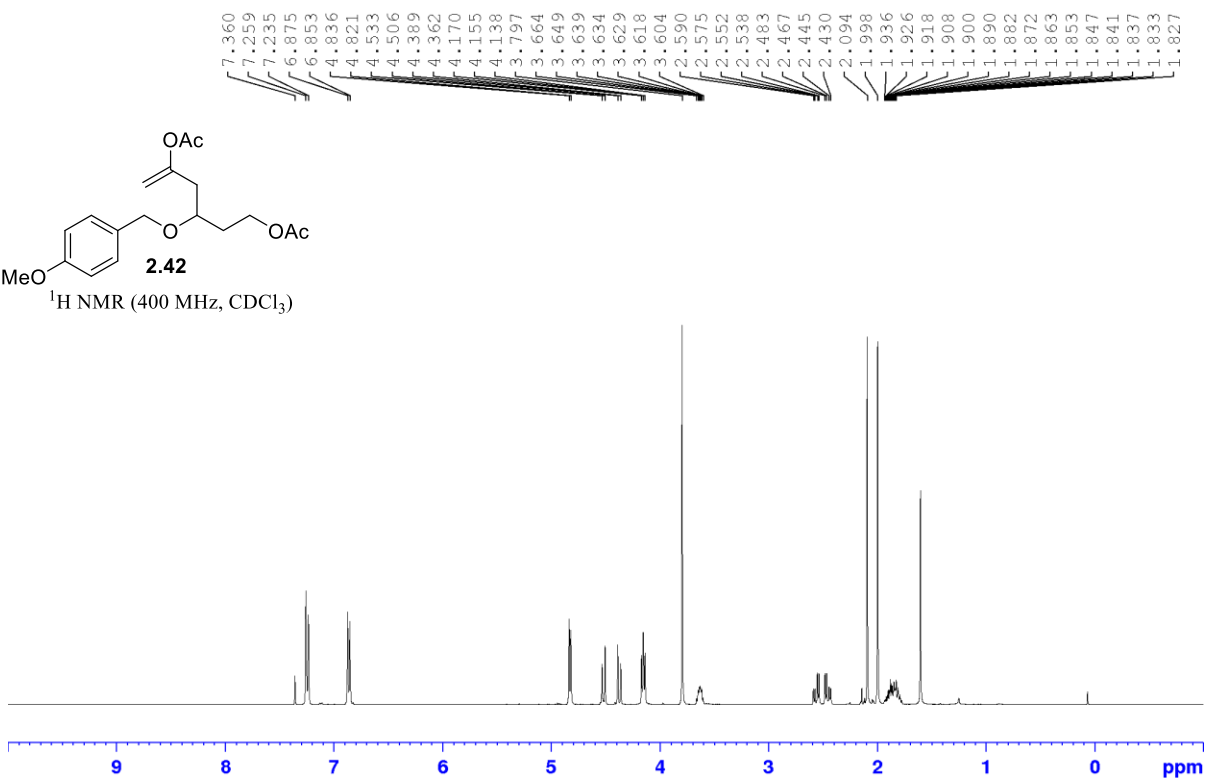
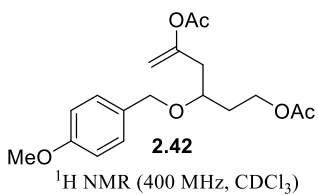
^1H NMR (400 MHz, CDCl_3)

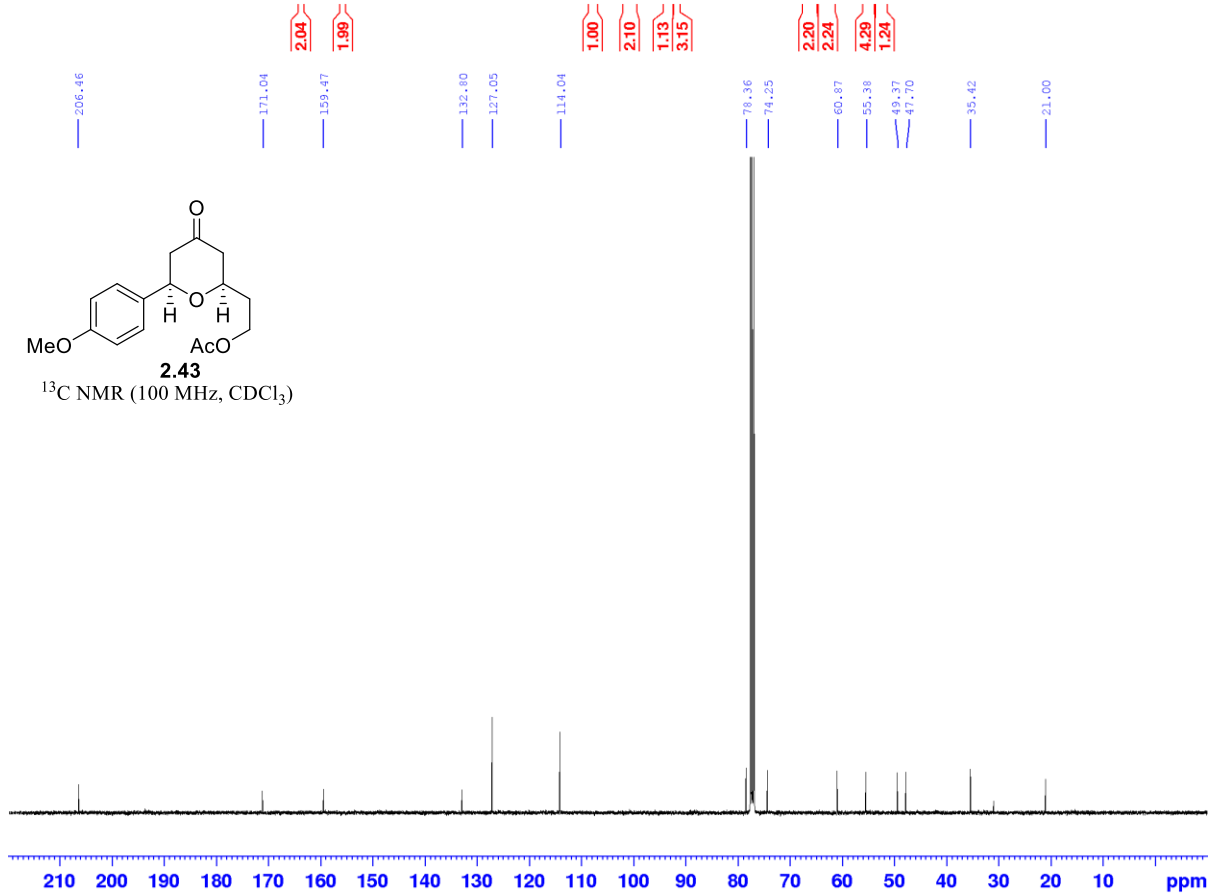
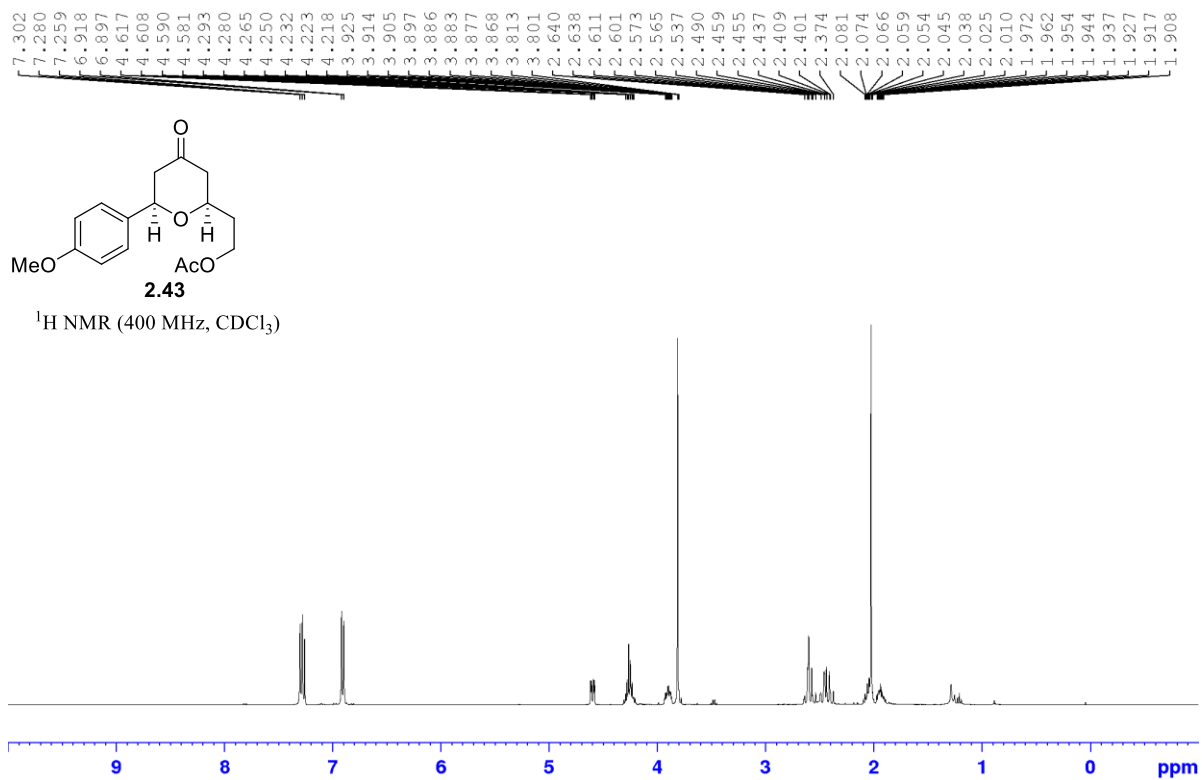


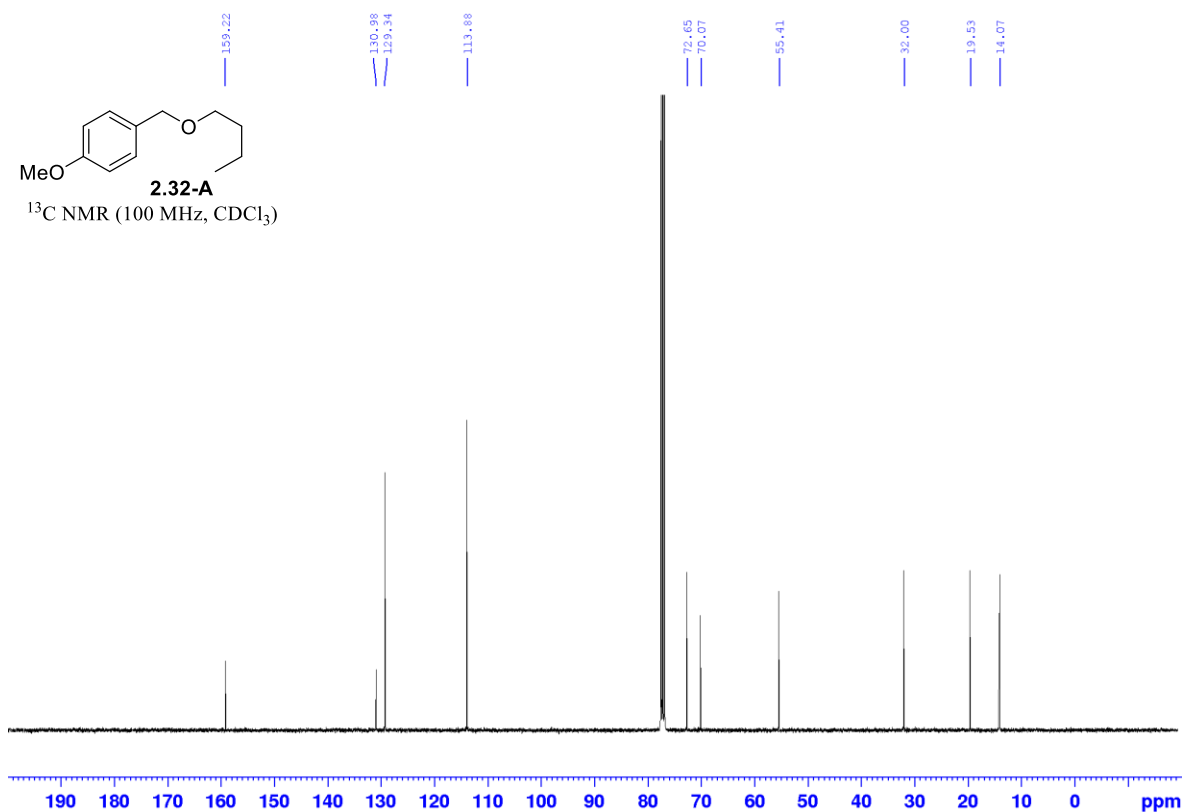
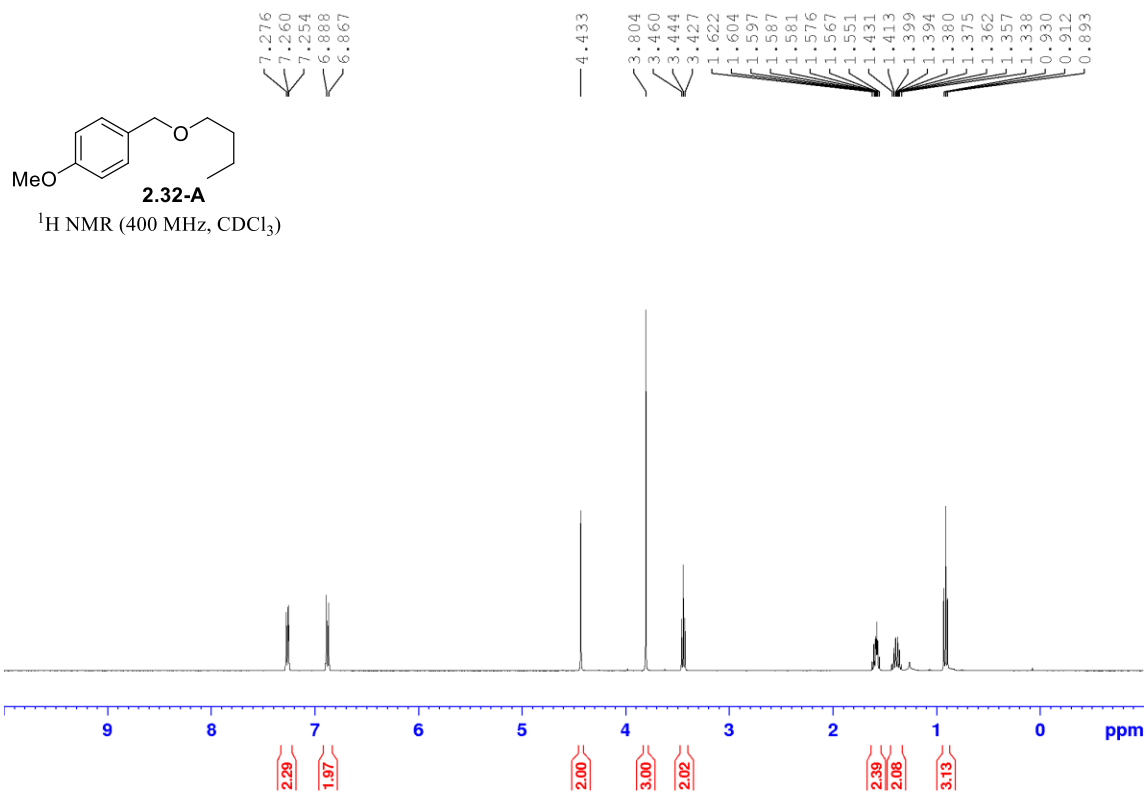
^{13}C NMR (100 MHz, CDCl_3)

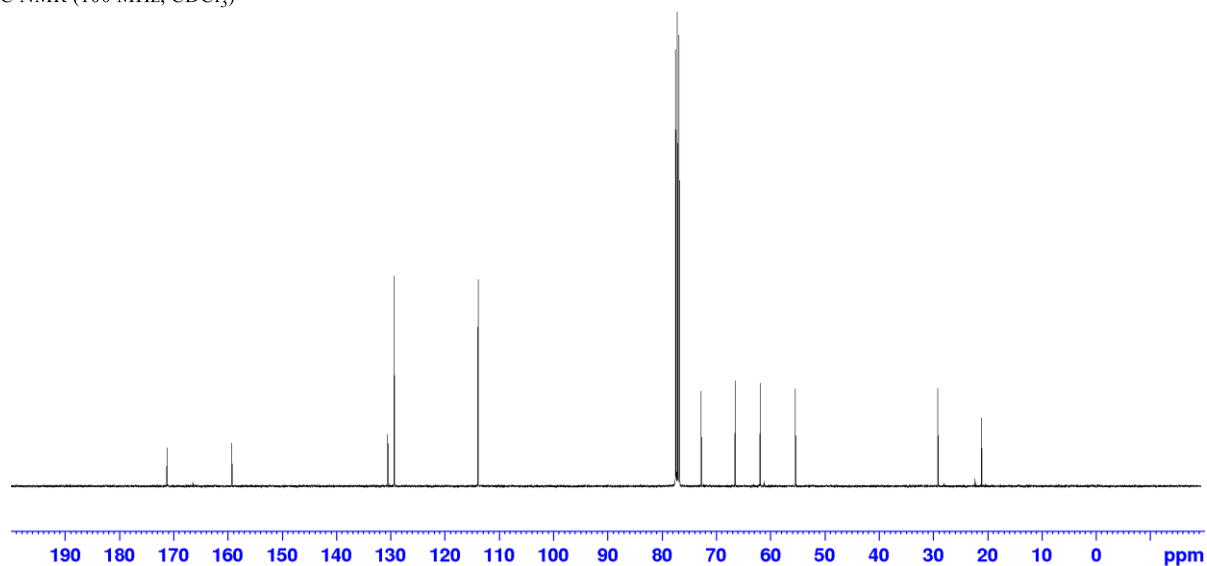
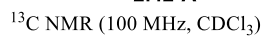
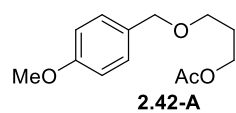
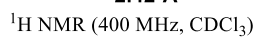


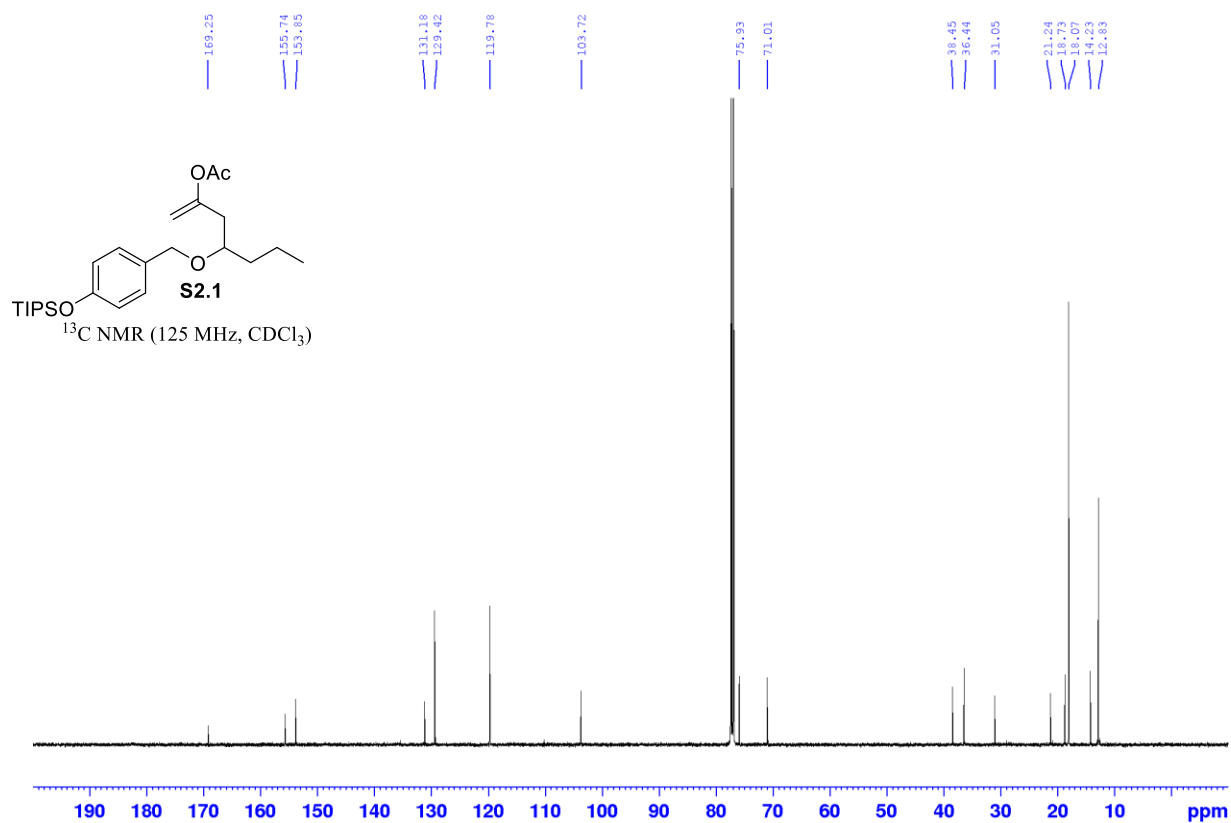
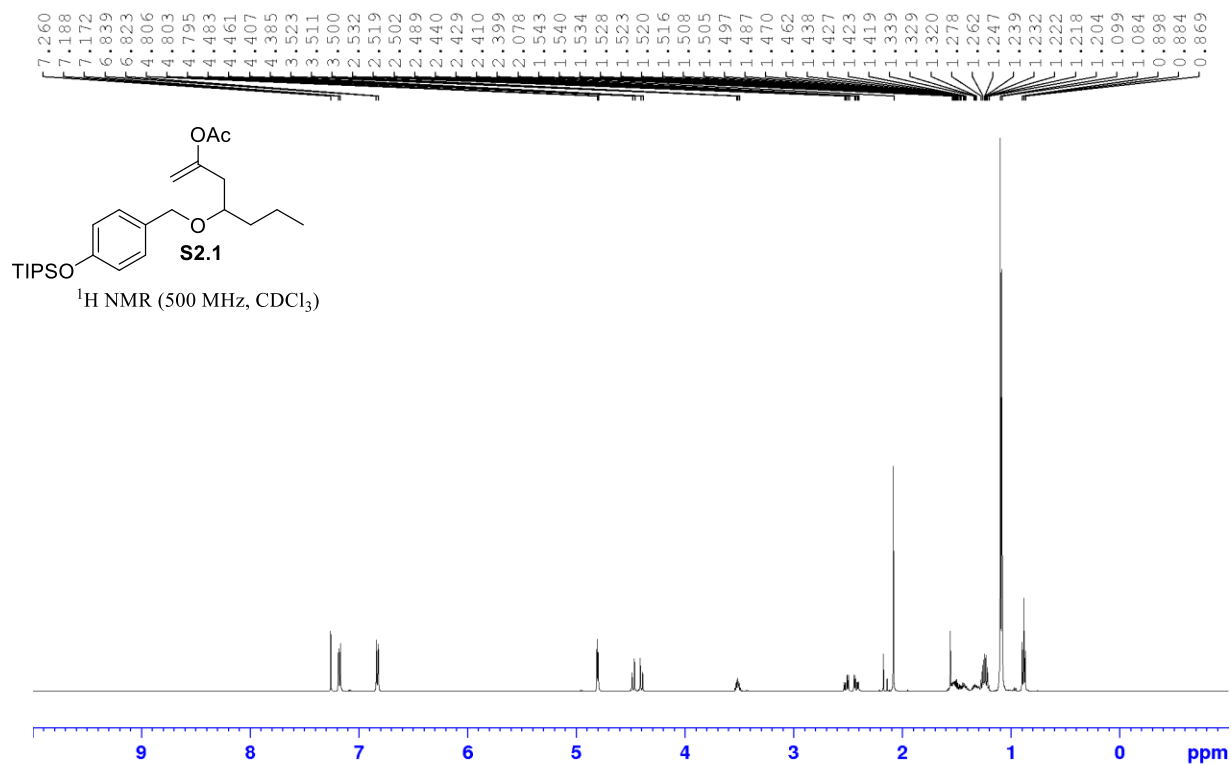


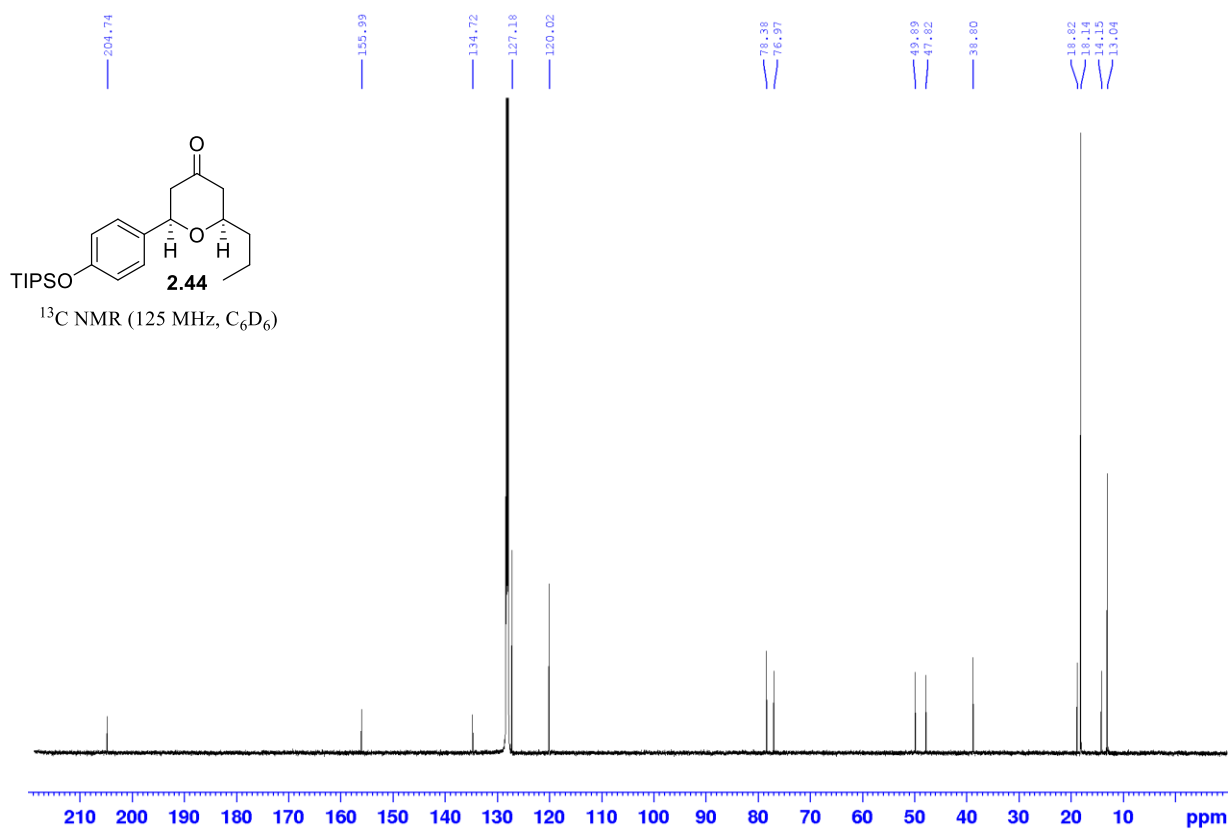
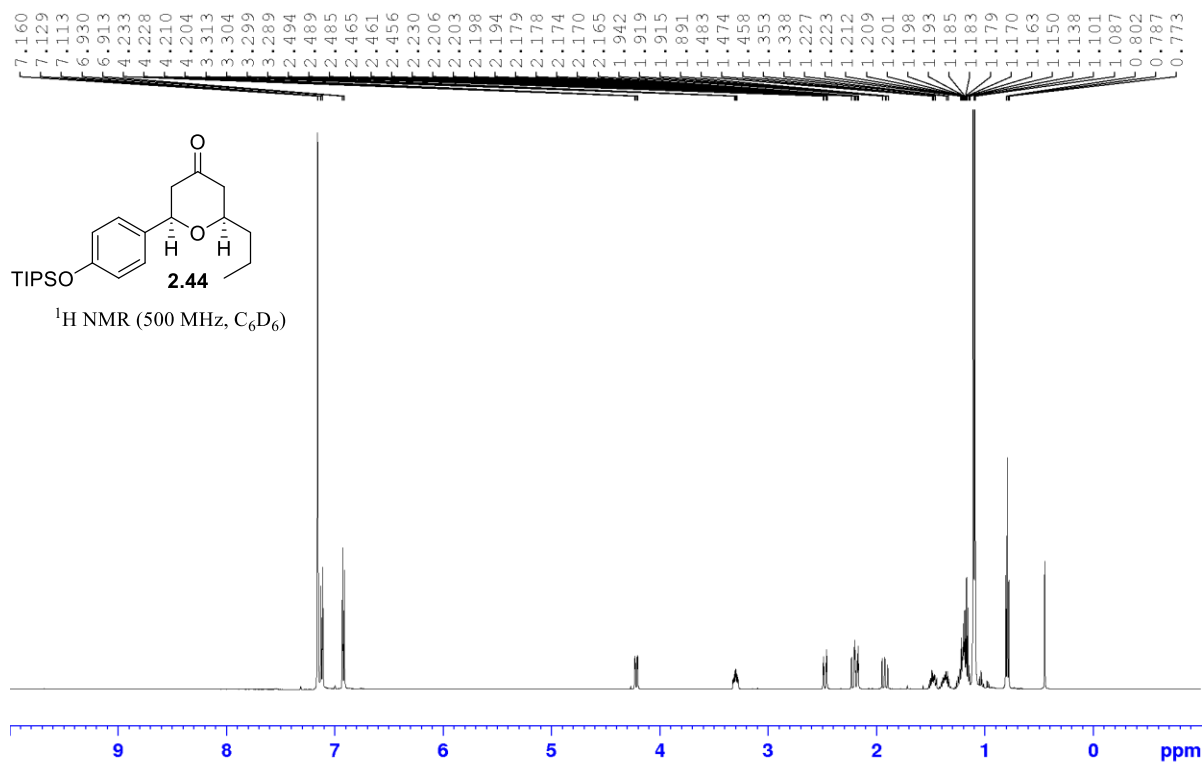


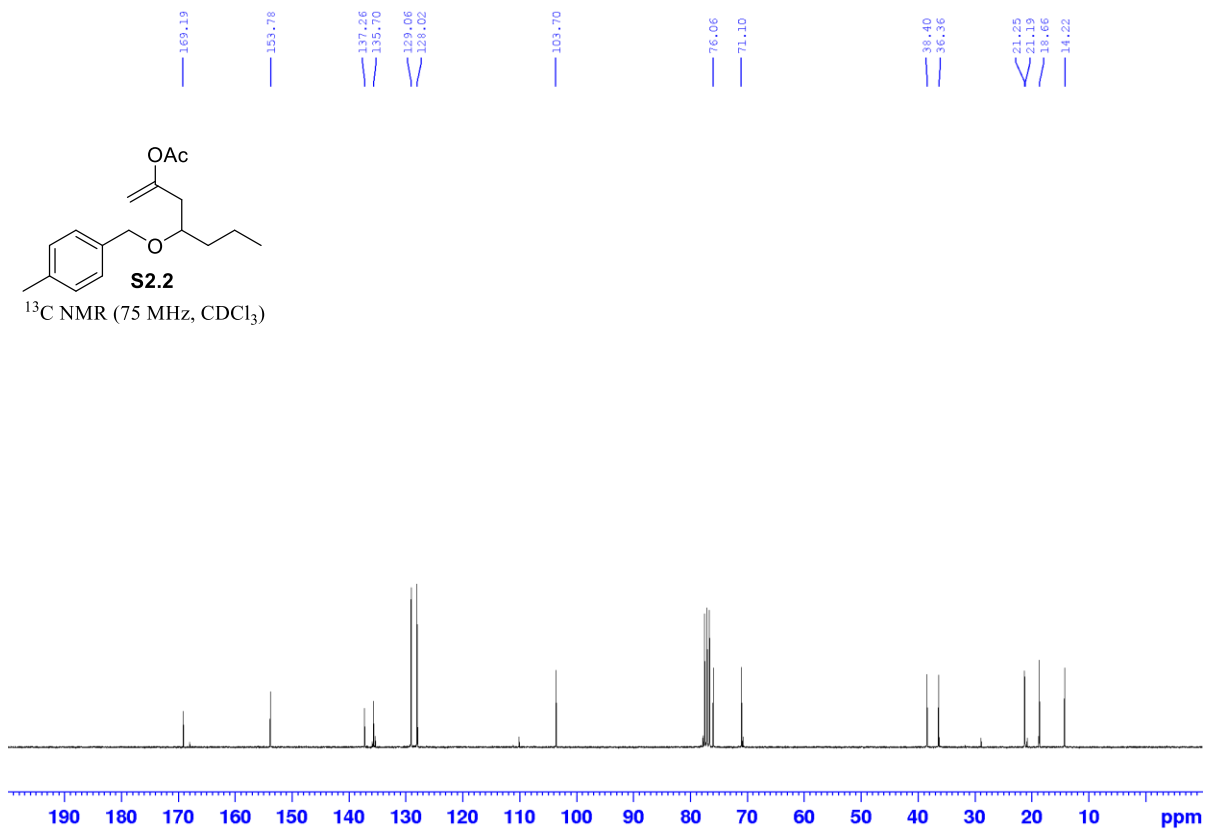
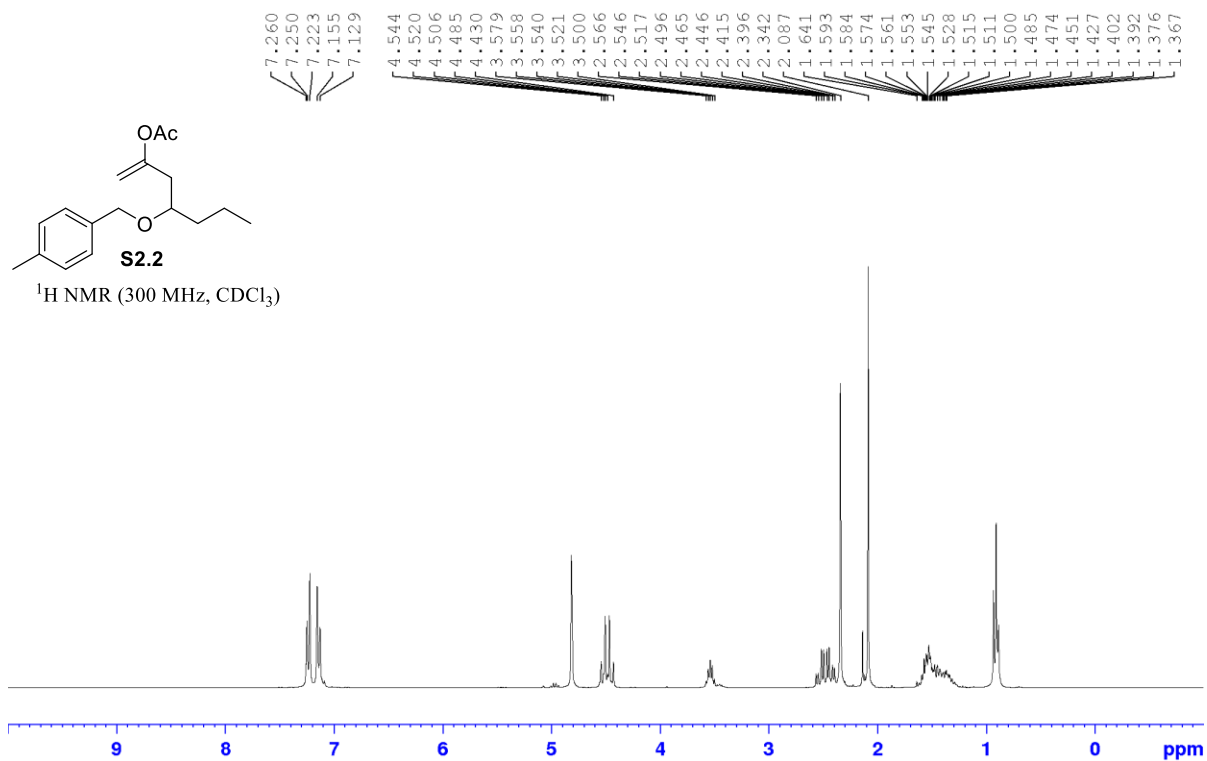


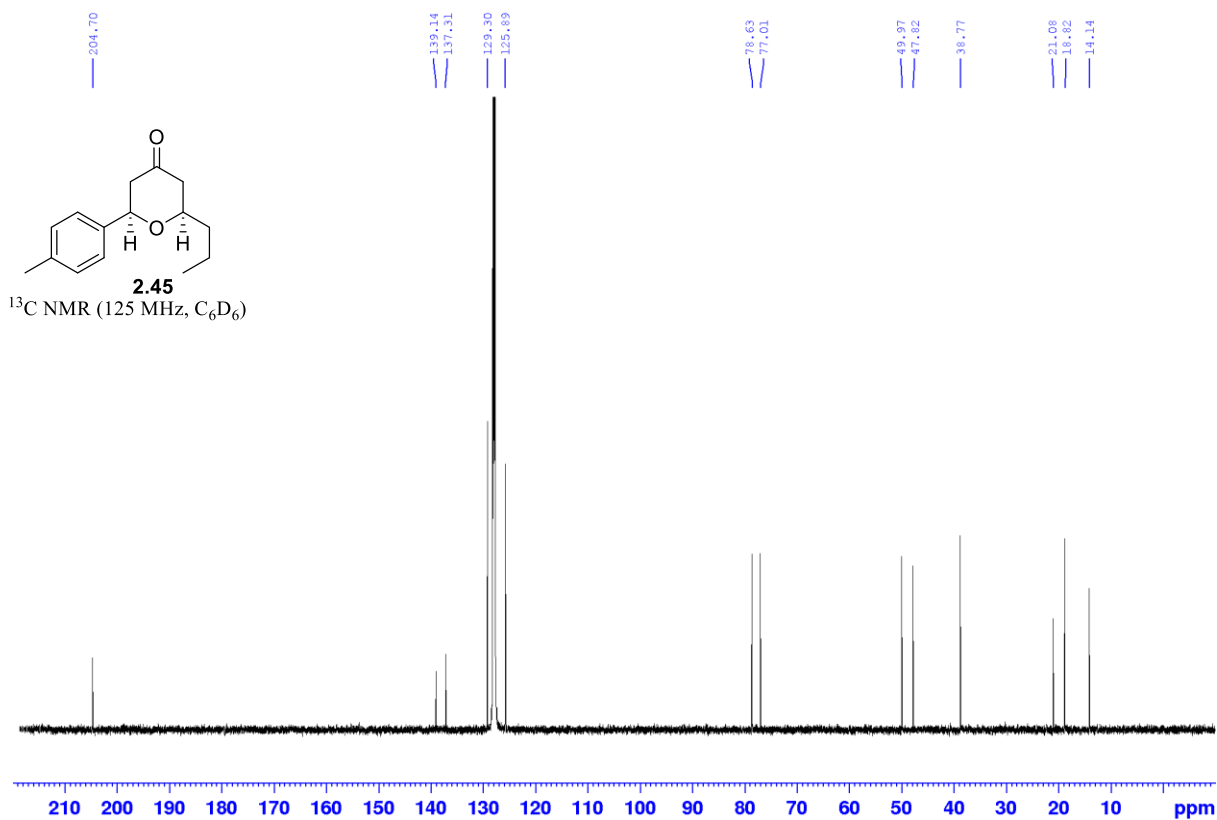
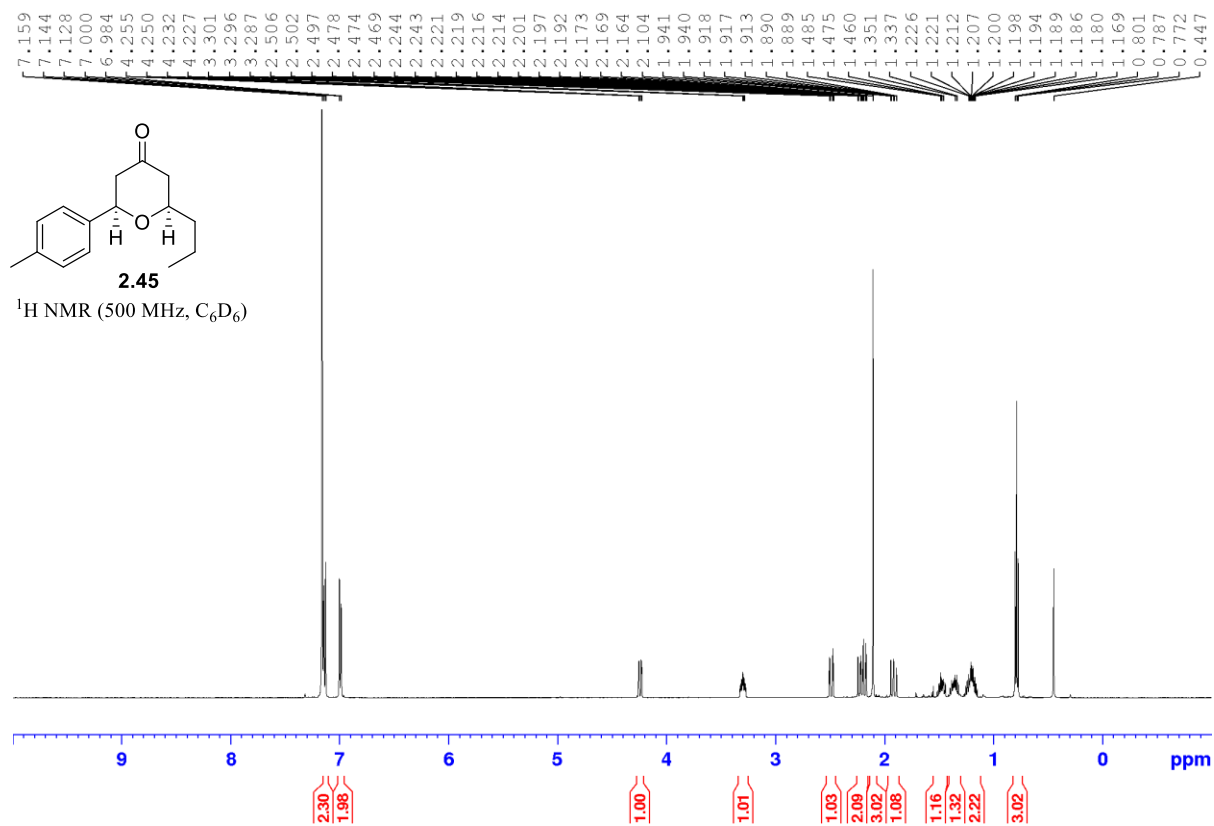


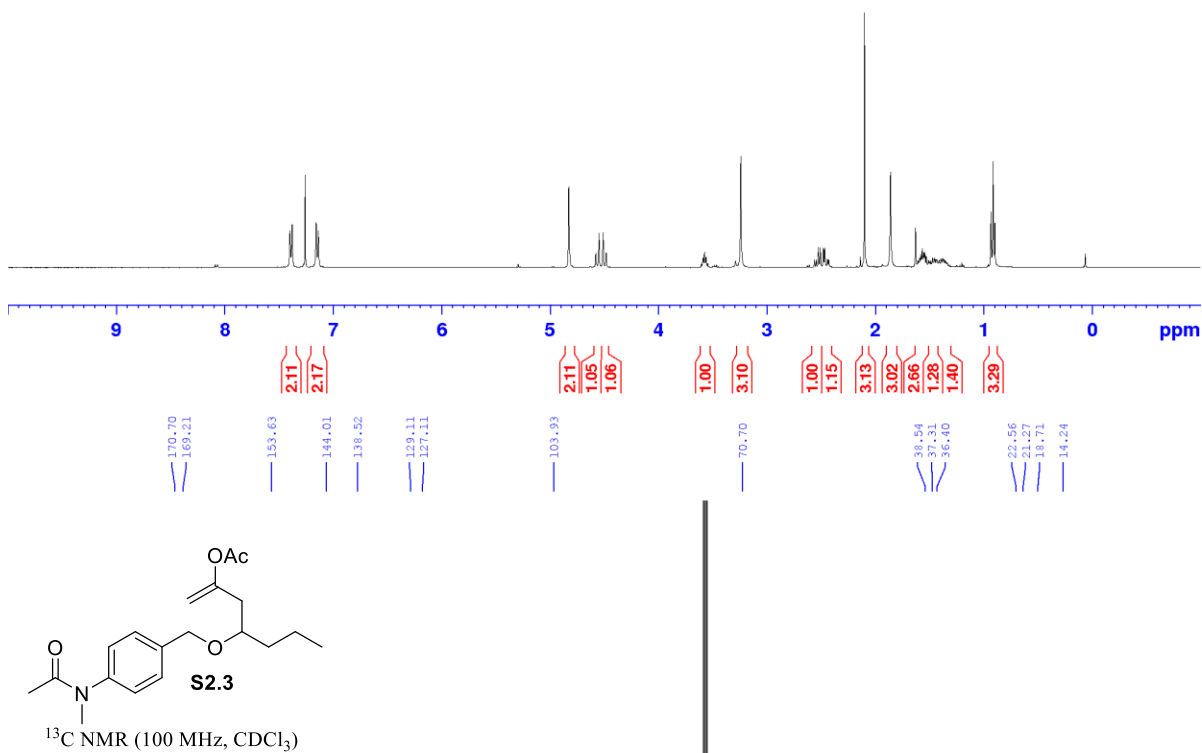
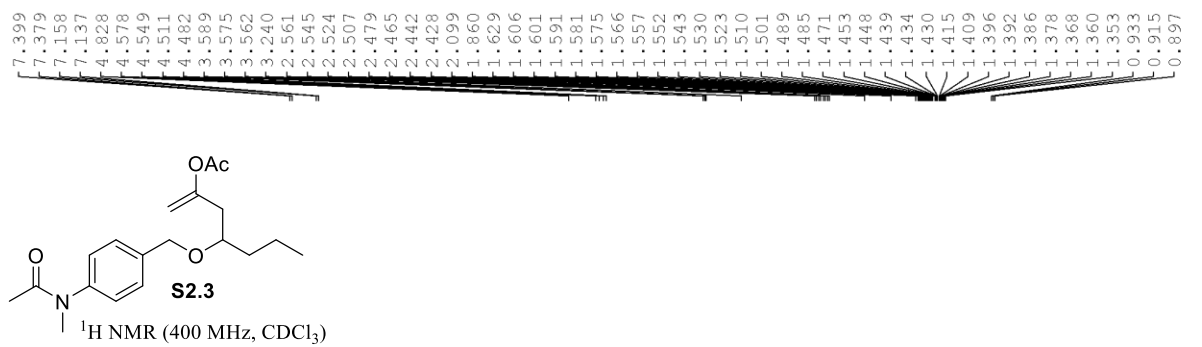


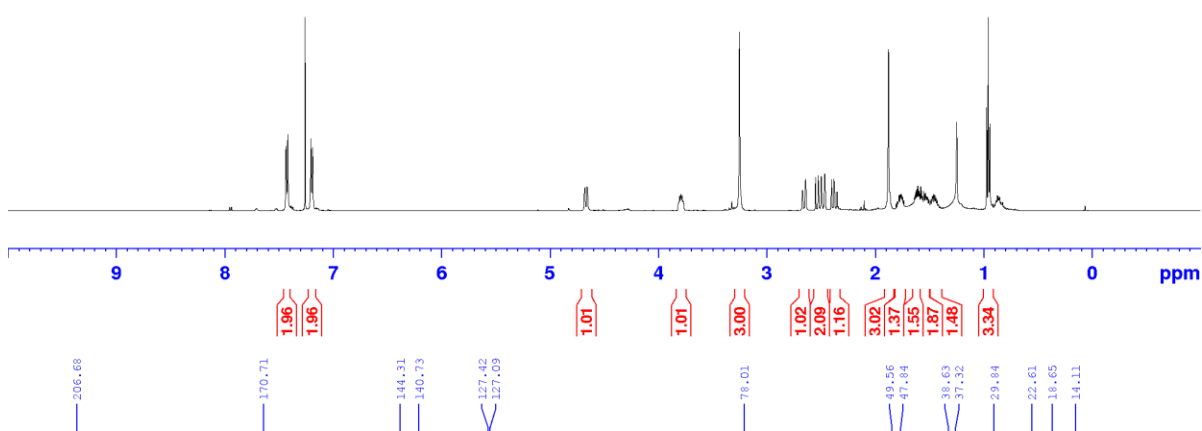
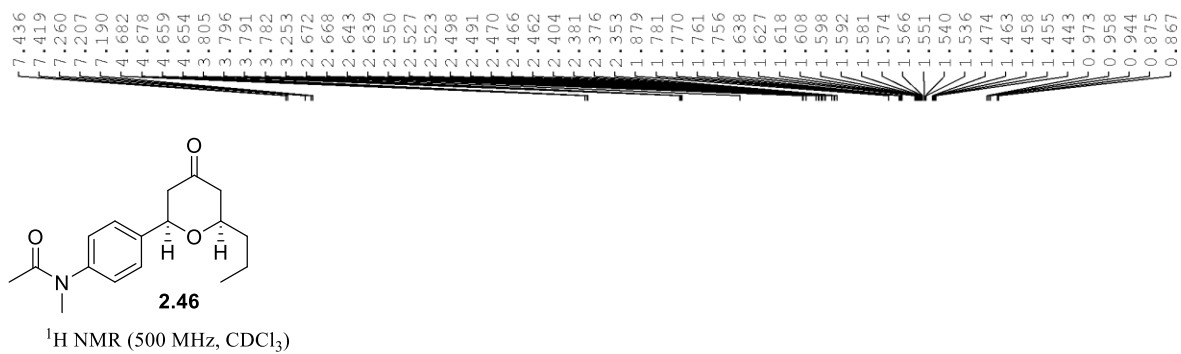


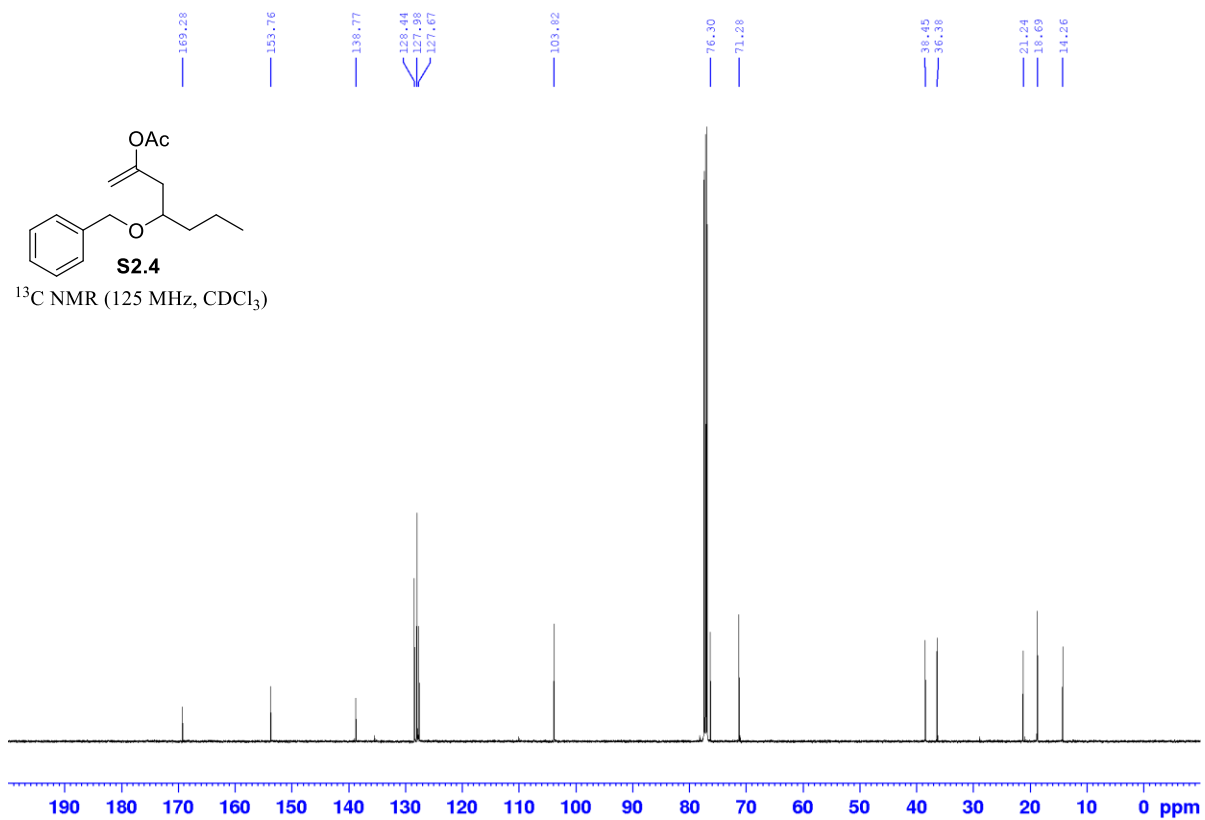
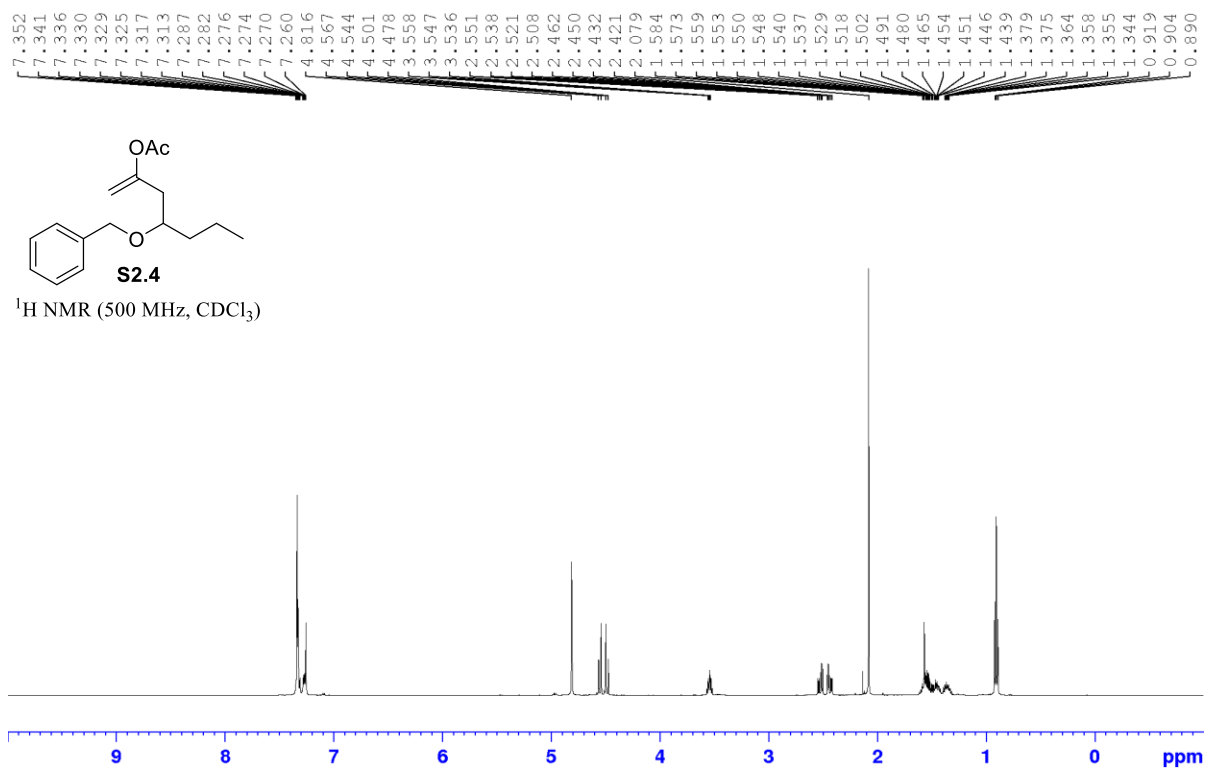


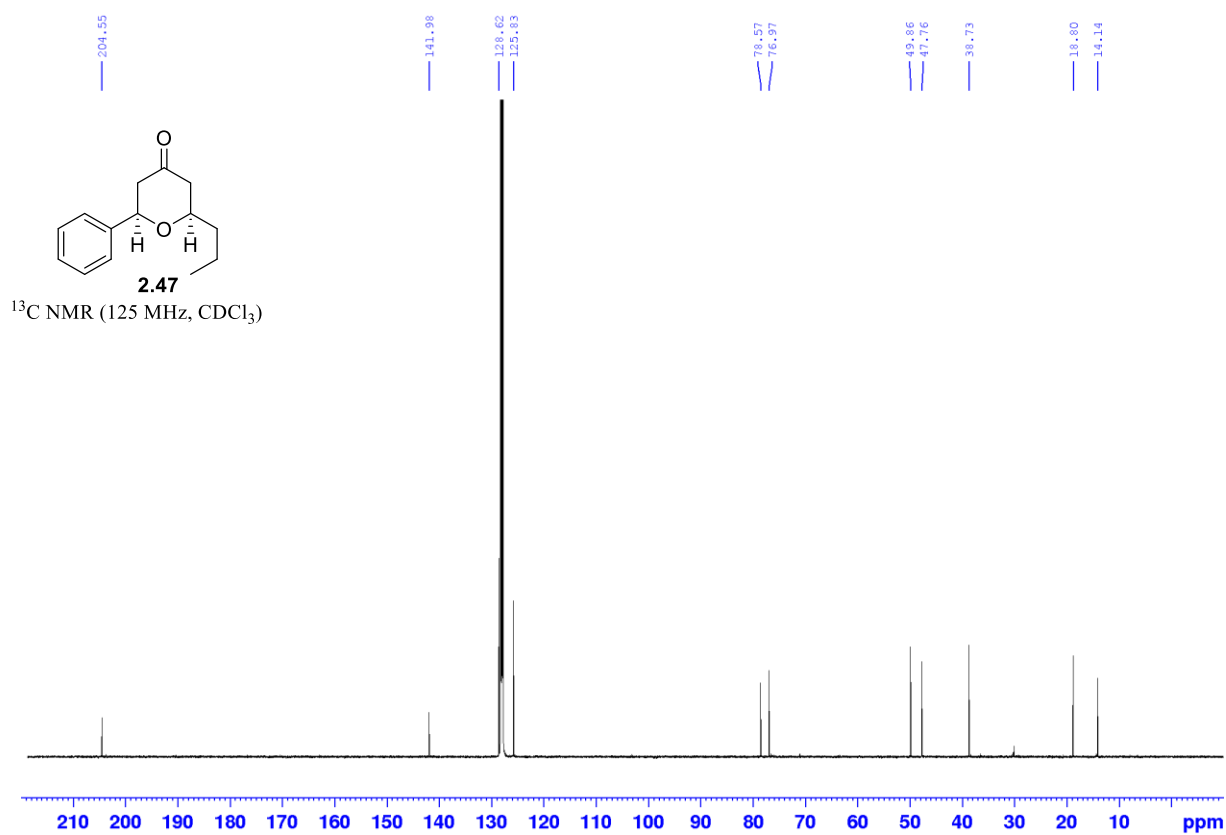
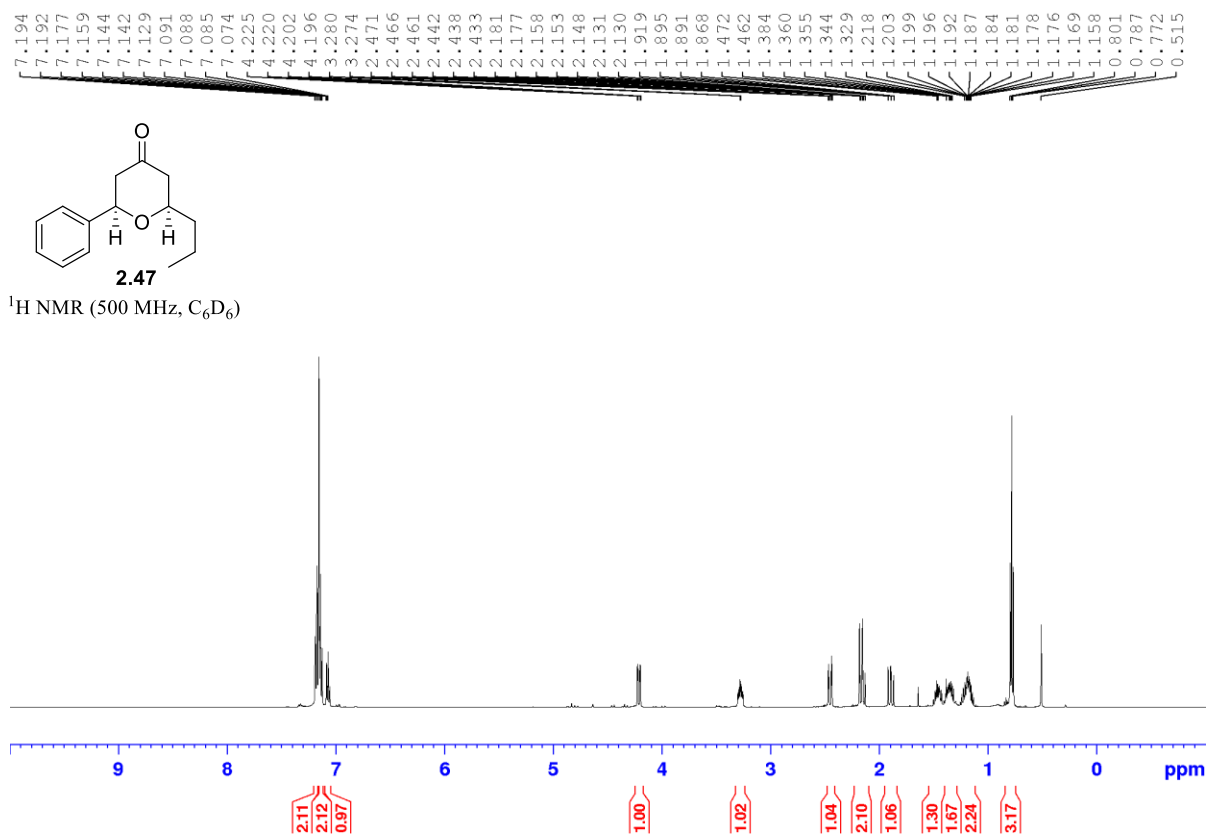


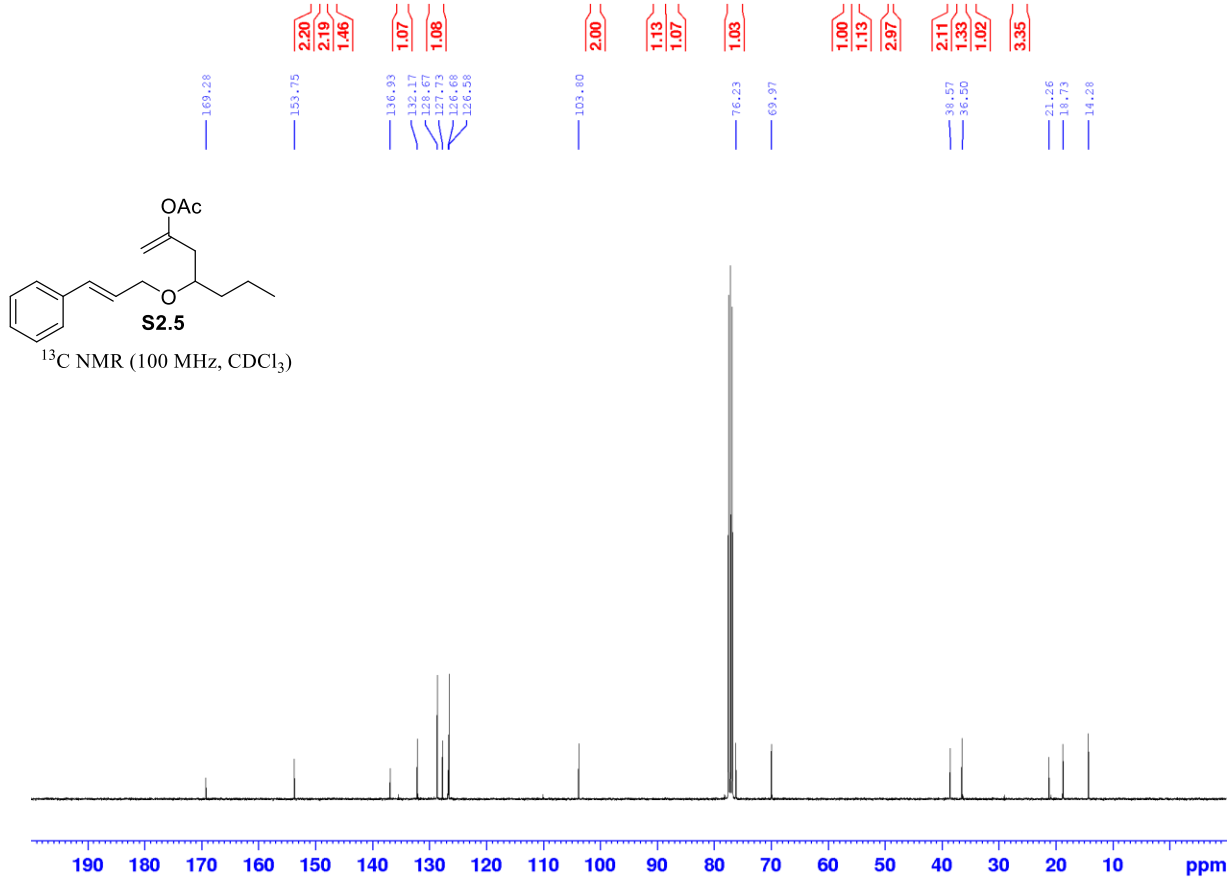
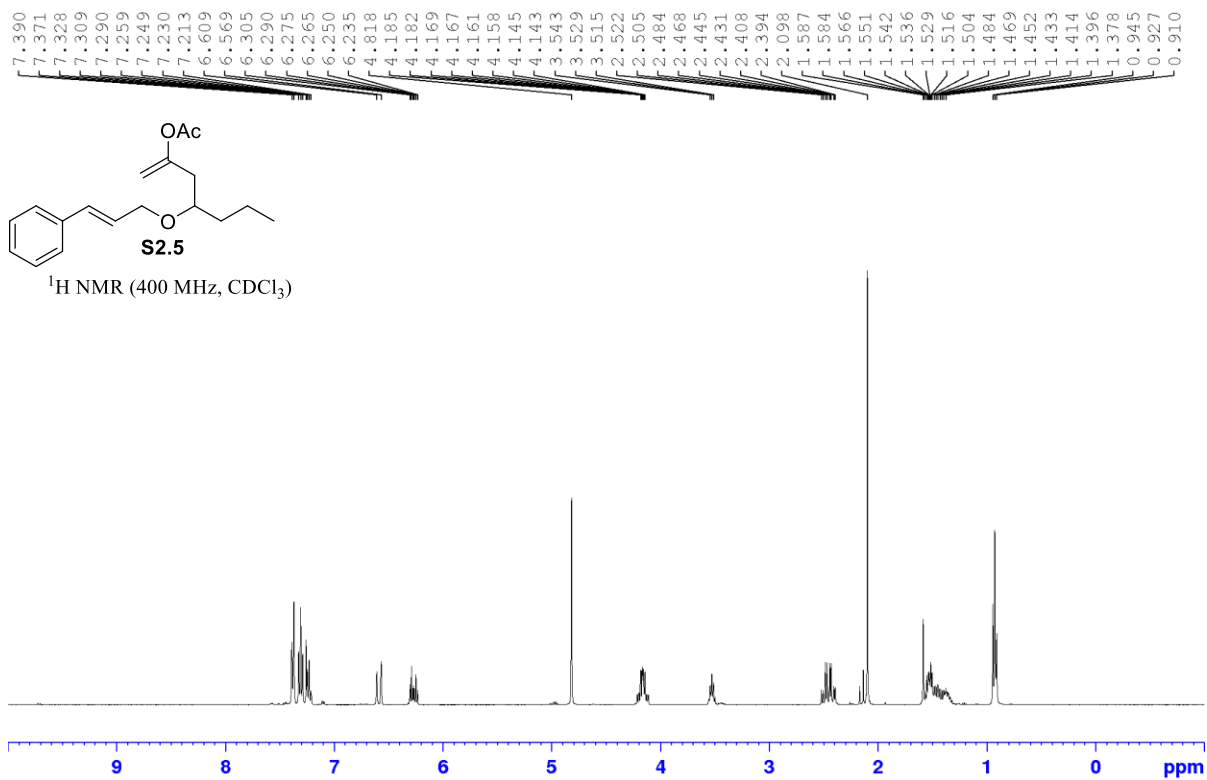


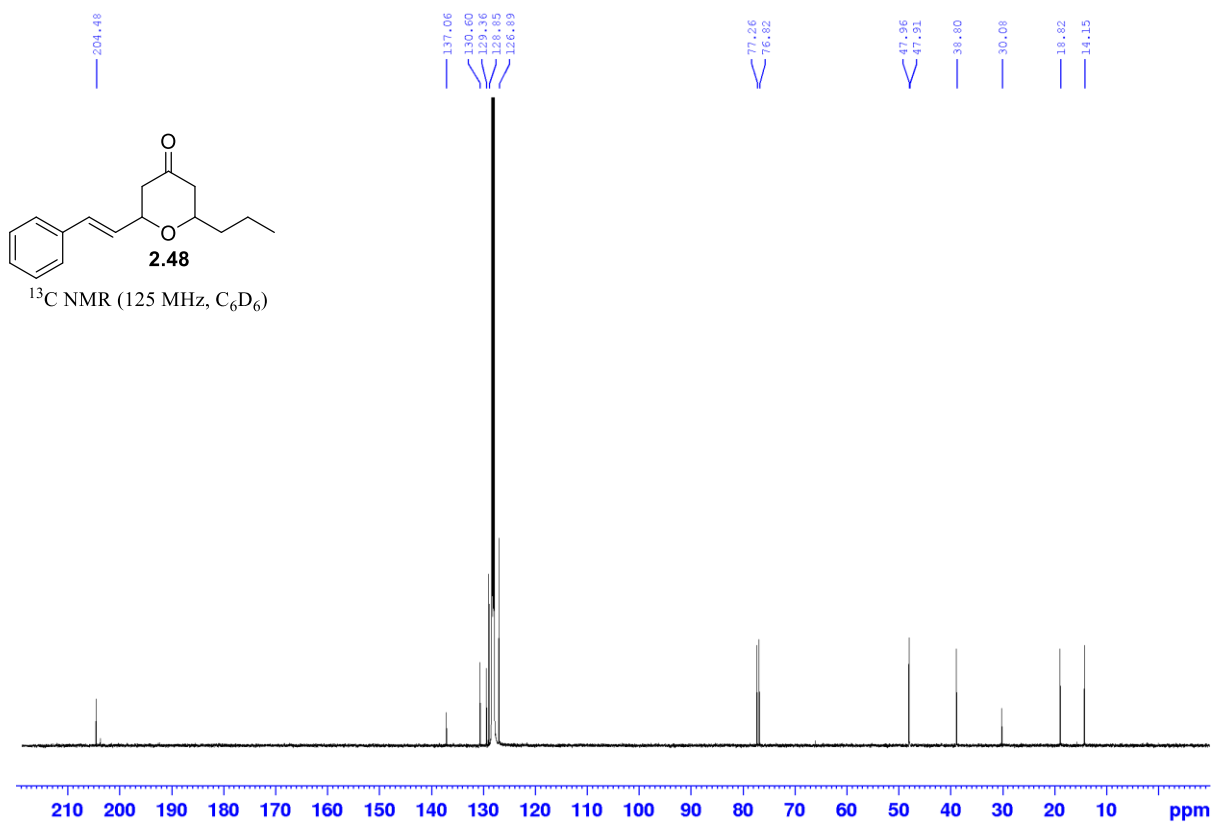
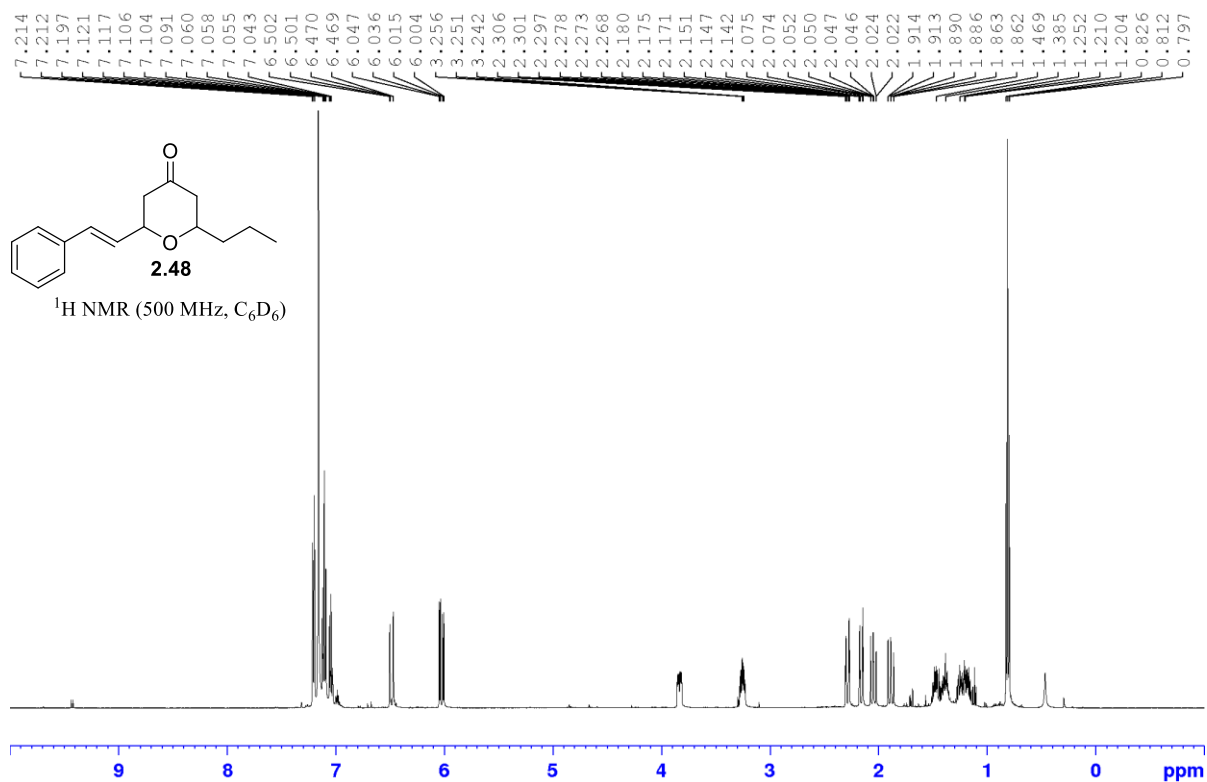


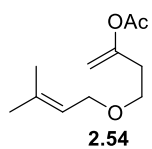




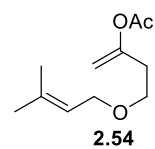
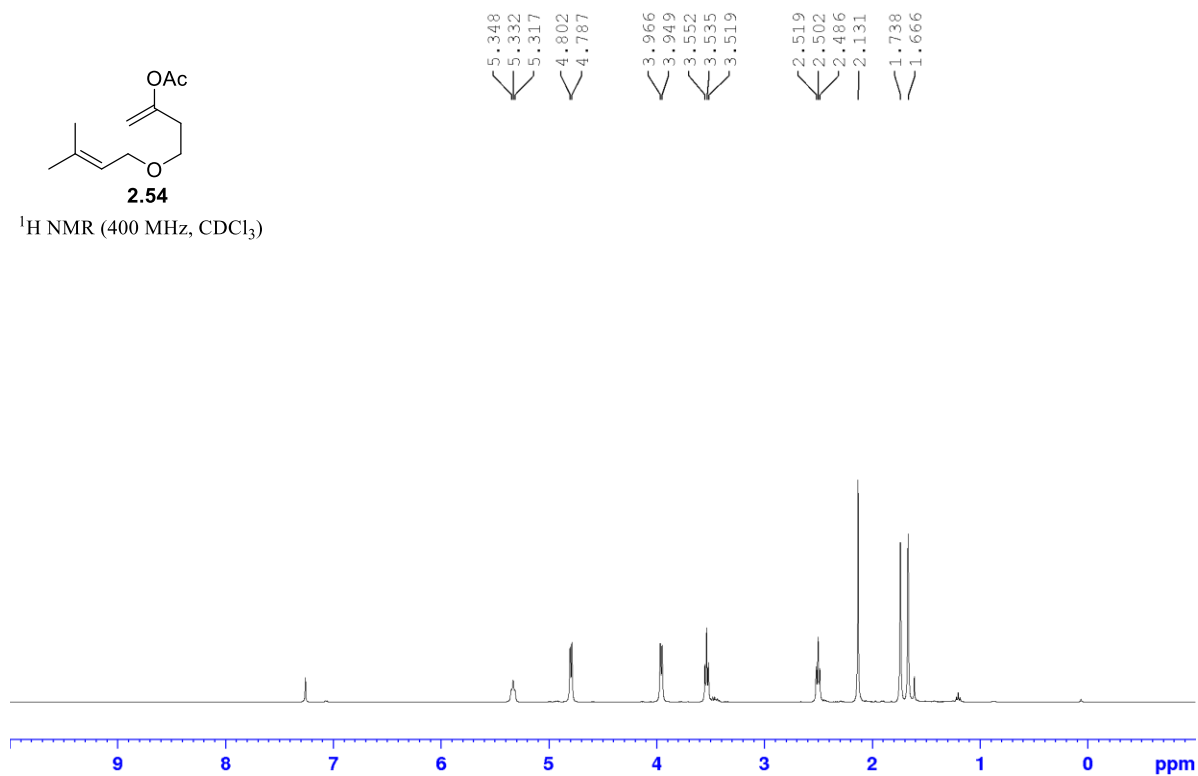




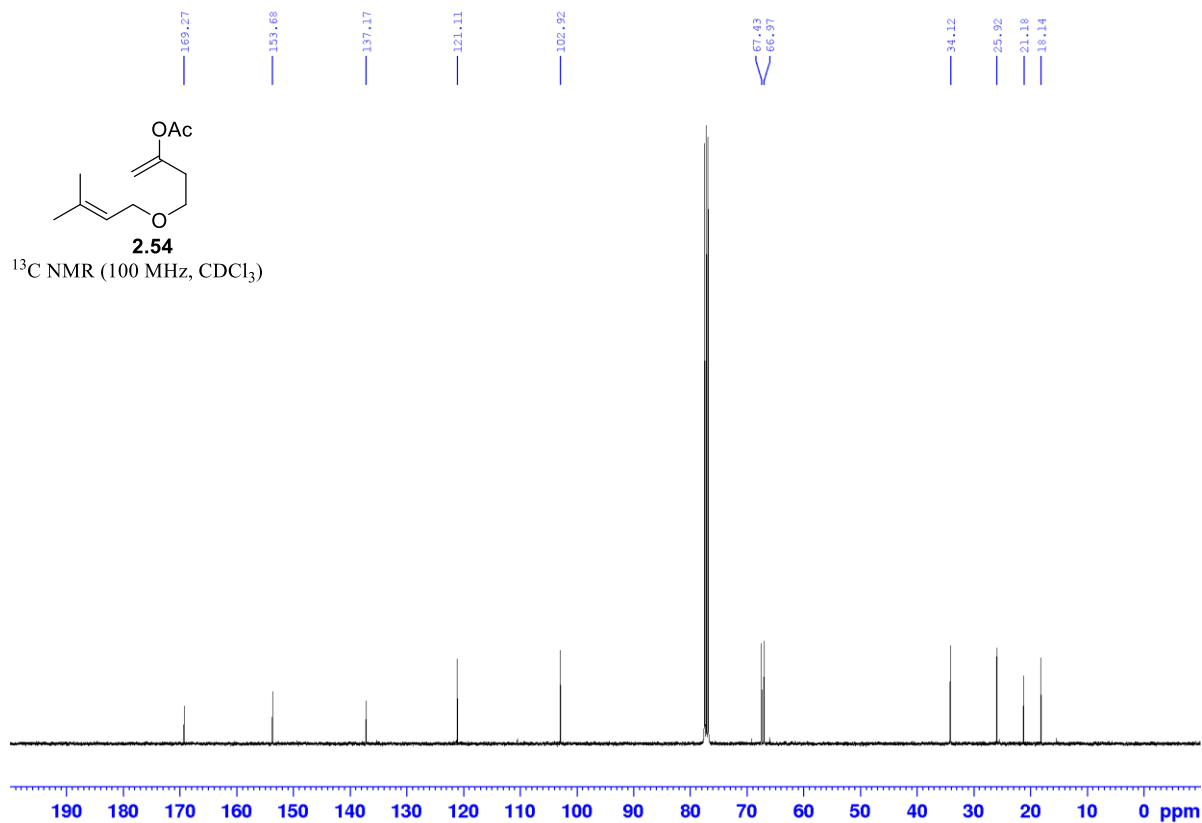


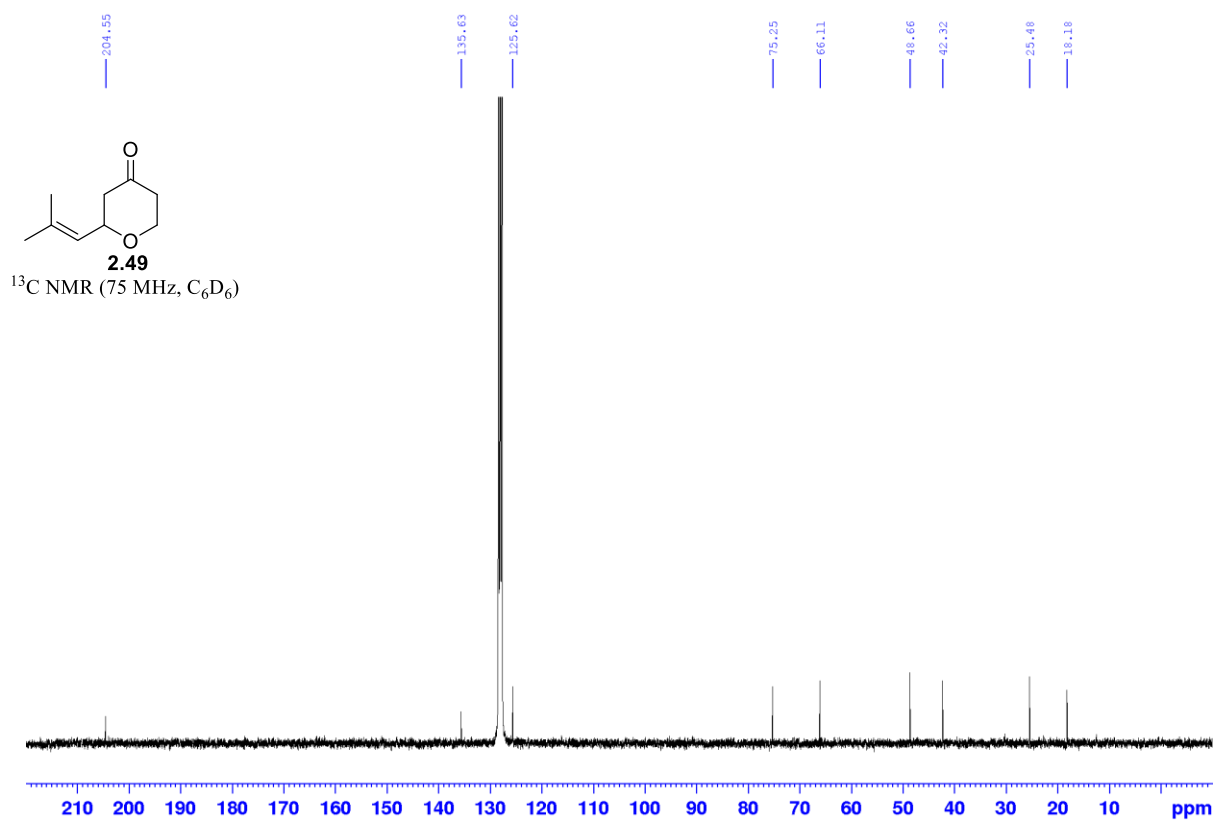
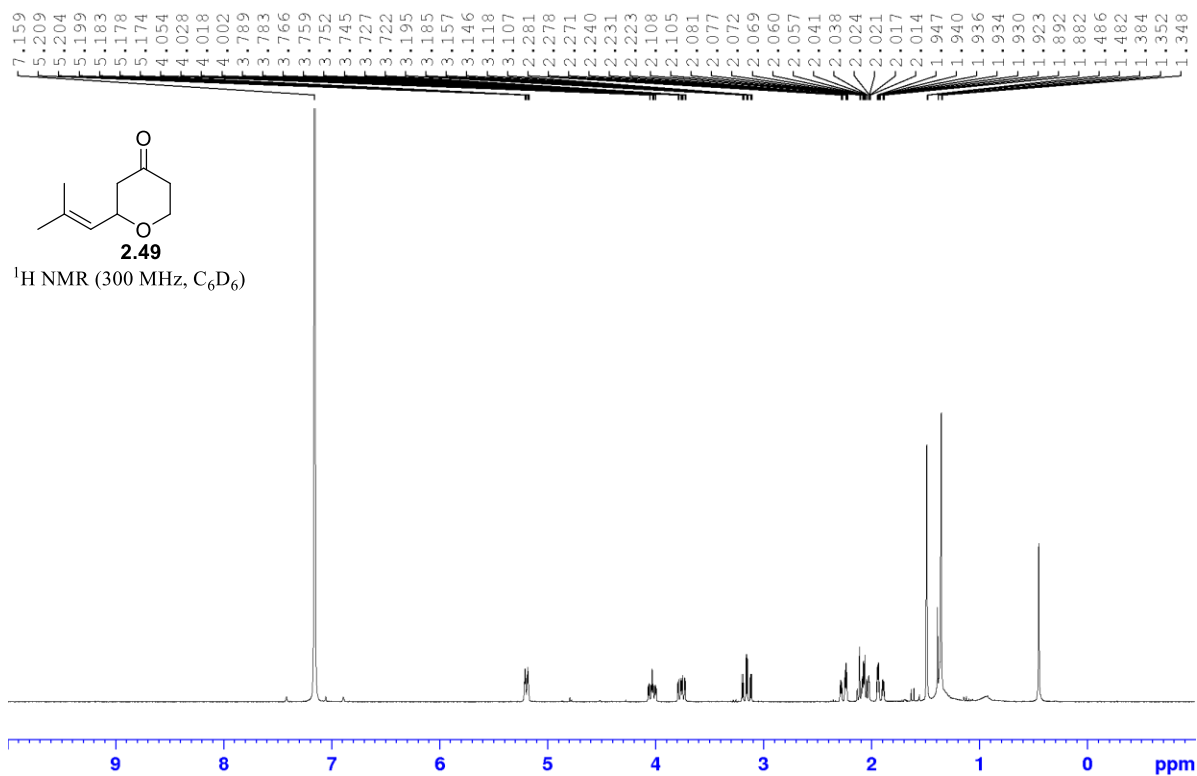


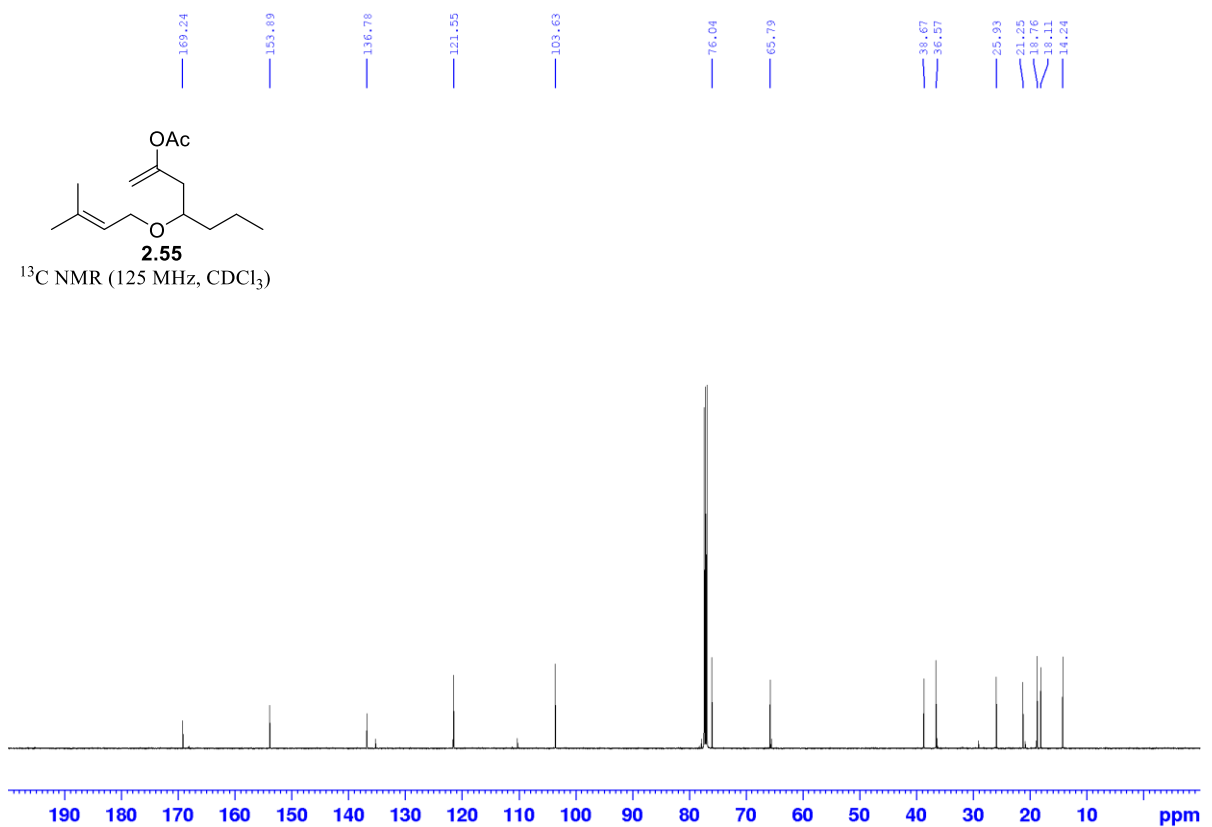
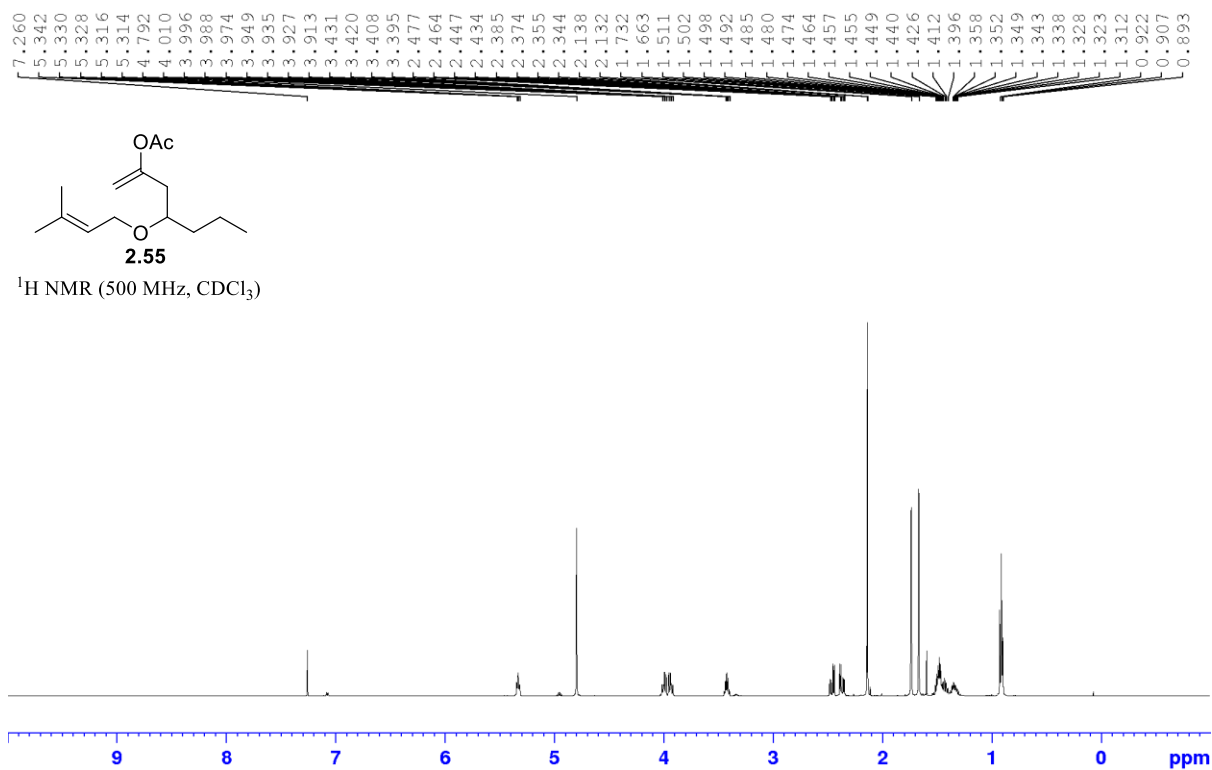
¹H NMR (400 MHz, CDCl₃)

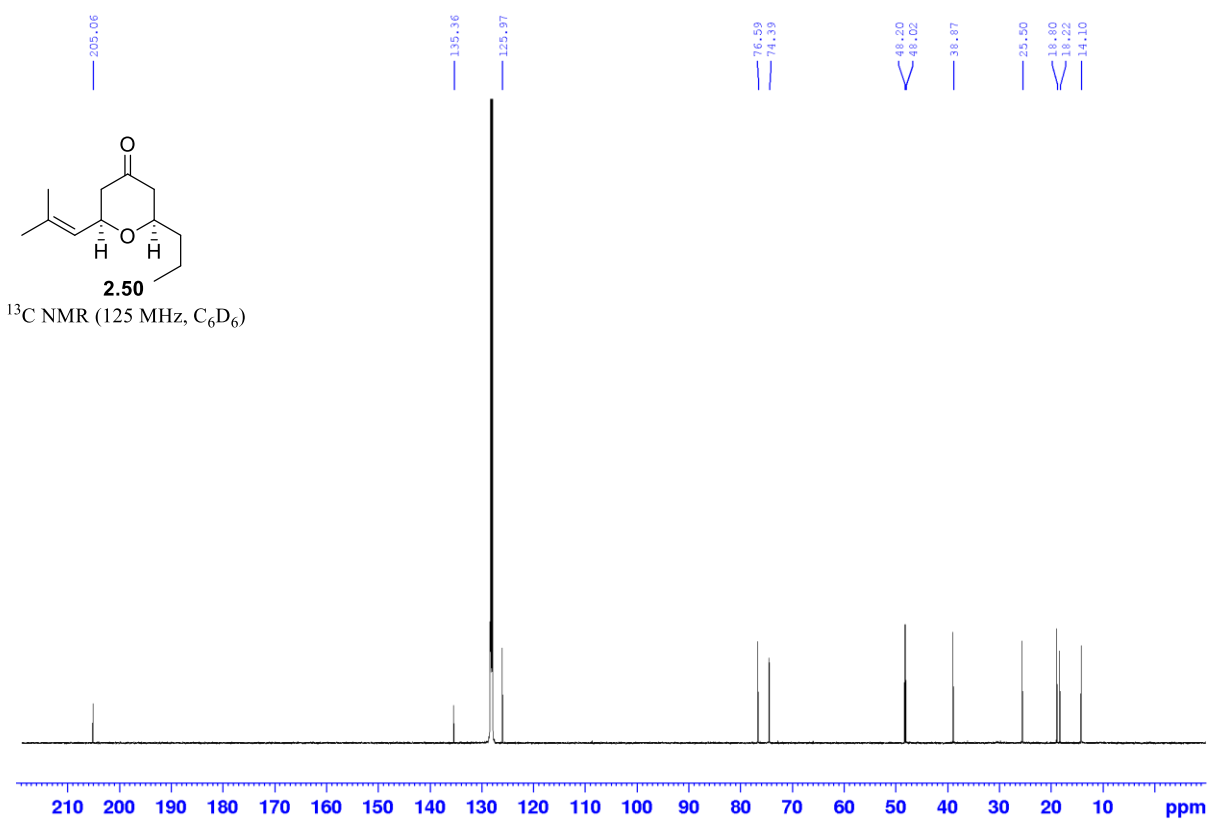
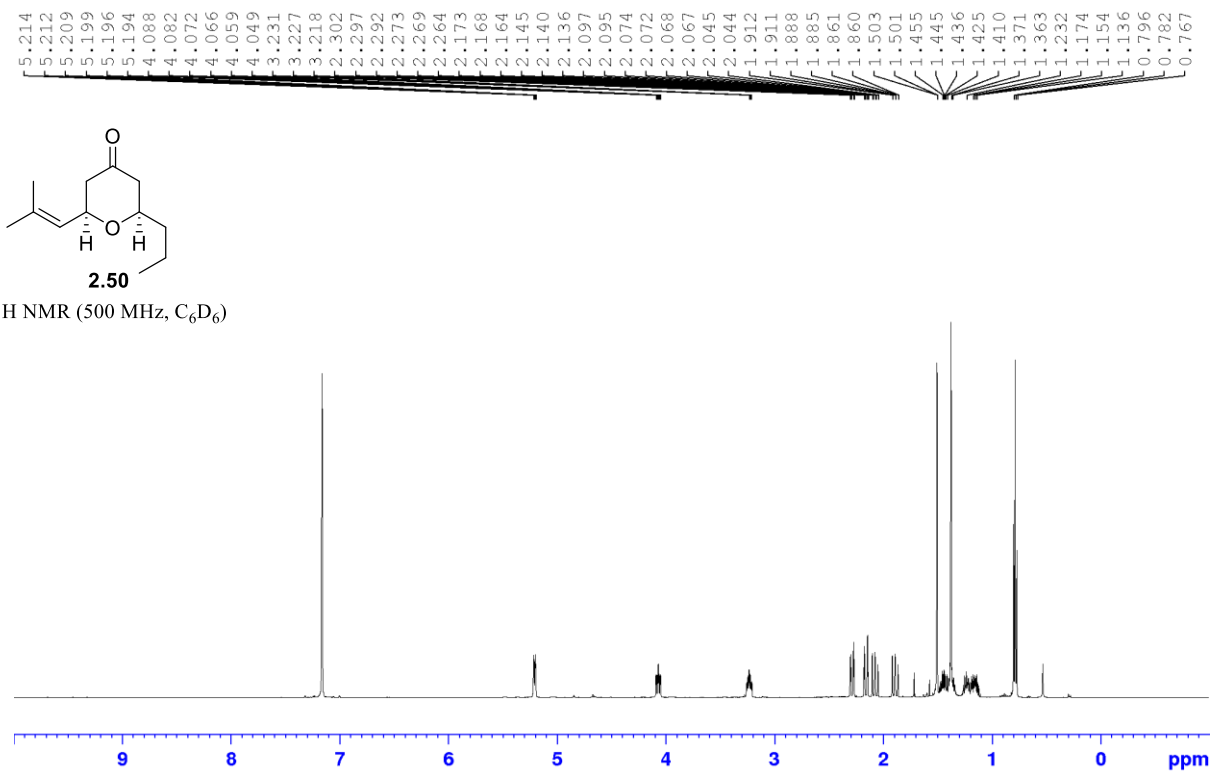


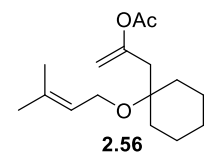
¹³C NMR (100 MHz, CDCl₃)



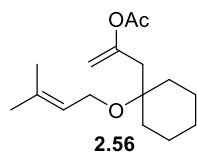
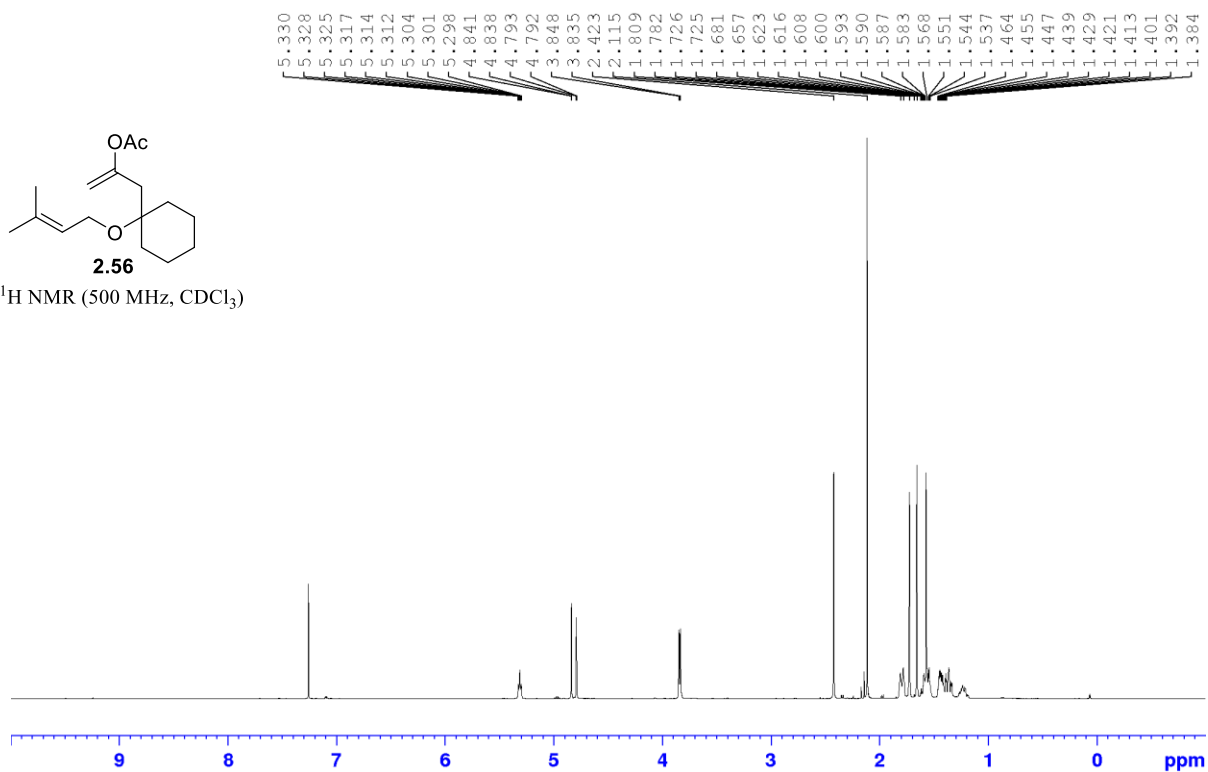




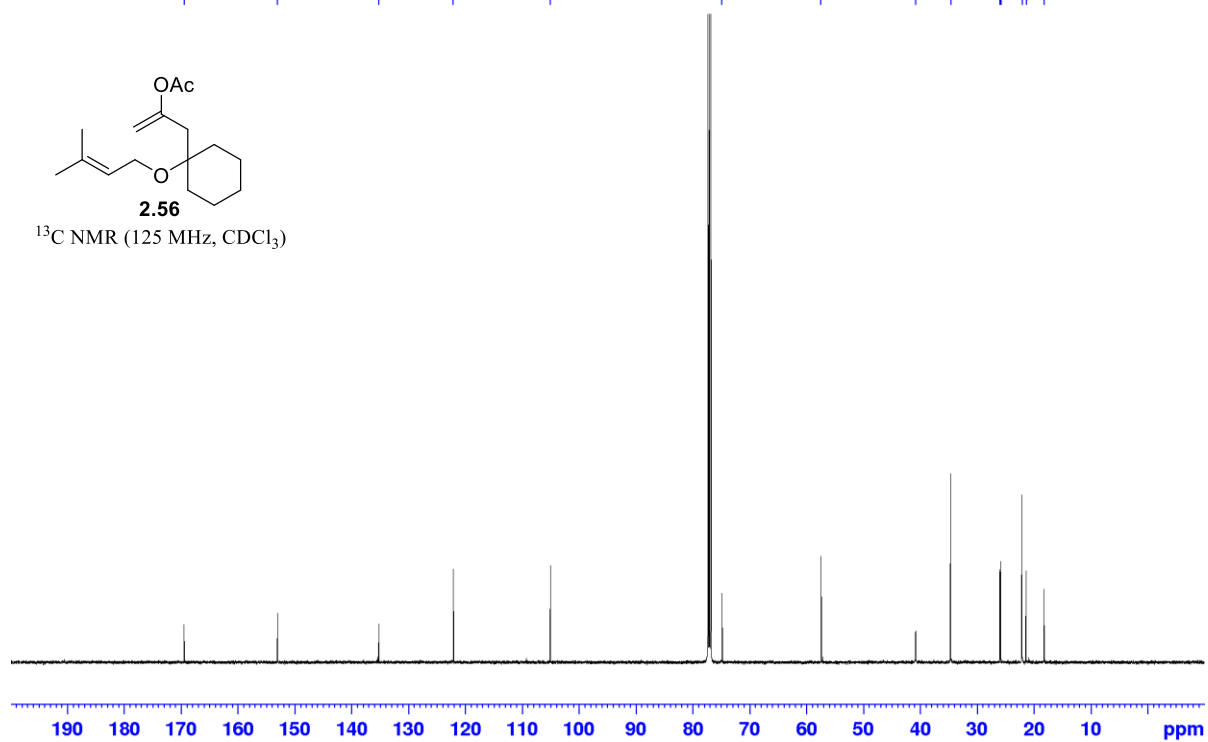


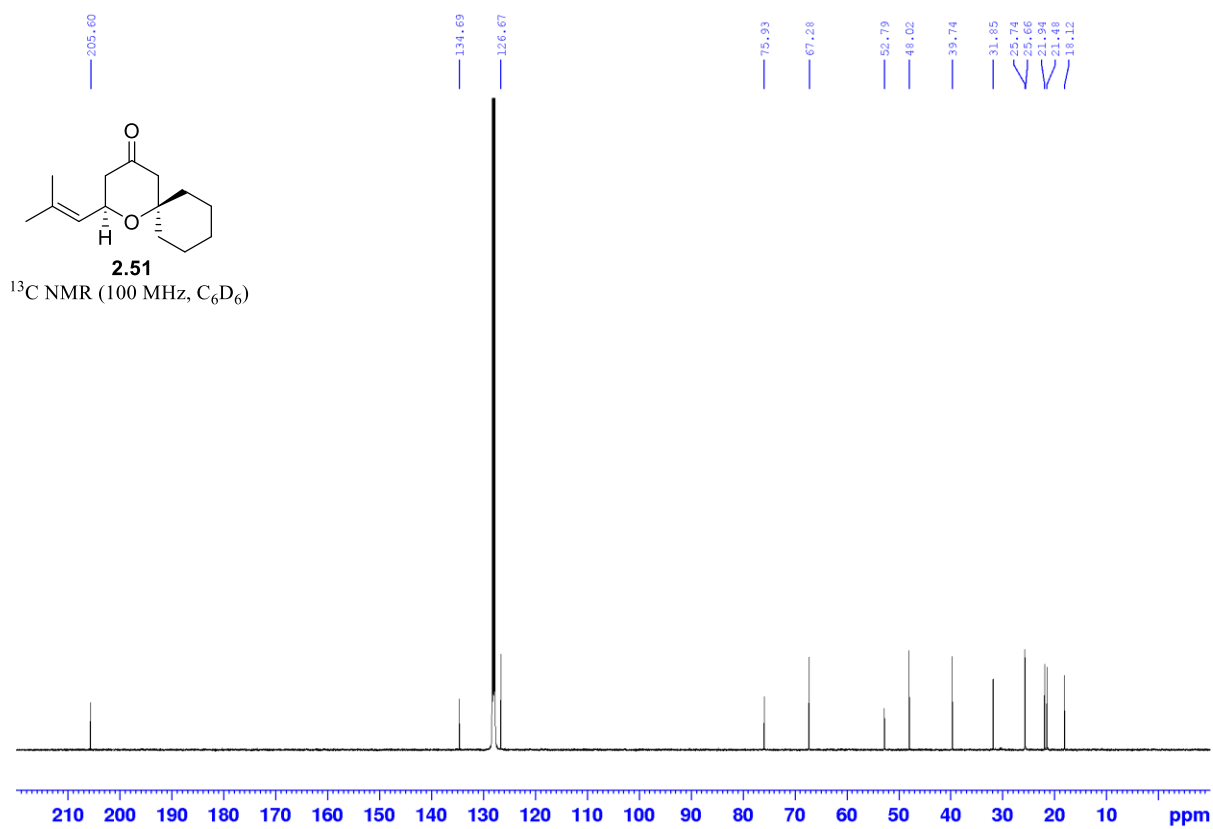
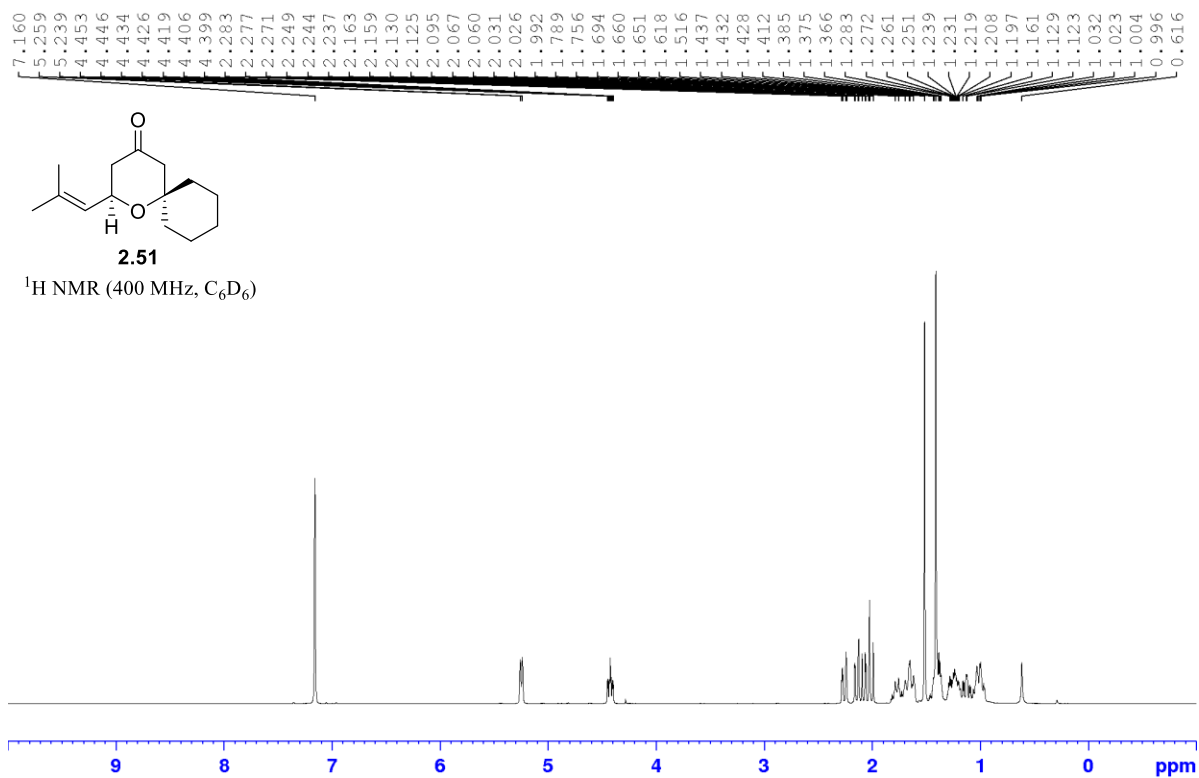


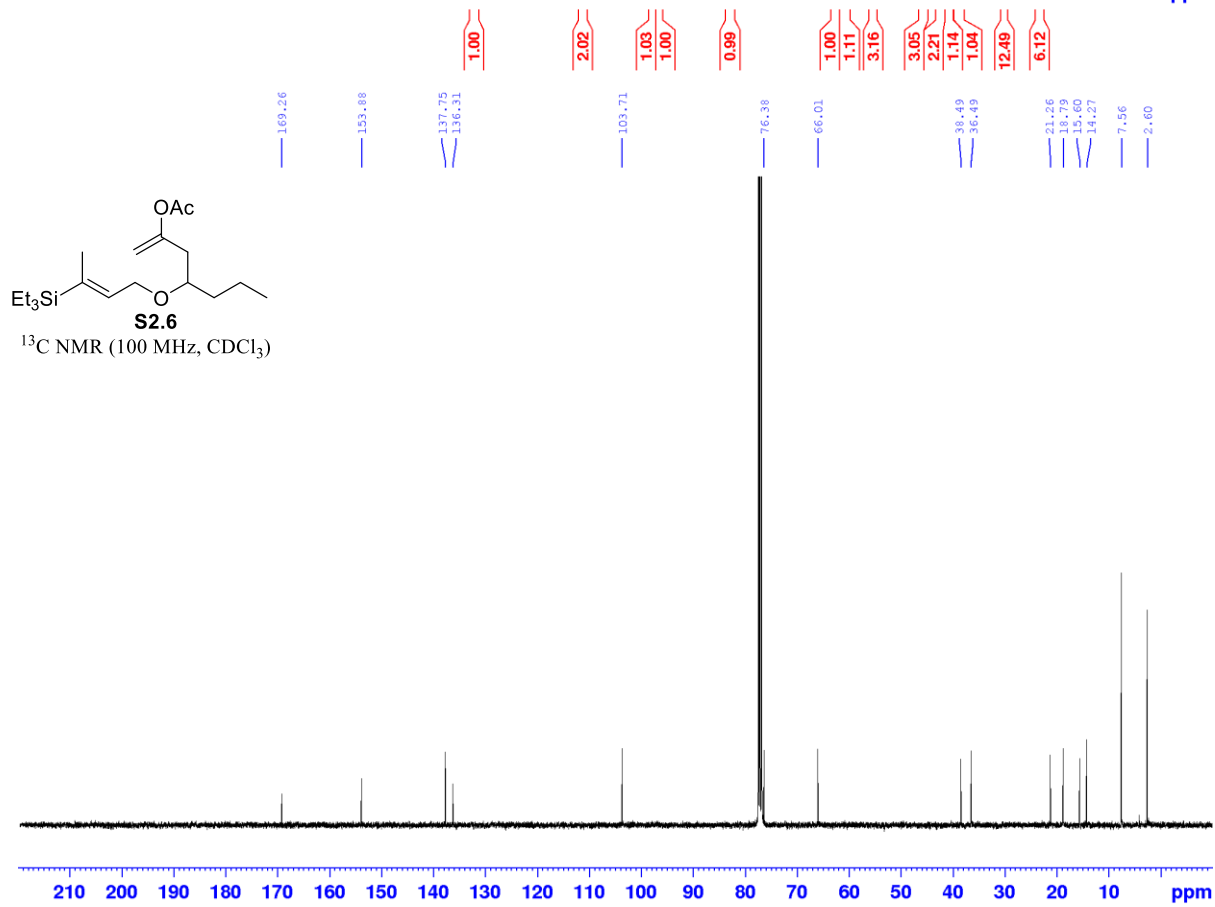
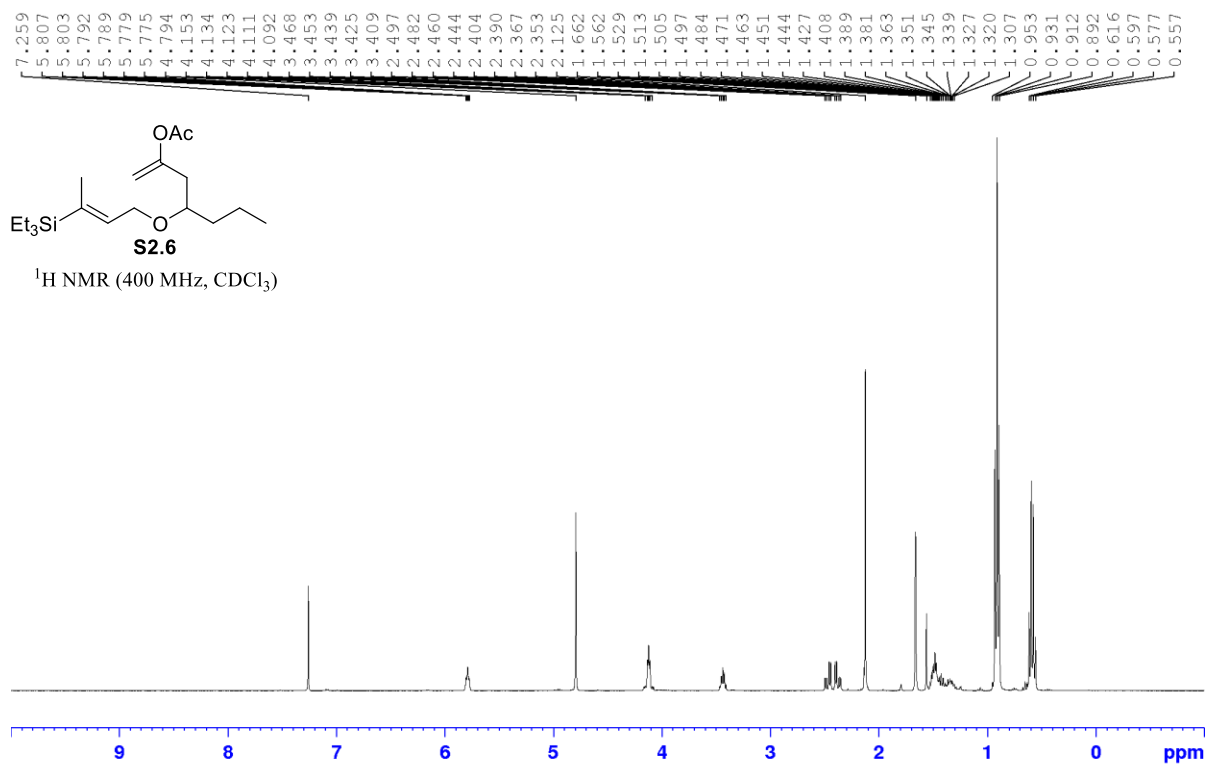
¹H NMR (500 MHz, CDCl₃)

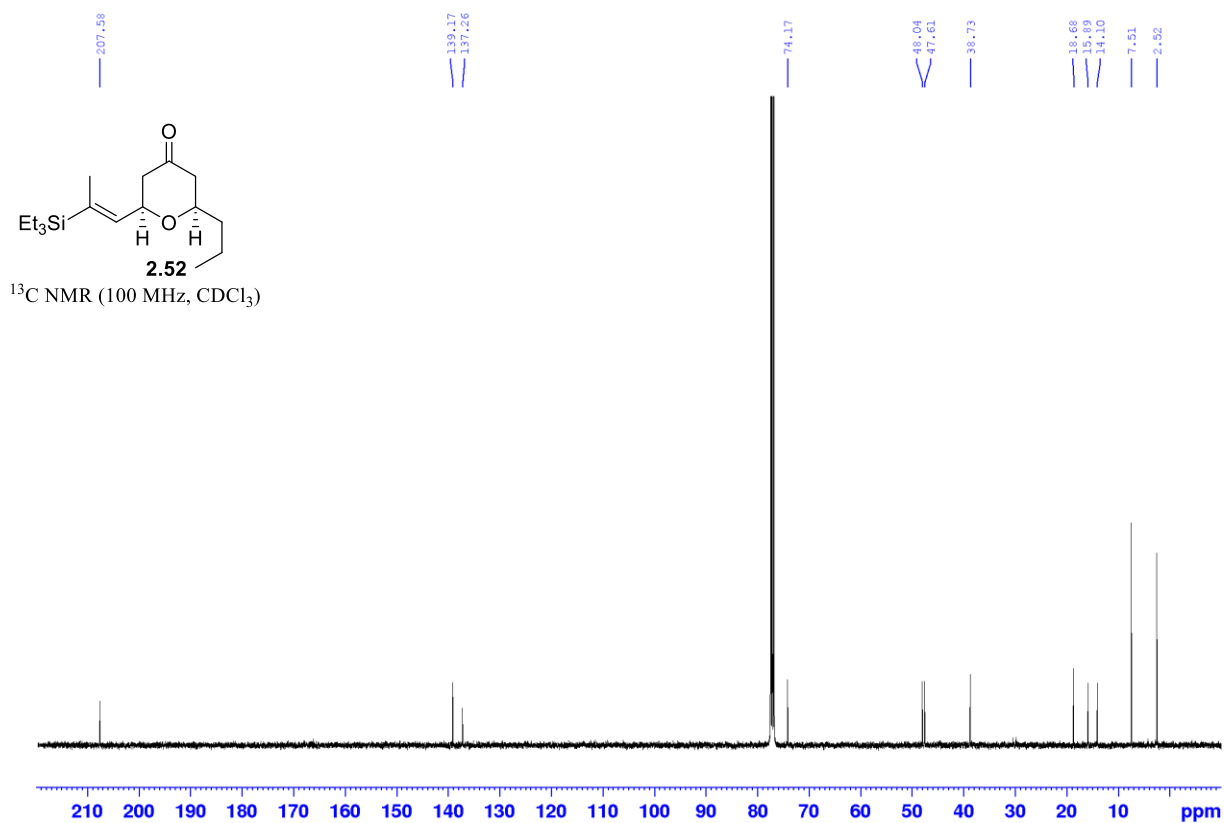
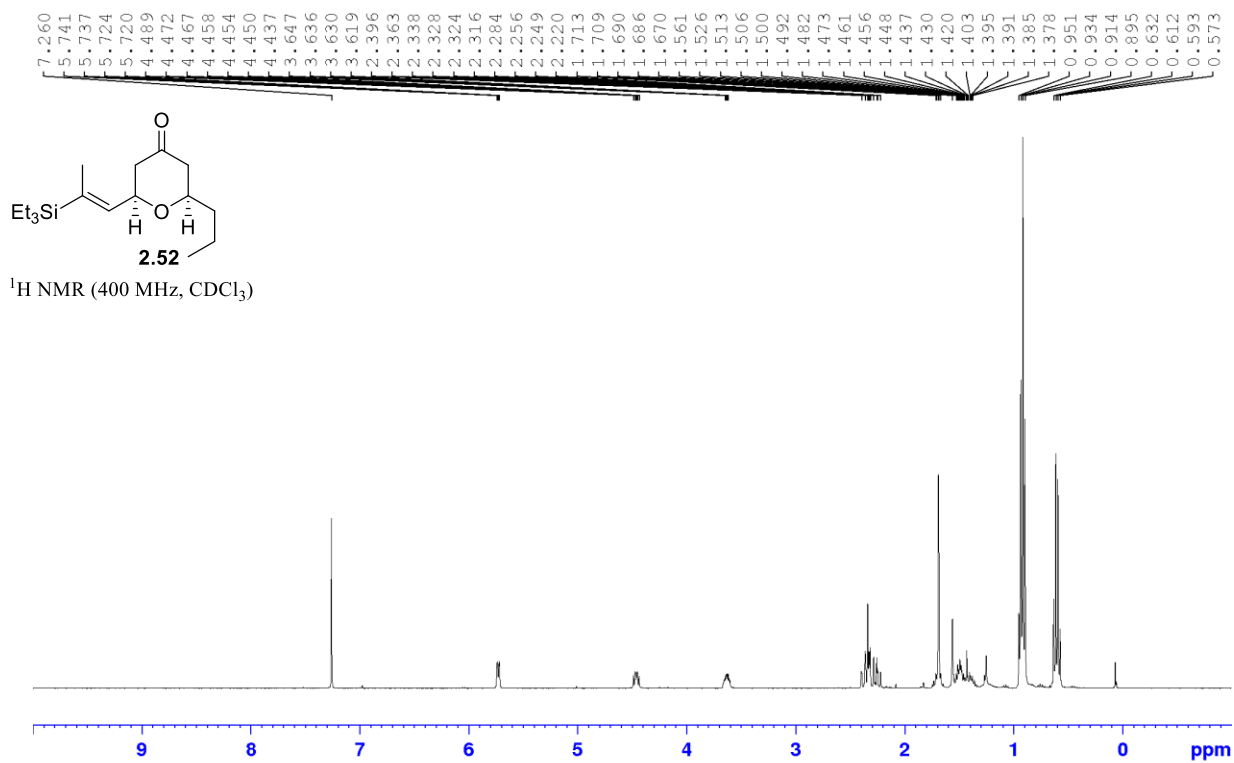


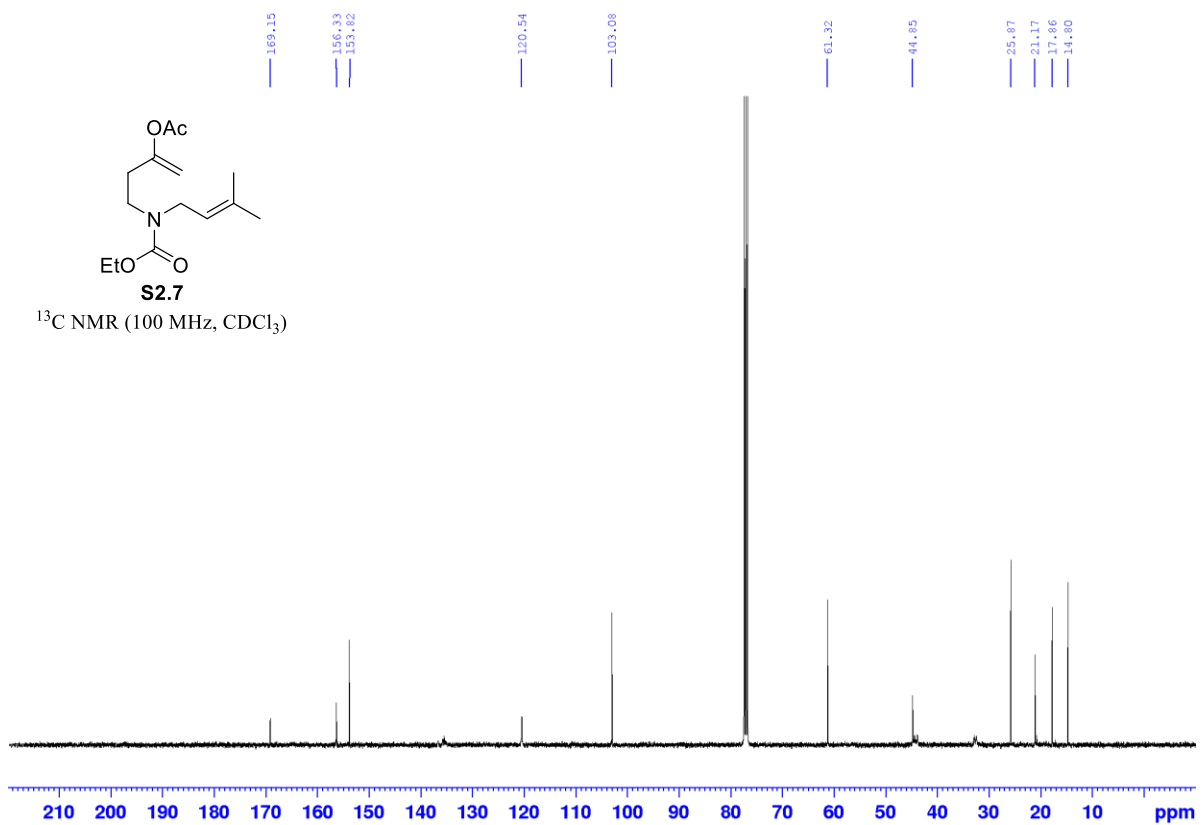
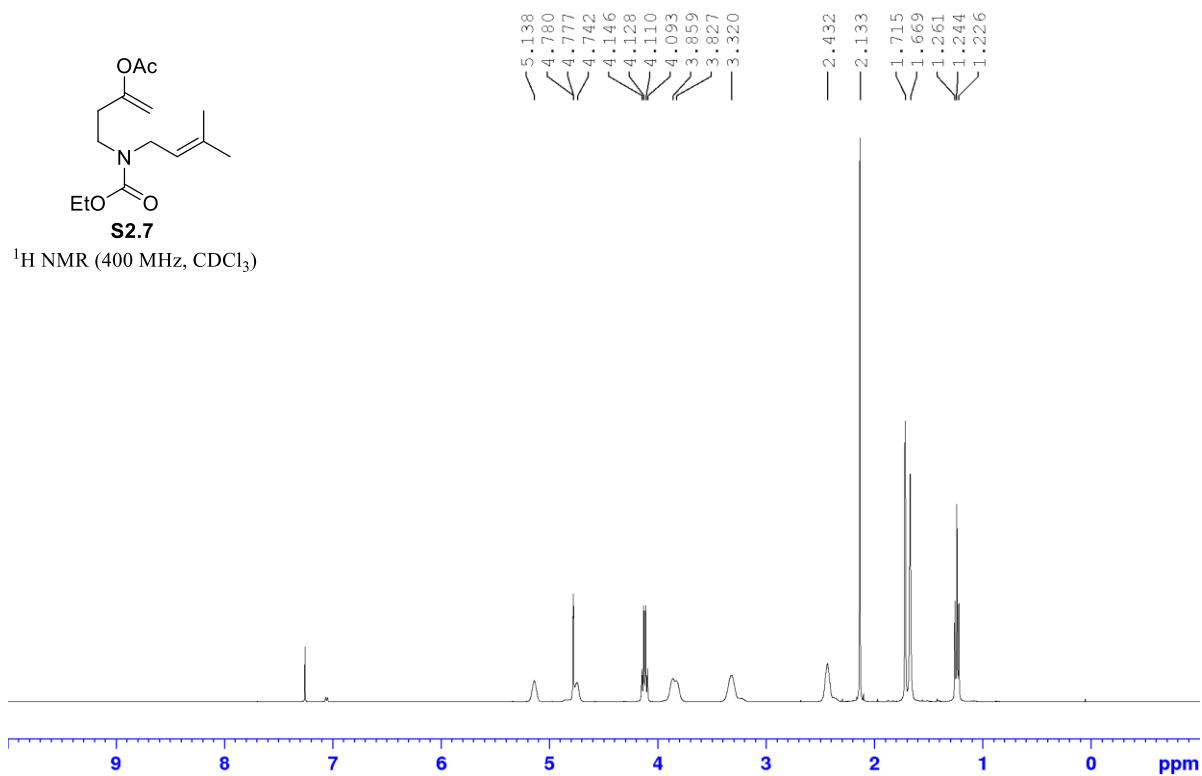
¹³C NMR (125 MHz, CDCl₃)

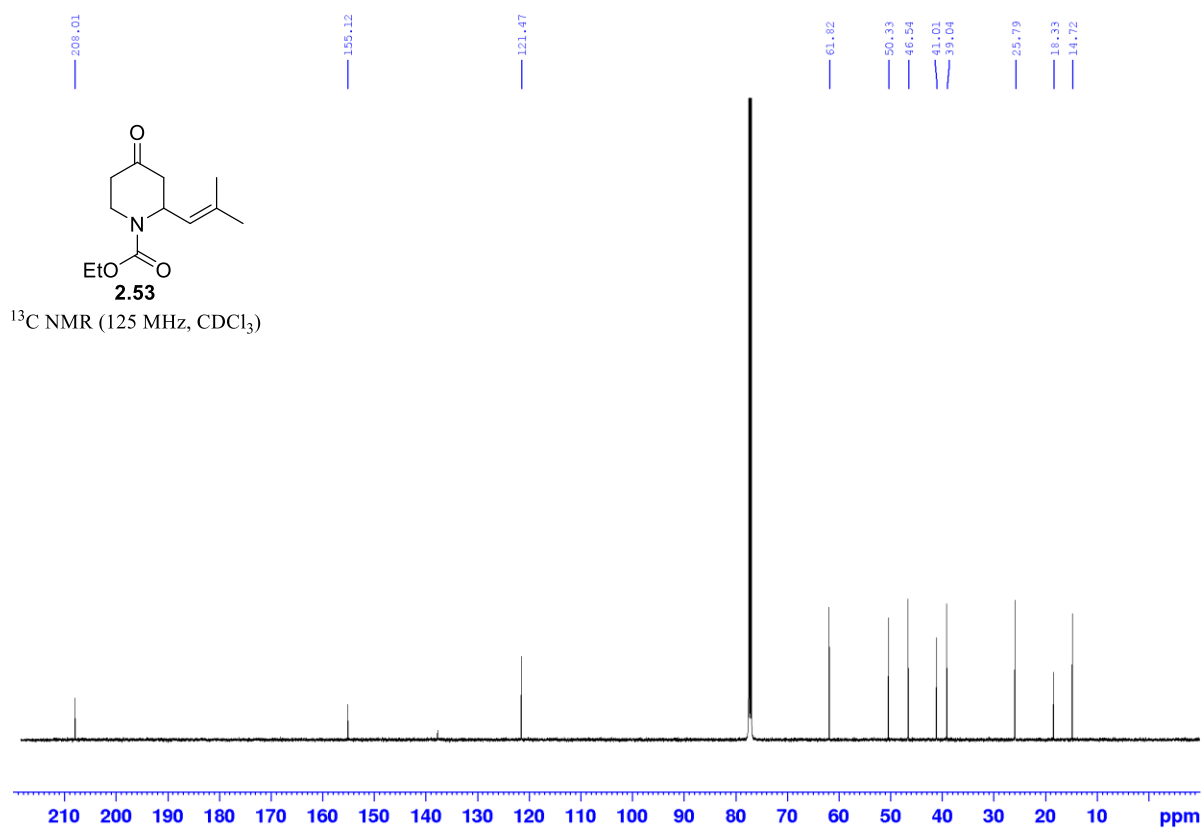
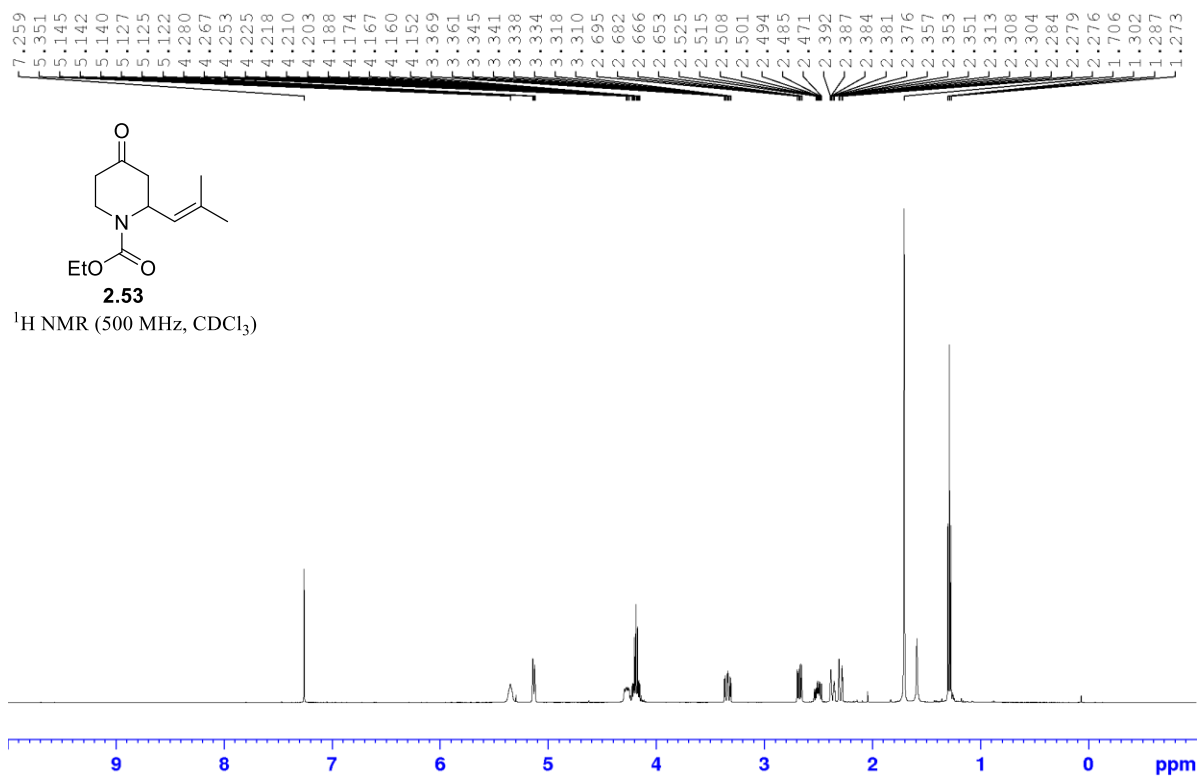


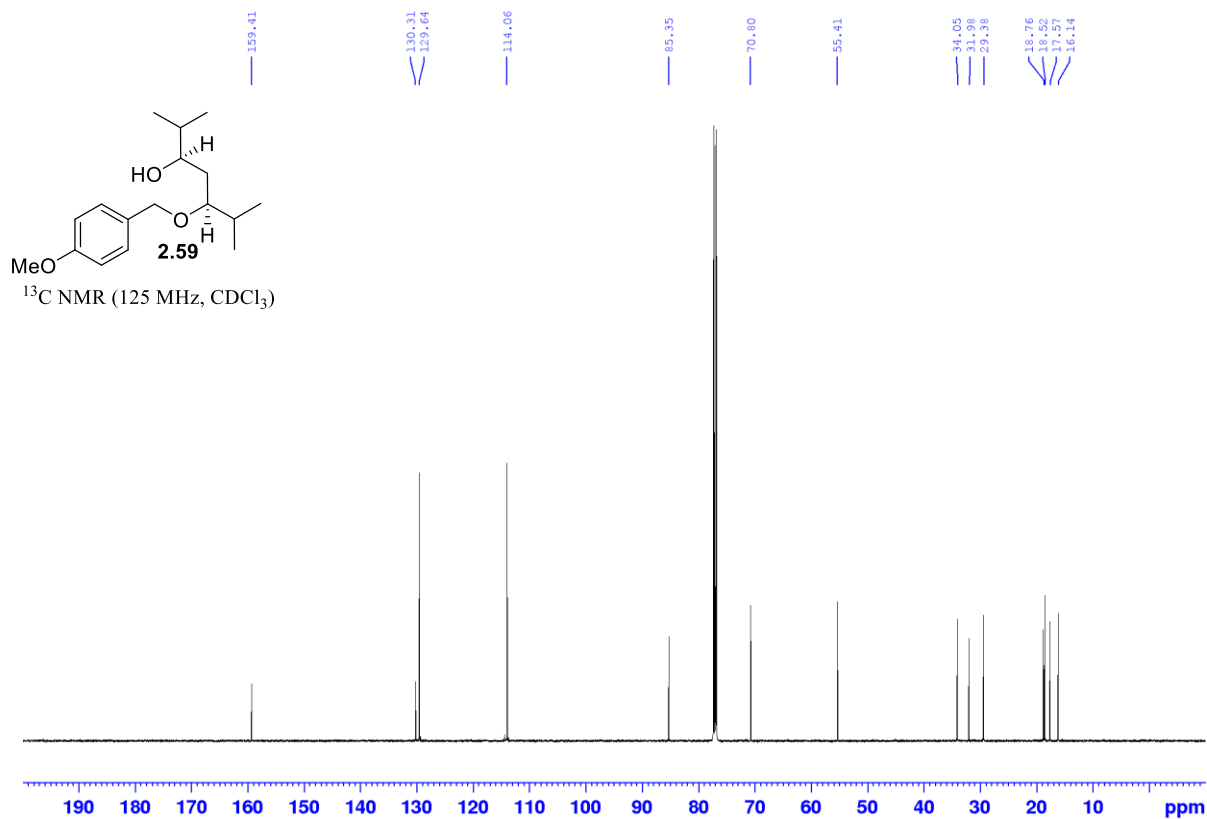
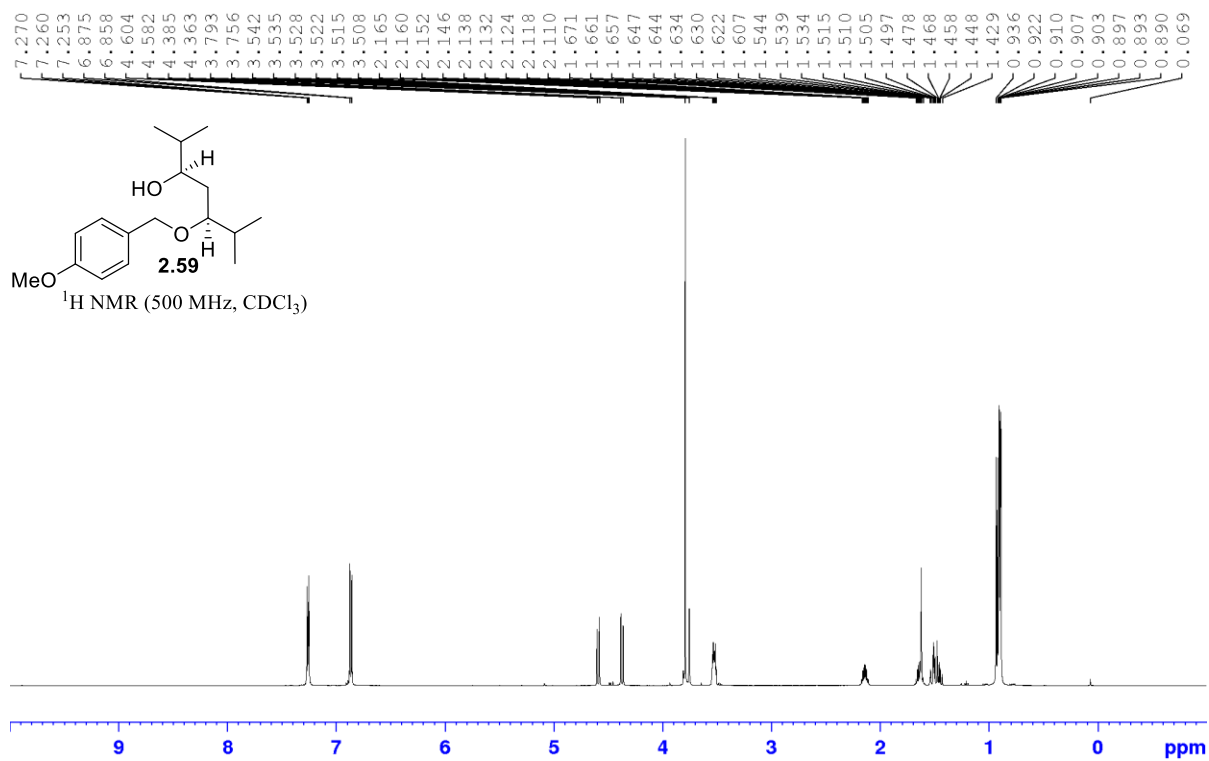


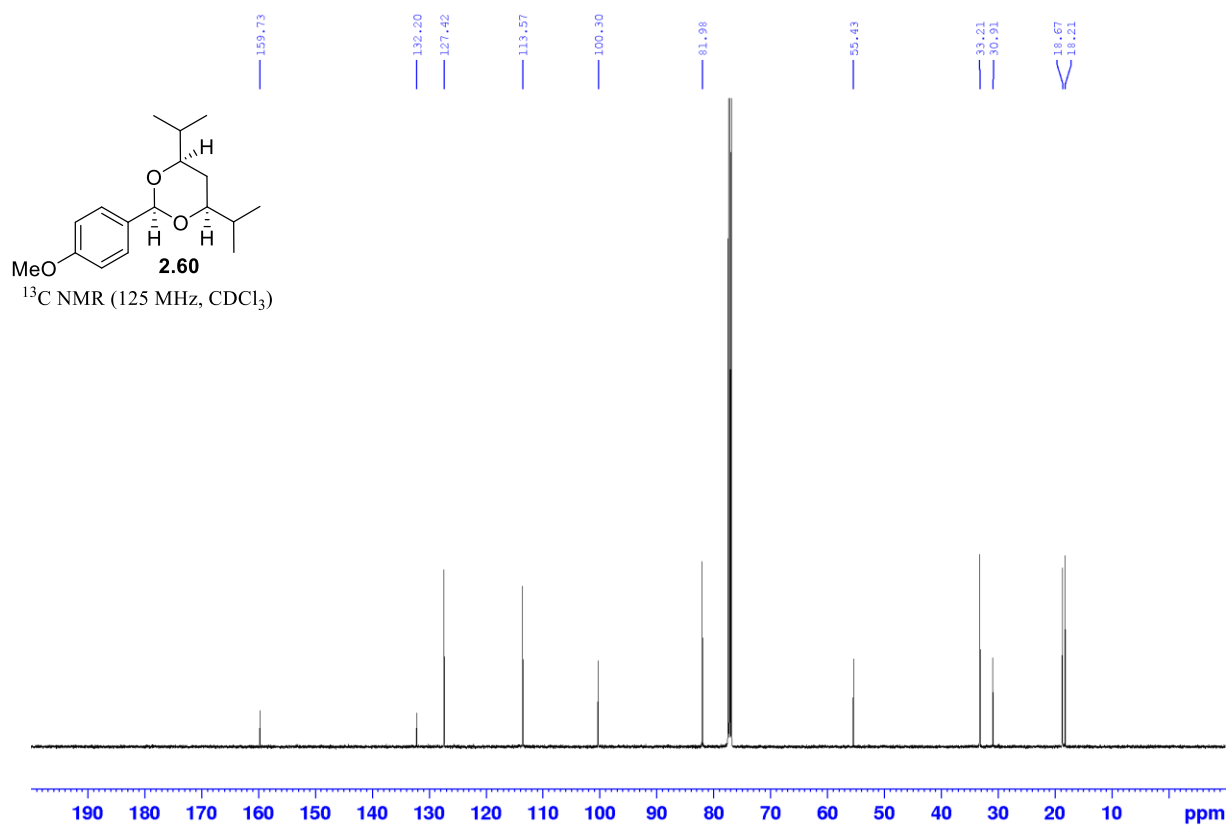
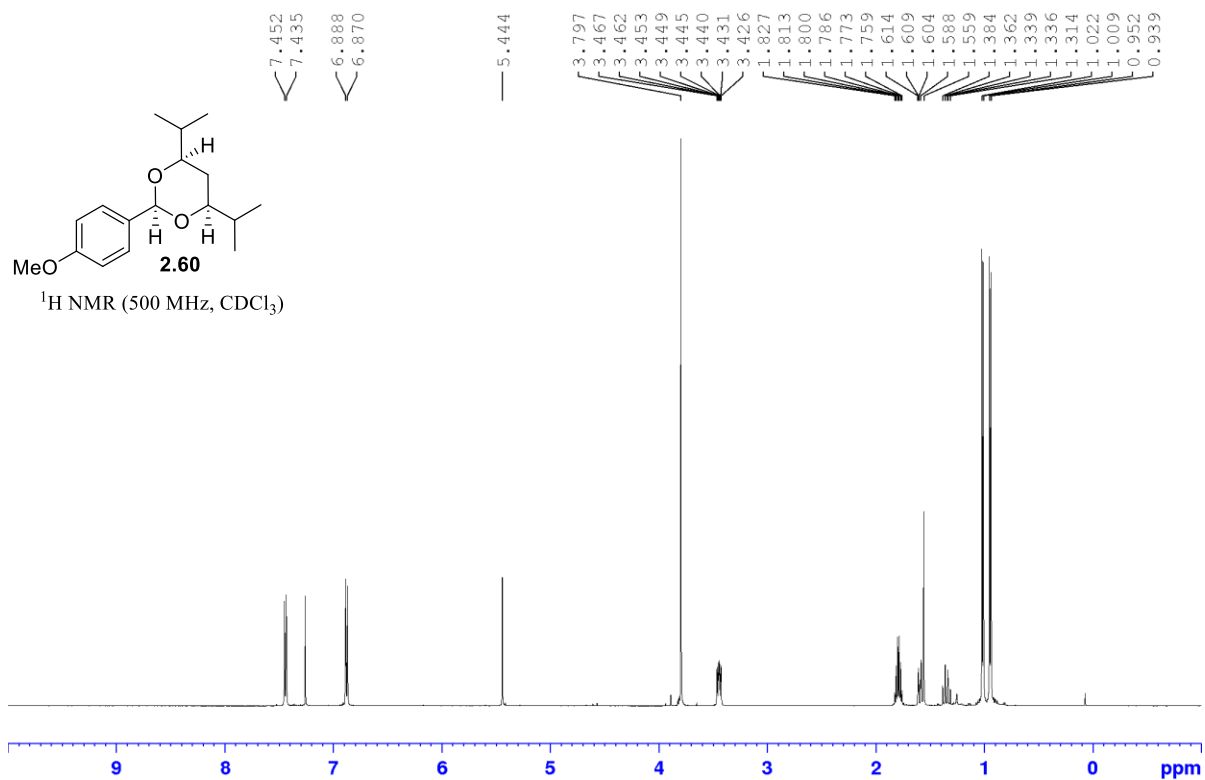


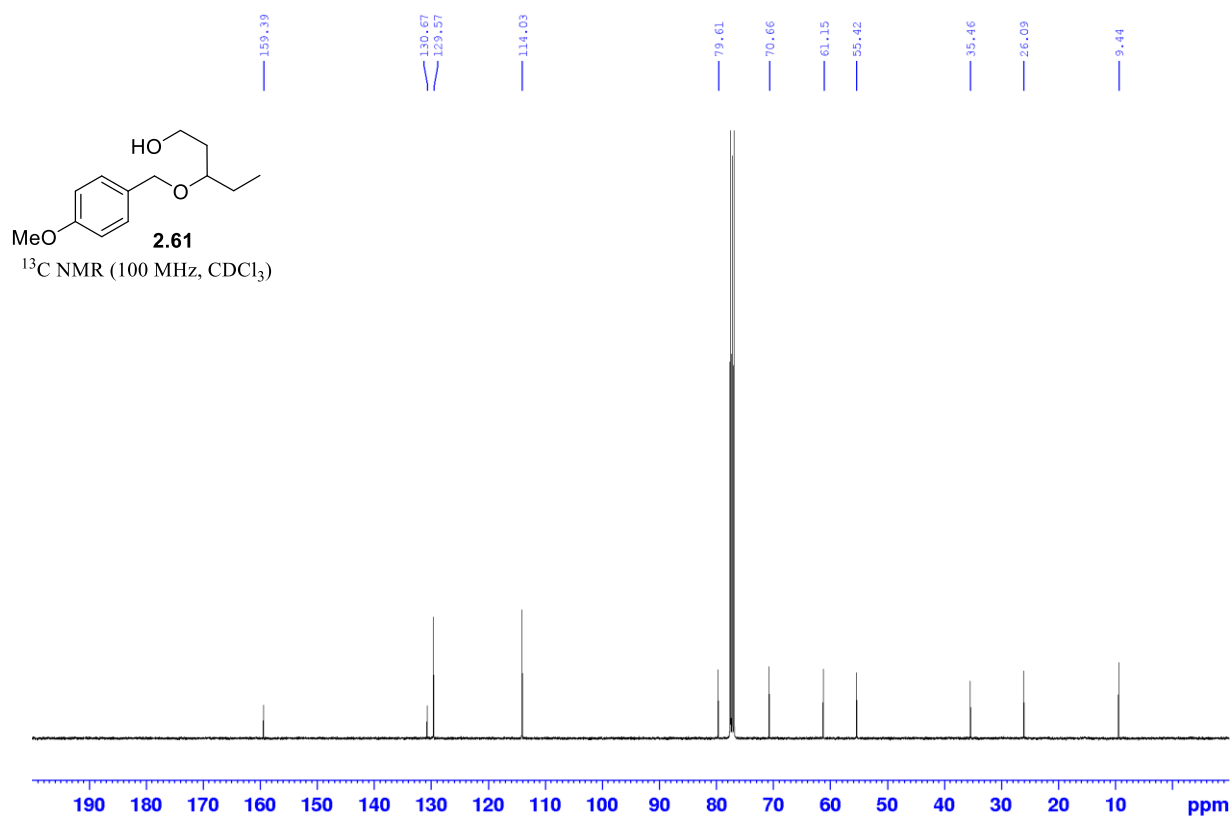
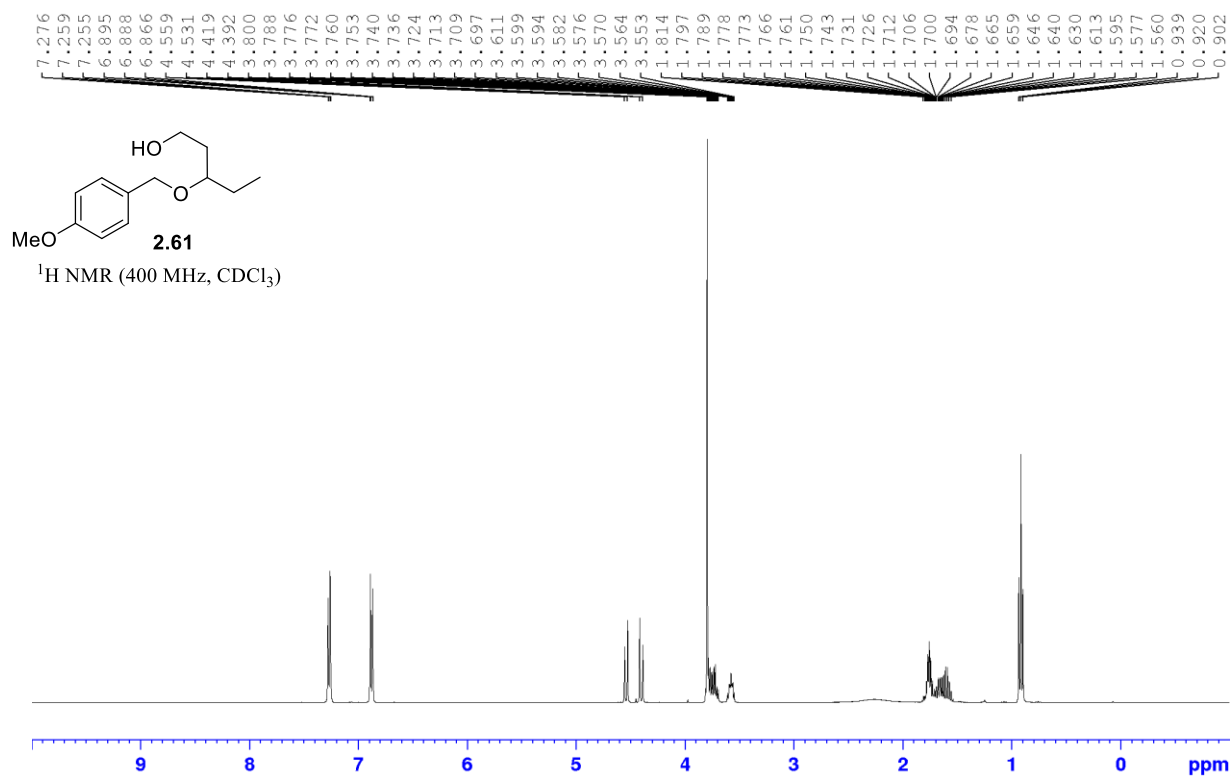


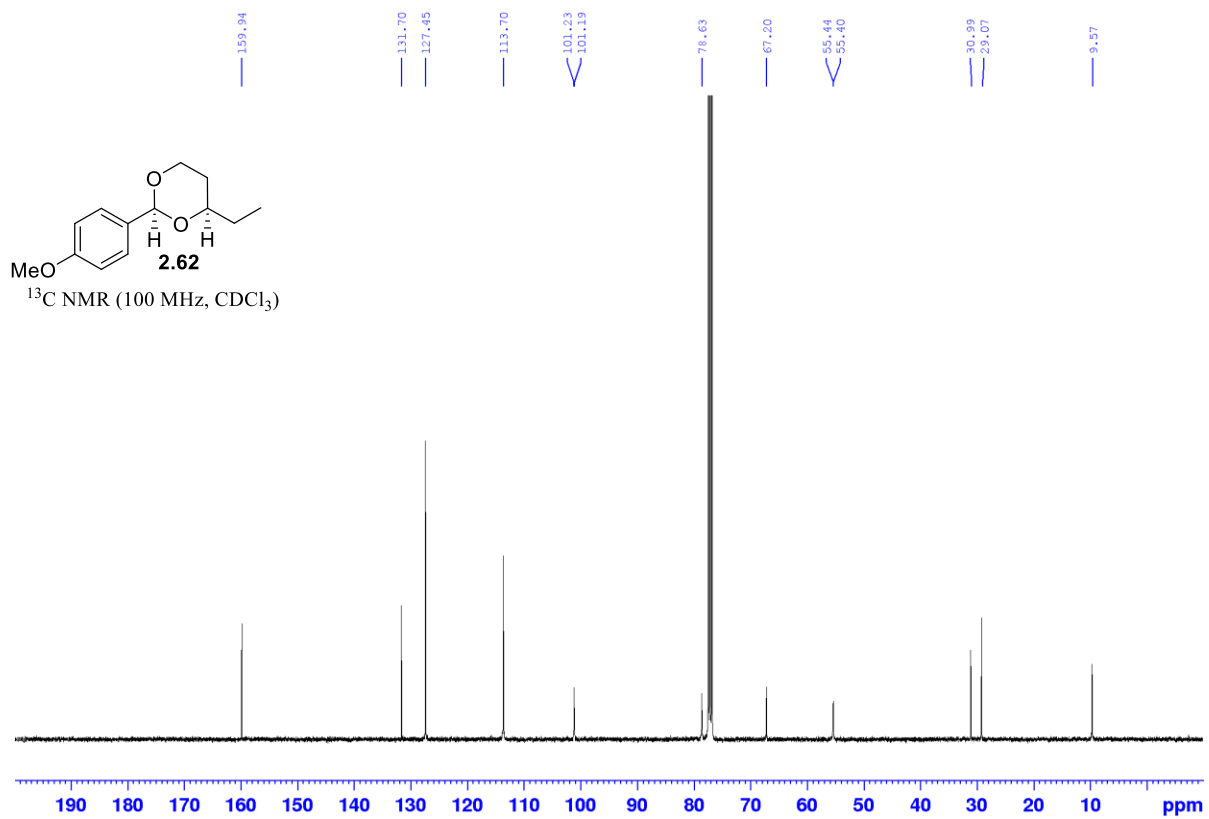
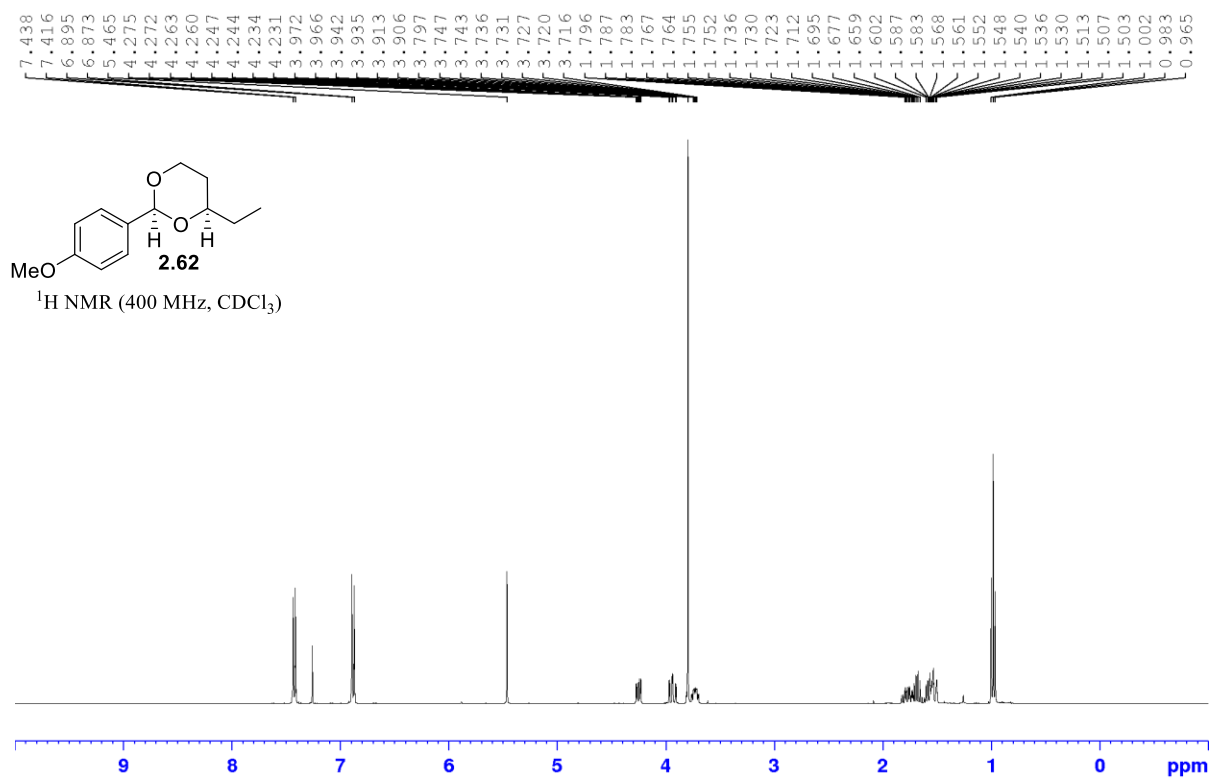


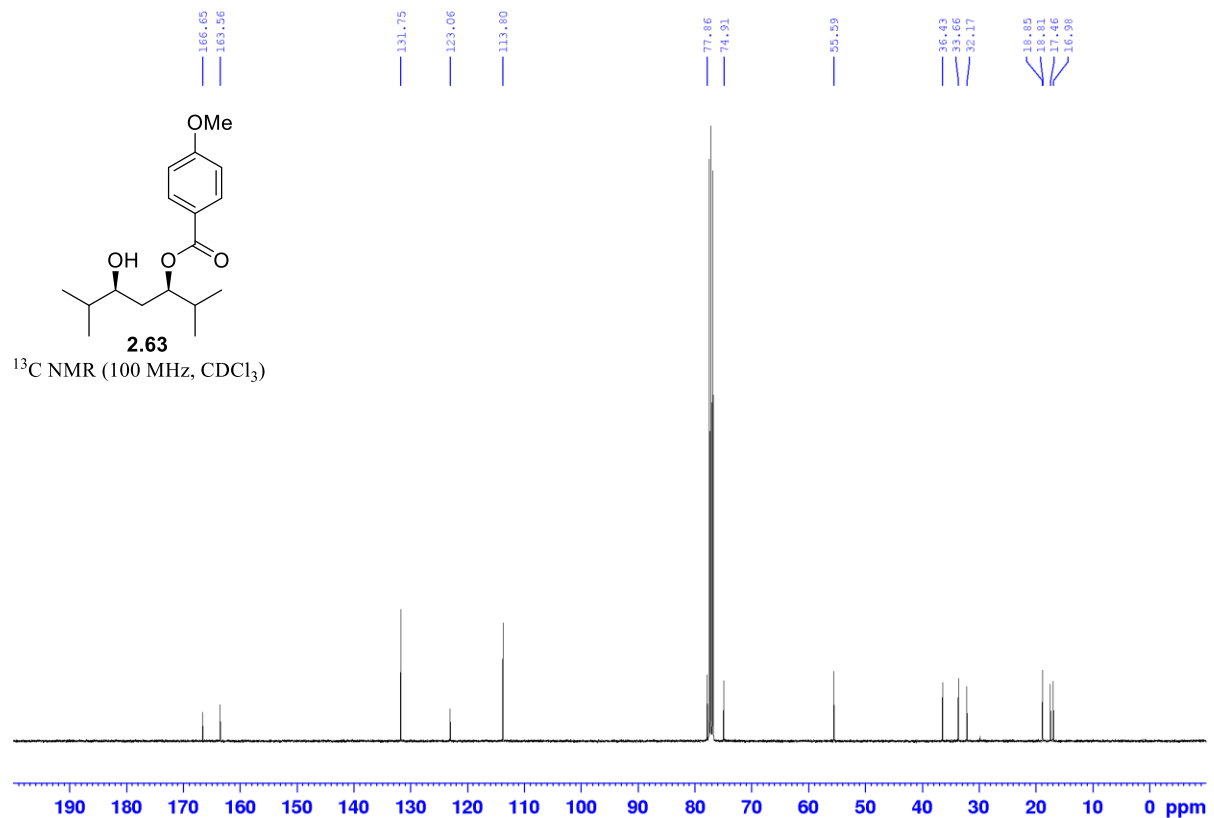
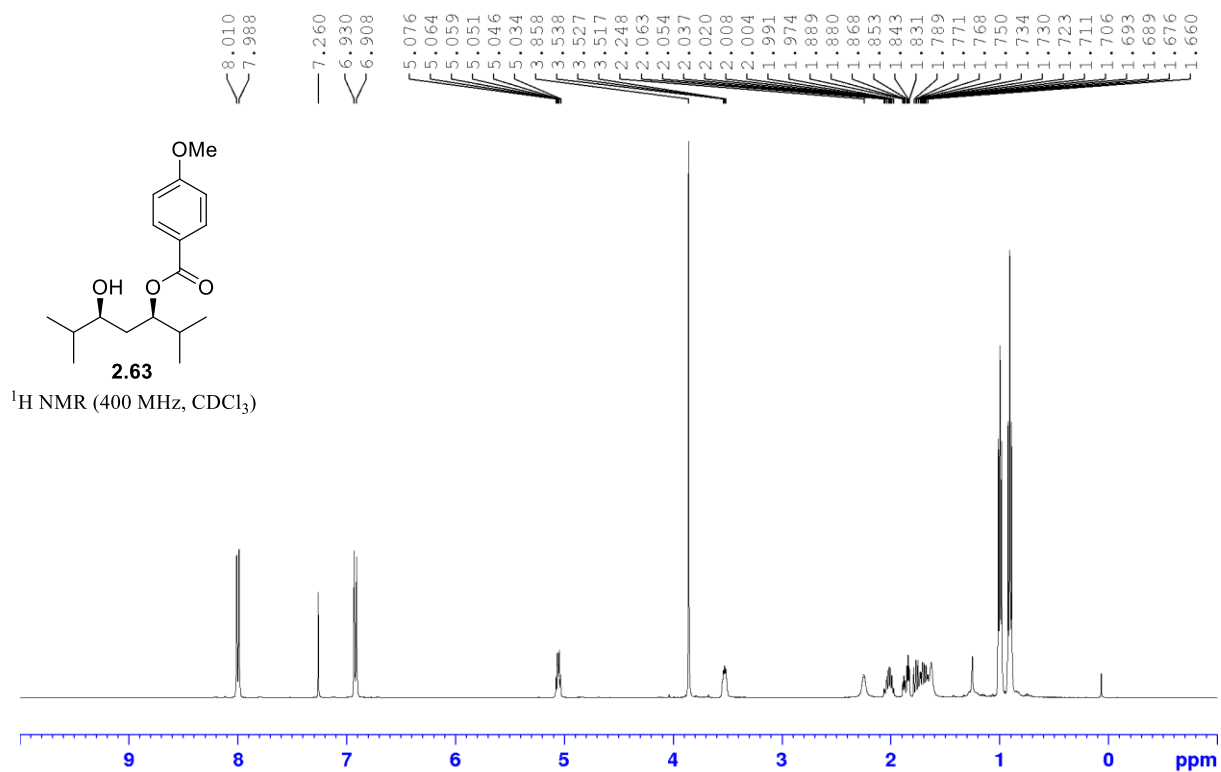


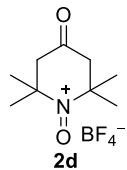




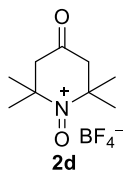
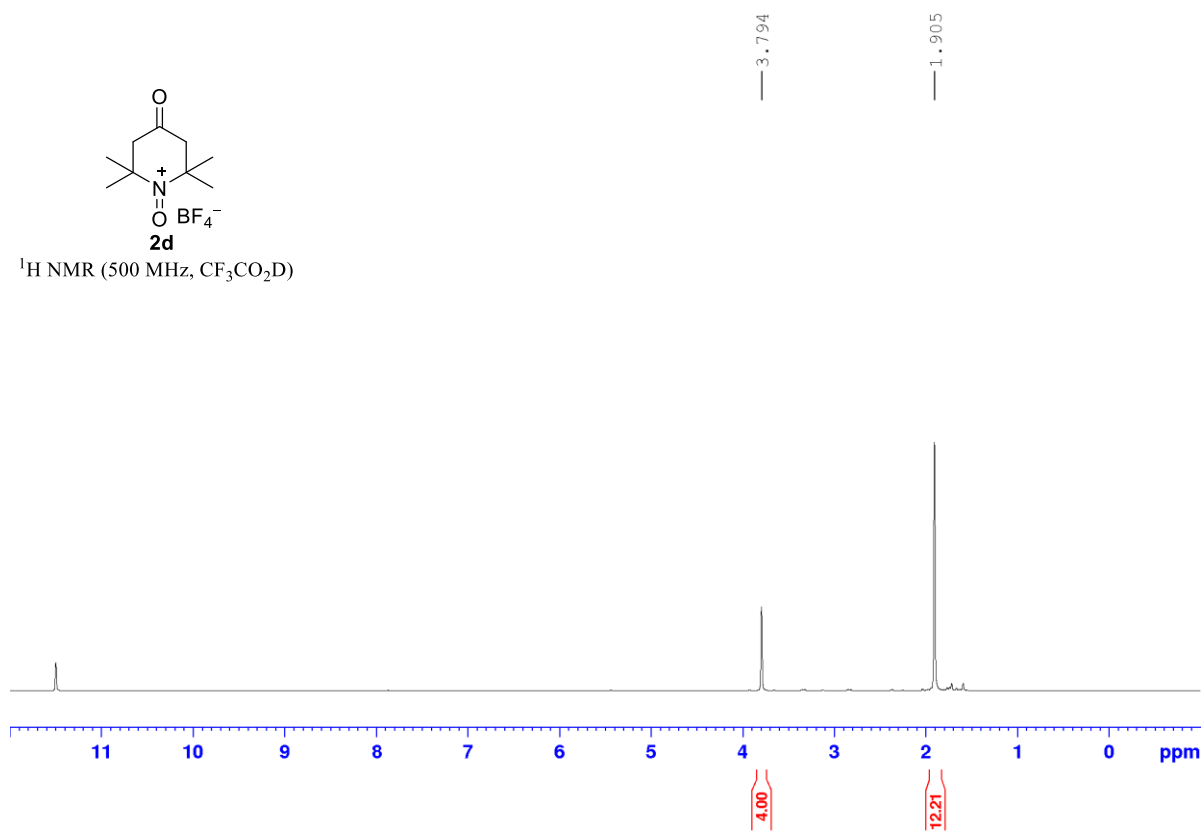




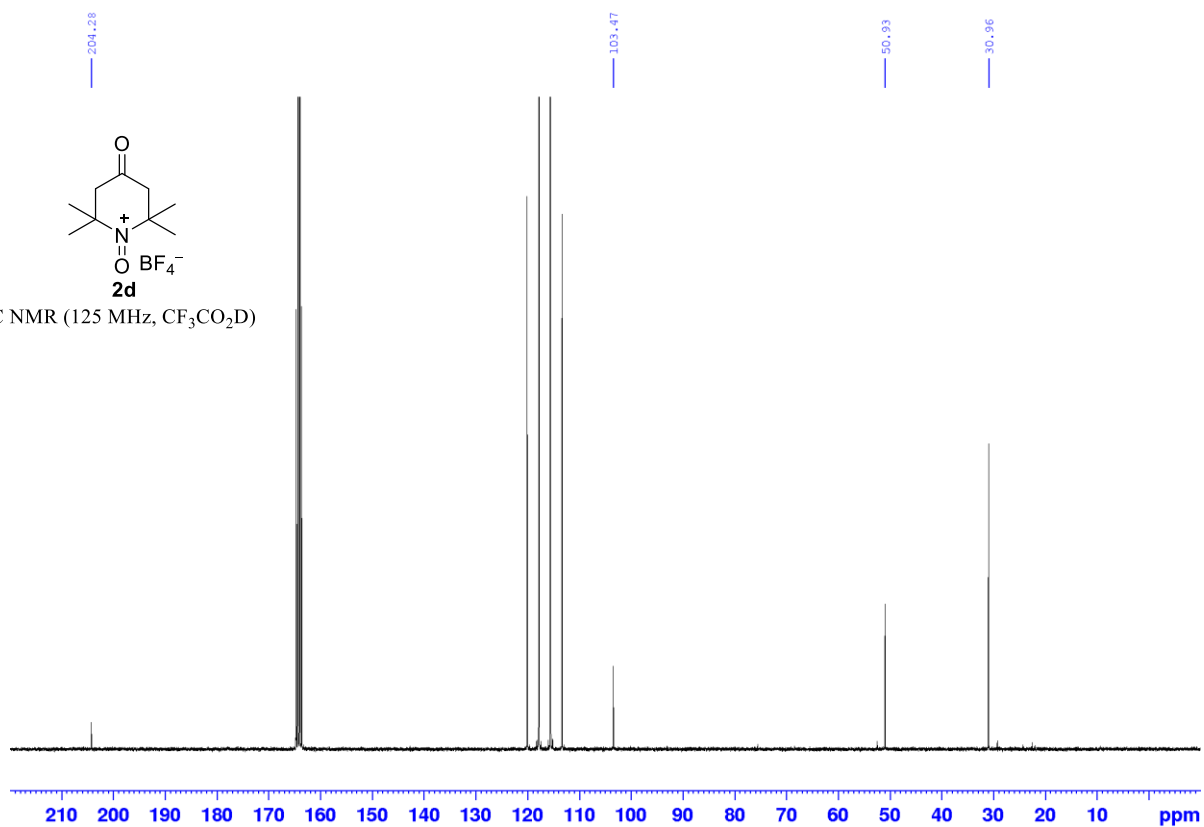


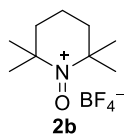


^1H NMR (500 MHz, $\text{CF}_3\text{CO}_2\text{D}$)

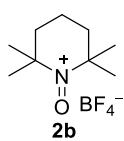
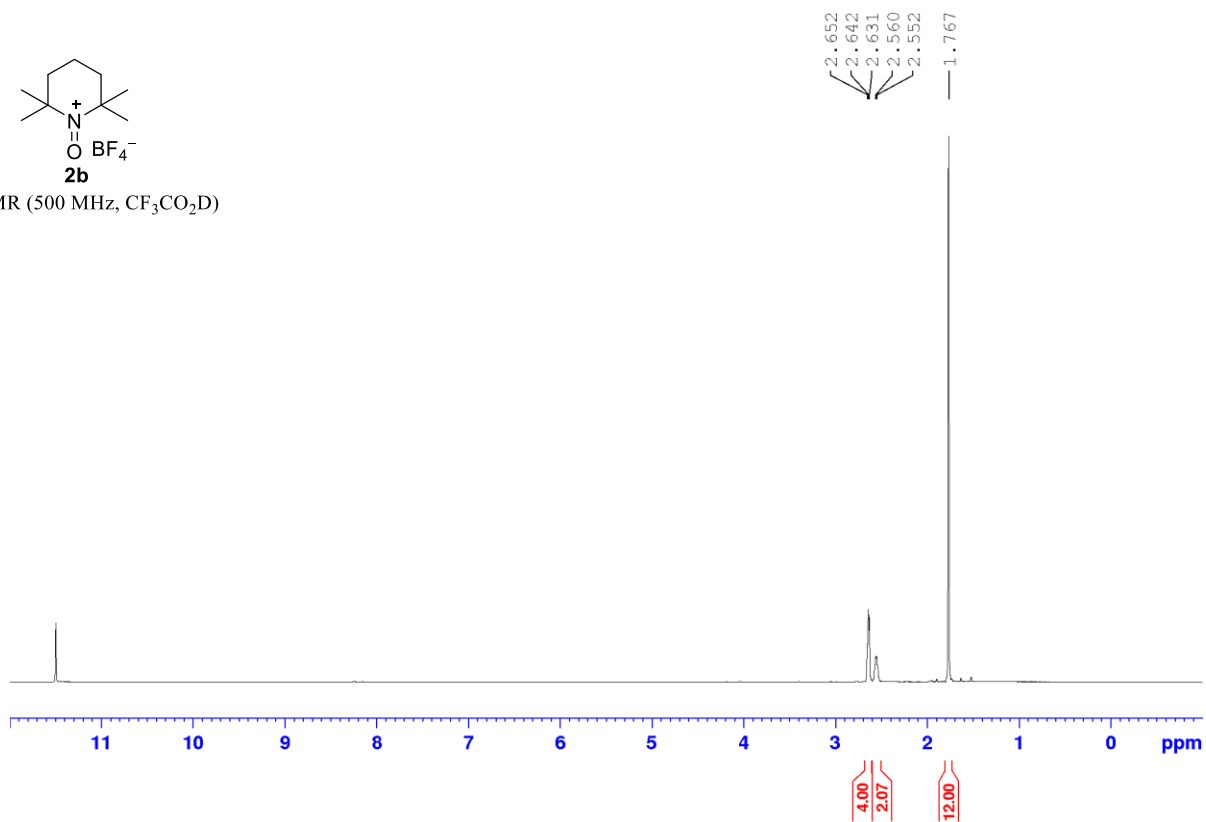


^{13}C NMR (125 MHz, $\text{CF}_3\text{CO}_2\text{D}$)

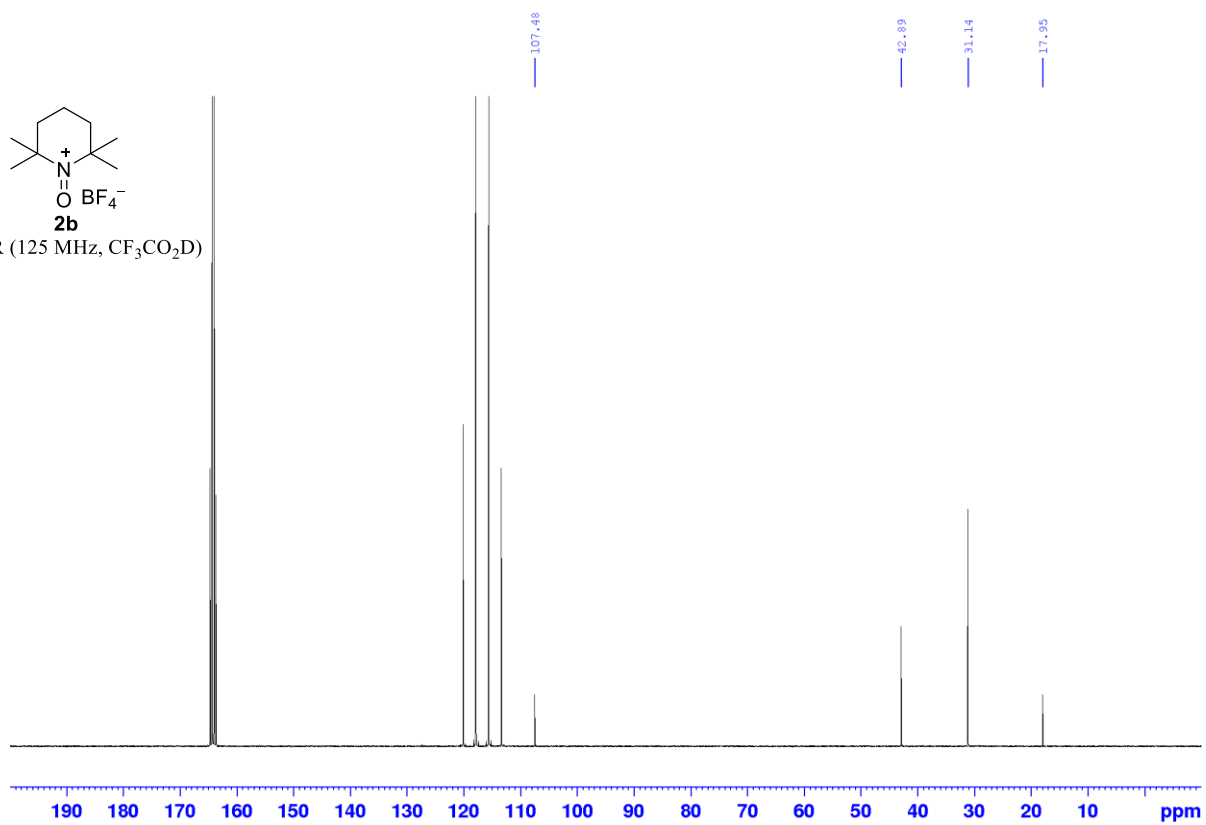


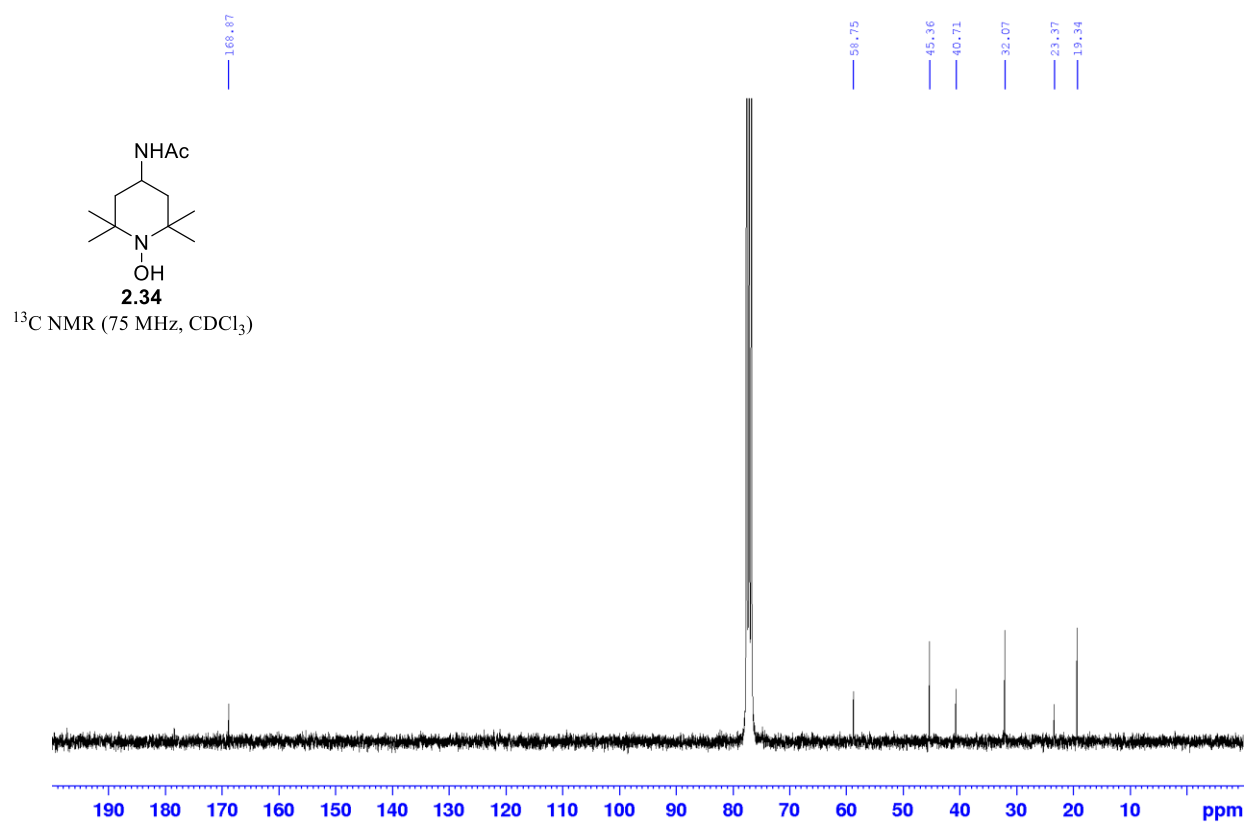
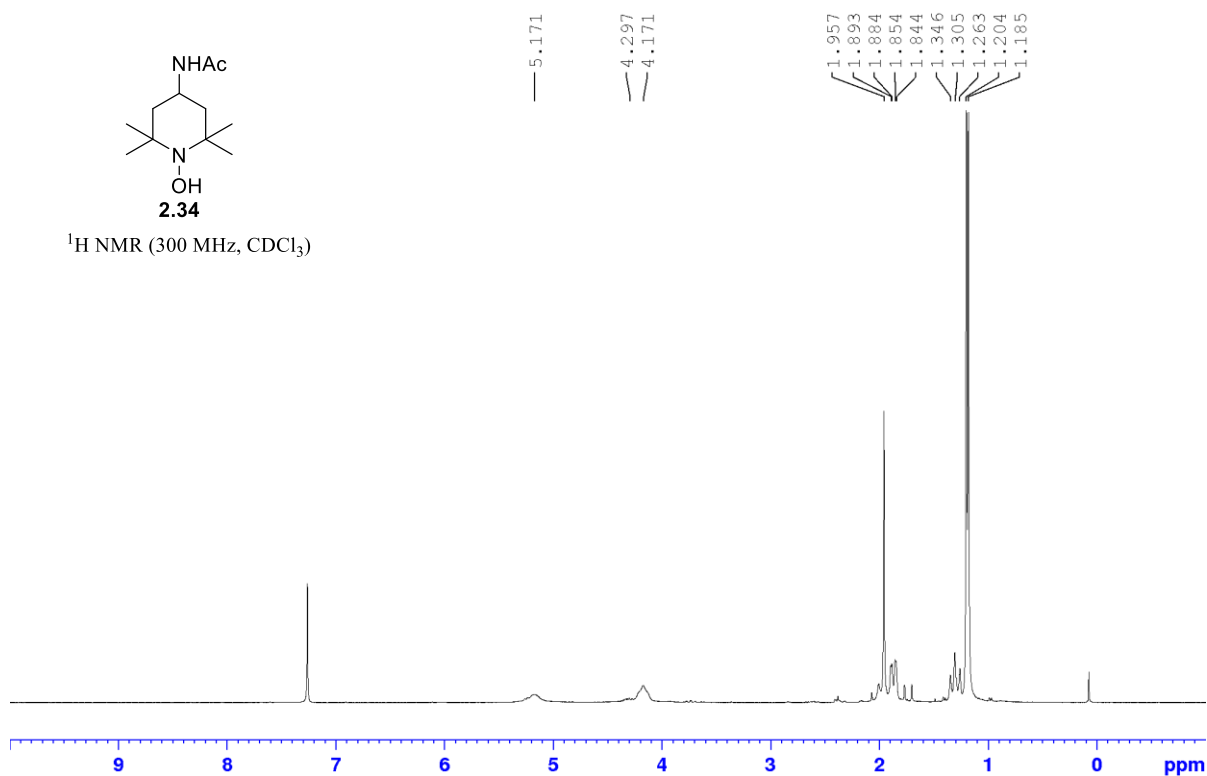


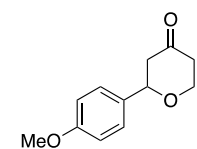
^1H NMR (500 MHz, $\text{CF}_3\text{CO}_2\text{D}$)



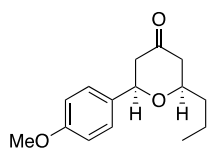
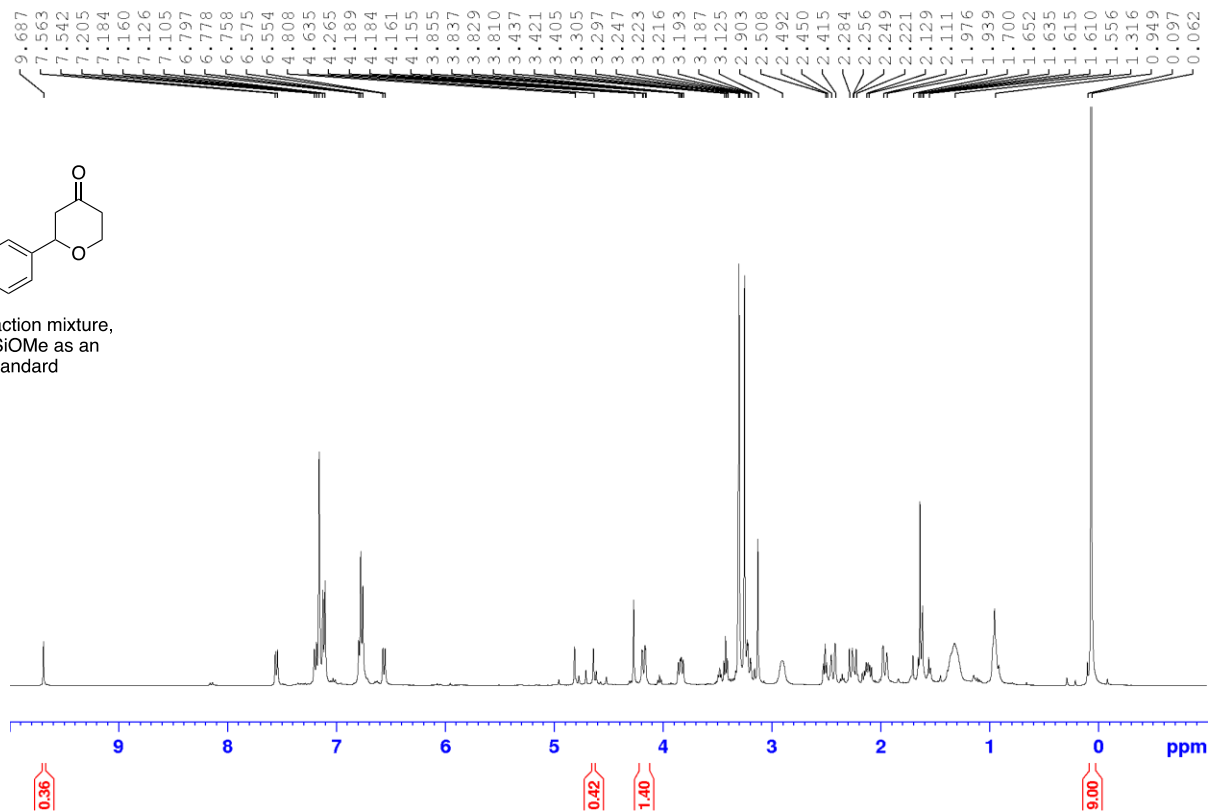
^{13}C NMR (125 MHz, $\text{CF}_3\text{CO}_2\text{D}$)



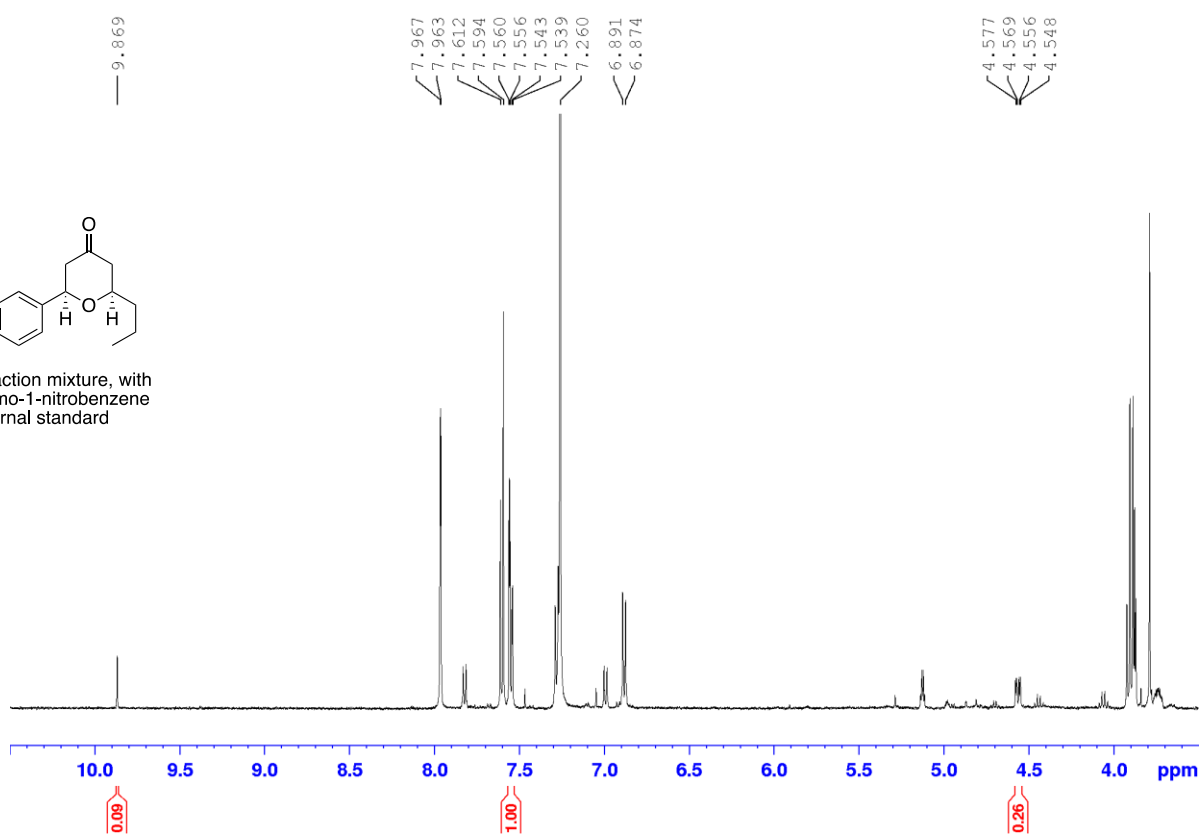


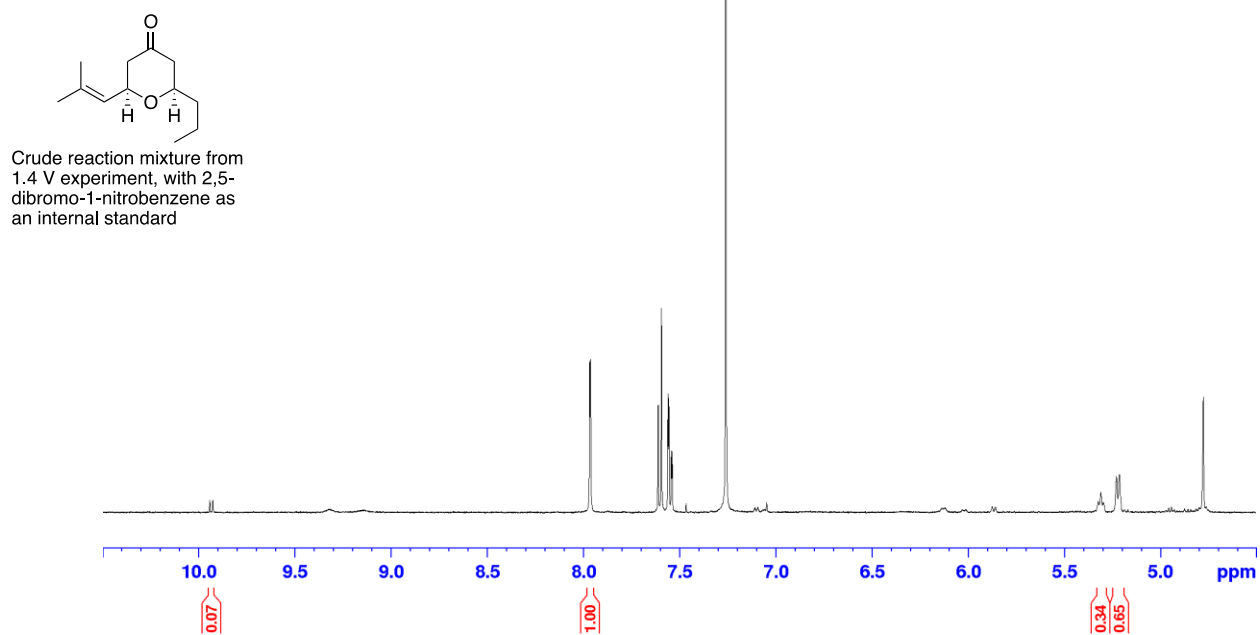
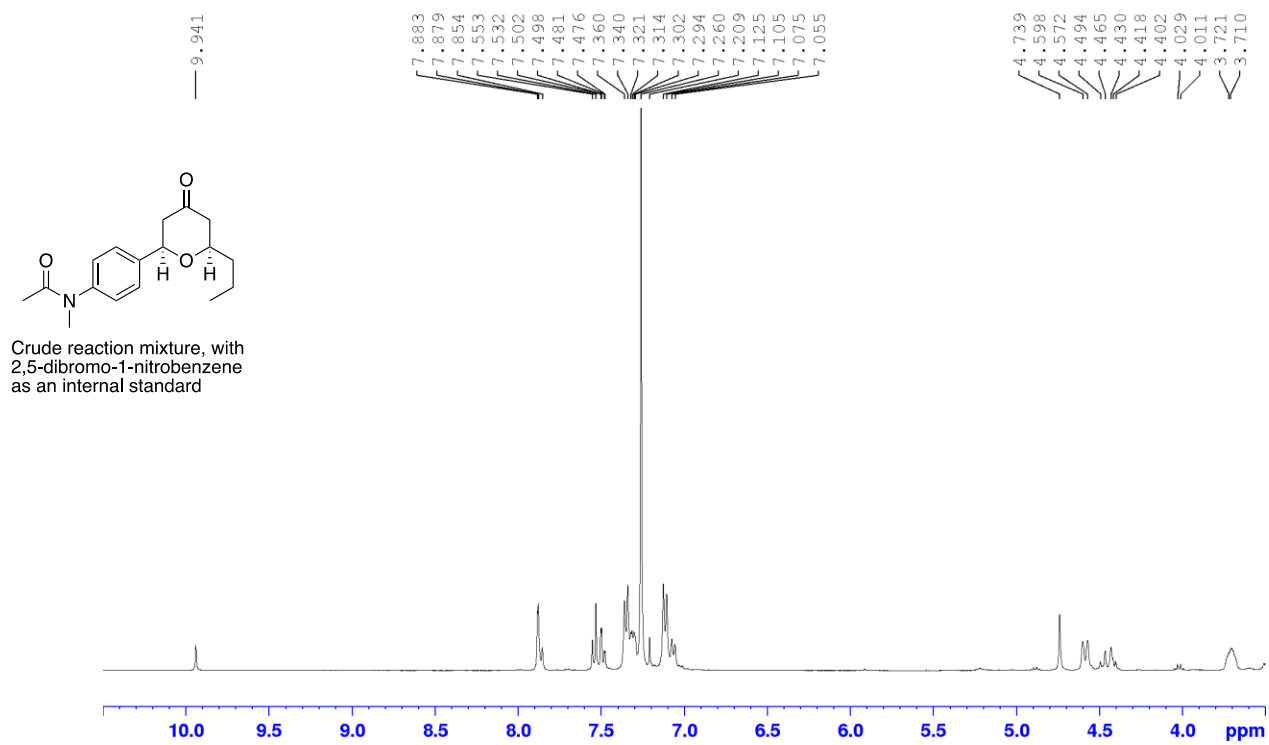


Crude reaction mixture,
with Me₃SiOMe as an
internal standard



Crude reaction mixture, with
2,5-dibromo-1-nitrobenzene
as an internal standard





Bibliography

1. Mooberry, S. L., Tien, G., Hernandez, A. H., Plubrukarn, A., Davidson, B. S., *Cancer Res.* **1999**, *59* (3), 653-60.
2. Nelson, S. G., Cheung, W. S., Kassick, A. J., Hilfiker, M. A., *J. Am. Chem. Soc.* **2002**, *124* (46), 13654-5.
3. Ghosh, A. K., Wang, Y., *J. Am. Chem. Soc.* **2000**, *122* (44), 11027-11028.
4. Smith, A. B., Dong, S., Brenneman, J. B., Fox, R. J., *J. Am. Chem. Soc.* **2009**, *131* (34), 12109-11.
5. Semeyn, C., Blaauw, R. H., Hiemstra, H., Speckamp, W. N., *J. Org. Chem.* **1997**, *62* (11), 3426-3427.
6. Yu, H., Lee, R., Kim, H., Lee, D., *Org. Lett.* **2021**, *23* (3), 1135-1140.
7. Hanessian, S., Focken, T., Oza, R., *Tetrahedron*, **2011**, *67* (51), 9870-9884.
8. Um, J. M., Houk, K. N., Phillips, A. J., *Org. Lett.* **2008**, *10* (17), 3769-3772.
9. Danishefsky, S. J., Selnick, H. G., Deninno, M. P., Zelle, R. E., *J. Am. Chem. Soc.* **1987**, *109* (5), 1572-1574.
10. Wierschke, S. G., Chandrasekhar, J., Jorgensen, W. L., *J. Am. Chem. Soc.* **1985**, *107* (6), 1496-1500.
11. Crimmins, M. T., Emmitte, K. A., *Org. Lett.* **1999**, *1* (12), 2029-2032.
12. Flamme, E. M., Roush, W. R., *Beilstein J. Org. Chem.* **2005**, *1*.
13. Vukovic, V. D., Richmond, E., Wolf, E., Moran, J., *Angew. Chem. Int. Ed.* **2017**, *56* (11), 3085-3089.

14. Aponick, A., Biannic, B., *Org. Lett.* **2011**, *13* (6), 1330-3.
15. Aponick, A., Li, C. Y., Biannic, B., *Org. Lett.* **2008**, *10* (4), 669-71.
16. Mukherjee, P., Widenhoefer, R. A., *Org. Lett.* **2011**, *13* (6), 1334-7.
17. Uenishi, J., Ohmi, M.; Ueda, A., *Tetrahedron: Asymmetry*, **2005**, *16* (7), 1299-1303.
18. Zeni, G., Larock, R. C., *Chem. Rev.* **2004**, *104* (5), 2285-2309.
19. Palimkar, S. S., Uenishi, J., *Org. Lett.* **2010**, *12* (18), 4160-3.
20. Hattori, Y., Furuhashi, S., Okajima, M., Konno, H., Abe, M., Miyoshi, H., Goto, T., Makabe, H., *Org. Lett.* **2008**, *10* (5), 717-720.
21. Guerinot, A., Serra-Muns, A., Bensoussan, C., Reymond, S., Cossy, J., *Tetrahedron*, **2011**, *67* (27-28), 5024-5033.
22. Guerinot, A., Serra-Muns, A., Gnam, C., Bensoussan, C., Reymond, S., Cossy, J., *Org. Lett.* **2010**, *12* (8), 1808-1811.
23. Guérinot, A., Serra-Muns, A., Gnam, C., Bensoussan, C., Reymond, S., Cossy, J., *Org. Lett.* **2010**, *12* (8), 1808-1811.
24. Matsubara, S., Okazoe, T., Oshima, K., Takai, K., Nozaki, H., *Bull. Chem. Soc. Jpn.* **1985**, *58* (3), 844-849.
25. Qin, H., Yamagiwa, N., Matsunaga, S., Shibasaki, M., *Angew. Chem. Int. Ed.* **2007**, *46* (3), 409-413.
26. Peyman Salehi, N. I., Farahnaz K. B., *Tetrahedron*, **1998**, *54*, 943-948.
27. Morrill, C., Grubbs, R. H., *J. Am. Chem. Soc.* **2005**, *127* (9), 2842-2843.
28. Chabardes, P., Kuntz, E., Varagnat, J., *Tetrahedron*, **1977**, *33* (14), 1775-1783.
29. Bellemin-Laponnaz, S., Gisie, H., LeNy, J. P., Osborn, J. A., *Angew. Chem. Int. Ed.* **1997**, *36* (9), 976-978.

30. Xie, Y., Floreancig, P. E., *Angew. Chem. Int. Ed.* **2014**, 53 (19), 4926-9.
31. Asari, A. H., Floreancig, P. E., *Angew. Chem. Int. Ed.* **2020**, 59 (16), 6622-6626.
32. Floreancig, P. E., *Synlett*, **2021**, 32 (14), 1406-1418.
33. Xie, Y., Floreancig, P. E., *Angew. Chem. Int. Ed.* **2013**, 52 (2), 625-8.
34. Lawrence, J. I. A., Floreancig, P. E., *Org. Lett.* **2020**, 22 (24), 9513-9517.
35. Qin, Q., Xie, Y., Floreancig, P. E., *Chem. Sci.* **2018**, 9 (45), 8528-8534.
36. Rodriguez Del Rey, F. O.; Floreancig, P. E., *Org. Lett.* **2021**, 23 (1), 150-154.
37. Rohrs, T. M., Qin, Q., Floreancig, P. E., *Angew. Chem. Int. Ed.* **2017**, 56 (36), 10900-10904.
38. Afeke, C., Xie, Y., Floreancig, P. E., *Org. Lett.* **2019**, 21 (13), 5064-5067.
39. Dischmann, M., Frassetto, T., Breuning, M. A.; Koert, U., *Chem. Eur. J.* **2014**, 20 (36), 11300-11302.
40. Mo, X. B., Yakiwchuk, J., Dansereau, J., McCubbin, J. A. Hall, D. G., *J. Am. Chem. Soc.* **2015**, 137 (30), 9694-9703.
41. Evans, D. A., Bartroli, J., Shih, T. L., *J. Am. Chem. Soc.* **1981**, 103 (8), 2127-2129.
42. Evans, D. A., Chapman, K. T., Carreira, E. M., *J. Am. Chem. Soc.* **1988**, 110 (11), 3560-3578.
43. Bruice, T. C., Pandit, U. K., *J. Am. Chem. Soc.*, **1960**, 82 (22), 5858-5865.
44. Hoye, T. R., Jeffrey, C. S., Shao, F., *Nat. Protoc.* **2007**, 2 (10), 2451-8.
45. Gao, G., Moore, D., Xie, R. G.; Pu, L. *Org Lett* **2002**, 4 (23), 4143-6.
46. Matsumura, K., Hashiguchi, S., Ikariya, T., Noyori, R., *J. Am. Chem. Soc.* **1997**, 119 (37), 8738-8739.
47. Kaise, H., Shimokawa, J., Fukuyama, T., *Org. Lett.* **2014**, 16 (3), 727-9.
48. Brown, C. A., Ahuja, V. K., *J. Org. Chem.*, **1973**, 38 (12), 2226-2230.
49. Winstein, S., Klinedinst, P. E., Robinson, G. C., *J. Am. Chem. Soc.* **1961**, 83 (4), 885-895.

50. Lewis, E. S., Boozer, C. E., *J. Am. Chem. Soc.* **1952**, *74* (2), 308-311.
51. Morimoto, Y., Iwai, T., *J. Am. Chem. Soc.* **1998**, *120* (7), 1633-1634.
52. Morimoto, Y., Iwai, T., Kinoshita, T., *J. Am. Chem. Soc.* **1999**, *121* (29), 6792-6797.
53. Sharkey, B. E., Jentoft, F. C., *ACS. Catal.* **2019**, *9* (12), 11317-11328.
54. Abrams, D. J., Provencher, P. A., Sorensen, E. J. *Chem. Soc. Rev.* **2018**, *47* (23), 8925-8967.
55. Gutekunst, W. R., Baran, P. S., *Chem. Soc. Rev.* **2011**, *40* (4), 1976-1991.
56. Ali, W., Prakash, G., Maiti, D., *Chem. Sci.* **2021**, *12* (8), 2735-2759.
57. Morales-Rivera, C. A., Floreancig, P. E., Liu, P., *J. Am. Chem. Soc.* **2017**, *139* (49), 17935-17944.
58. Tu, W., Liu, L., Floreancig, P. E., *Angew. Chem. Int. Ed.* **2008**, *47* (22), 4184-4187.
59. Gotta, M. F., Mayr, H., *J. Org. Chem.* **1998**, *63* (26), 9769-9775.
60. Caplan, S. M.; Floreancig, P. E., Total Synthesis of Divergolides E and H. *Angew Chem Int Ed Engl* **2018**, *57* (48), 15866-15870.
61. Cui, Y., Floreancig, P. E., *Org. Lett.* **2012**, *14* (7), 1720-1723.
62. Han, X., Floreancig, P. E., *Angew. Chem. Int. Ed.* **2014**, *53* (41), 11075-11078.
63. Han, X.; Floreancig, P. E., *Org. Lett.* **2012**, *14* (14), 3808-3811.
64. Liu, L., Floreancig, P. E., *Angew. Chem. Int. Ed.* **2010**, *49* (17), 3069-3072.
65. Liu, L., Floreancig, P. E., *Org. Lett.* **2010**, *12* (20), 4686-4689.
66. Liu, L., Floreancig, P. E., *Org. Lett.* **2009**, *11* (14), 3152-3155.
67. Liu, L., Floreancig, P. E., *Angew. Chem. Int. Ed.* **2010**, *49* (34), 5894-5897.
68. Peh, G., Floreancig, P. E., *Org. Lett.* **2015**, *17* (15), 3750-3753.
69. Cavedon, C., Sletten, E. T., Madani, A., Niemeyer, O., Seeberger, P. H., Pieber, B., *Org. Lett.* **2021**, *23* (2), 514-518.

70. Hou, Z.-W., Li, L., Wang, L., *Org. Chem. Front.* **2021**, 8 (17), 4700-4705.
71. Ghosh, A. K., Cheng, X., *Tetrahedron Lett.* **2012**, 53 (20), 2568-2570.
72. Miller, J. L., Zhou, L., Liu, P.; Floreancig, P. E., *Chem. Eur. J.* **2022**, 28 (1), e202103078.
73. Bailey, W. F., Bobbitt, J. M., Wiberg, K. B., *J. Org. Chem.* **2007**, 72 (12), 4504-4509.
74. Kelly, C. B., Ovian, J. M., Cywar, R. M.; Gosselin, T. R., Wiles, R. J.; Leadbeater, N. E., *Org. Biomol. Chem.* **2015**, 13 (14), 4255-4259.
75. Pradhan, P. P., Bobbitt, J. M., Bailey, W. F., *J. Org. Chem.* **2009**, 74 (24), 9524-9527.
76. Lucio Anelli, P., Biffi, C., Montanari, F., Quici, S., *J. Org. Chem.* **1987**, 52 (12), 2559-2562.
77. Hoover, J. M., Ryland, B. L., Stahl, S. S., *J. Am. Chem. Soc.* **2013**, 135 (6), 2357-2367.
78. Das, A., Stahl, S. S., *Angew. Chem. Int. Ed.* **2017**, 56 (30), 8892-8897.
79. Rafiee, M., Alherech, M., Karlen, S. D., Stahl, S. S., *J. Am. Chem. Soc.* **2019**, 141 (38), 15266-15276.
80. Rafiee, M., Konz, Z. M., Graaf, M. D., Koolman, H. F., Stahl, S. S., *ACS Catal.* **2018**, 8 (7), 6738-6744.
81. Rafiee, M., Miles, K. C., Stahl, S. S., *J. Am. Chem. Soc.* **2015**, 137 (46), 14751-14757.
82. Goes, S. L., Mayer, M. N., Nutting, J. E., Hooper-Burkhardt, L. E., Stahl, S. S., Rafiee, M., *J. Chem. Ed.* **2021**, 98 (2), 600-606.
83. Wang, F., Rafiee, M., Stahl, S. S., *Angew. Chem. Int. Ed.* **2018**, 57 (22), 6686-6690.
84. Nutting, J. E., Gerken, J. B., Stamoulis, A. G., Bruns, D. L., Stahl, S. S., *J. Org. Chem.* **2021**, 86 (22), 15875-15885.
85. Clausen, D. J., Floreancig, P. E., *J. Org. Chem.* **2012**, 77 (15), 6574-6582.
86. Jung, H. H., Floreancig, P. E., *Tetrahedron*, **2009**, 65 (52), 10830-10836.
87. Jung, H. H., Seiders, J. R., Floreancig, P. E., *Angew. Chem. Int. Ed.* **2007**, 46 (44), 8464-7.

88. Gerken, J. B., Pang, Y. Q., Lauber, M. B., Stahl, S. S., *J. Org. Chem.* **2018**, 83 (14), 7323-7330.
89. Nutting, J. E., Rafiee, M., Stahl, S. S., *Chem. Rev.* **2018**, 118 (9), 4834-4885.
90. Zhong, X., Hoque, M. A., Graaf, M. D., Harper, K. C., Wang, F., Genders, J. D., Stahl, S. *S. Org. Process Res. Dev.* **2021**, 25 (12), 2601-2607.
91. Lennox, A. J. J., Goes, S. L., Webster, M. P., Koolman, H. F., Djuric, S. W., Stahl, S. S., *J. Am. Chem. Soc.*, **2018**, 140 (36), 11227-11231.
92. Lawrence, J.-M. I. A., Floreancig, P. E., *Chem. Eur. J.* **2022**, e202200335.
93. Gholap, S. P., Jangid, D., Fernandes, R. A., *J. Org. Chem.* **2019**, 84 (6), 3537-3551.
94. Goossen, L. J., Paetzold, J., Koley, D., *Chem. Commun.* **2003**, (6), 706-707.
95. Neveux, M., Bruneau, C., Dixneuf, P. H., *J. Chem. Soc., Perkin Trans.* **1991**, 1 (5), 1197.
96. Costentin, C., Drouet, S., Robert, M., Savéant, J.-M., *J. Am. Chem. Soc.*, **2012**, 134 (27), 11235-11242.
97. Kingston, C., Palkowitz, M. D., Takahira, Y., Vantourout, J. C., Peters, B. K., Kawamata, Y., Baran, P. S., *Acc. Chem. Res.* **2020**, 53 (1), 72-83.
98. Heard, D. M., Lennox, A. J. J., *Angew. Chem. Int. Ed.* **2020**, 59 (43), 18866-18884.
99. Liu, K., Wu, J., Deng, Y., Song, C., Song, W., Lei, A., *Chem. Electrochem.* **2019**, 6 (16), 4173-4176.
100. Wang, F., Stahl, S. S., *Angew. Chem. Int. Ed.* **2019**, 58 (19), 6385-6390.
101. Deprez, N. R., Clausen, D. J., Yan, J. X., Peng, F., Zhang, S., Kong, J., Bai, Y., *Org. Lett.* **2021**, 23 (22), 8834-8837.
102. Liu, C., Szostak, M., *Chem. Eur. J.* **2017**, 23 (30), 7157-7173.

103. Narasaka, K., Pai, F.-C., *Tetrahedron*, **1984**, 40 (12), 2233-2238.
104. Kim, M. C., Machado, H., Jang, K. H., Trzoss, L., Jensen, P. R., Fenical, W., *J. Am. Chem. Soc.* **2018**, 140 (34), 10775-10784.
105. Yu, J.-L., Wang, H., Zou, K.-F., Zhang, J.-R., Gao, X., Zhang, D.-W., Li, Z.-T., *Tetrahedron* **2013**, 69 (1), 310-315.
106. Merbouh, N., Bobbitt, J. M., Brückner, C., *Org. Prep. Proced. Int.* **2004**, 36 (1), 1-31..
107. Bobbitt, J. M., Eddy, N. A., Cady, C. X., Jin, J., Gascon, J. A., Gelpí-Dominguez, S., Zakrzewski, J., Morton, M. D., *J. Org. Chem.* **2017**, 82 (18), 9279-9290.